

CA84006665

52033

# **Interseasonal Changes of Wind Stress and Ekman Upwelling: North Atlantic, 1950-1980**

Keith R. Thompson and Mark G. Hazen

Department of Oceanography  
Dalhousie University  
Halifax, Nova Scotia B3H 4J1  
(Published by: Ocean Science and Surveys,  
Atlantic, Department of Fisheries and  
Oceans)

October 1983

**Canadian Technical Report of  
Fisheries and Aquatic Sciences  
No. 1214**



Government of Canada  
Fisheries and Oceans

Gouvernement du Canada  
Pêches et Océans

## **Canadian Technical Report of Fisheries and Aquatic Sciences**

These reports contain scientific and technical information that represents an important contribution to existing knowledge but which for some reason may not be appropriate for primary scientific (i.e. *Journal*) publication. Technical Reports are directed primarily towards a worldwide audience and have an international distribution. No restriction is placed on subject matter and the series reflects the broad interests and policies of the Department of Fisheries and Oceans, namely, fisheries management, technology and development, ocean sciences, and aquatic environments relevant to Canada.

Technical Reports may be cited as full publications. The correct citation appears above the abstract of each report. Each report will be abstracted in *Aquatic Sciences and Fisheries Abstracts* and will be indexed annually in the Department's index to scientific and technical publications.

Numbers 1-456 in this series were issued as Technical Reports of the Fisheries Research Board of Canada. Numbers 457-714 were issued as Department of the Environment, Fisheries and Marine Service, Research and Development Directorate Technical Reports. Numbers 715-924 were issued as Department of Fisheries and the Environment, Fisheries and Marine Service Technical Reports. The current series name was changed with report number 925.

Details on the availability of Technical Reports in hard copy may be obtained from the issuing establishment indicated on the front cover.

## **Rapport technique canadien des sciences halieutiques et aquatiques**

Ces rapports contiennent des renseignements scientifiques et techniques qui constituent une contribution importante aux connaissances actuelles mais qui, pour une raison ou pour une autre, ne semblent pas appropriés pour la publication dans un journal scientifique. Il n'y a aucune restriction quant au sujet, de fait, la série reflète la vaste gamme des intérêts et des politiques du Ministère des Pêches et des Océans, notamment gestion des pêches, techniques et développement, sciences océaniques et environnements aquatiques, au Canada.

Les Rapports techniques peuvent être considérés comme des publications complètes. Le titre exact paraîtra au haut du résumé de chaque rapport, qui sera publié dans la revue *Aquatic Sciences and Fisheries Abstracts* et qui figurera dans l'index annuel des publications scientifiques et techniques du Ministère.

Les numéros 1-456 de cette série ont été publiés à titre de Rapports techniques de l'Office des recherches sur les pêcheries du Canada. Les numéros 457-714, à titre de Rapports techniques de la Direction générale de la recherche et du développement, Service des pêches et de la mer, ministère de l'Environnement. Les numéros 715-924 ont été publiés à titre de Rapports techniques du Service des pêches et de la mer, Ministère des Pêches et de l'Environnement. Le nom de la série a été modifié à partir du numéro 925.

La page couverture porte le nom de l'établissement auteur où l'on peut se procurer les rapports sous couverture cartonnée.

*CA8404665*

CANADIAN TECHNICAL REPORT OF  
FISHERIES AND AQUATIC SCIENCES NO. 1214

October 1983

INTERSEASONAL CHANGES OF WIND STRESS AND EKMAN UPWELLING:  
NORTH ATLANTIC, 1950-80.

by

Keith R. Thompson and Mark G. Hazen

Department of Oceanography  
Dalhousie University  
Halifax, Nova Scotia B3H 4J1

Published by:

Ocean Science and Surveys, Atlantic  
Department of Fisheries and Oceans  
Bedford Institute of Oceanography  
P. O. Box 1006  
Dartmouth, Nova Scotia B2Y 4A2

(c) Minister of Supply and Services Canada 1983

Cat. No. Fs 97-6/1214

ISSN 0706-6457

## TABLE OF CONTENTS

Abstract/Résumé . . . . .	iv
1. INTRODUCTION . . . . .	1
2. METHOD . . . . .	5
3. SEASONAL AND DECADAL MEAN MAPS . . . . .	9
4. SEASONAL ANOMALY MAPS . . . . .	10
5. SELECTED TIME SERIES . . . . .	11
Acknowledgements . . . . .	12
References . . . . .	13
(Figures) . . . . .	19

CA84ff665

## ABSTRACT

Thompson, Keith R. and Mark G. Hazen. 1983. Interseasonal changes of wind stress and Ekman upwelling: North Atlantic, 1950-80. Can. Tech. Rep. Fish. Aquat. Sci. No. 1214: 175 pp.

Wind stress and Ekman upwelling maps are presented for the 124 individual seasons covering the period 1950-80. They were calculated using a method recently devised by Thompson et al. (1983). The maps both update and improve upon those previously available. Time series of wind stress and Ekman upwelling at selected locations are also given to illustrate the temporal variability.

## RÉSUMÉ

Thompson, Keith R. and Mark G. Hazen. 1983. Interseasonal changes of wind stress and Ekman upwelling: North Atlantic, 1950-80. Can. Tech. Rep. Fish. Aquat. Sci. No. 1214: 175 pp.

Ce rapport présente les cartes décrivant la tension éolienne et l'upwelling d'Ekman pour 124 saisons, de 1950 à 1980. Ces résultats ont été obtenus à l'aide d'une méthode mise au point par Thompson et al. (1983). Ces cartes constituent une mise à jour et une amélioration de celles disponibles auparavant. Des séries temporelles de données de la tension éolienne et de l'upwelling d'Ekman en des endroits particuliers sont présentées afin d'en illustrer la variation temporelle.

## 1 Introduction

It has been suggested that North Atlantic plankton abundance and fish recruitment exhibit large scale patterns of variability. This has encouraged biologists to search for a link with environmental changes. (A detailed review has recently been given by Cushing, 1982). Colebrook (1978), for example, reported similarity in the low frequency fluctuations of north-east Atlantic and North Sea zooplankton abundance. Garrod and Colebrook (1978) found evidence for synchronous changes in the recruitment of widely separated fish stocks of the North Atlantic. Doubts concerning the reality of such large scale patterns, and the role of the environment, have been raised (Akenhead et al, 1981). However, it is not our intention to enter such a debate in this report - we simply hope to provide indices which may prove useful in future attempts to clarify the role of the environment on the North Atlantic ecosystem.

Several indices have previously been used to describe the environmental variability. Colebrook (1978) used North Atlantic sea surface temperature patterns and 'the frequency of days per year of westerly weather type over the United Kingdom' to account for changes in zooplankton abundance. Garrod and Colebrook (1978) used air pressure as an index of North Atlantic wind patterns to explain the common variability in the recruitment of Arctic Cod and North Sea plaice. Although statistically

significant empirical relationships were reportedly found between the environmental and biological time series, the underlying causal relationships were not obvious.

A major problem in such empirical studies is the choice of suitable environmental indices. One important consideration is clearly data availability if decadal changes are to be examined. On the other hand, if too obscure an index is chosen the study may not necessarily advance our understanding of the driving mechanism. One obvious candidate is wind stress and its associated spatial derivatives. Wind stress is known to play an important role in the circulation of shelf seas and the surface layers of the deep ocean (i.e. the Ekman flux) and is thus associated with advection of plankton. Convergences and divergences of the Ekman flux result in Ekman upwelling which drives a vertical flux of nutrients and also large scale horizontal currents according to the well known Sverdrup relationship. (On a seasonal time scale the Sverdrup relationship must be modified to take account of the influence of bottom topography - see Gill (1982) for details). Interseasonal changes of these two indices, namely wind stress and Ekman upwelling, are reported here. (They were originally determined by one of us - KRT - in a study of the relationship between the sea level and circulation of the North Atlantic).

In the first of a series of data reports, Fofonoff and Dobson (1963) produced monthly stress and upwelling estimates for the

North Atlantic. Geostrophic winds were calculated from monthly air pressure charts and then substituted into a quadratic stress law to give the wind stress. As Fofonoff noted 'an error is encountered in using the square of the mean velocity rather than the mean of the velocity squared in the stress law'.

There are several methods of calculating mean stress fields over the open ocean. The most laborious yet most accurate method is to calculate stresses on a 6 hr time scale from observed winds and then form the mean. The main problem with this approach is the paucity of reliable wind observations, particularly in the southern hemisphere or for periods prior to 1950. Even for the North Atlantic the data coverage is by no means uniform through space or time and this hampers attempts to determine interseasonal changes of the large scale features of the stress field. An alternative method is to determine the mean wind field from air pressure maps and then calculate the stress. The major advantage of using geostrophy is the resolution of the large scale features of the mean wind and hence stress field. The main disadvantage to date has been a systematic error due to the use of mean winds. In Section 2 we describe an estimation procedure which overcomes this problem. The seasonal stress and upwelling estimates given in this report thus update and improve on those previously available. In Section 3 decadal and seasonal distributions are given, followed in Section 4 by seasonal anomaly distributions for the period 1950-80. Selected time series of coastal wind stress and open ocean upwelling are plotted in Section 5.

We hope that the information contained in this report will prove useful to both physical and biological oceanographers. For that reason we will supply the interested reader, on request, with a copy of the seasonal anomaly data on magnetic tape.

## 2 METHOD

(The method outlined below is essentially that of Wright and Thompson (1983) and Thompson et al (1983). The interested reader is referred to those papers for a more detailed description).

Mean wind stress, averaged over a period of several hours, is most simply determined from a bulk aerodynamic formula of the form

$$\tilde{\tau} = \rho_a c_d (\| \tilde{v} \|) \| \tilde{v} \| \tilde{v} \quad (2.1)$$

where  $\tilde{\tau}$  is the surface wind stress,  $\rho_a$  is the density of air,  $\tilde{v}$  is the mean wind (usually recorded at 10 m) and  $c_d$  is an empirically determined drag coefficient. Recent measurements of  $c_d$  show a significant dependence on  $\| \tilde{v} \|$ . Large and Pond (1981), for example, suggest the following form for  $c_d$  over the open ocean

$$10^3 c_d = \begin{cases} 1.14 & 4 < \| \tilde{v} \| < 10 \text{ ms}^{-1} \\ 0.49 + 0.065 \| \tilde{v} \| & 10 \leq \| \tilde{v} \| < 26 \text{ ms}^{-1}. \end{cases} \quad (2.2)$$

This drag coefficient was used in this report.

As noted in the Introduction, it has long been recognised that a non-linear stress law such as (2.1) will underestimate the stress if the winds are first averaged over a period of two days or longer - account must be taken of the fluctuations occurring

within the averaging period. The underestimation can be quantified by first expressing the wind vector as

$$\mathbf{v} = \mathbf{\tilde{v}}_0 + \mathbf{\tilde{v}}_1$$

where suffix 0 and 1 denote the mean and fluctuating components respectively. The mean, or expected stress is then given by

$$\tau_0 = \rho_a \iint_{-\infty}^{\infty} c_d(|\mathbf{\tilde{v}}|) |\mathbf{\tilde{v}}| \mathbf{\tilde{v}} P(u_1, v_1) du_1 dv_1 \quad (2.3)$$

where  $P$  is the probability density function (pdf) of the fluctuating winds. If we assume that  $P$  is an isotropic Gaussian pdf with variance  $\sigma^2$  i.e.

$$P = P_g = (2\pi\sigma^2)^{-1} \exp [-|\mathbf{\tilde{v}}_1|^2/(2\sigma^2)] \quad (2.4)$$

then  $\tau_0$  may be accurately approximated by  $\hat{\tau}_0$  where

$$\begin{aligned} \hat{\tau}_0 &= \rho_a c_d(a) a \mathbf{\tilde{v}}_0 \\ a^2 &= |\mathbf{\tilde{v}}_0|^2 + 4\sigma^2 \end{aligned} \quad (2.5)$$

The relationship between  $|\mathbf{\tilde{v}}_0|$ ,  $\sigma$  and  $|\tau_0|$ , according to (2.2), (2.3) and (2.4) is shown in Figure 1. Clearly the stress will be seriously underestimated if just the mean wind is substituted into (2.1), i.e.  $\sigma=0$  in (2.5). This is in accord

with the quote by Fofonoff given in the Introduction.

Thompson et al (1983) have shown that the temporal changes of  $\sigma$  are dominated by a seasonal cycle with an amplitude that varies with location. They calculated the seasonal  $\sigma$  fields for the North Atlantic shown in Figure 2, using wind statistics published by the U.S. Navy.

A well tried and successful method of estimating large scale mean wind patterns over the open ocean is to first calculate the geostrophic wind vector from surface air pressure maps and then apply an empirically determined contraction and rotation to obtain the surface wind vector. This is the approach used in this report. The monthly pressure data were obtained from the publications of 'Die Grosswetterlagen Europas', Deutscher Wetterdienst, Offenbach.

The stresses given in this report have been estimated from (2.5), using the above seasonal  $\sigma$  and wind fields. Stresses were calculated every 1 degree of latitude and 2 degrees of longitude over the North Atlantic.

Ekman upwelling,  $w_e$ , is defined by

$$w_e = \text{curl}_z(\underline{\tau}/\rho f) \quad (2.6)$$

where  $f$  is the Coriolis parameter and  $\rho$  is the density of water. Upwelling was estimated using Green's theorem i.e. integrating

the tangential component of  $\zeta/\rho f$  around the periphery of a 2 (latitude) by 4 (longitude) degree region. (This approach was as accurate, but more convenient, than that of using finite difference approximations to the curl operator).

The significant difference in stress that results from ignoring the spatial and temporal changes of  $\sigma$  is clear from Figure 1. To illustrate the effect of ignoring  $\sigma$  in the estimation of  $w_e$ , we have plotted the mean seasonal Sverdrup transport across approximately 30N according to (i) Leetmaa and Bunker (1978) (ii) Fofonoff and Dobson (1963) and (iii) the present method (Figure 3). Leetmaa and Bunker's estimate was based on all available wind data for the North Atlantic, 1948-1972 - approximately 8 million observations. This is probably the most accurate of all the curves in Figure 3. The transport variation calculated by the present method is encouragingly close to that of Leetmaa and Bunker. (A  $c_d$  similar to that of Leetmaa and Bunker was used in (2.5) to facilitate comparison). Fofonoff's estimate, which is based on a constant drag coefficient and ignores  $\sigma$ , differs significantly from the others in both the mean and degree of seasonality.

### 3 SEASONAL AND DECADAL MEAN MAPS

To provide a background against which to view the seasonal anomalies, we have calculated both the mean seasonal (Dec-Feb, Mar-May, Jun-Aug, Sep-Nov) and decadal mean (1951-60, 61-70, 71-80) wind stress and upwelling distributions. They are shown in Figure 4 and Figure 5. The seasonal maps were calculated from the mean seasonal  $\bar{v}_0$  distributions. The decadal means were calculated from the mean of the 40 seasonal distributions within the given decade.

#### 4 SEASONAL ANOMALY MAPS

In order to highlight the interseasonal changes of wind stress and Ekman upwelling, we have removed the mean seasonal distributions given in Figure 4 from each individual 3-month pattern. The resulting anomaly distributions are given in Figure 6.

## 5 SELECTED TIME SERIES

To illustrate the temporal changes of wind stress and Ekman upwelling, time series from selected locations are given in Figure 9 and 10 respectively. The low-frequency component in each series is also plotted. It was obtained by applying a lowpass filter with the response function shown in Figure 7.

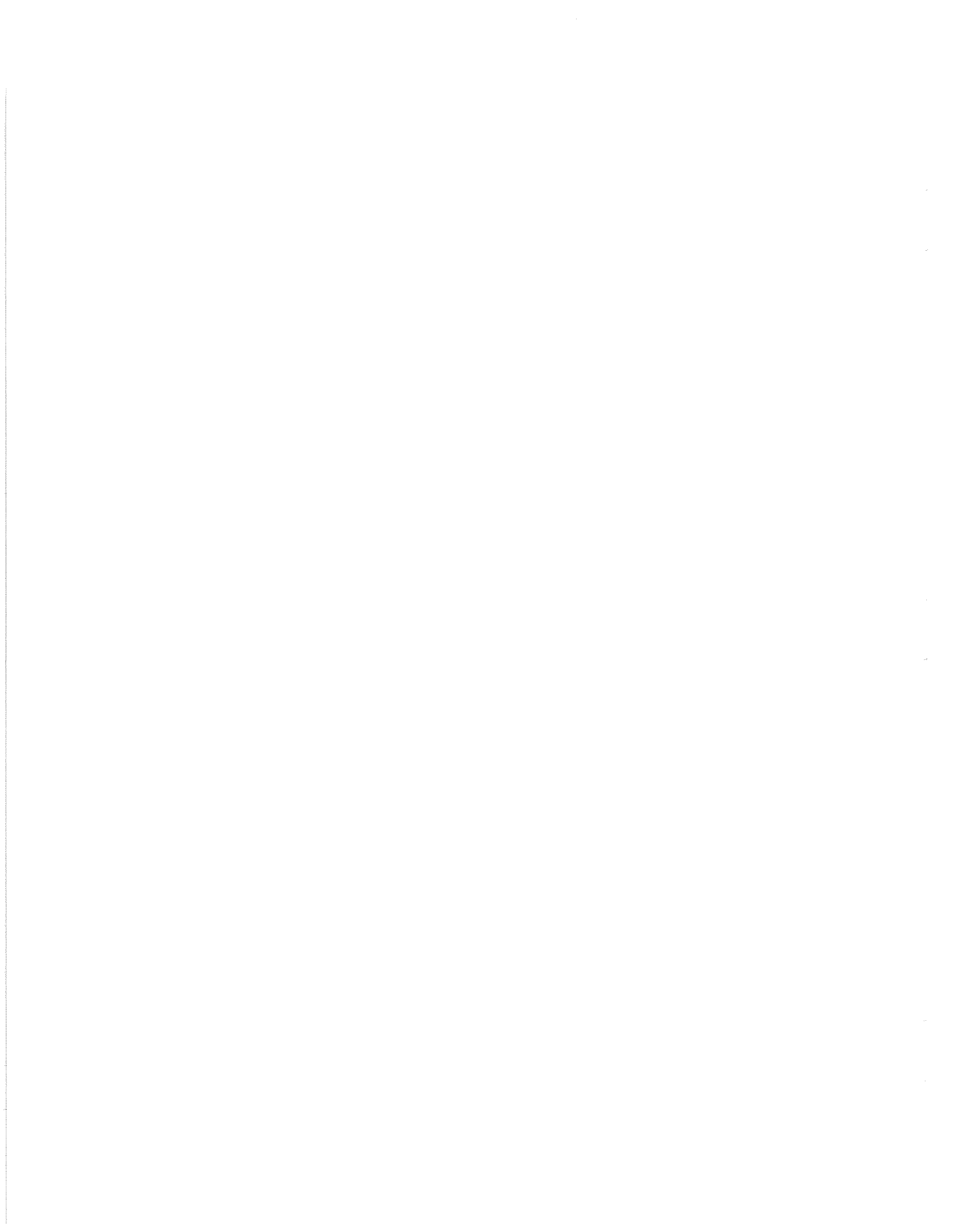
The wind stress locations correspond to coastal areas of the North Atlantic where local stress is known to have an important influence on the circulation (e.g. northwest European continental shelf) and possibly coastal upwelling (e.g. coasts of Labrador and Portugal). The coordinate system has been rotated to coincide with the orientation of the coastline as shown in Figure 8. The upwelling locations are for the open ocean.

#### Acknowledgements

We thank both Claire MacDonald and Roz Ernst for their care and patience in the early stages of data preparation and checking. This work was funded in part by a Strategic Grant awarded by the Natural Sciences and Engineering Research Council of Canada and also the Institute of Oceanographic Sciences, Great Britain.

## References

- Akenhead, S. A., Petrie, B. D., Ross, C. K. and D. M. Ware, 1981. Ocean Climate and the Marine Fisheries of Atlantic Canada: An Assessment. Bedford Institute of Oceanography Report Series /BI-R-81-8/ 121pp.
- Colebrook, J. M. 1978. Continuous Plankton Records: Zooplankton and Environment, North-East Atlantic and North Sea, 1948-1975. Oceanologica Acta, 1, 9-23.
- Cushing, D. H. 1982. Climate and Fisheries. Academic Press. 373pp.
- Fofonoff, N. P. and F. W. Dobson, 1963. Transport Computations for the North Atlantic Ocean 1950-1959: 10 year Means and Standard Deviations by Months. Fisheries Research Board of Canada. Manuscript Report Series, 162.
- Gill, A. E. 1982. Atmosphere-Ocean Dynamics. Academic Press. 662pp.
- Garrod, D. J. and J. M. Colebrook, 1978. Biological Effects of Variability in the North Atlantic Ocean. Rapp. P.-v. Reun. Cons. int. Explor. Mer, 173, 128-144.
- Large, W. F. and S. Pond, 1981. Open Ocean Momentum Flux Measurements in Moderate to Strong Winds. Journal of Physical Oceanography, 11, 324-336.
- Leetmaa, A. and A. F. Bunker, 1978. Updated Charts of the Mean Annual Wind Stress, Convergence in the Ekman Layers and Sverdrup Transports in the North Atlantic. Journal of Marine Research, 36, 311-321.
- Thompson, K. R., Marsden, R. F. and D. G. Wright, 1983. Estimation of Low-Frequency Wind Stress Fluctuations over the Open Ocean. Journal of Physical Oceanography, 13, 1003-1011.
- Wright, D. G. and K. R. Thompson, 1983. Time Averaged Forms of the Non-Linear Stress Law. Journal of Physical Oceanography, 13, 341-345.



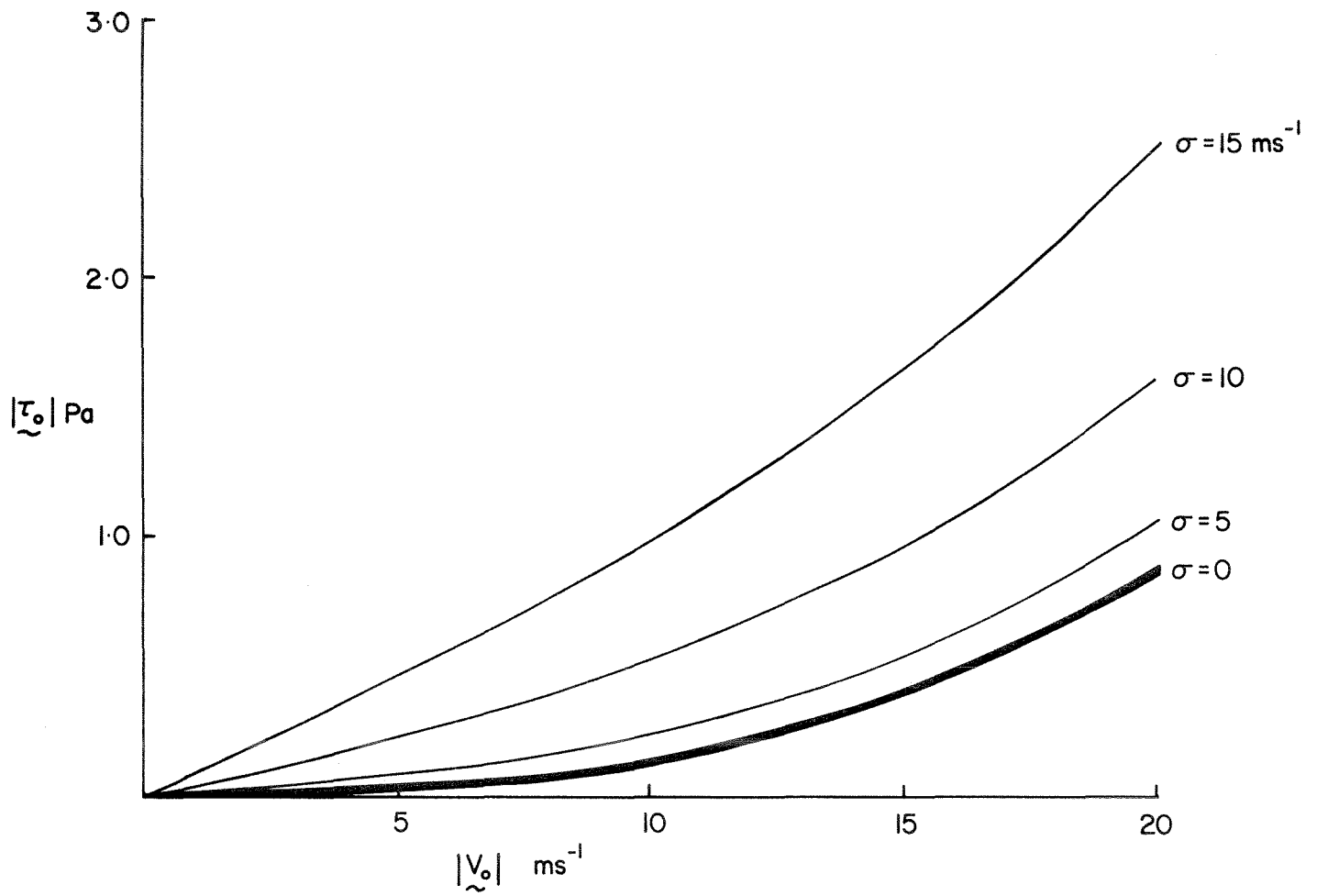


**FIGURE 1**

Mean stress  $|\tilde{\tau}_0|$  as a function of  $|\tilde{v}_0|$  and  $\sigma$ , according to (2.2), (2.3) and (2.4).

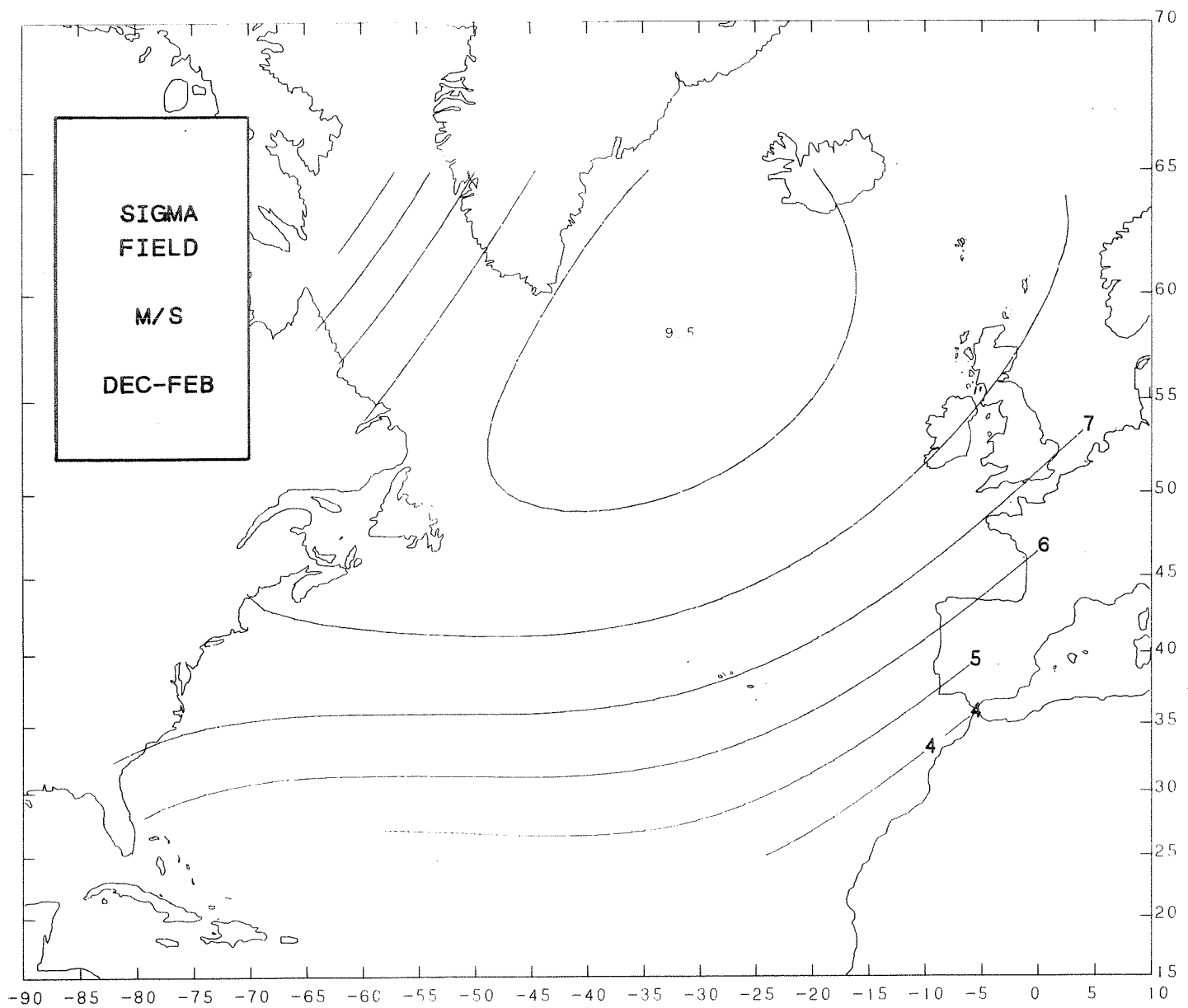
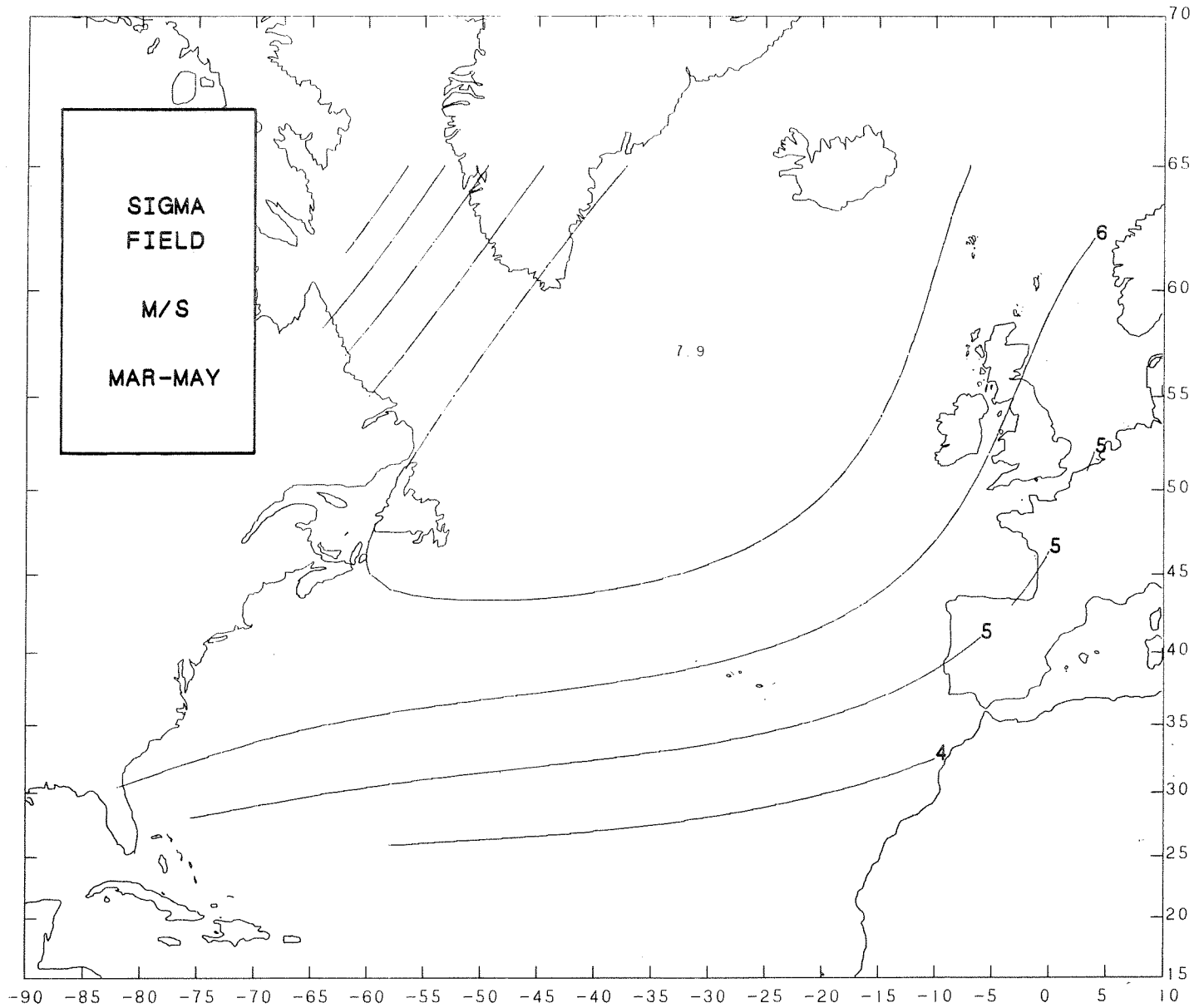


FIGURE 2

Seasonal  $\sigma$  fields for the North Atlantic.

(a) Winter (December–February).



**Figure 2b**

**Spring (March-May).**

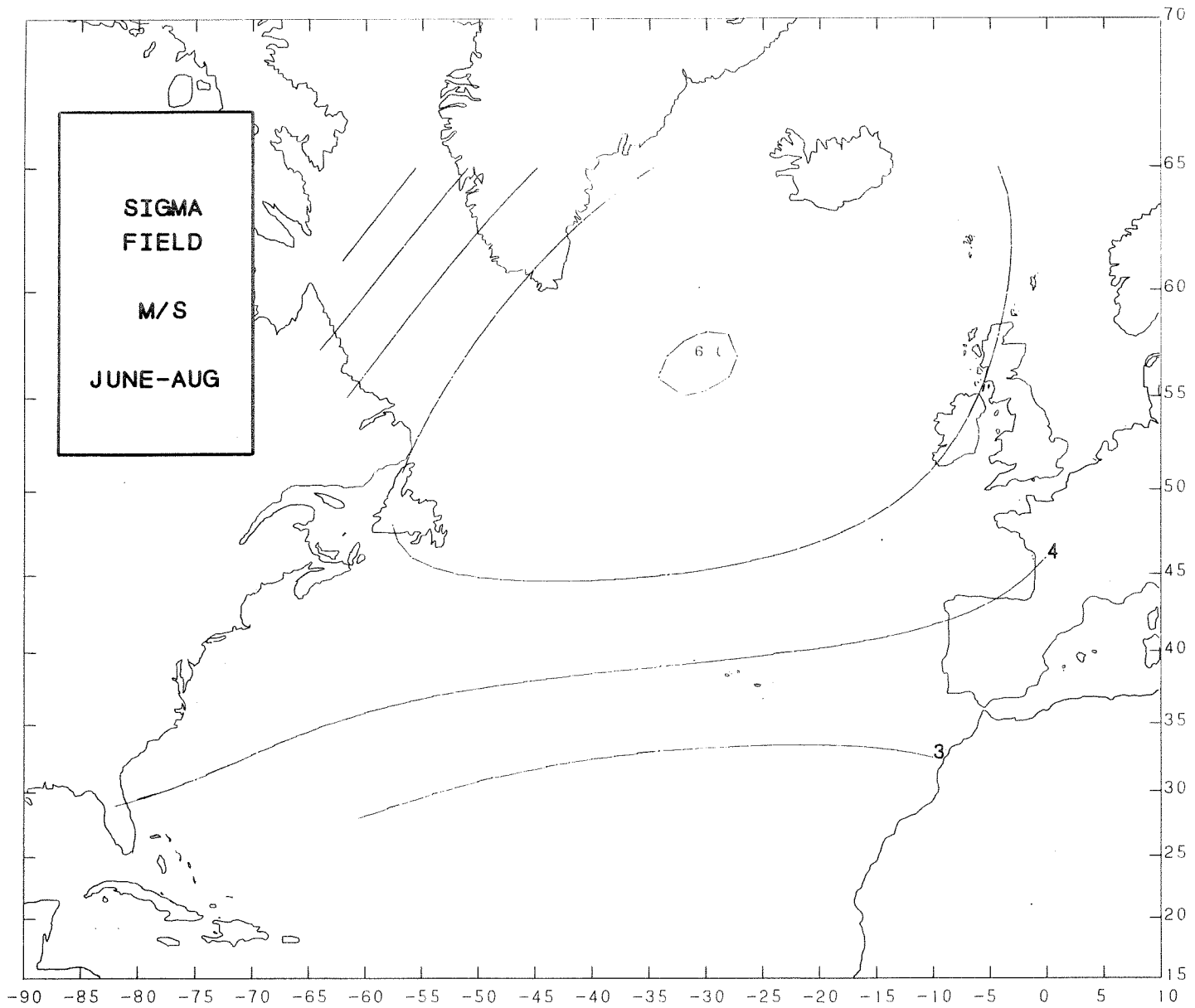


**Figure 2c**

**Summer (June-August).**

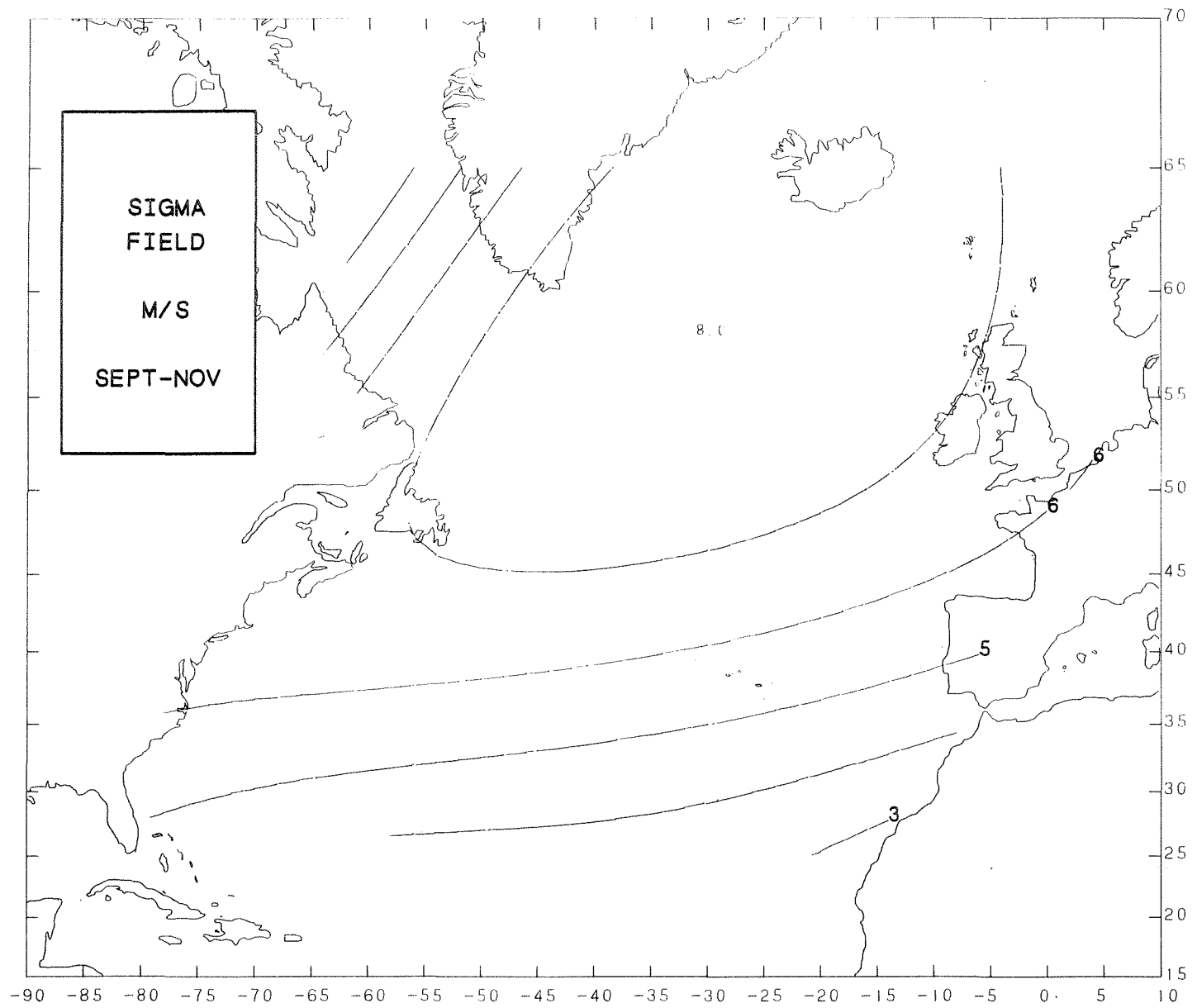


Figure 2d

Fall (September-November).

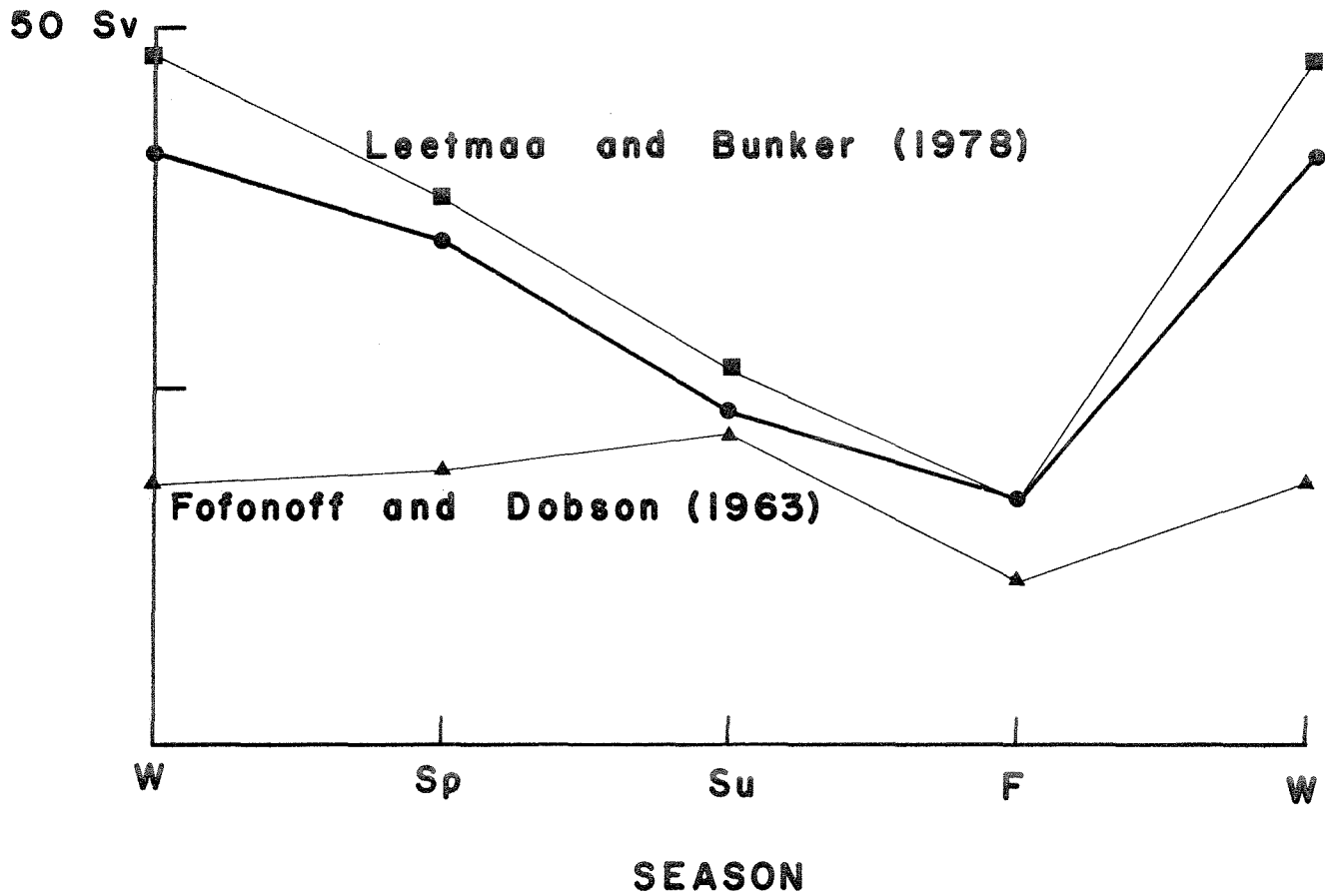
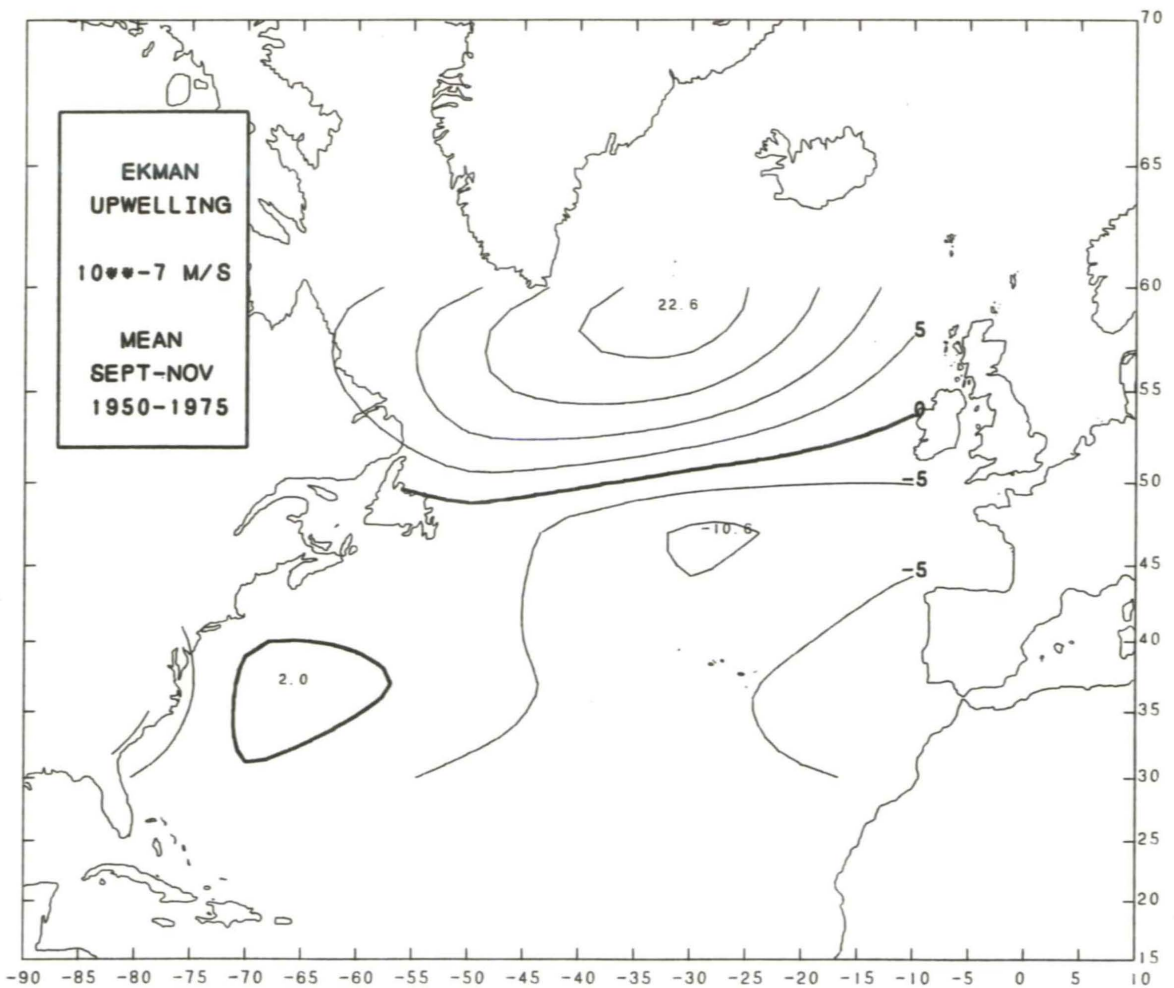
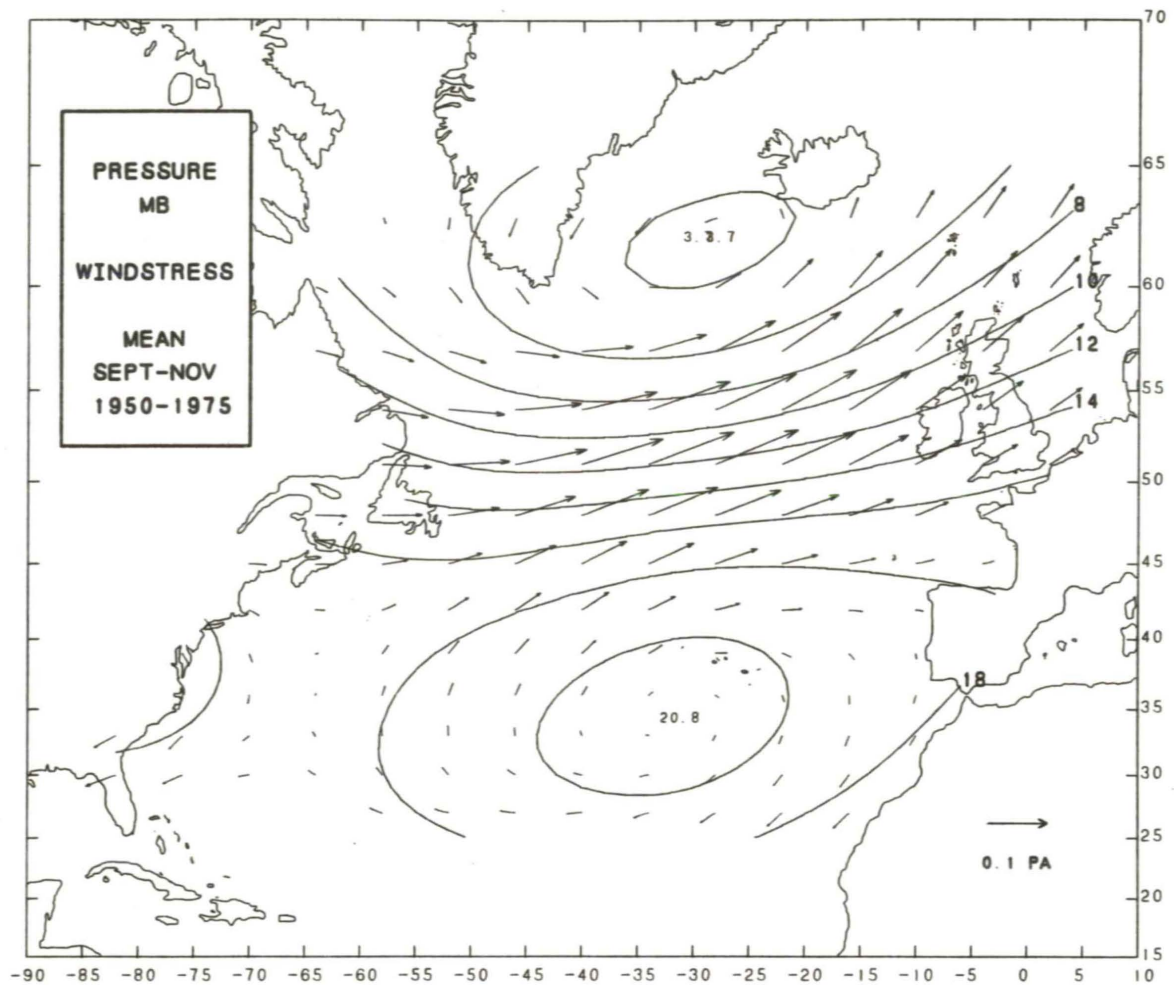


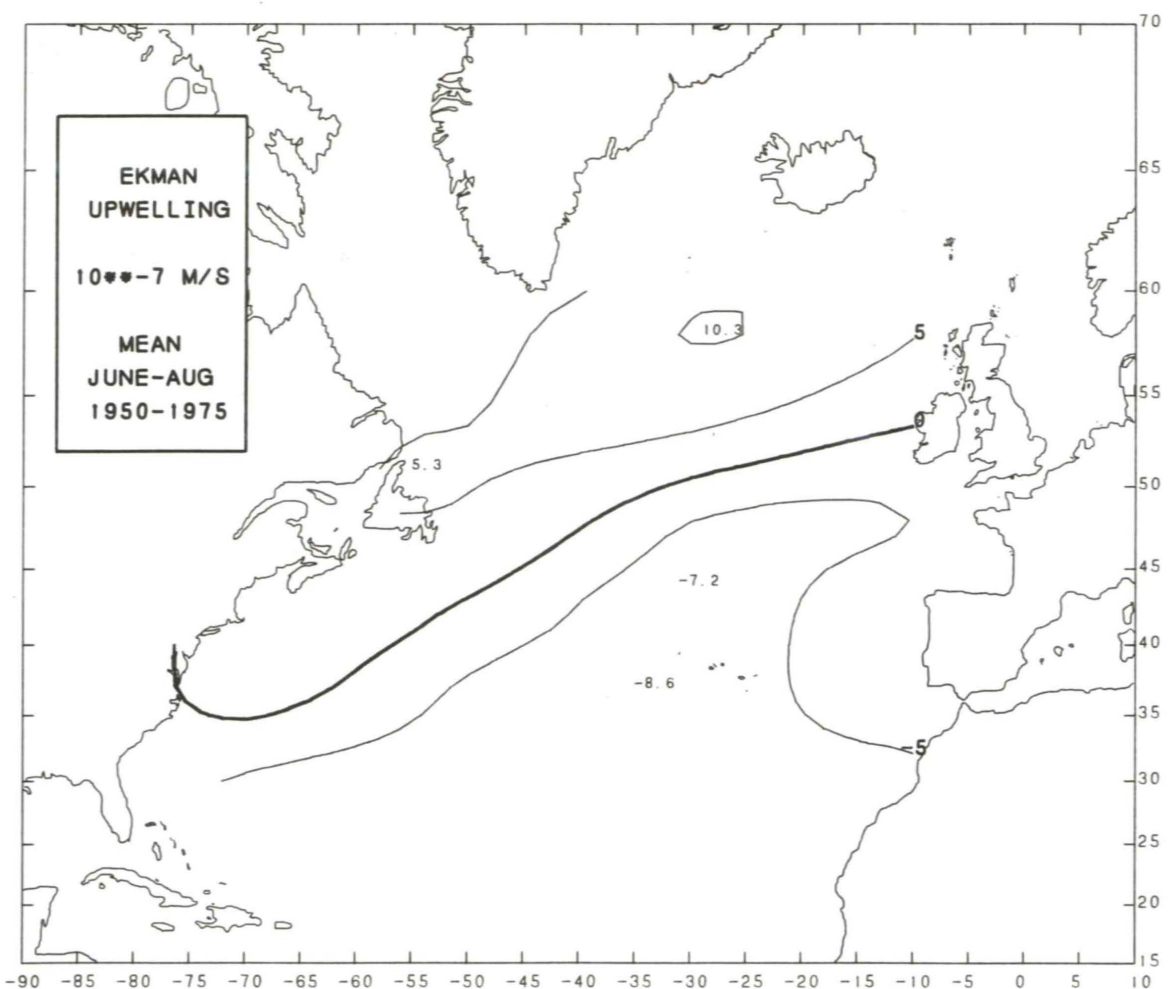
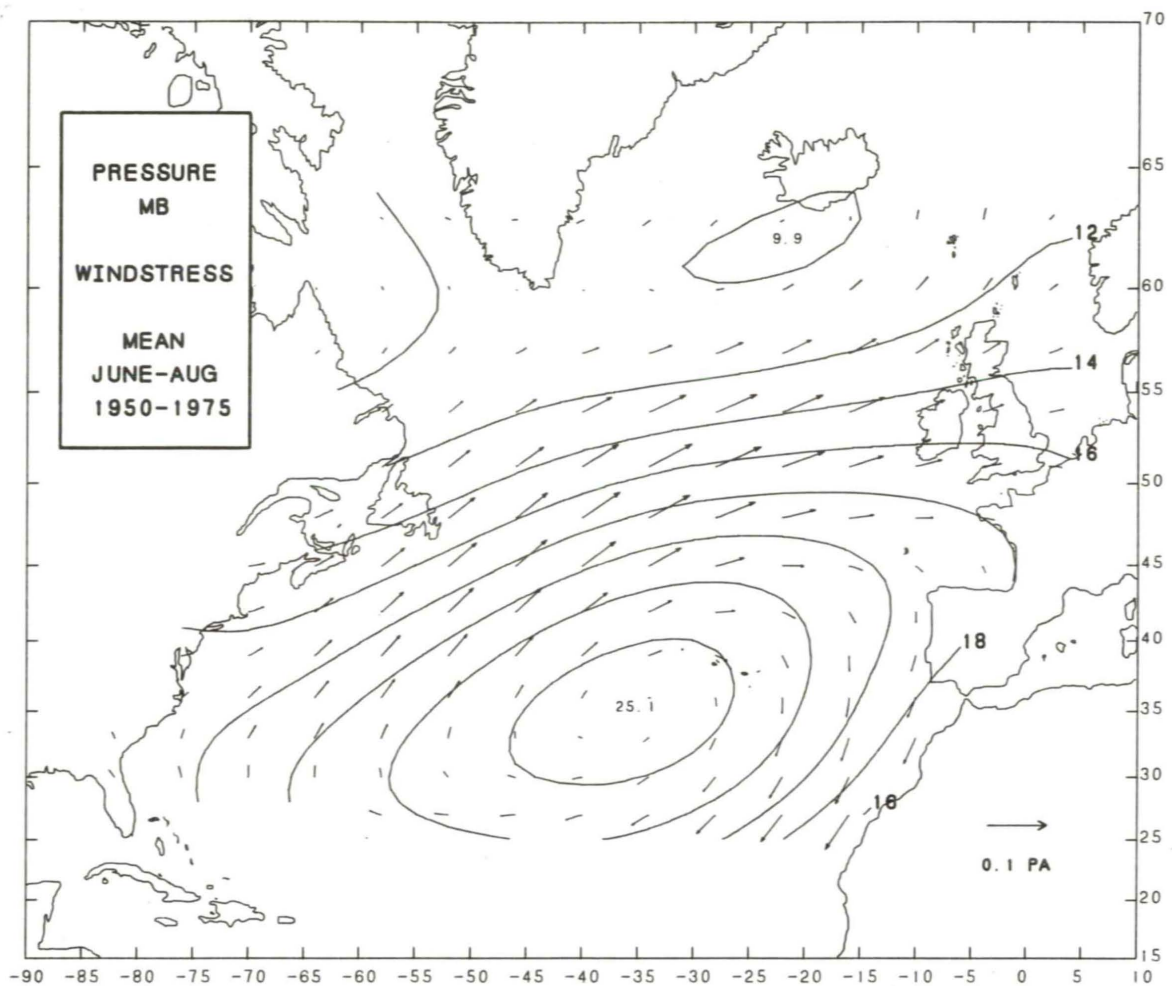
Figure 3.

Sverdrup transport across 31N calculated by Leetmaa and Bunker (1978) and the present method. (A similar  $c_d$  to that used by Leetmaa and Bunker was employed in the present method to facilitate comparison). The Fofonoff and Dobson estimate was for 30N and the period 1950-1959. (Winter corresponds to December-February etc.)

Figure 4

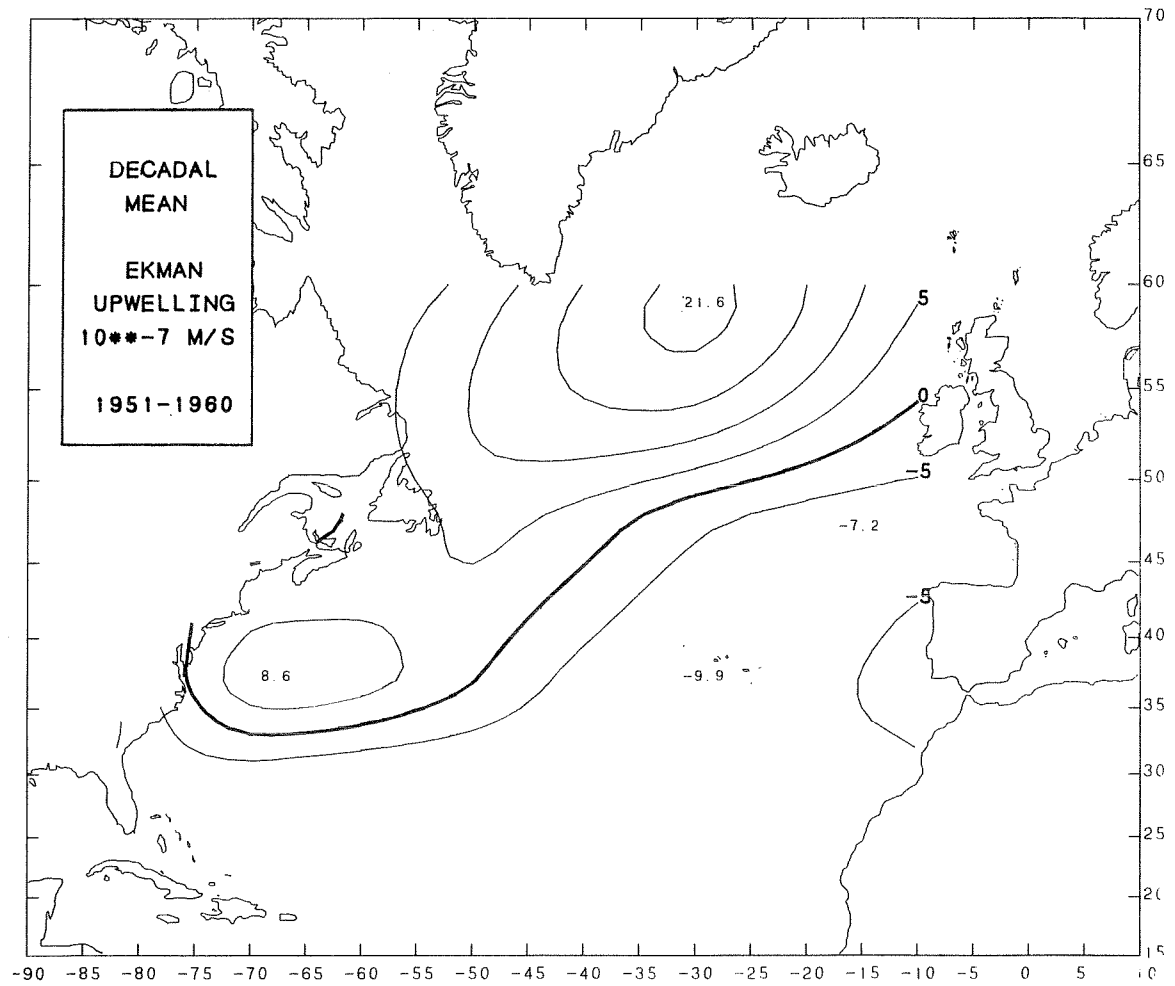
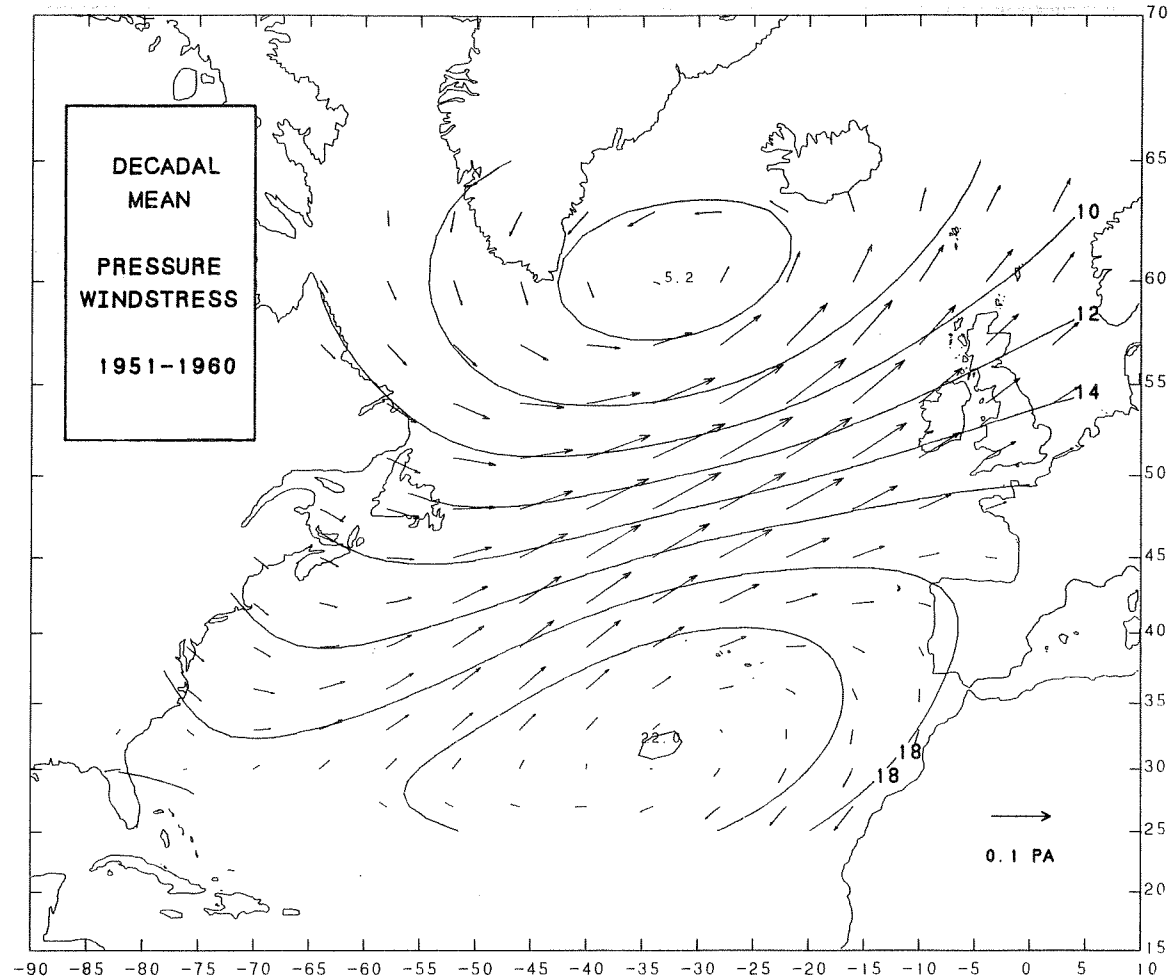
Mean seasonal air pressure, wind stress (top panel) and Ekman upwelling (bottom panel), 1950-75. The mean seasonal  $\bar{v}_0$  distributions were used.

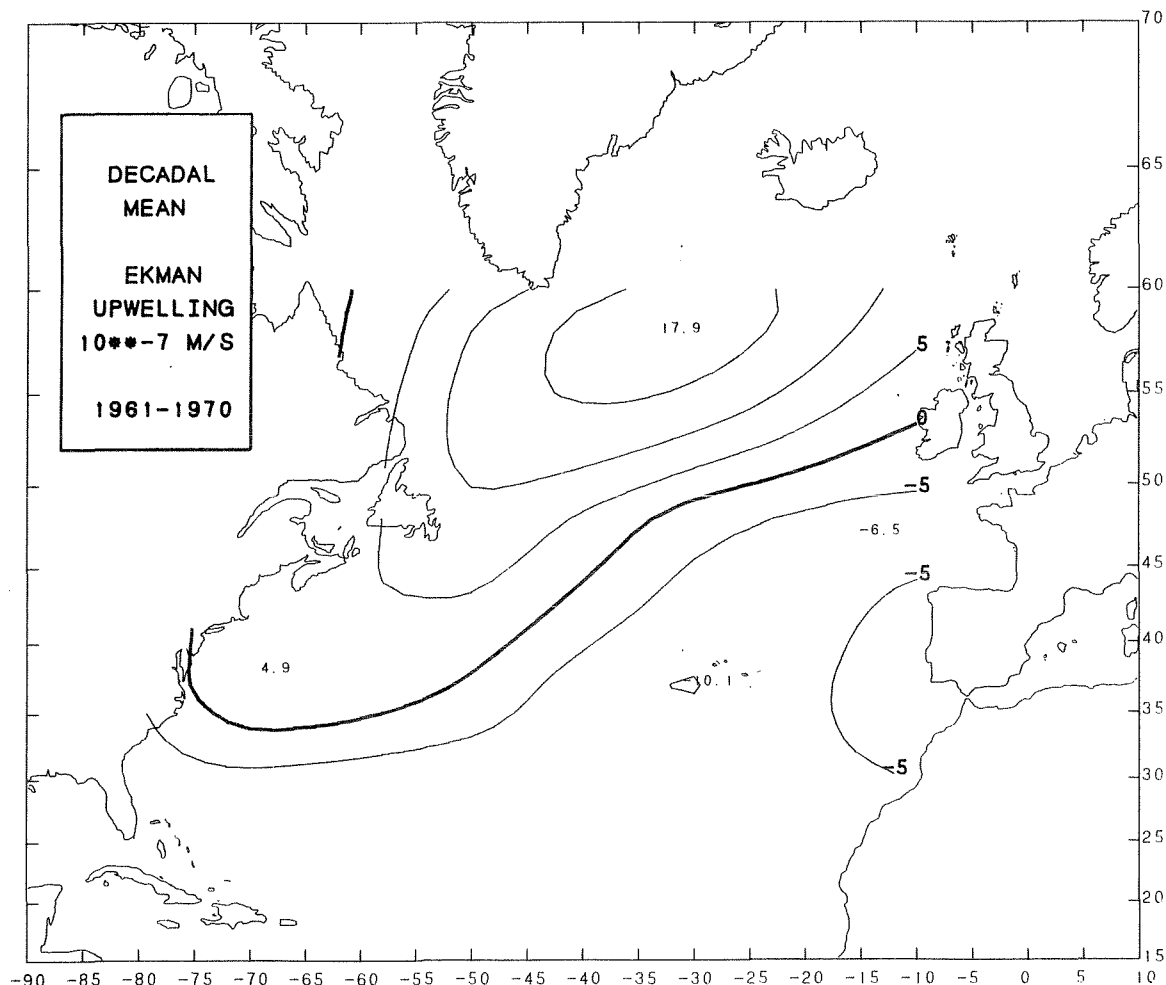
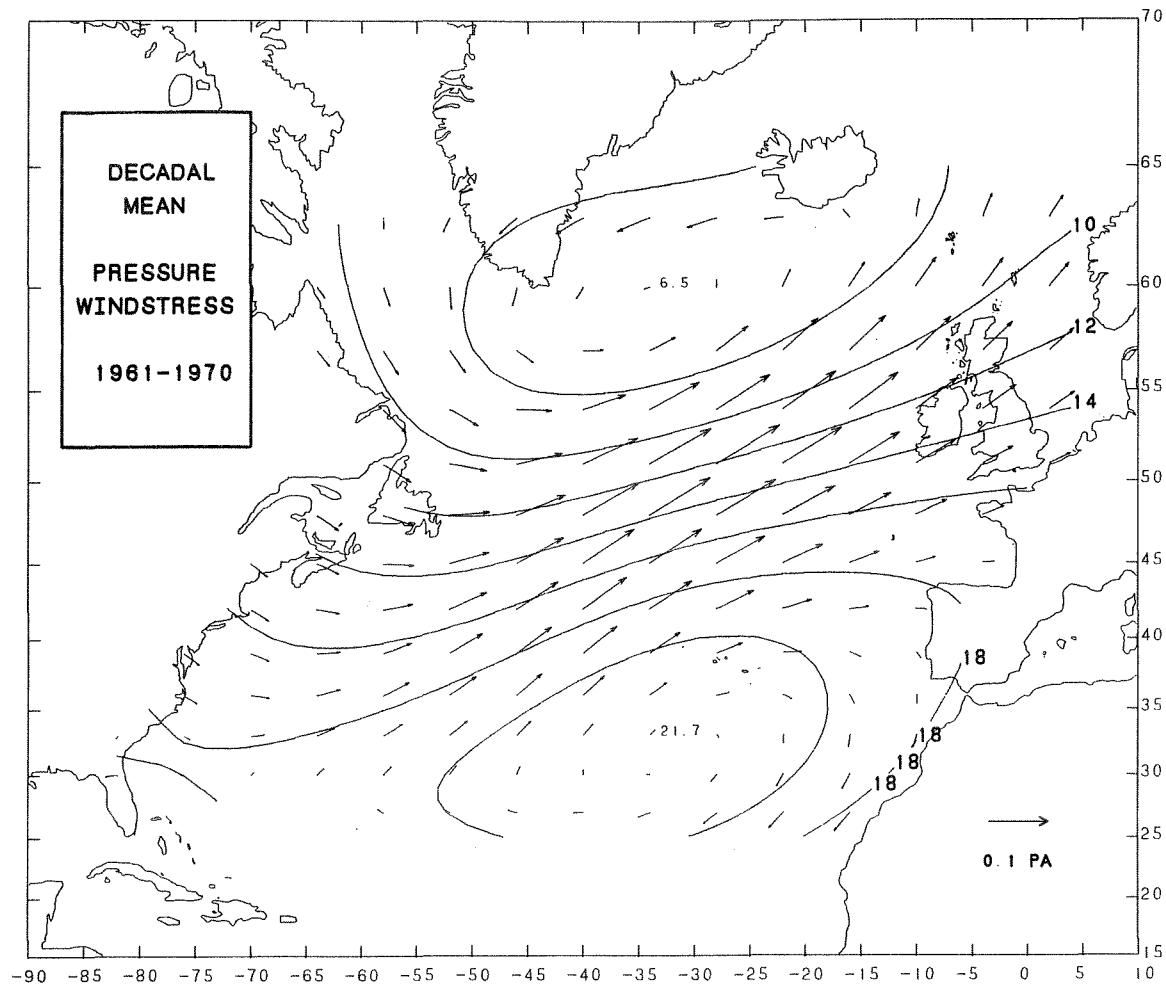


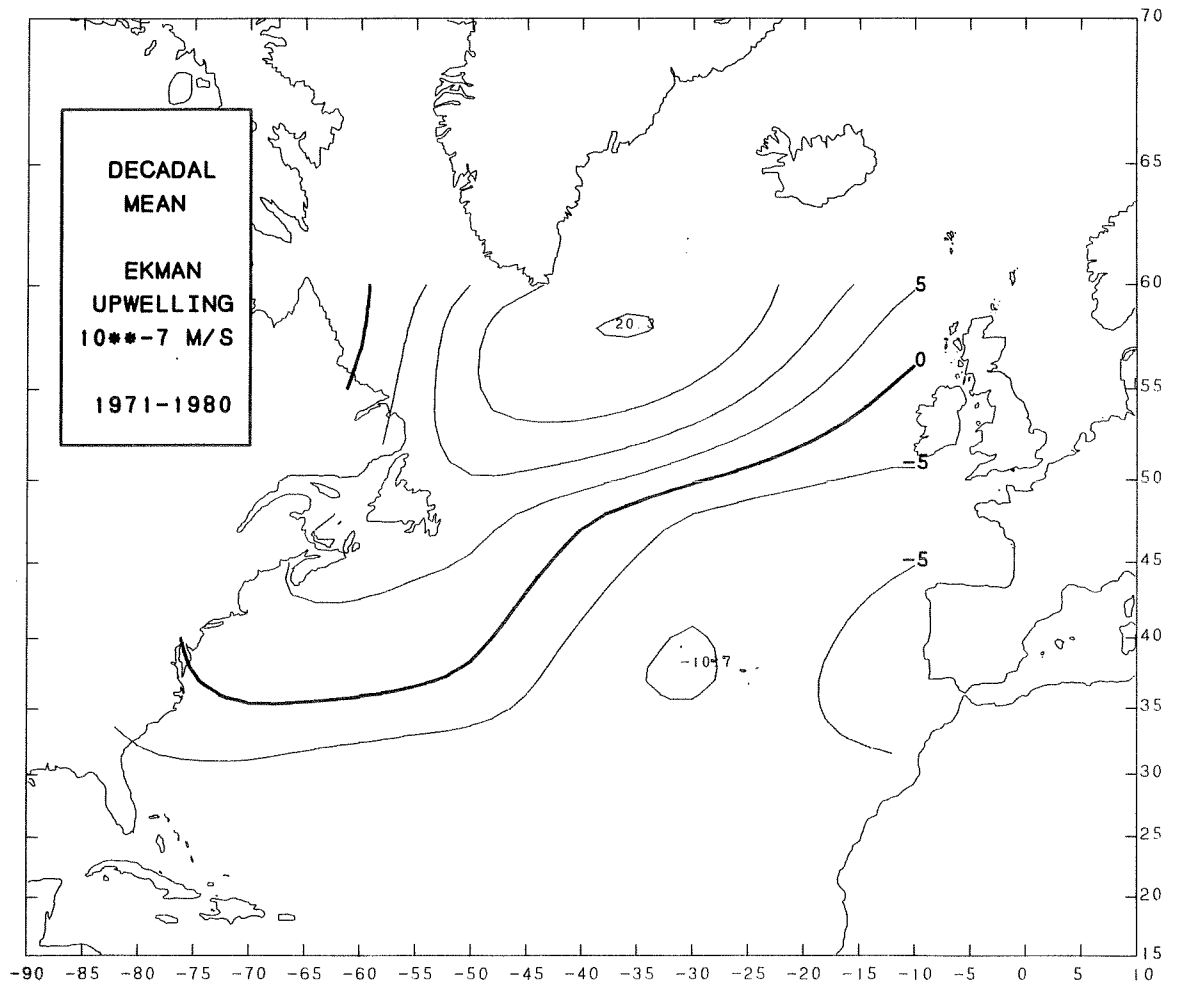
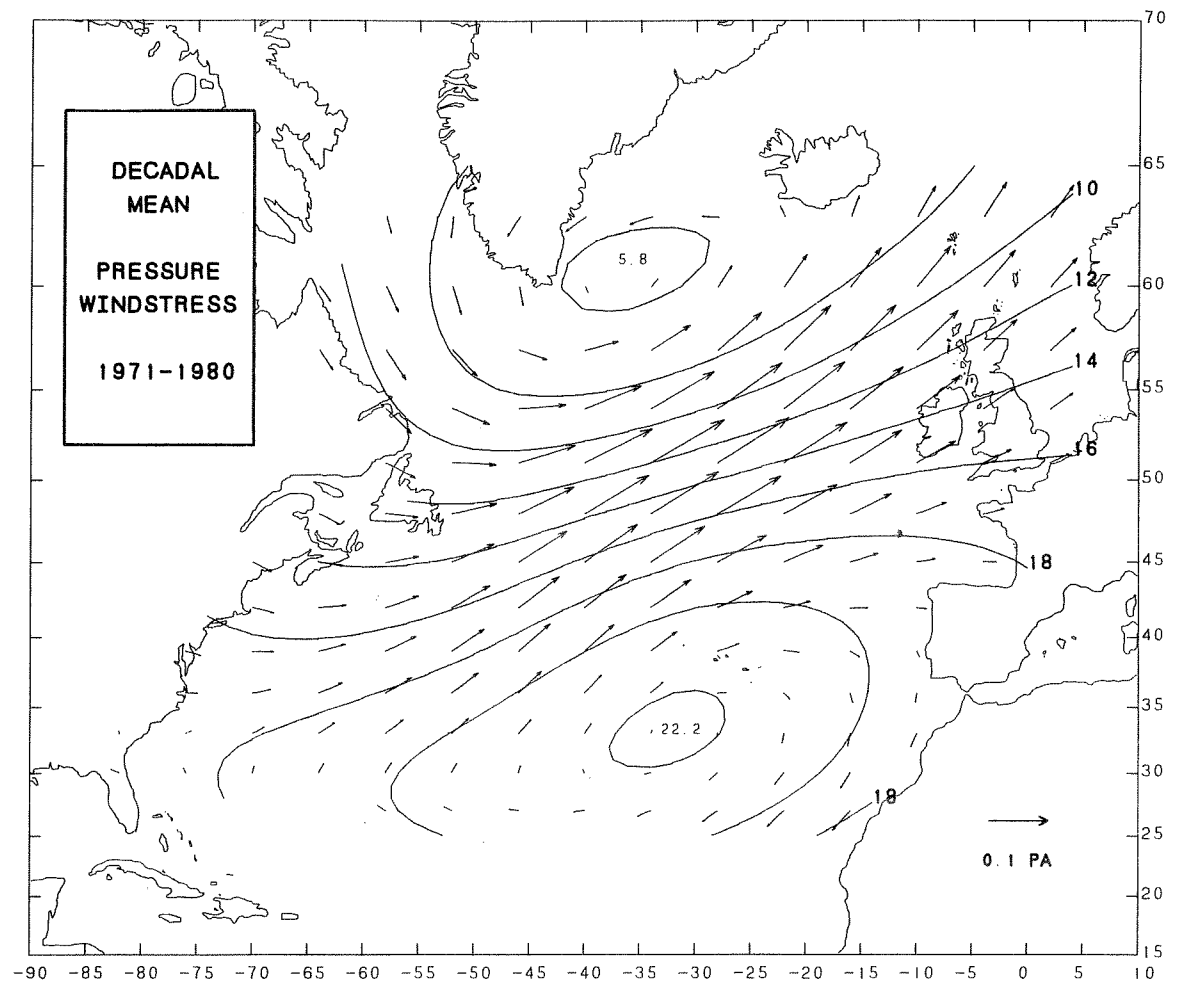


**Figure 5**

Decadal mean air pressure, wind stress and Ekman upwelling, 1951-1960, 1961-1970, 1971-1980. The distributions are the mean of the 40 seasonal maps within the given decade.



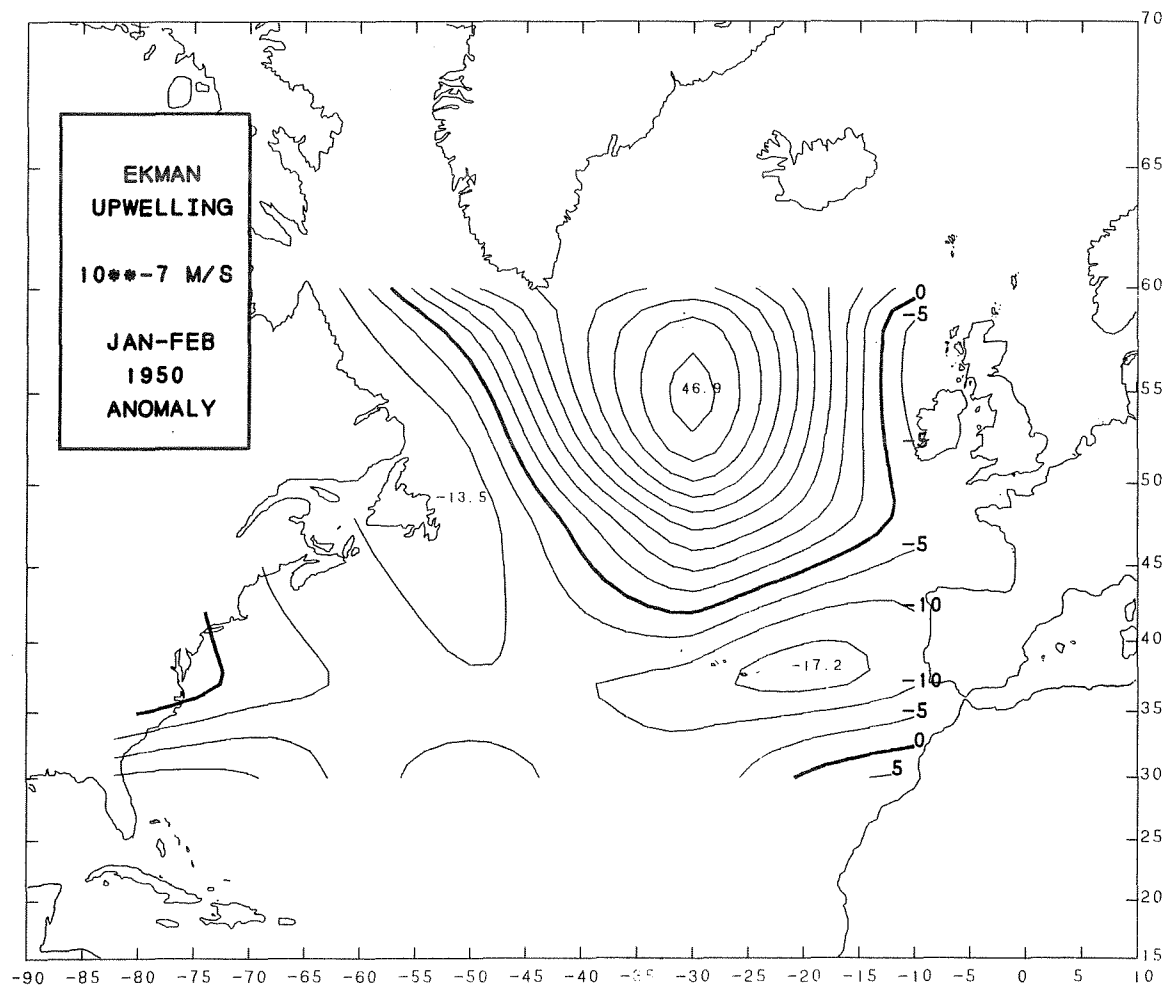
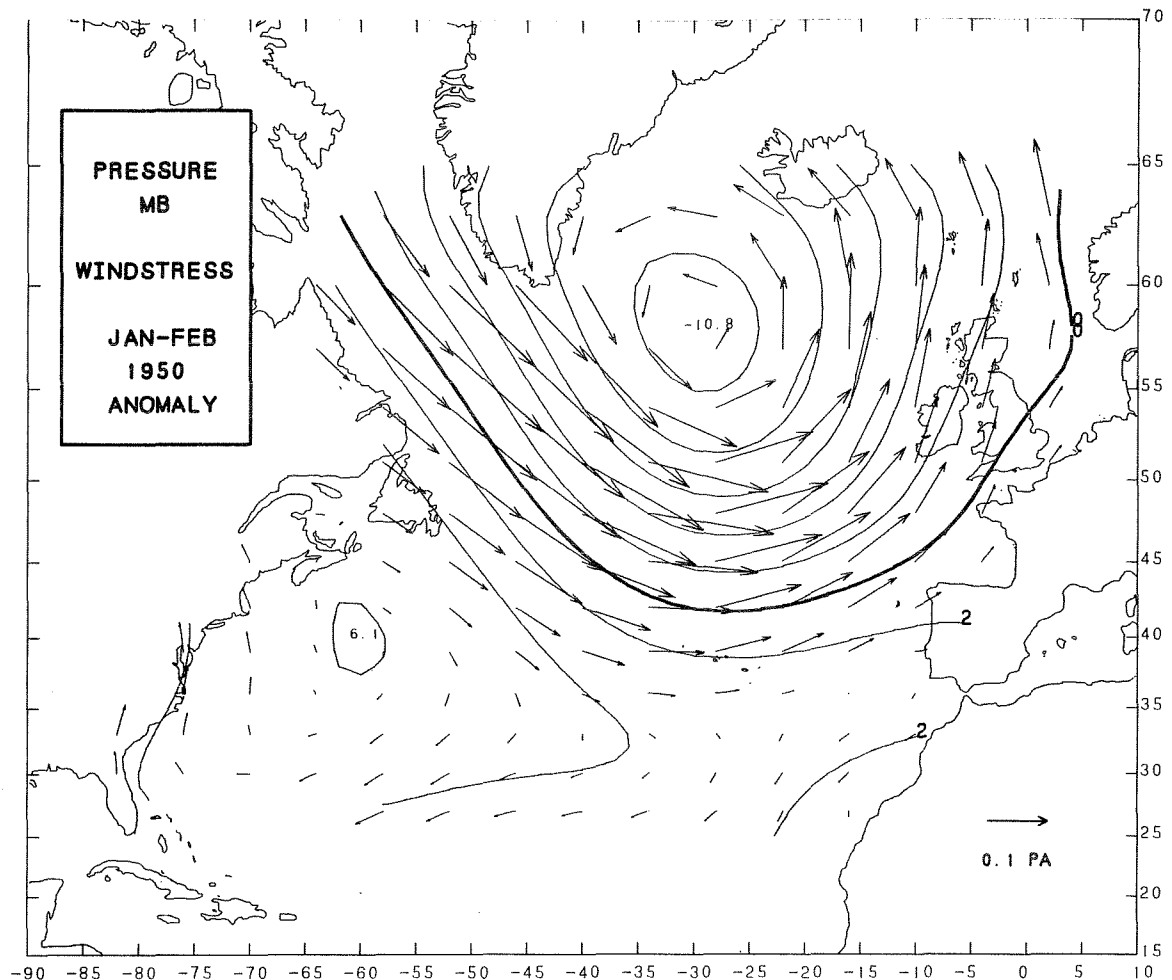


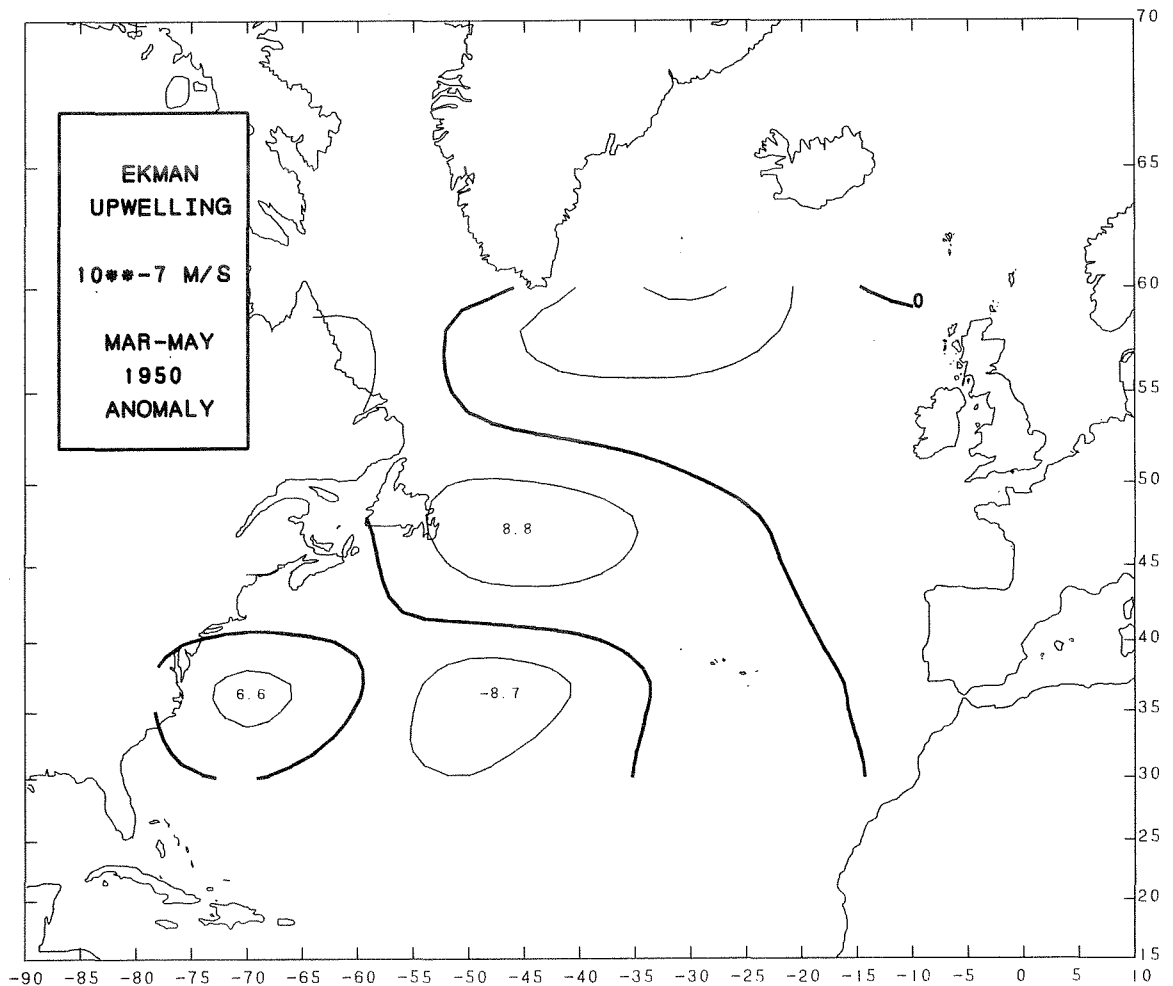
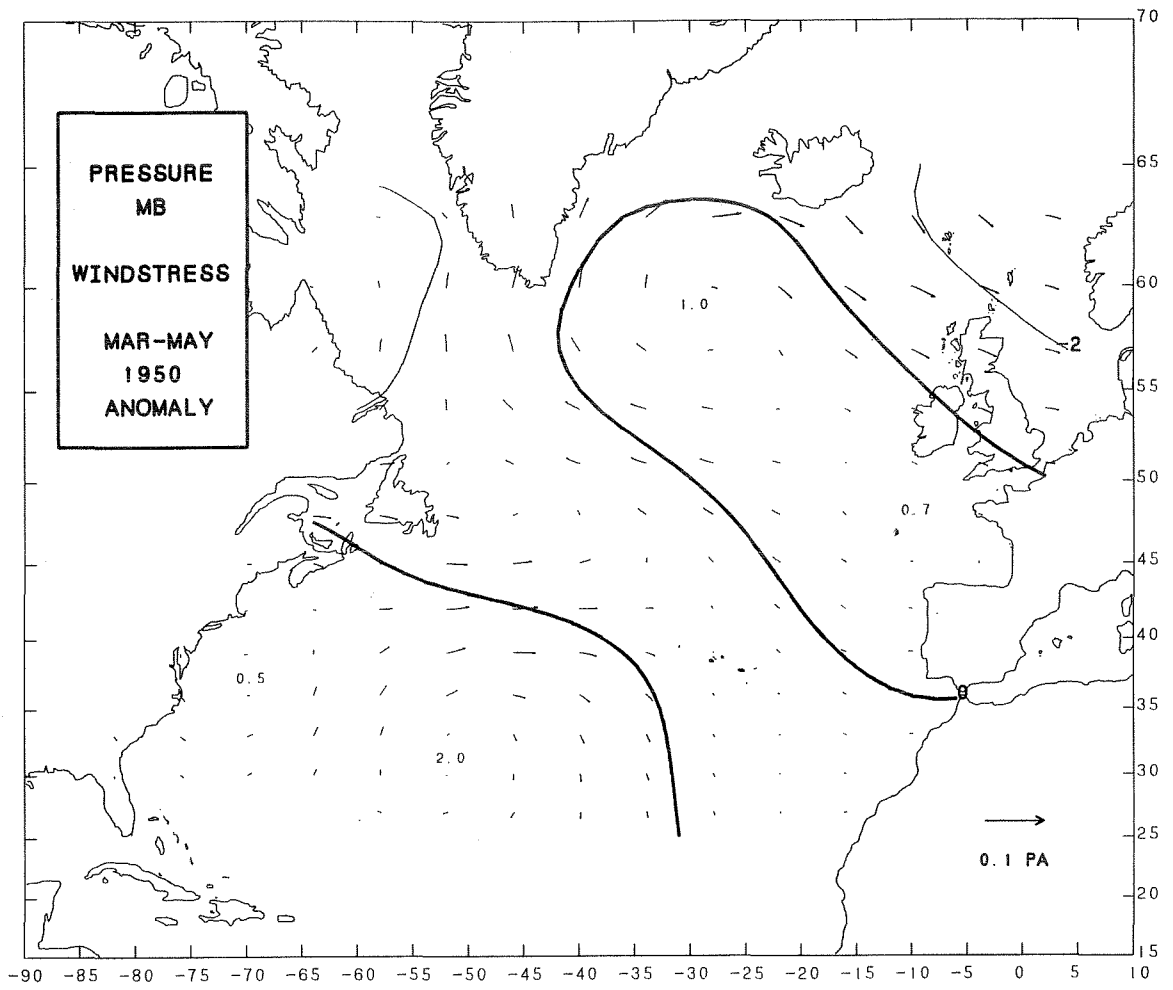


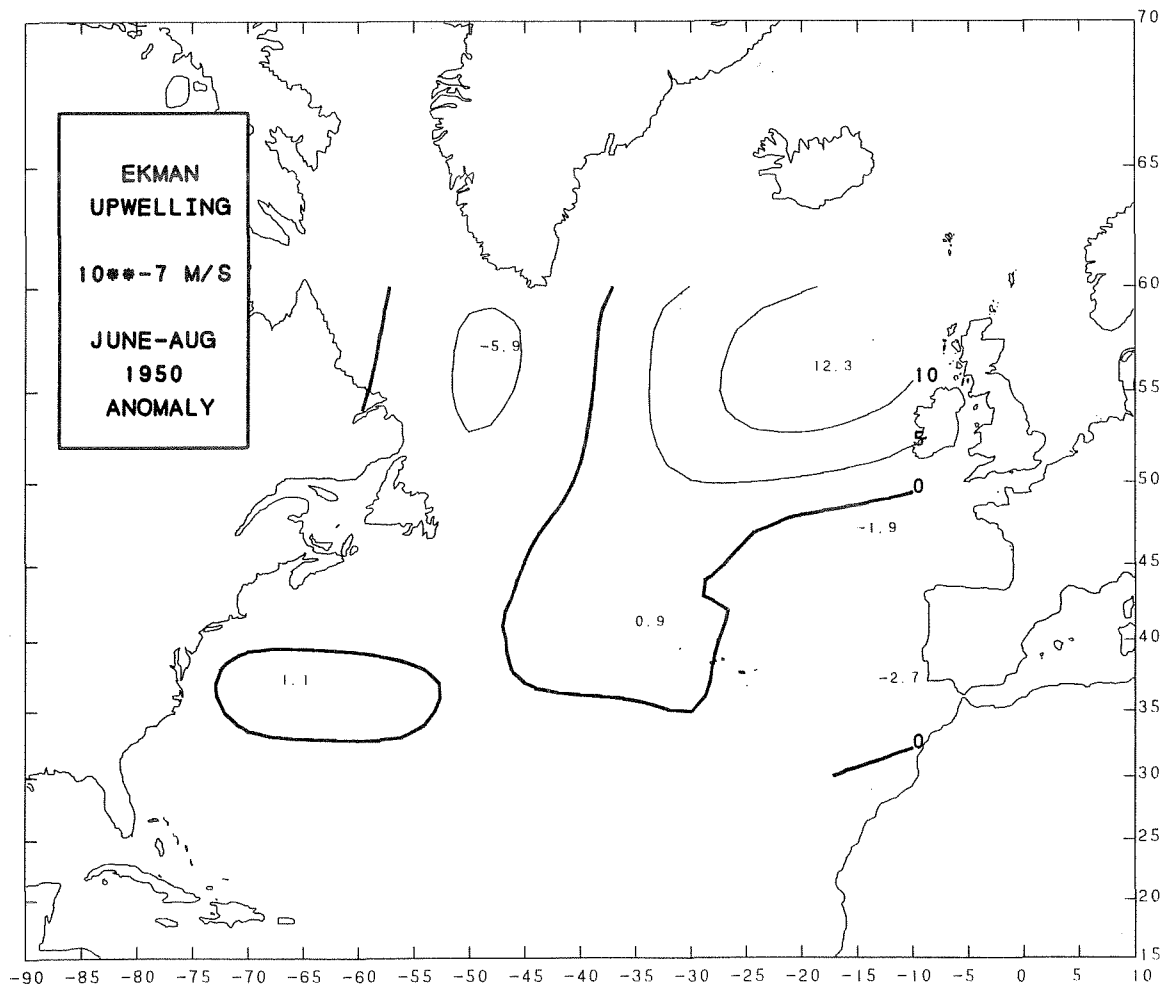
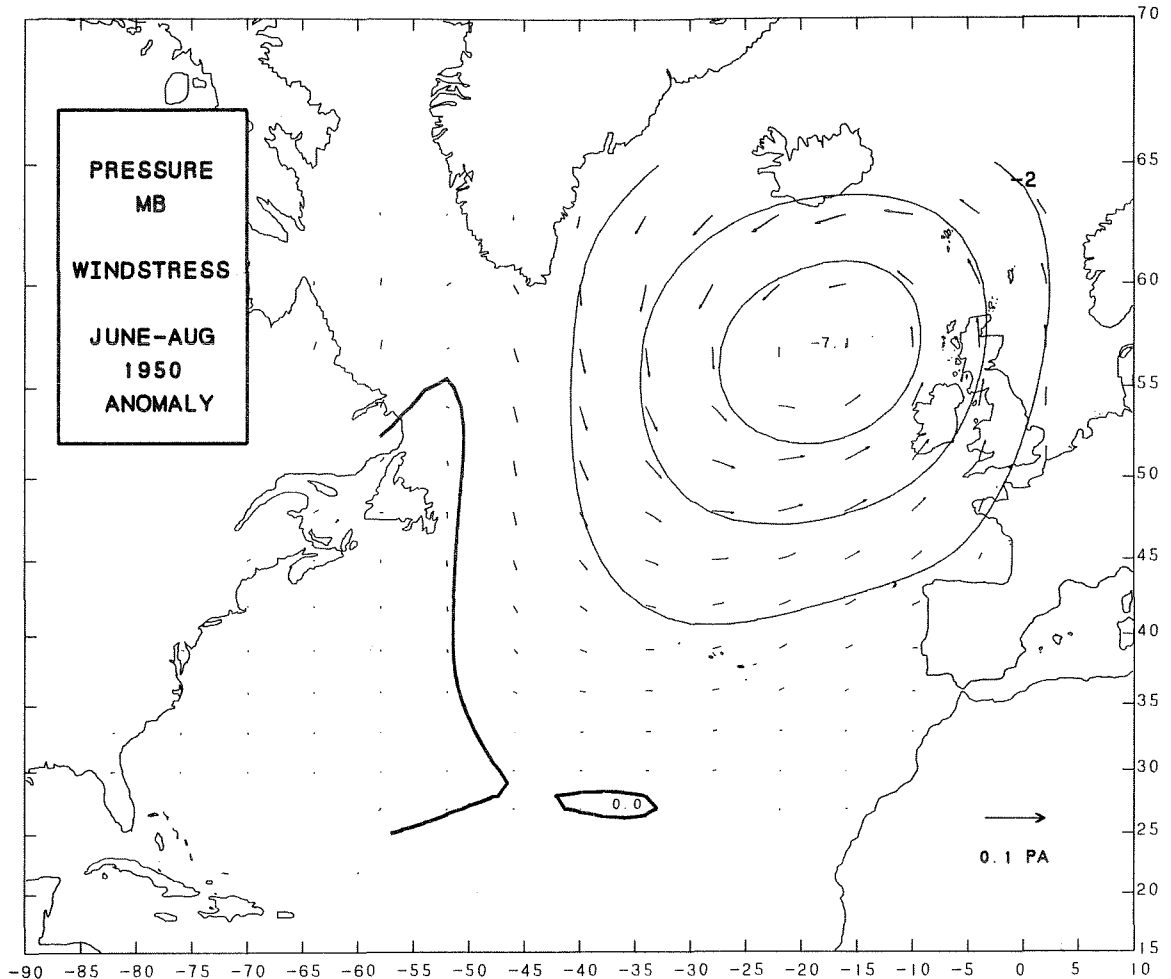


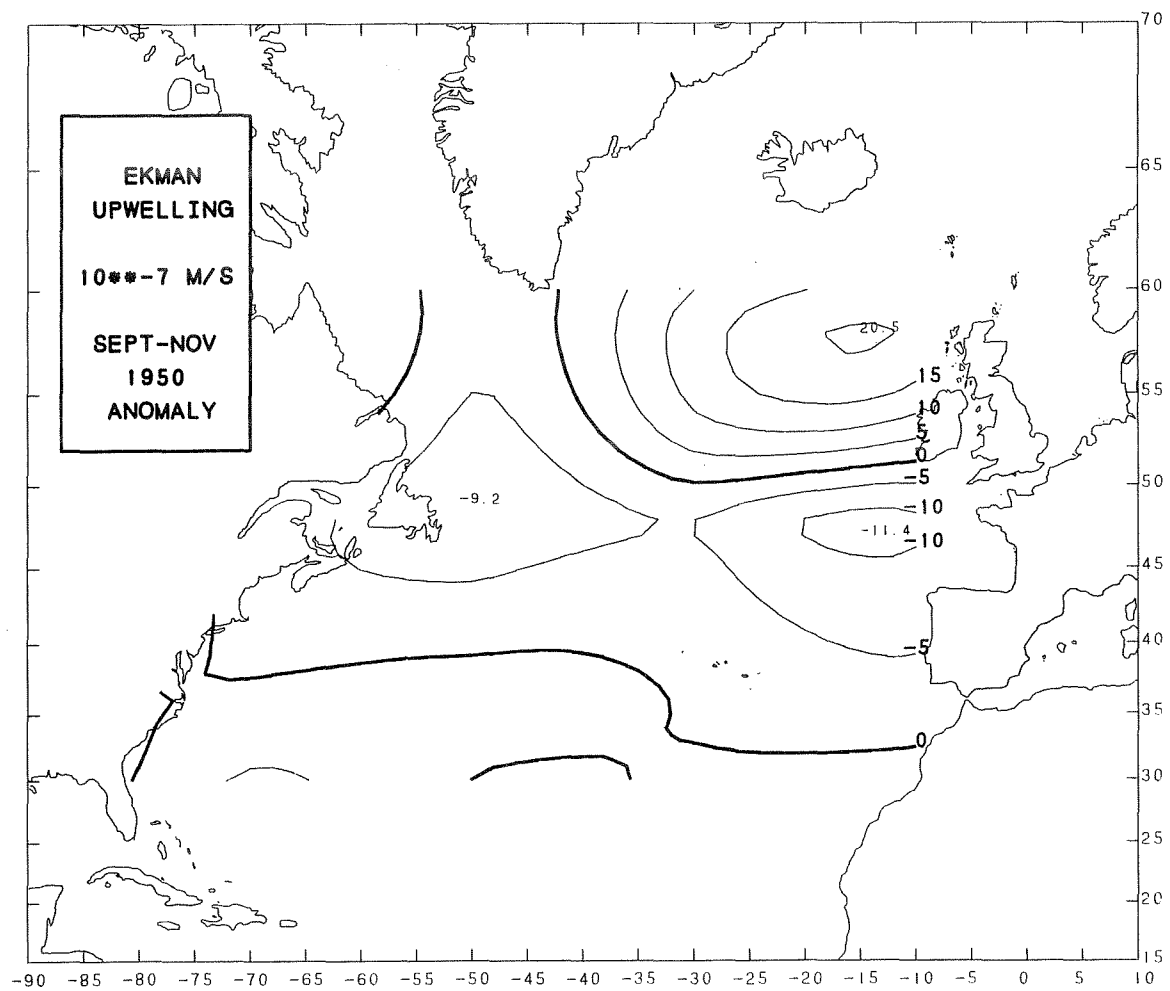
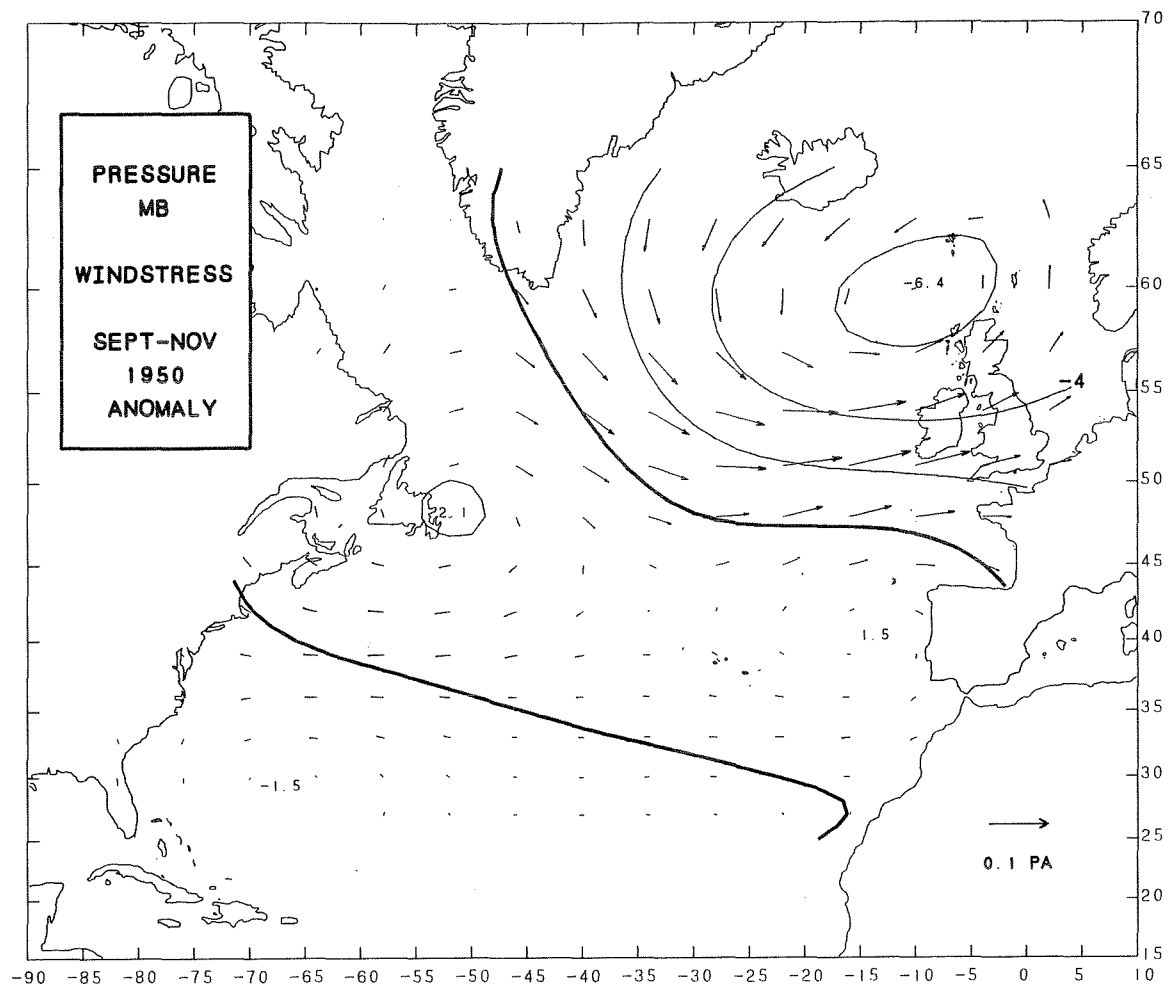
**Figure 6**

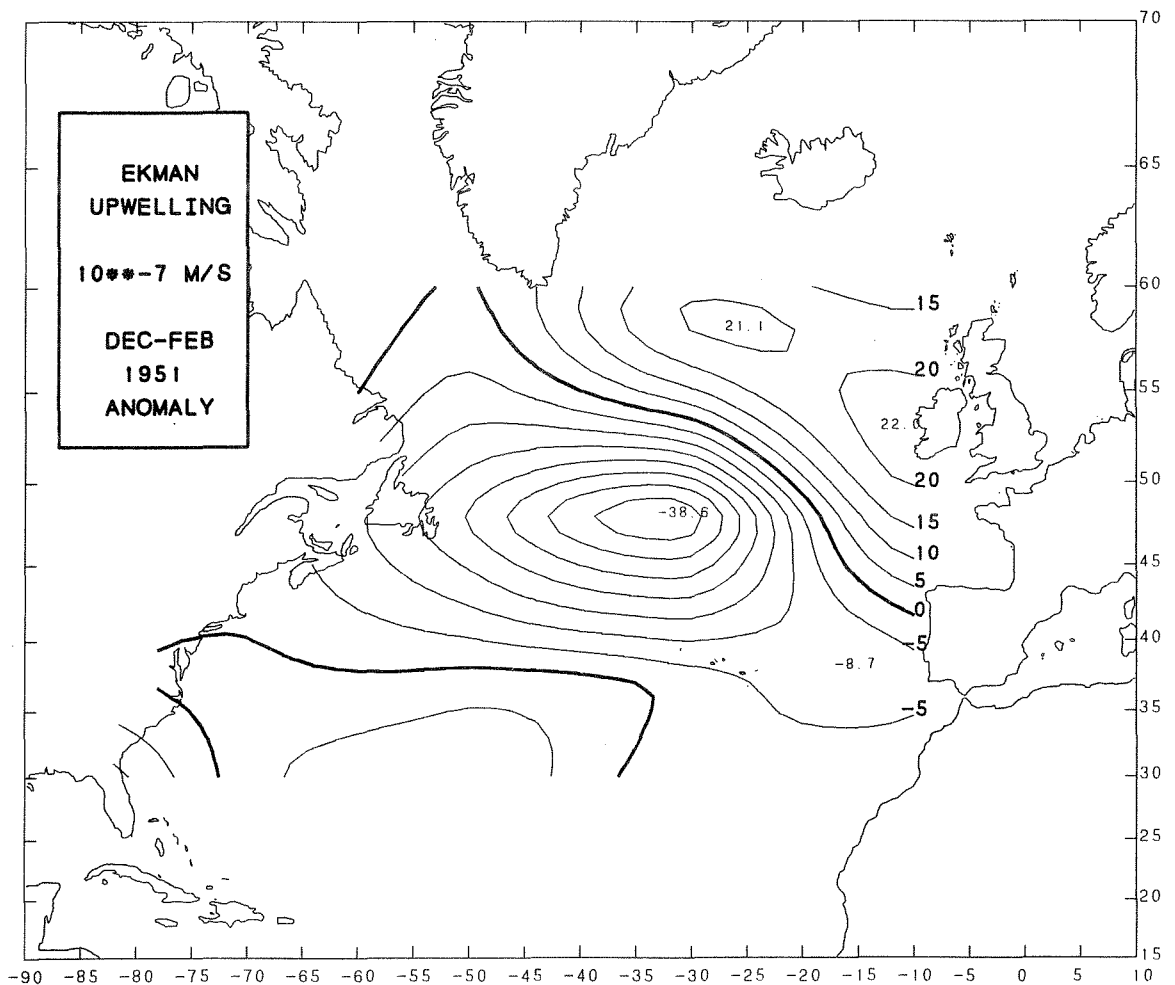
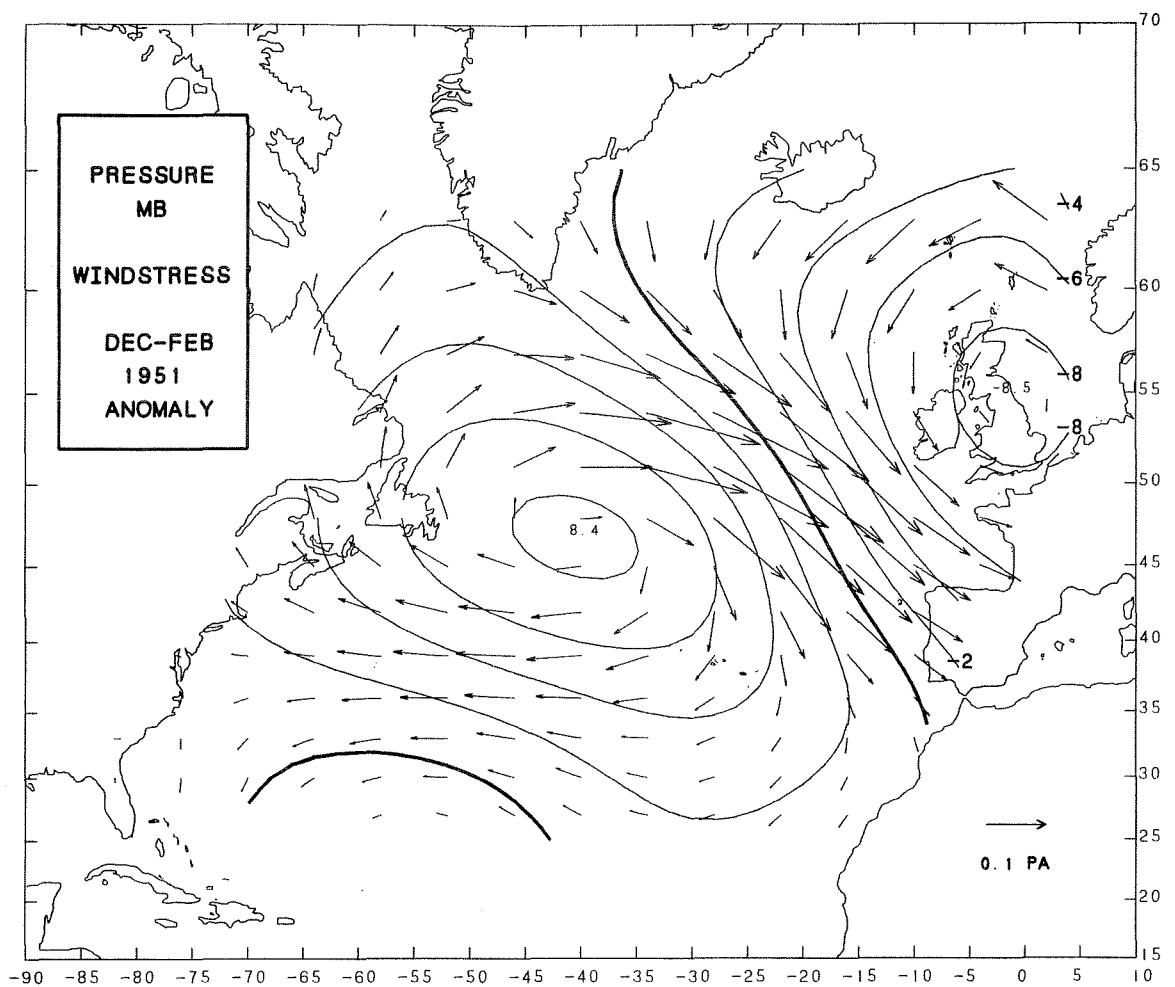
Seasonal anomaly maps of air pressure, wind stress and Ekman upwelling. The appropriate seasonal mean in Figure 4 has been removed from each 3 month mean to obtain the anomaly map.

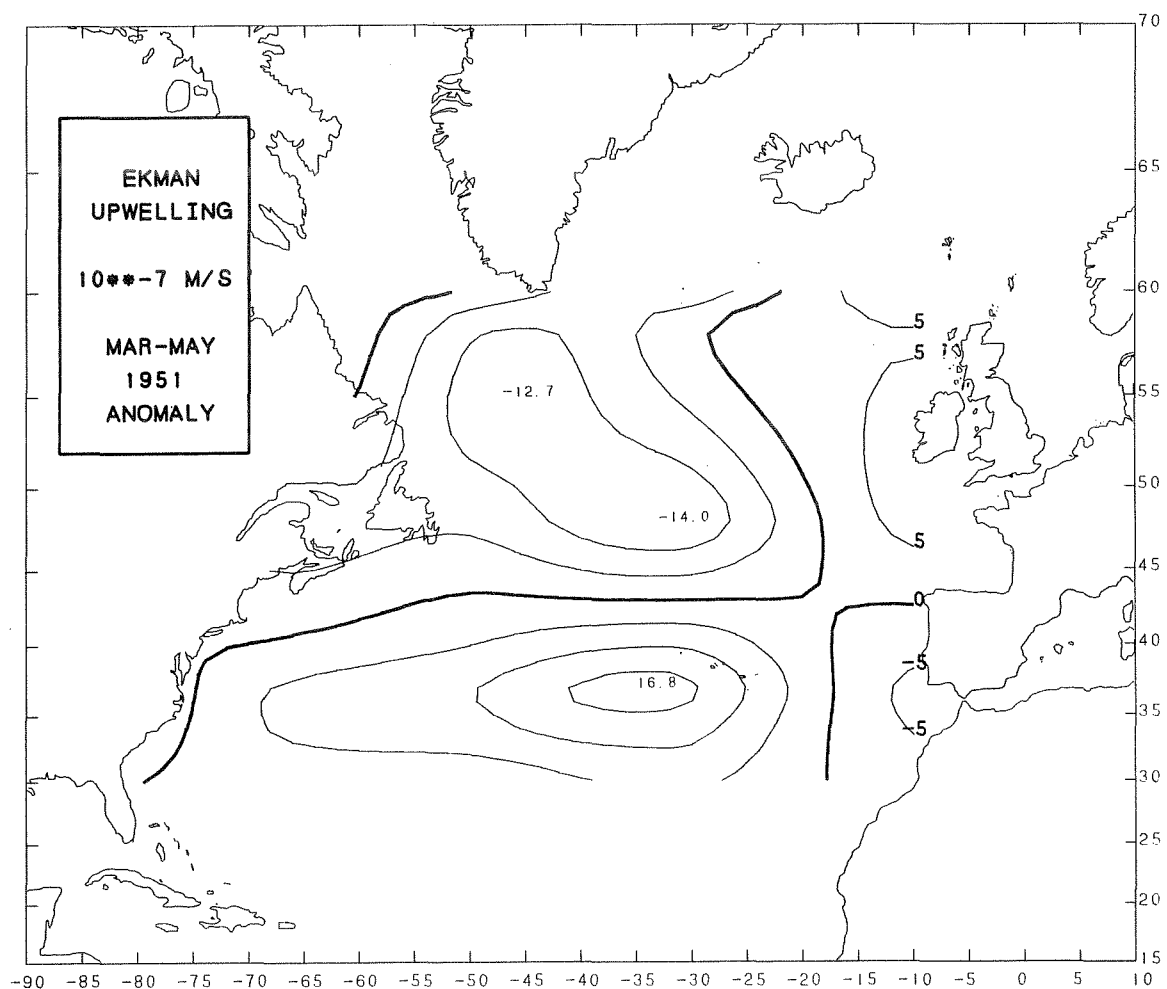
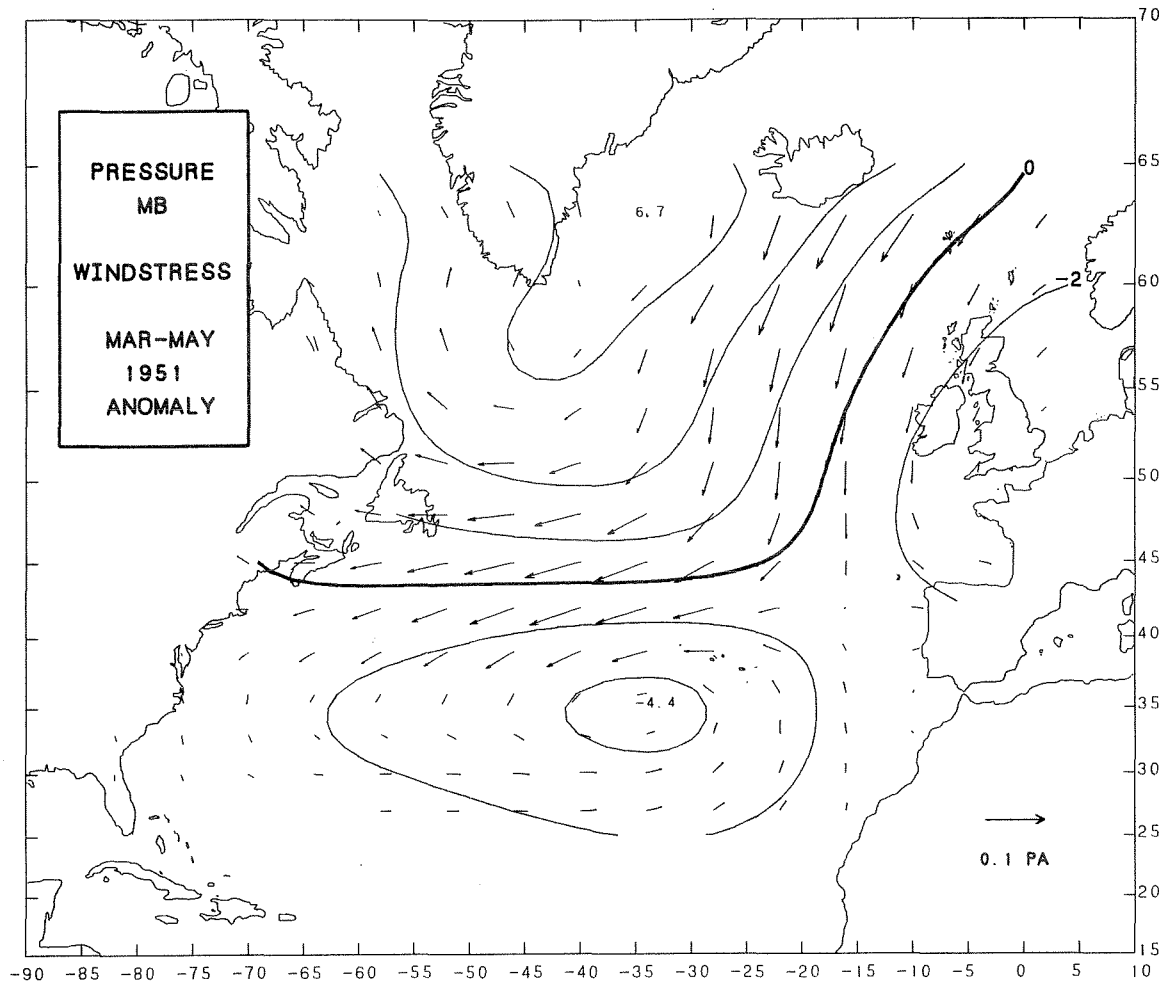


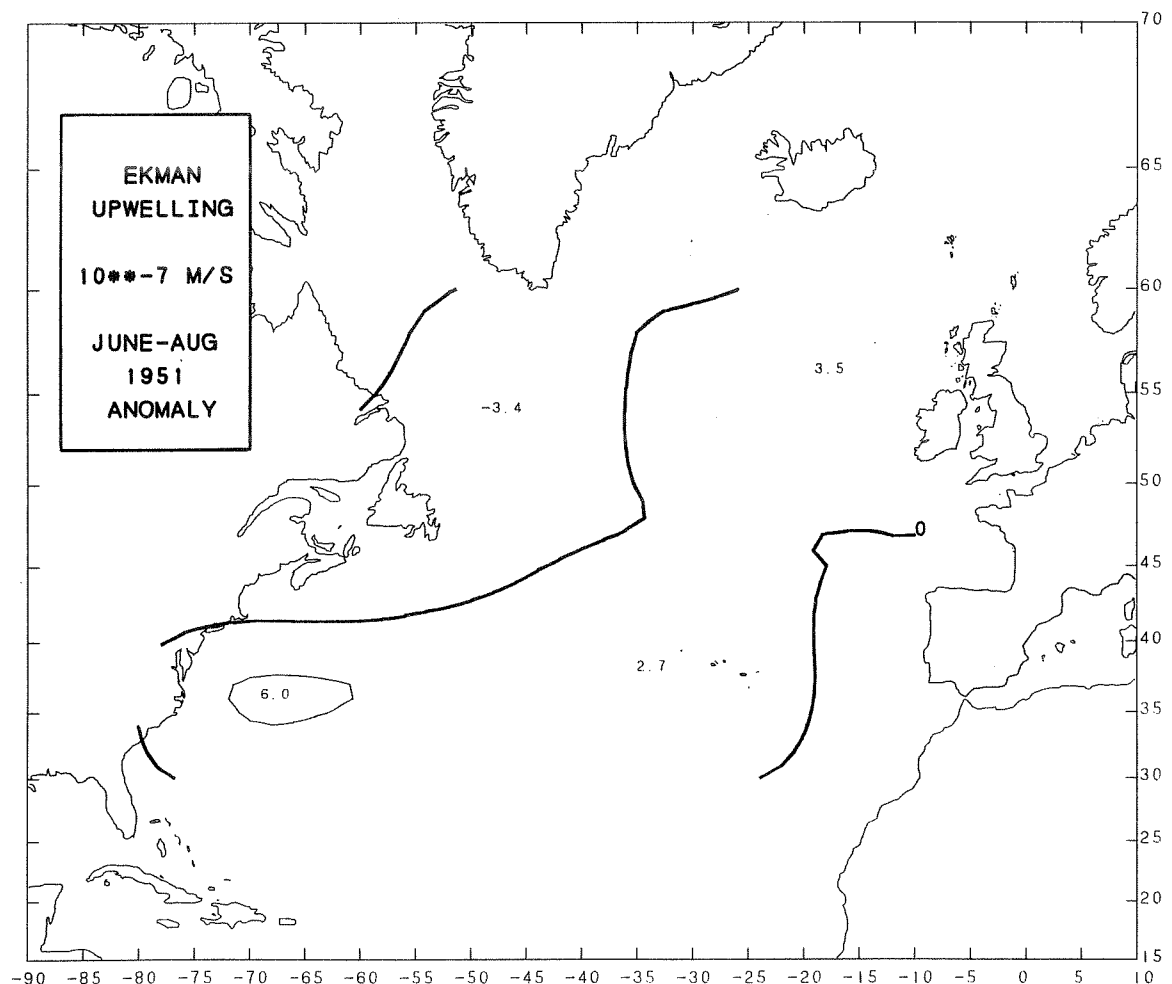
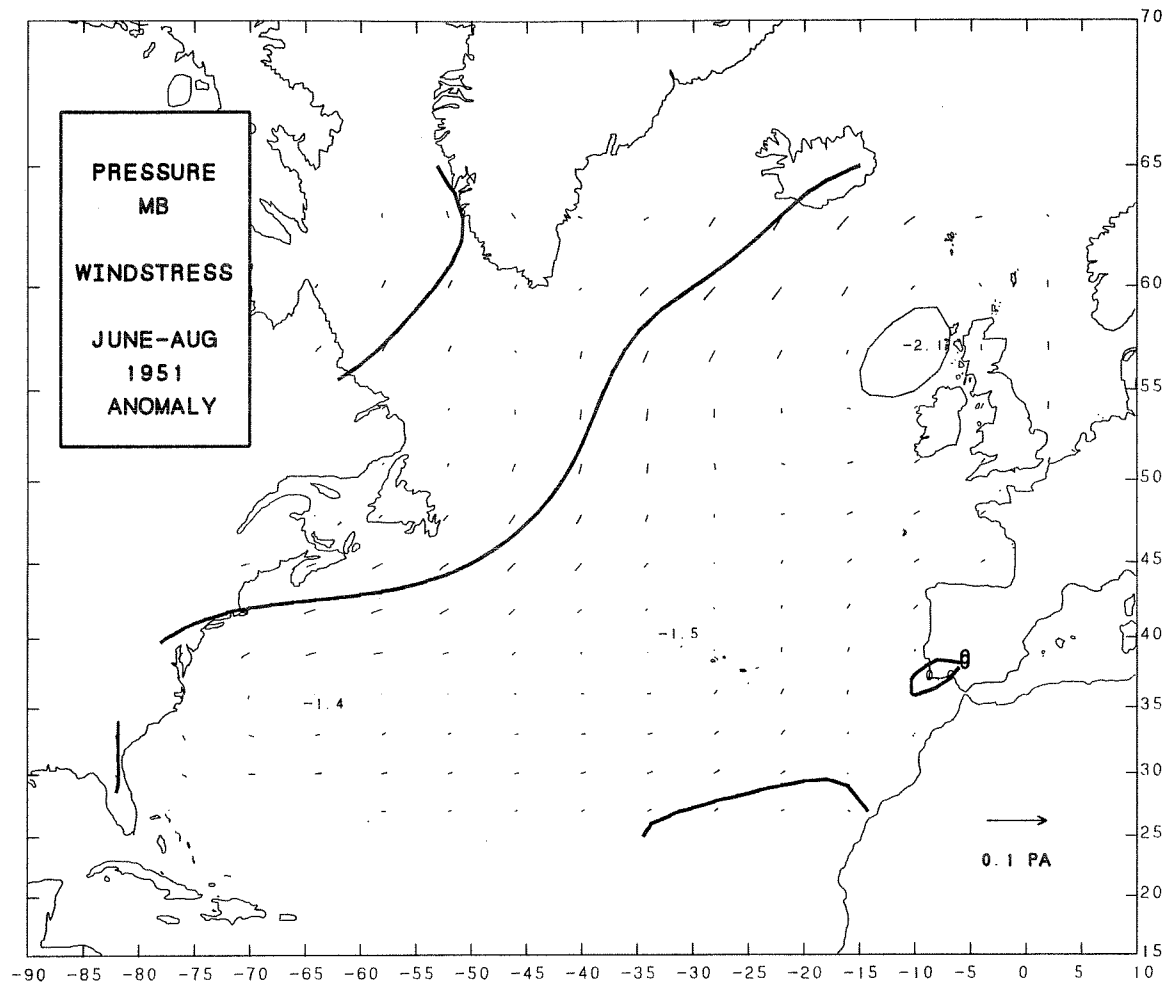


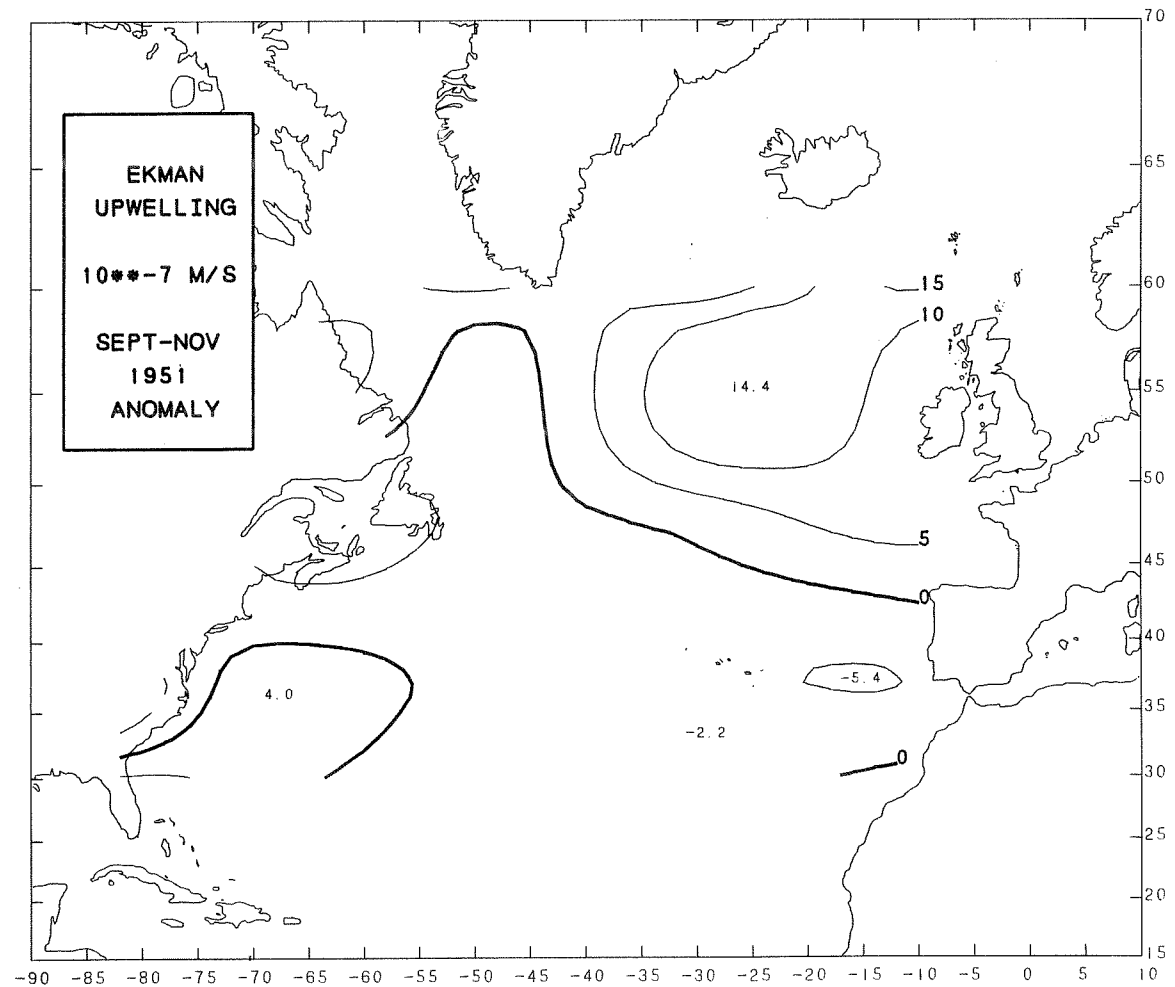
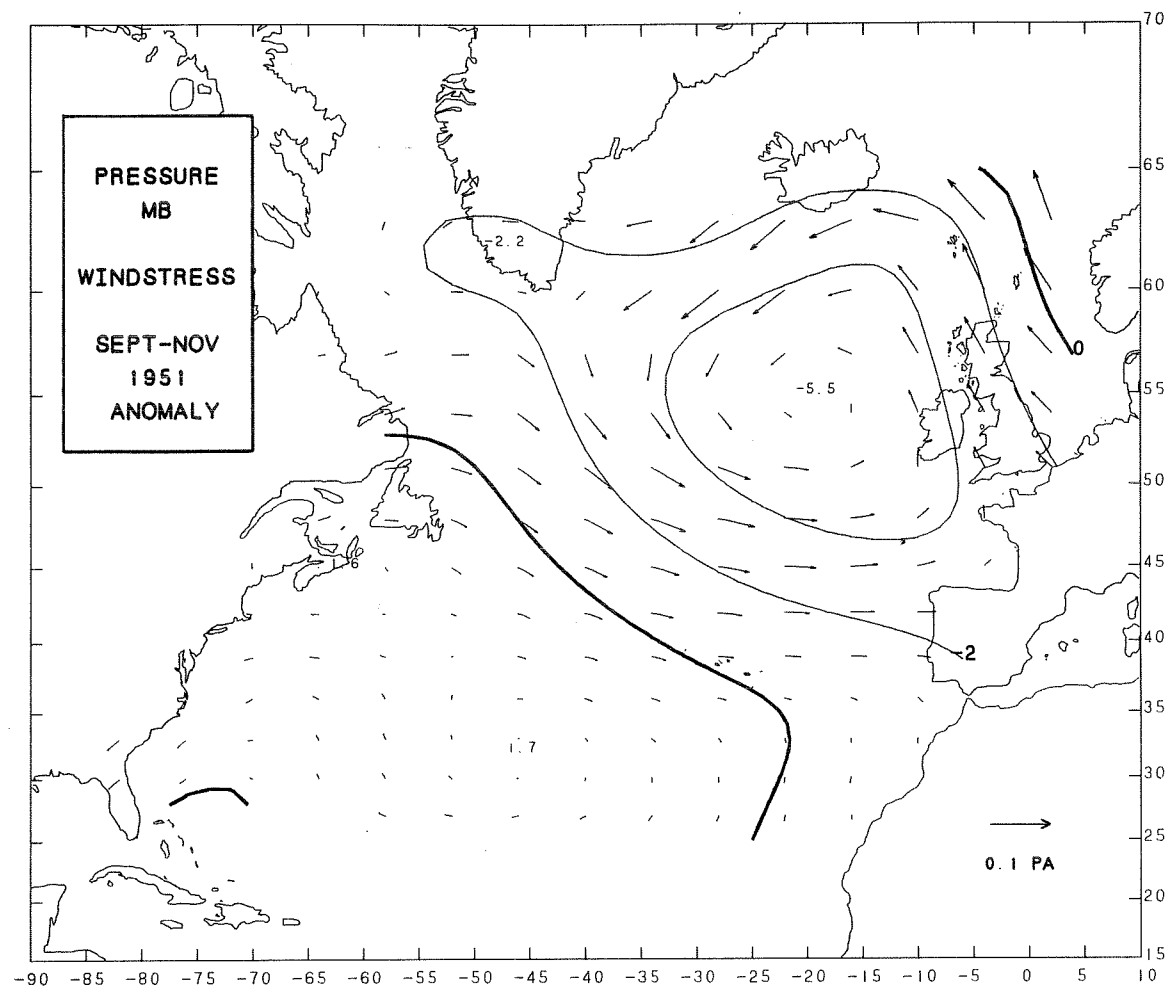


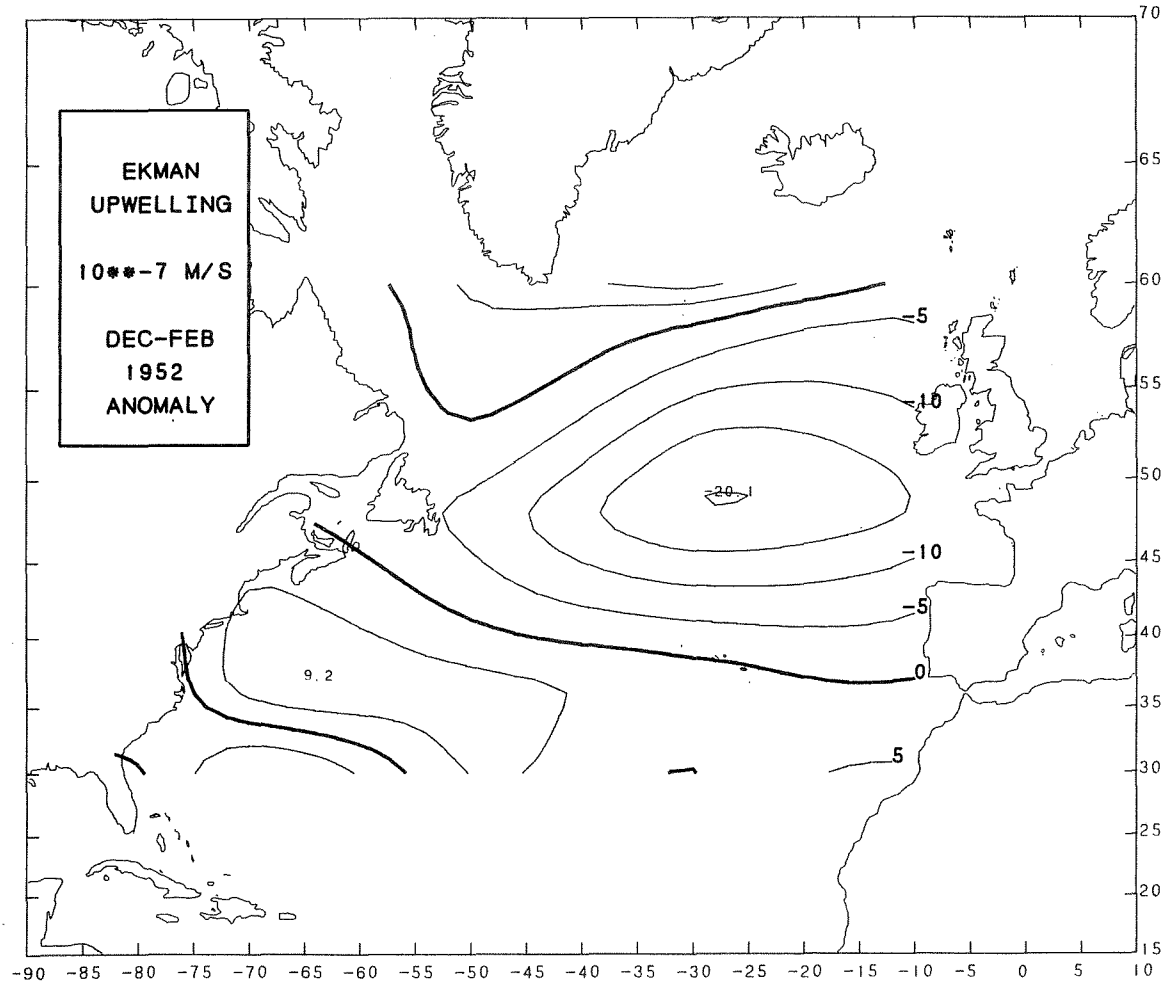
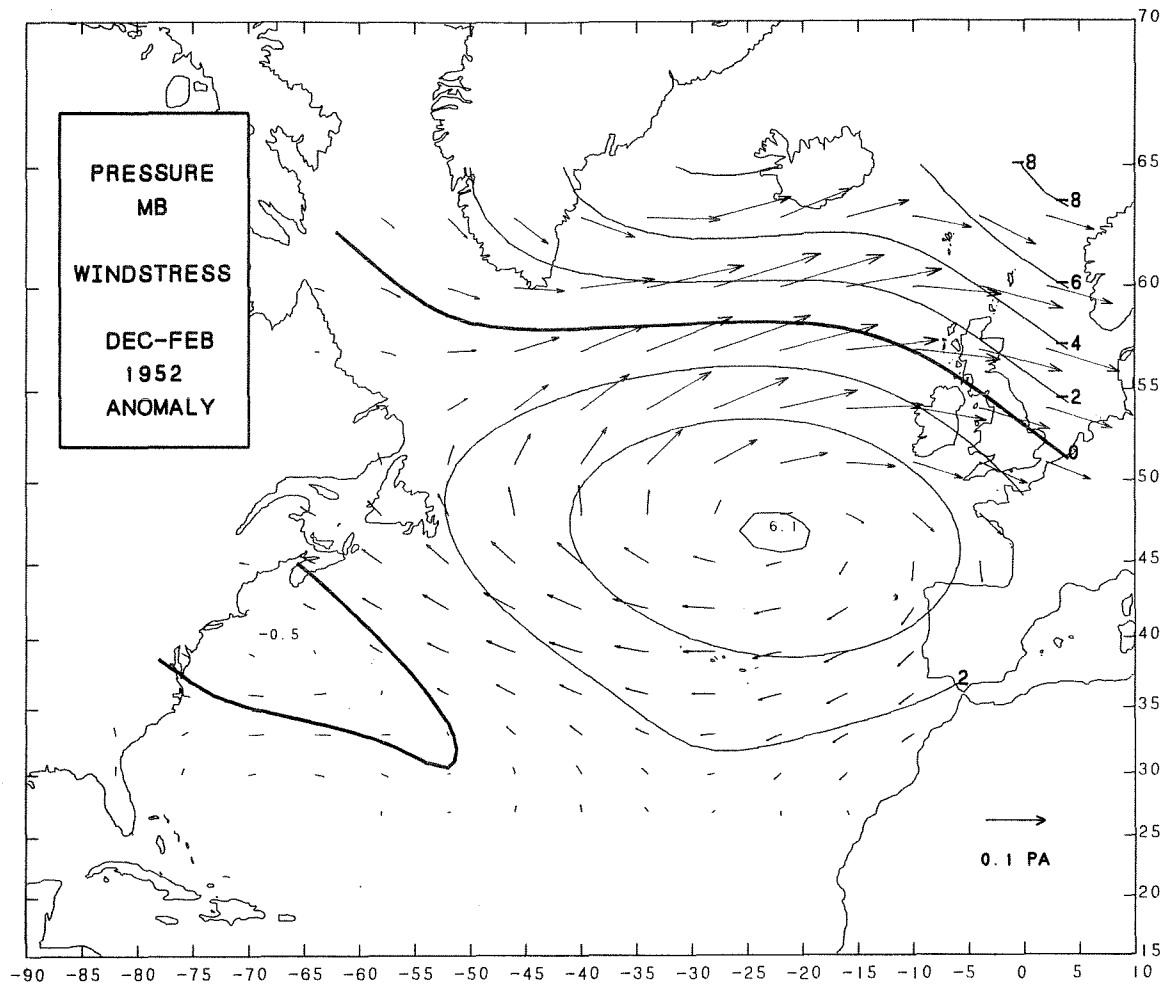


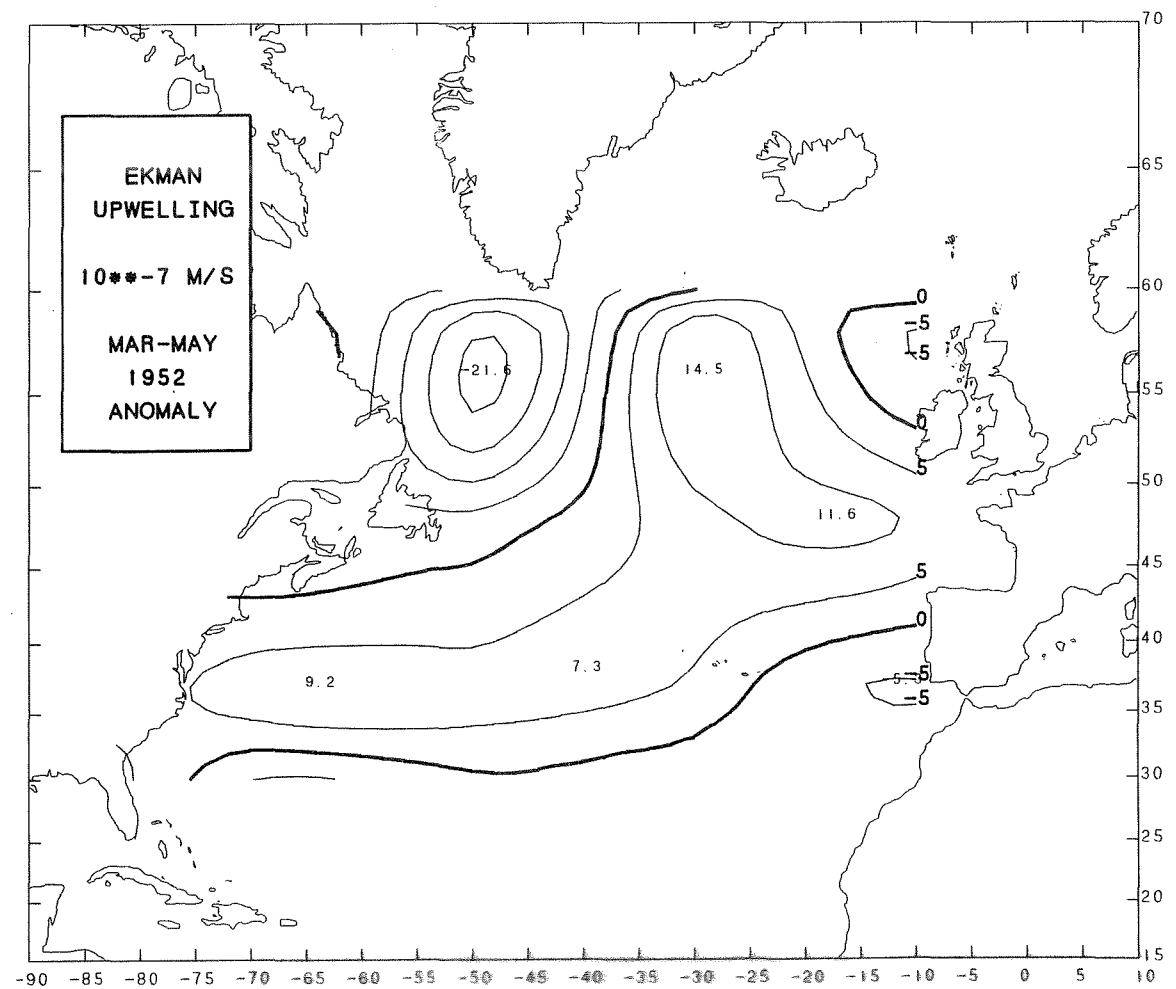
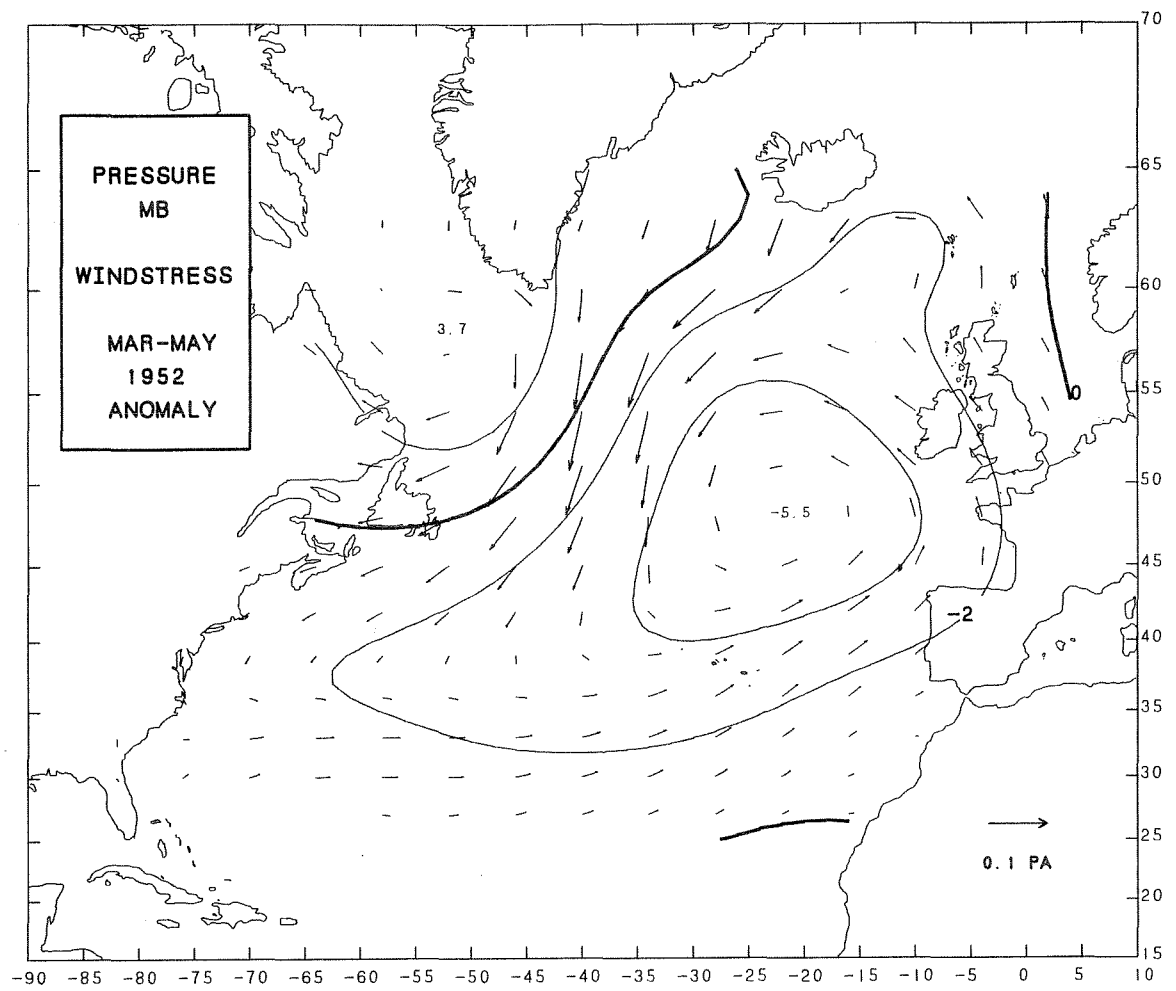


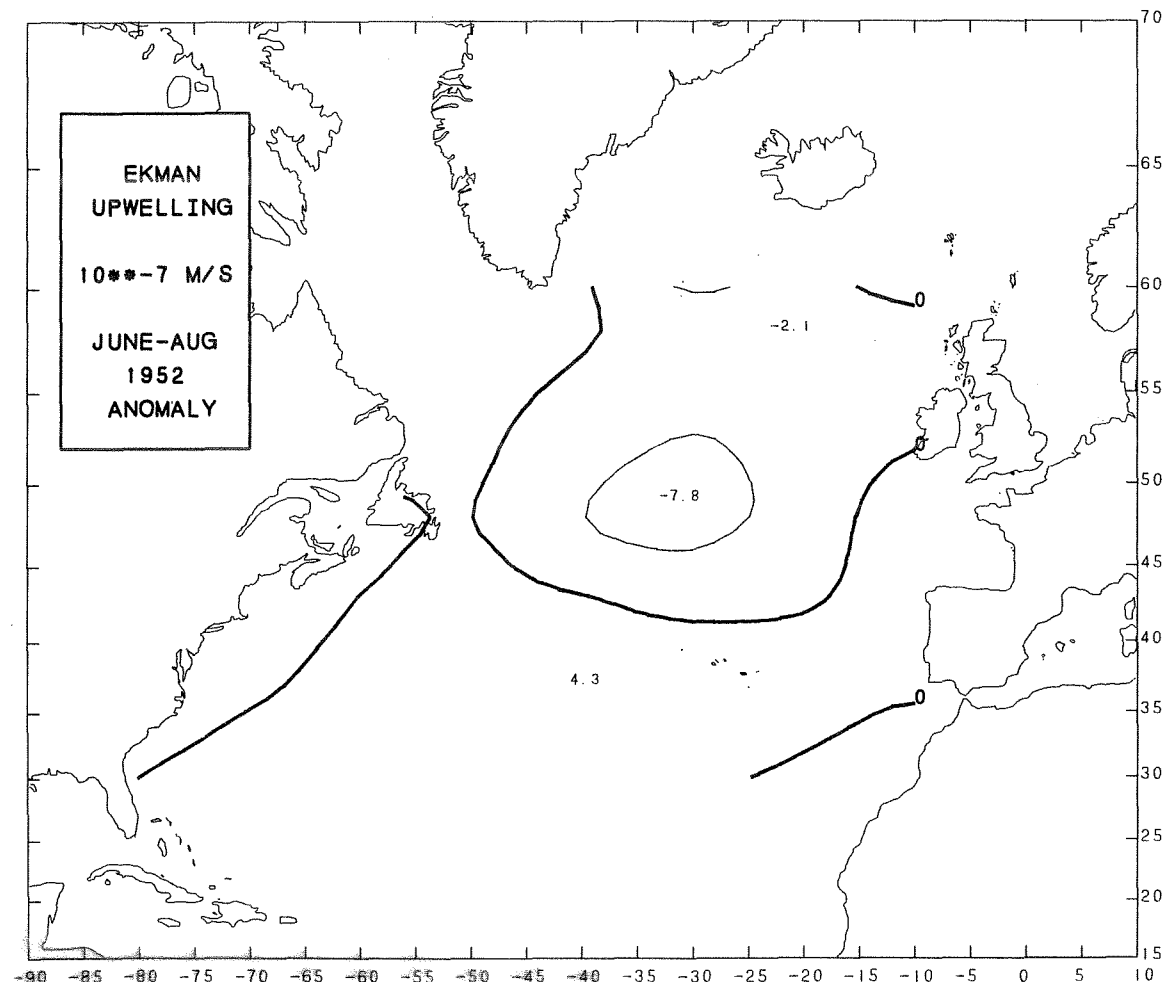
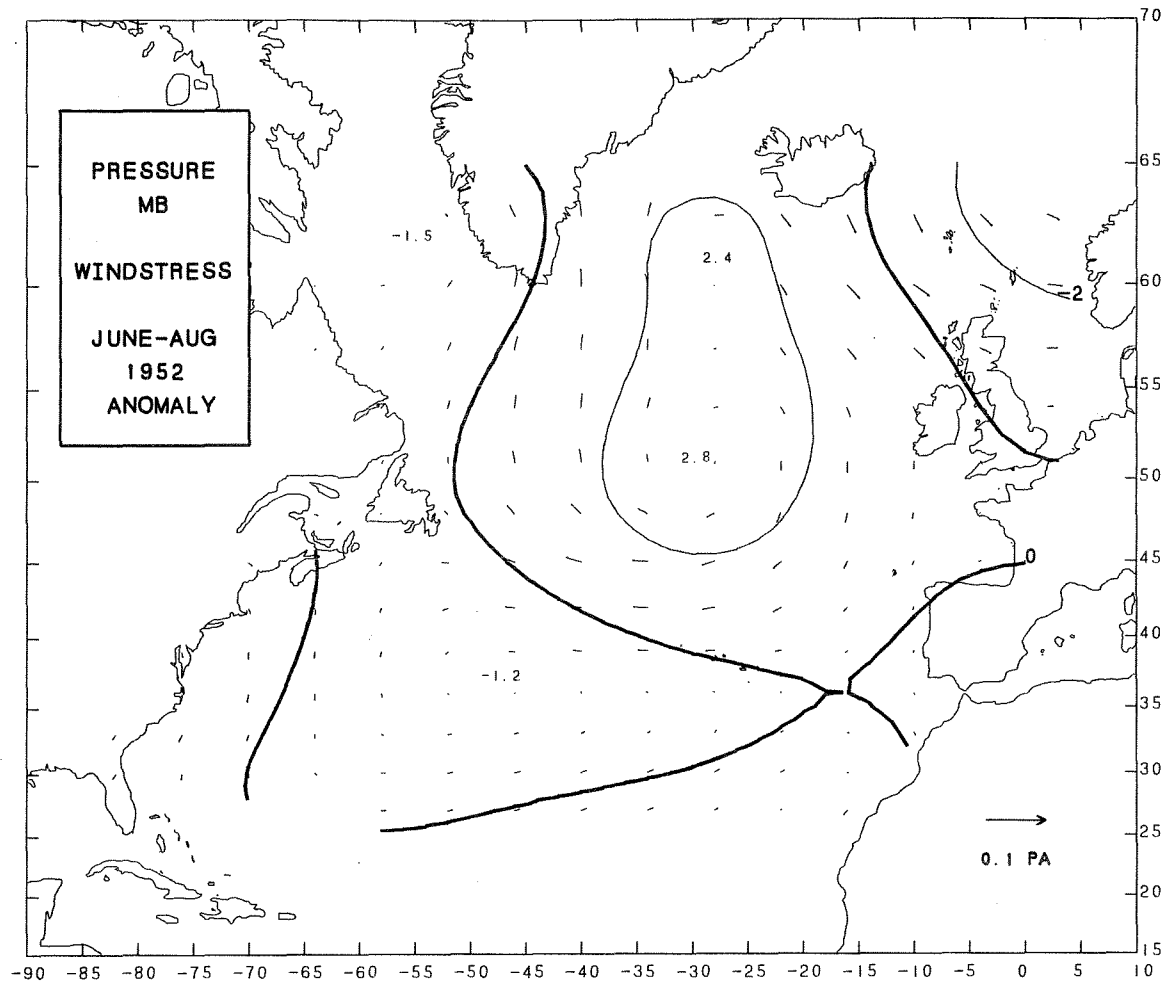


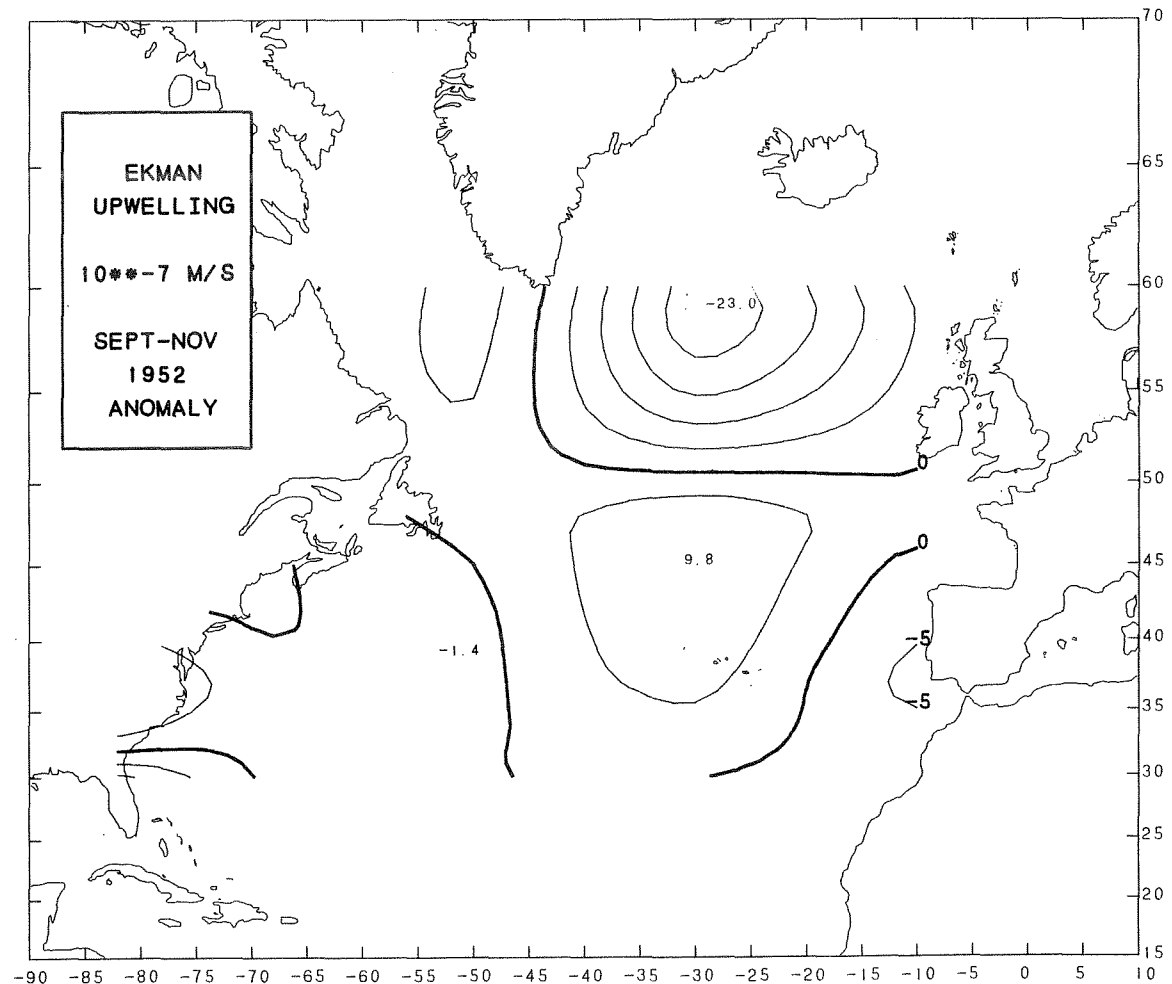
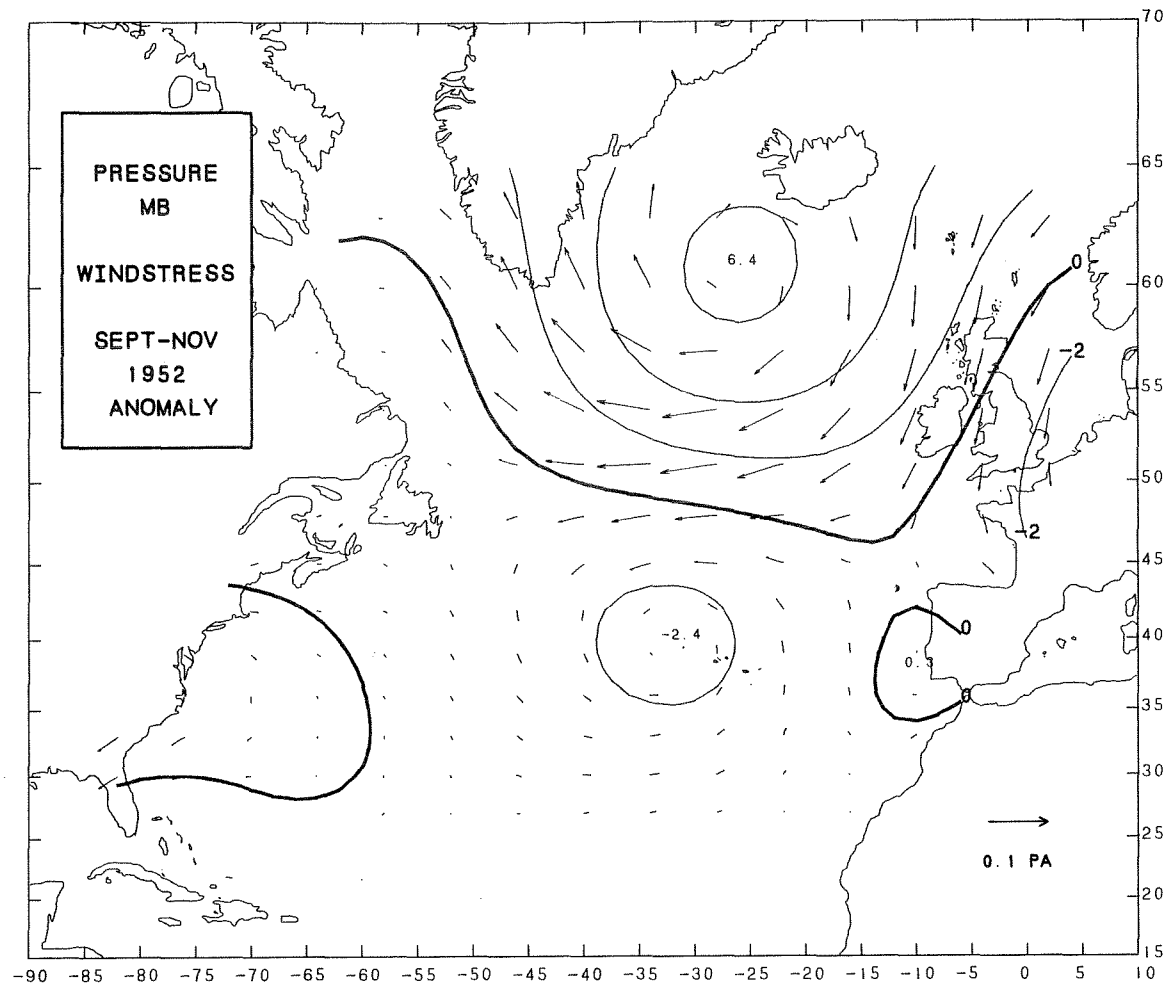


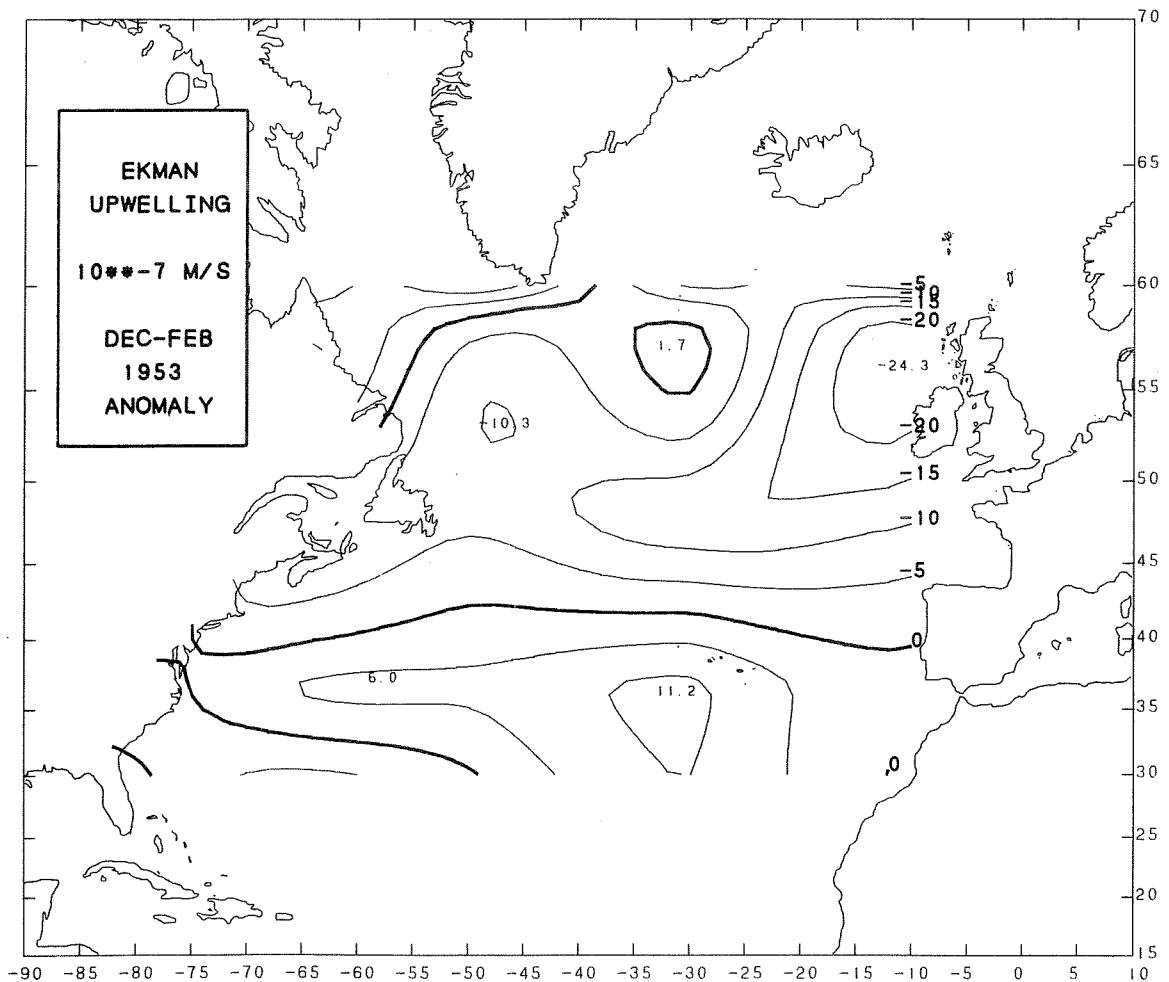
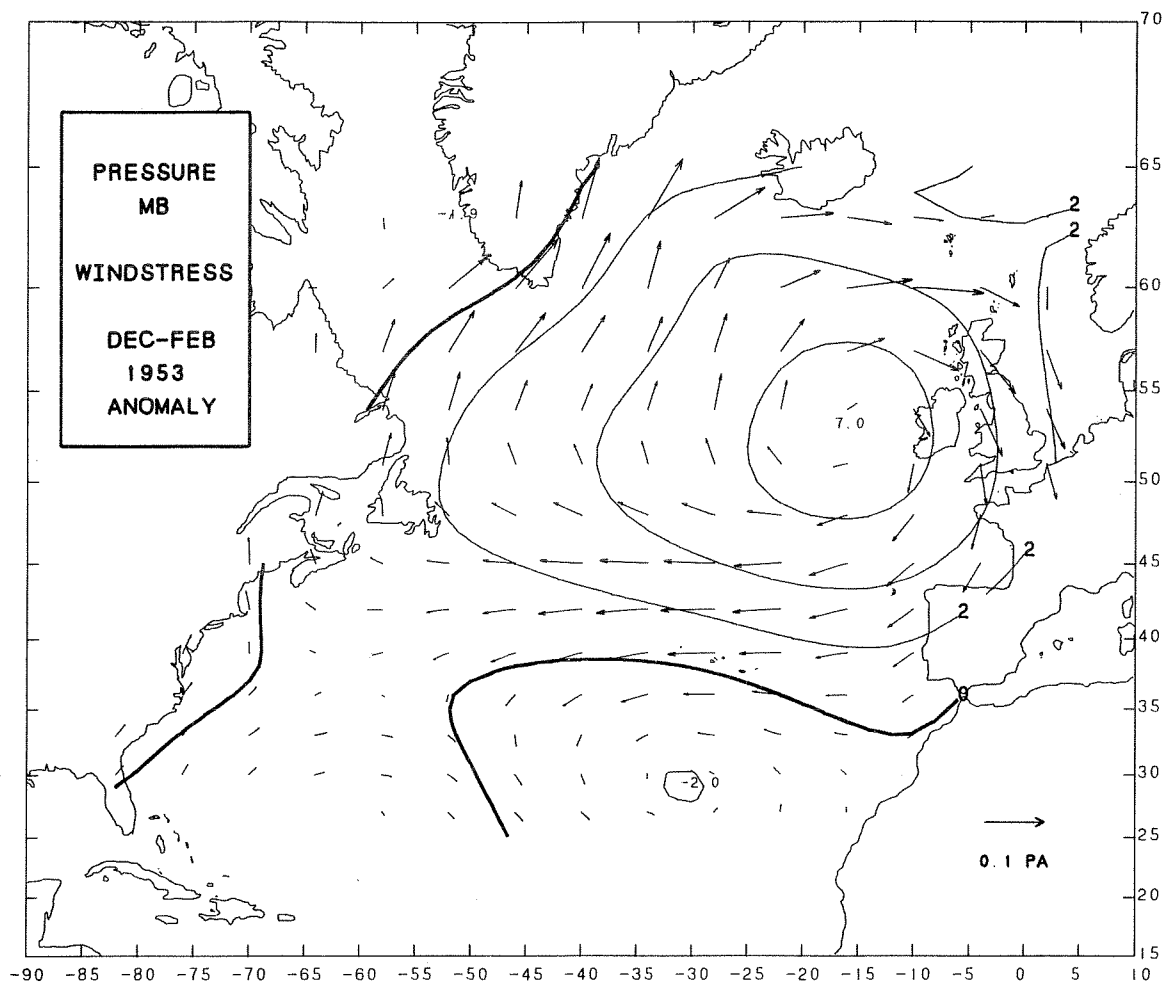


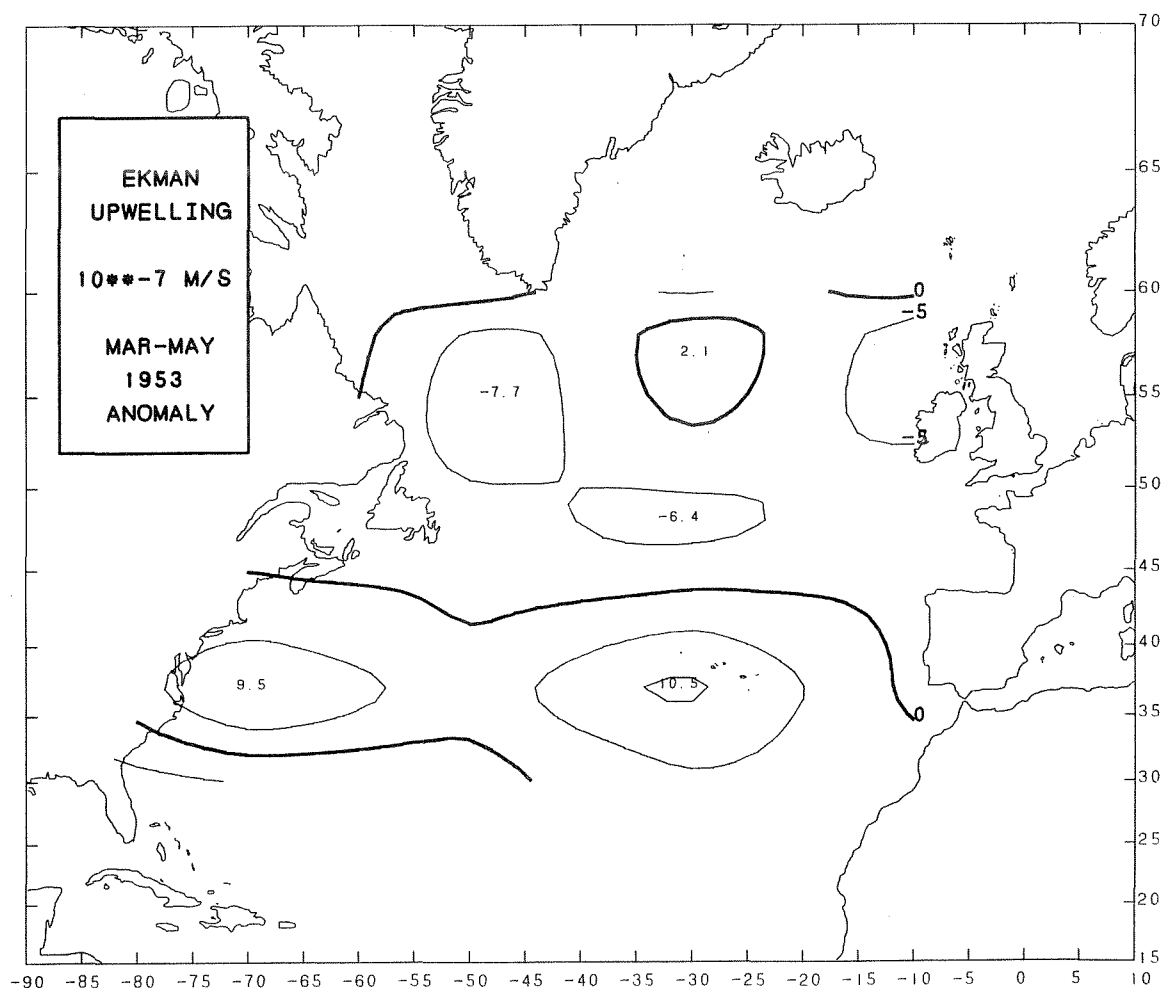
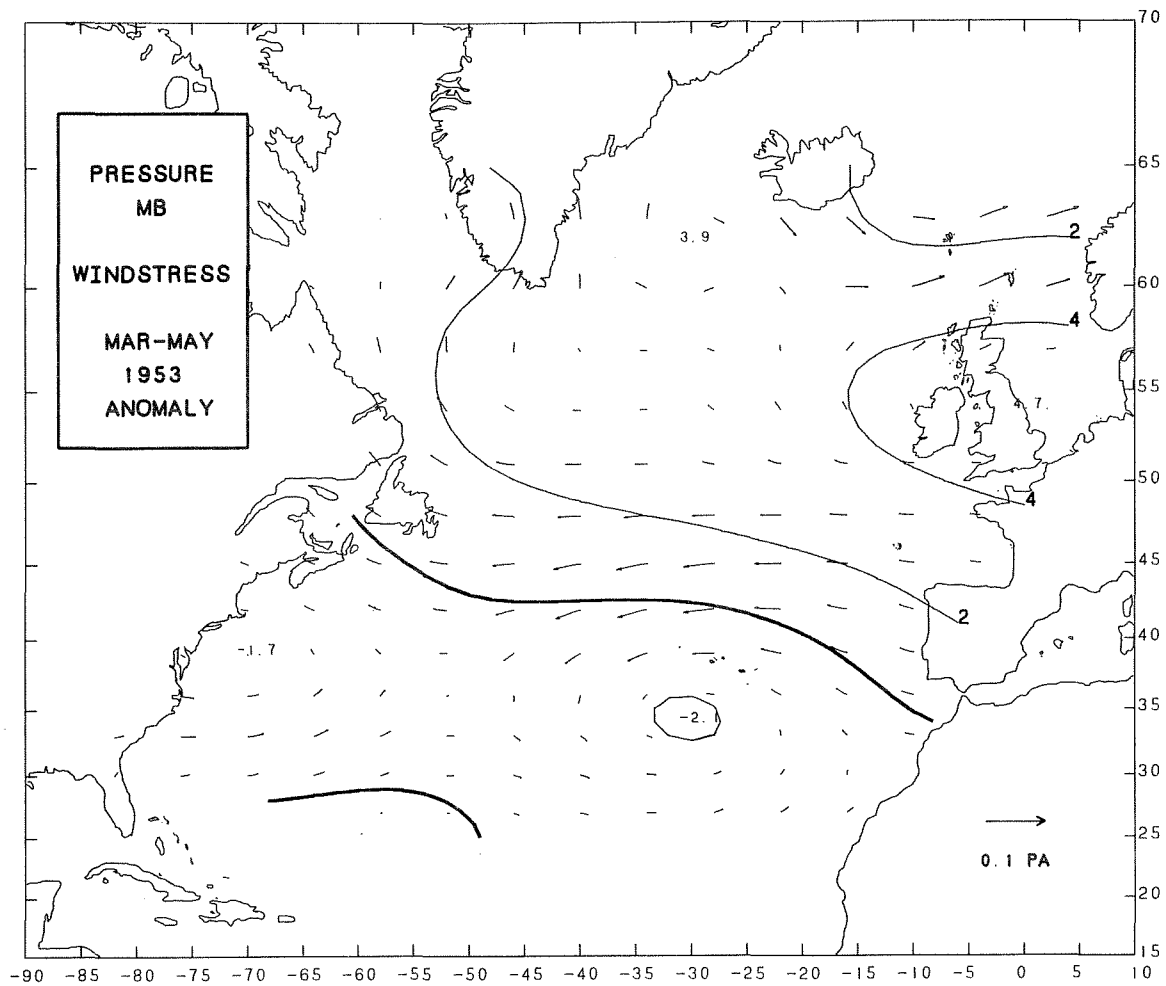


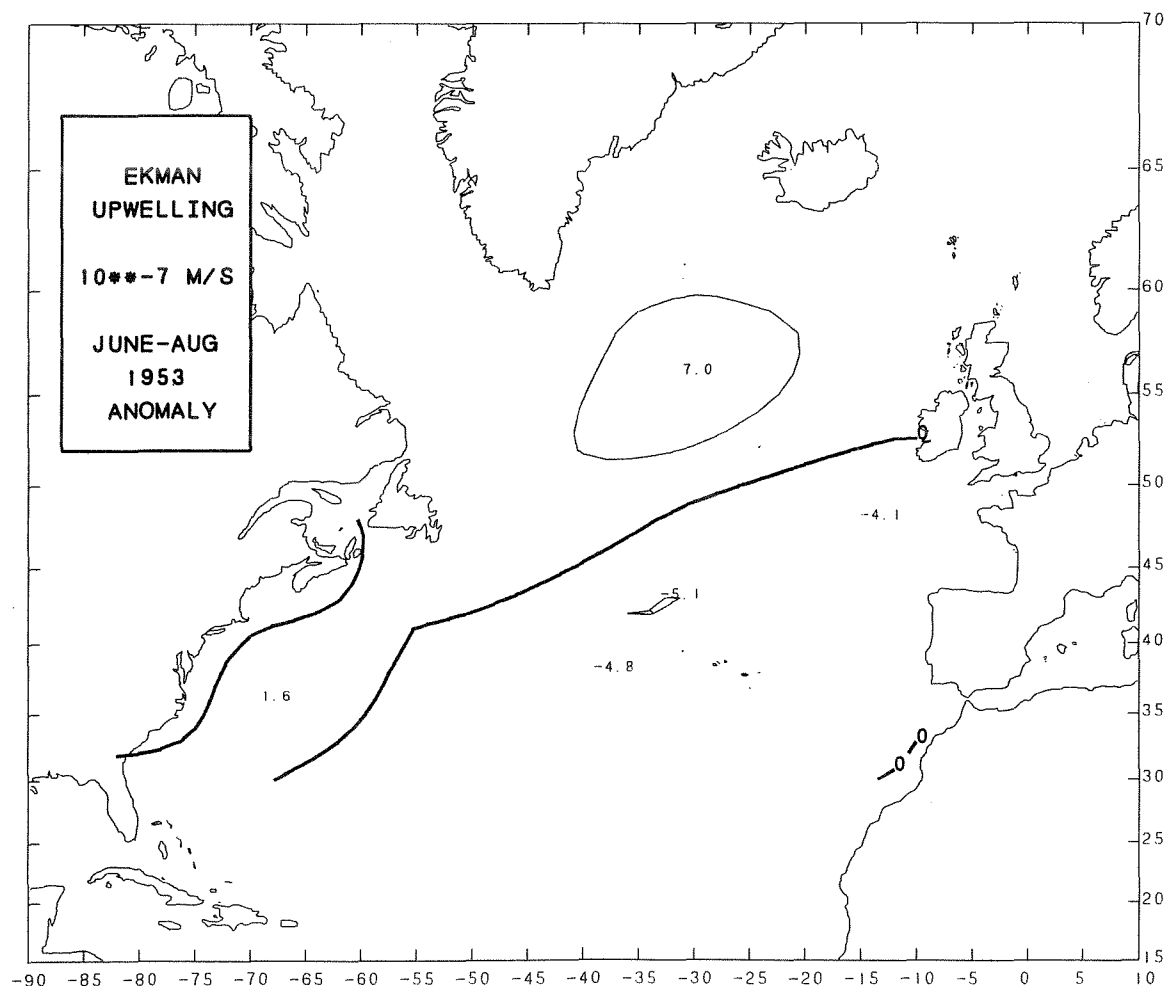
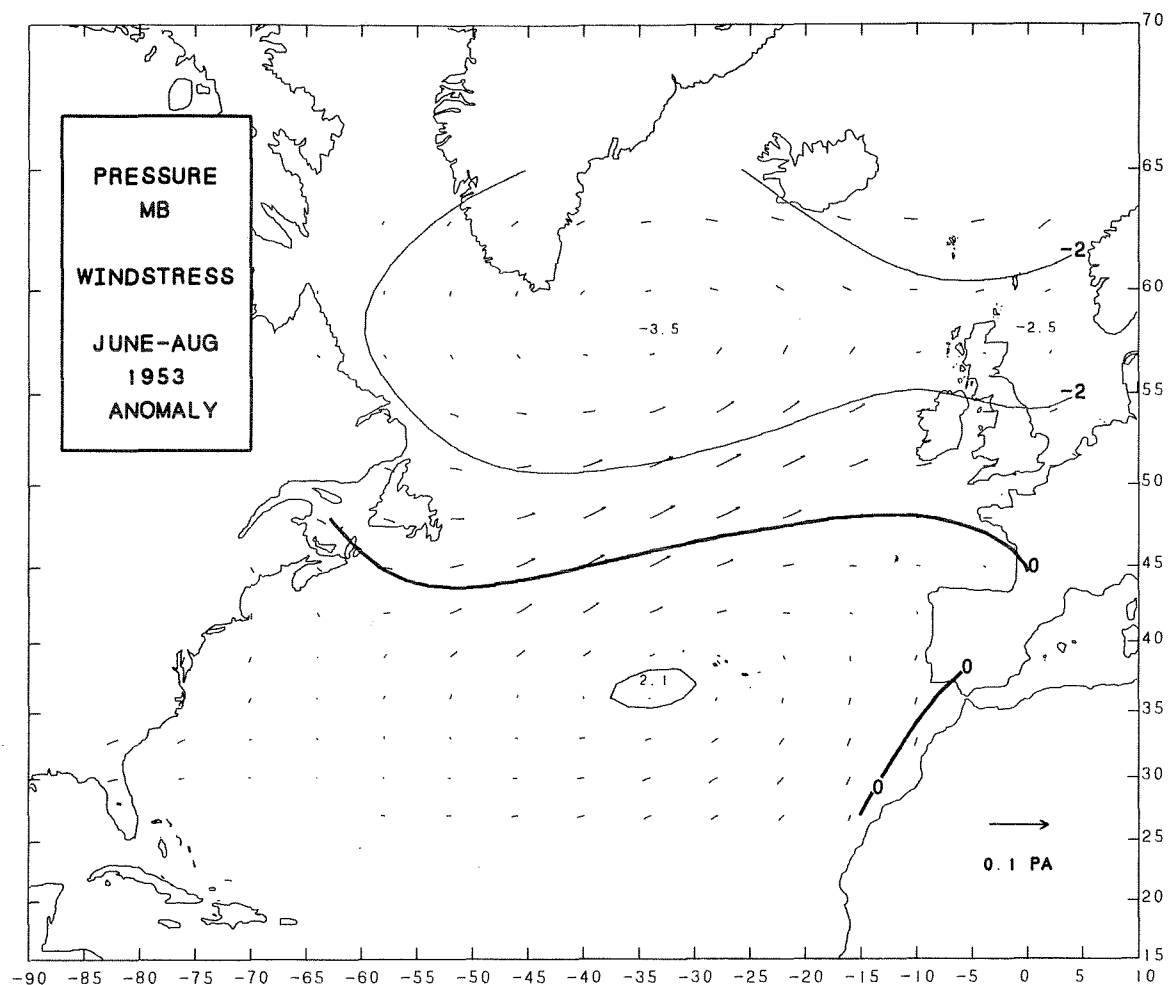


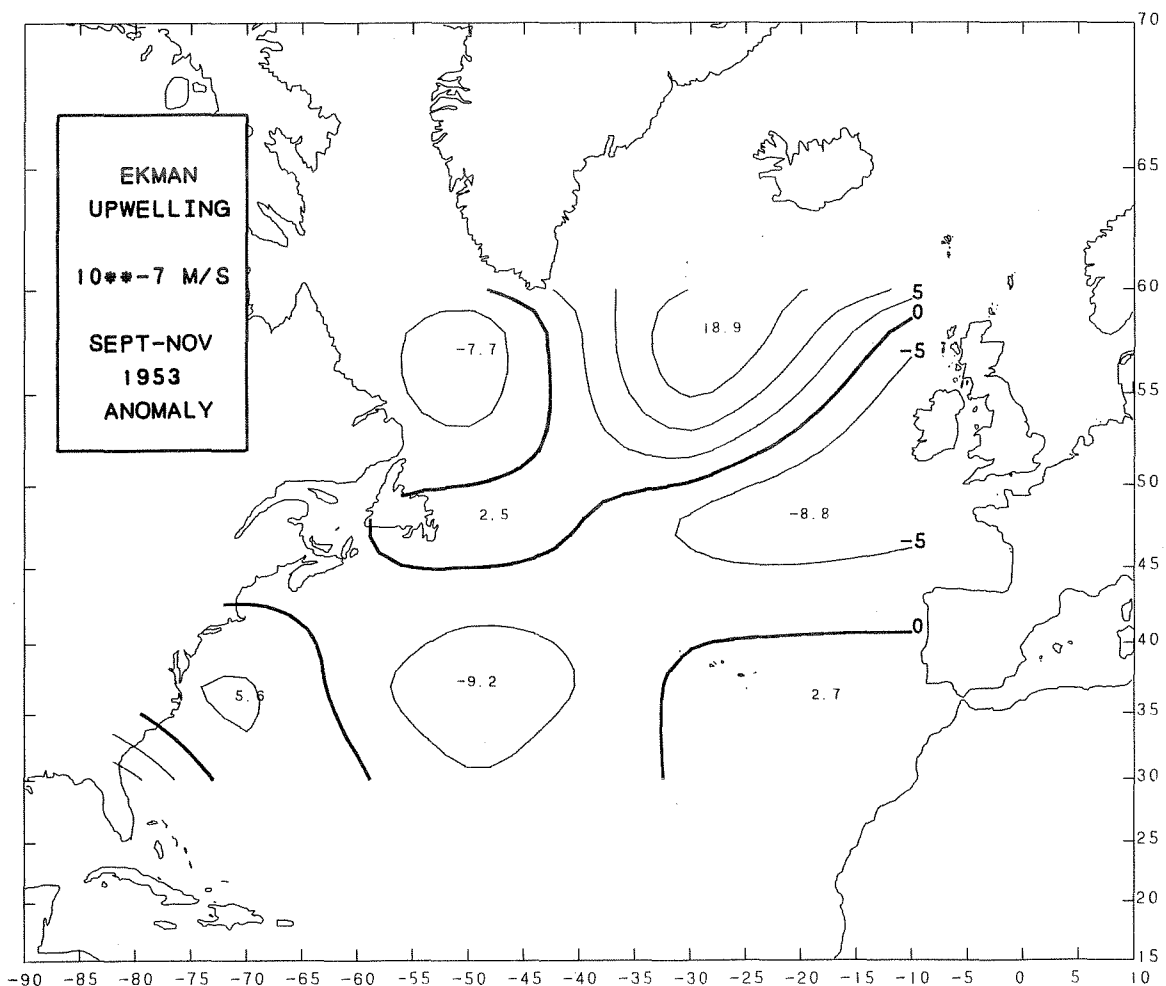
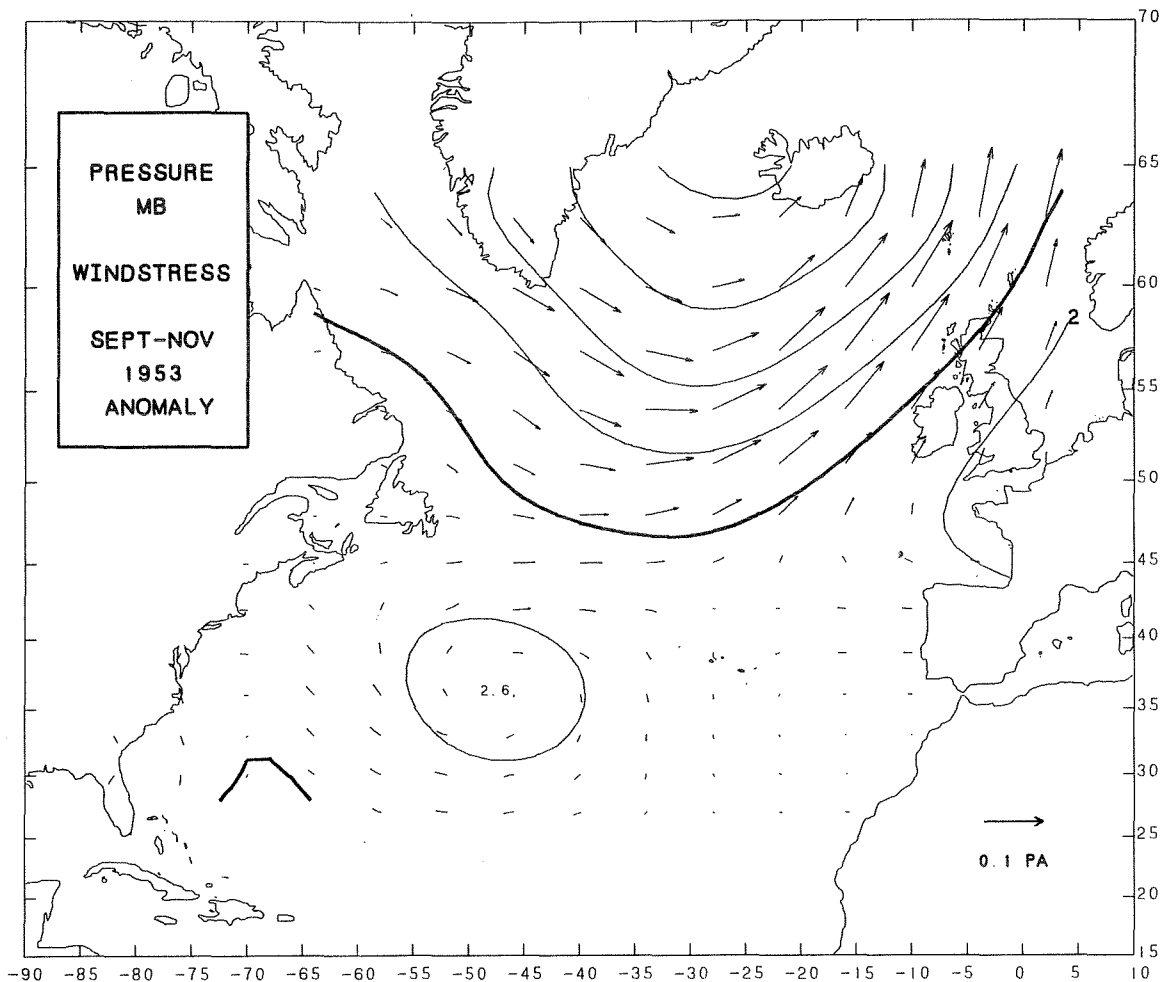


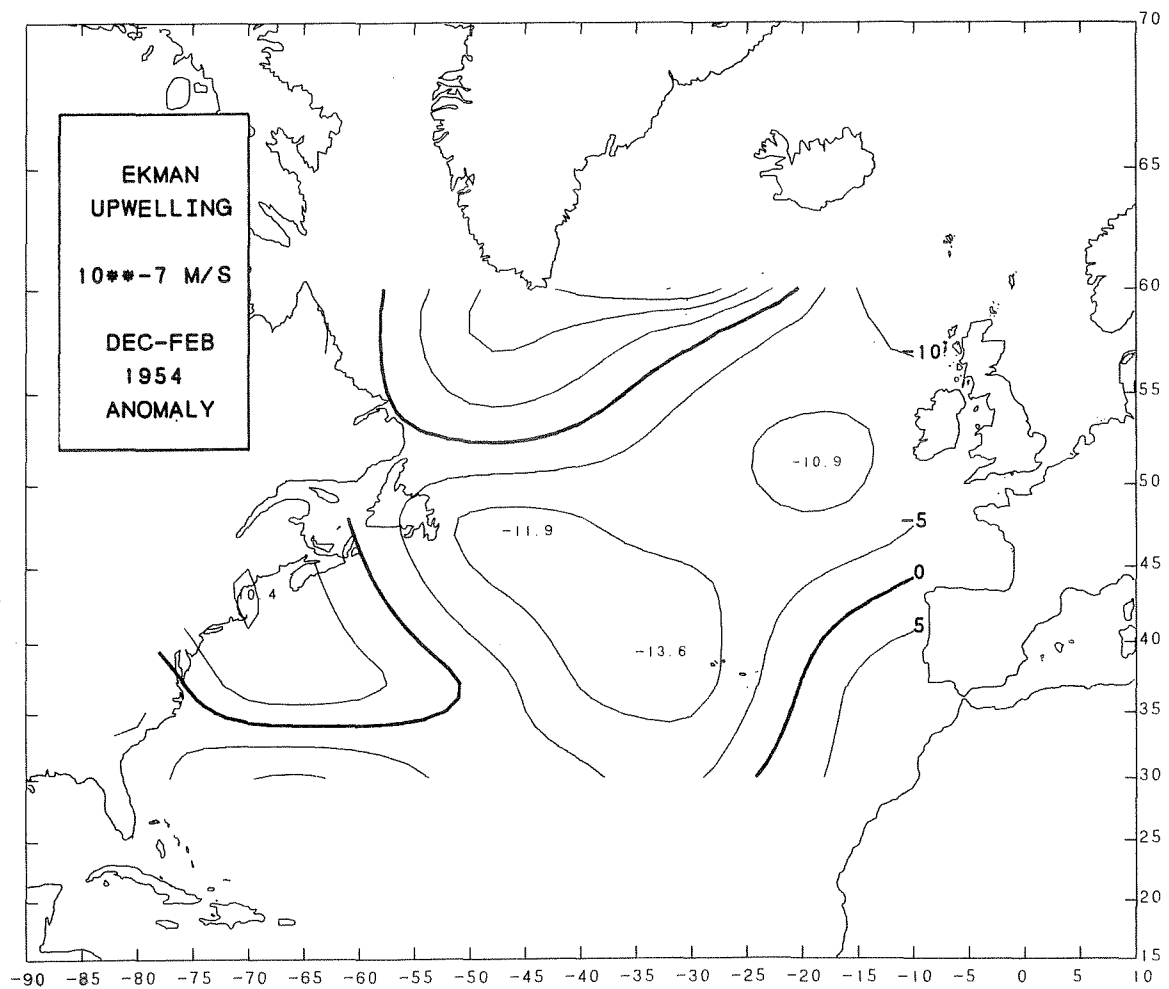
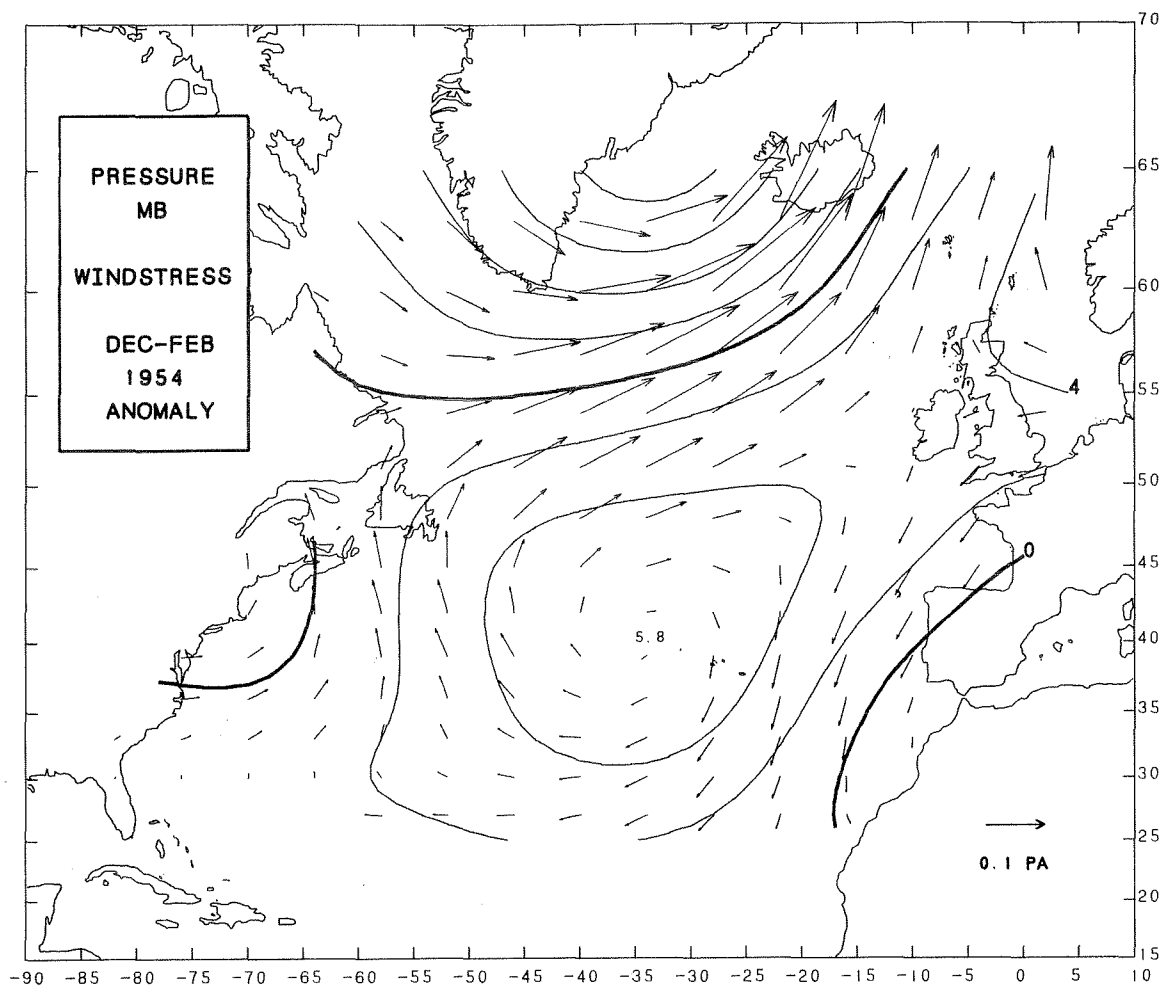


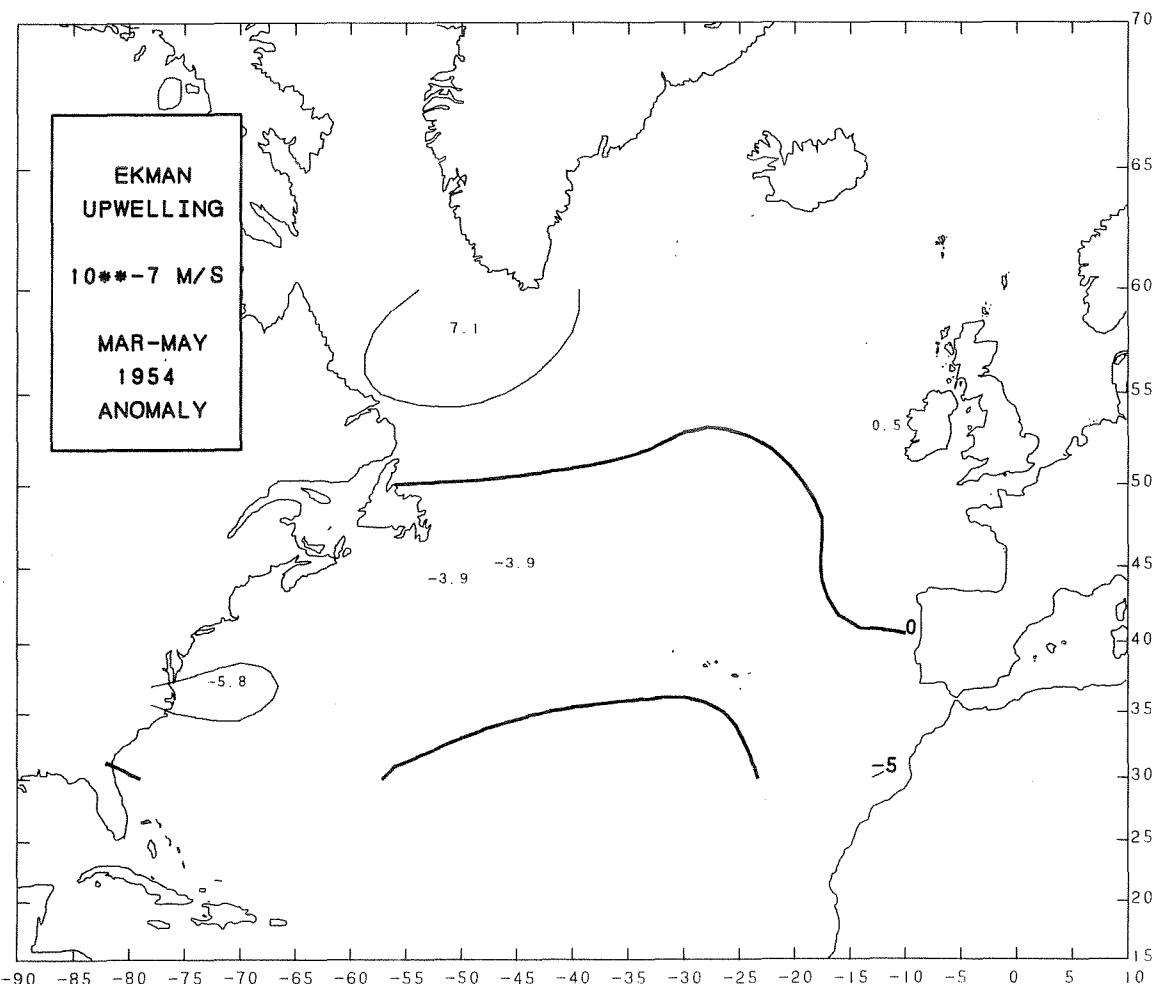
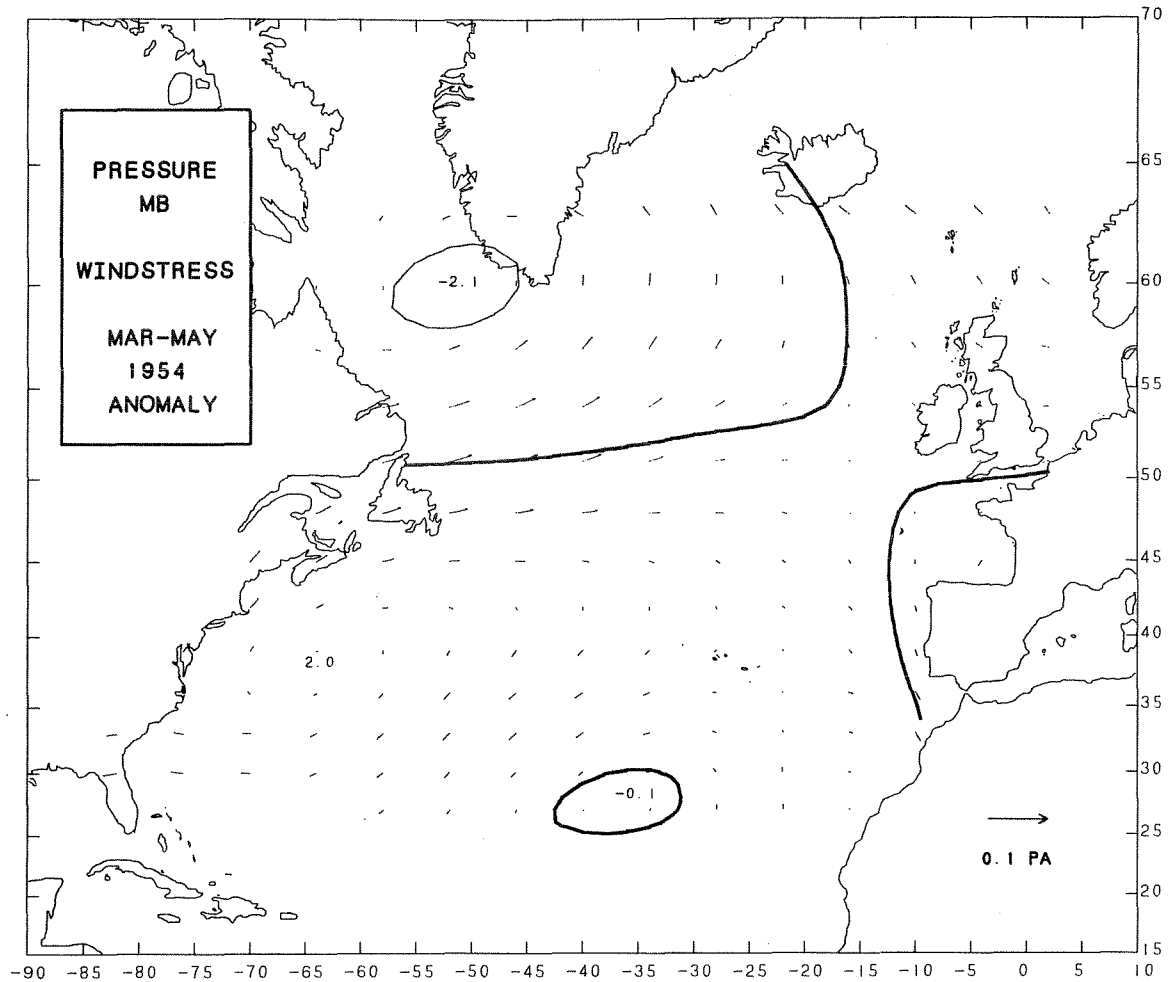


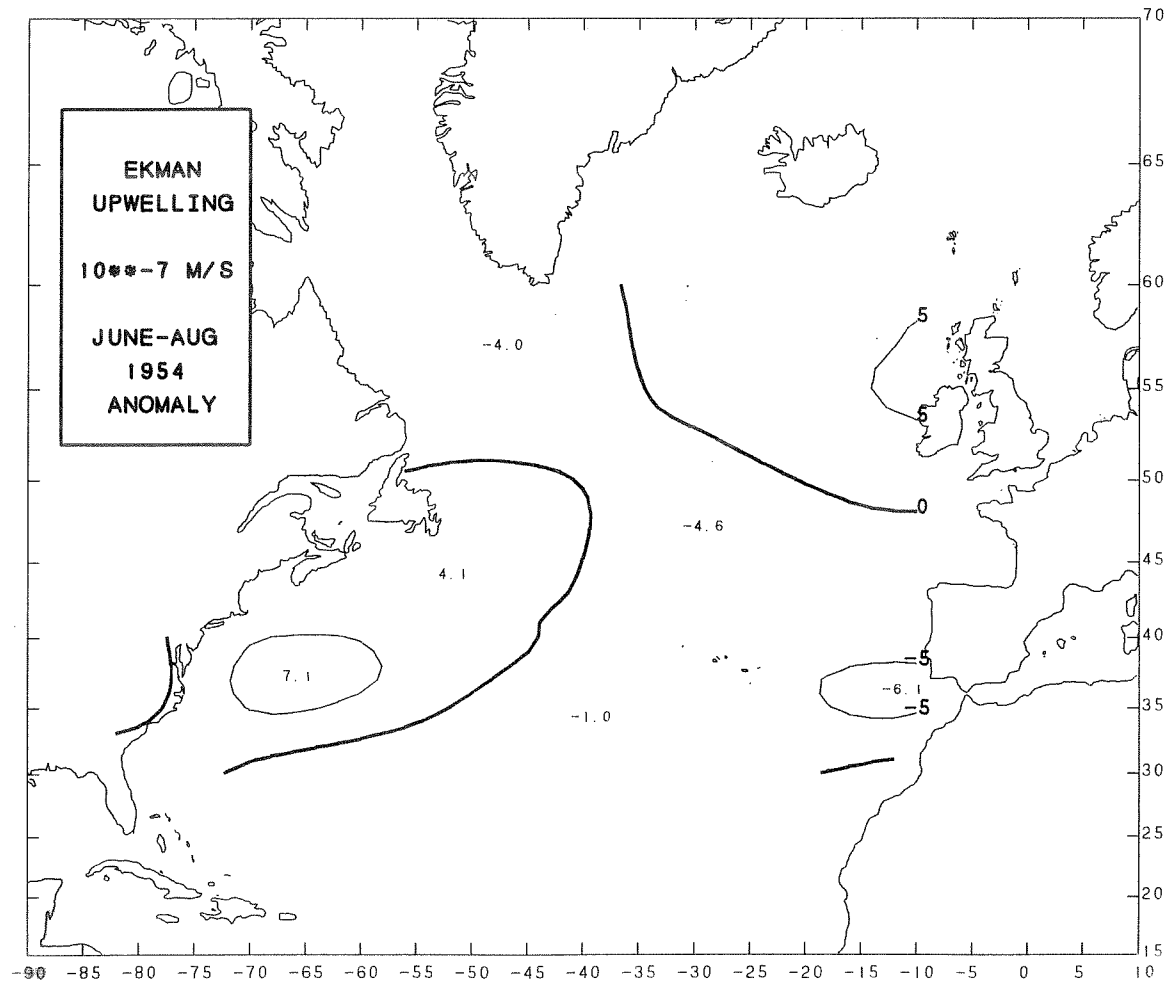
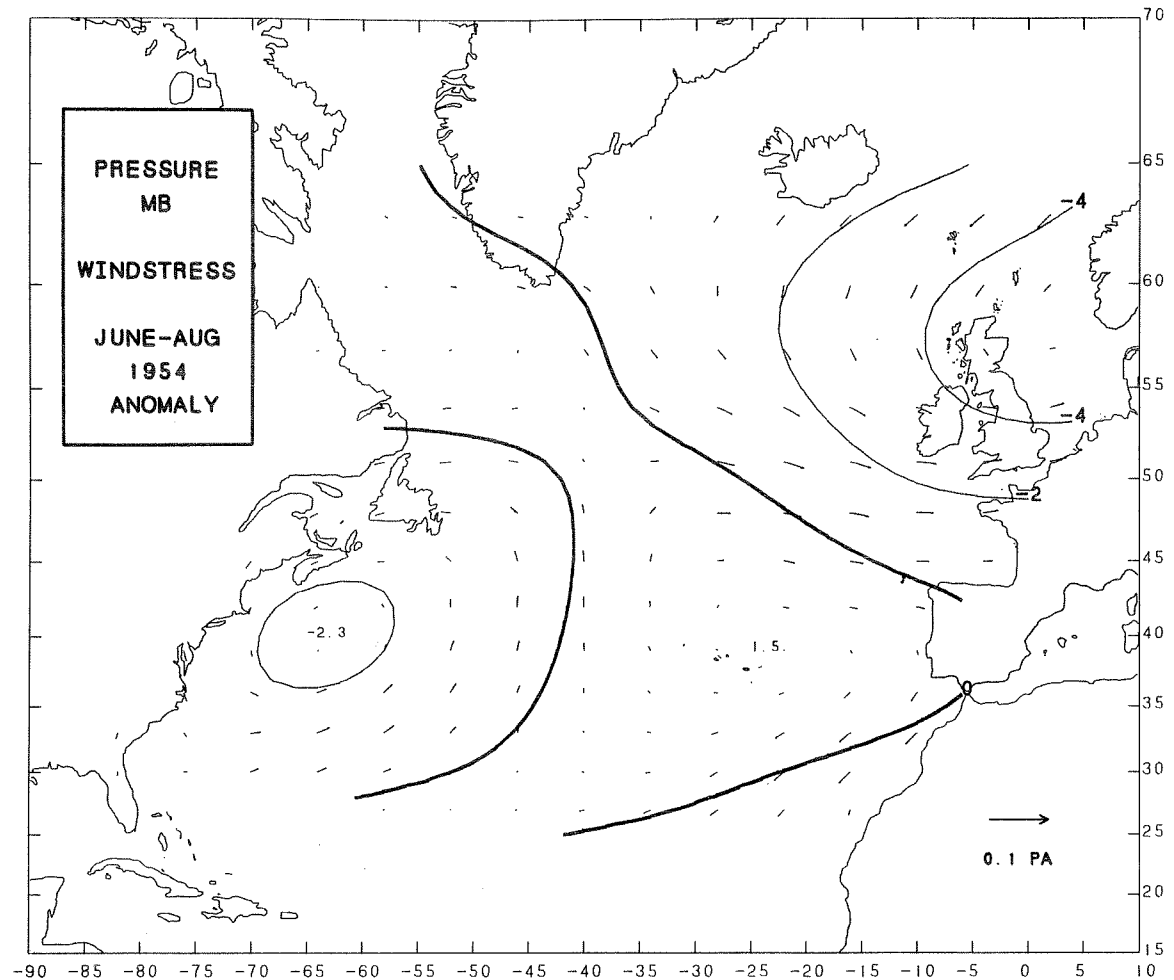


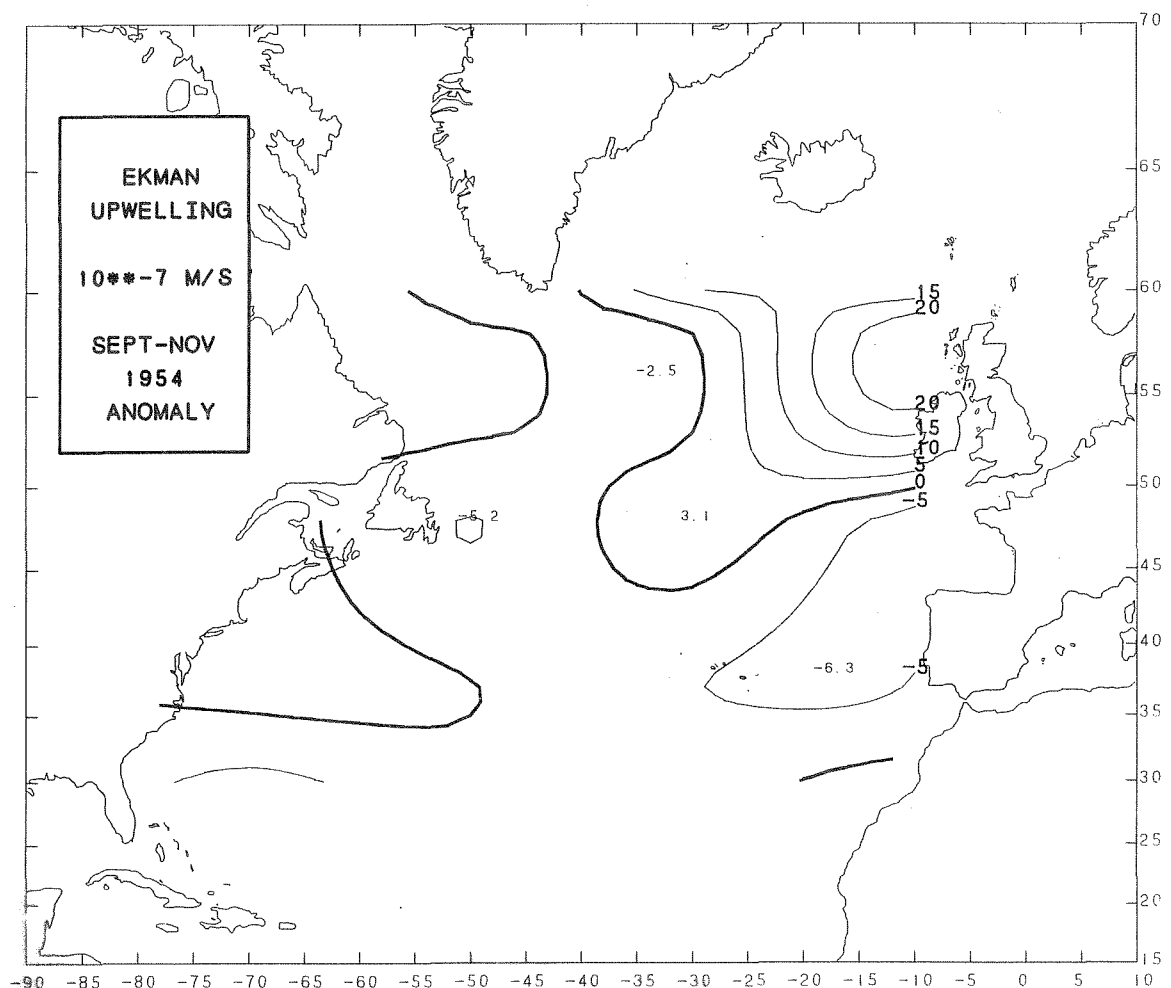
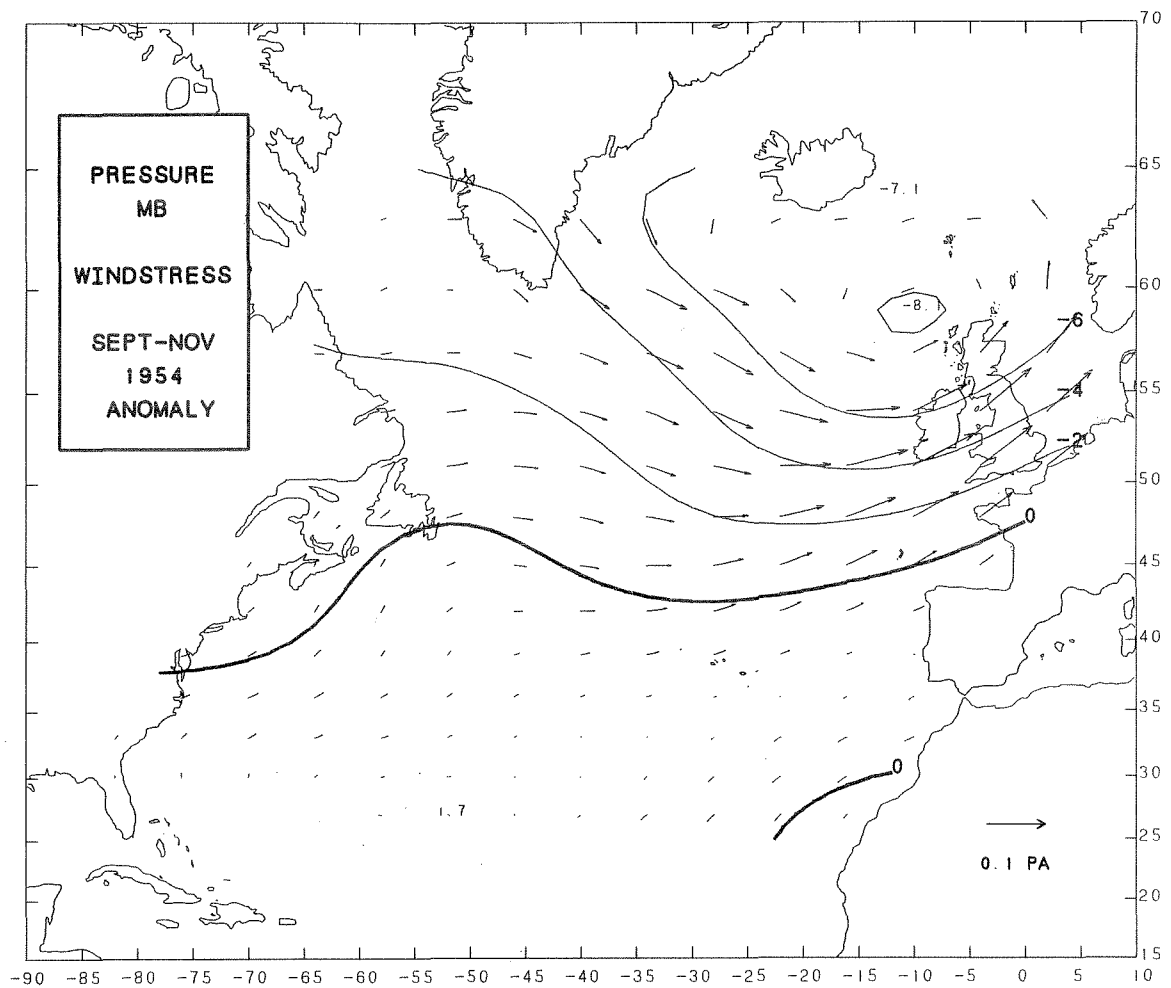


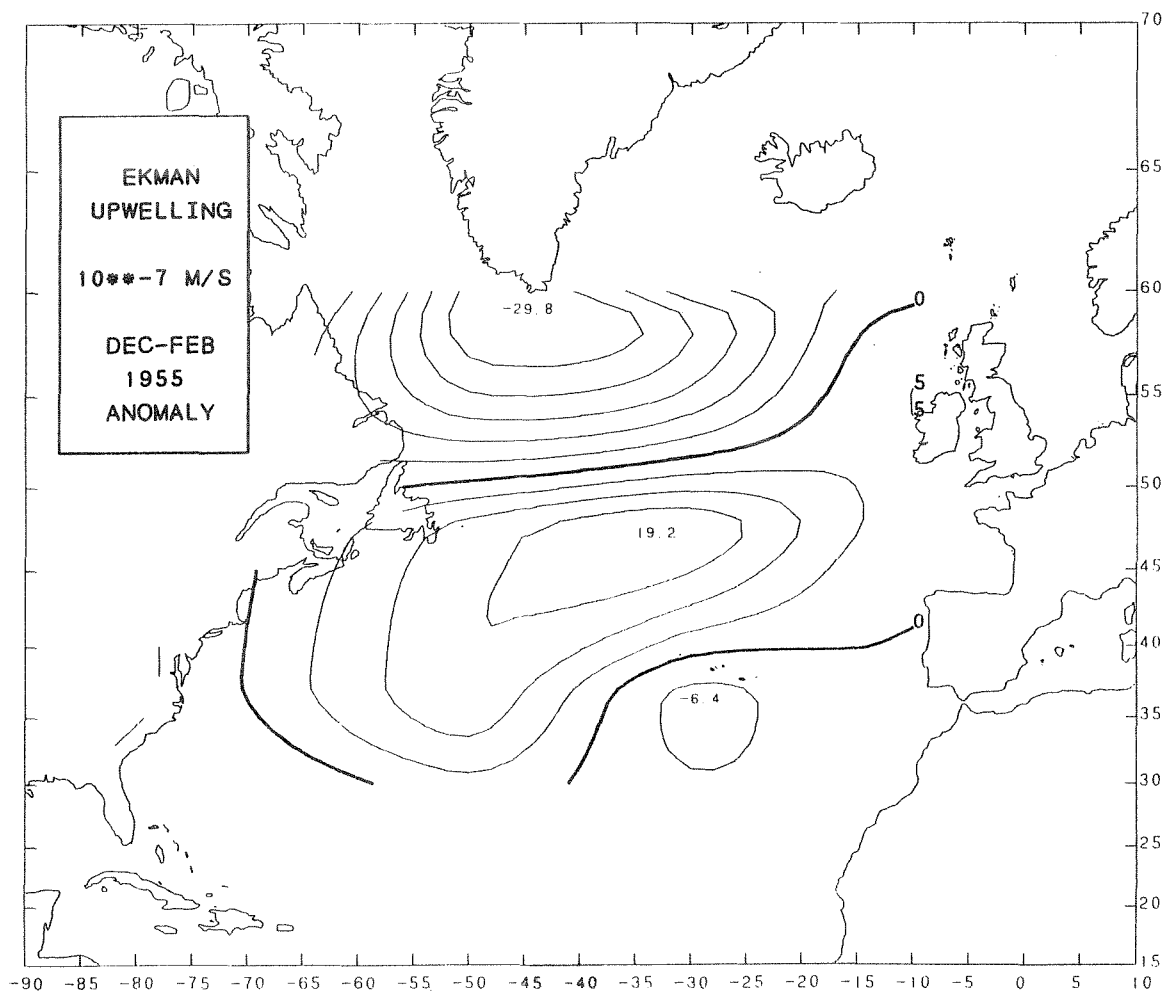
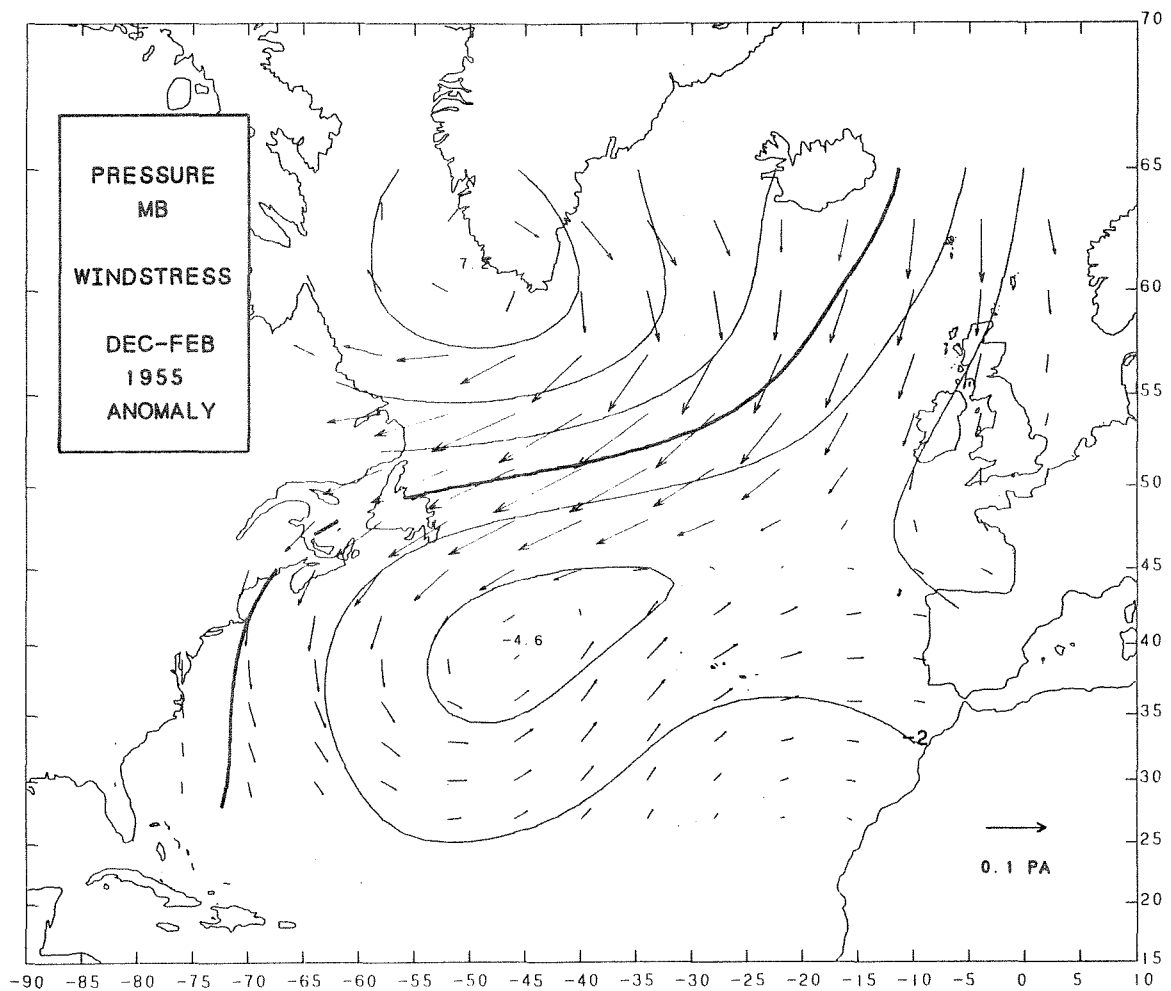


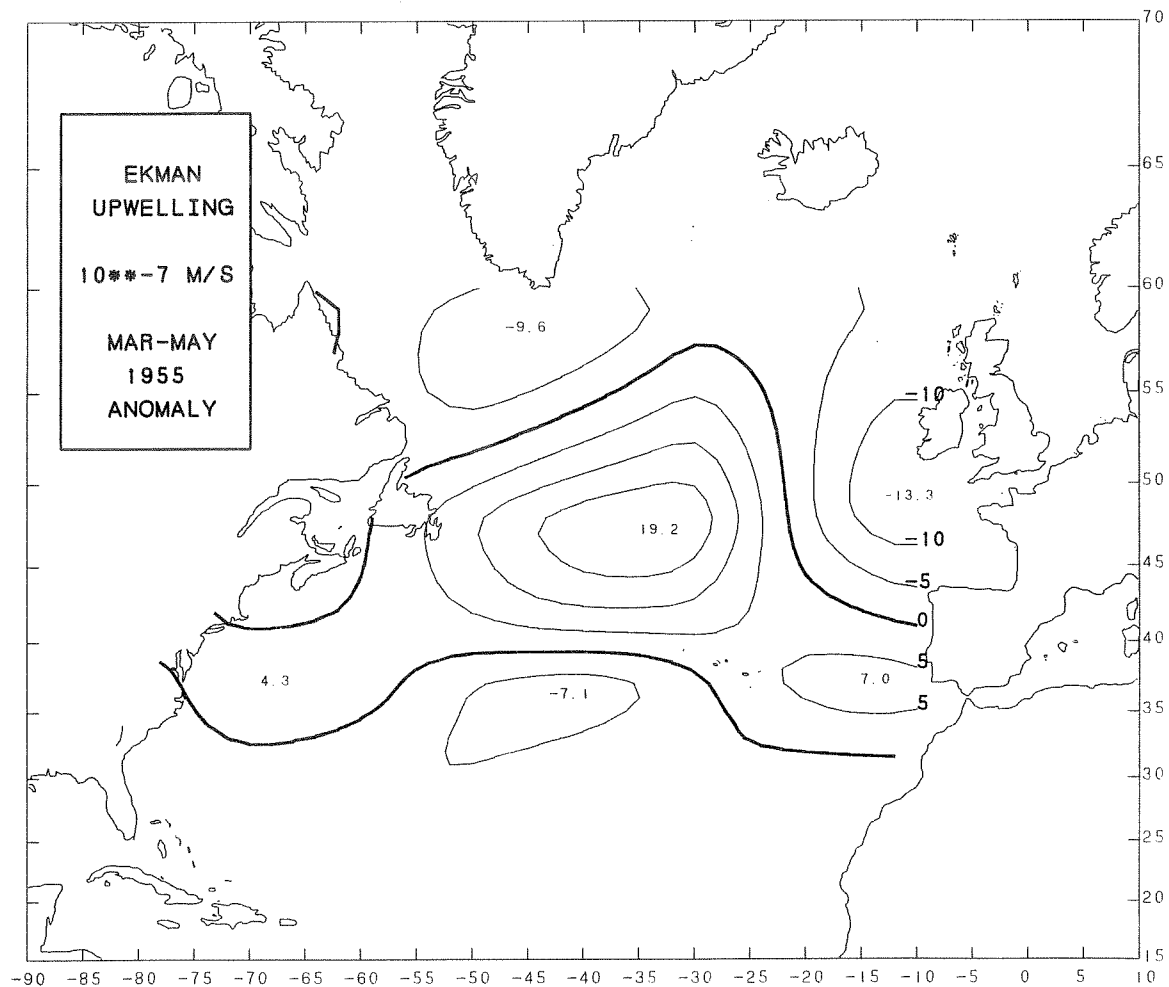
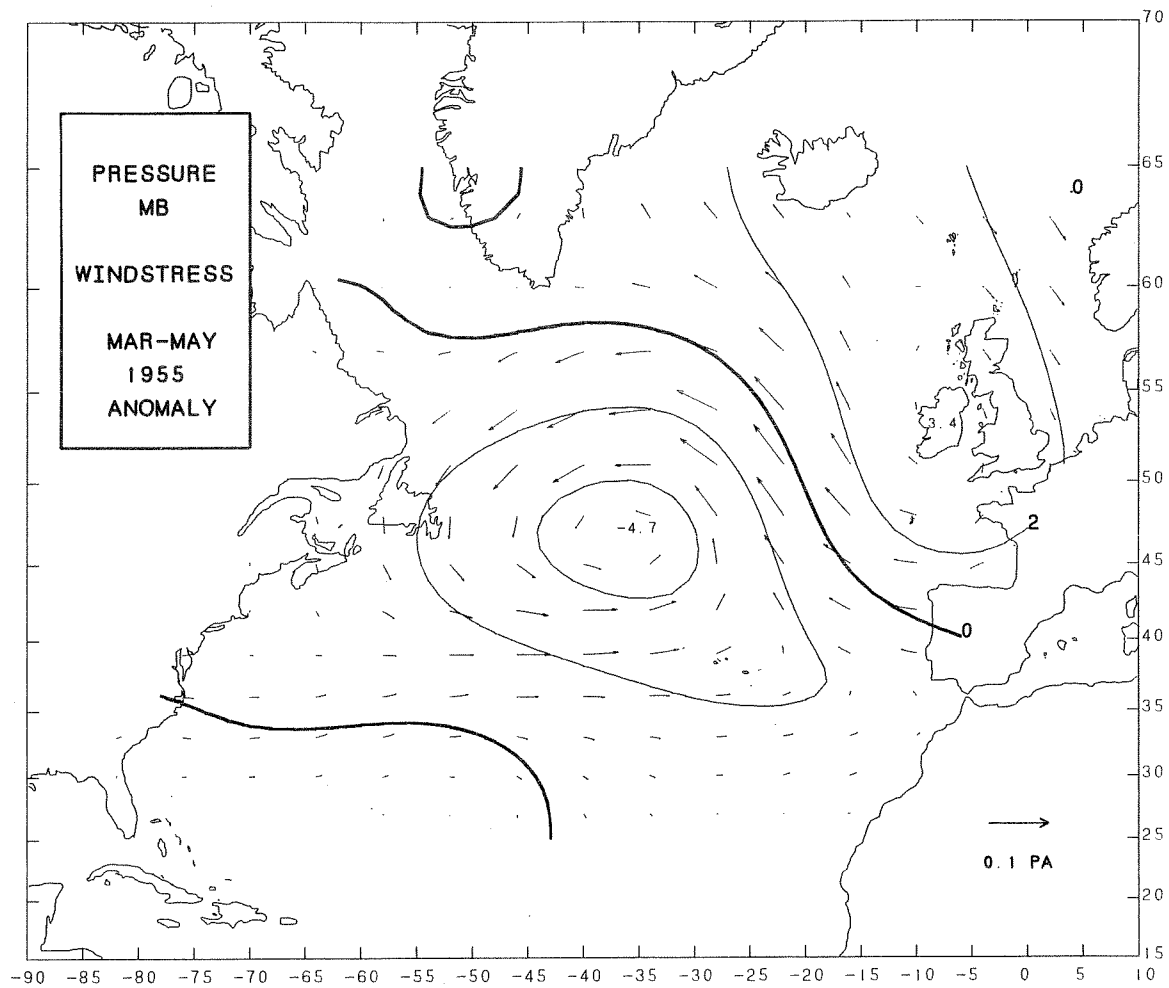


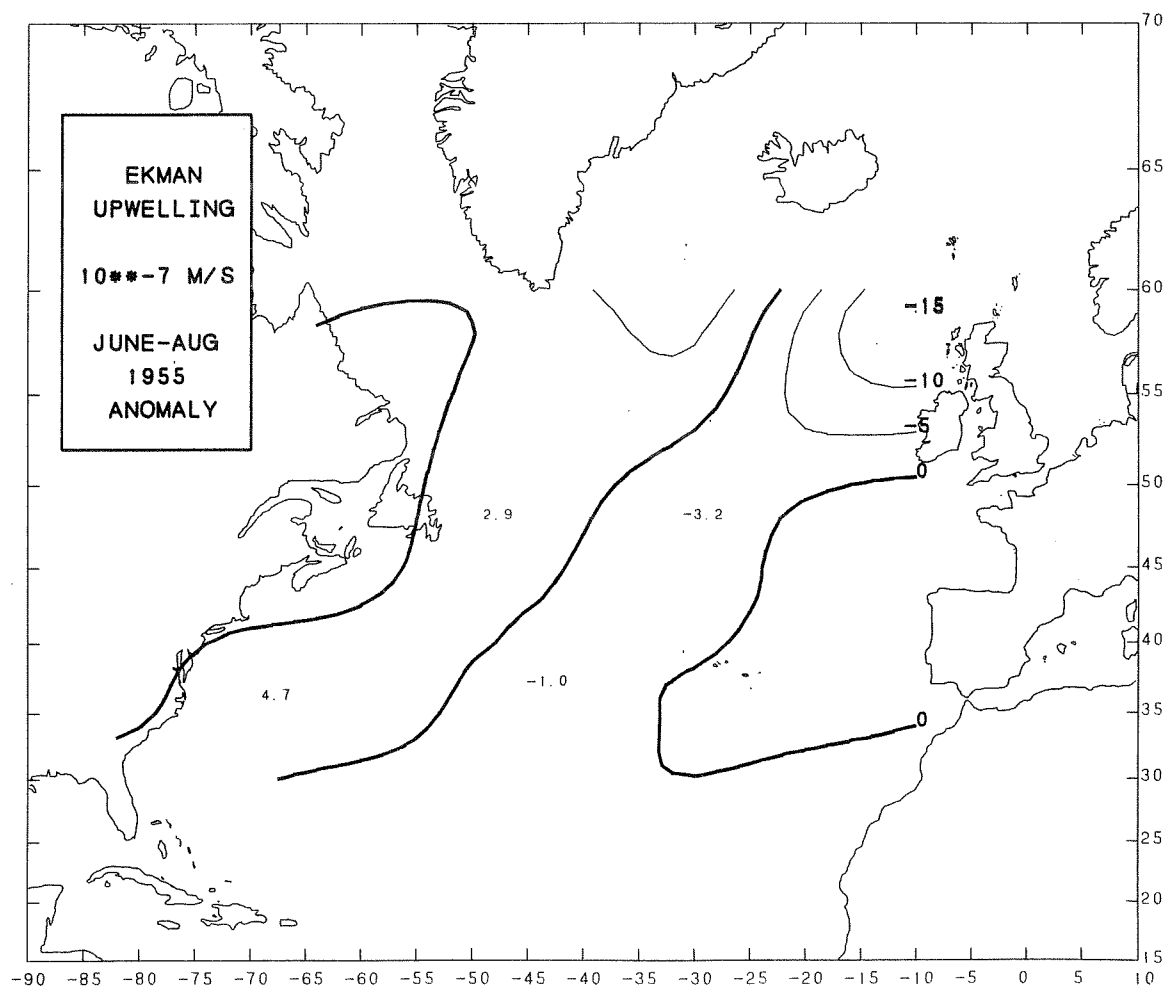
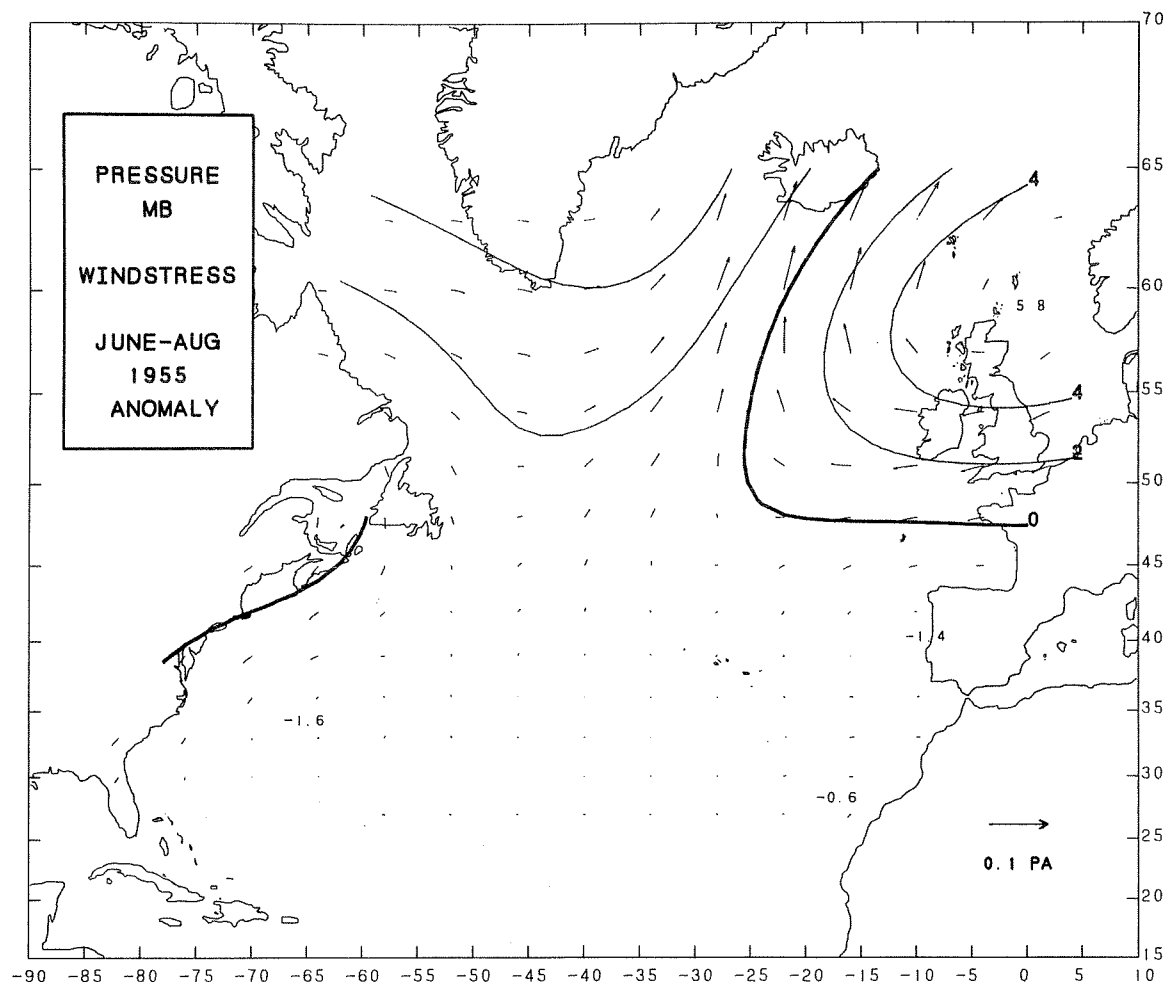


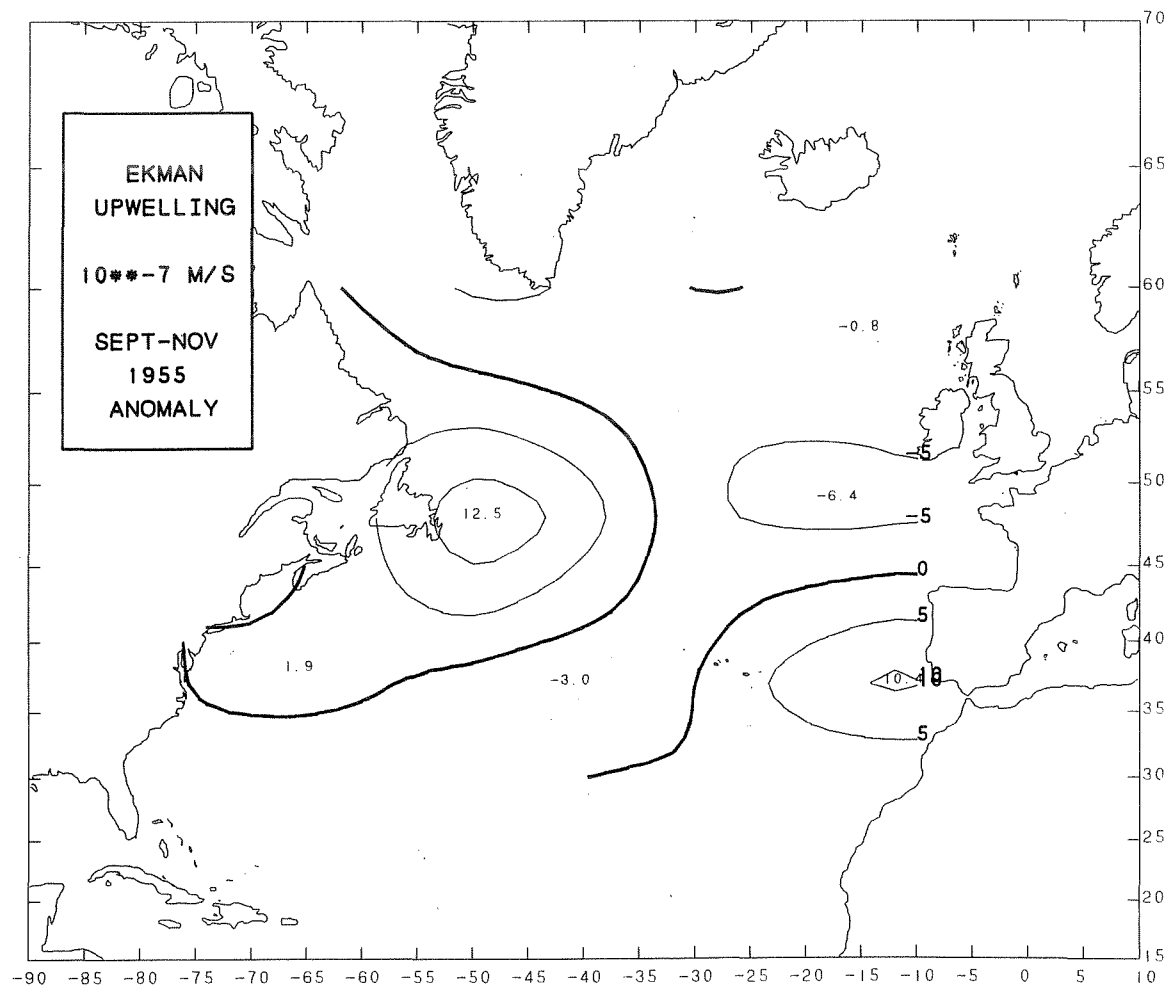
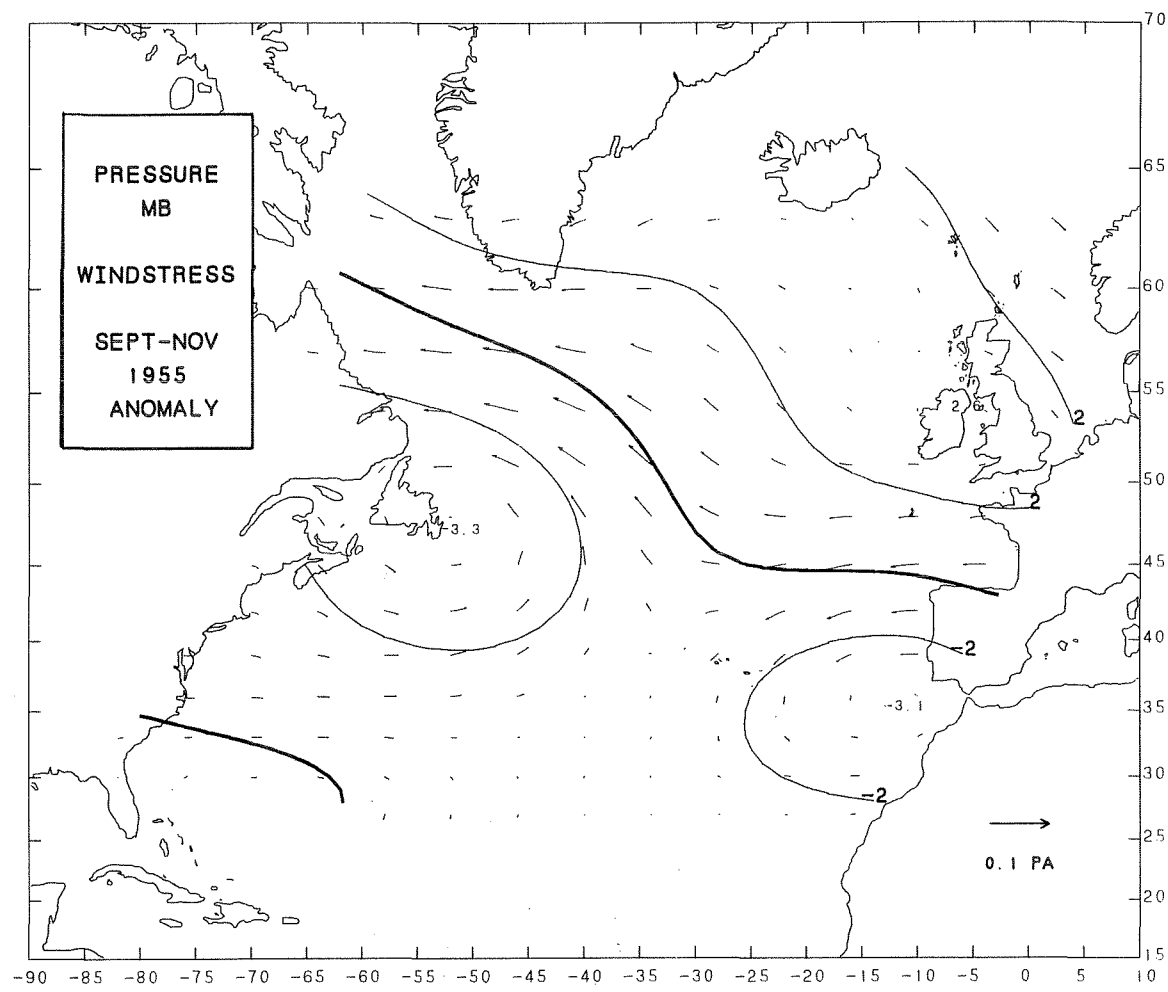


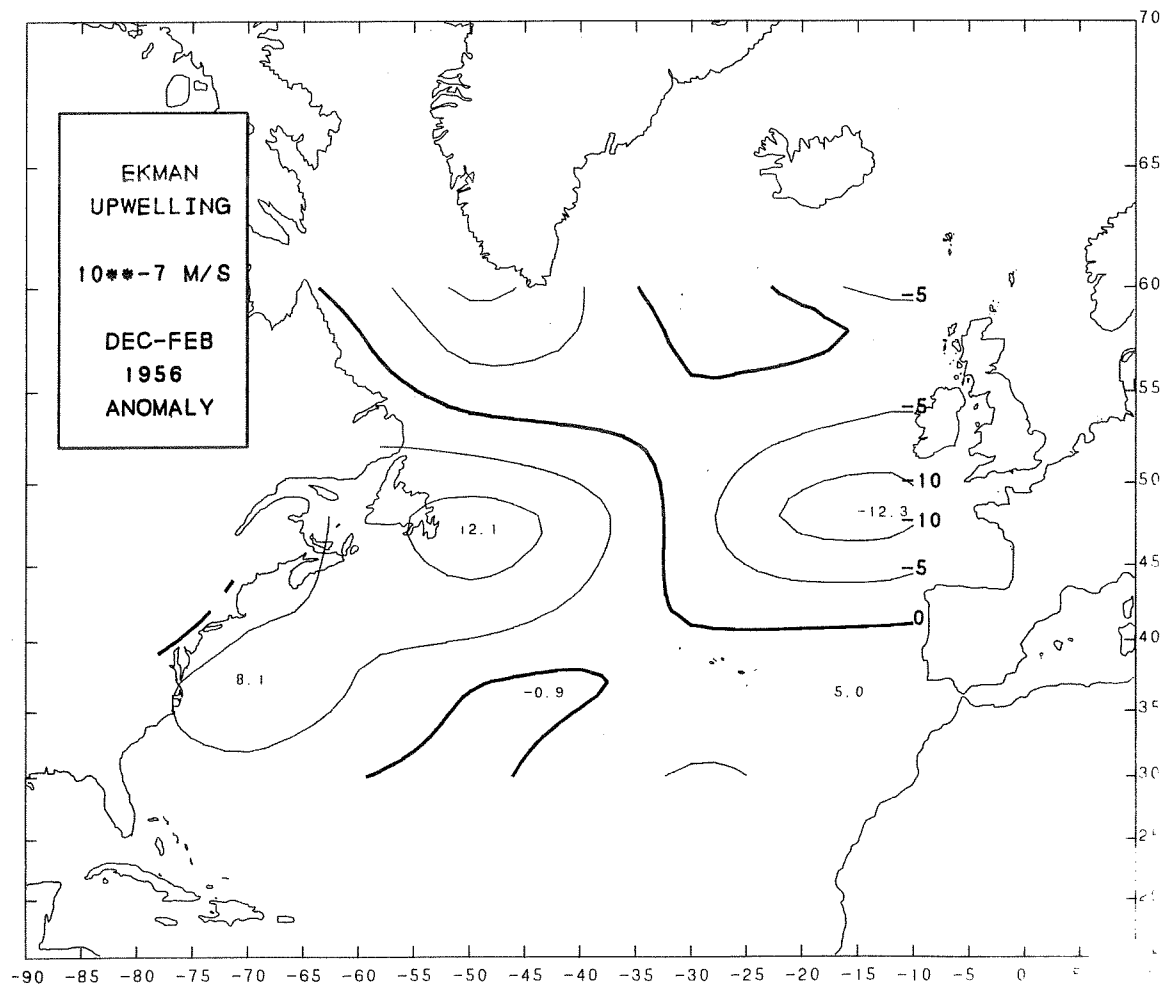
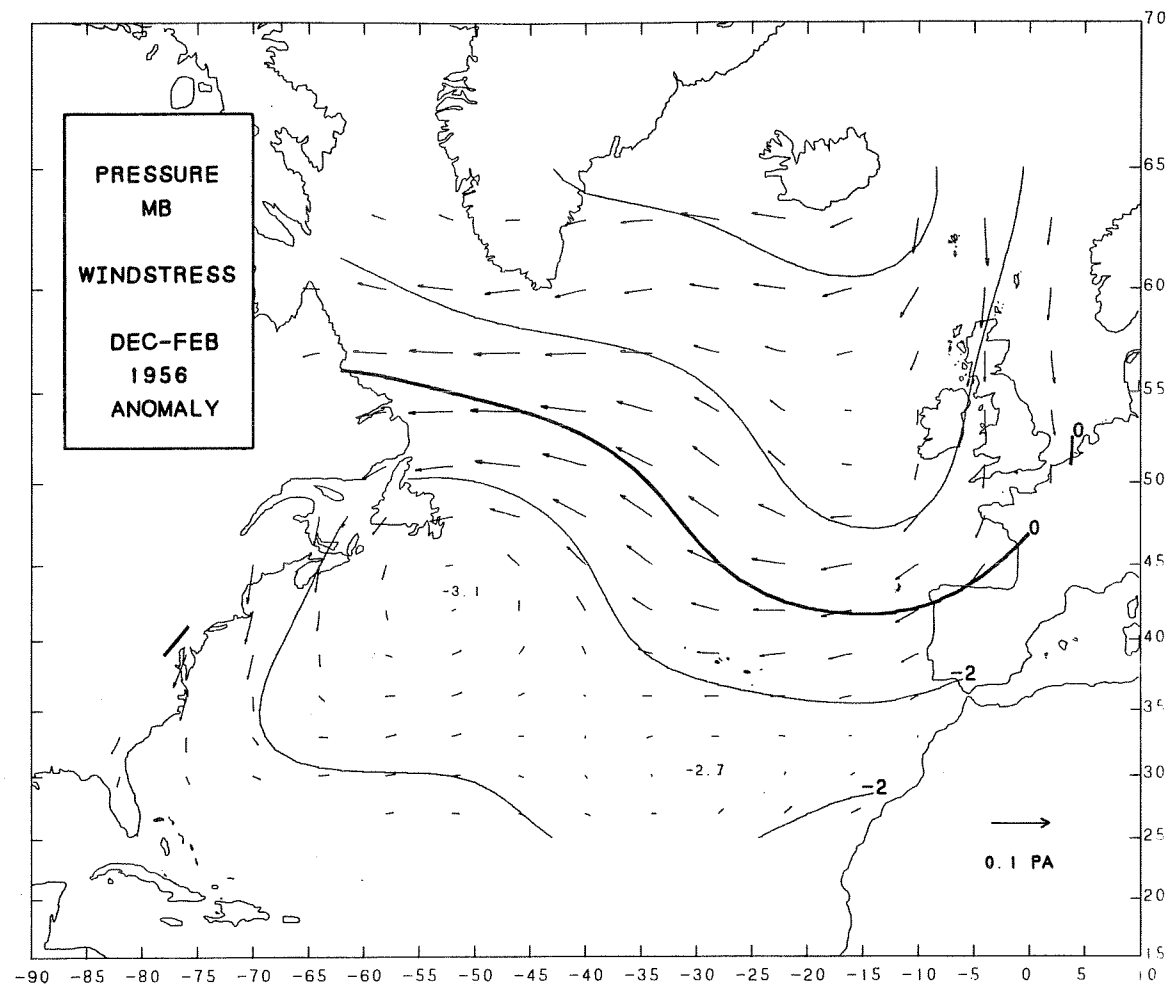


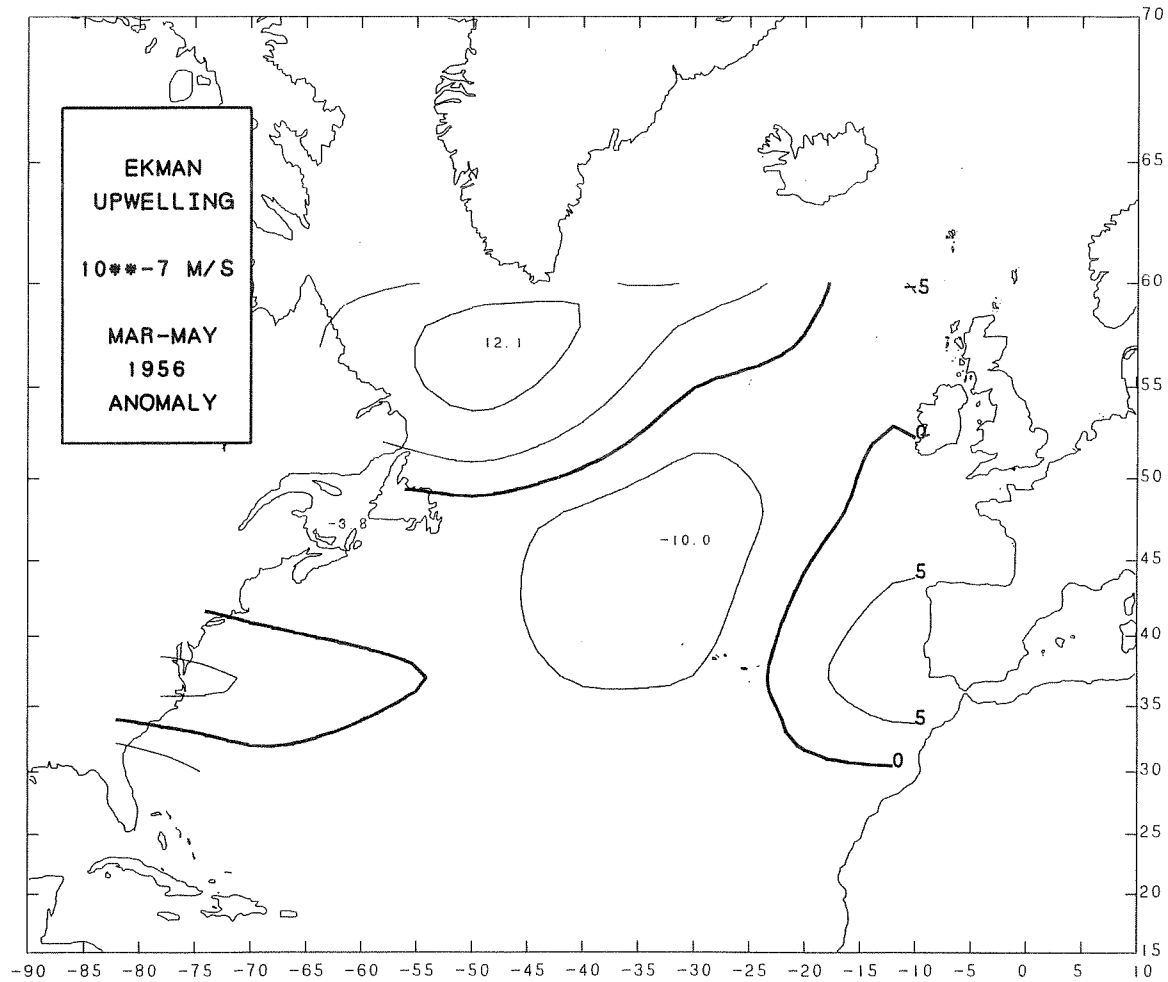
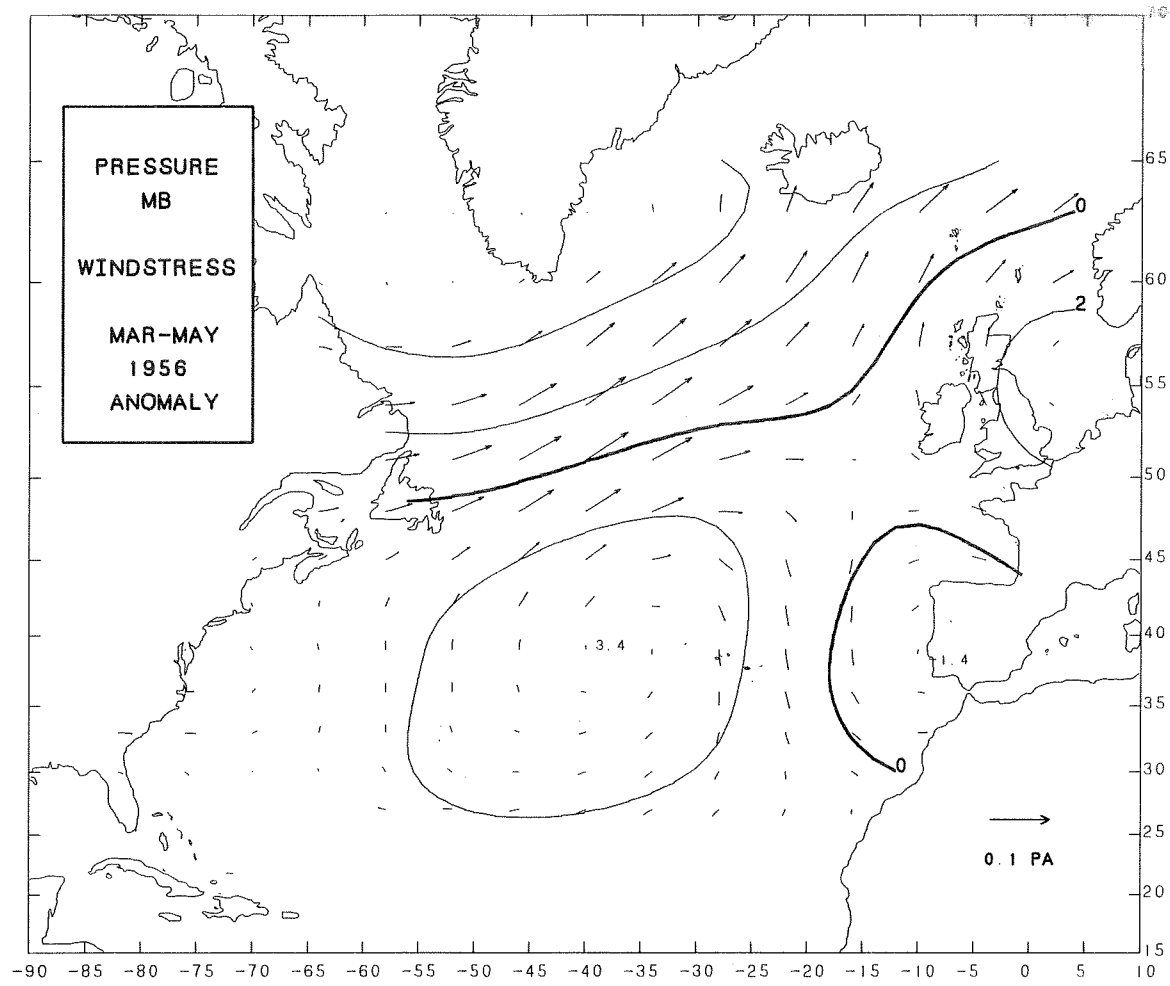


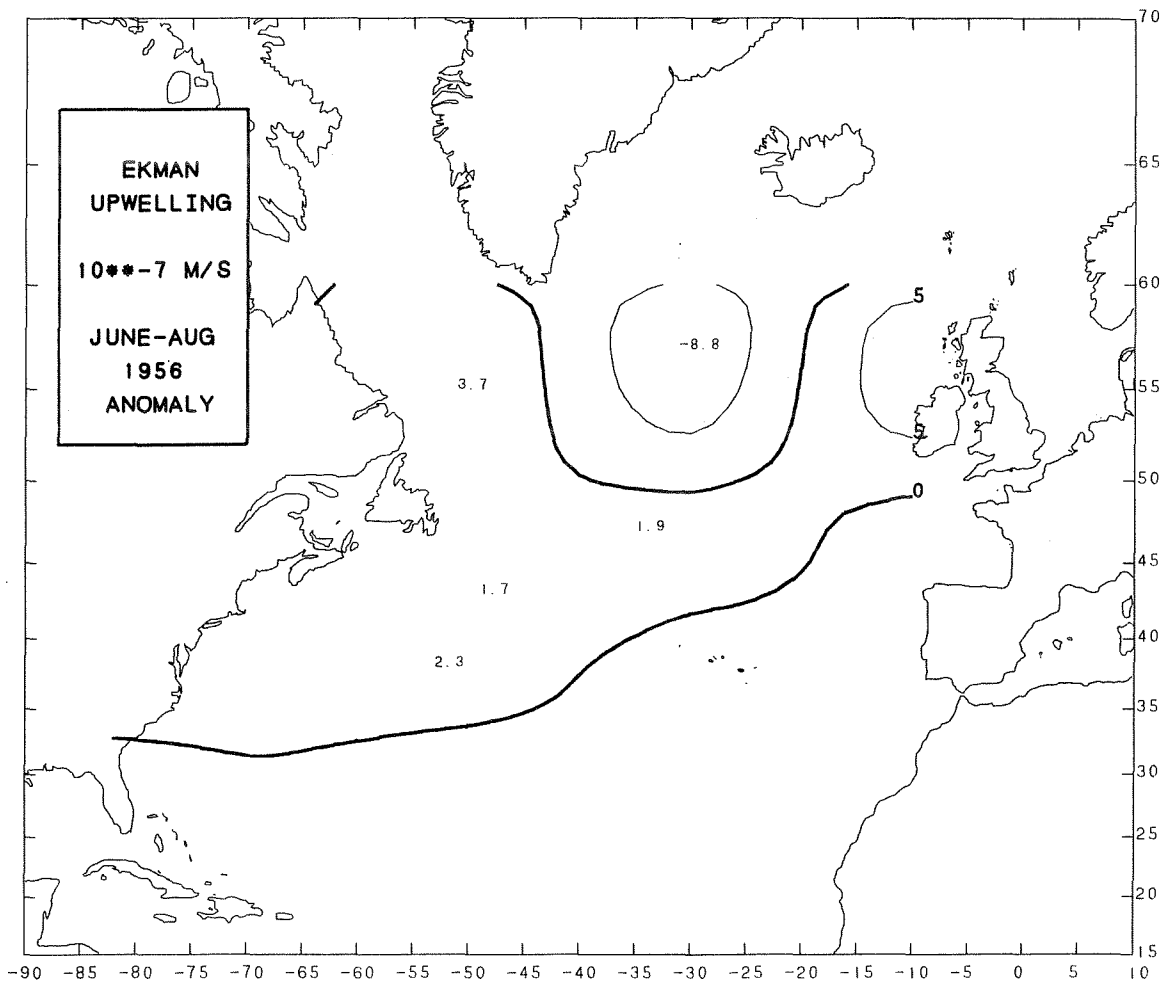
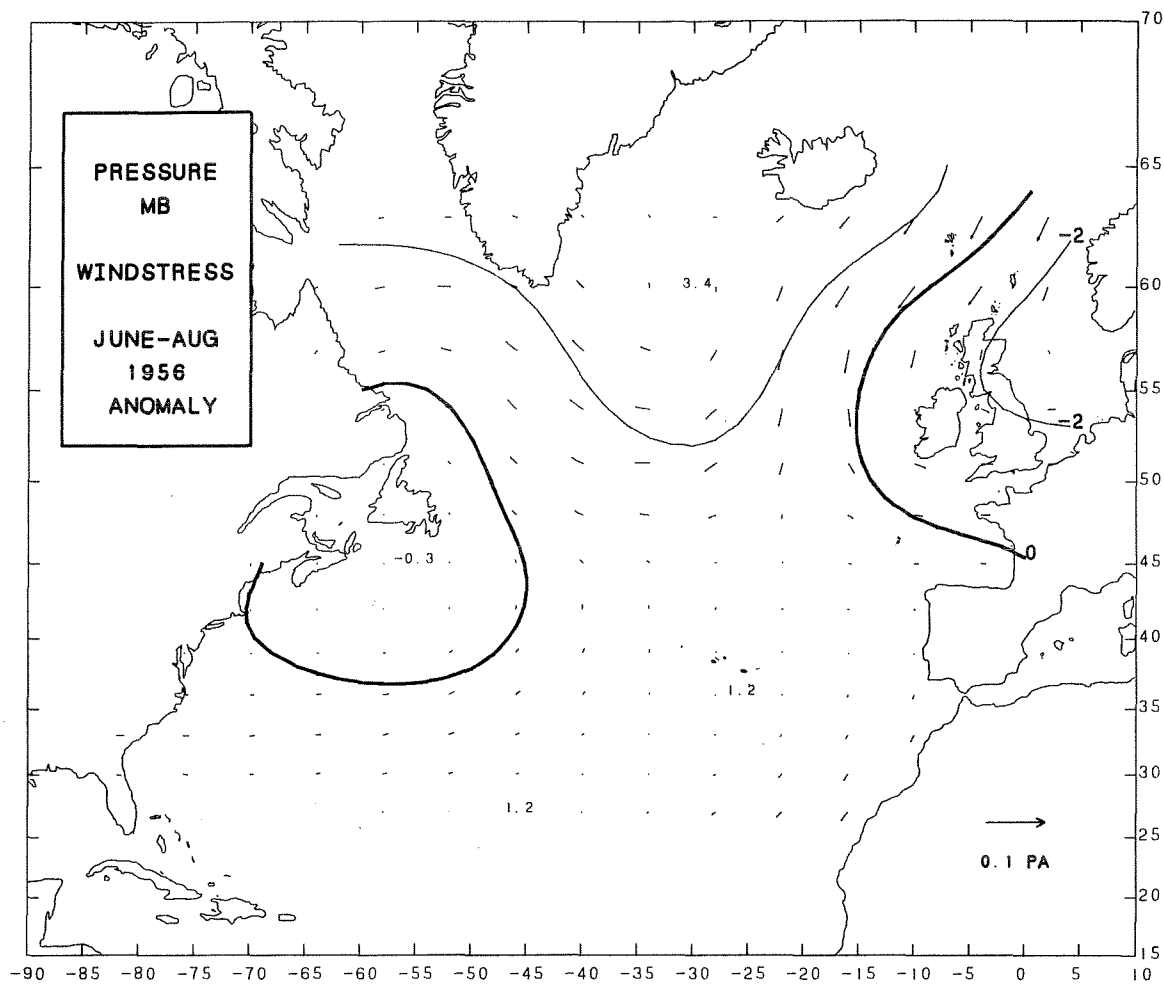


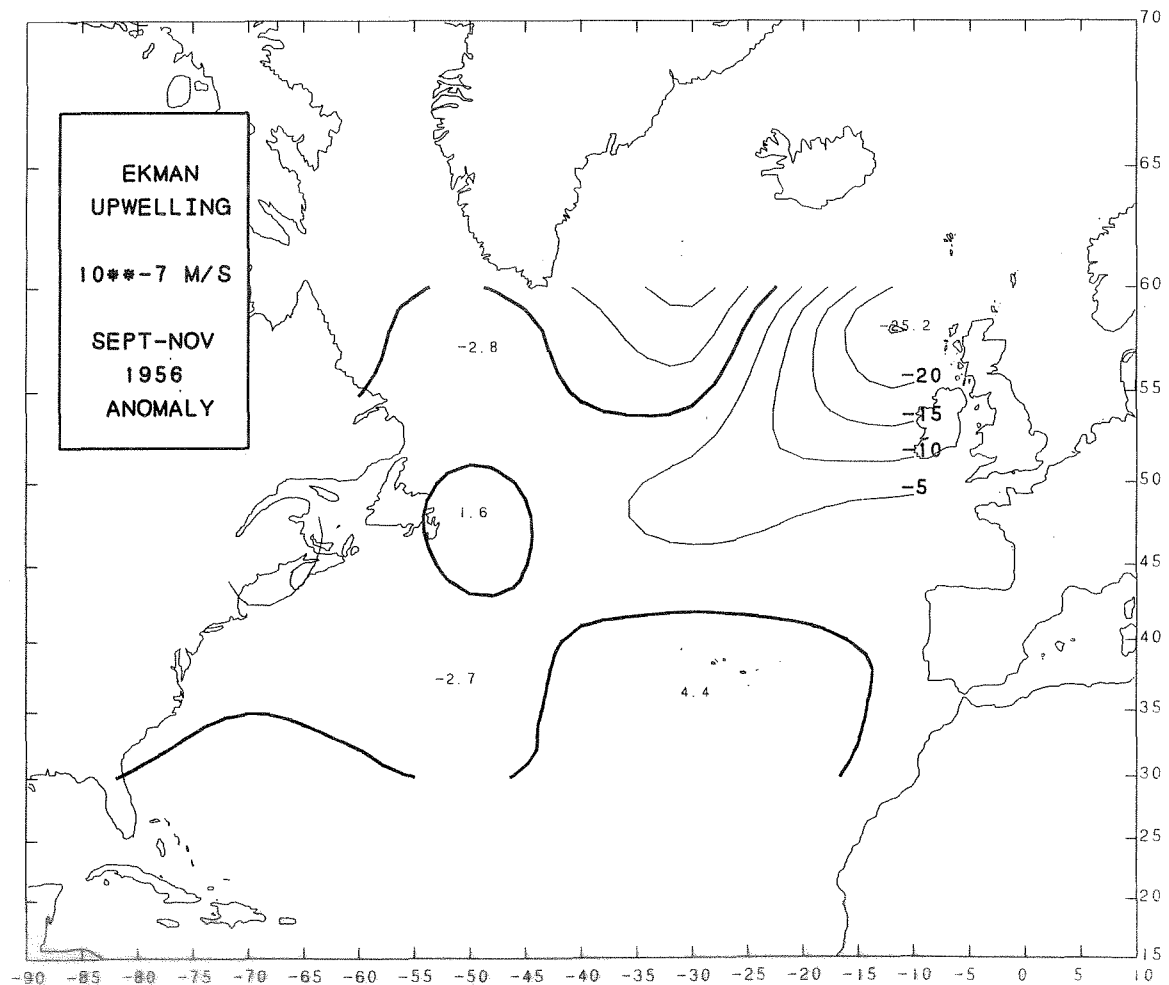
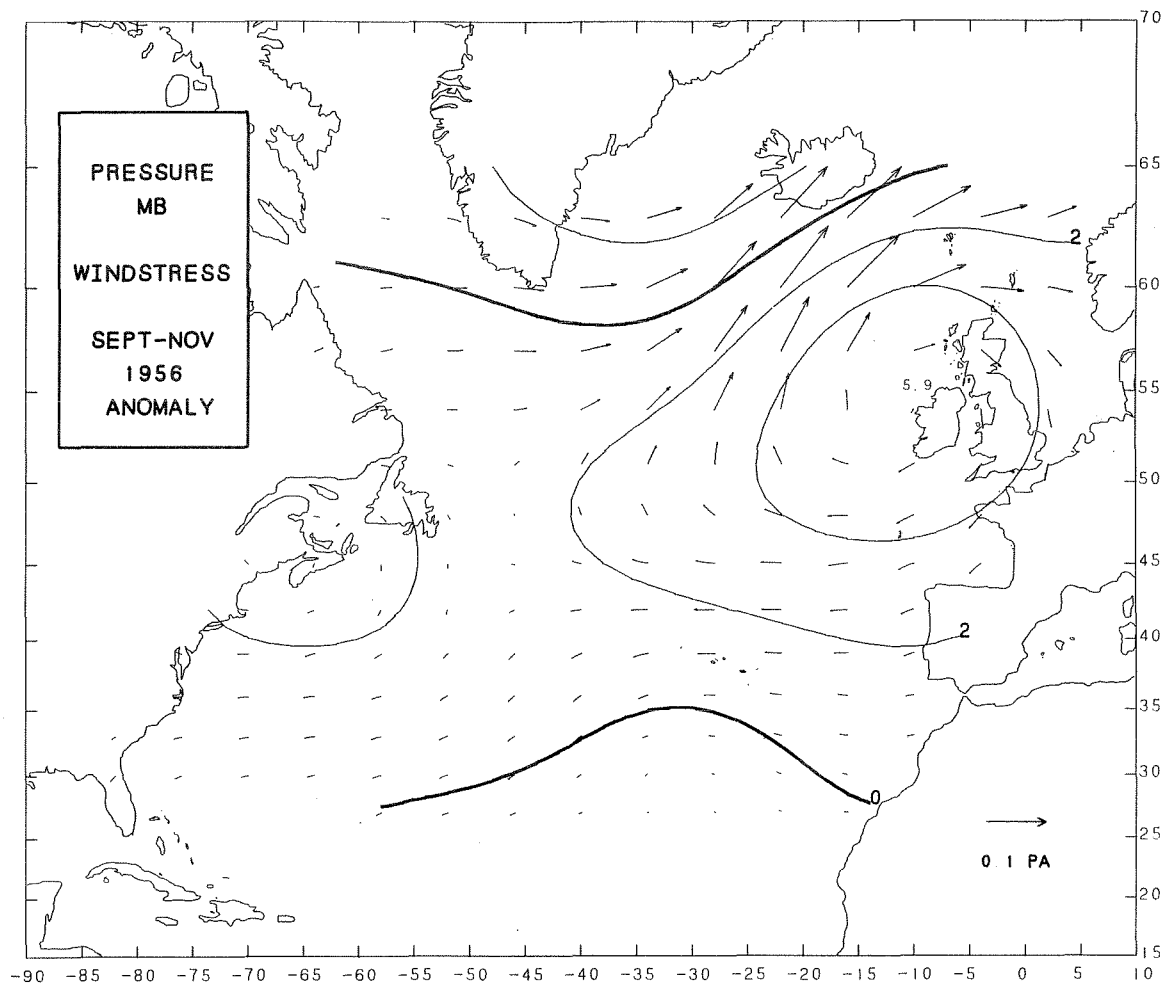


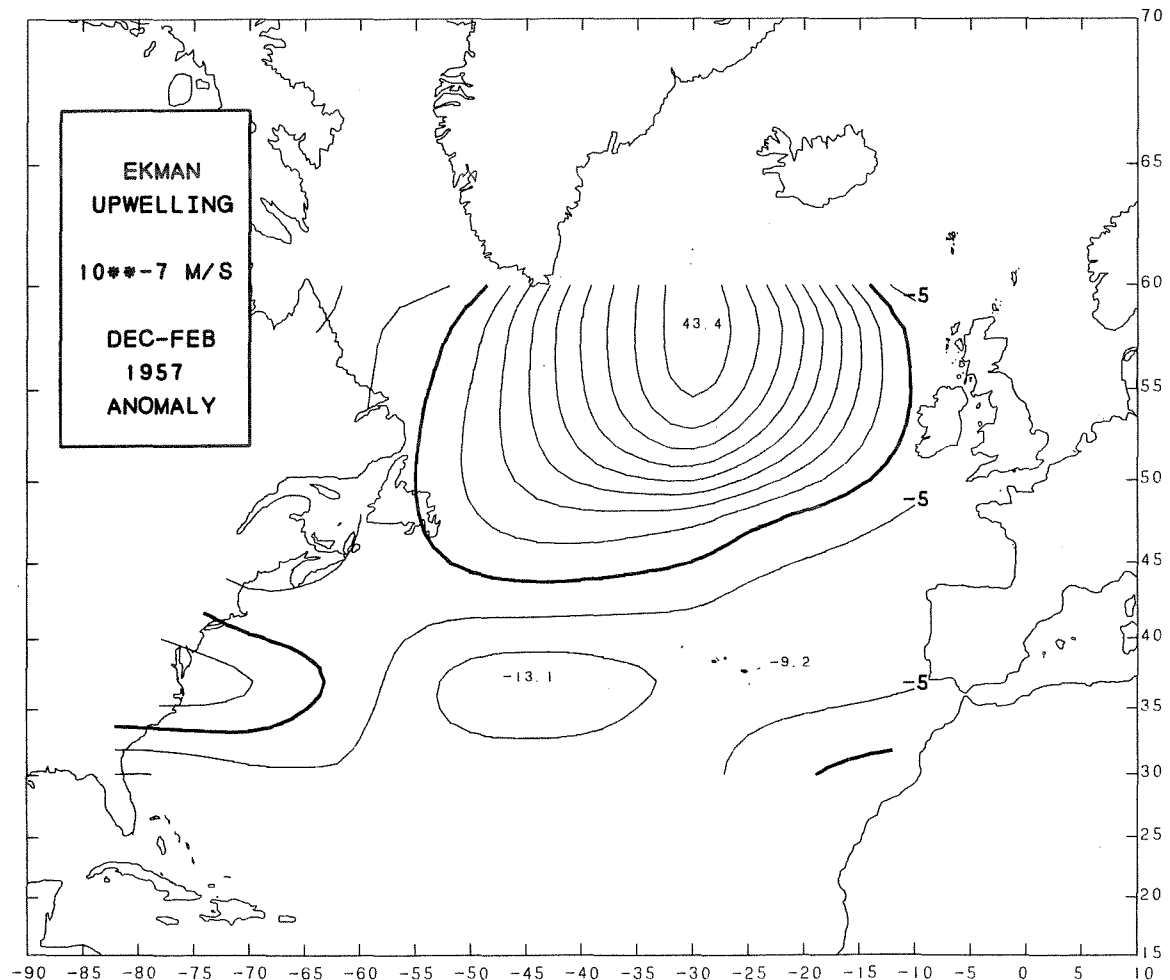
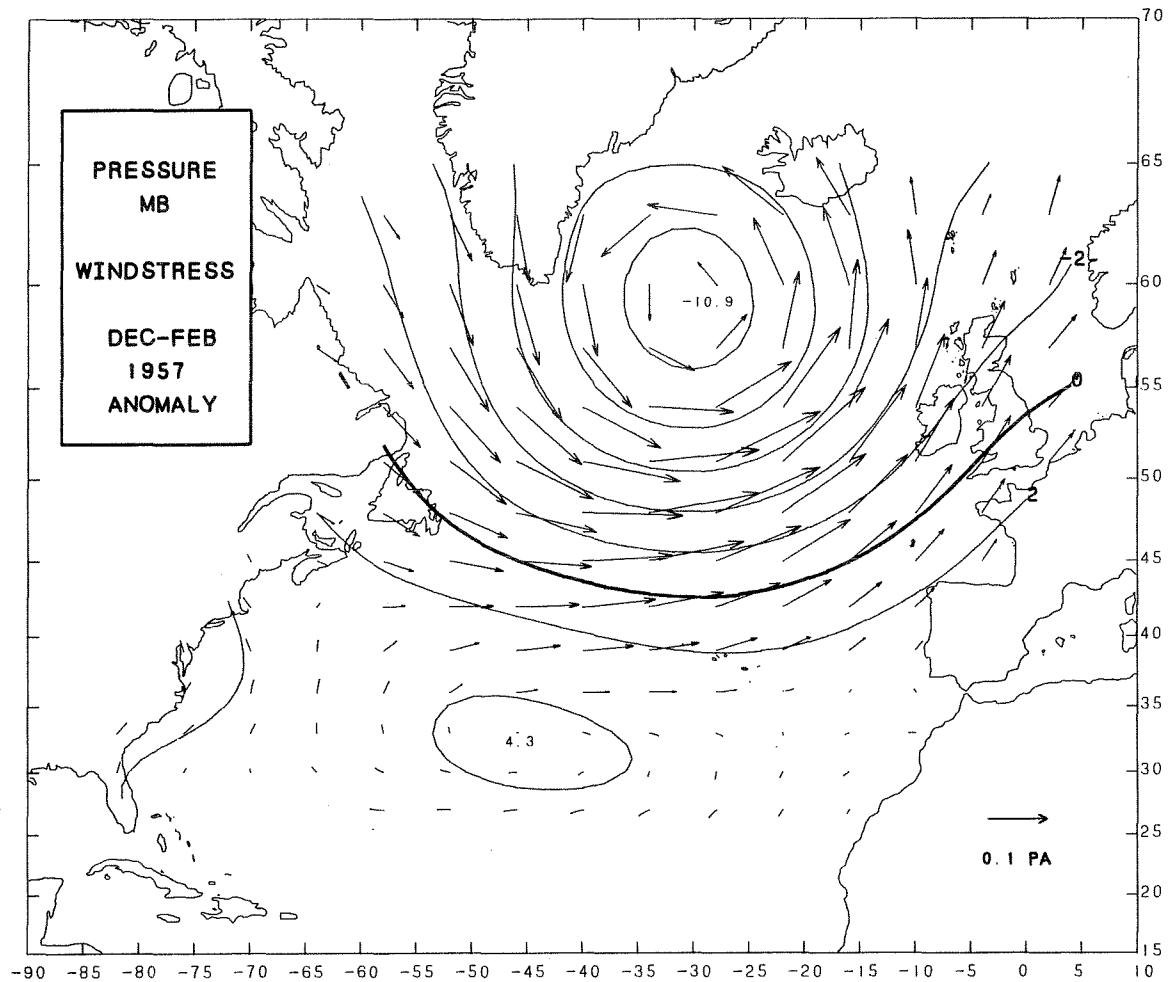


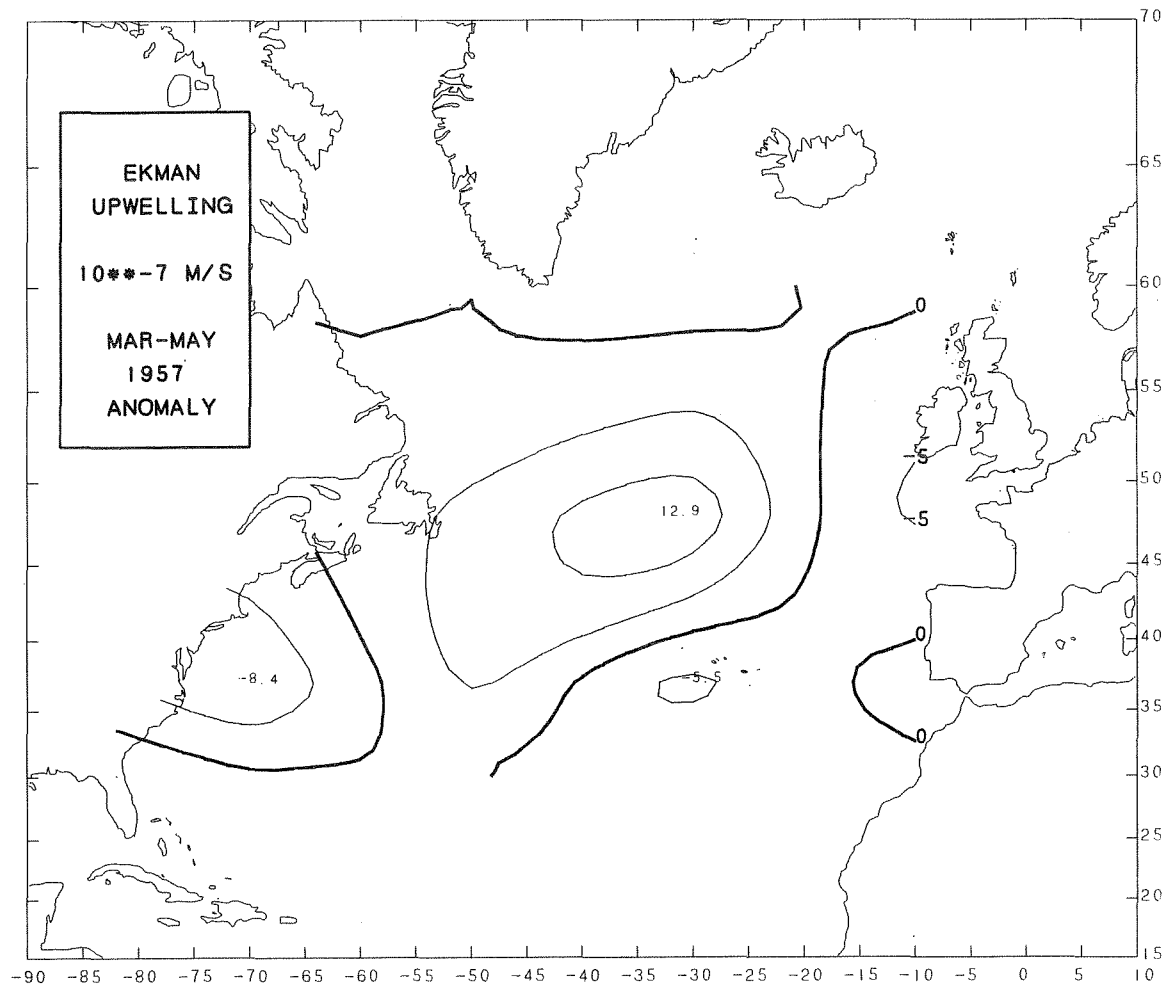
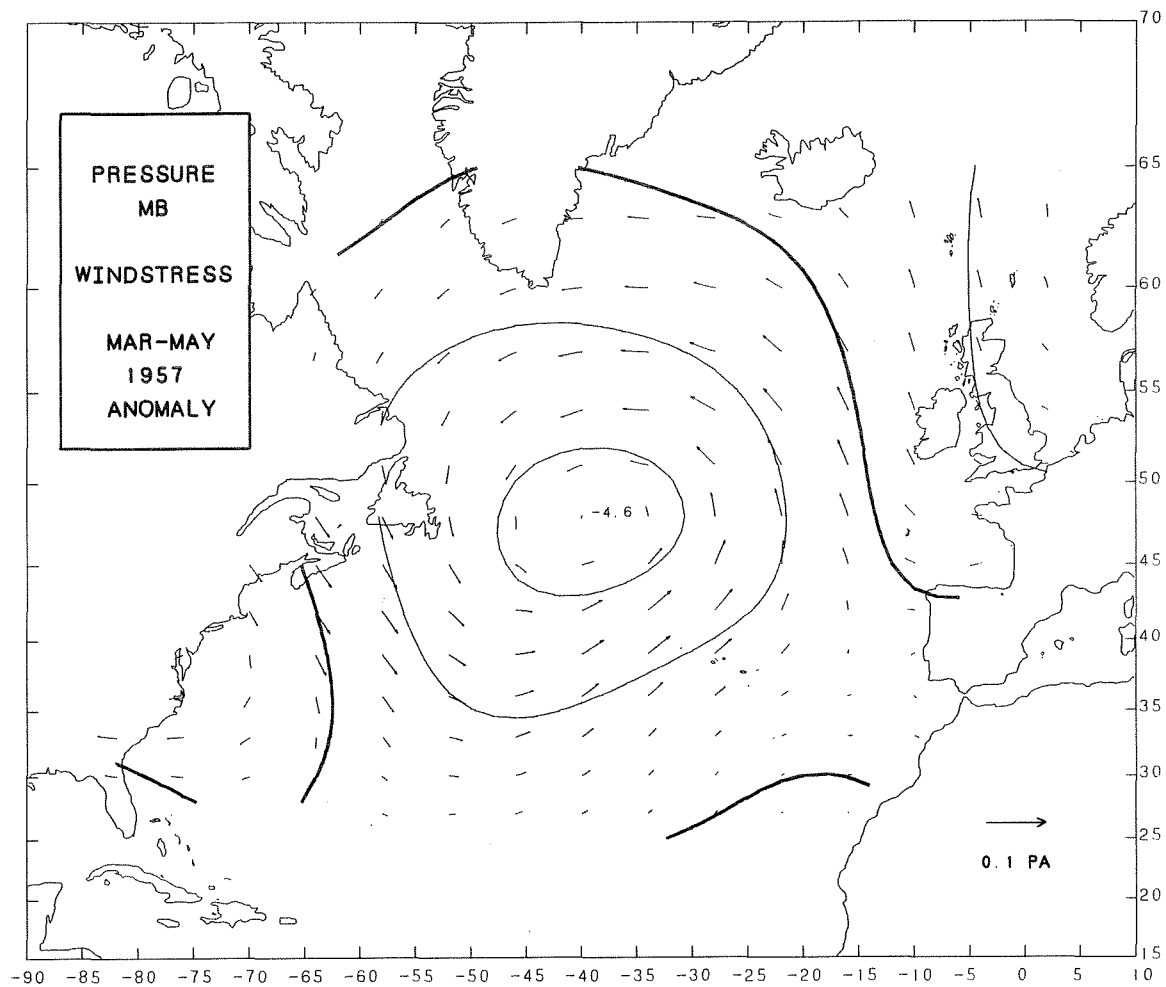


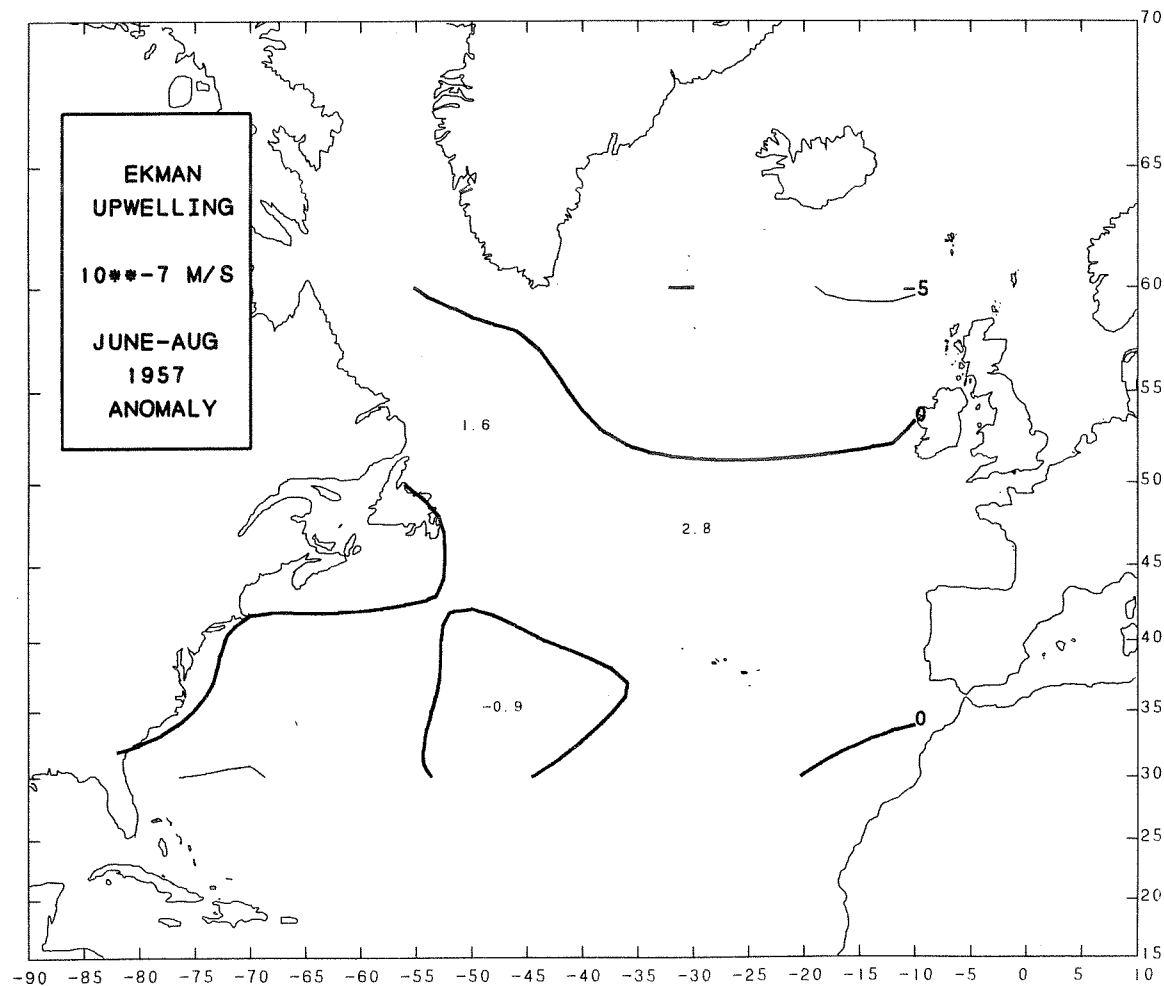
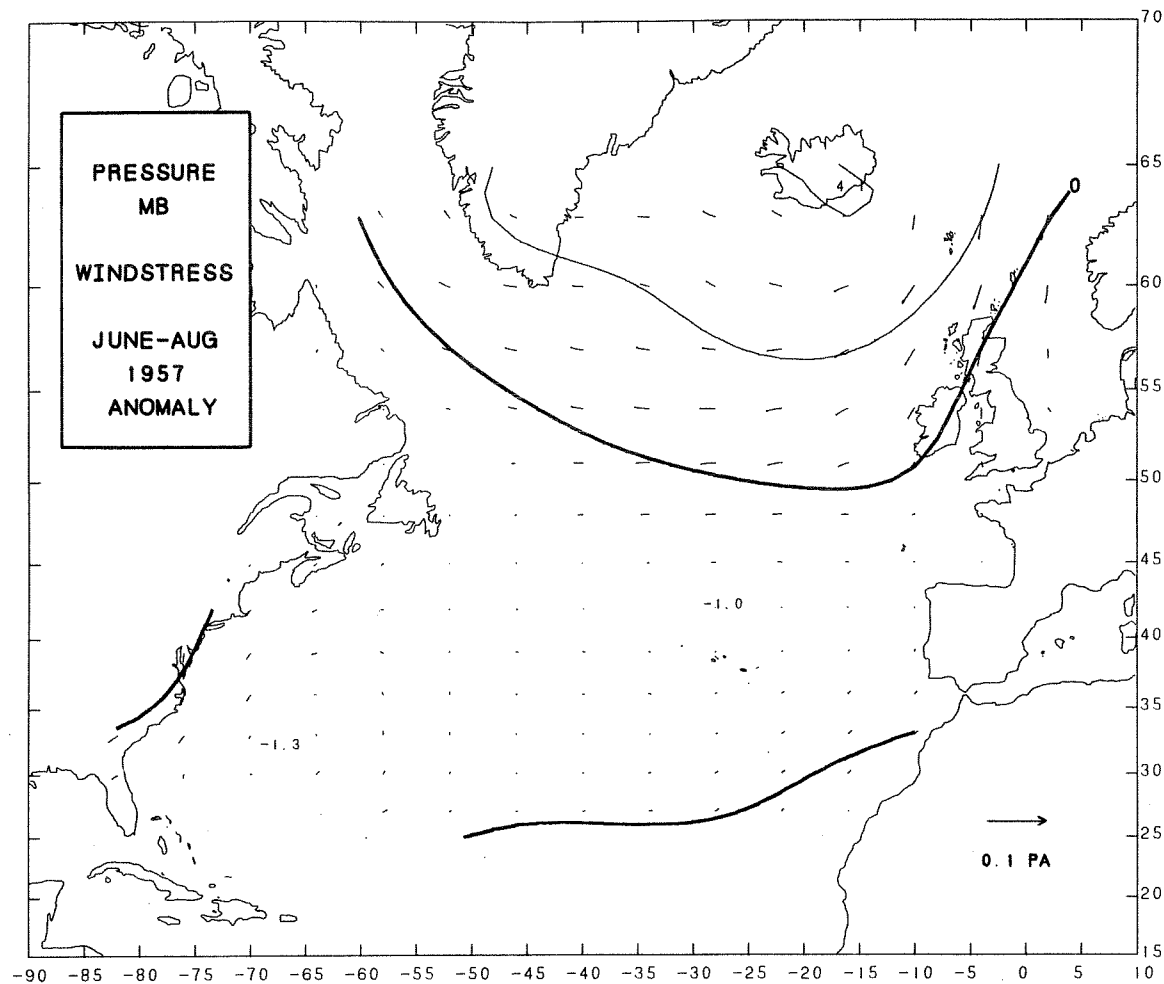


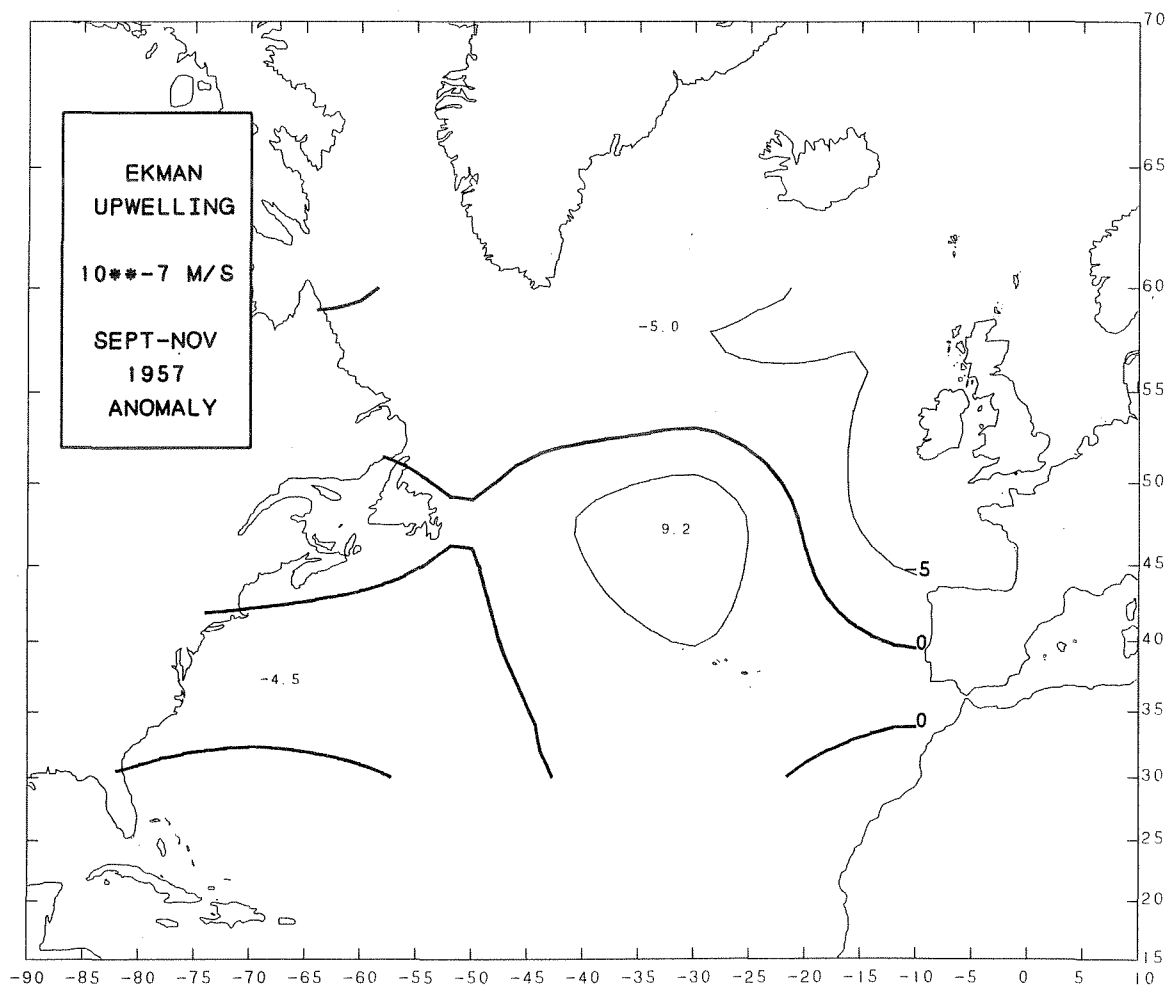
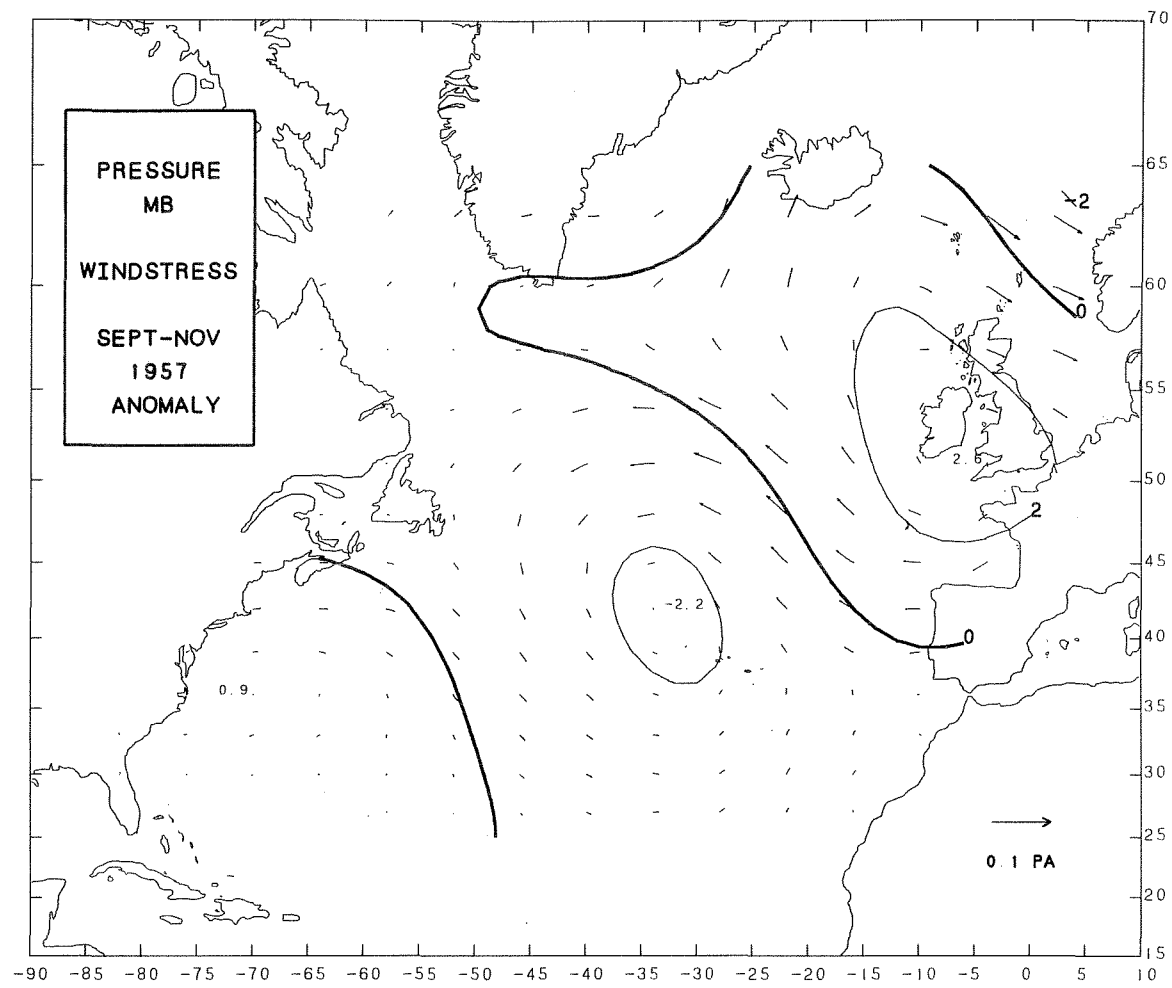


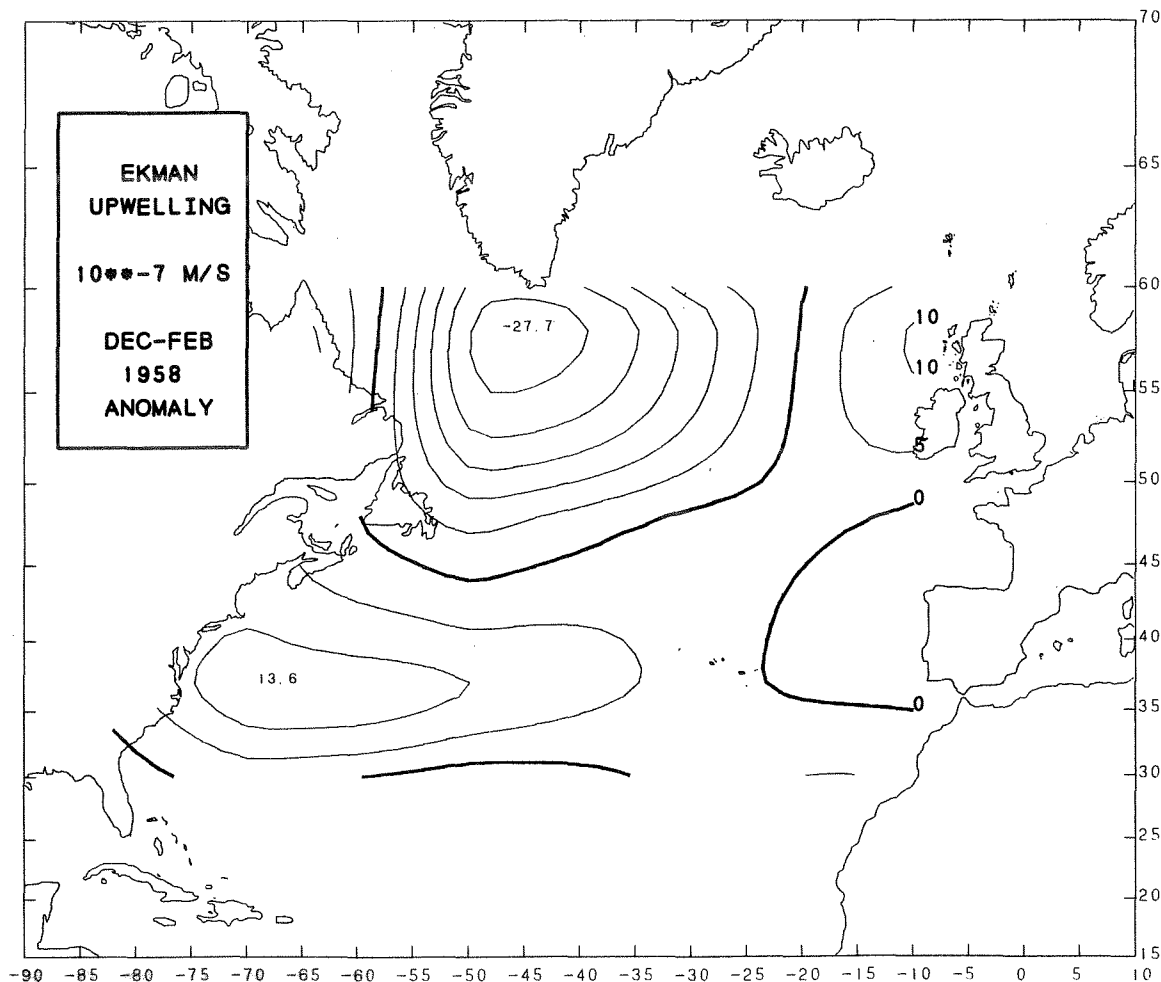
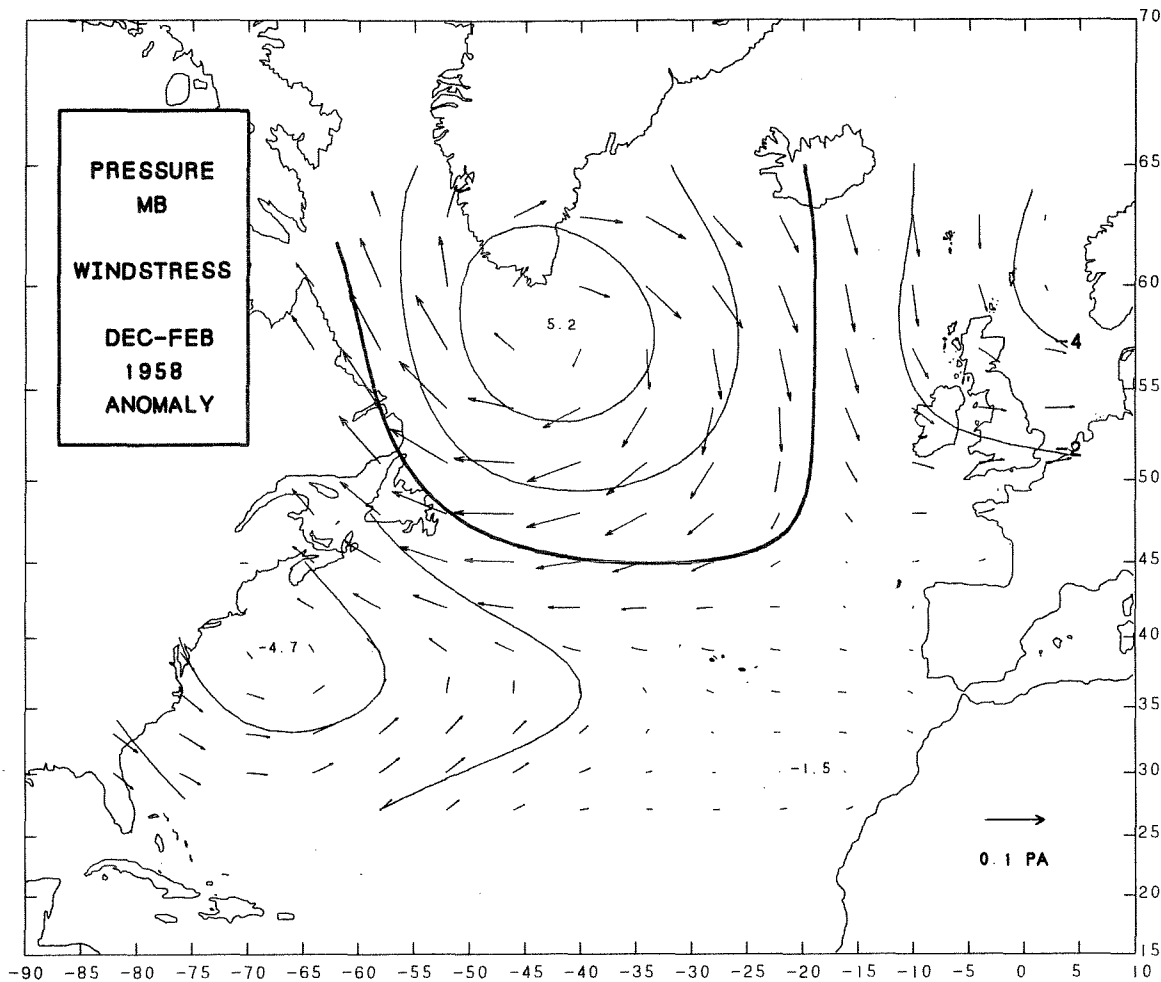


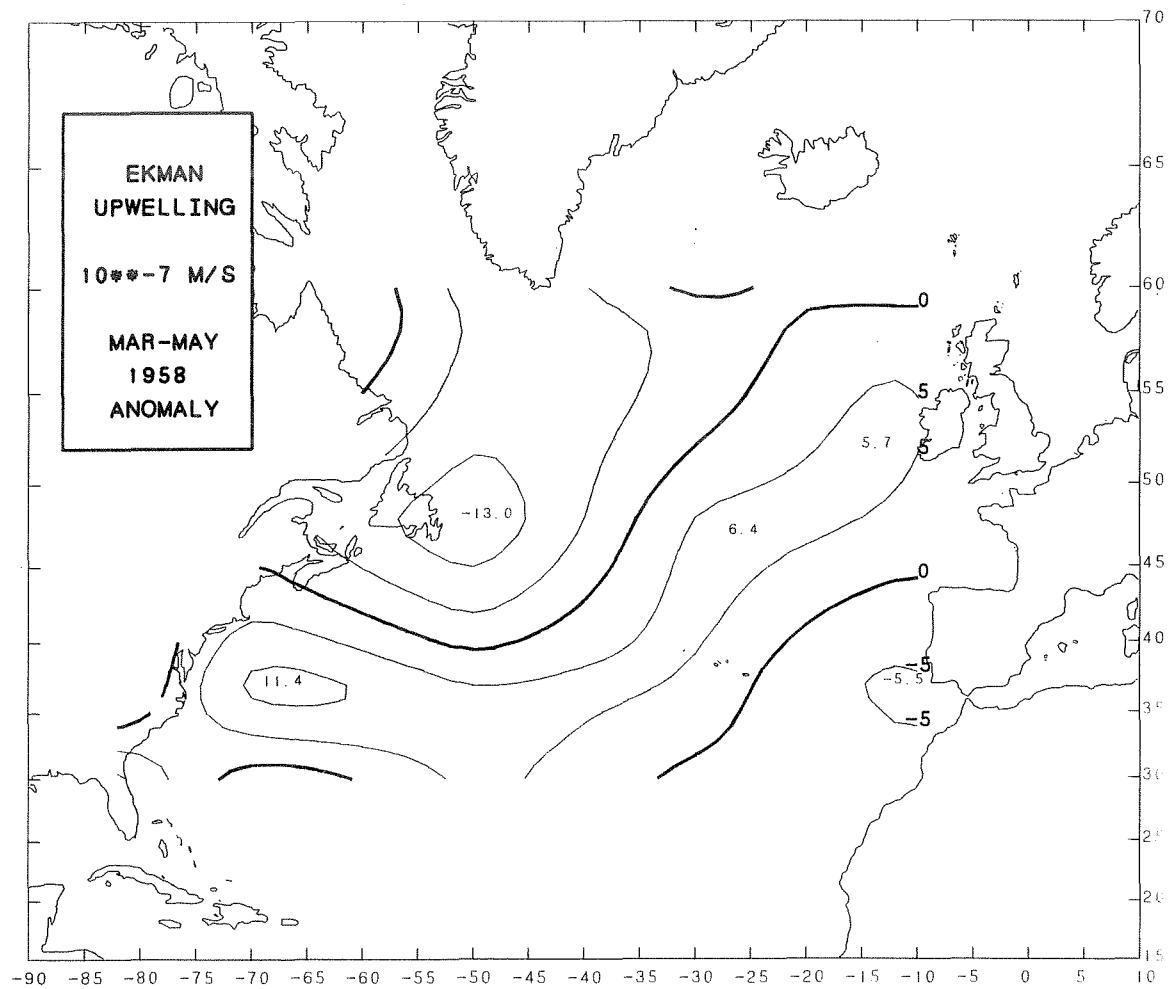
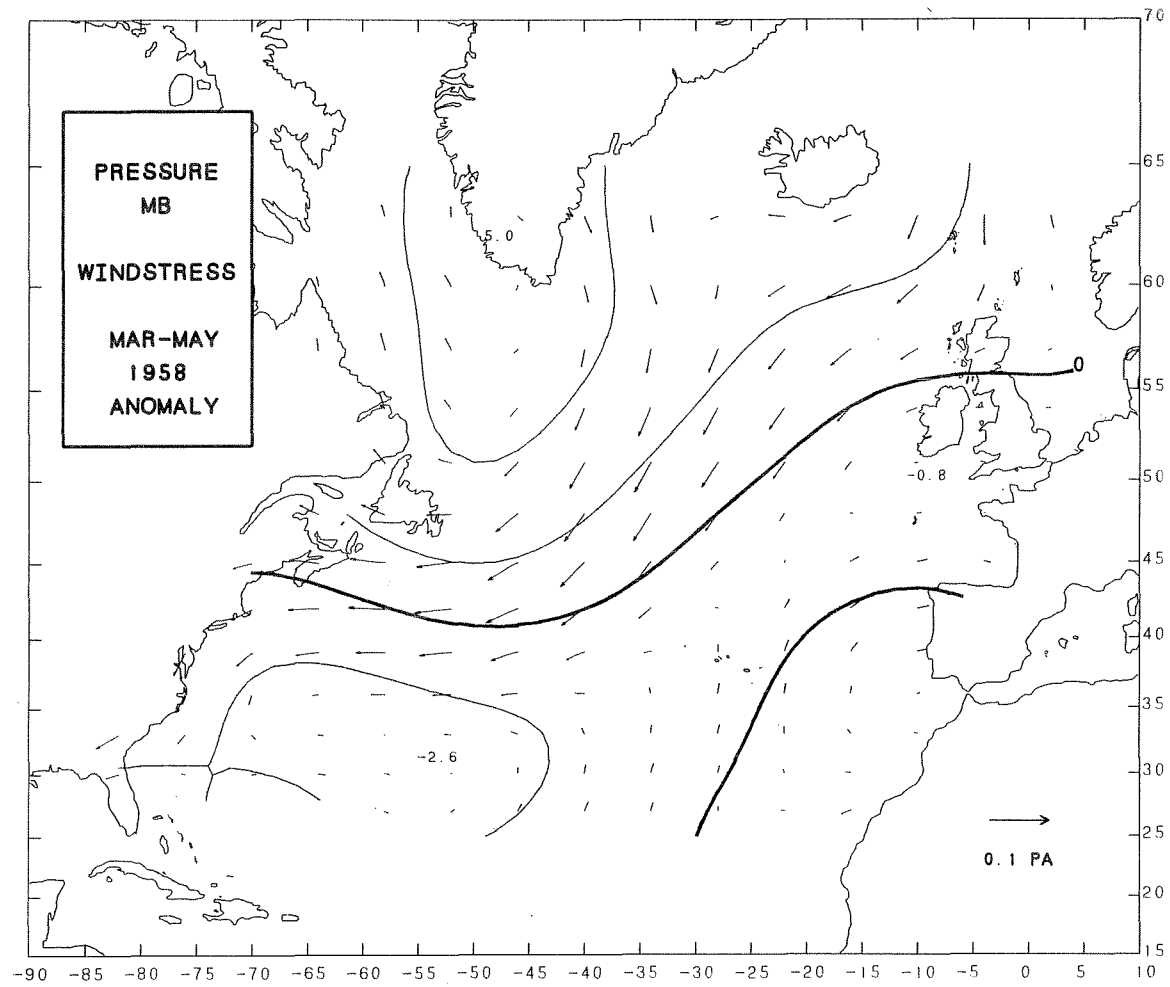


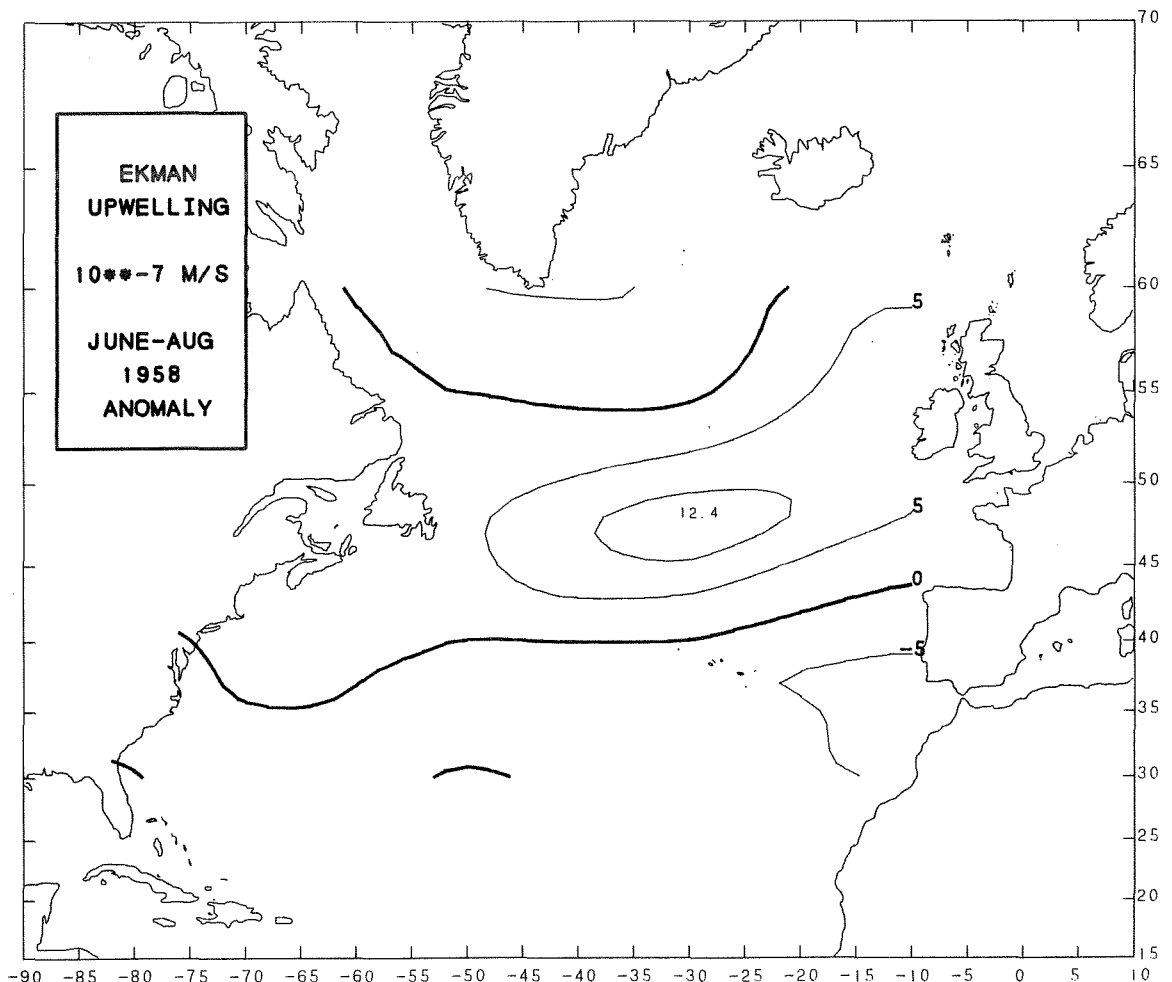
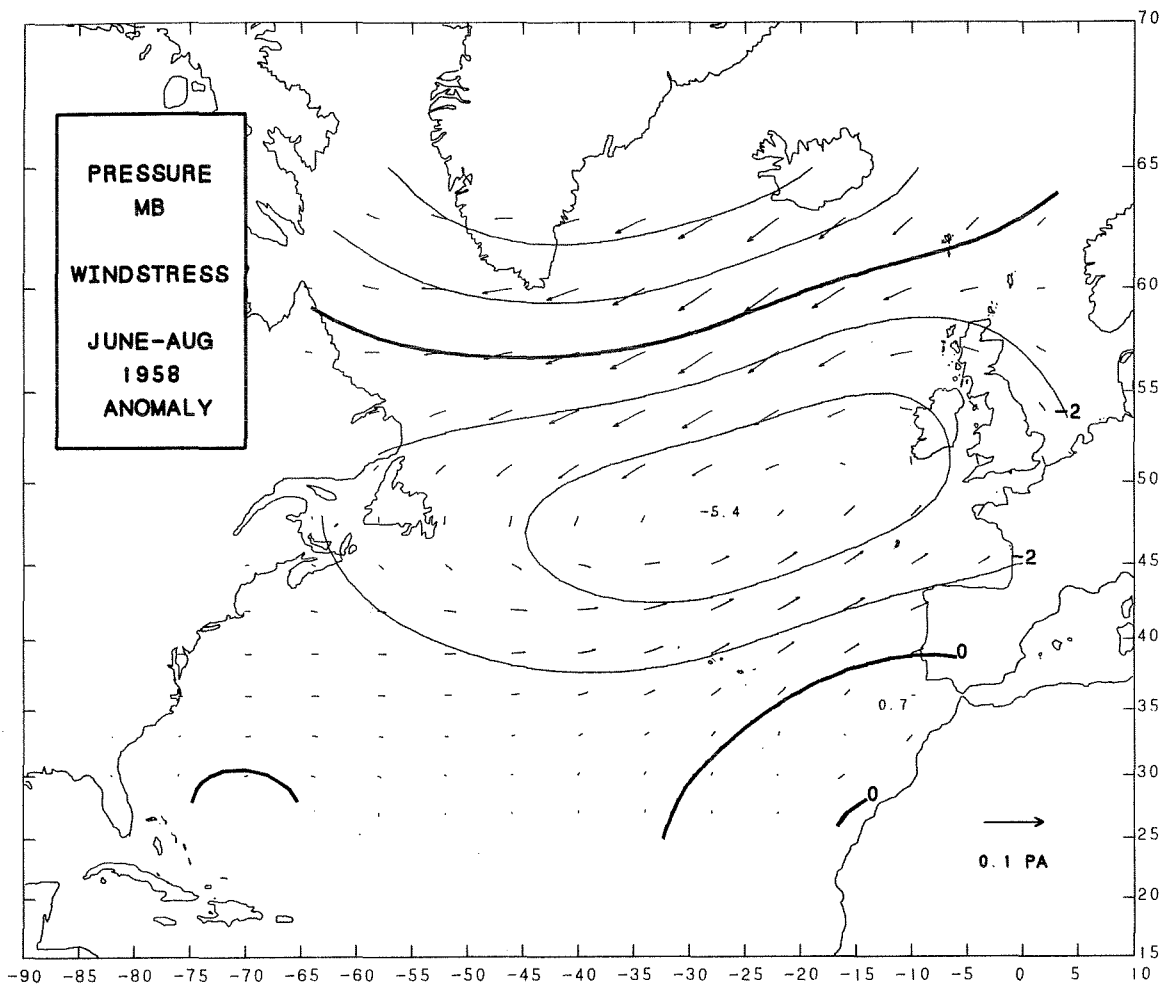


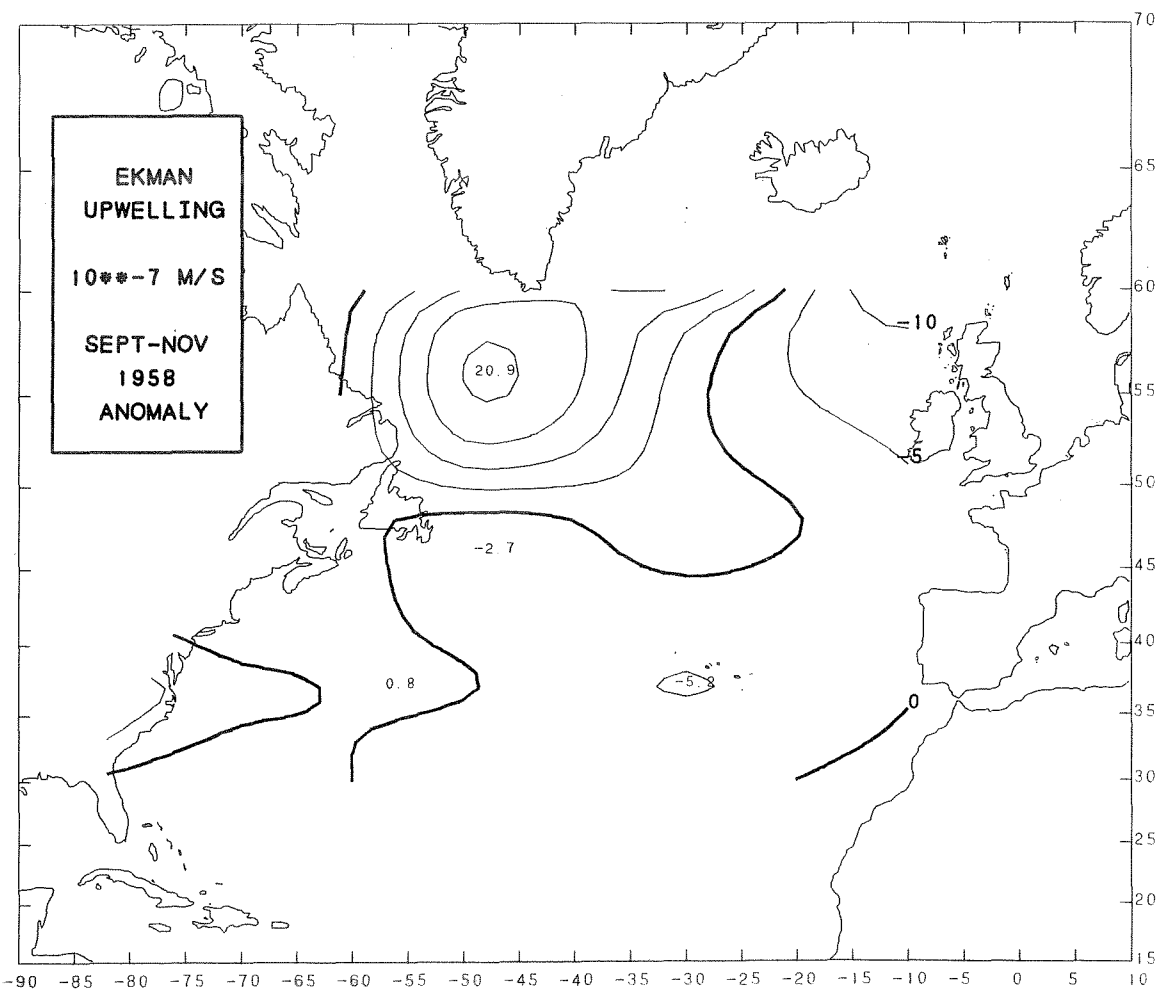
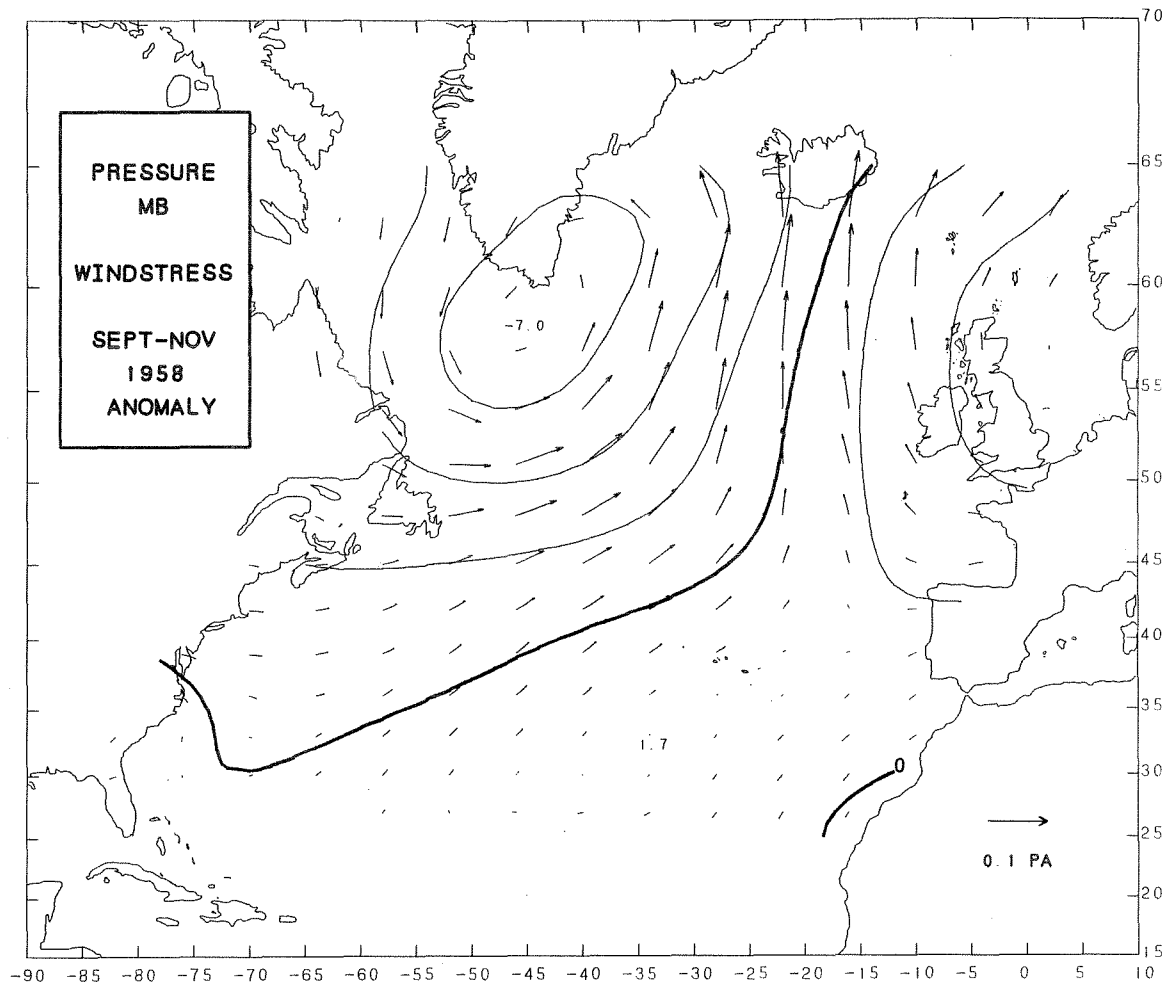


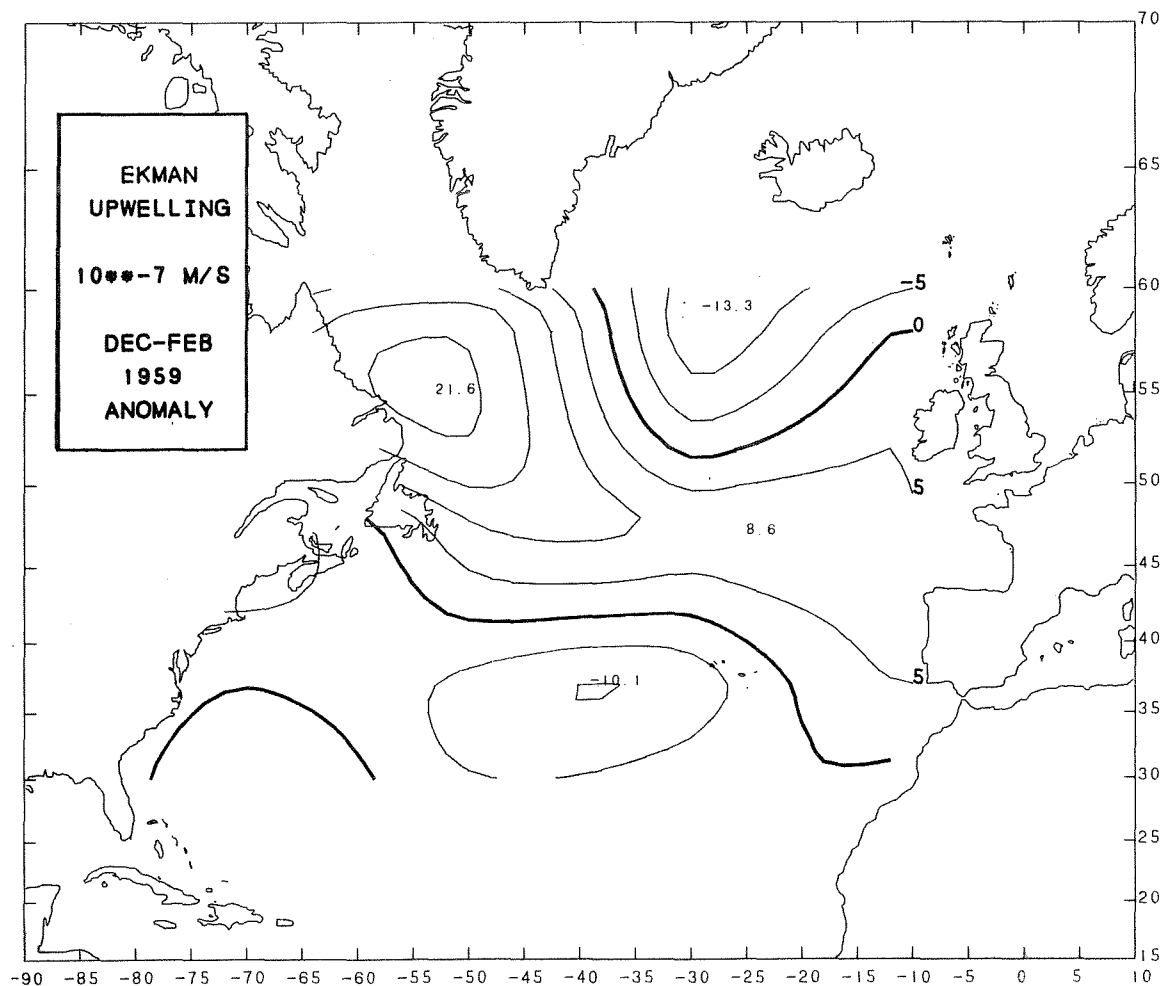
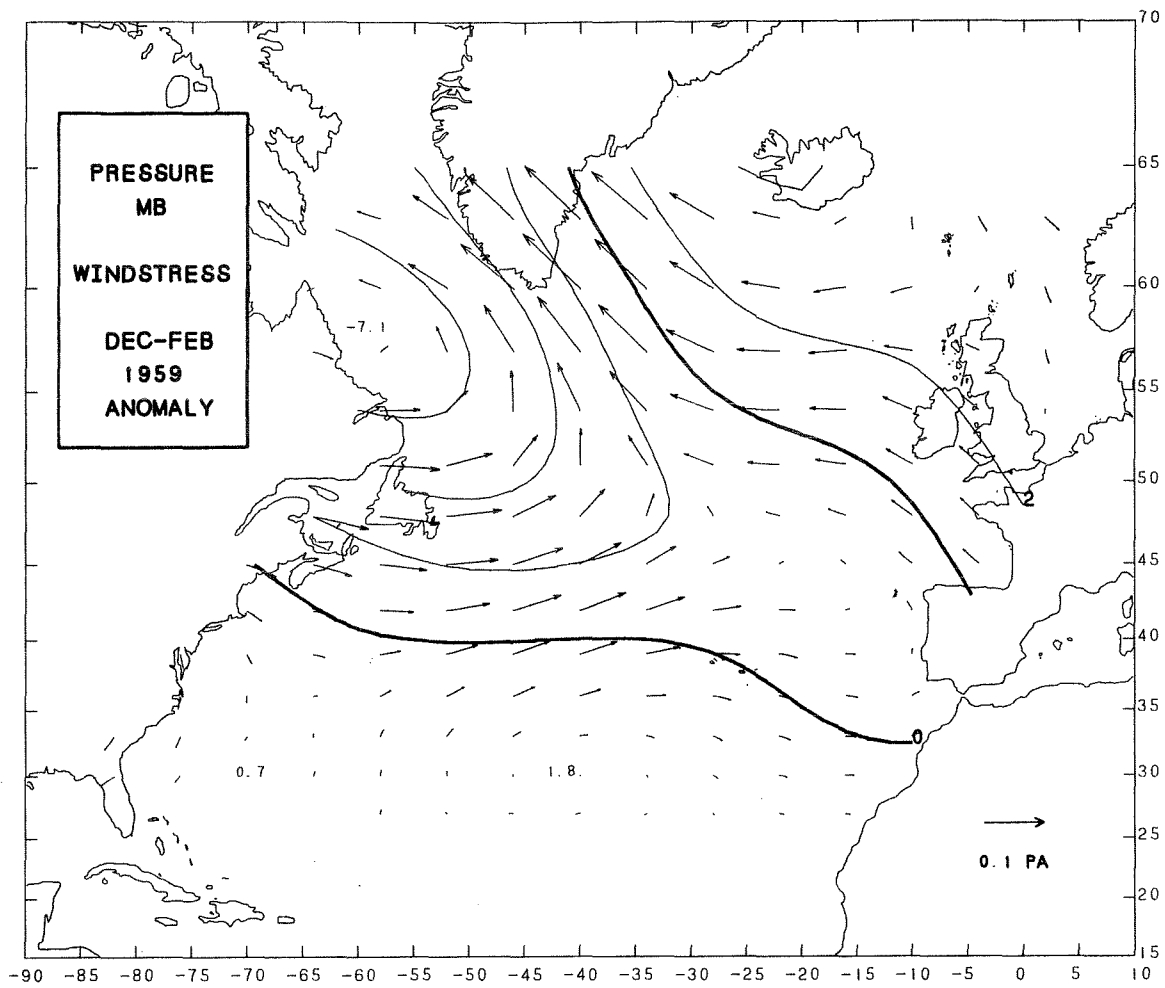


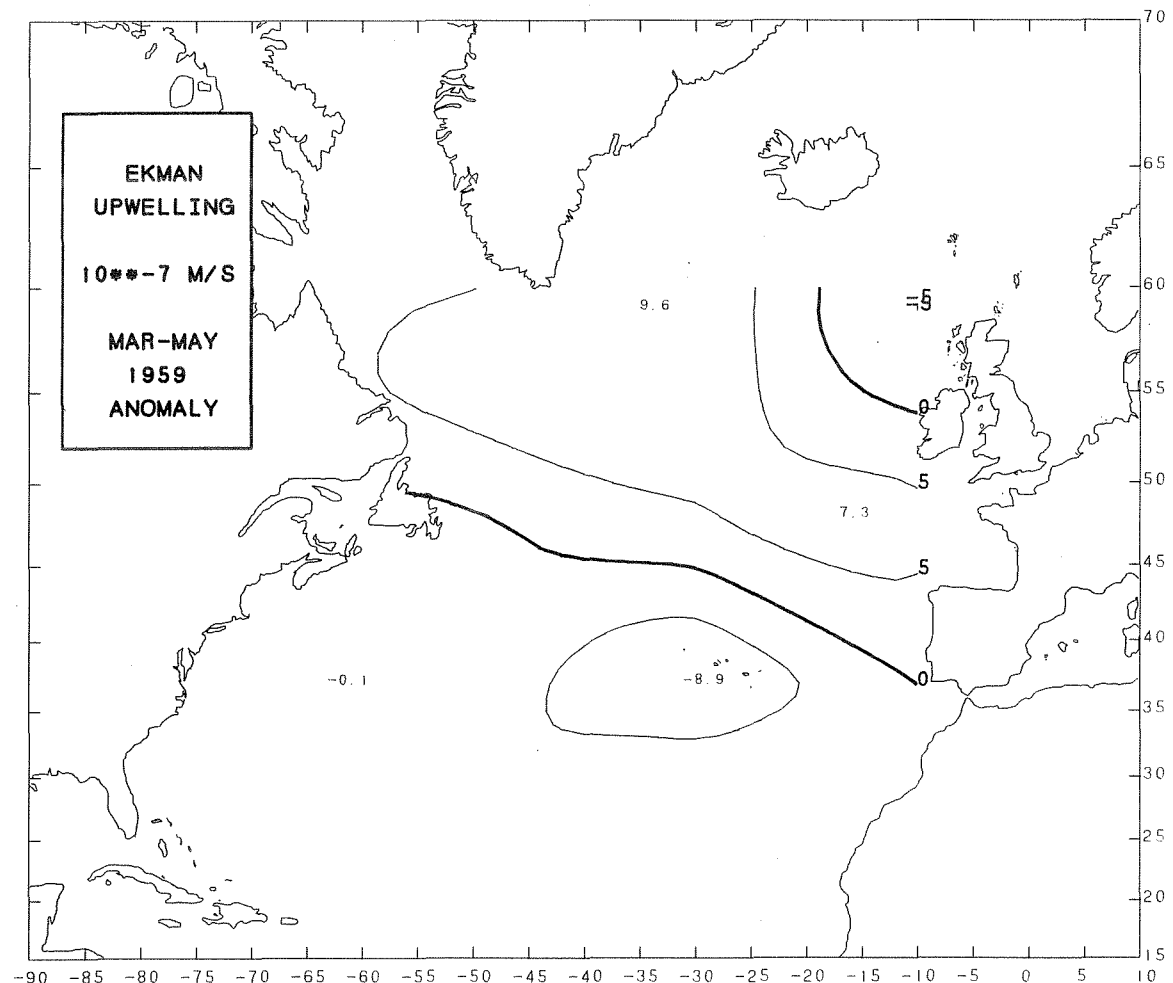
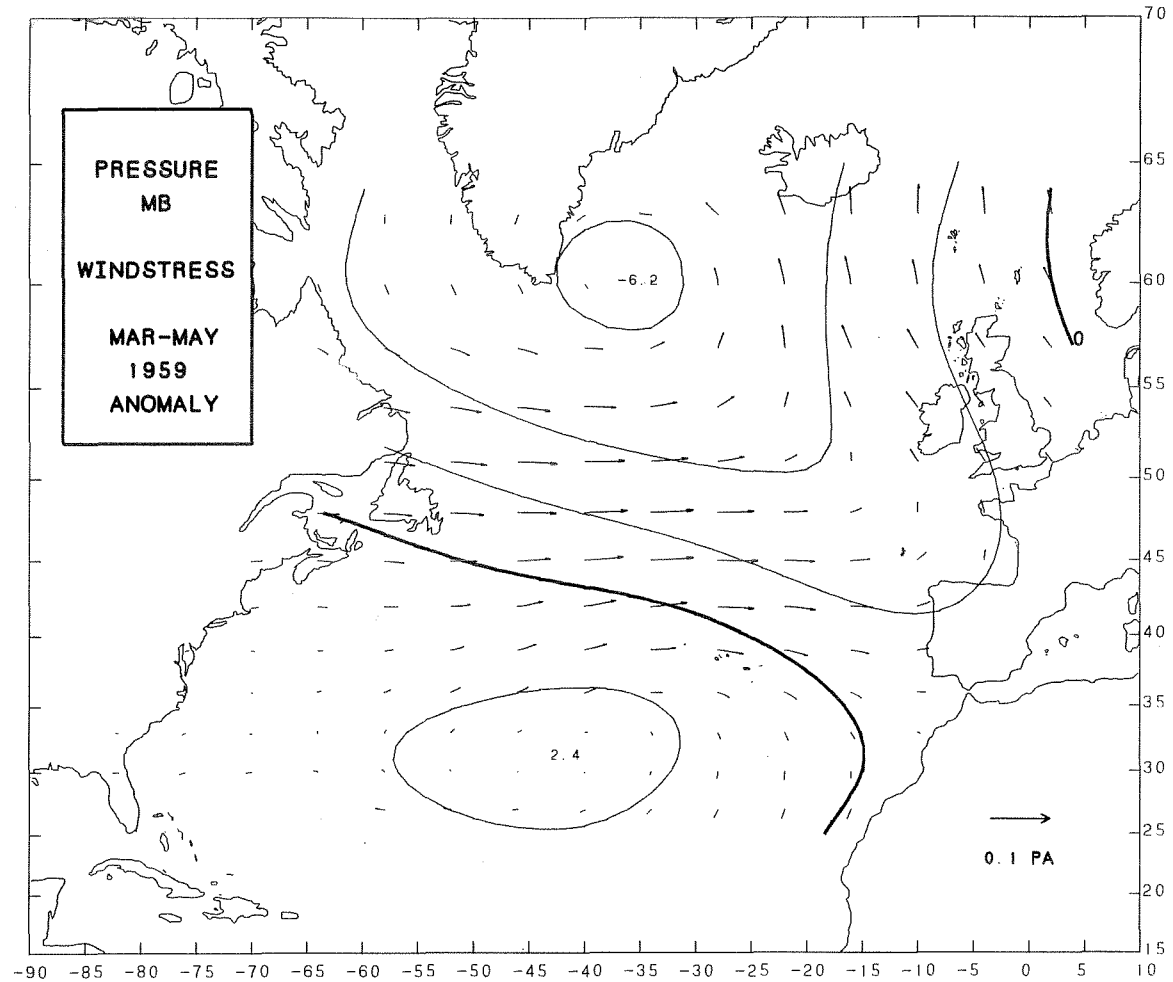


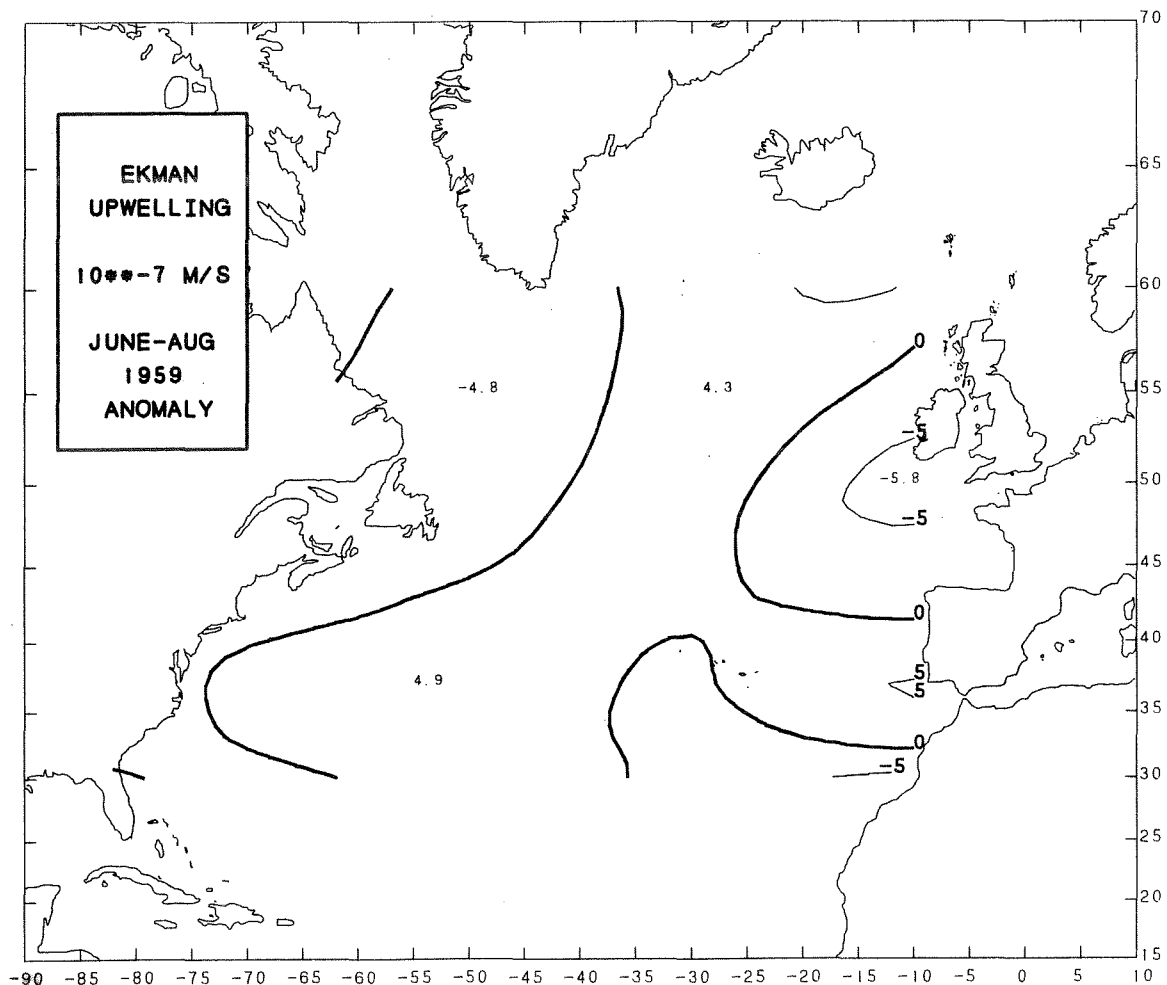
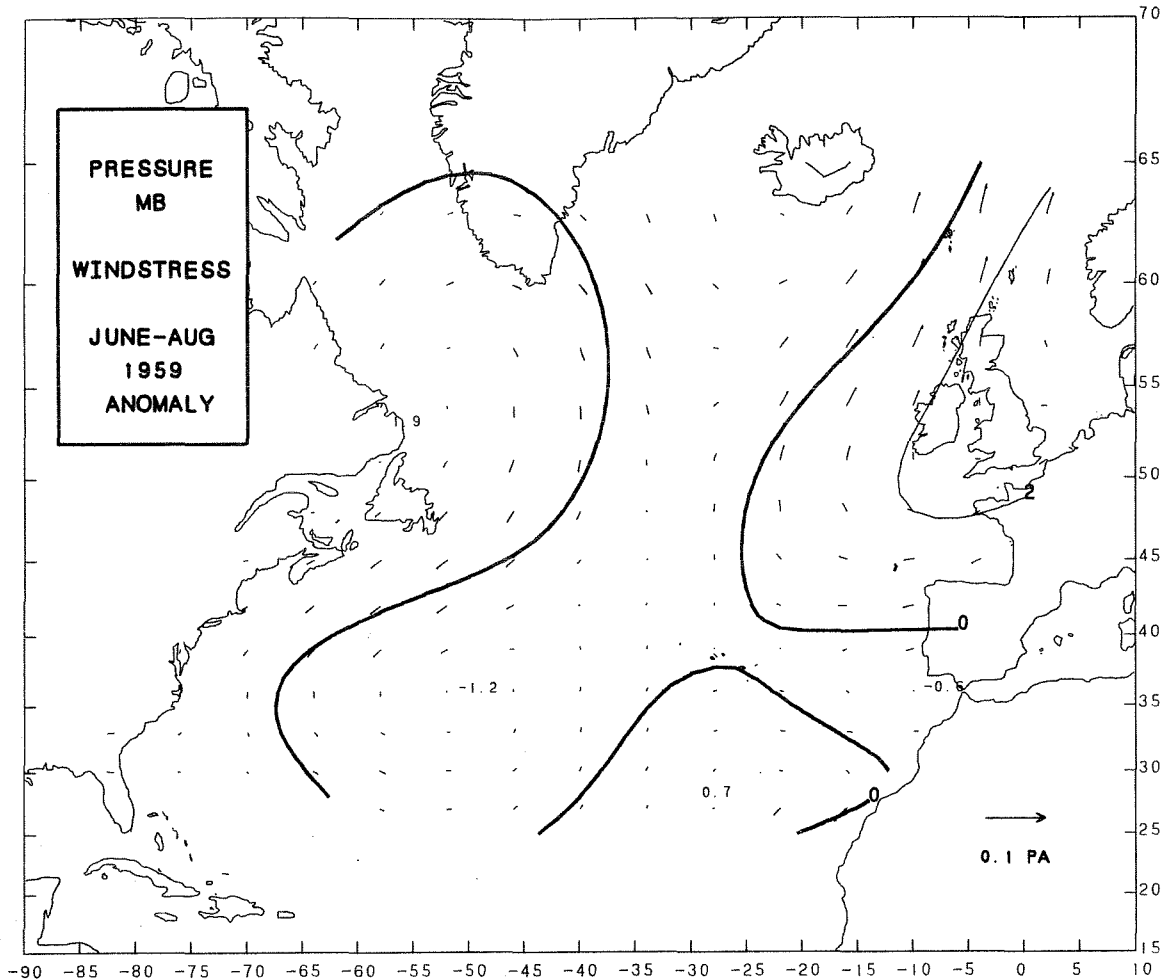


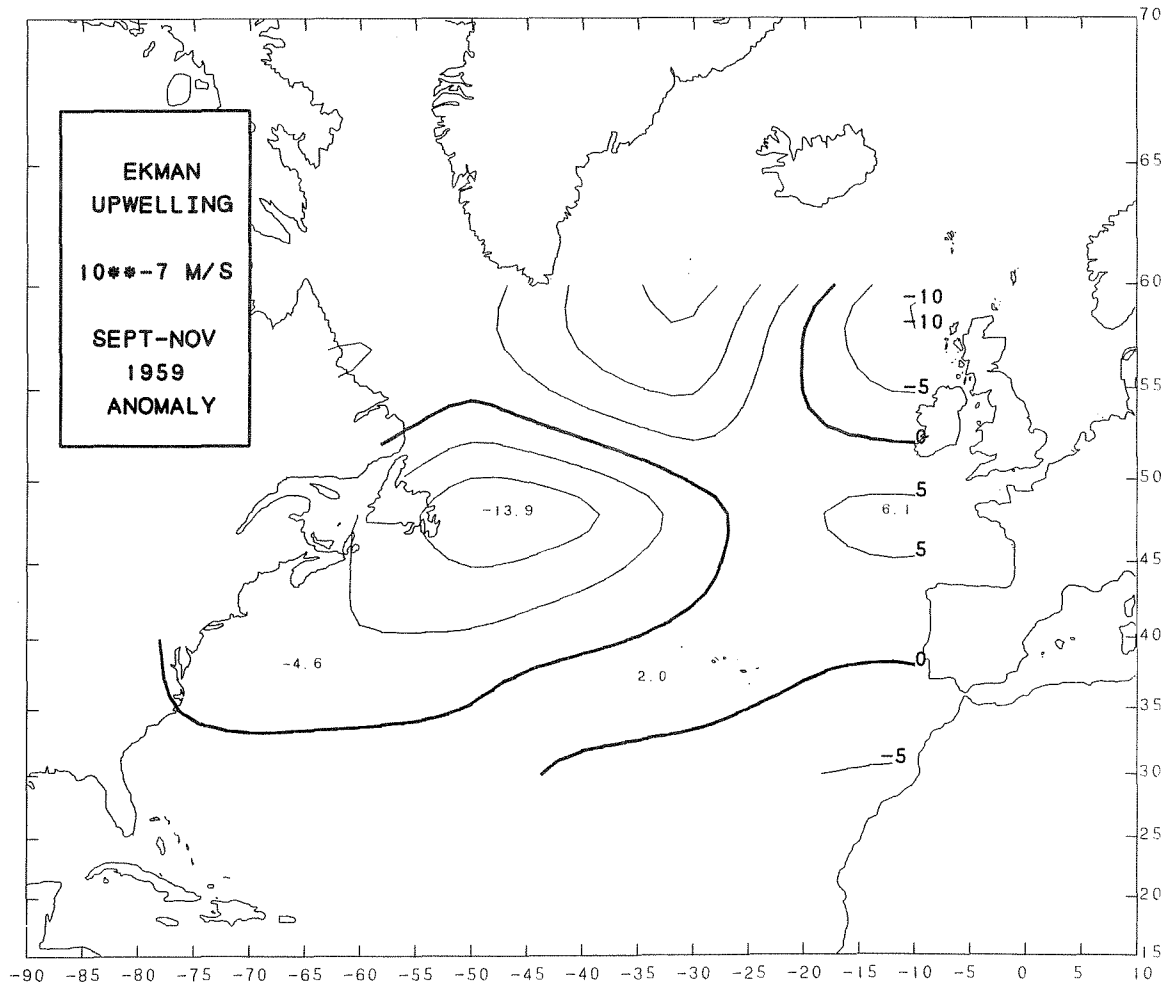
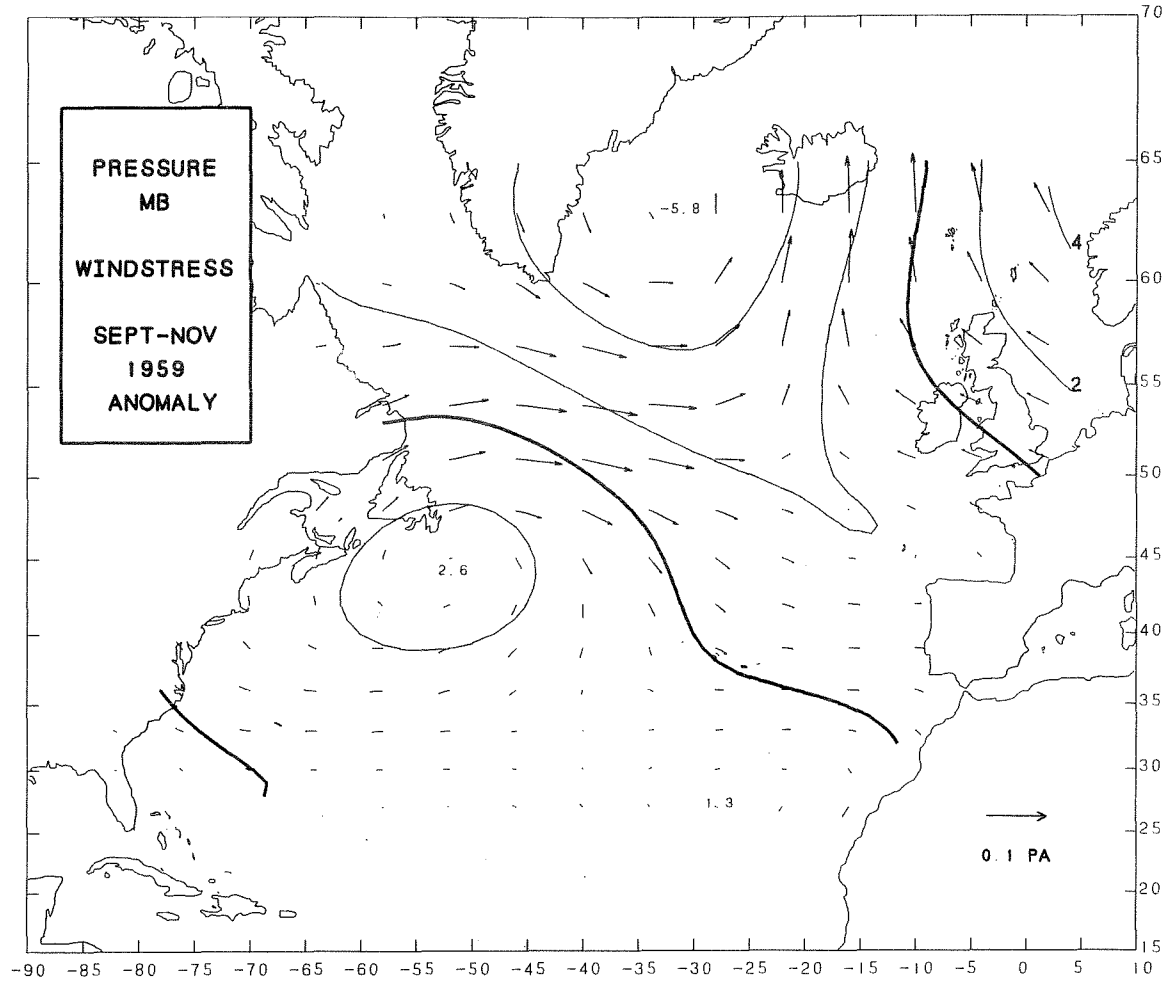


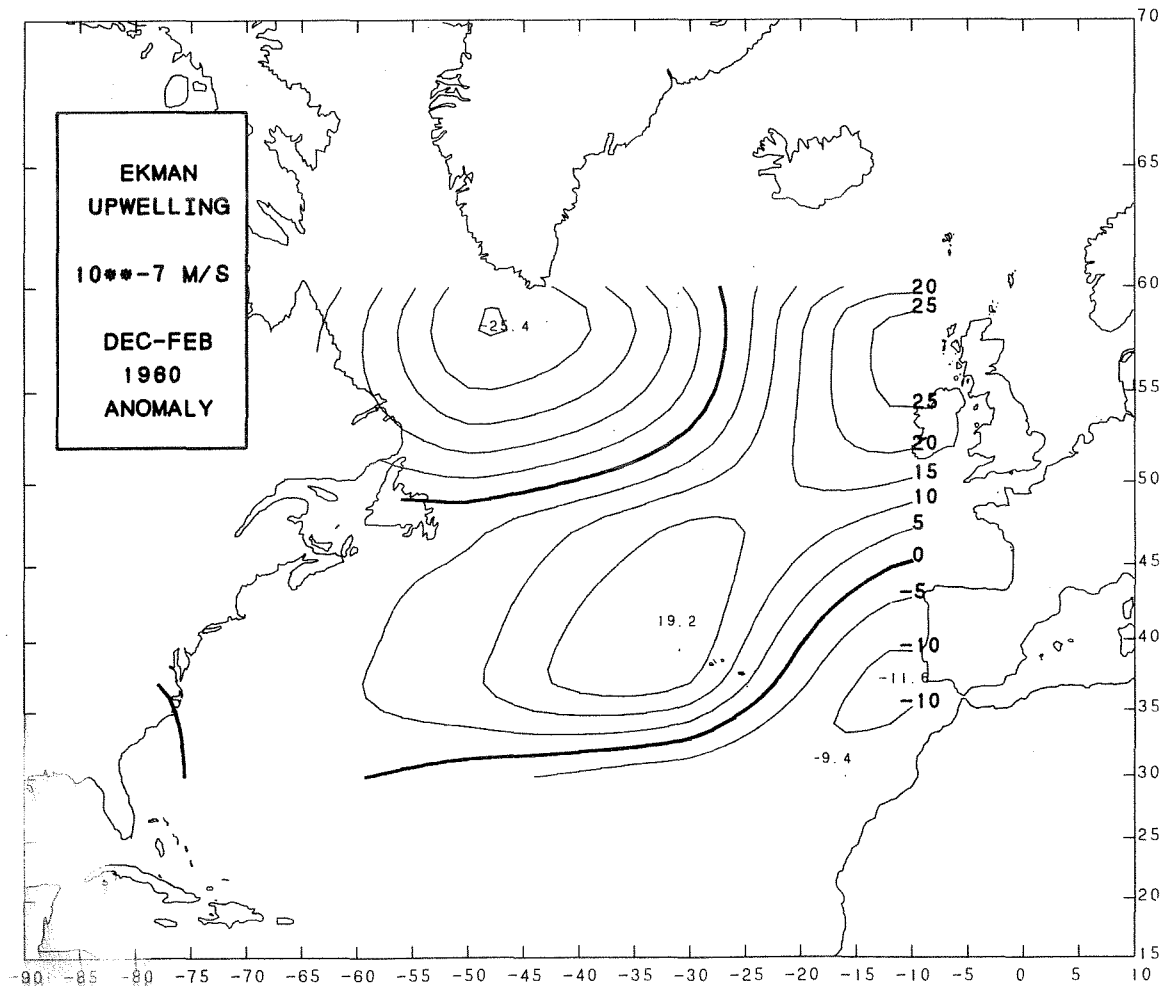
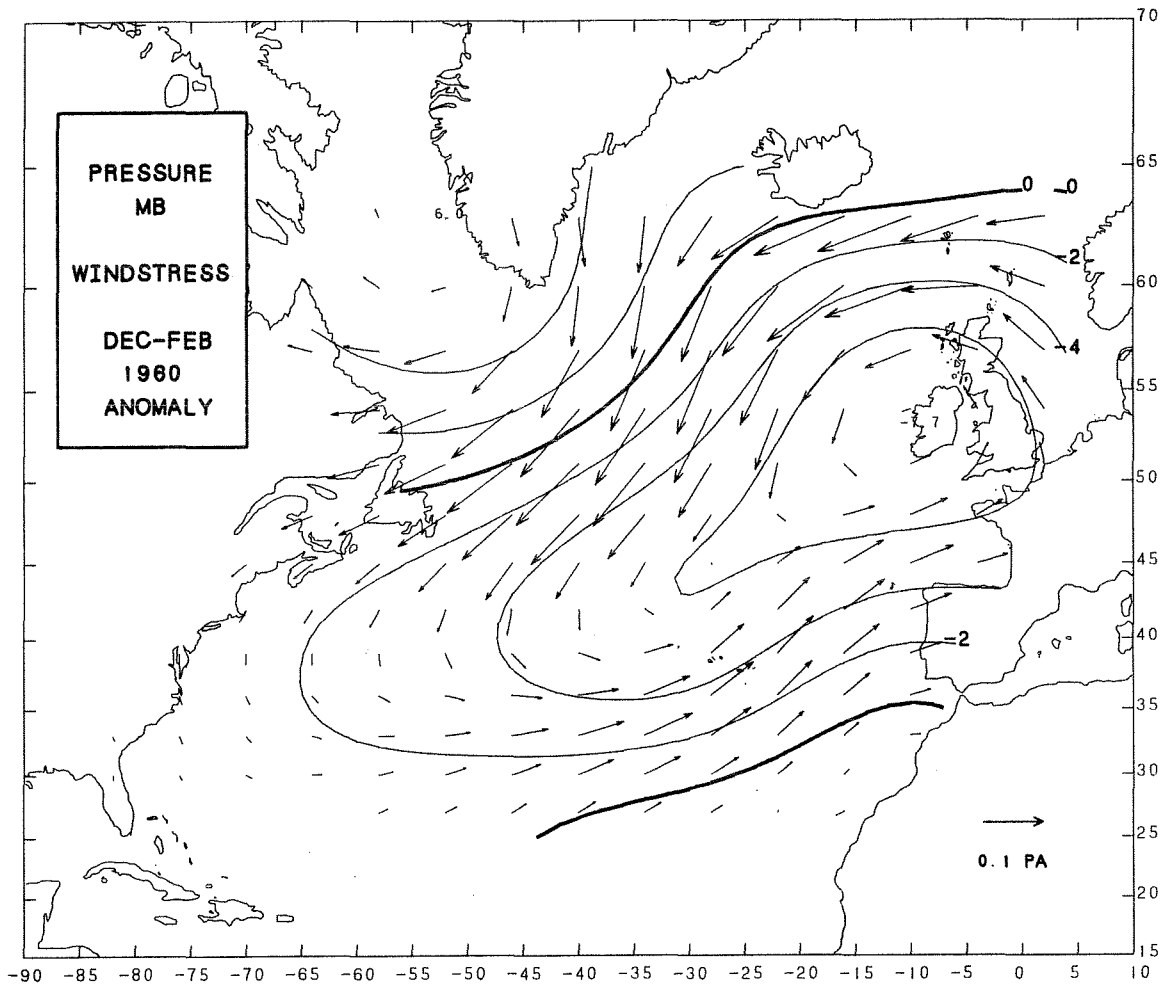


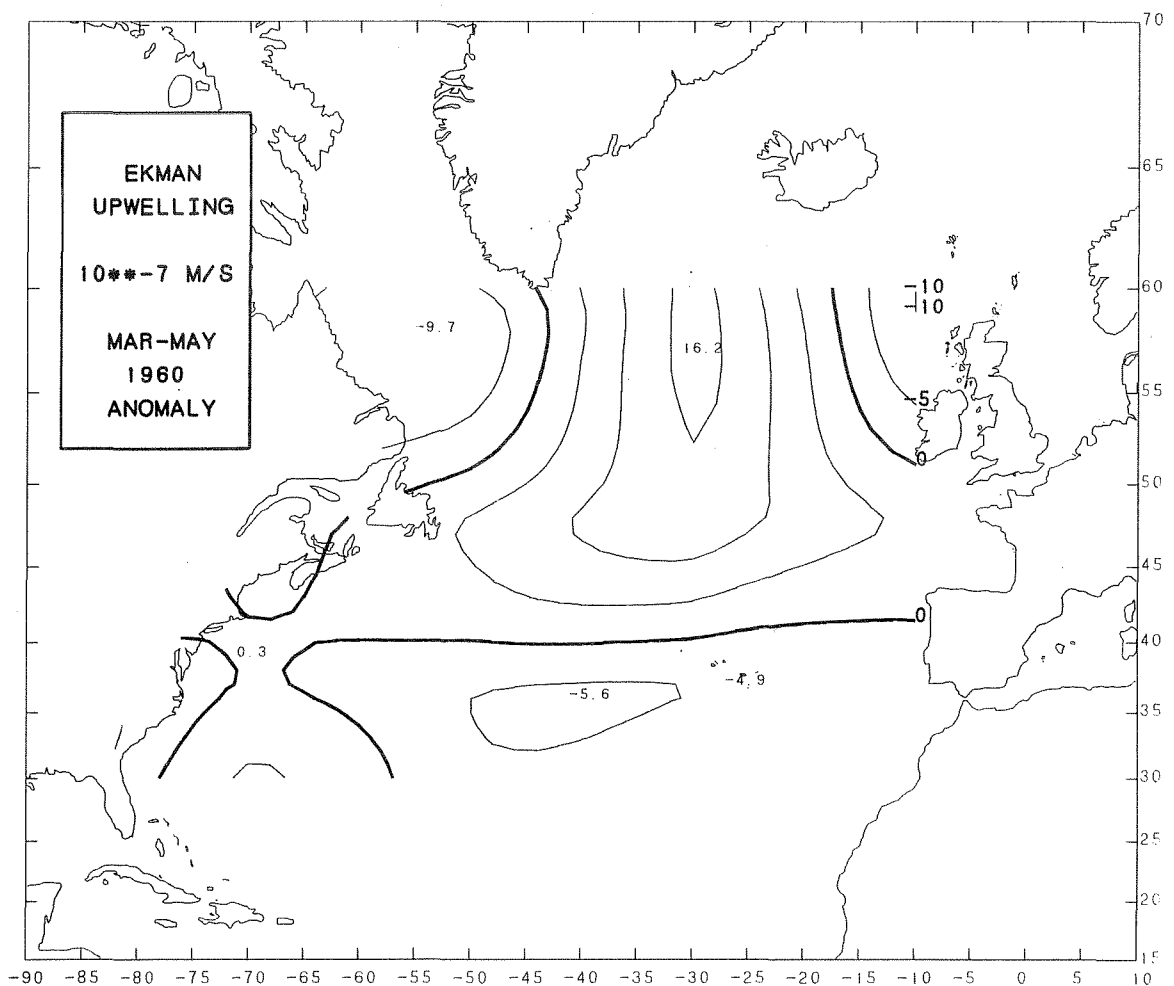
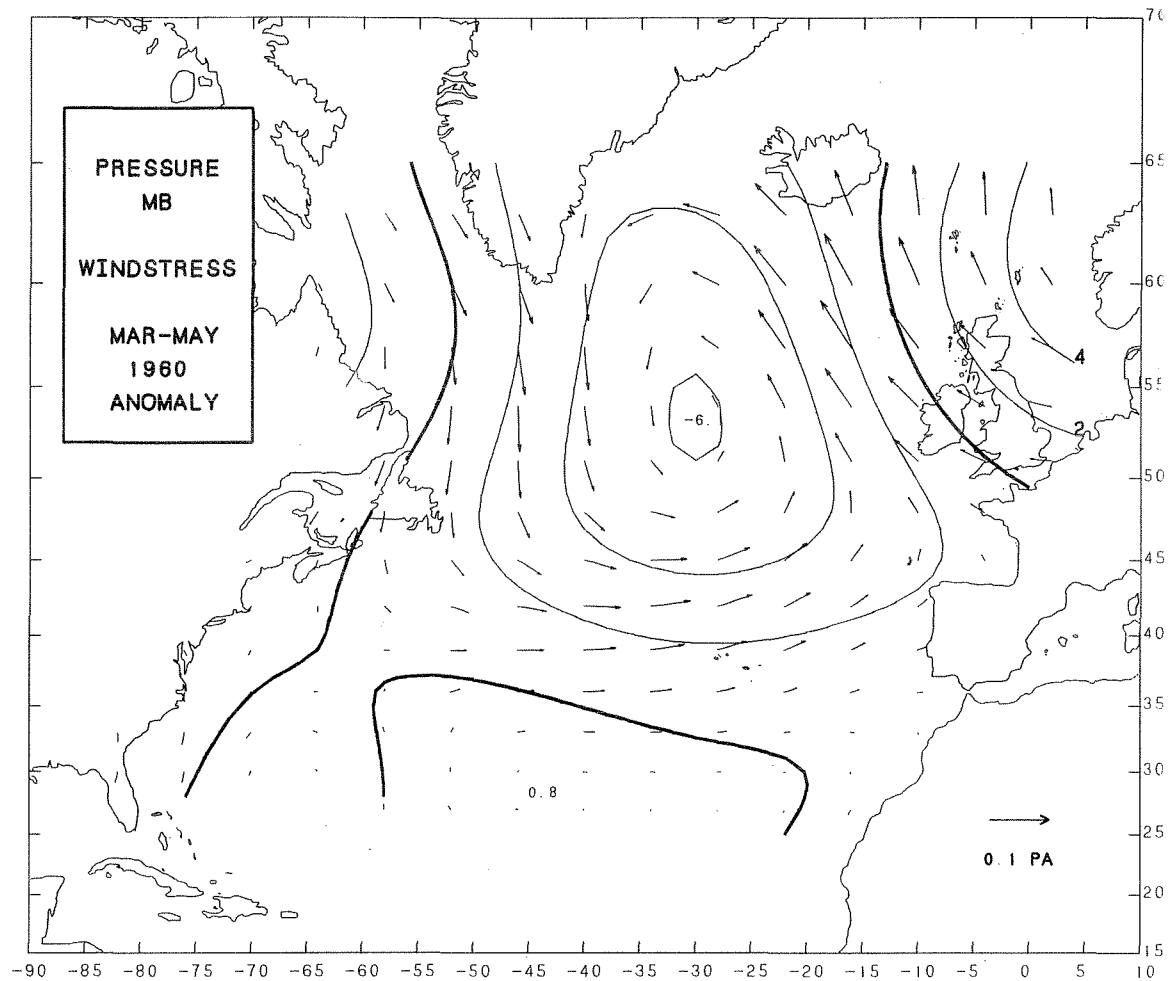


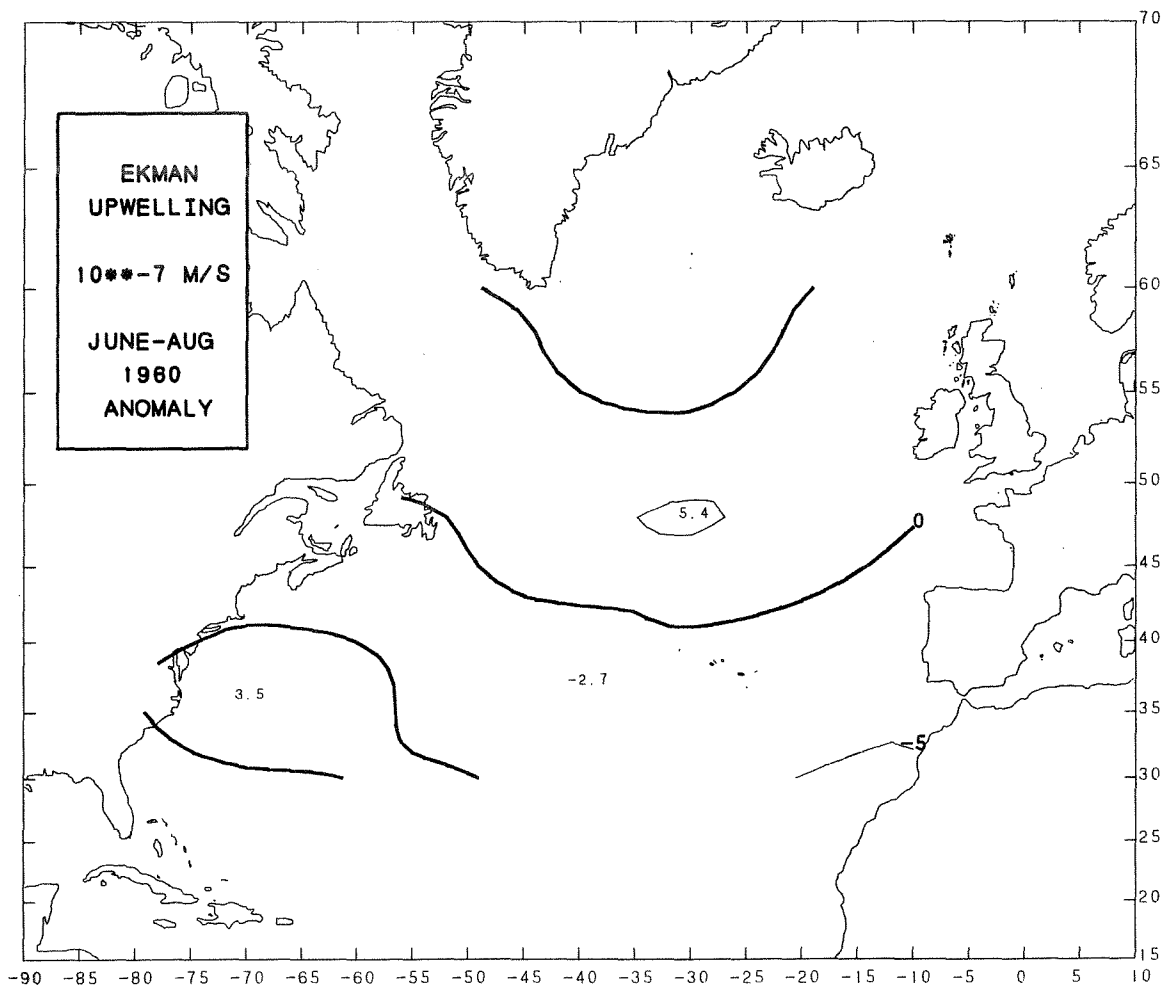
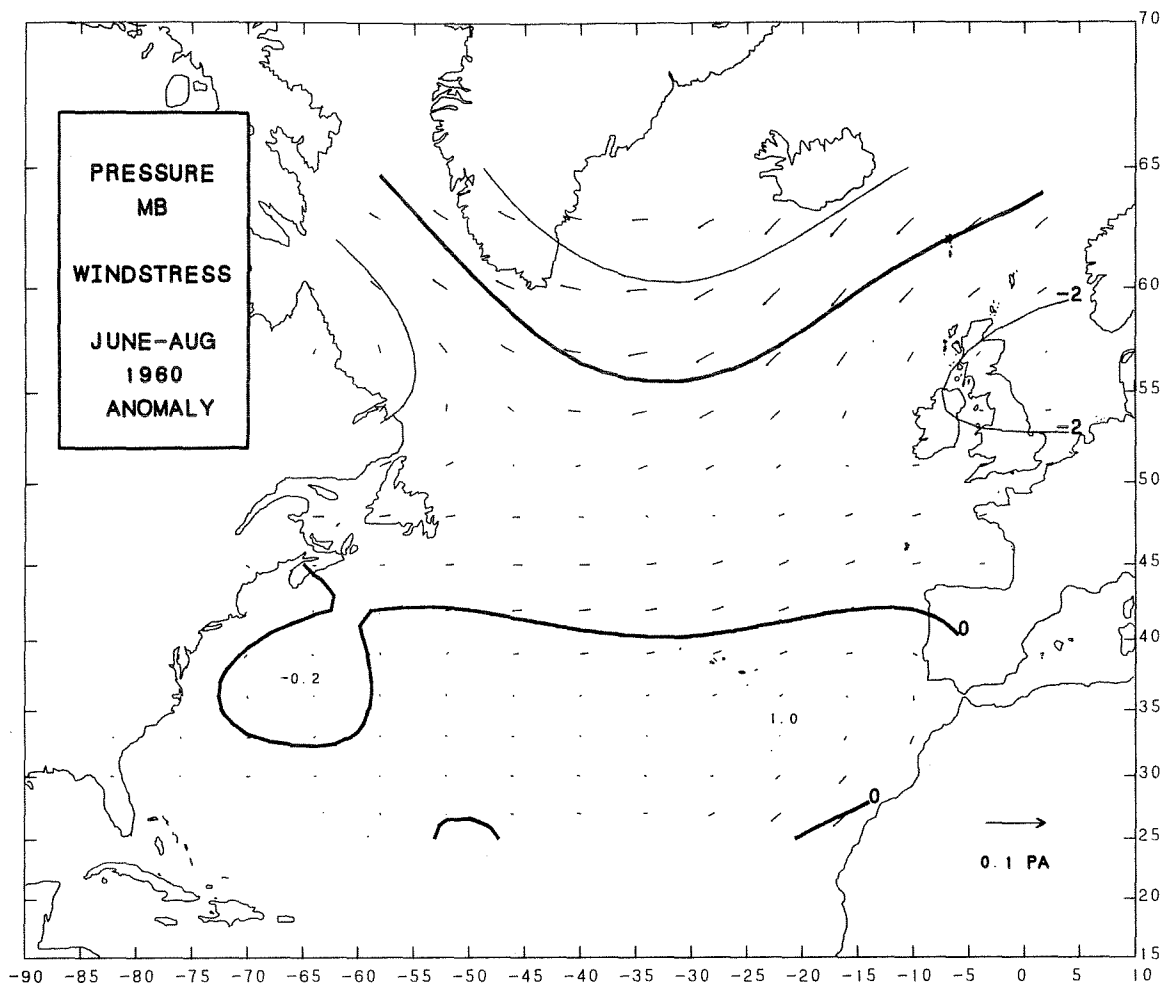


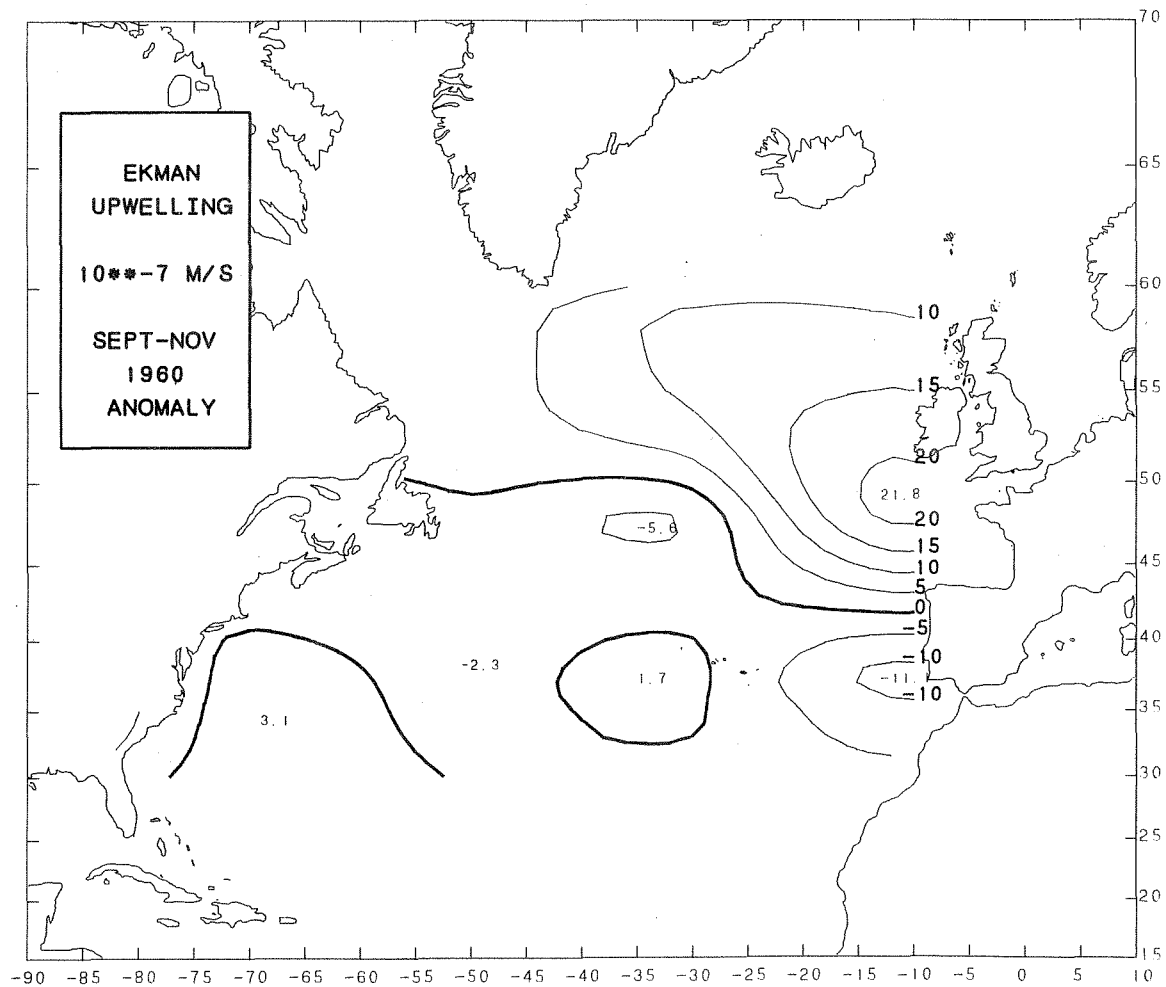
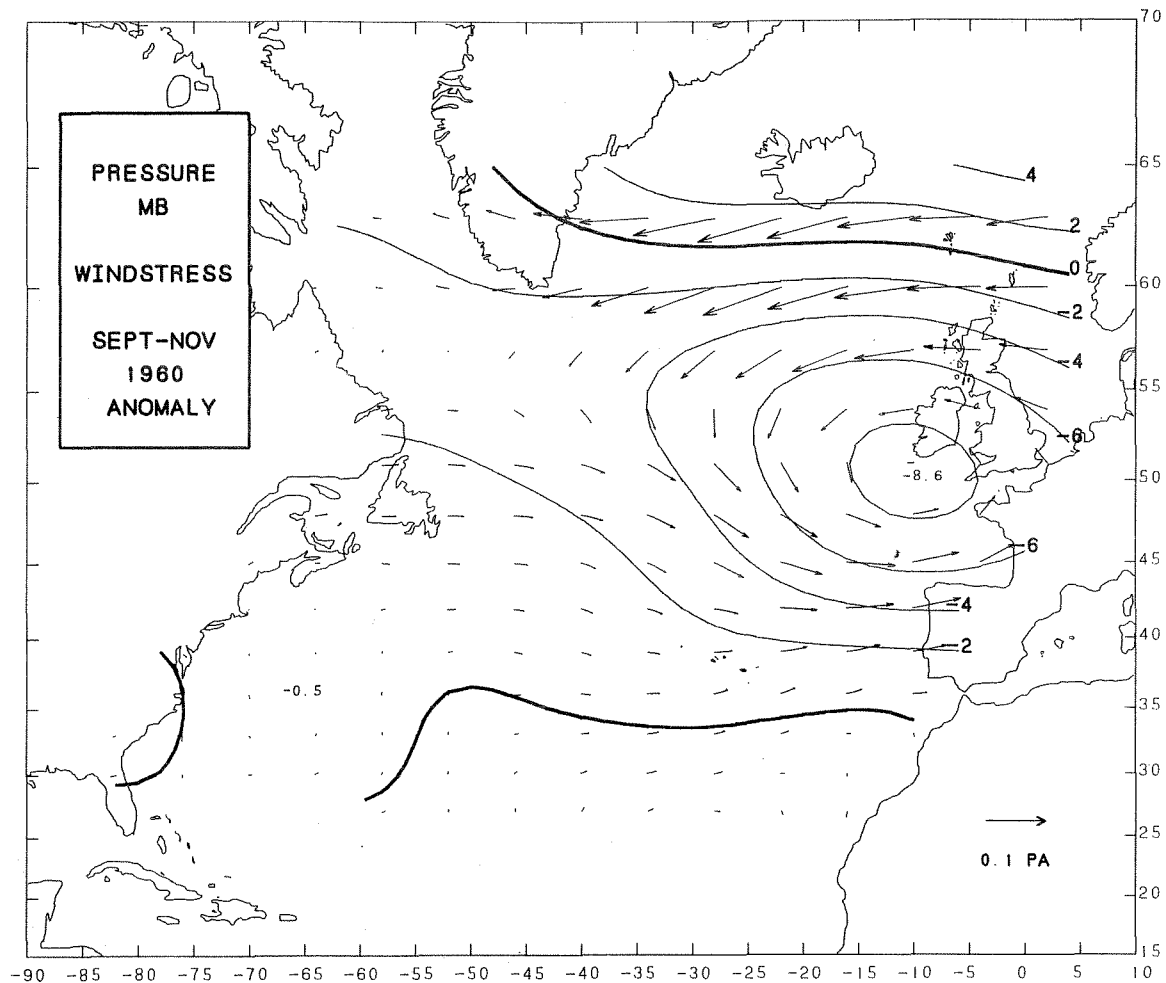


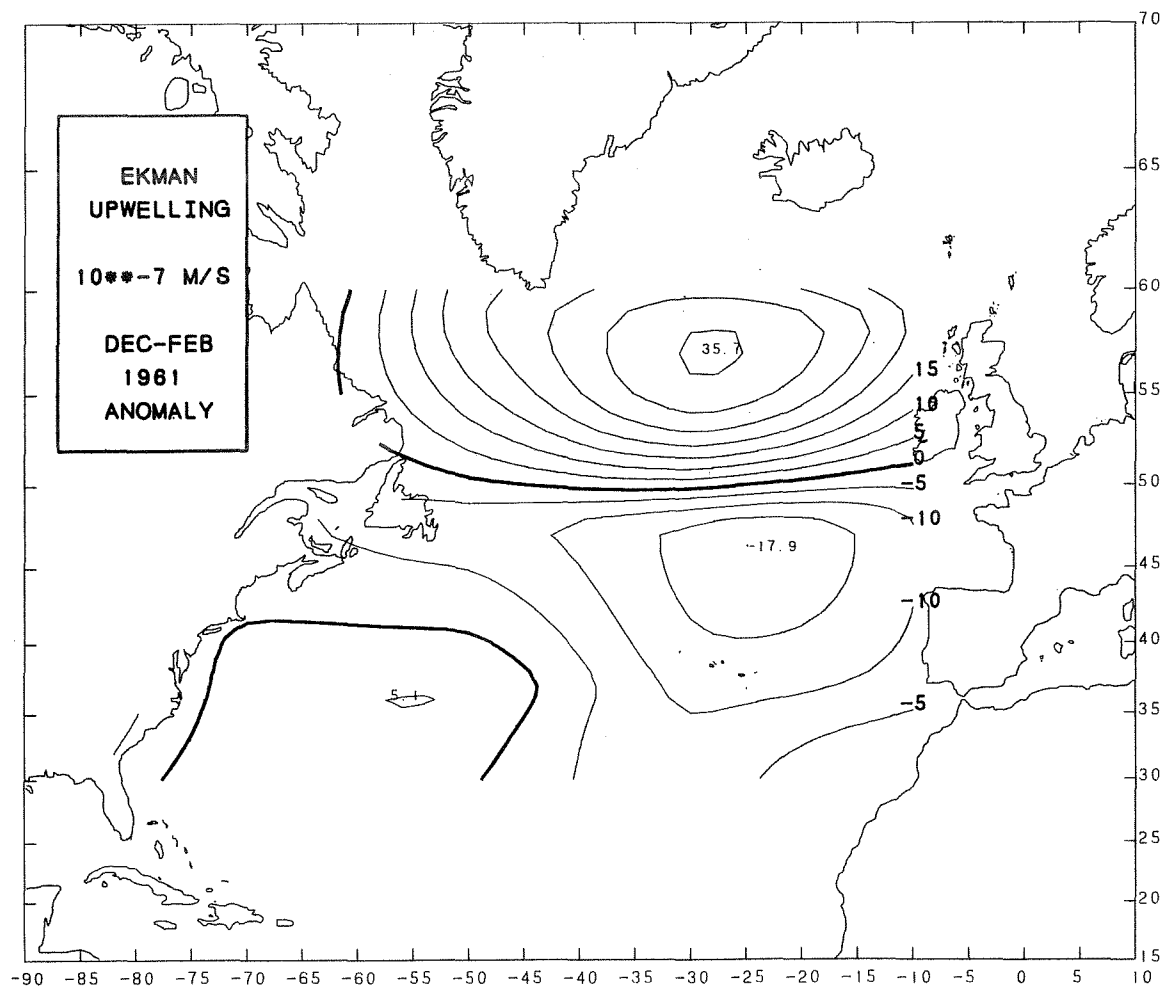
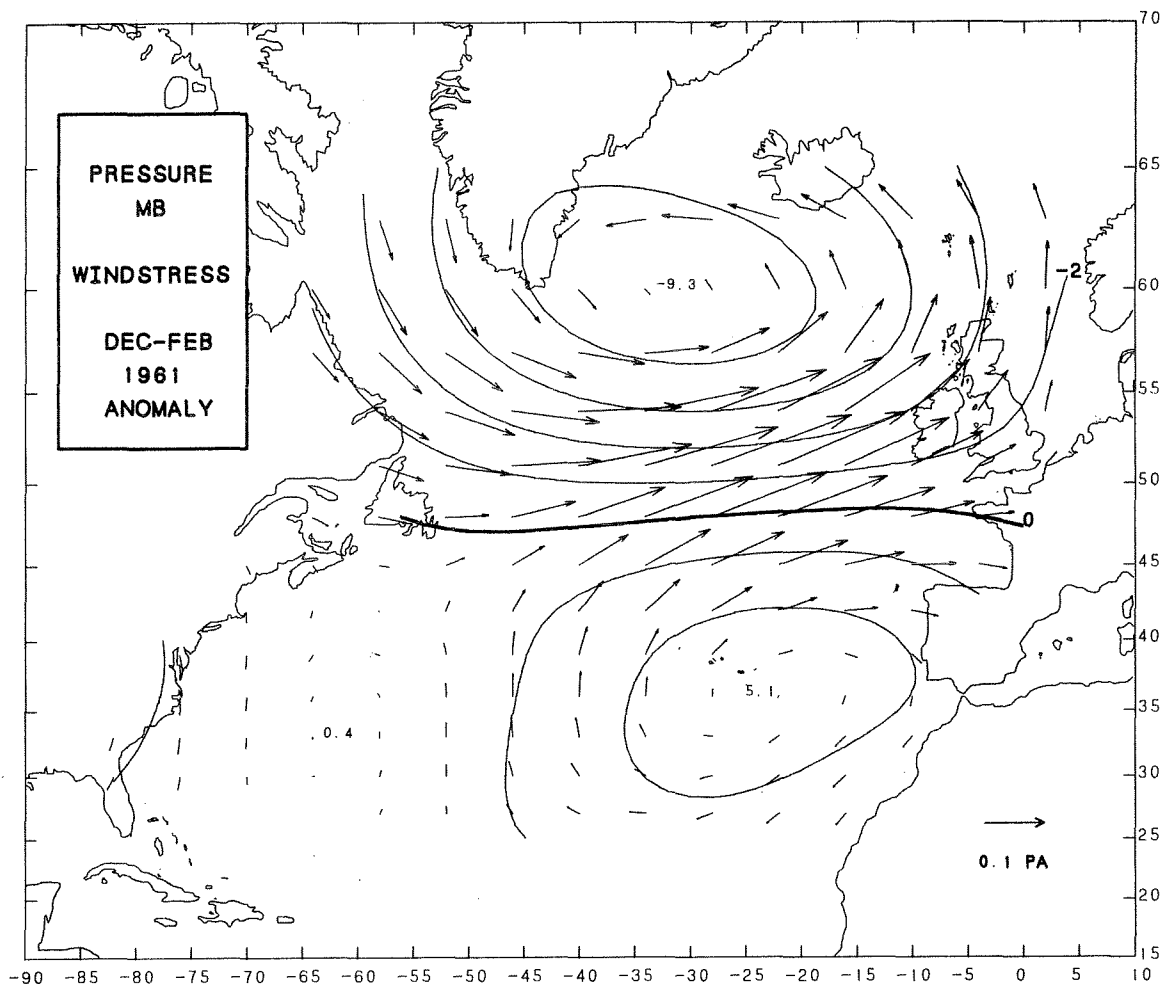


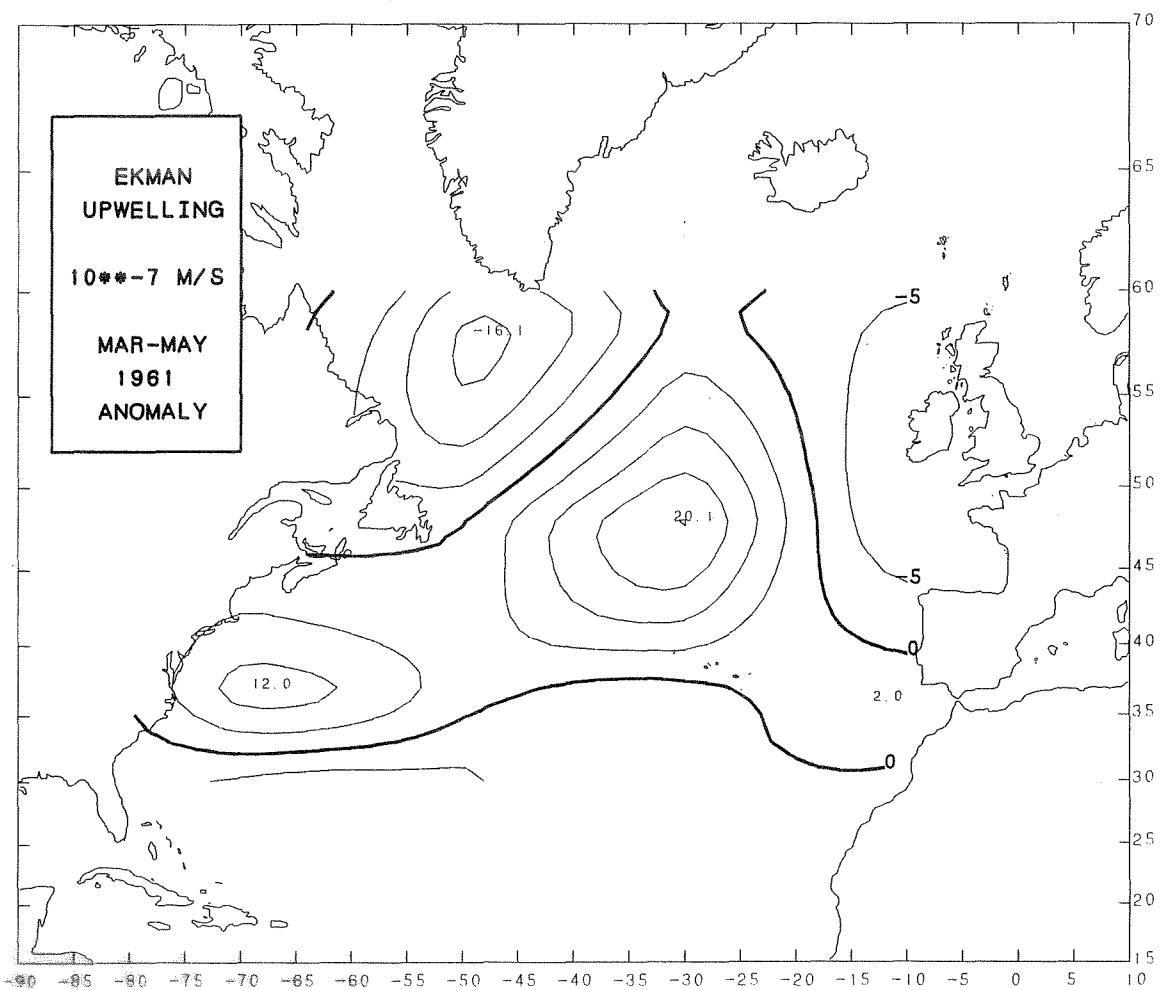
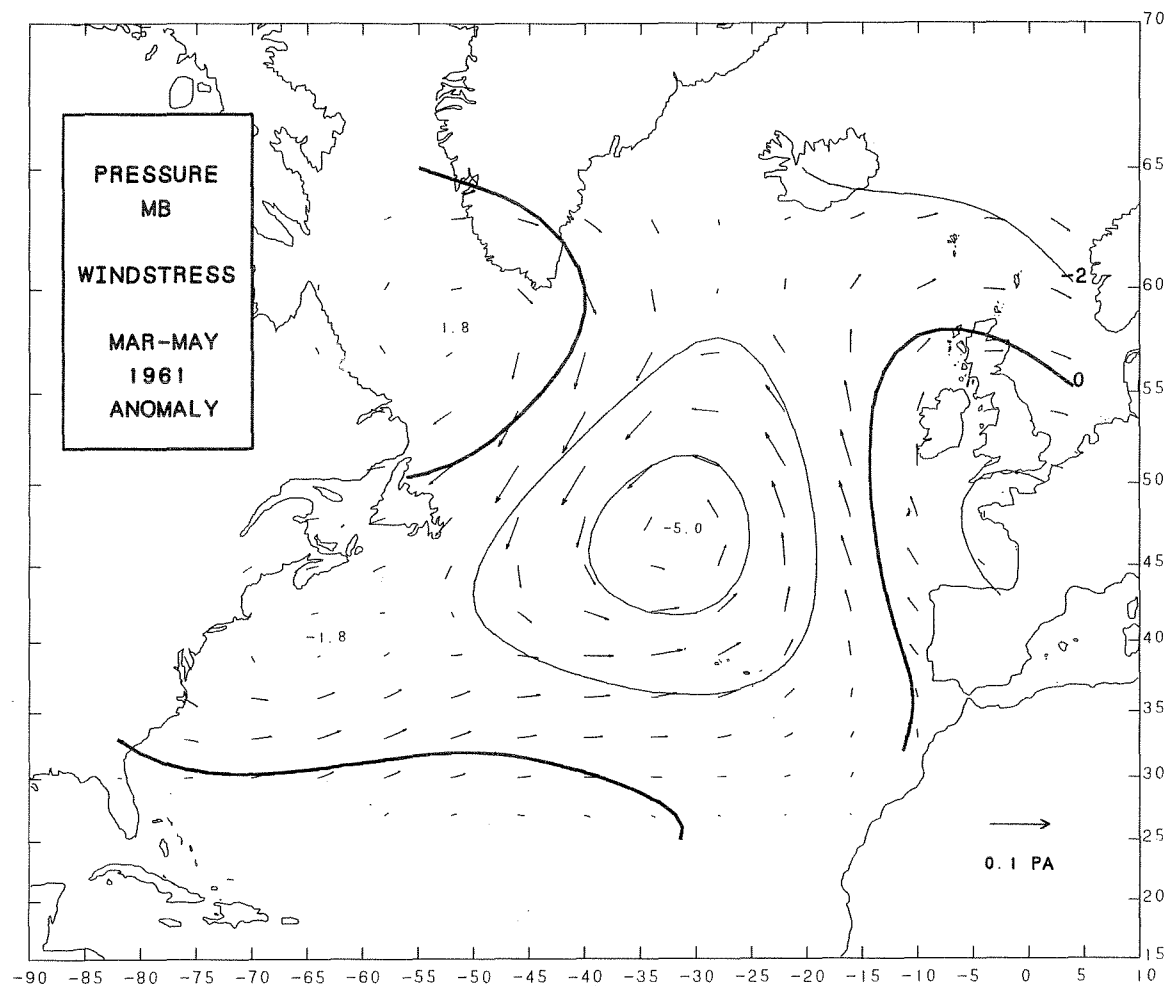


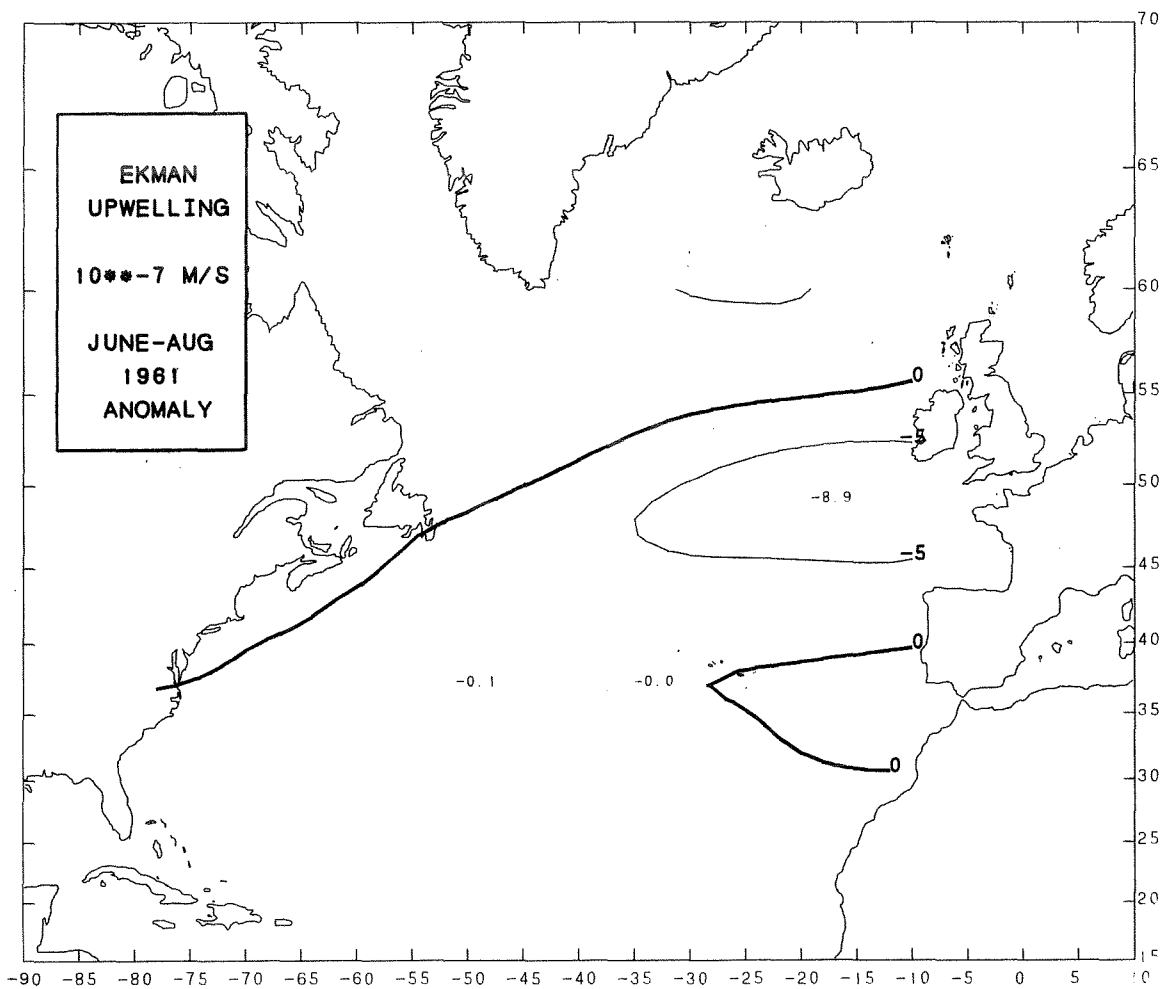
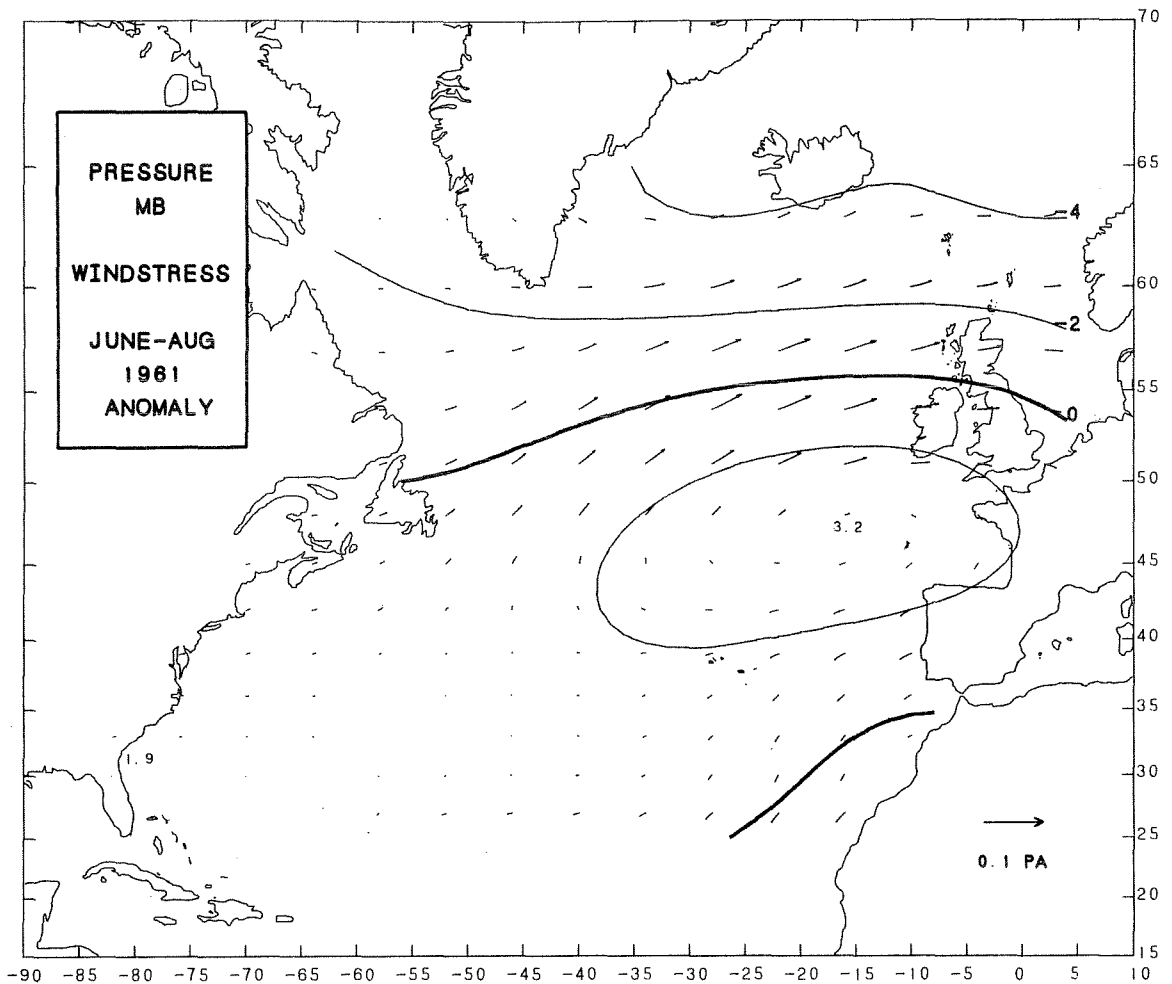


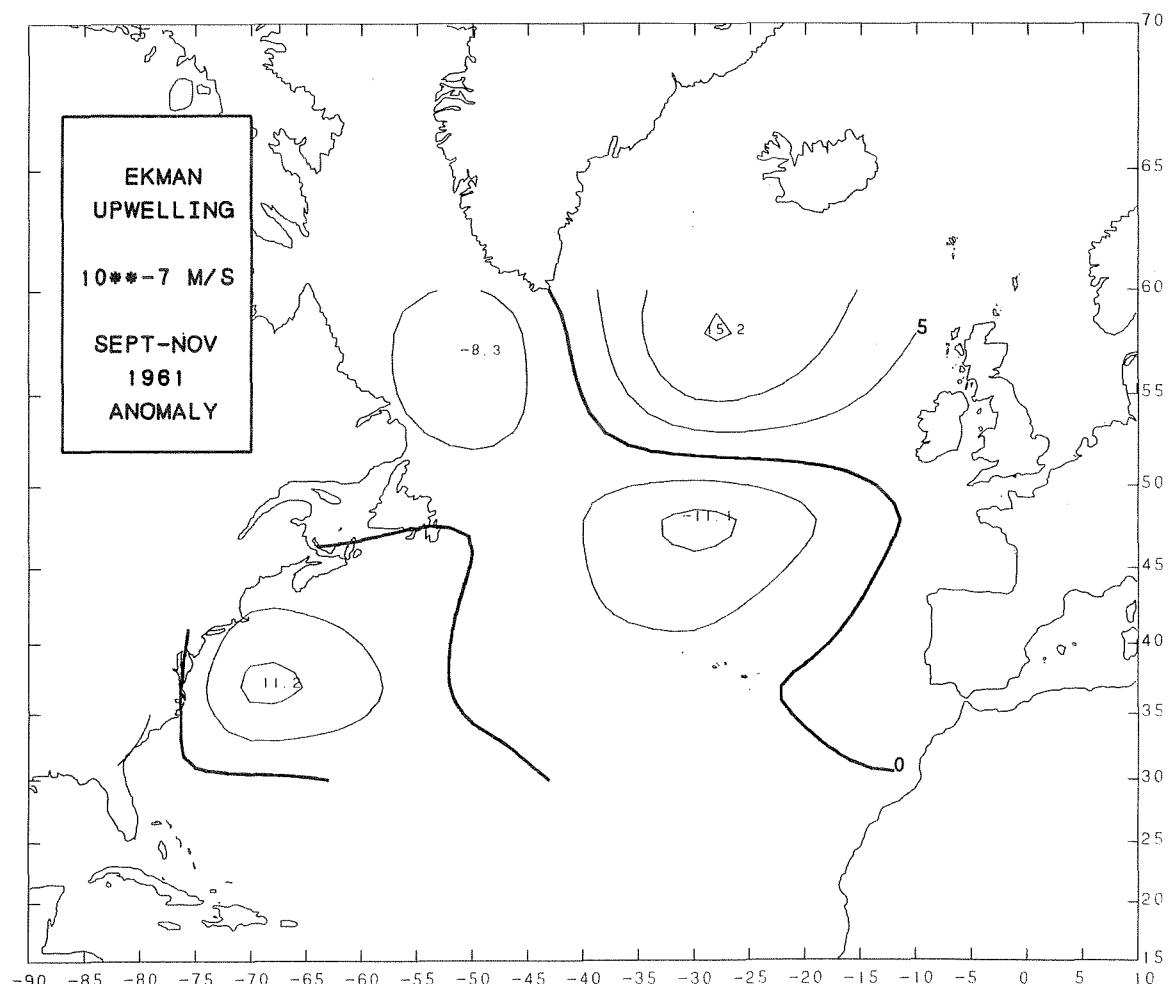
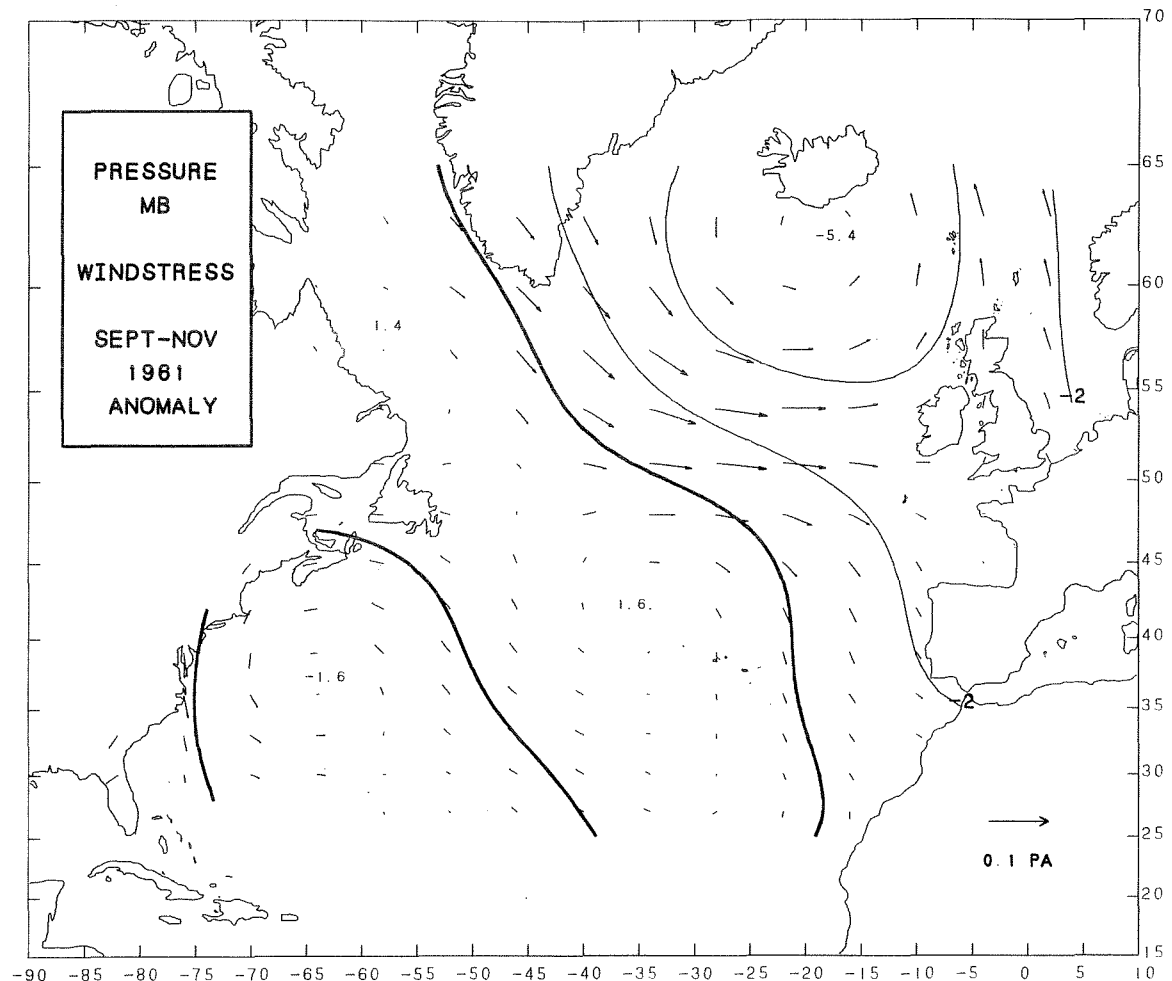


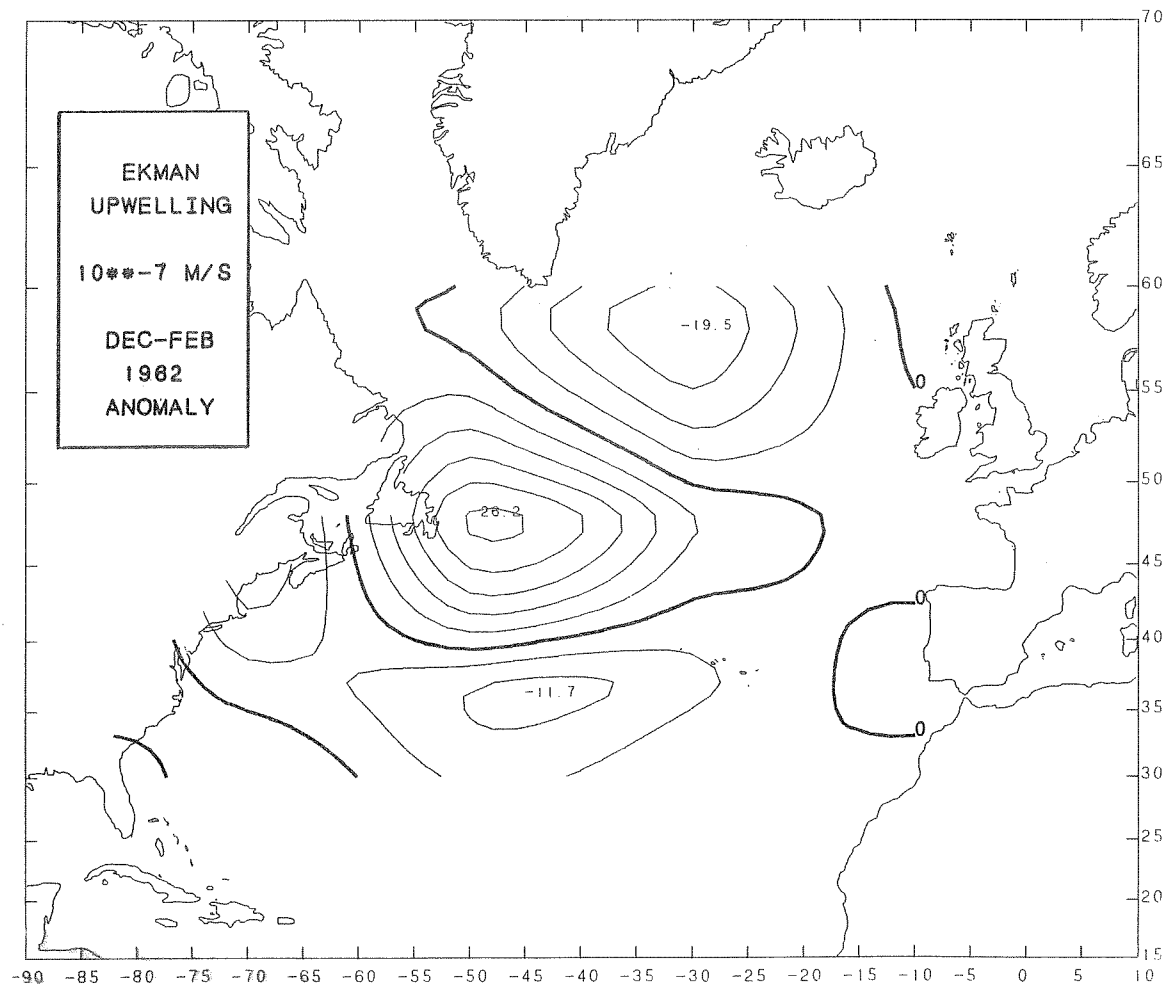
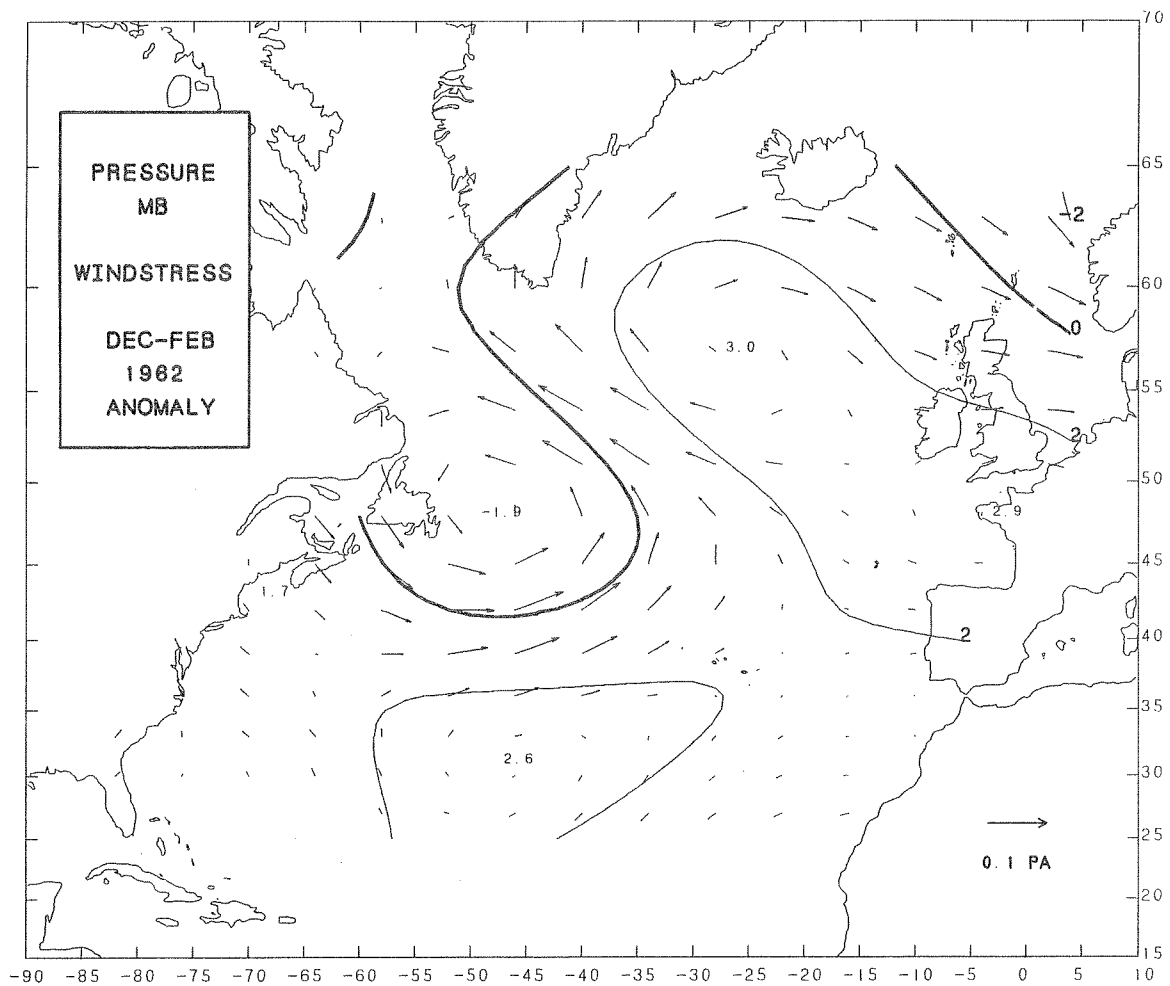


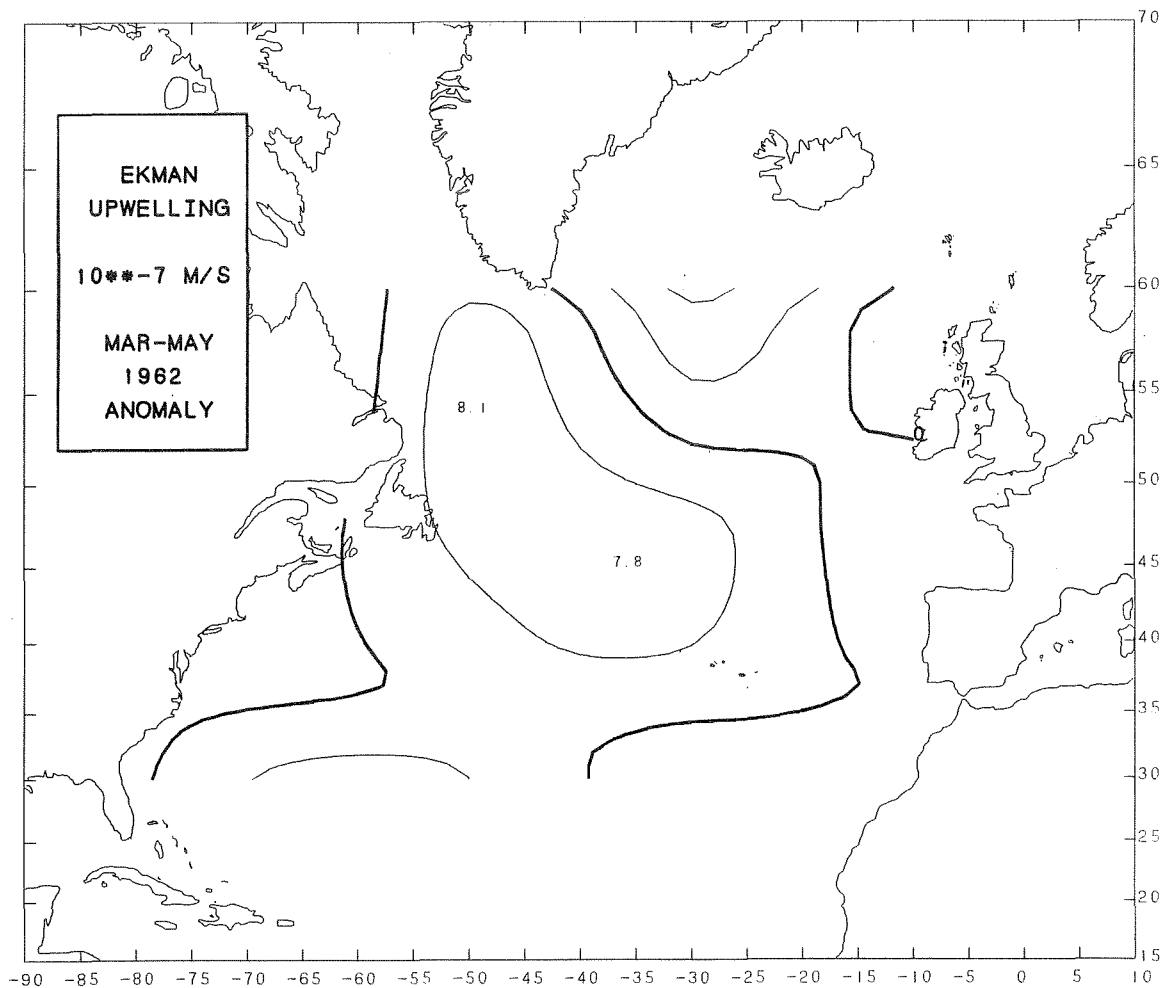
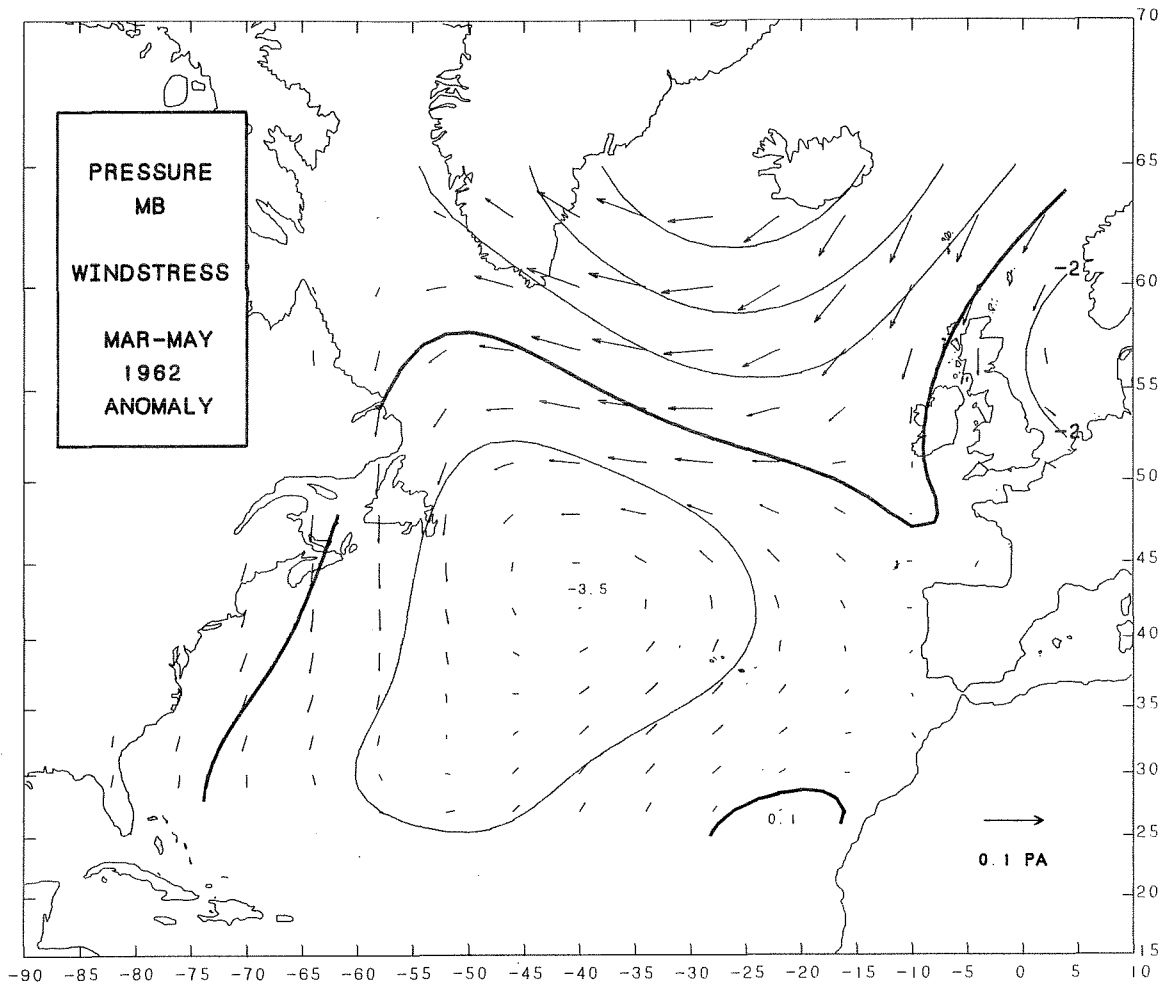


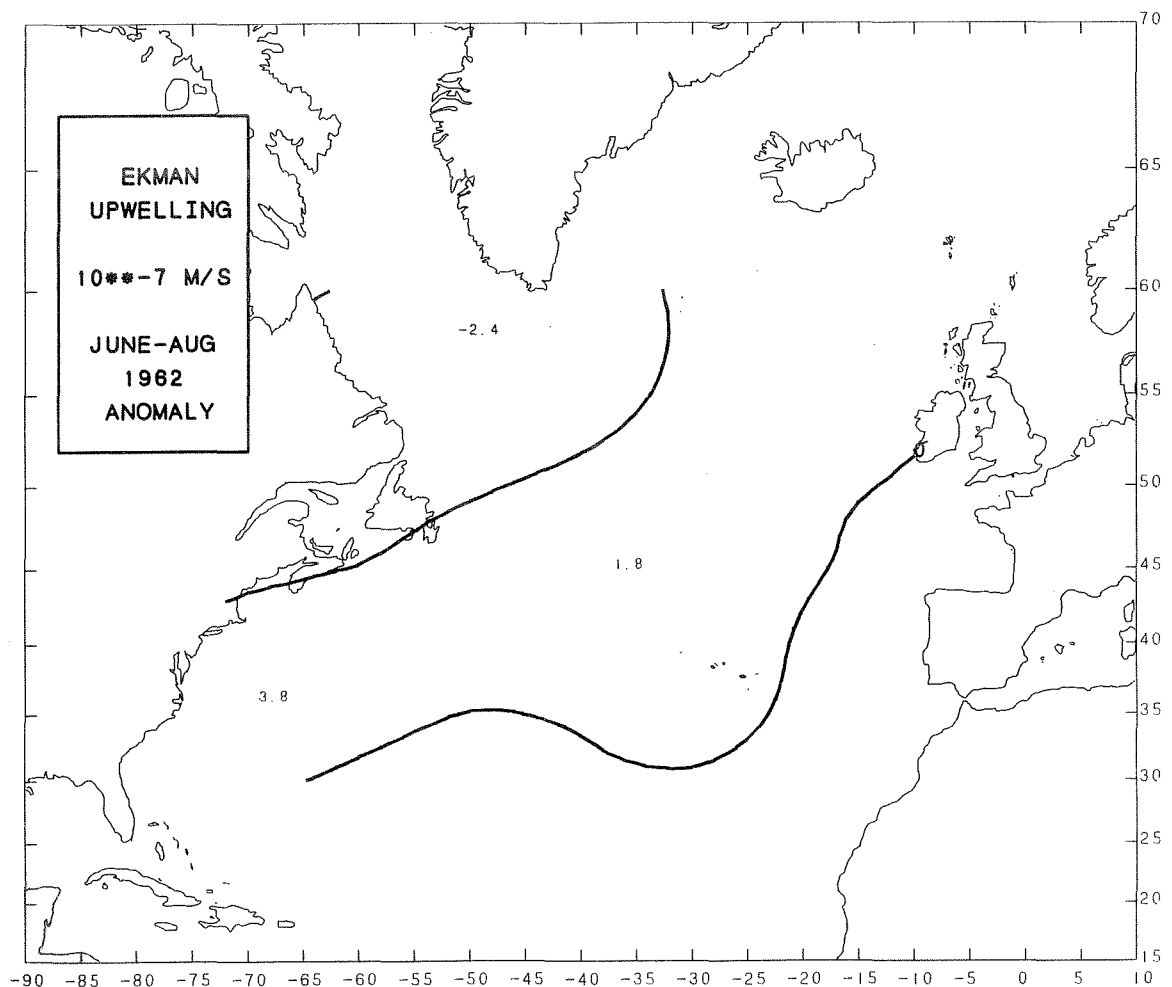
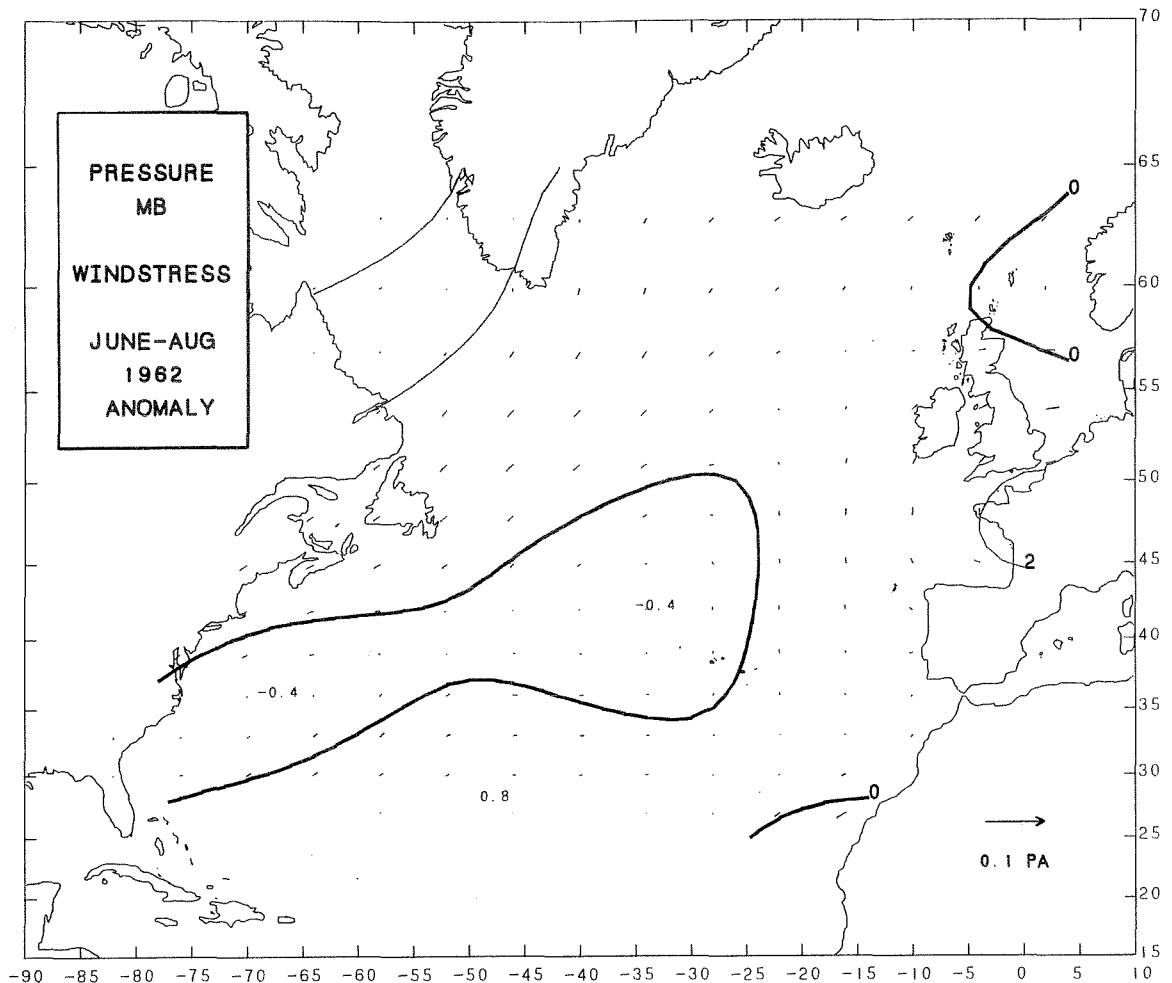


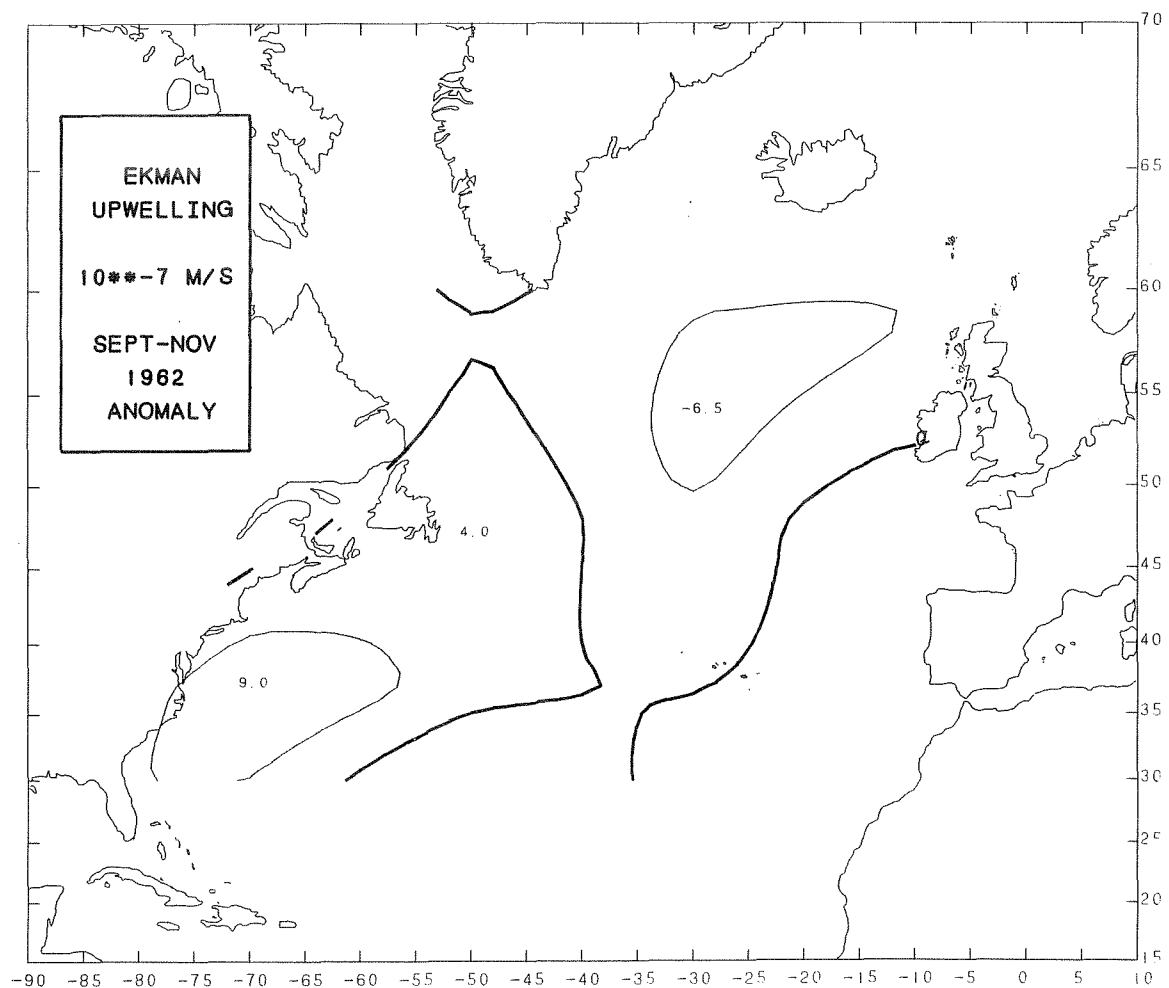
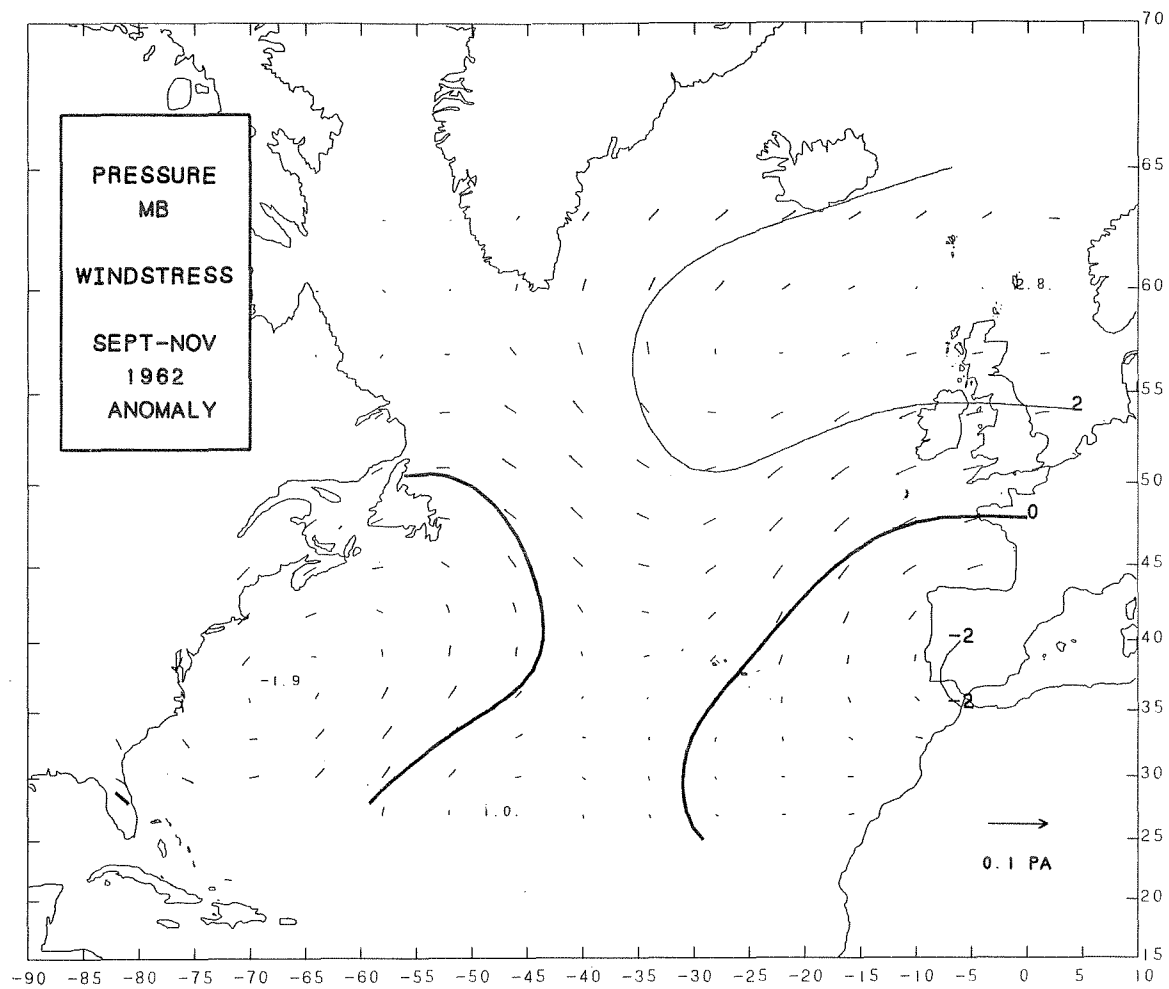


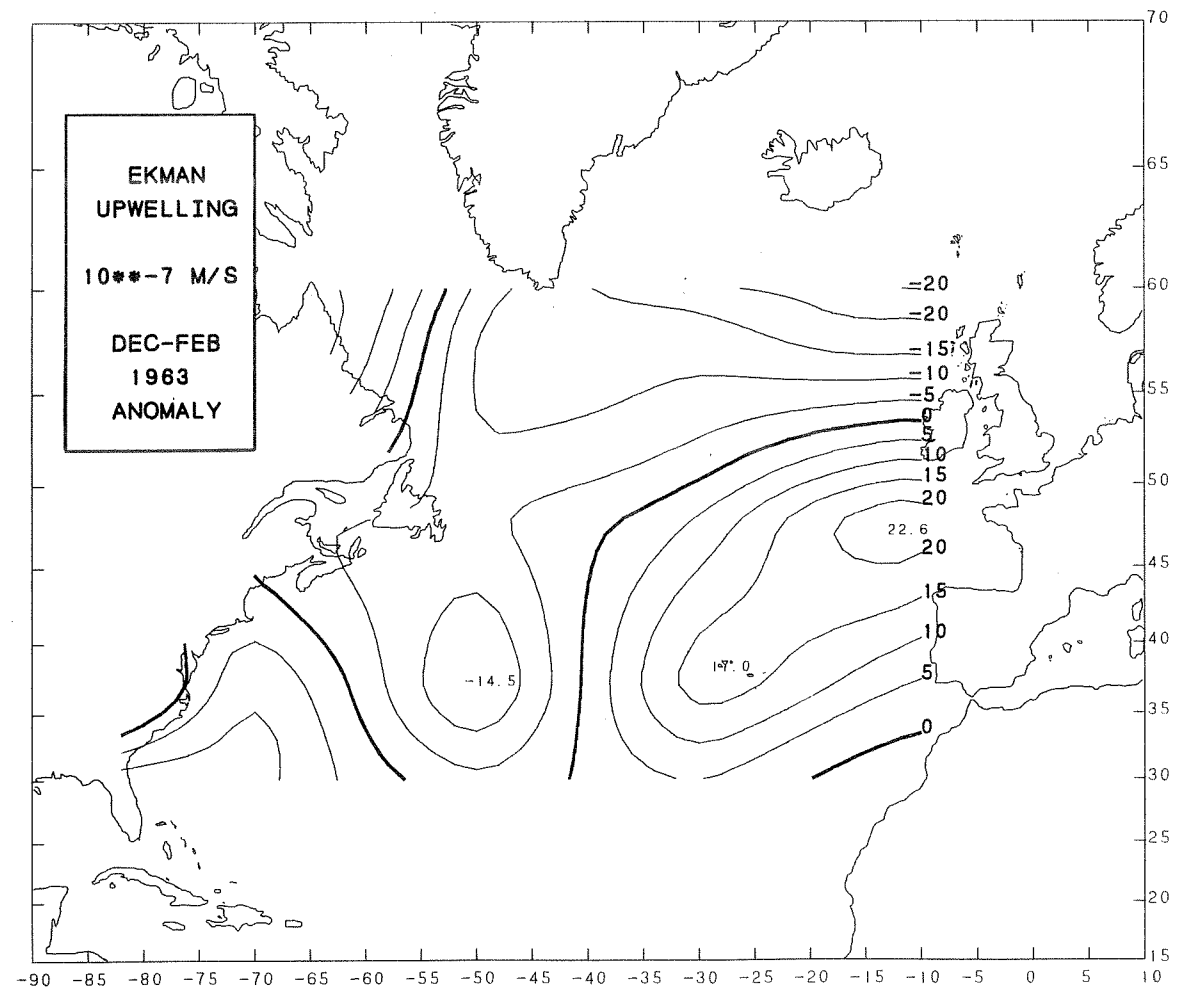
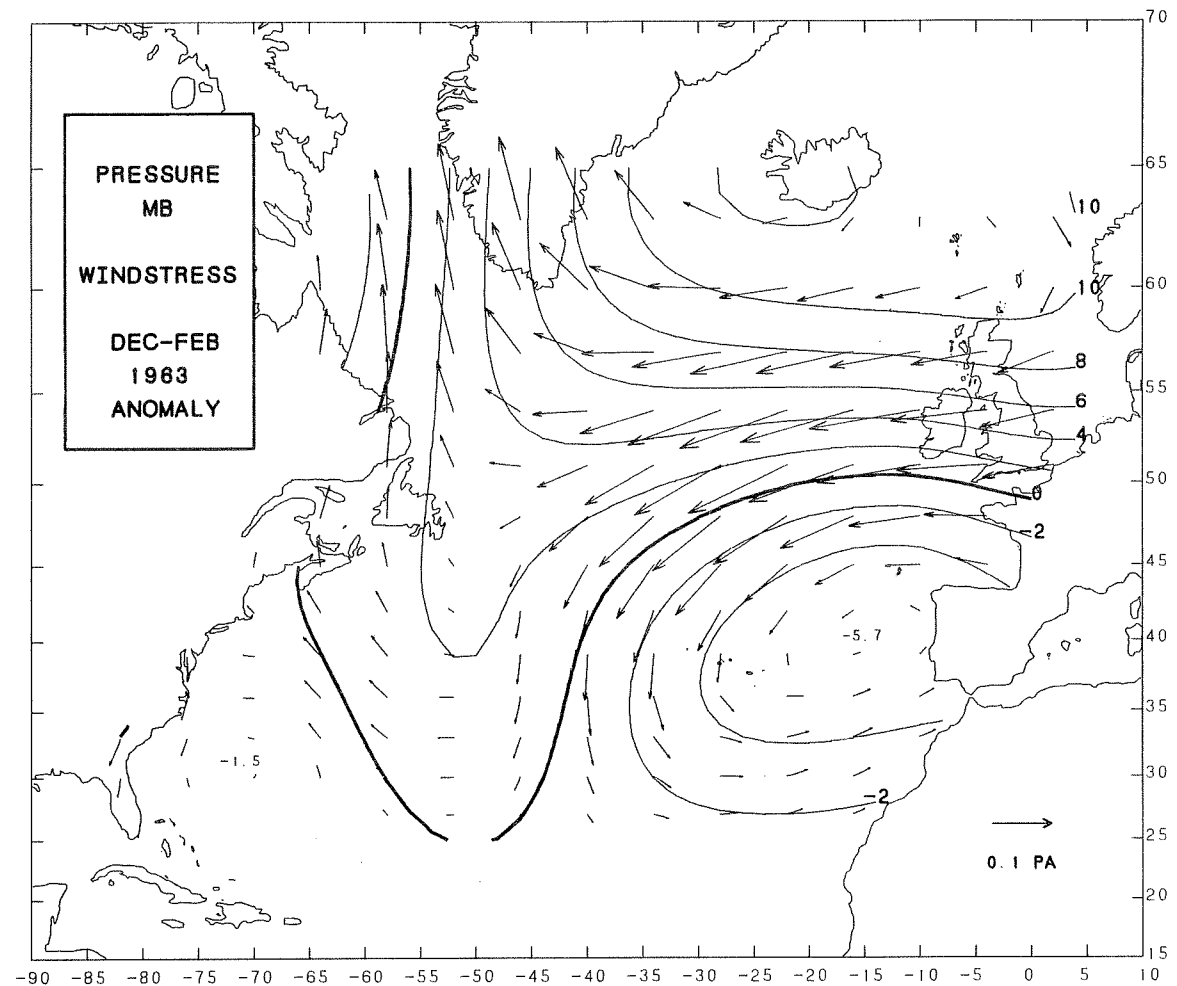


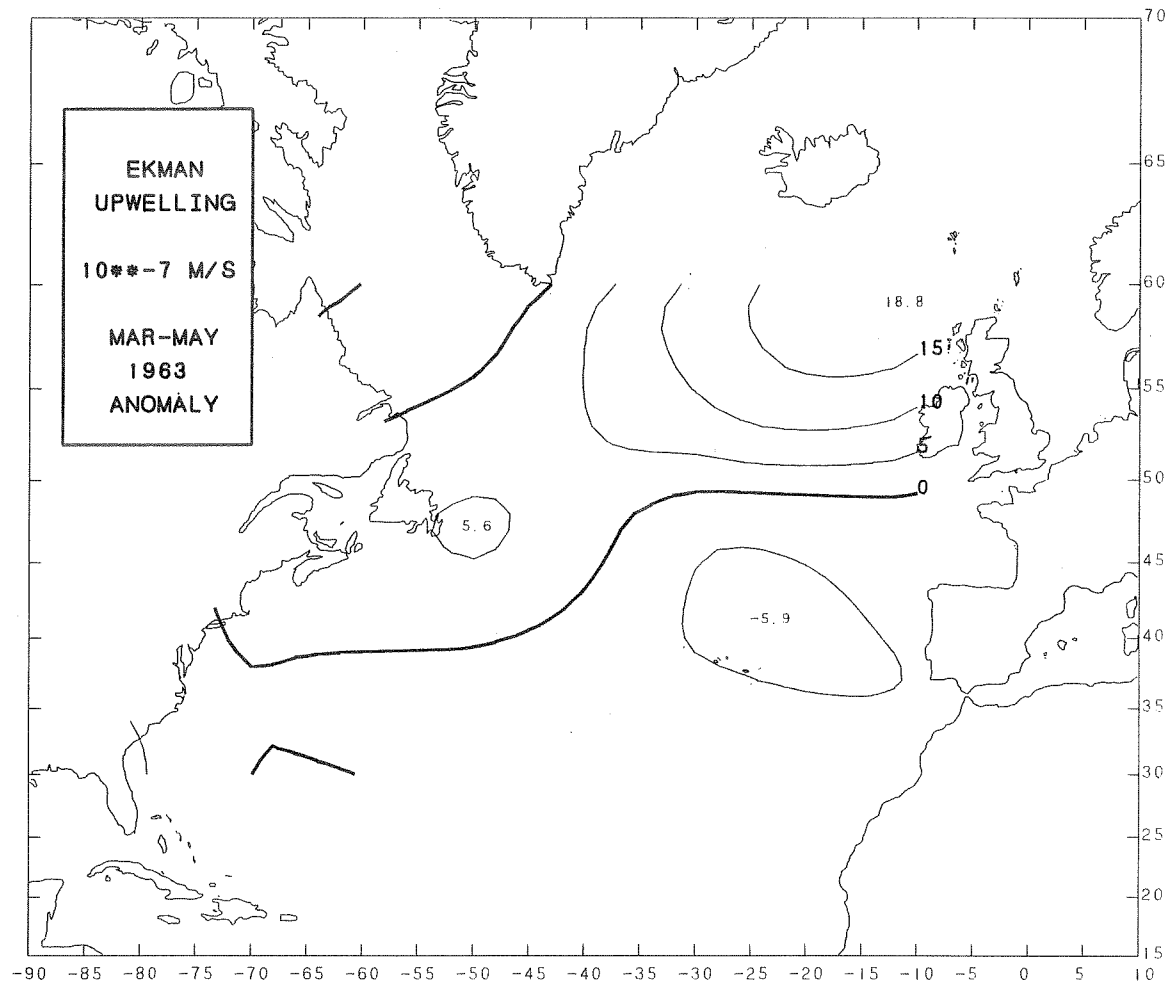
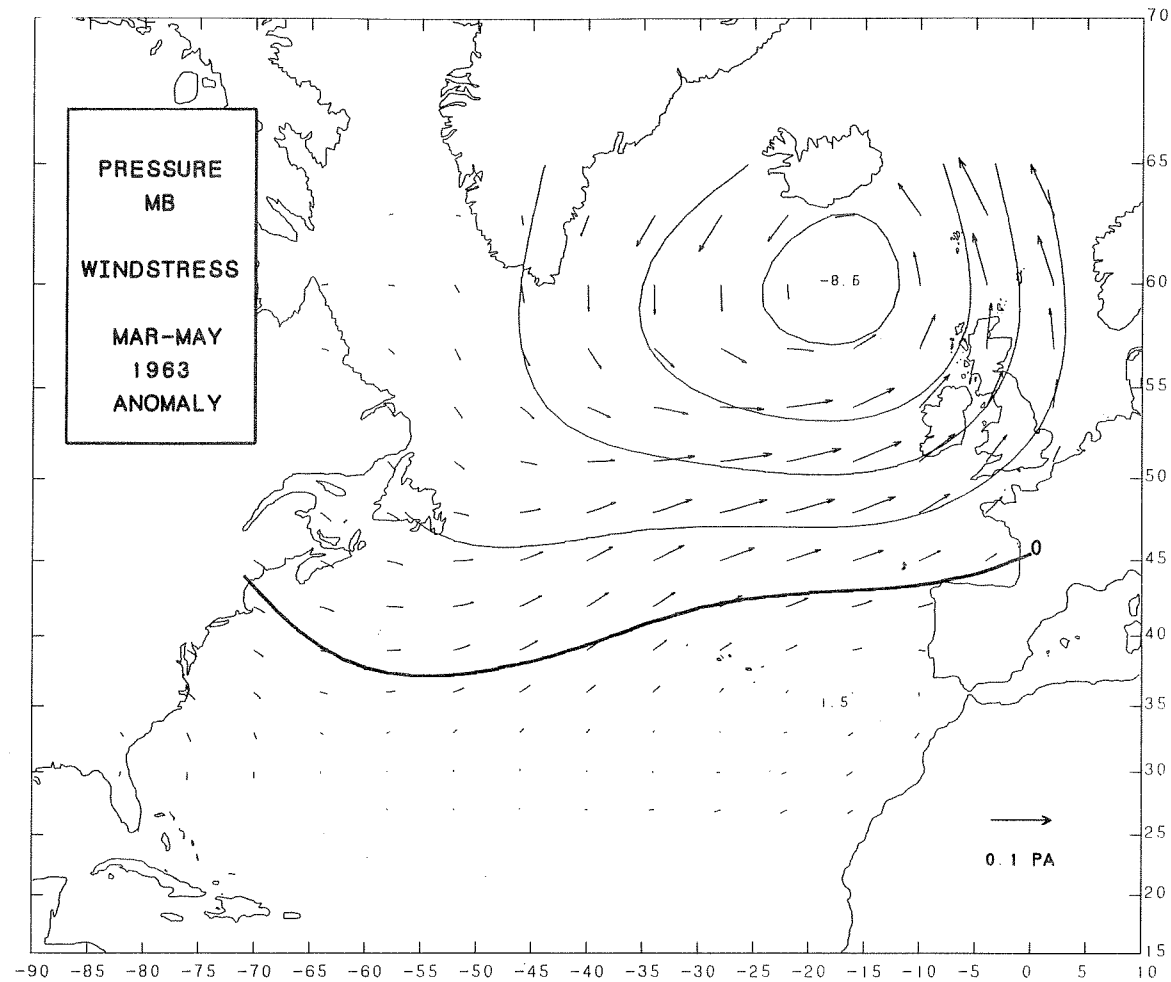


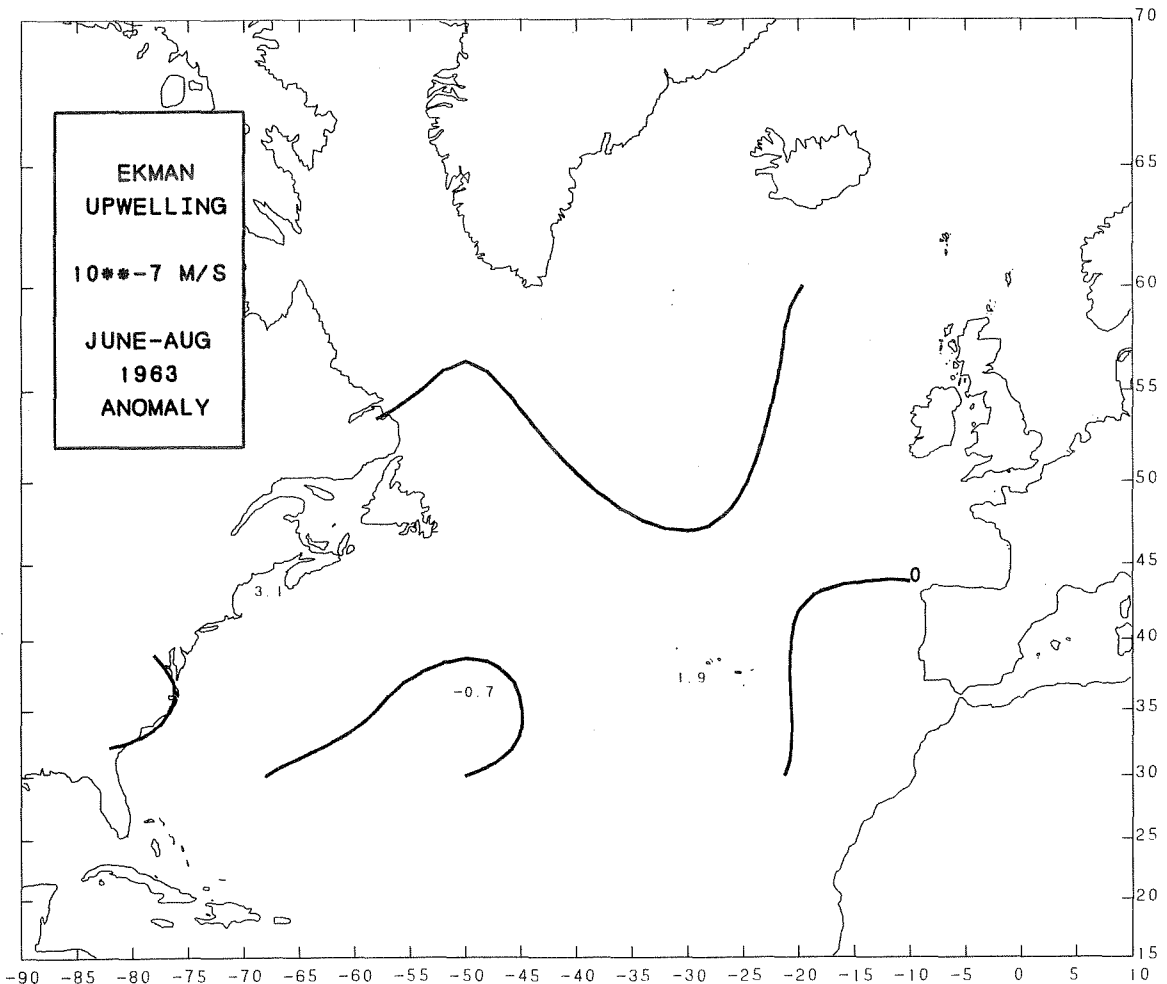
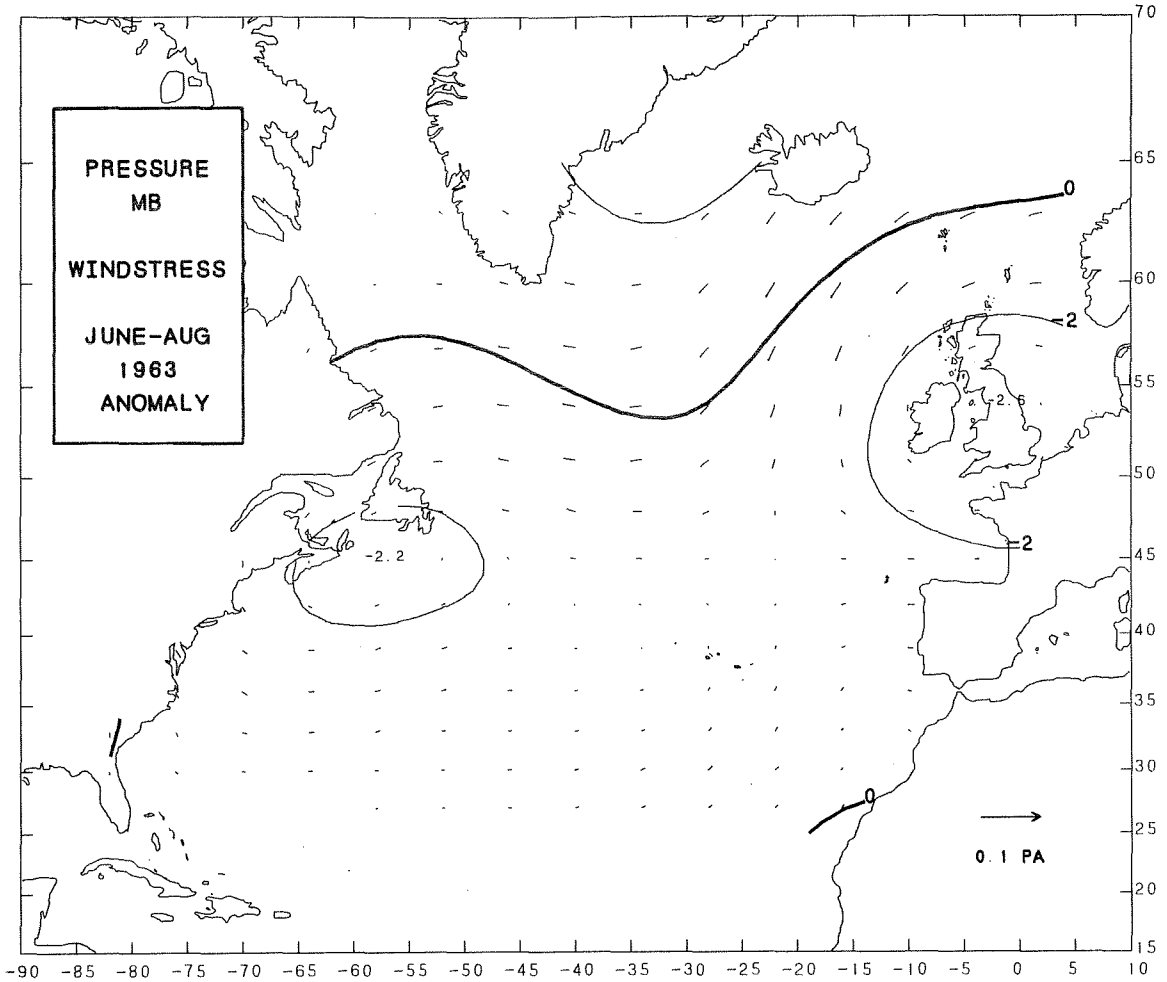


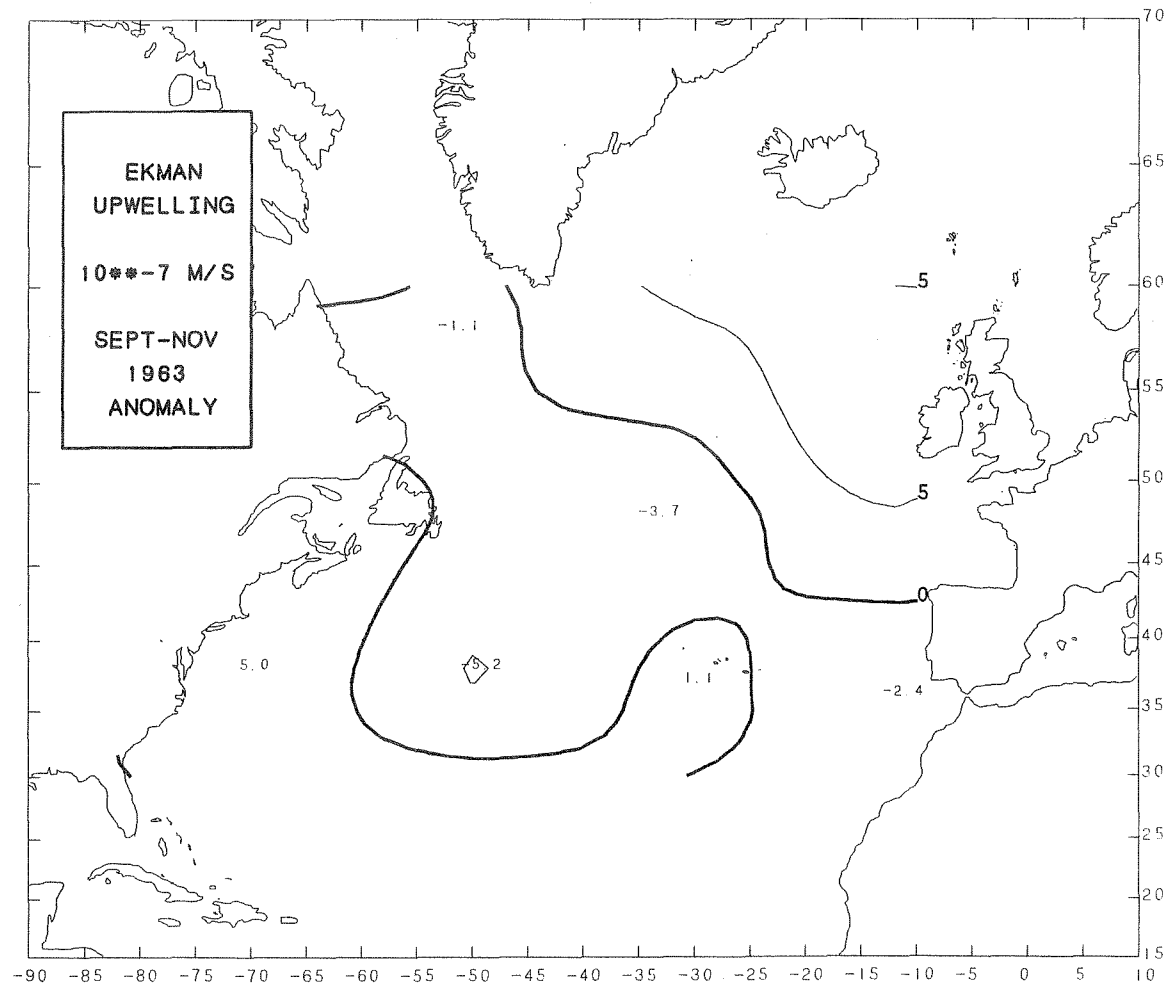
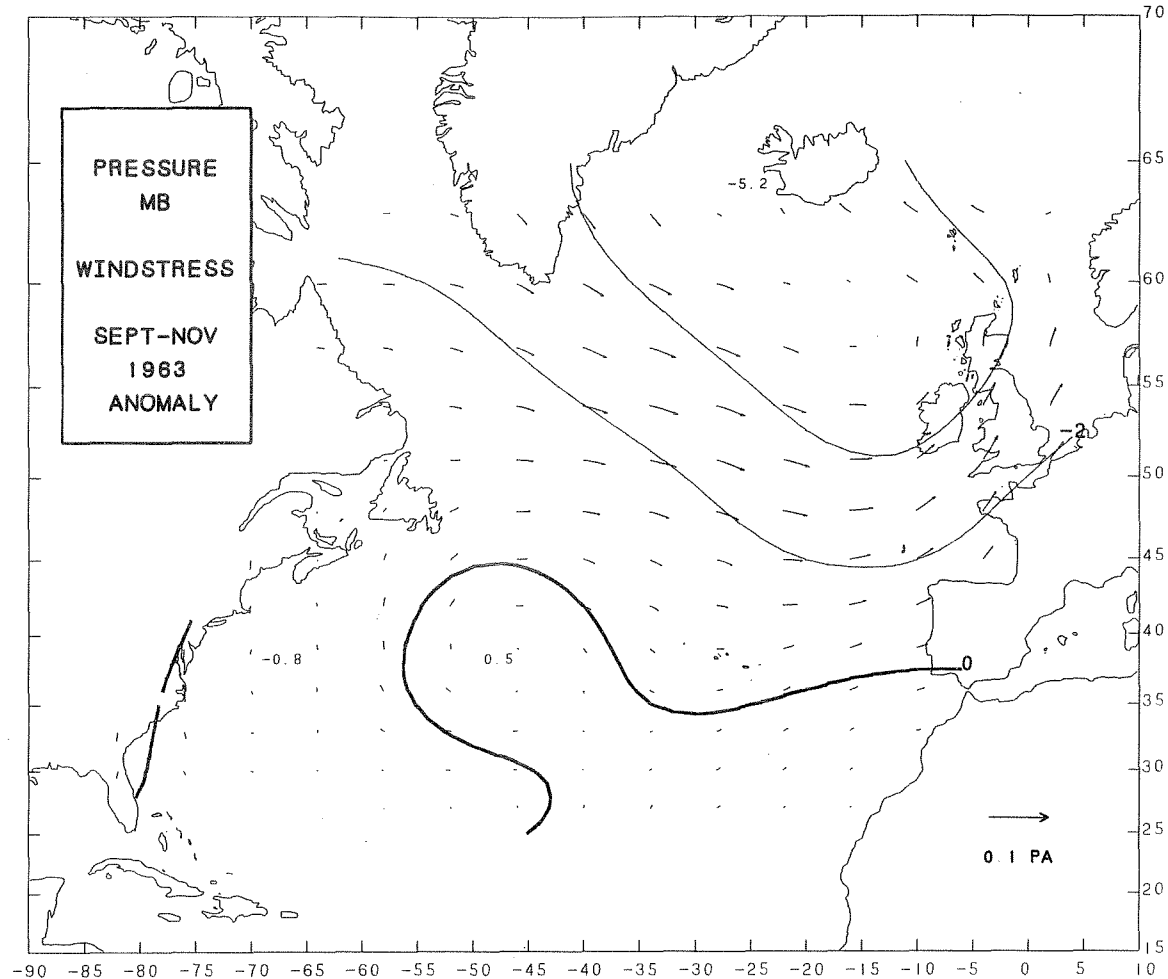


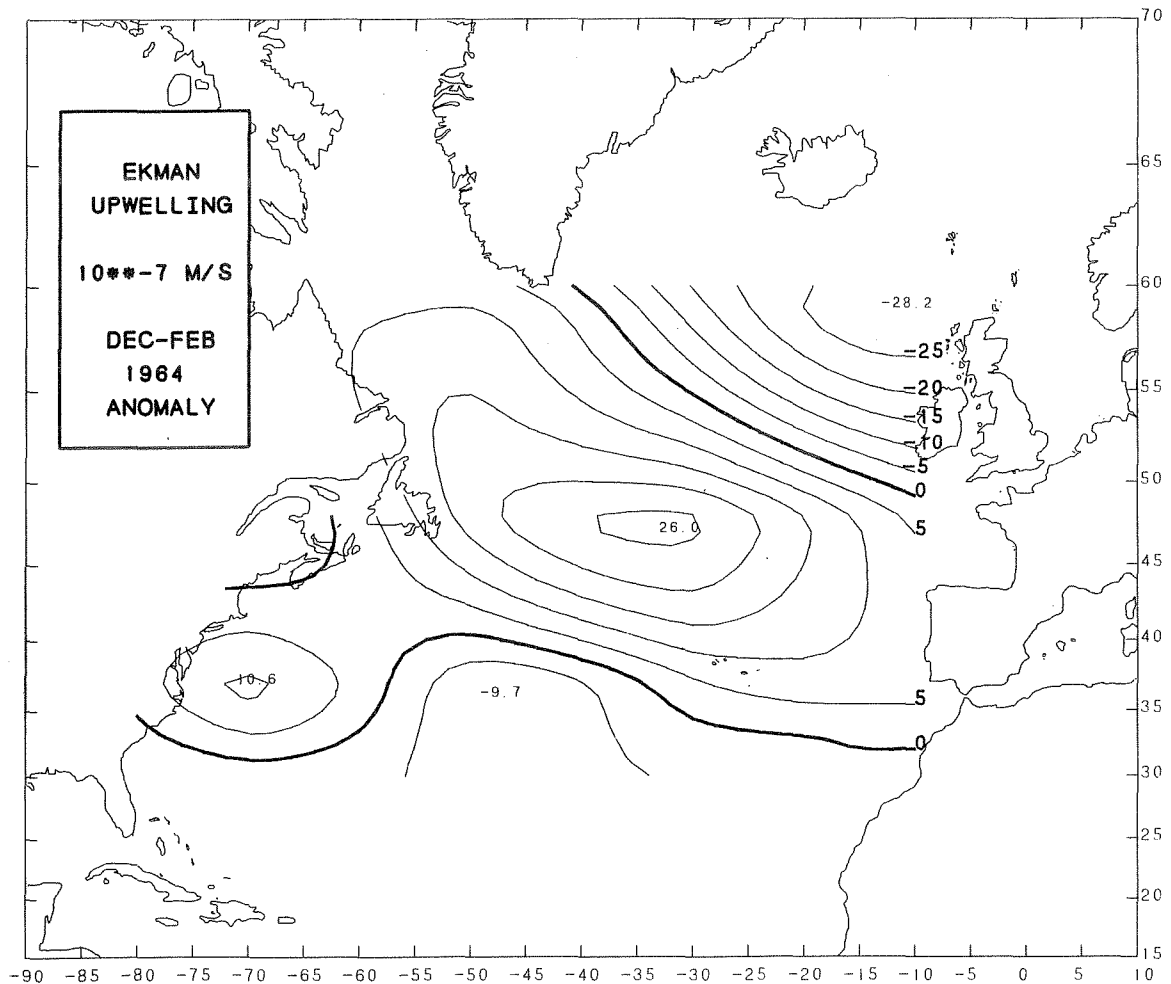
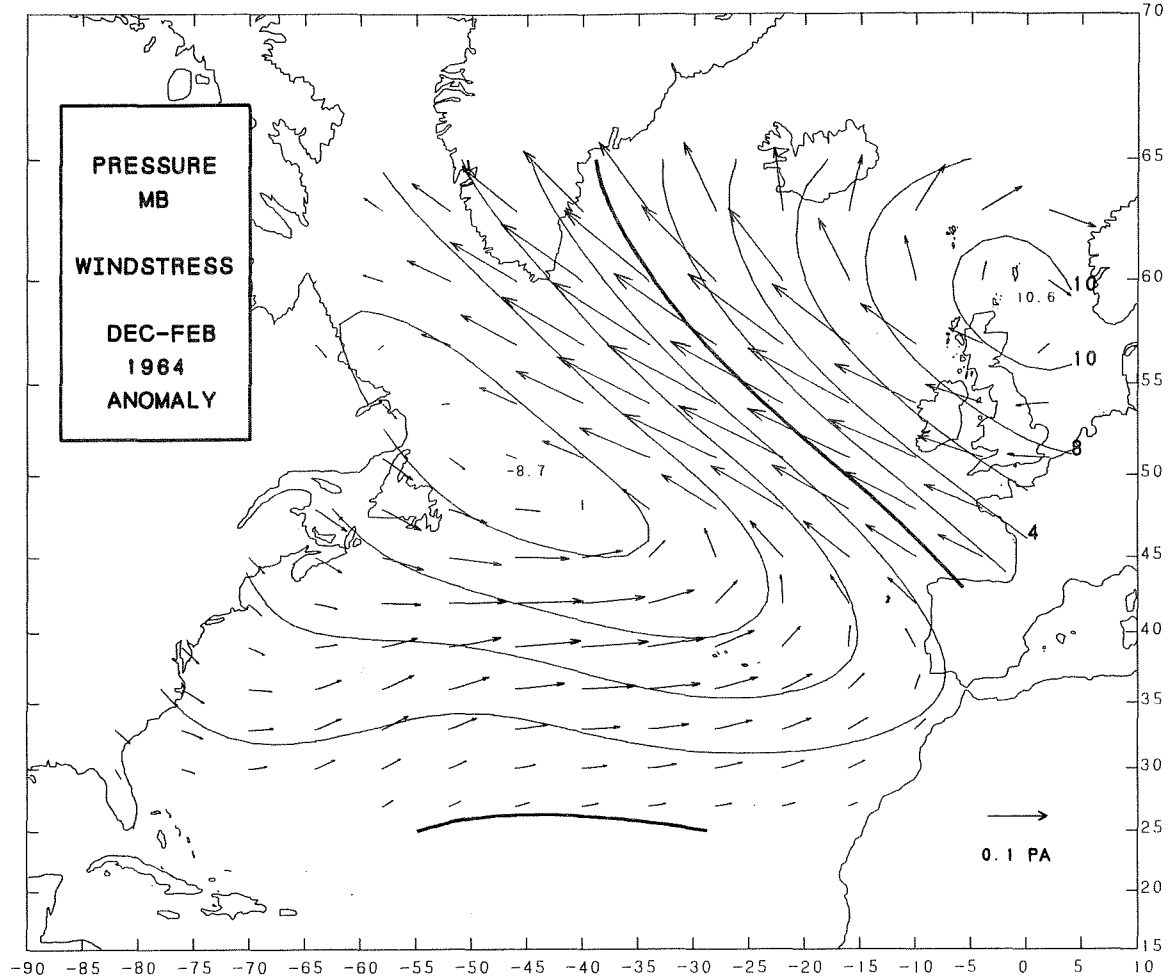


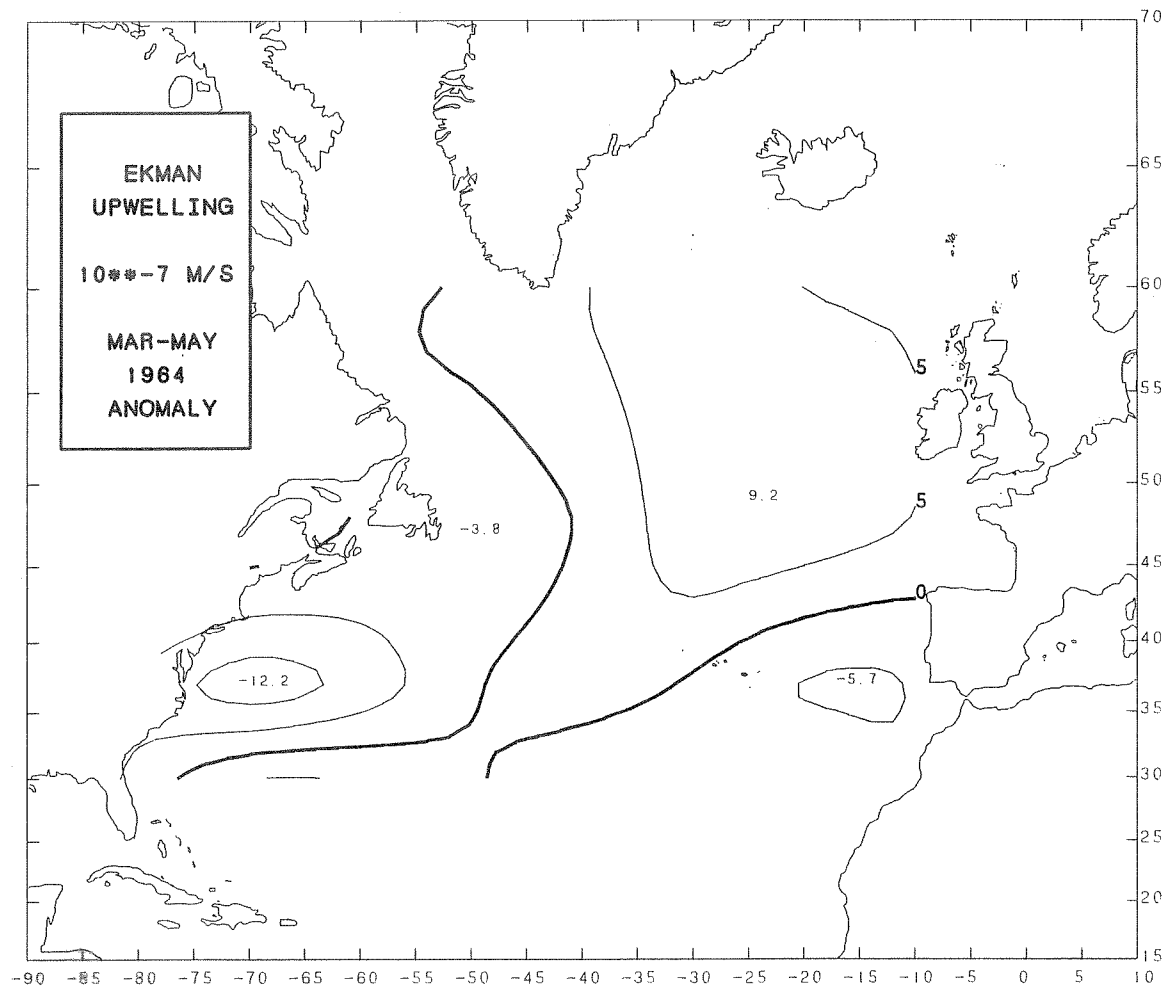
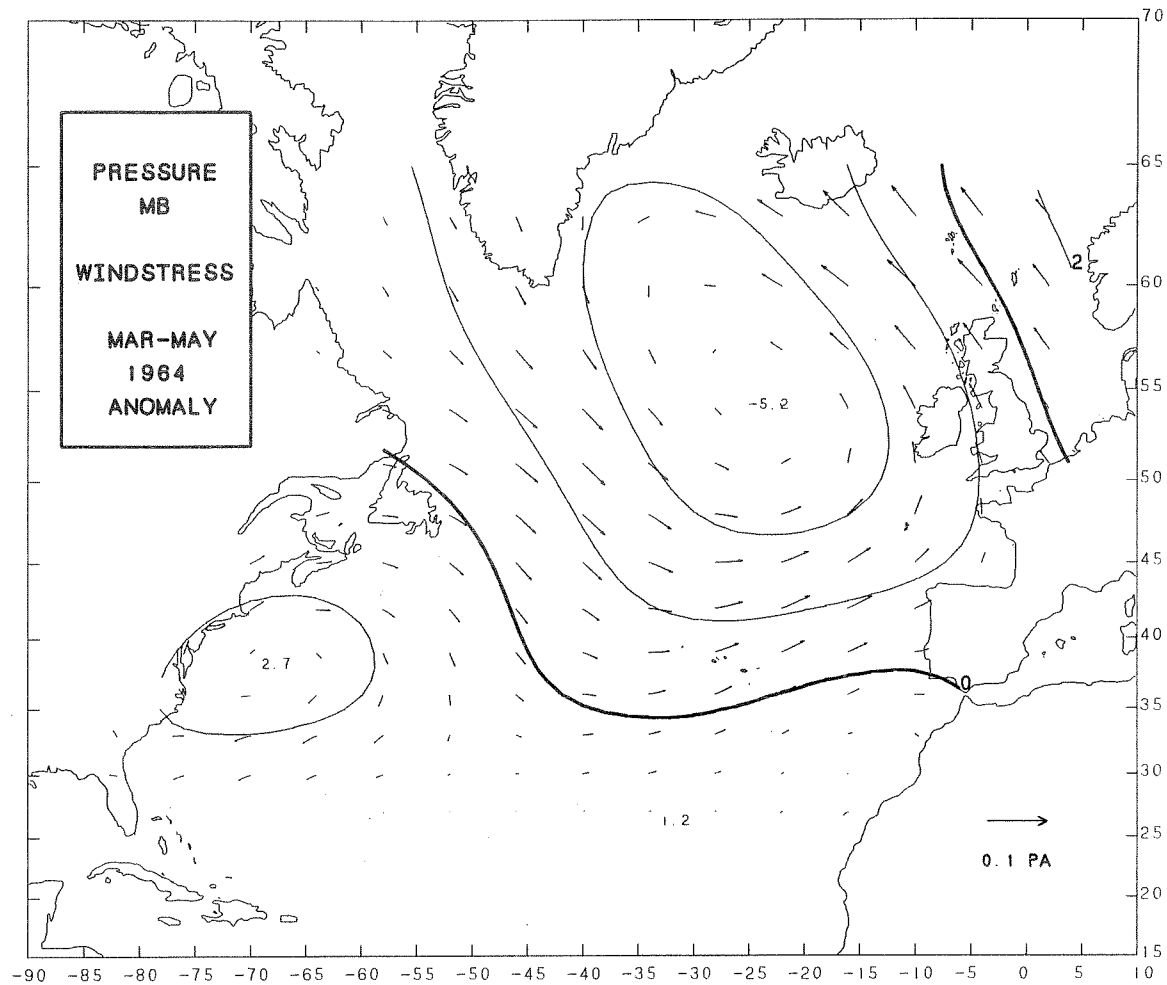


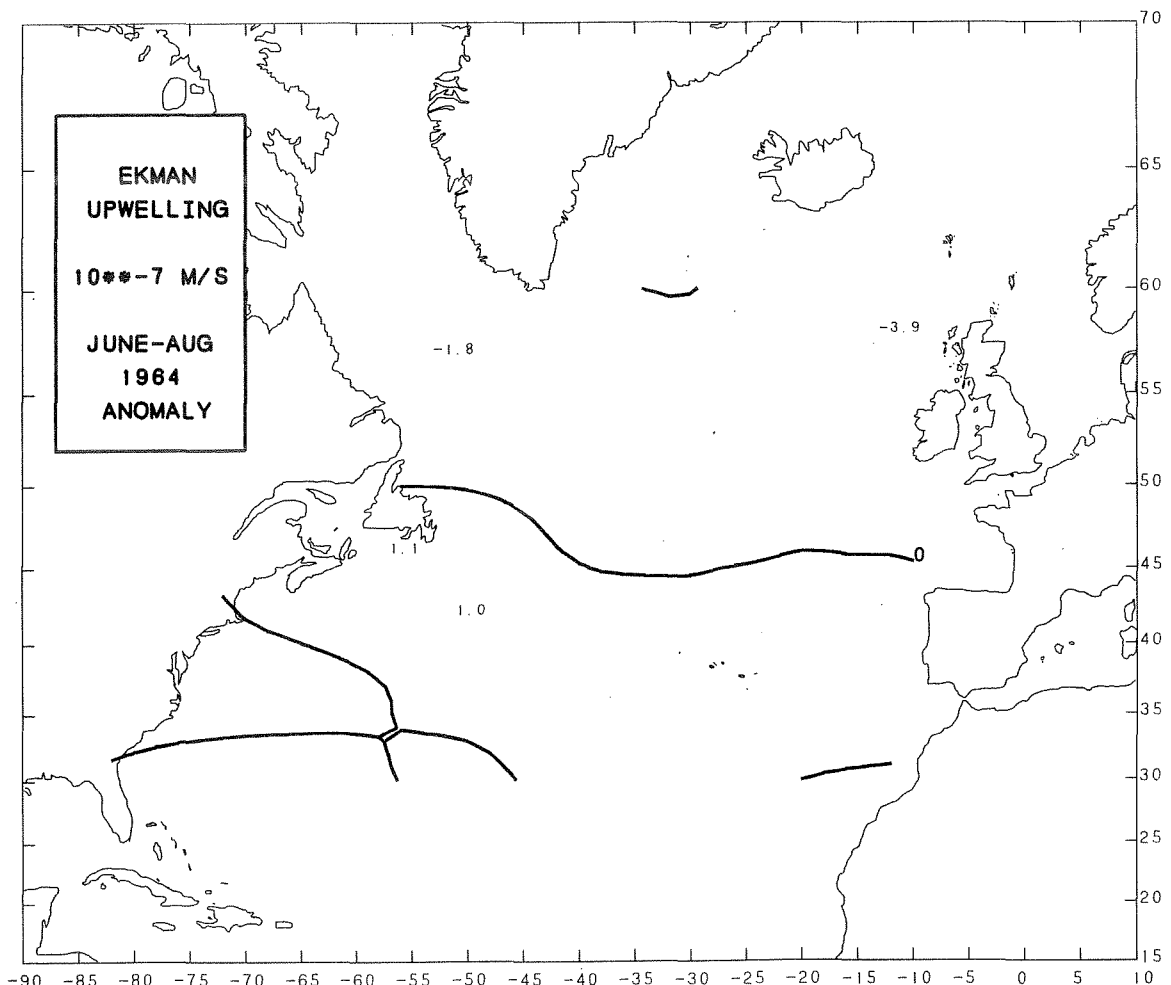
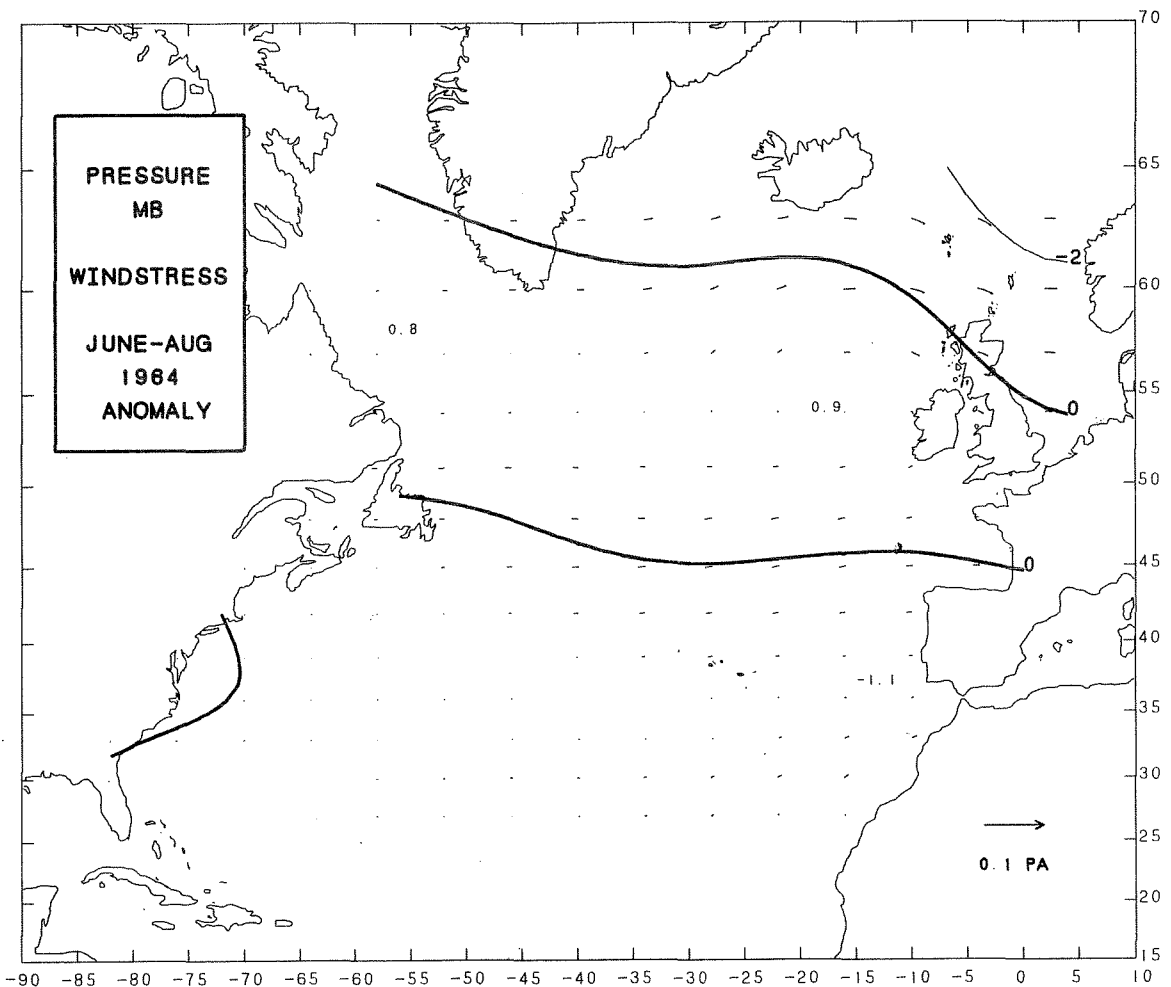


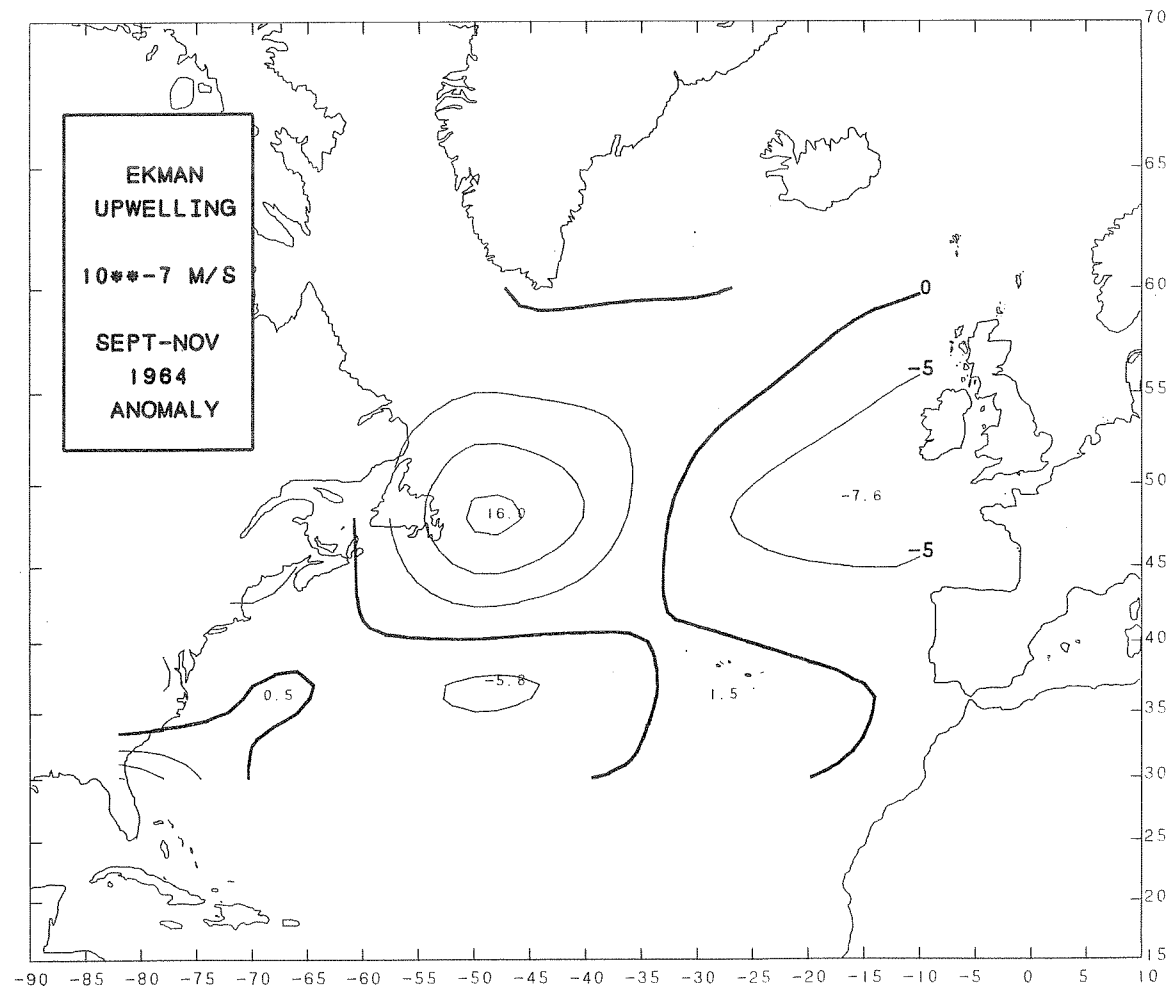
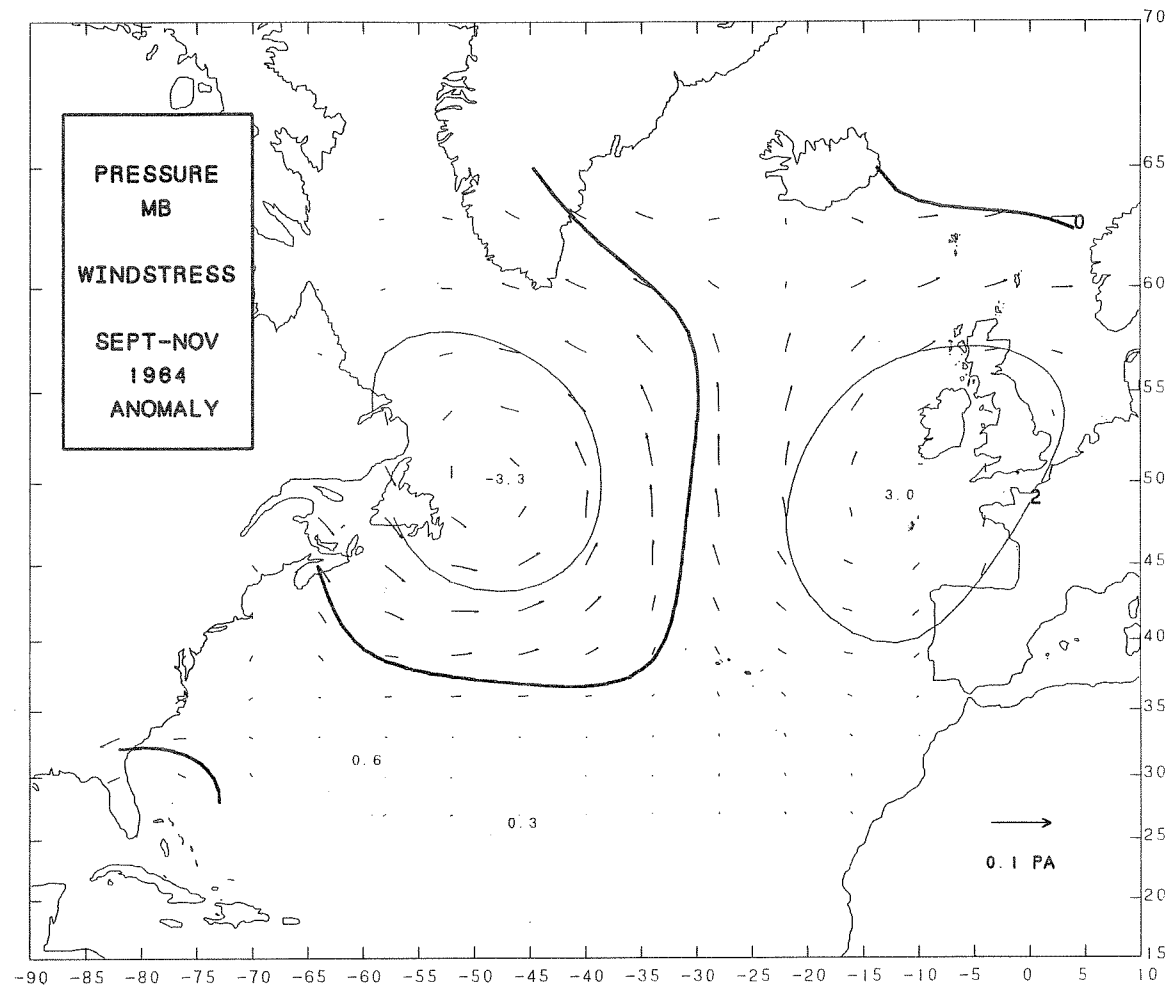


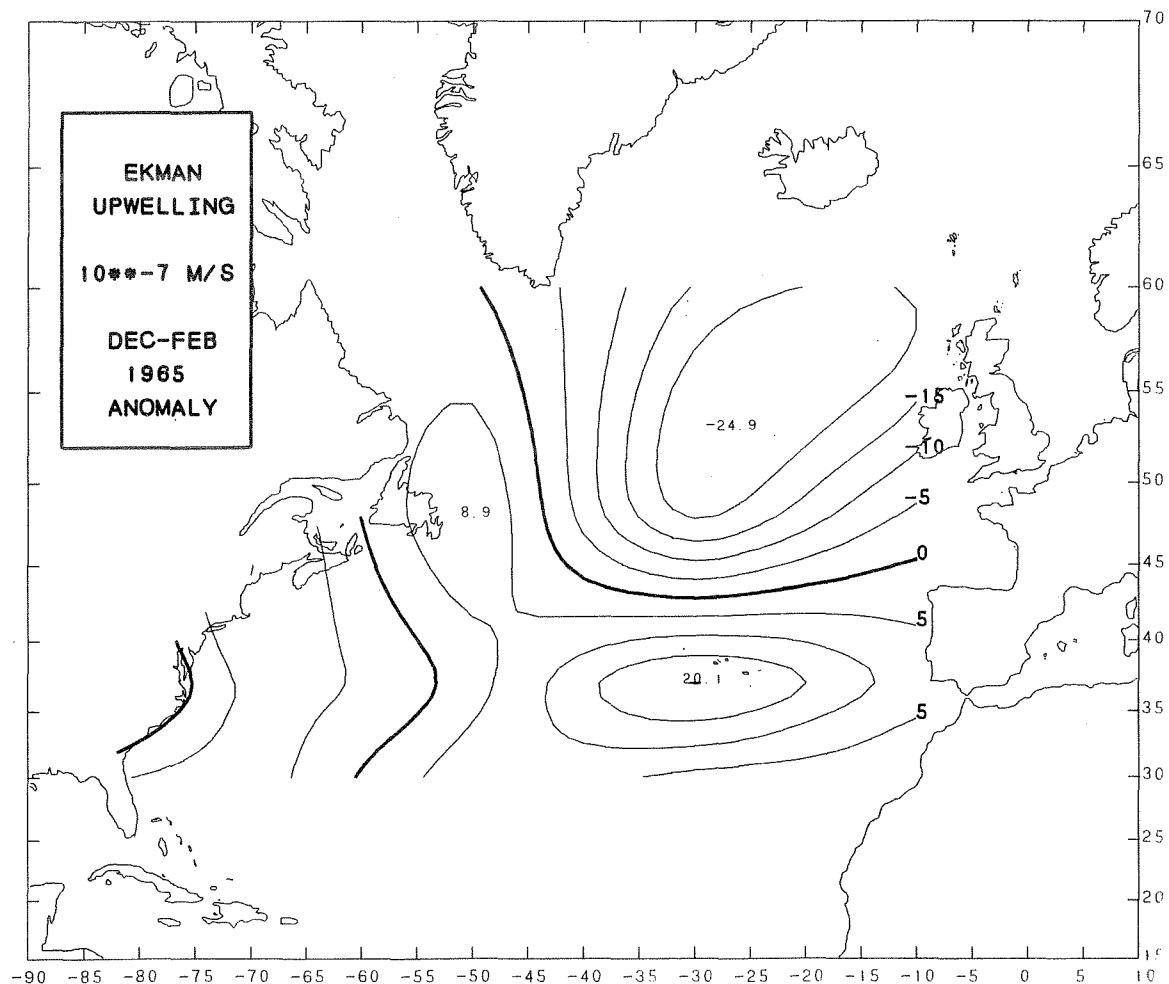
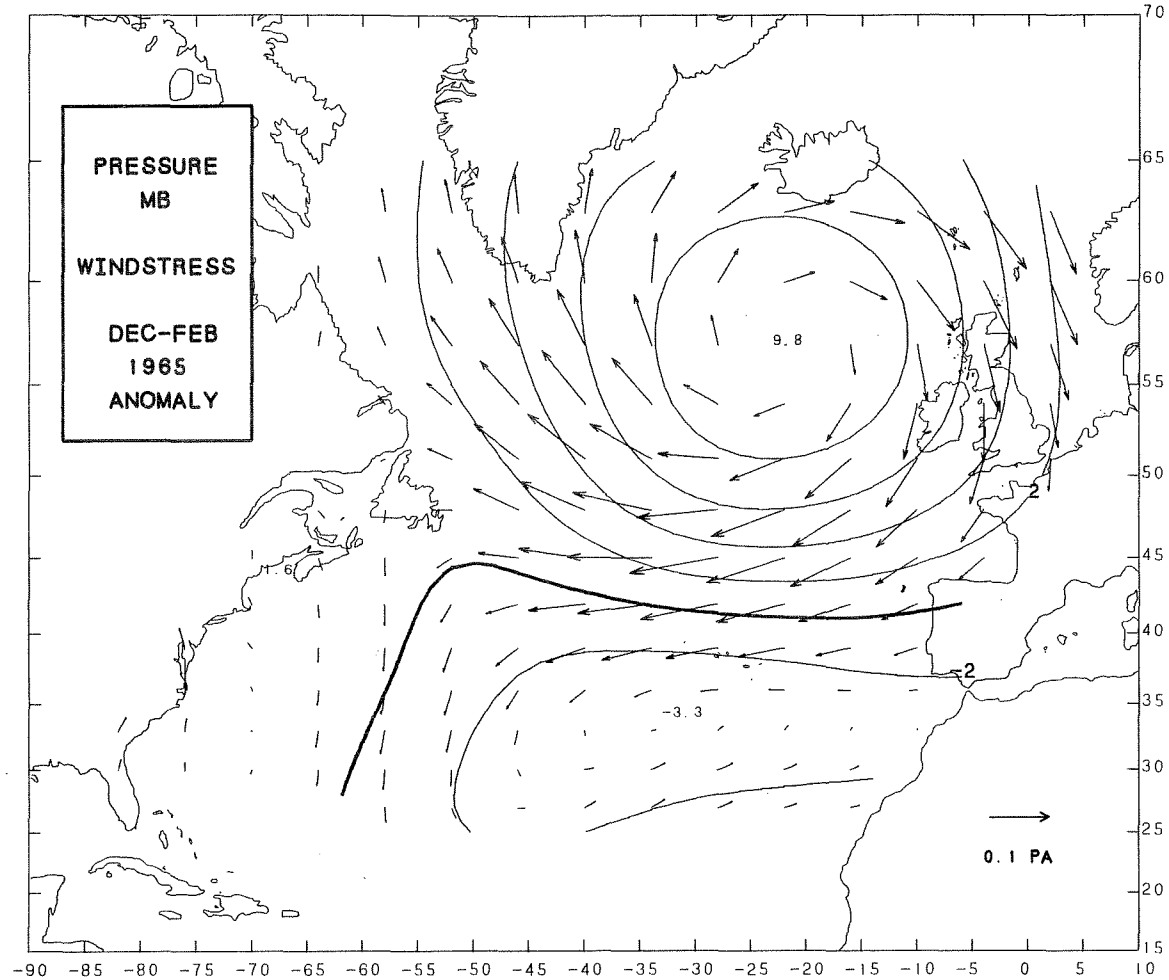


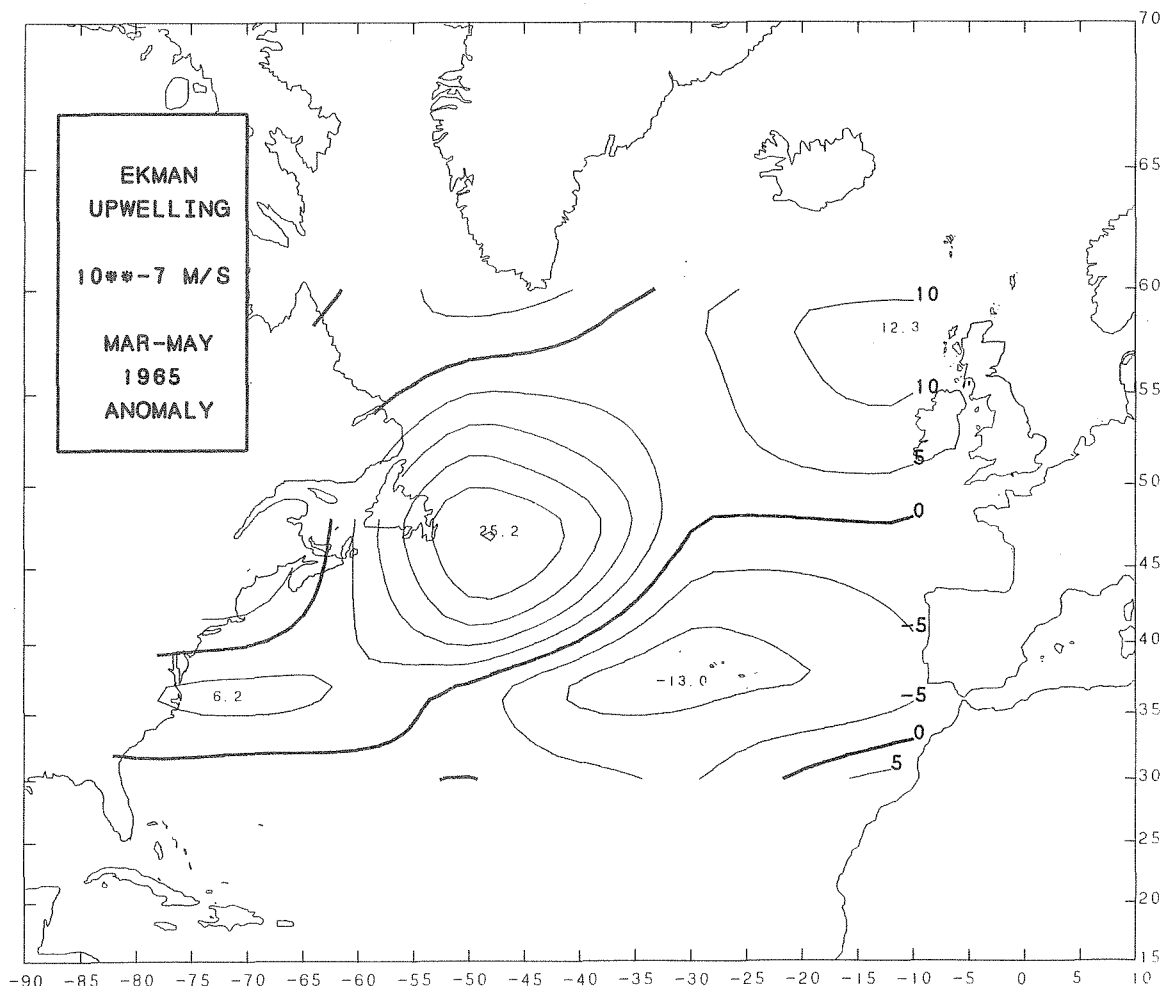
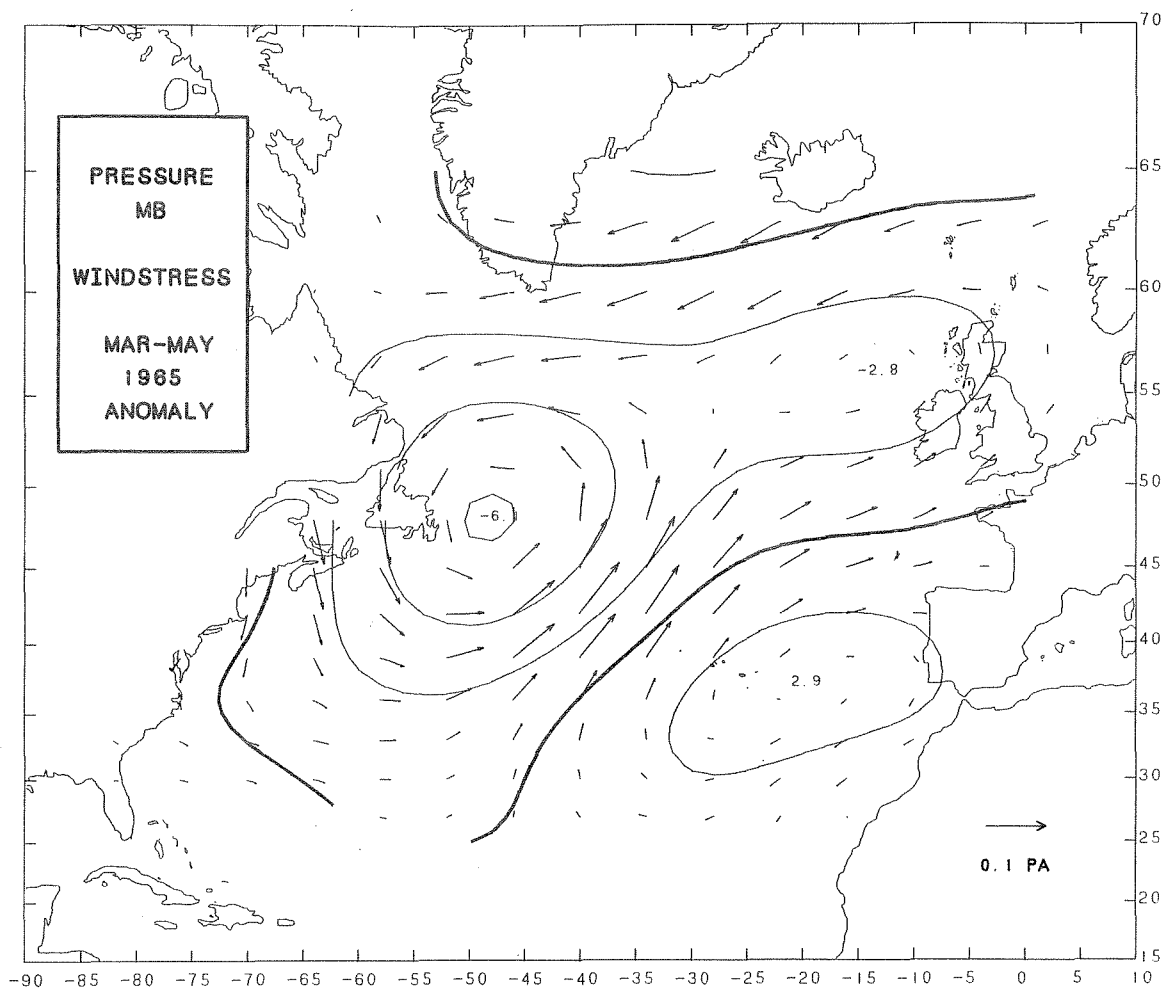


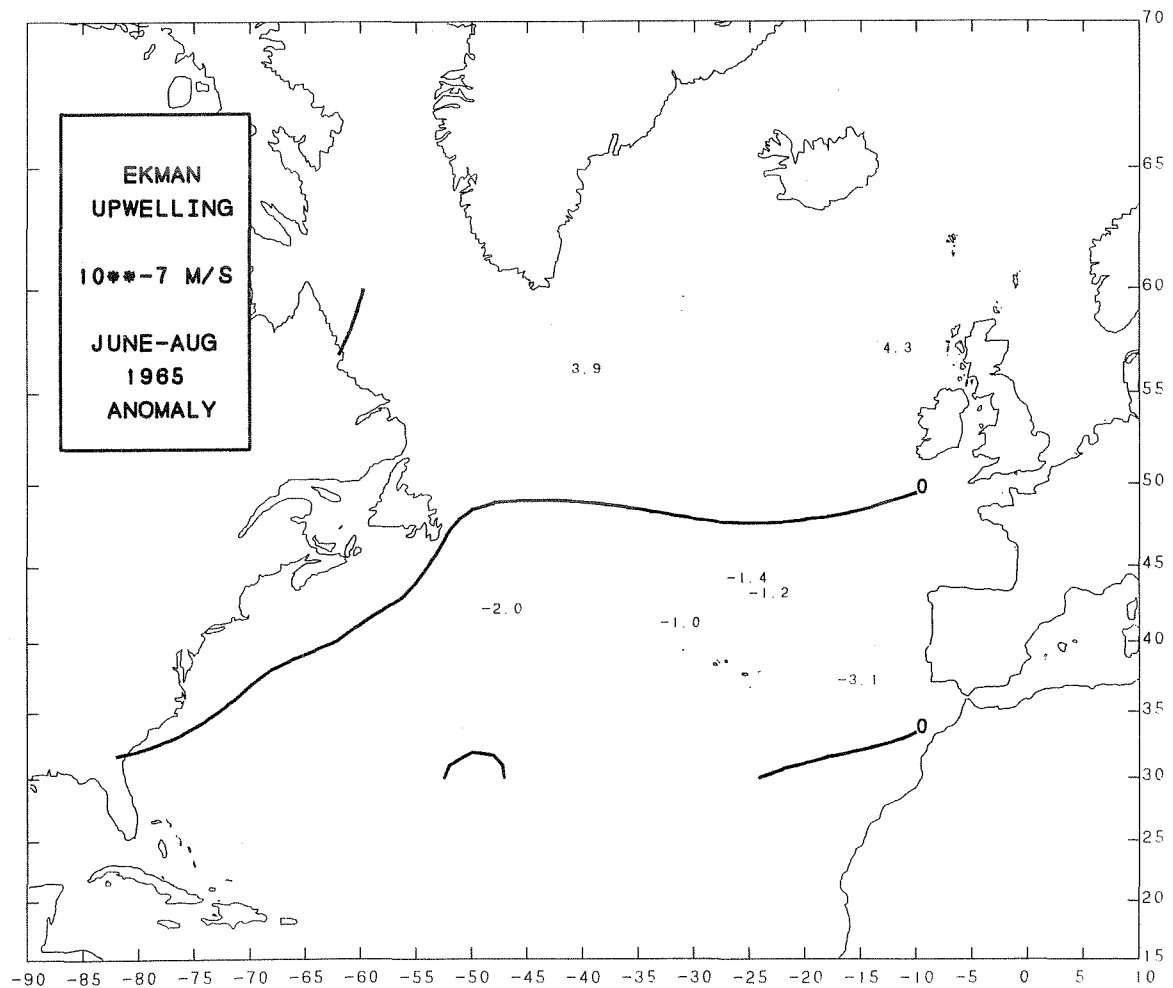
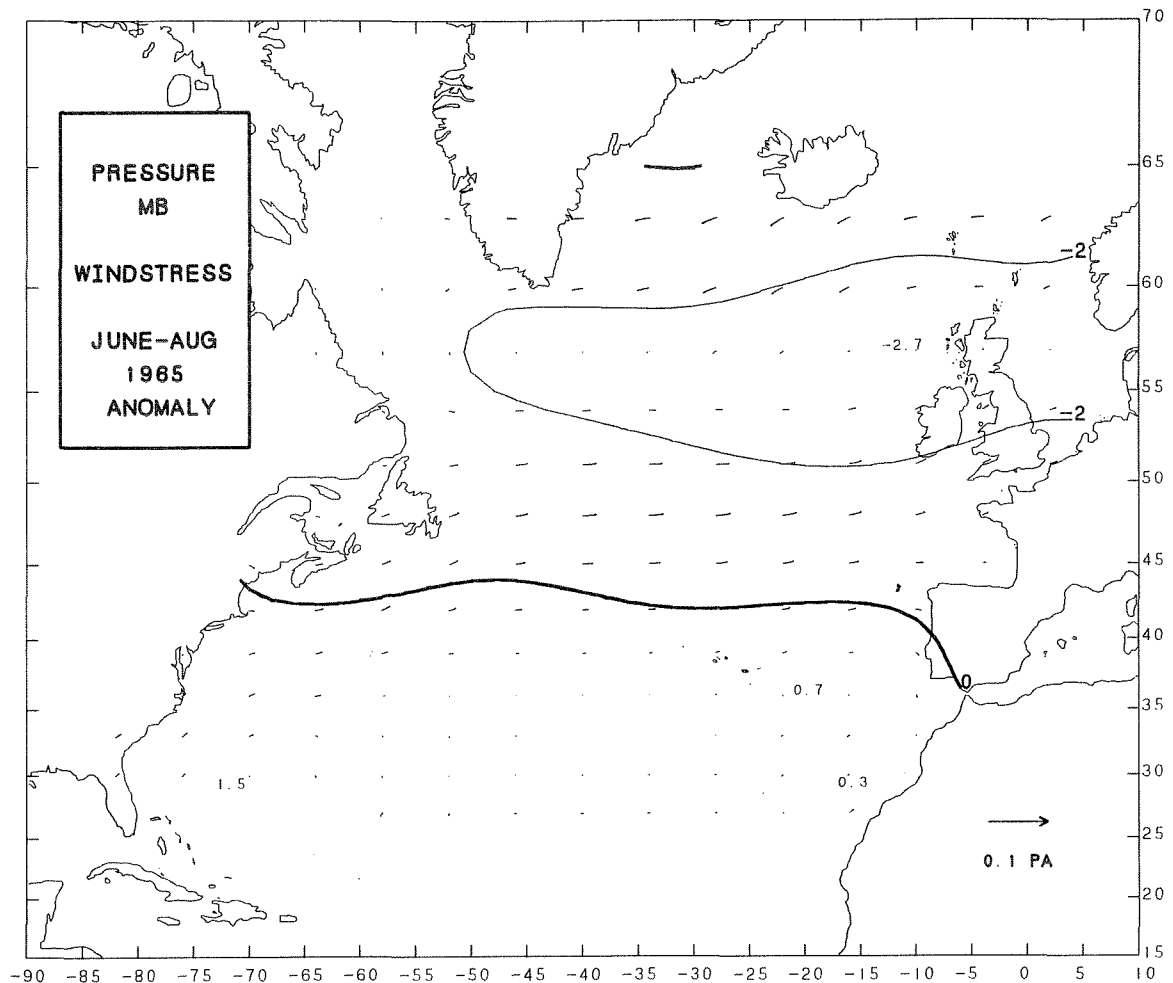


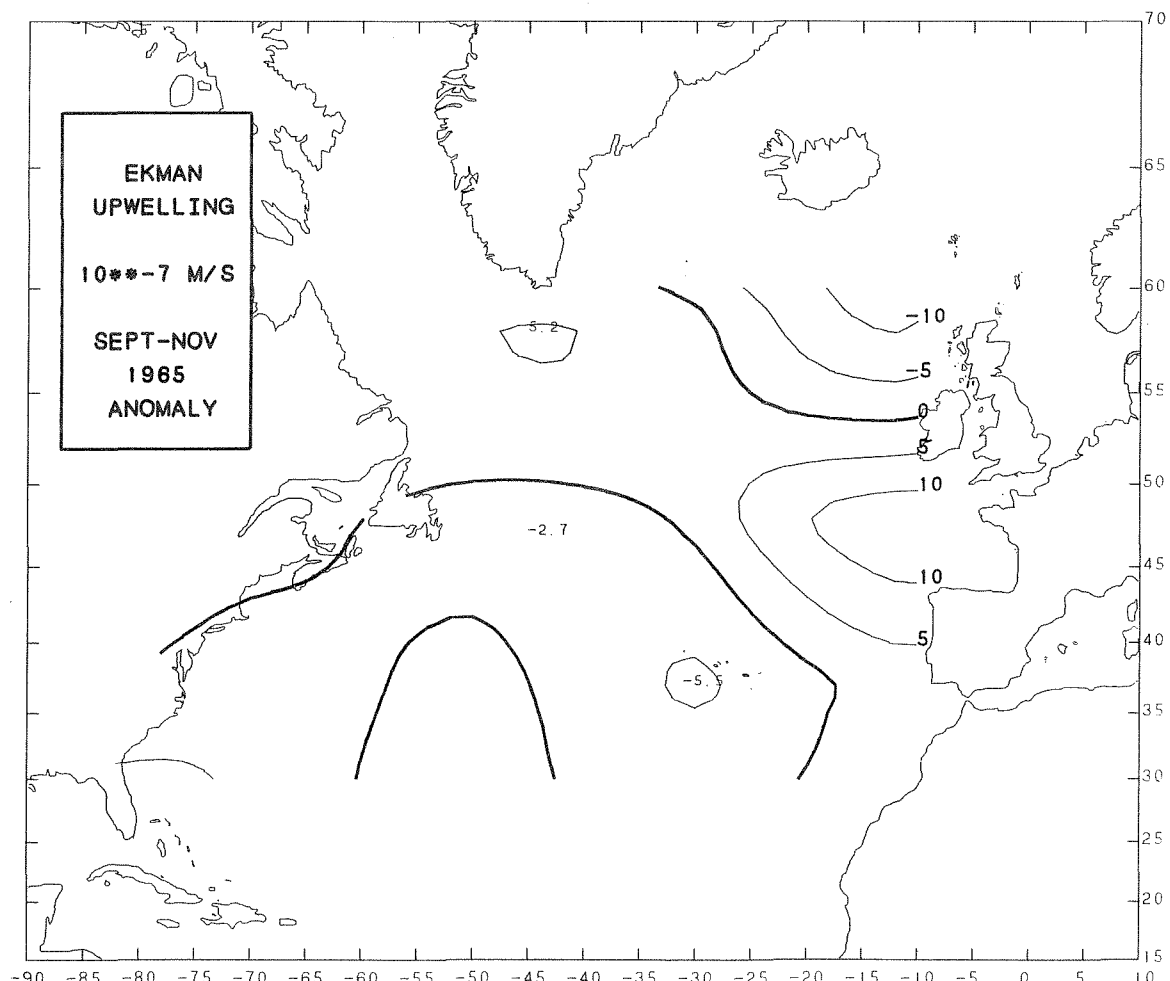
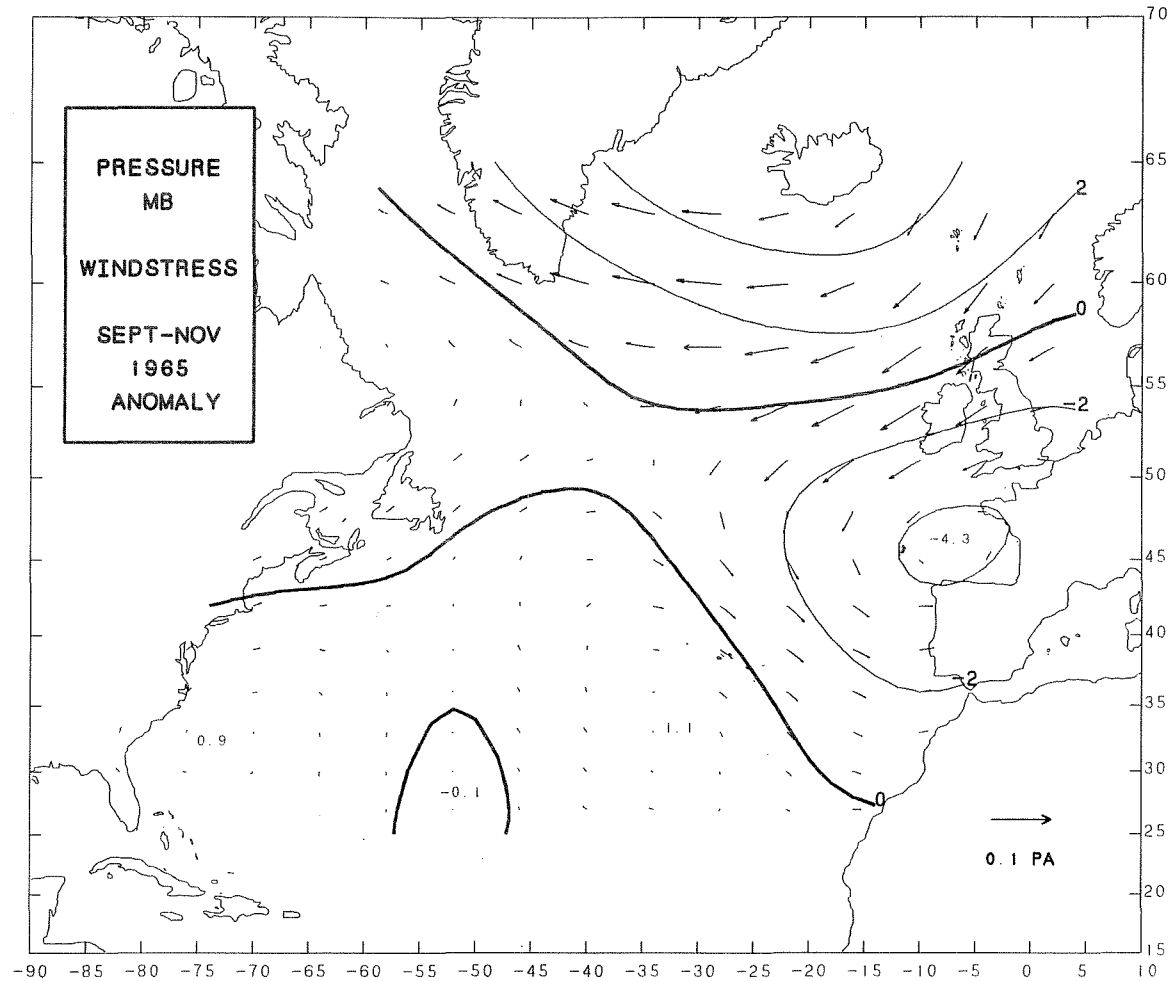


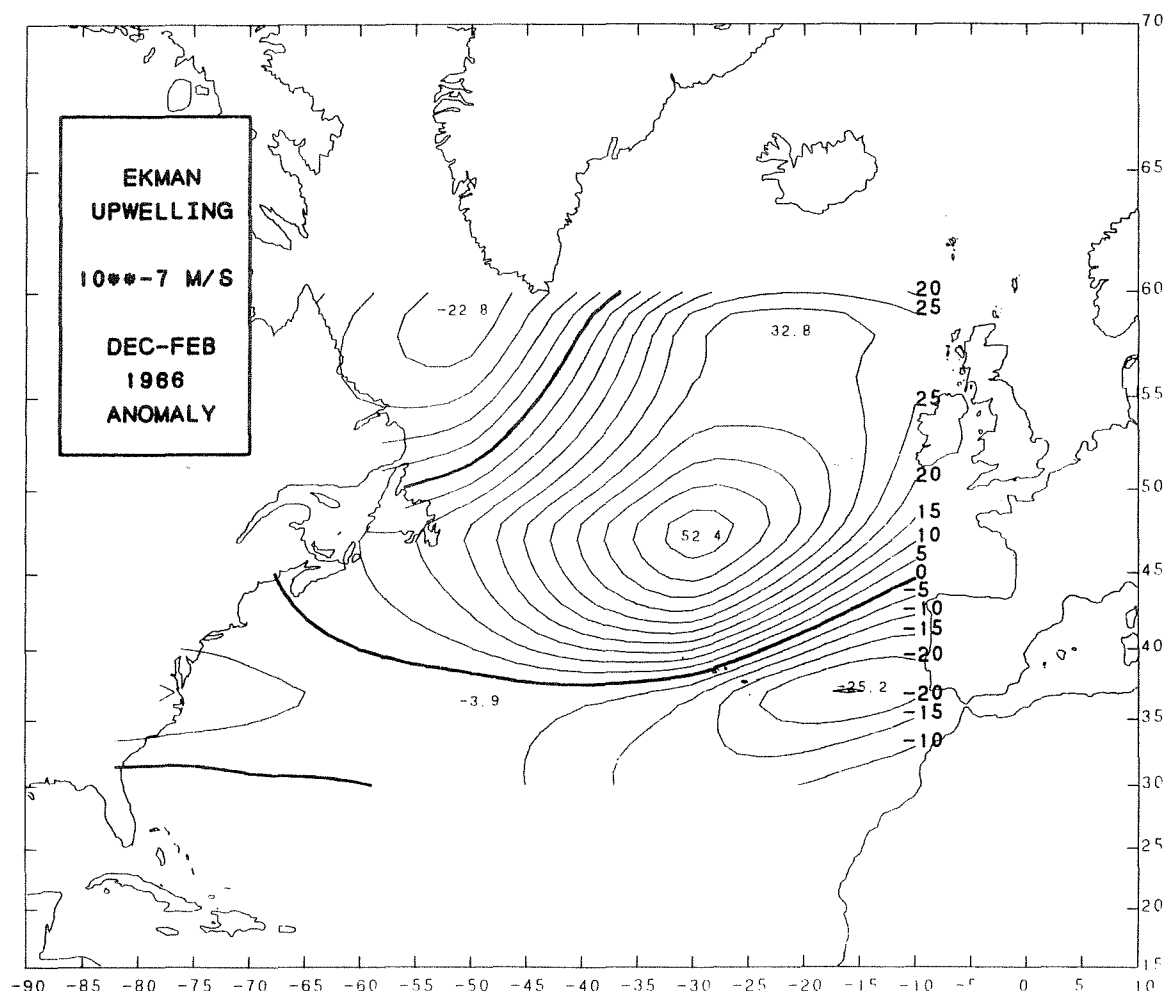
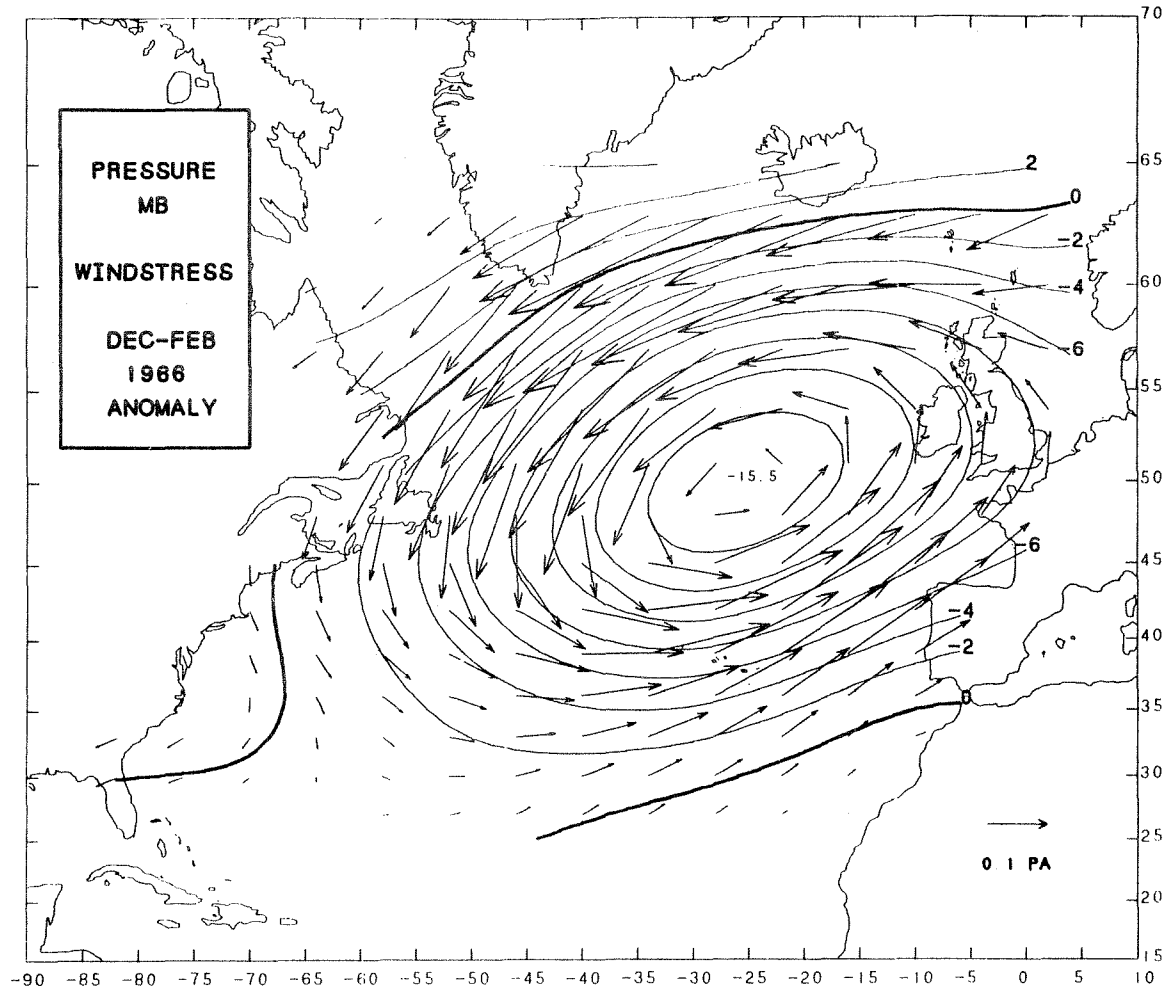


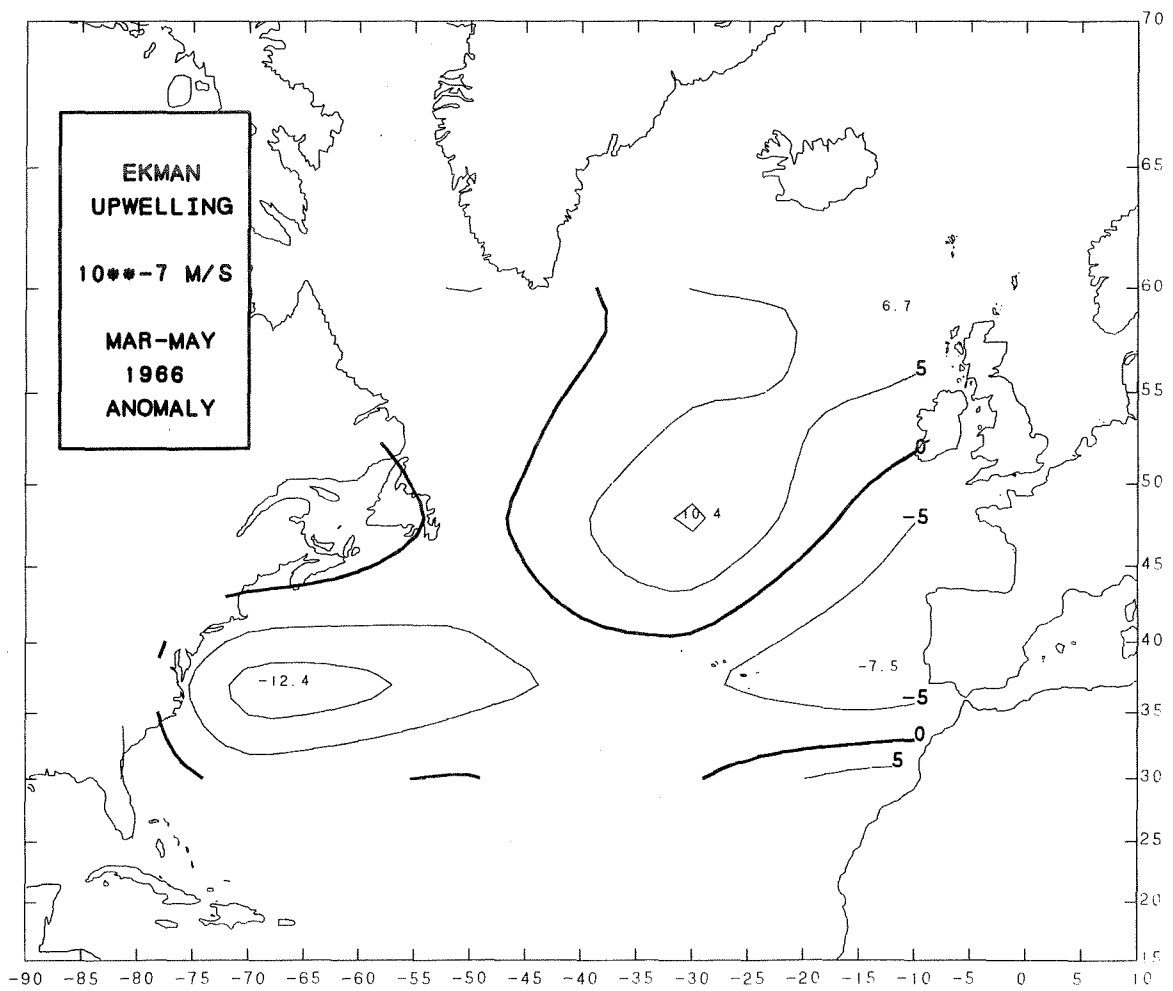
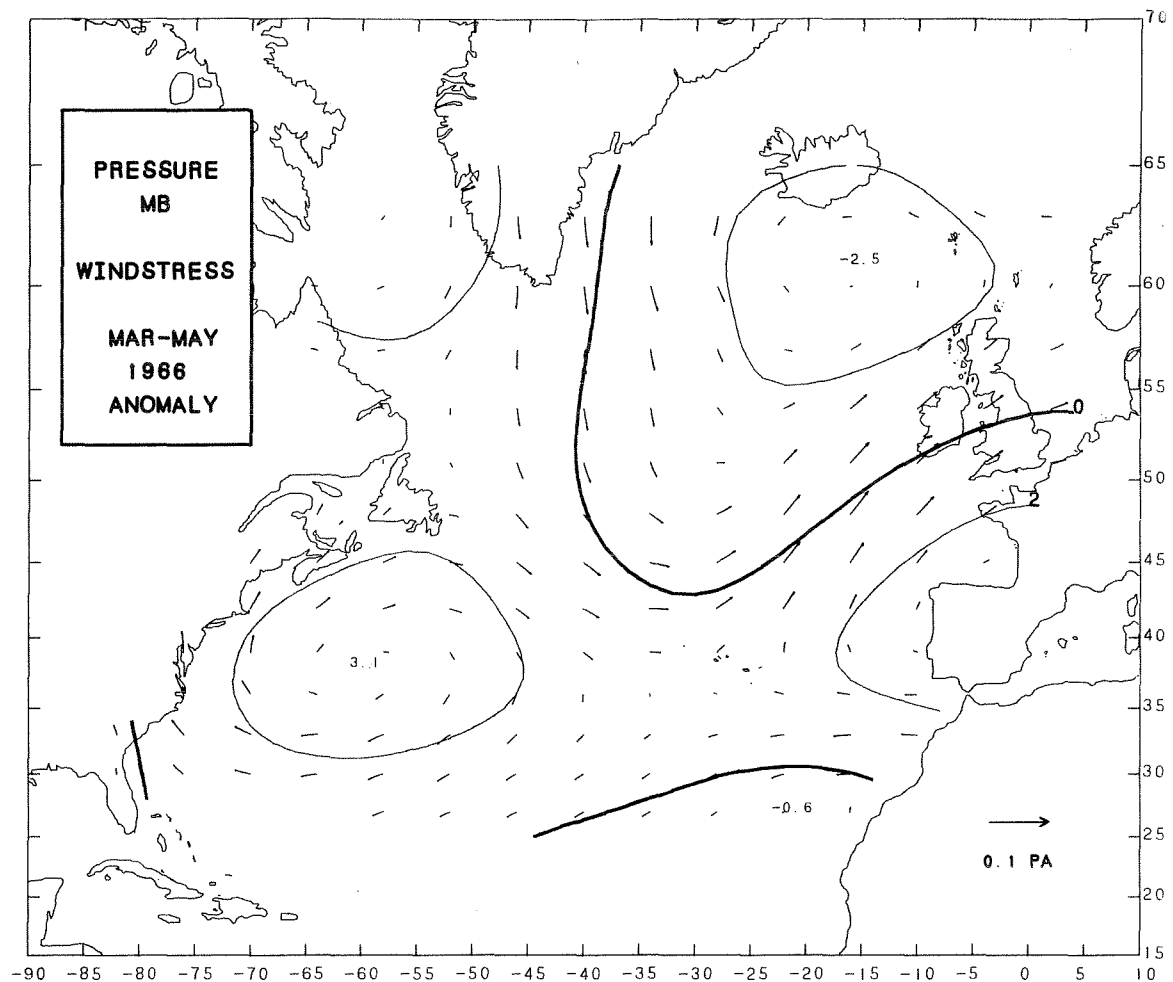


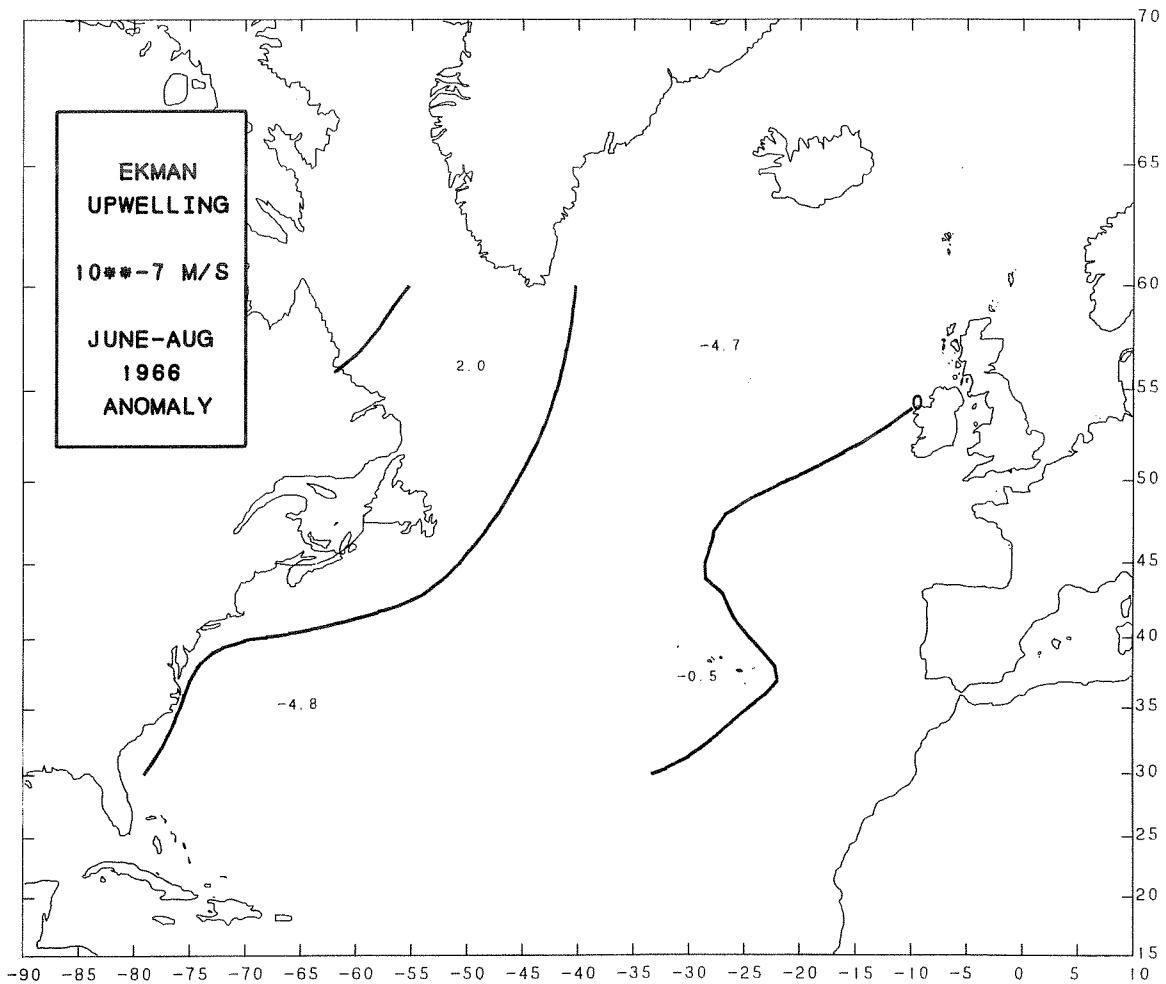
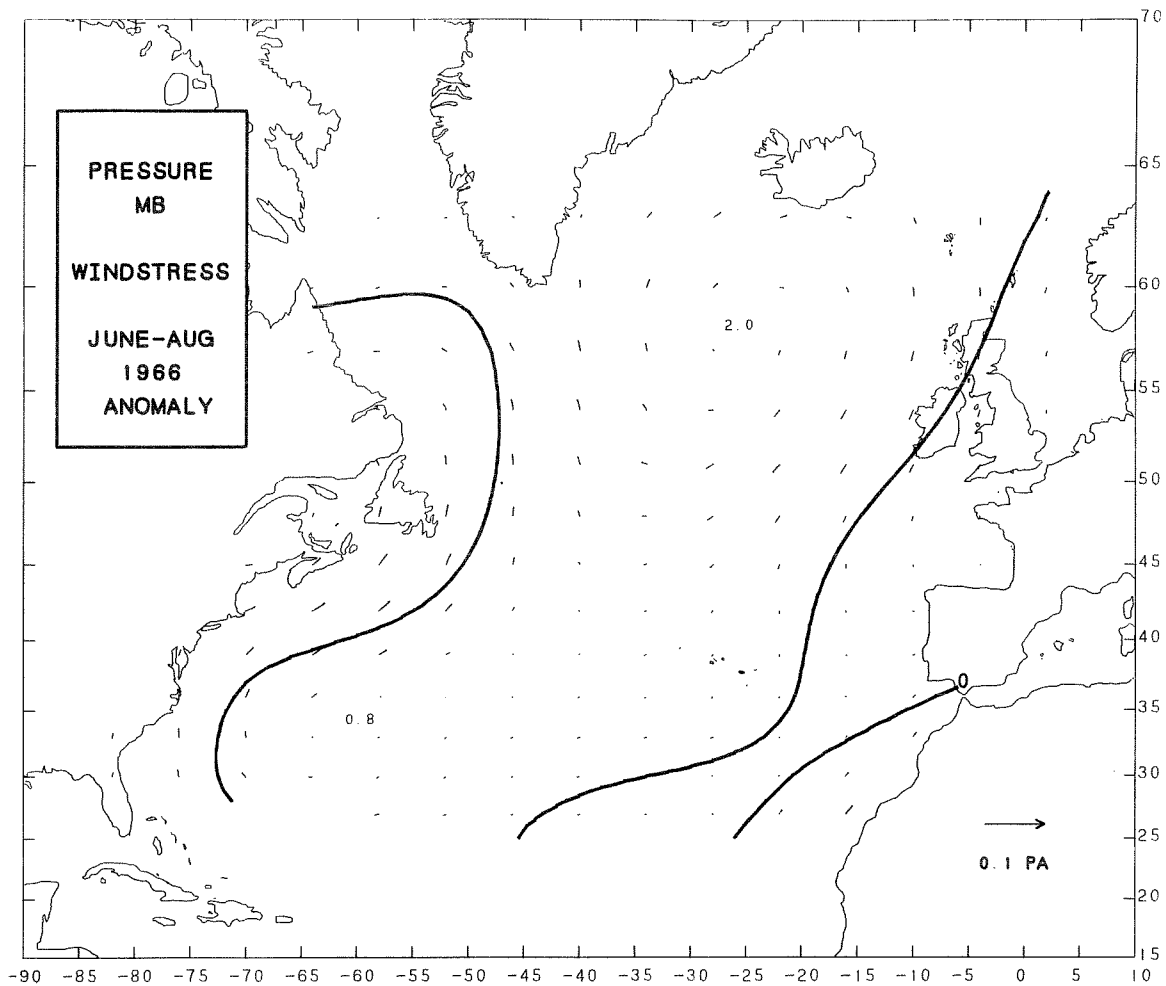


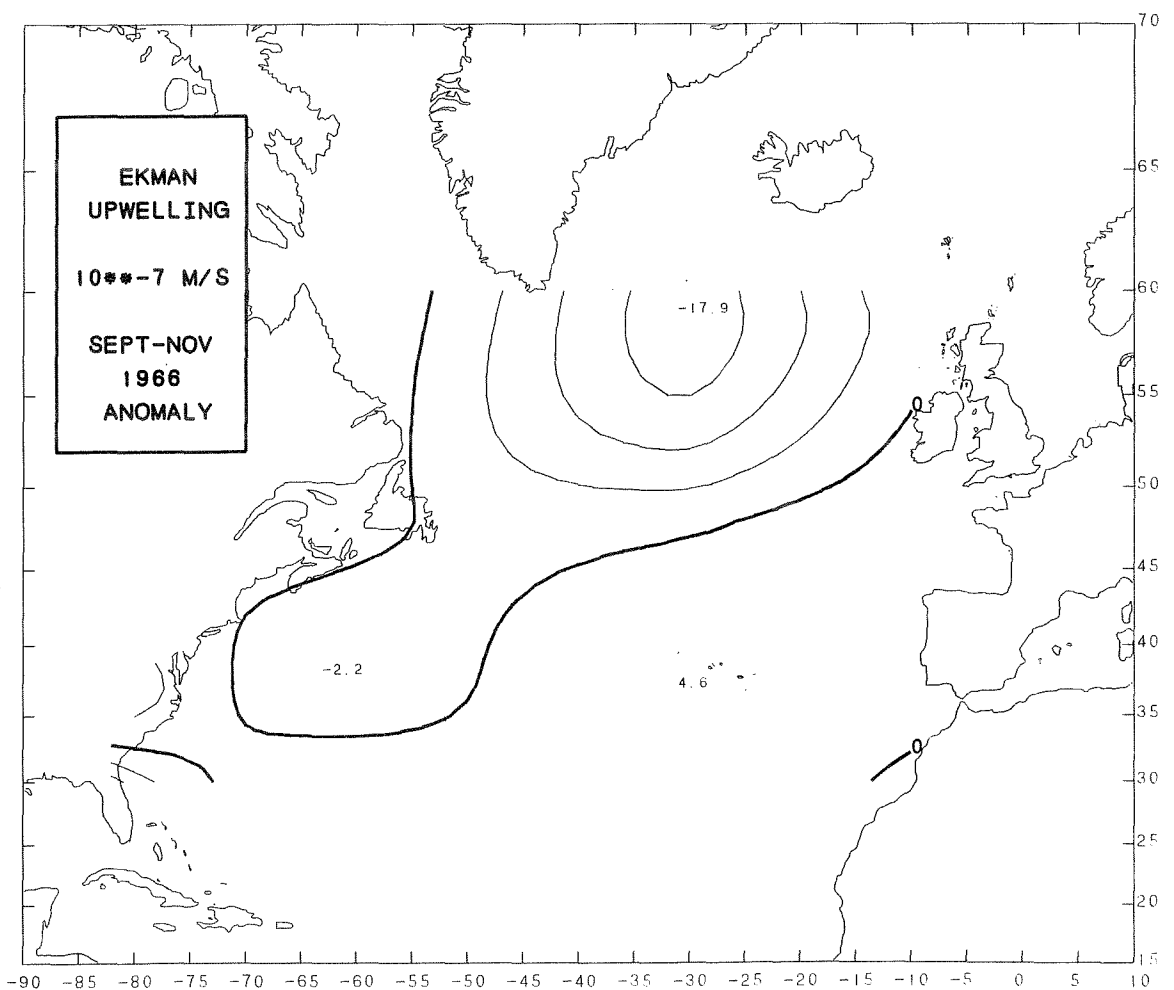
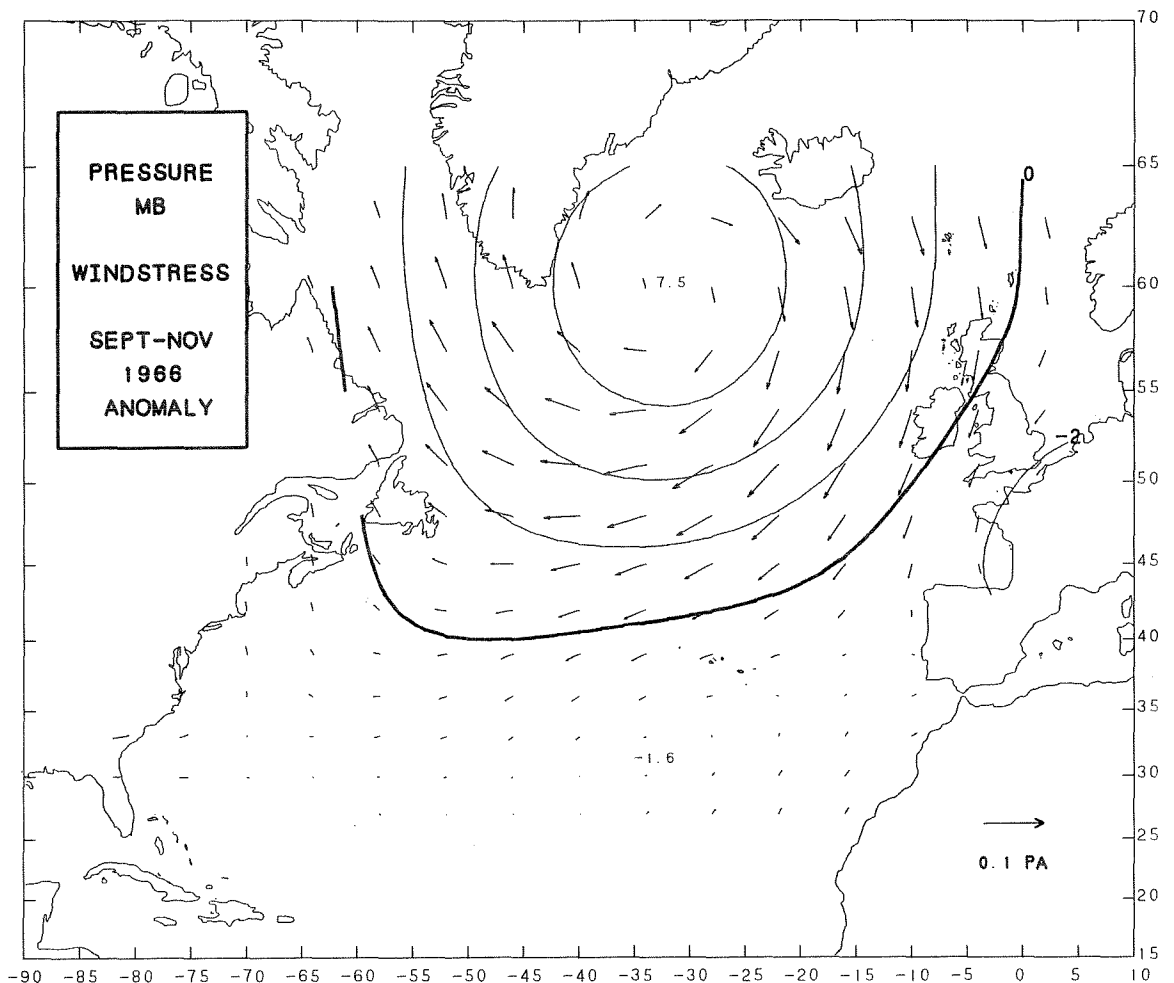


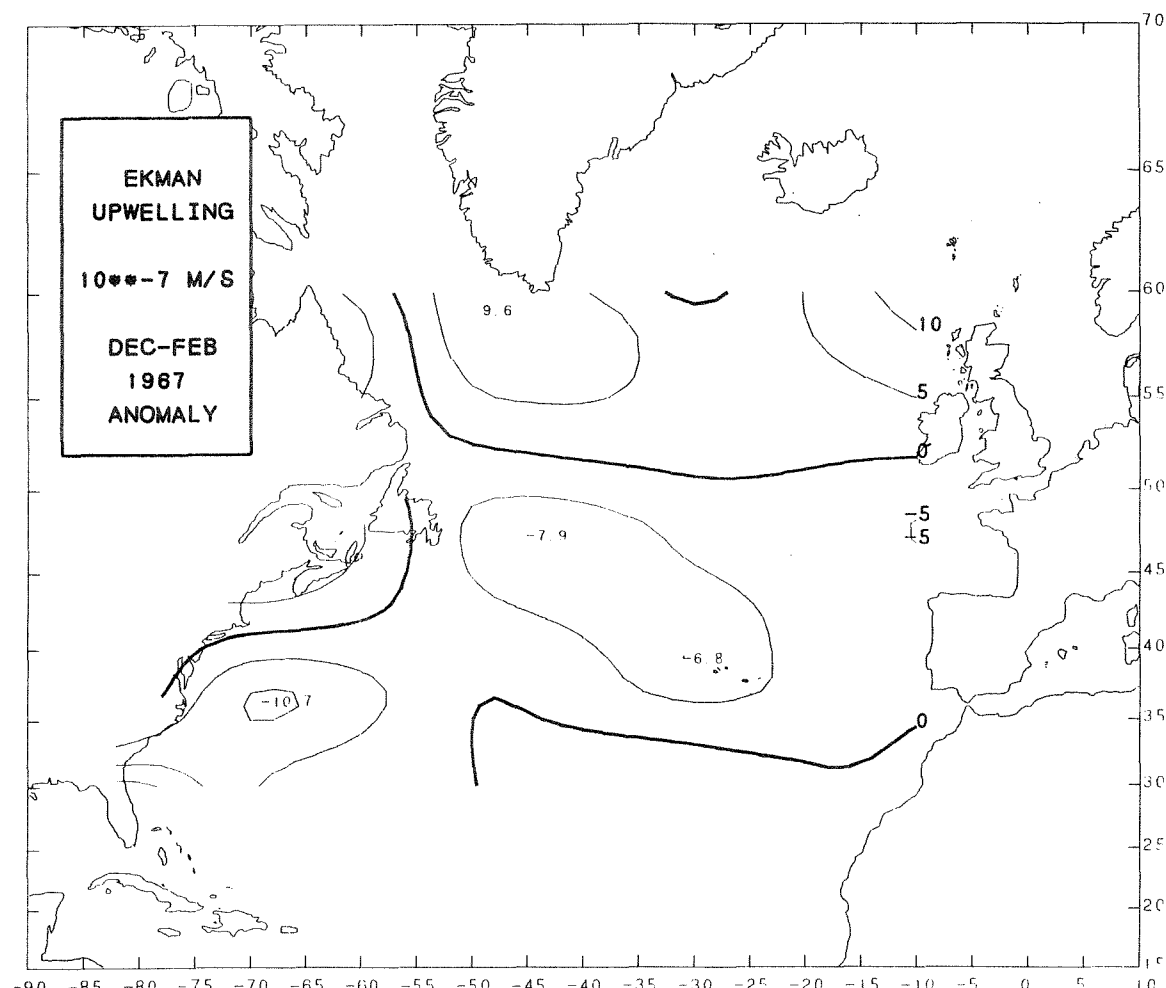
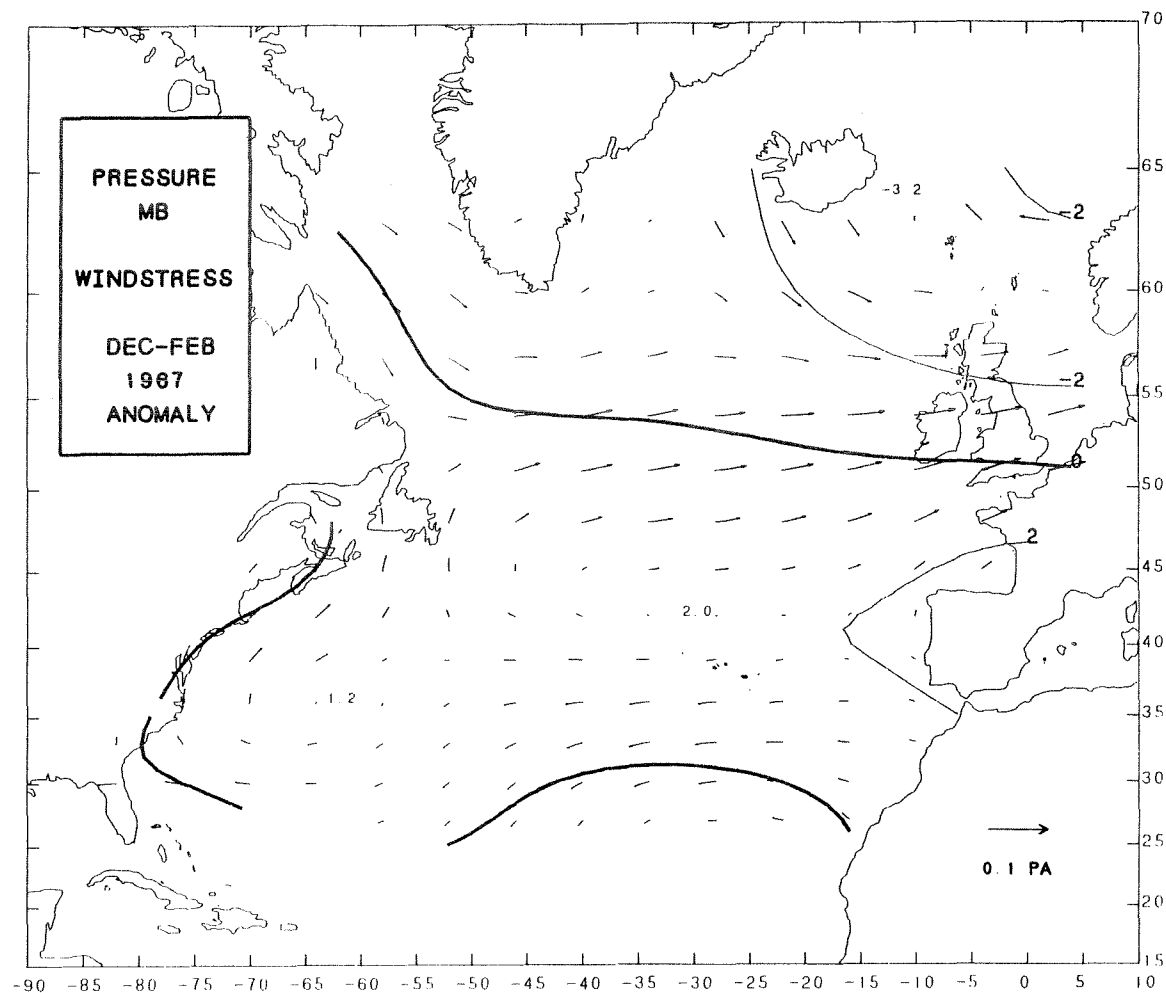


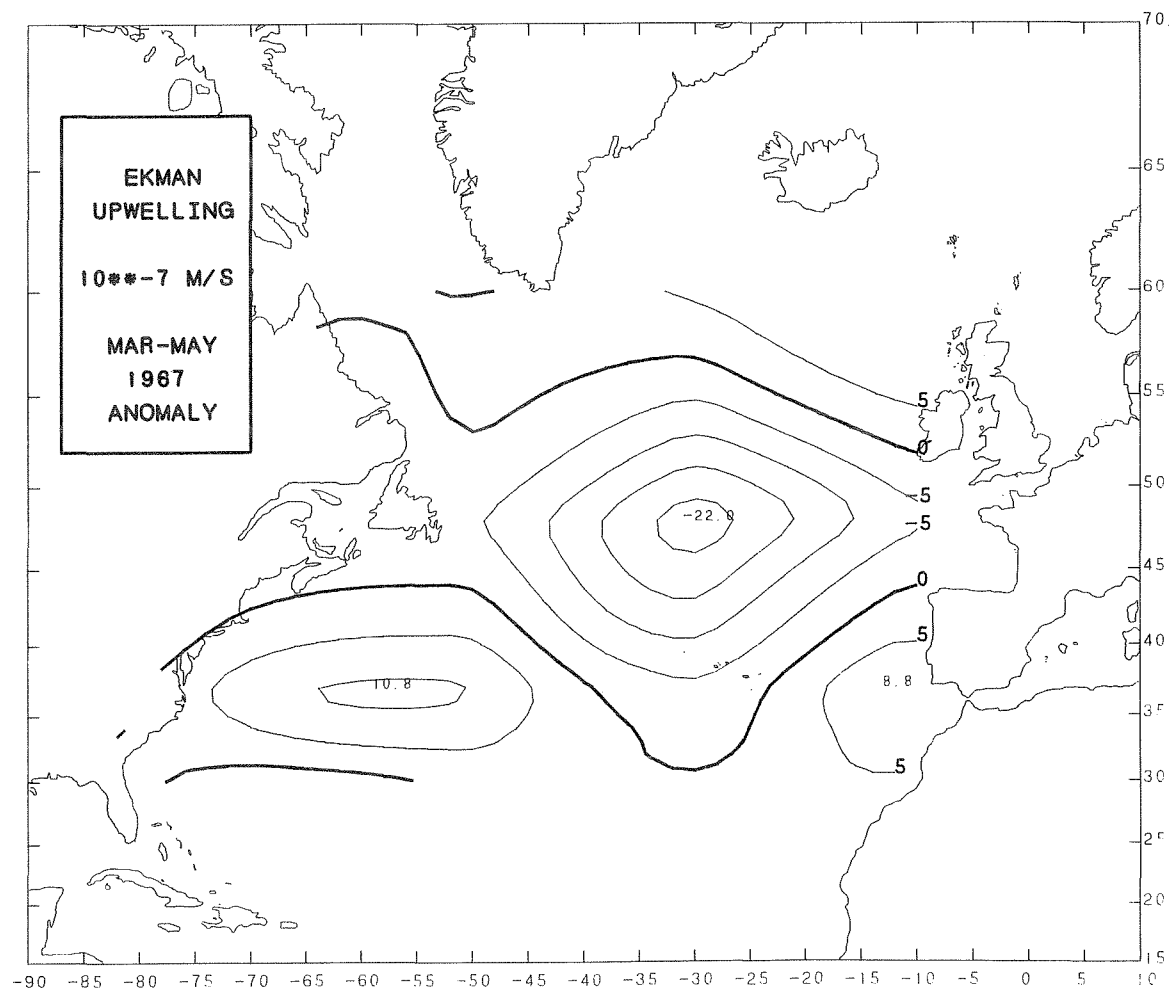
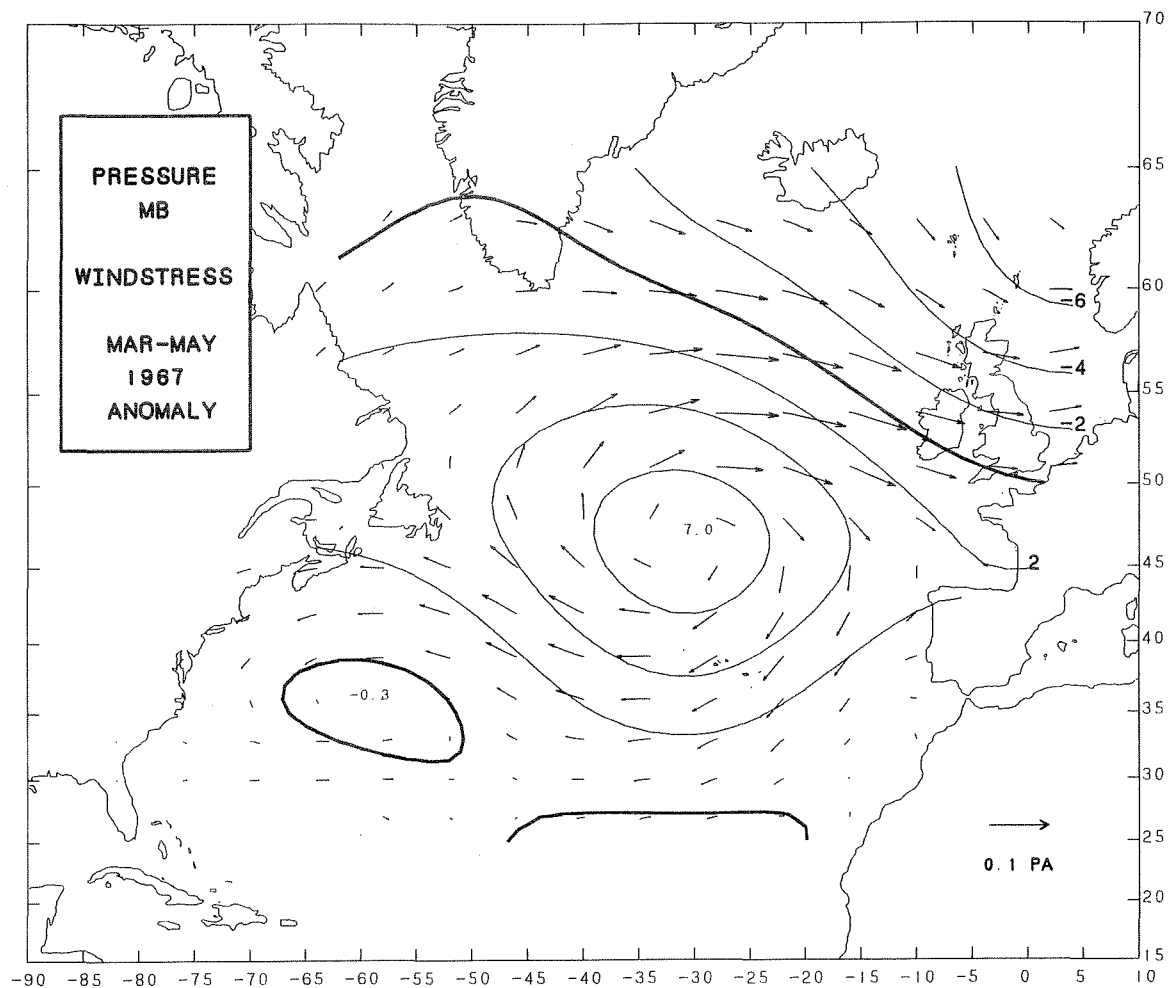


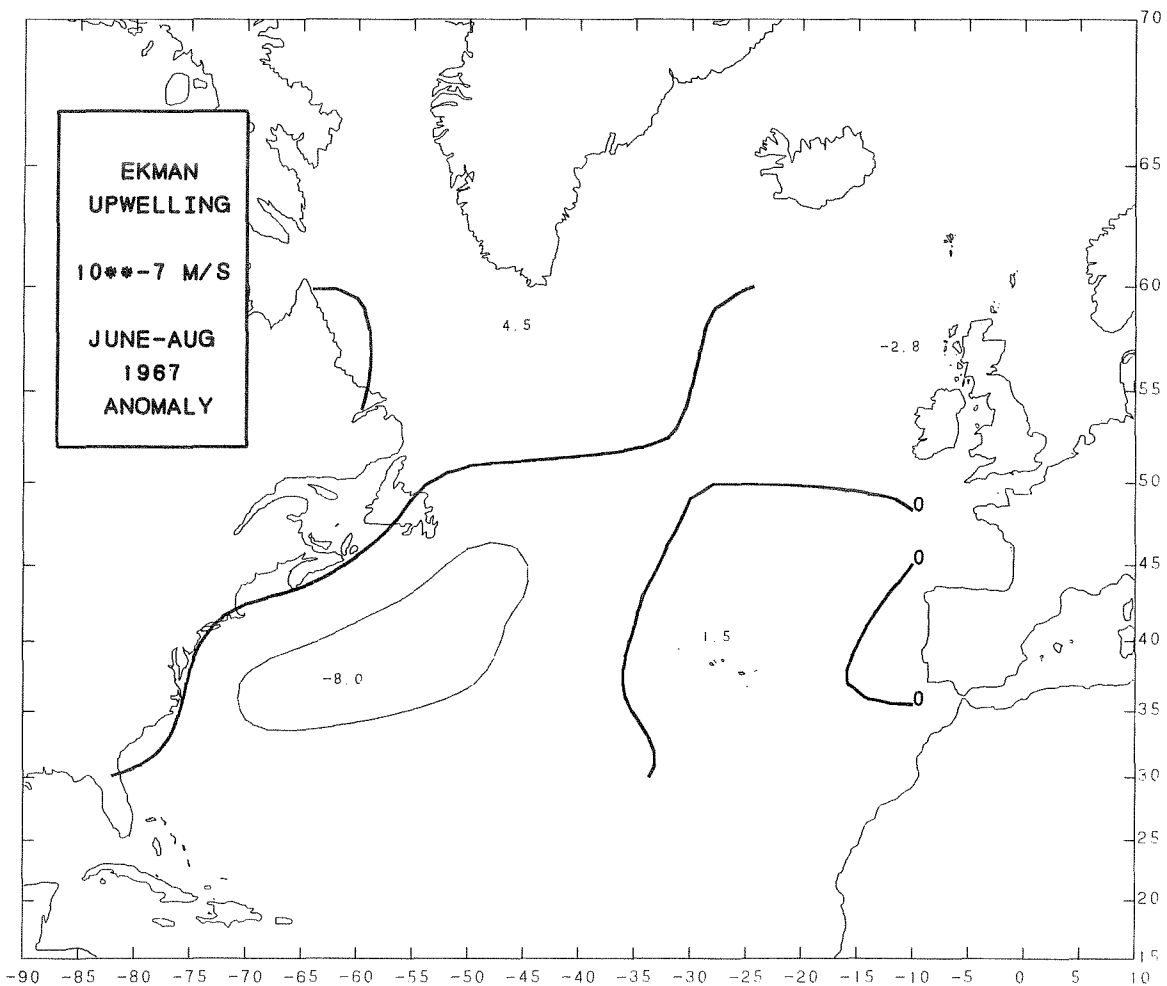
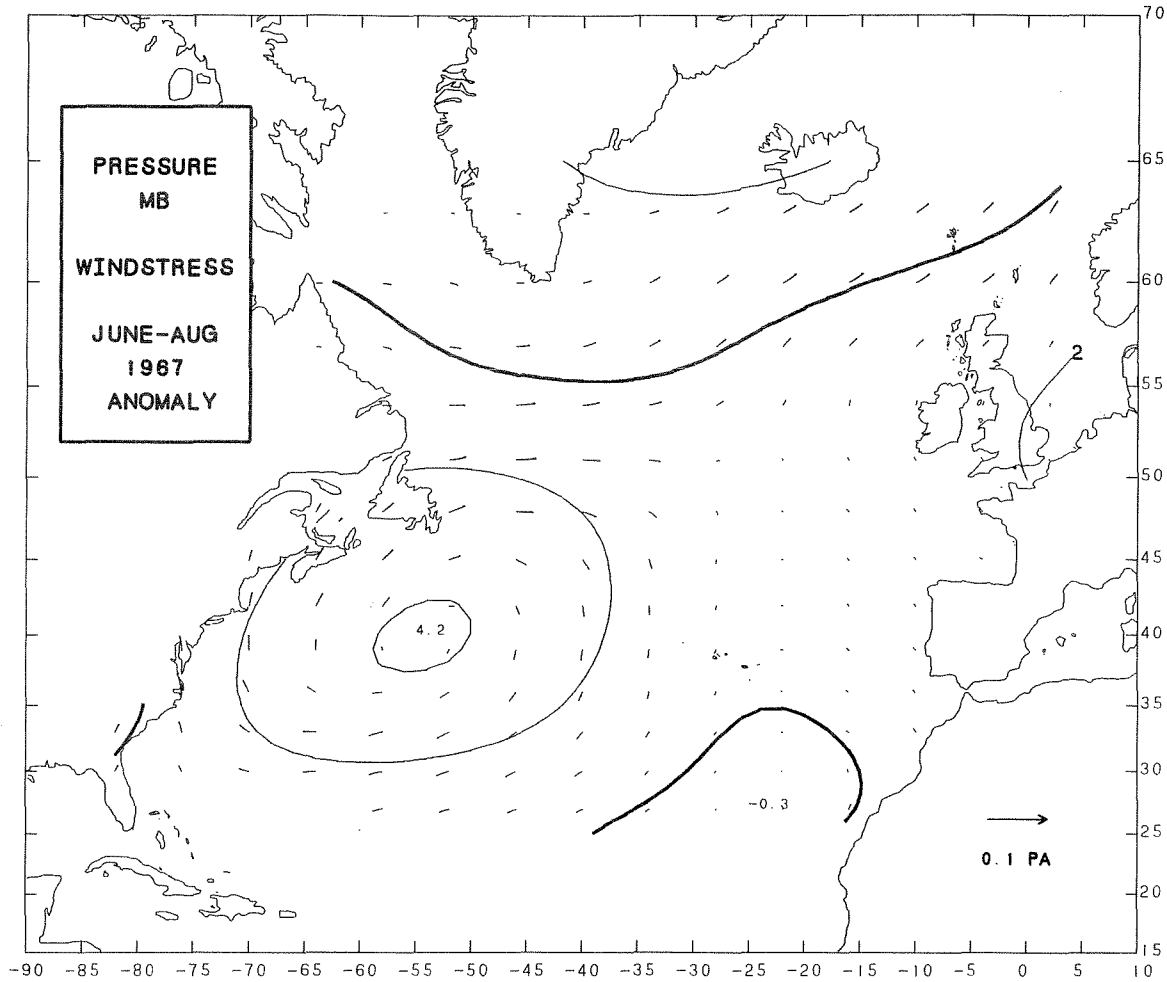


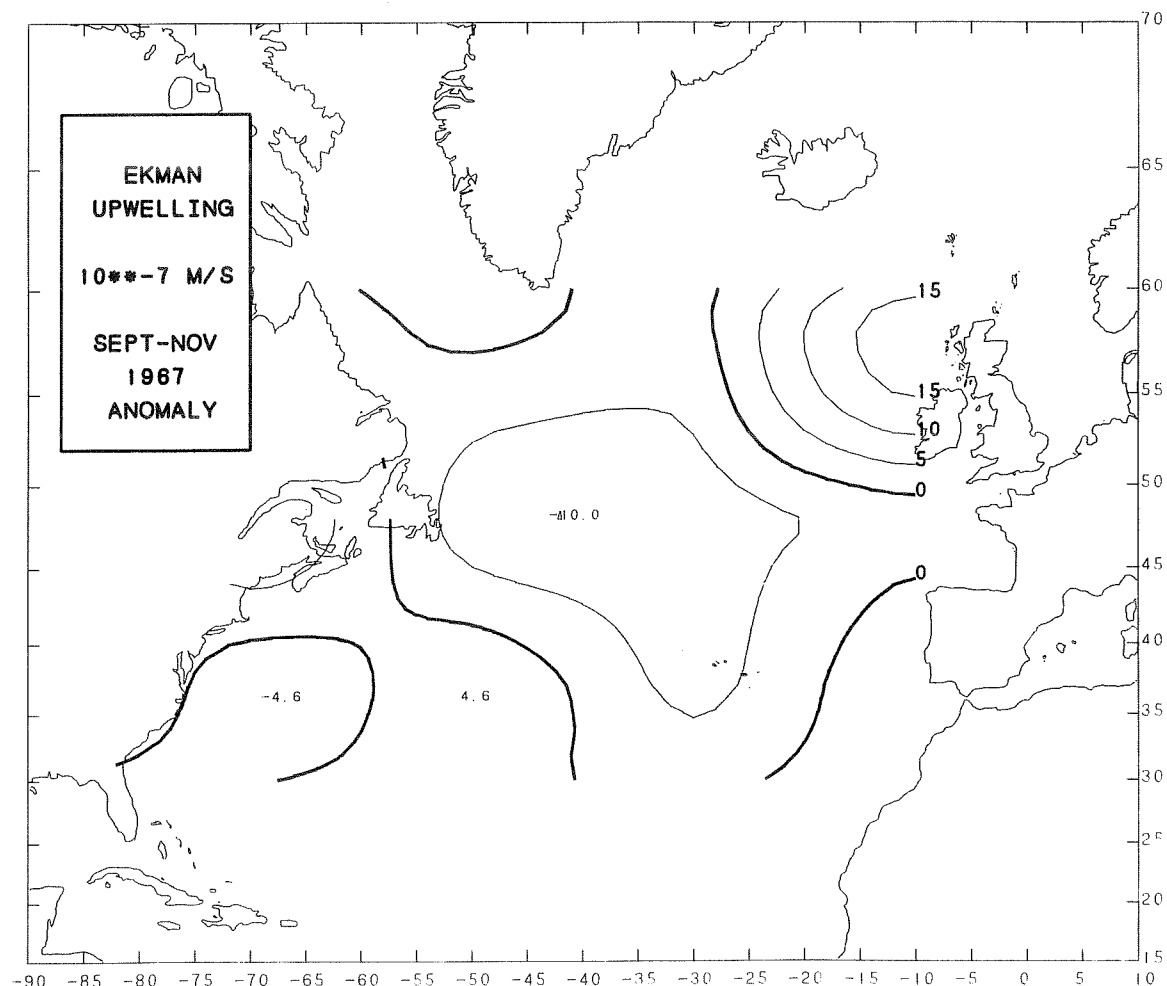
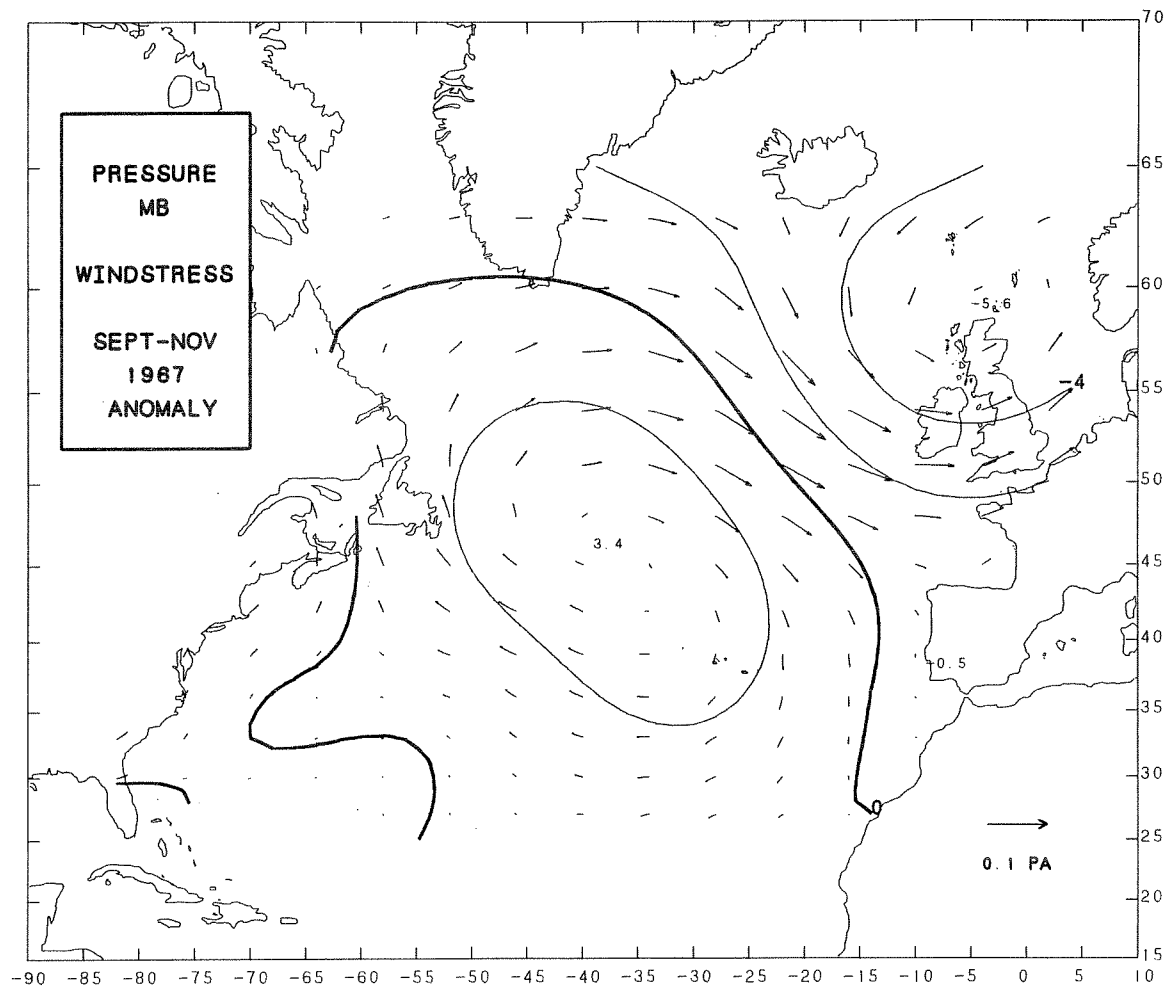


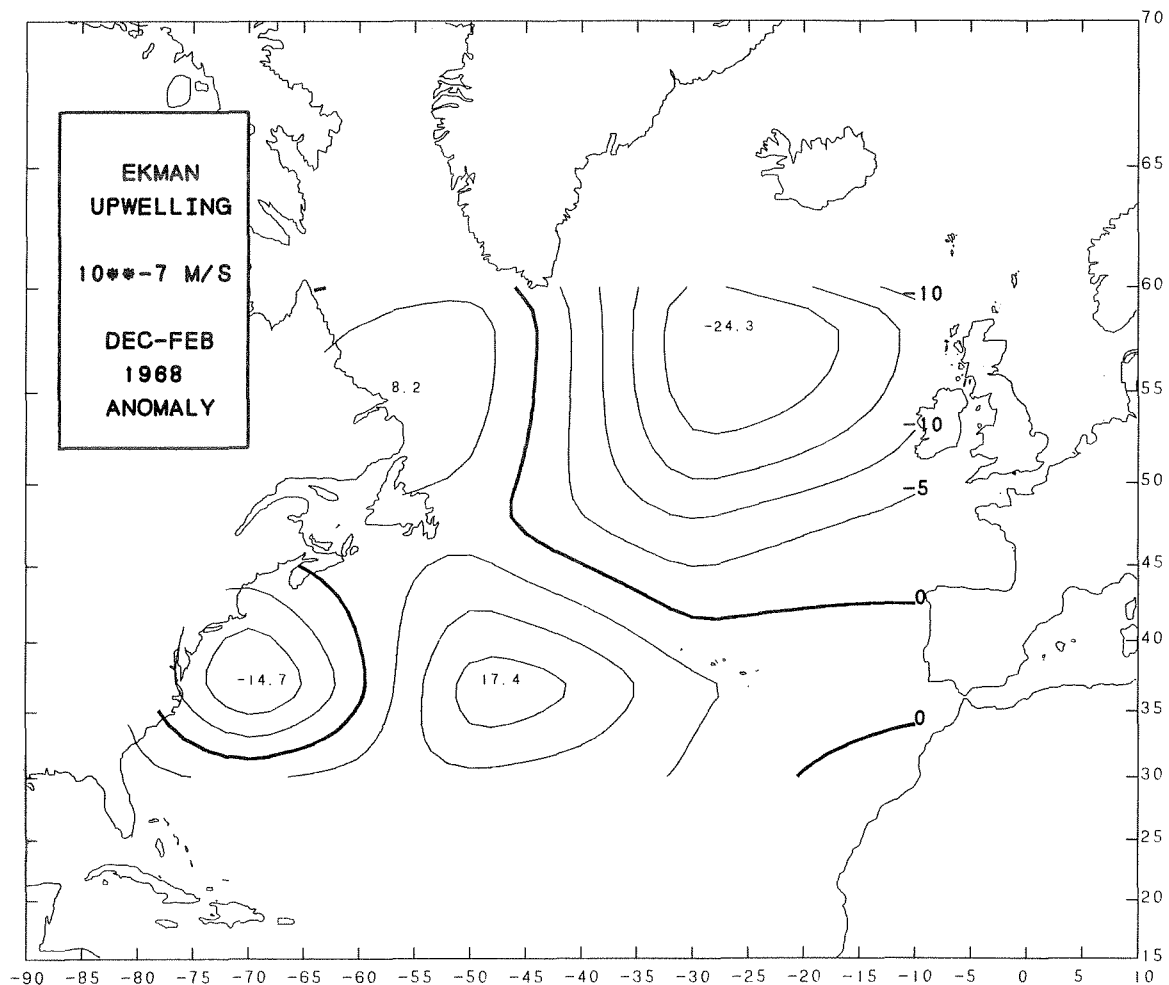
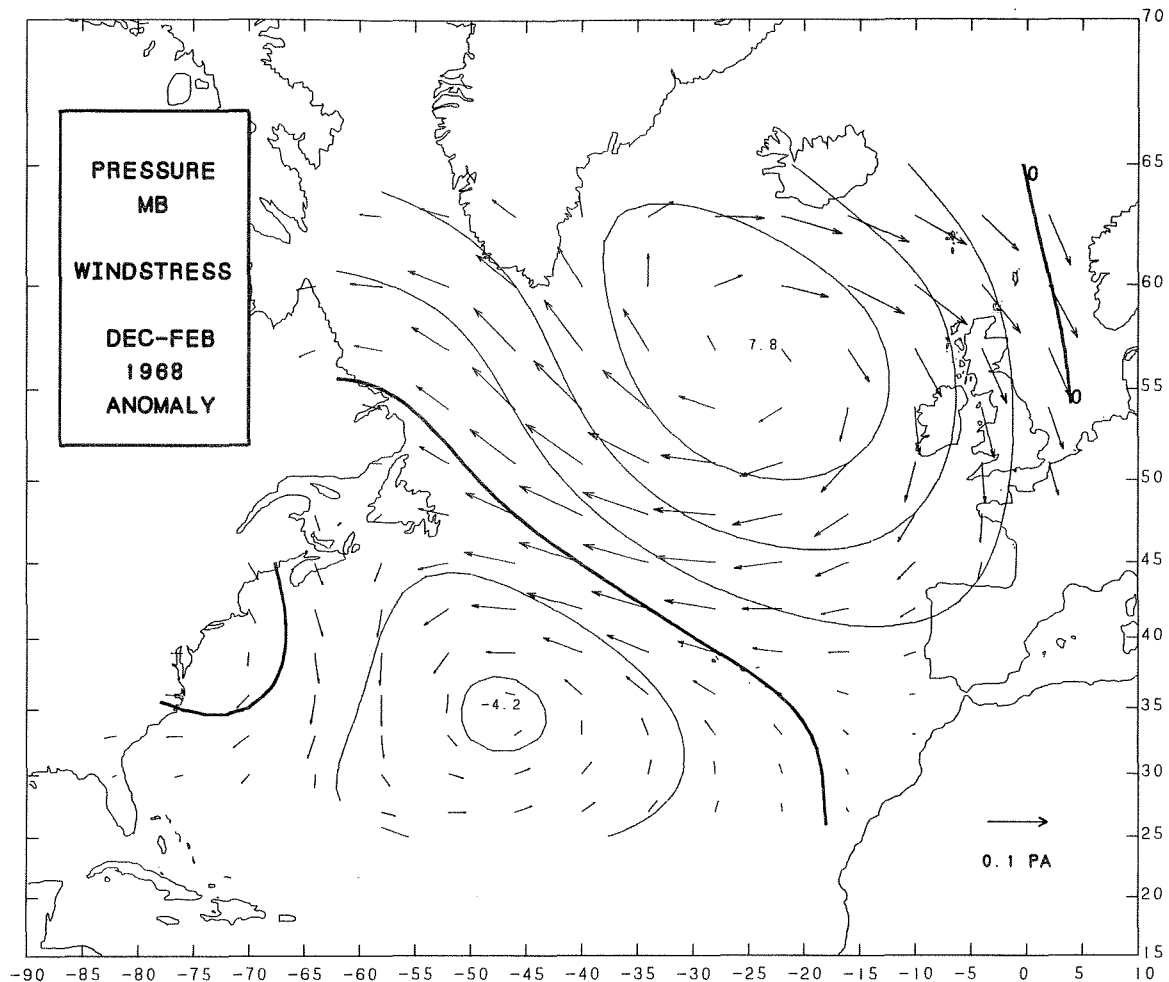


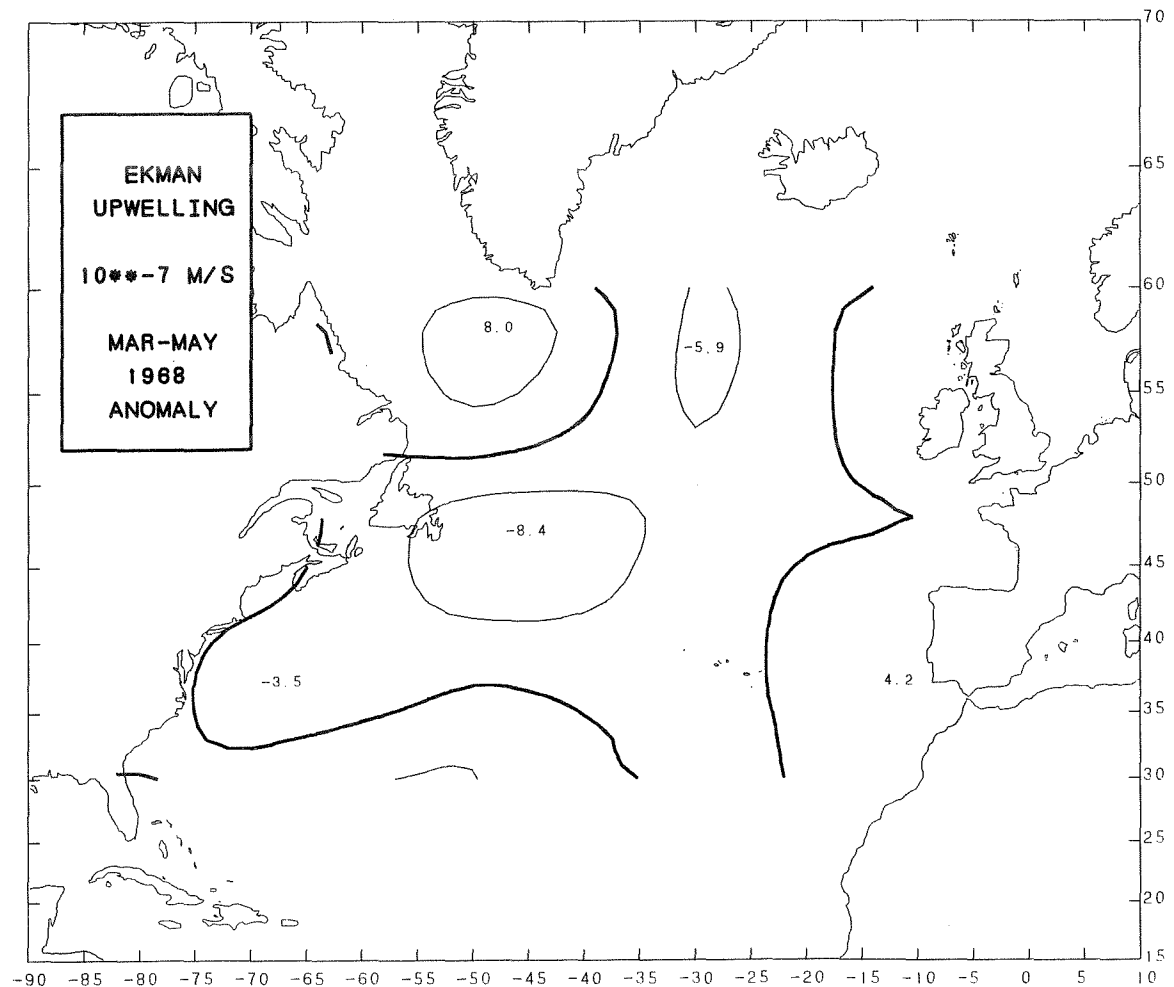
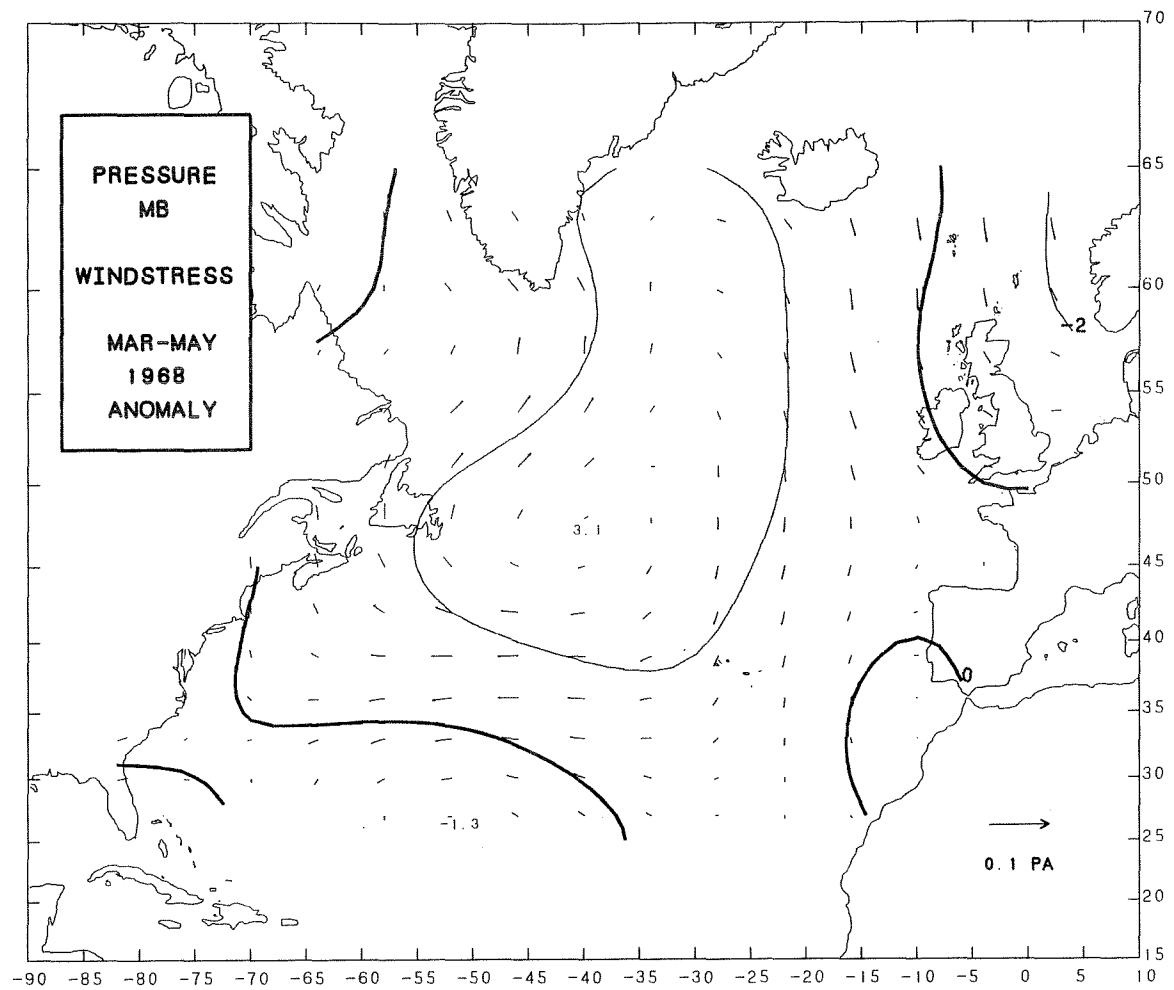


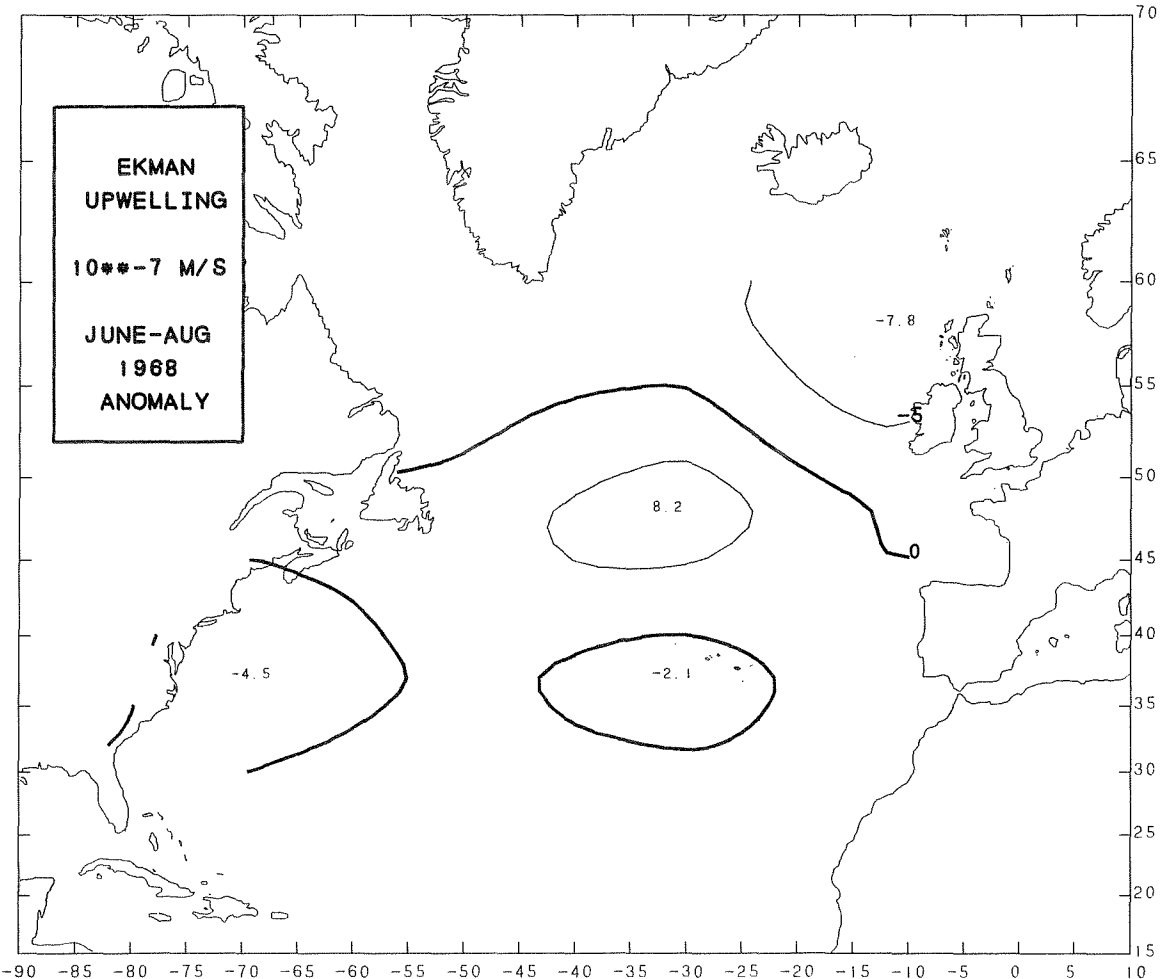
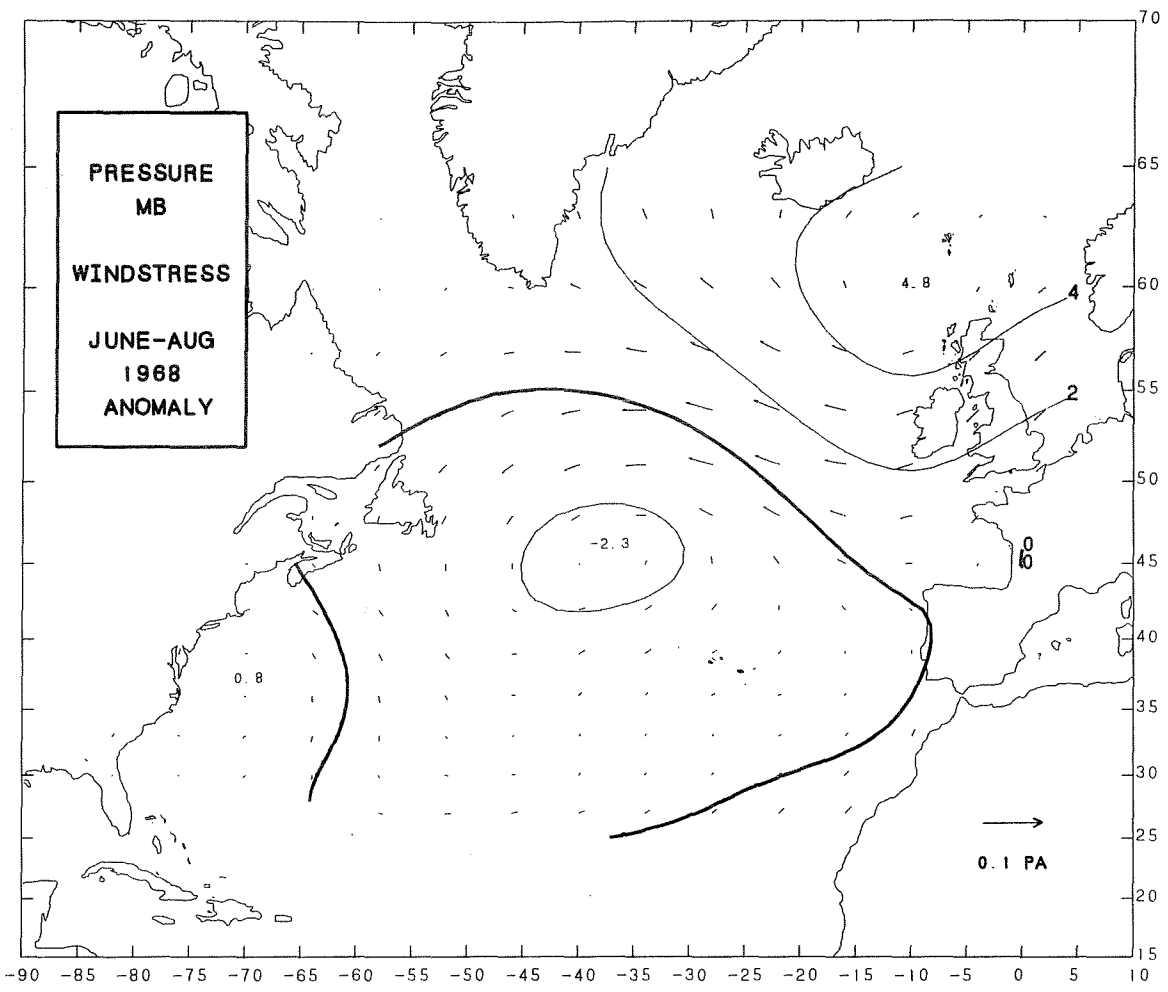


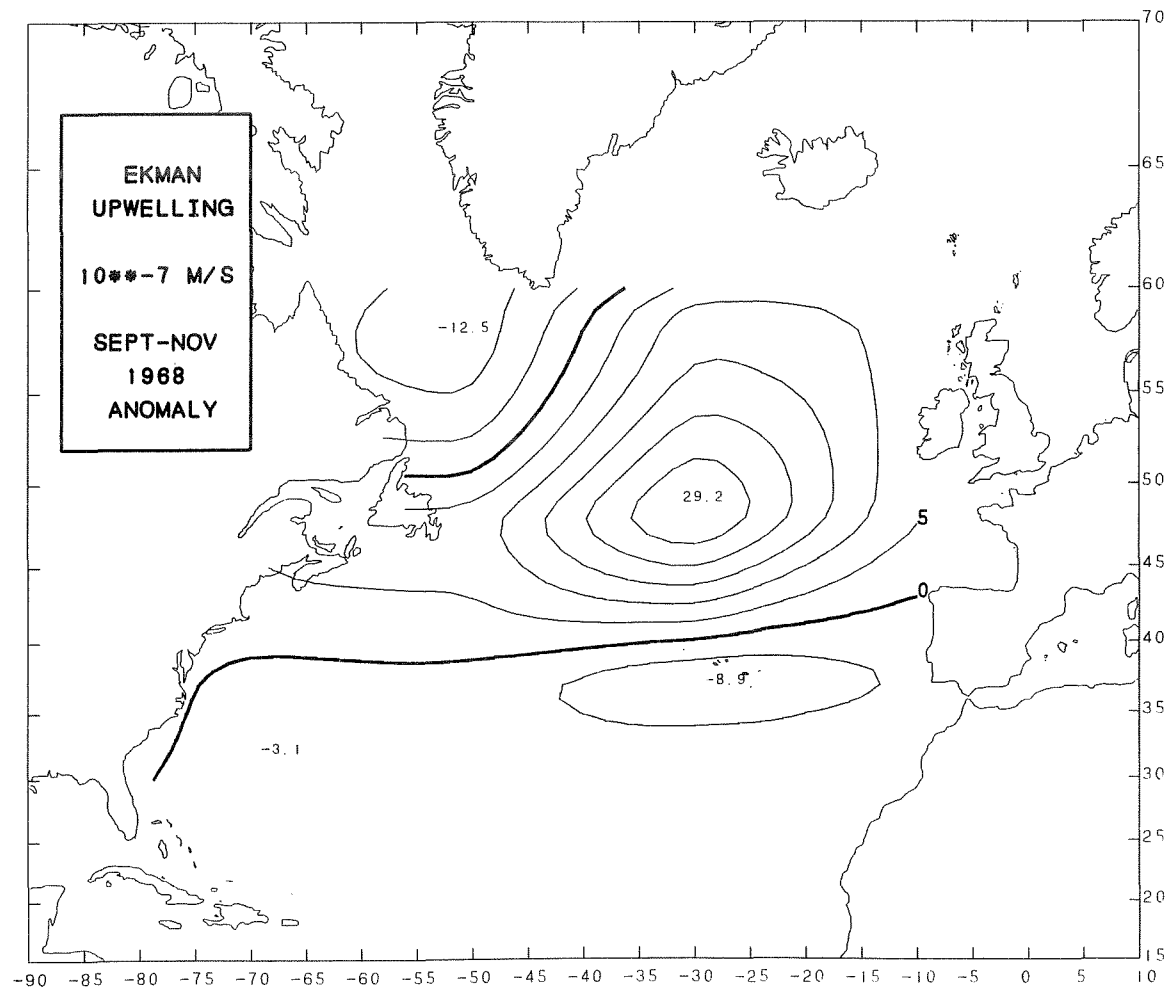
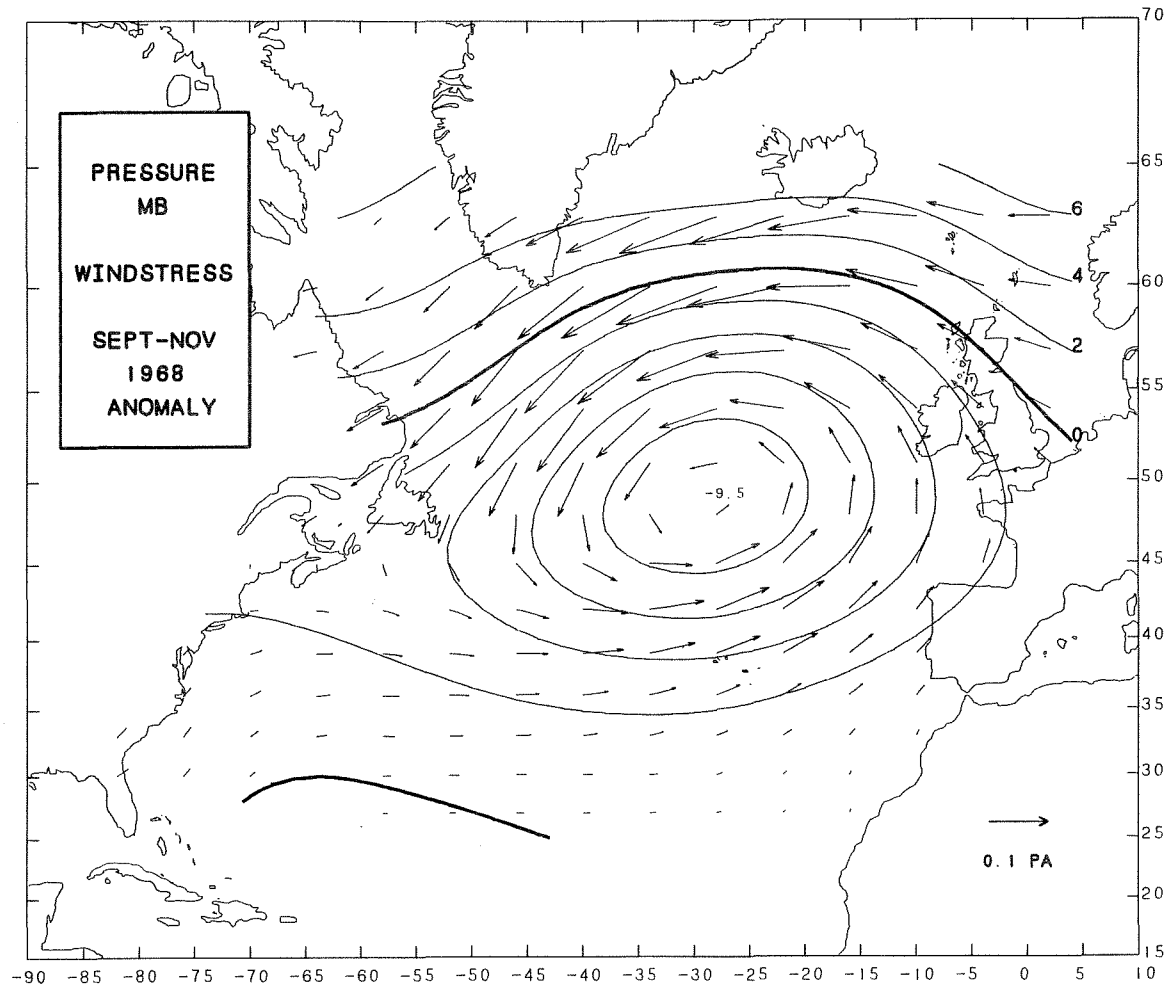


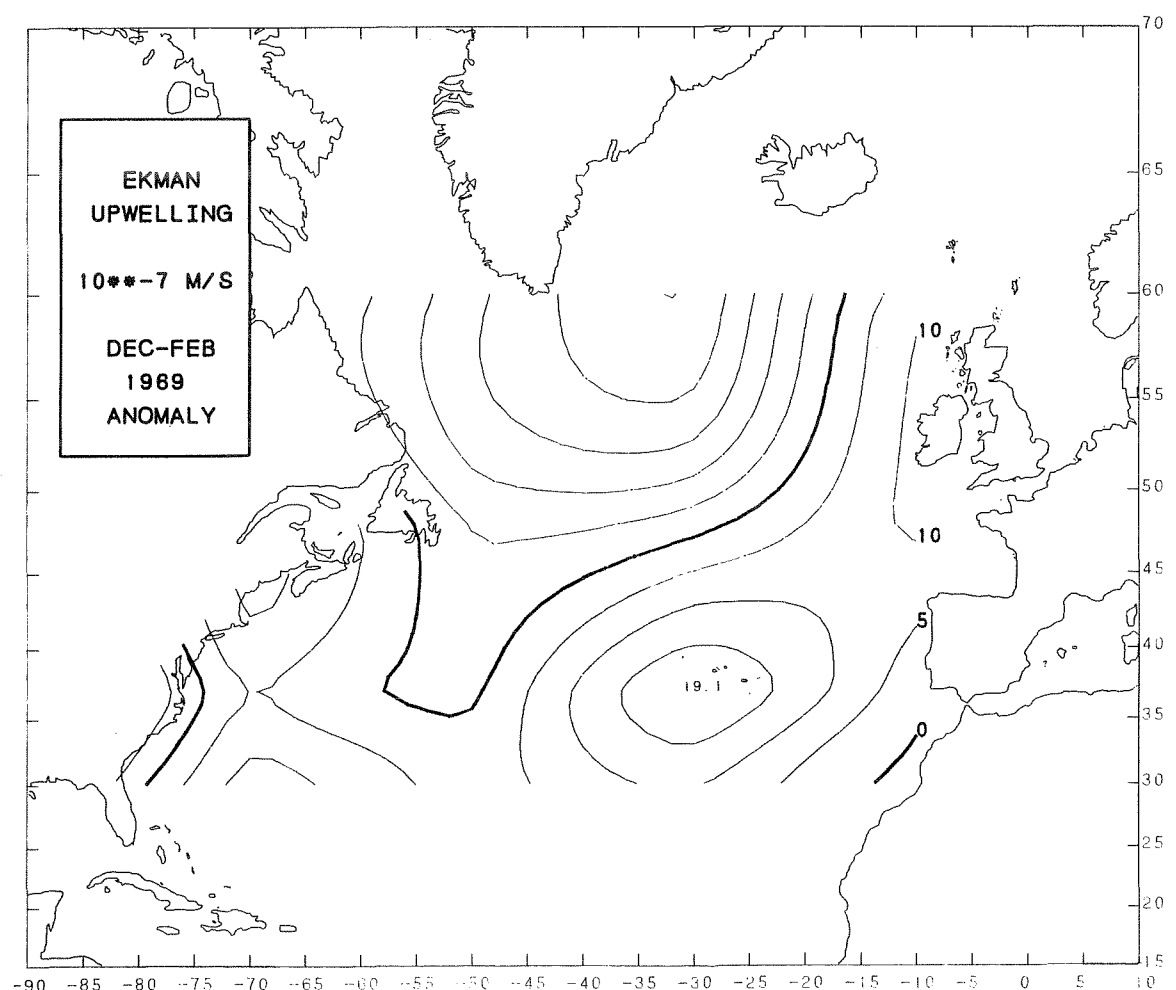
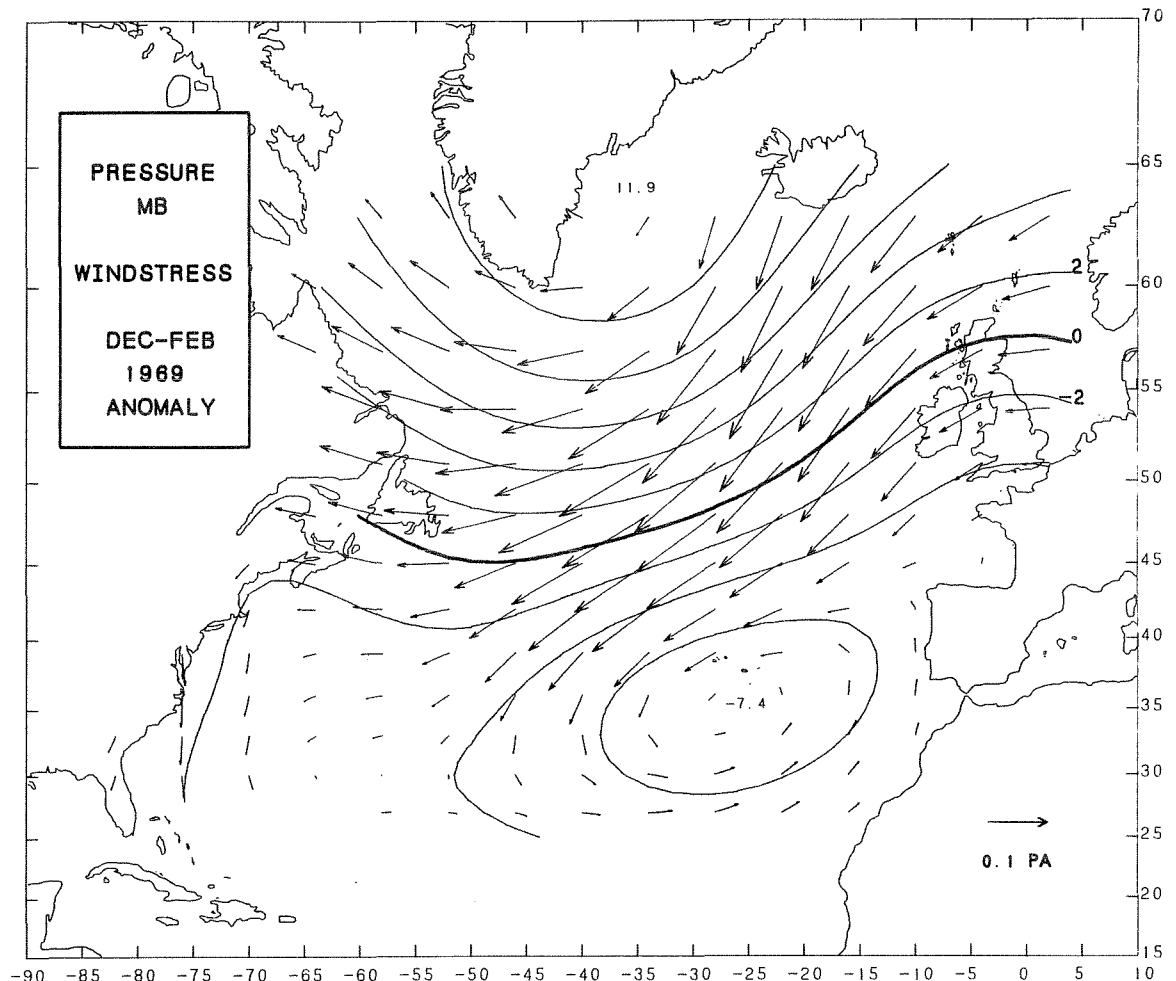


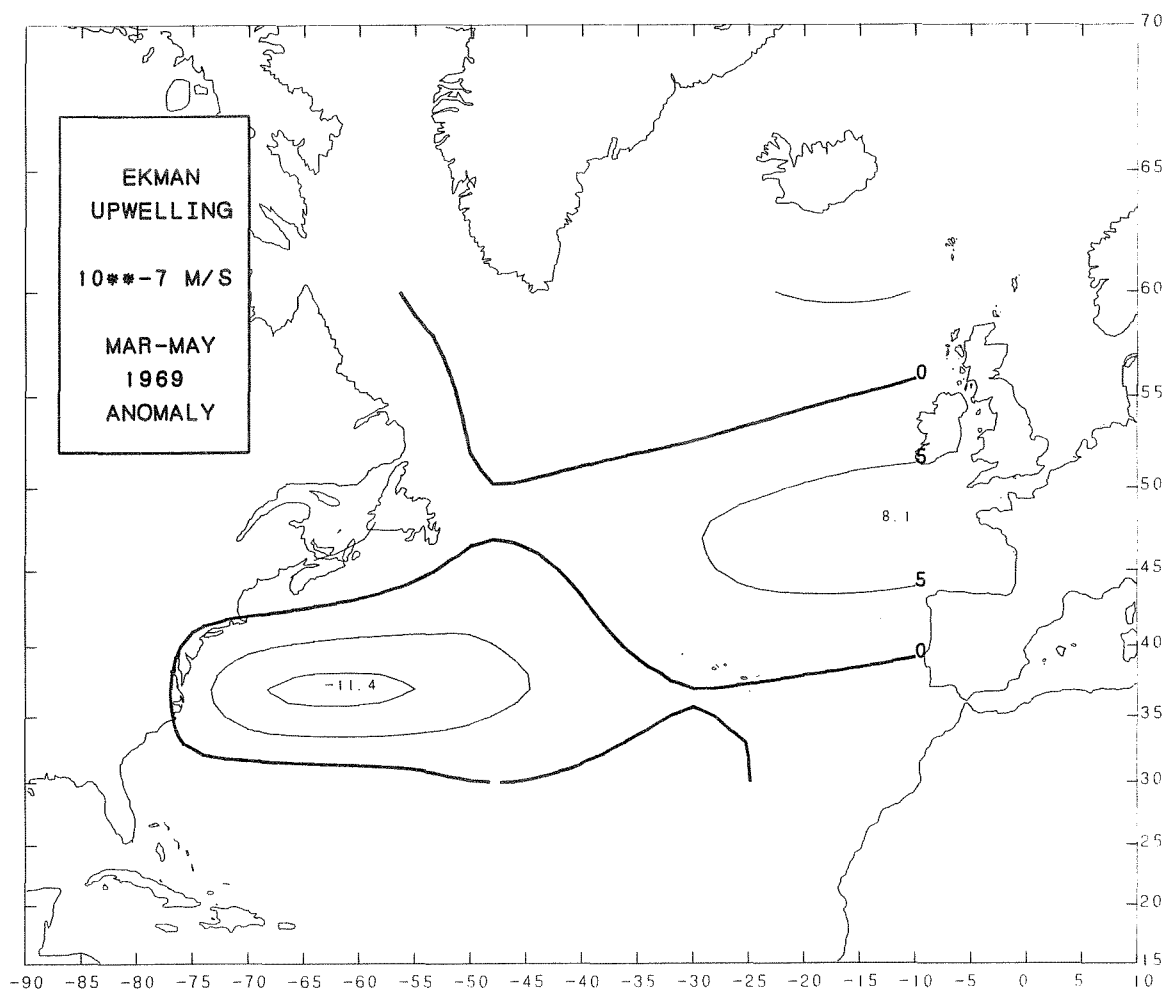
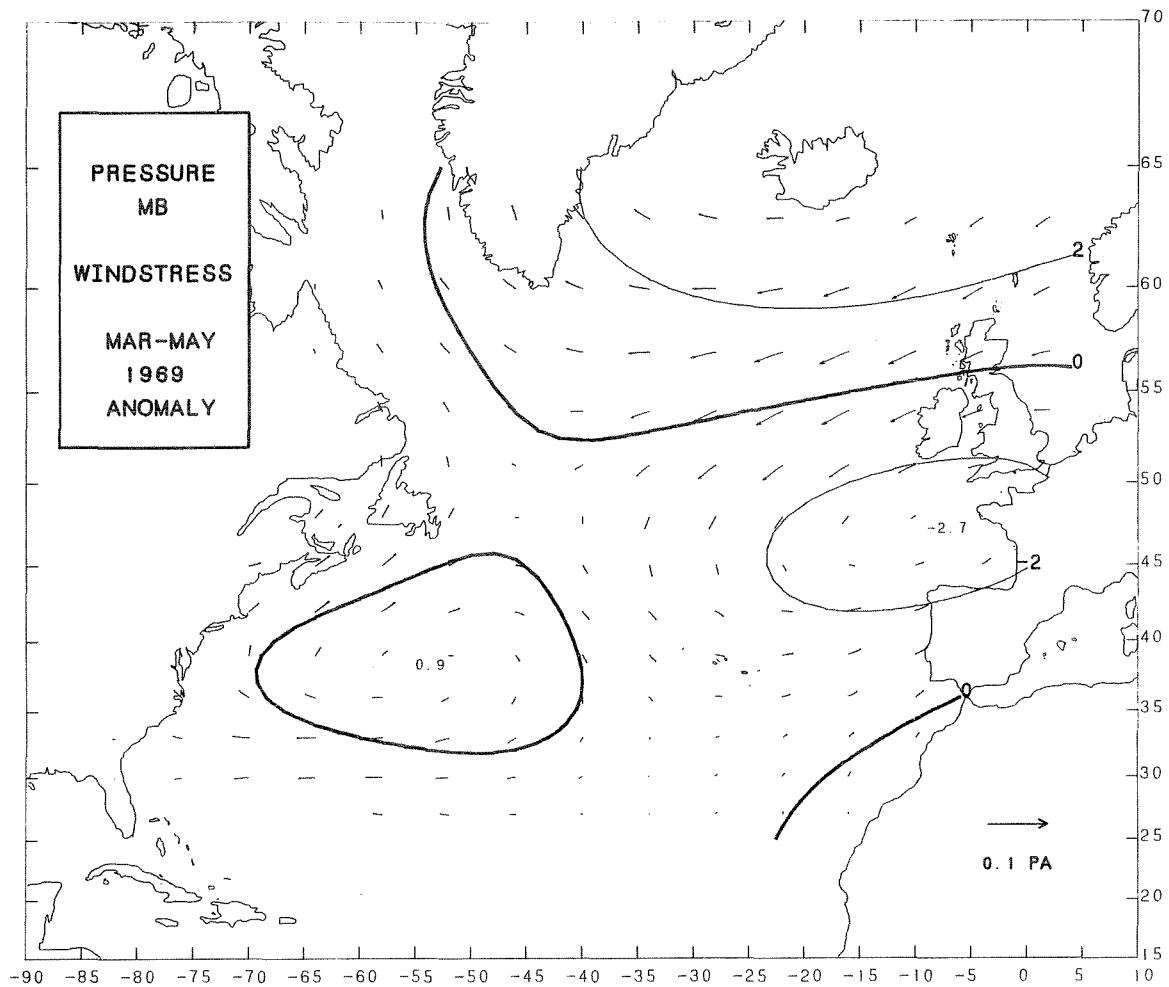


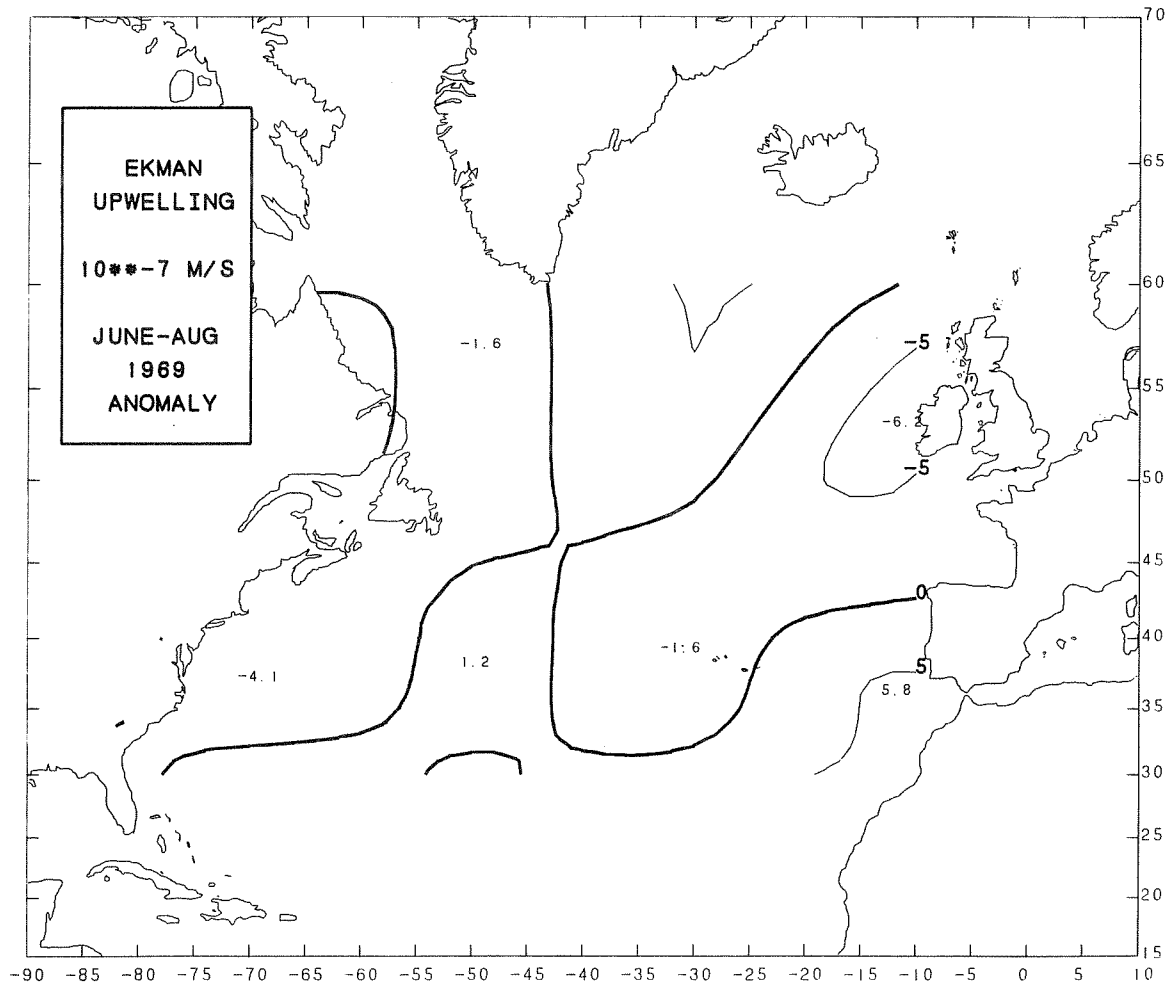
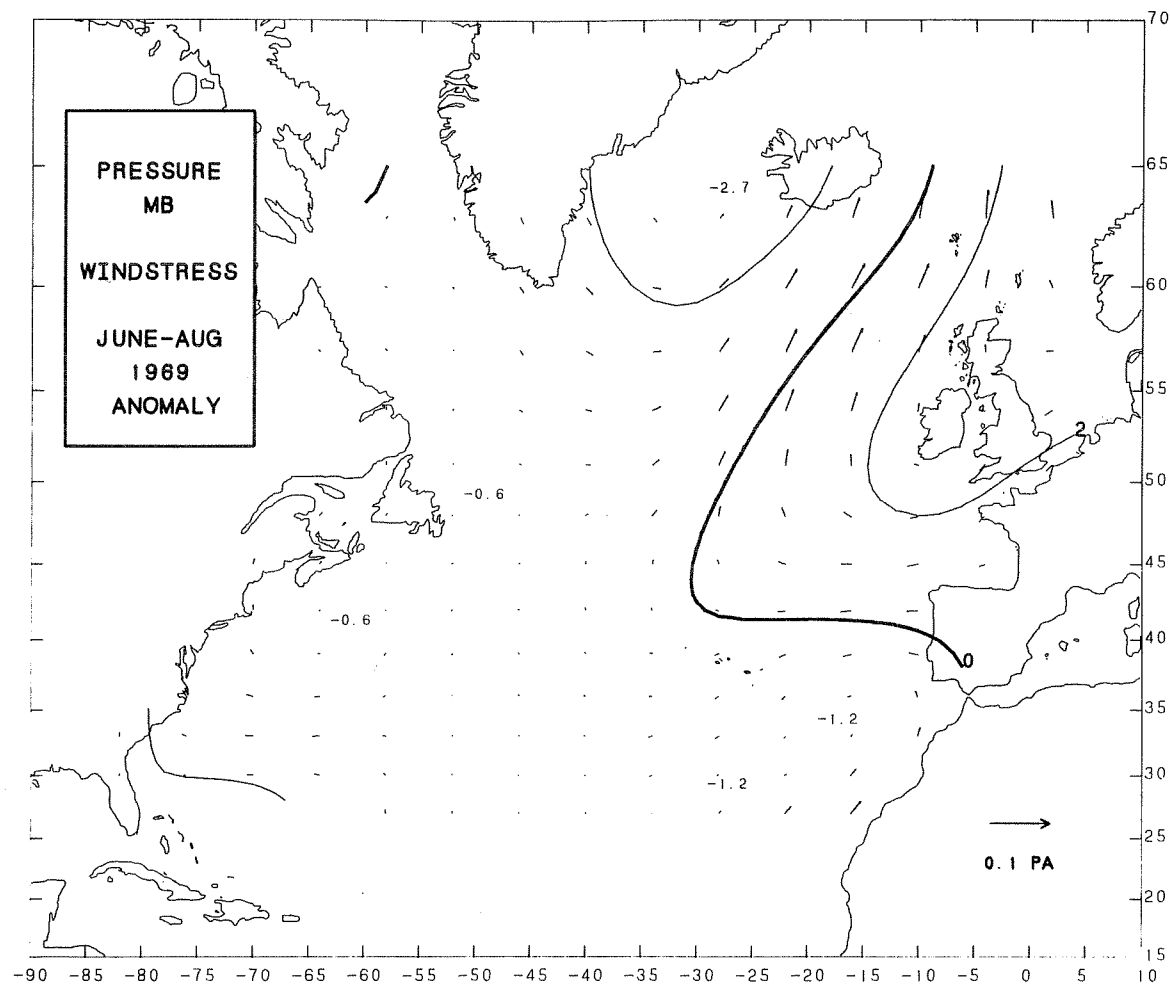


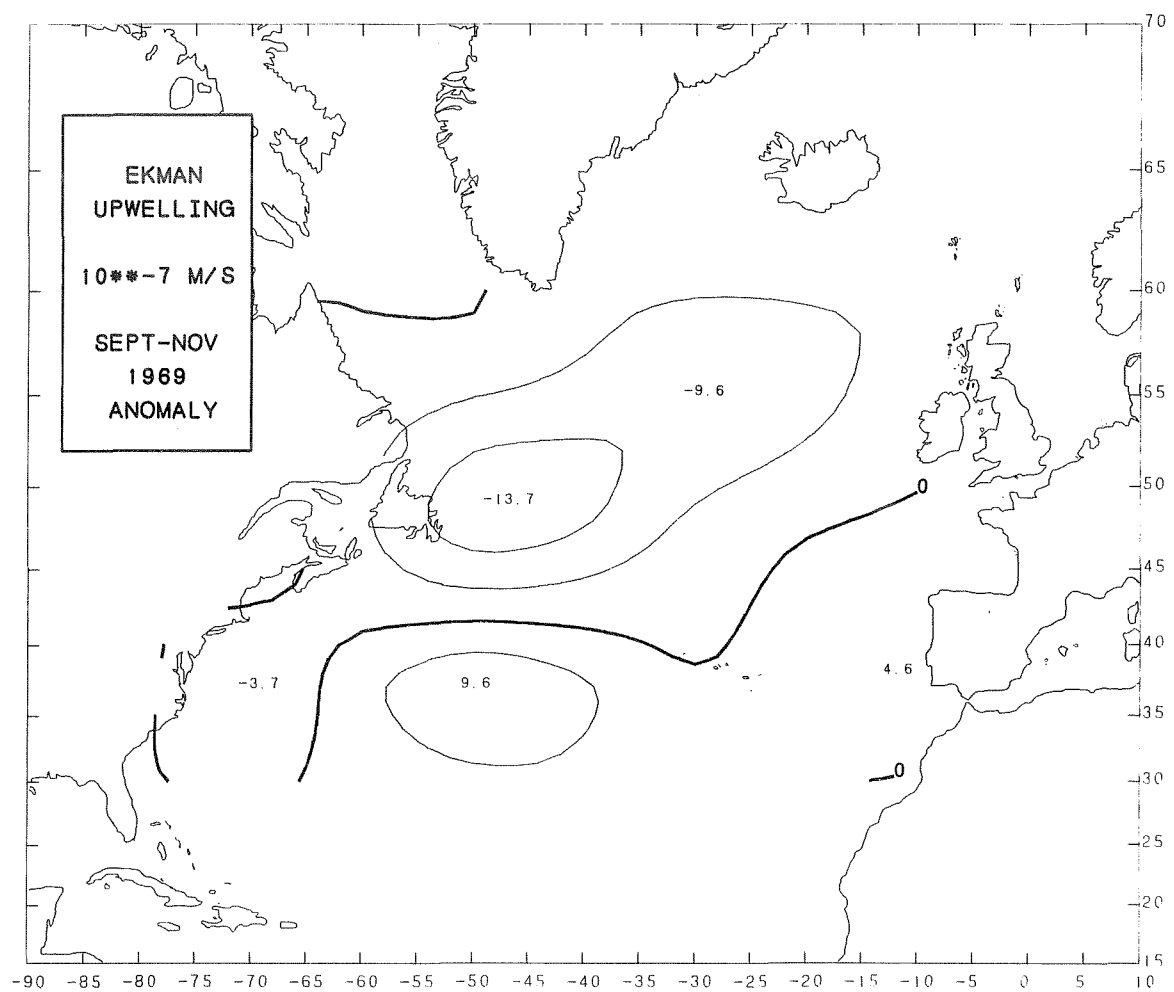
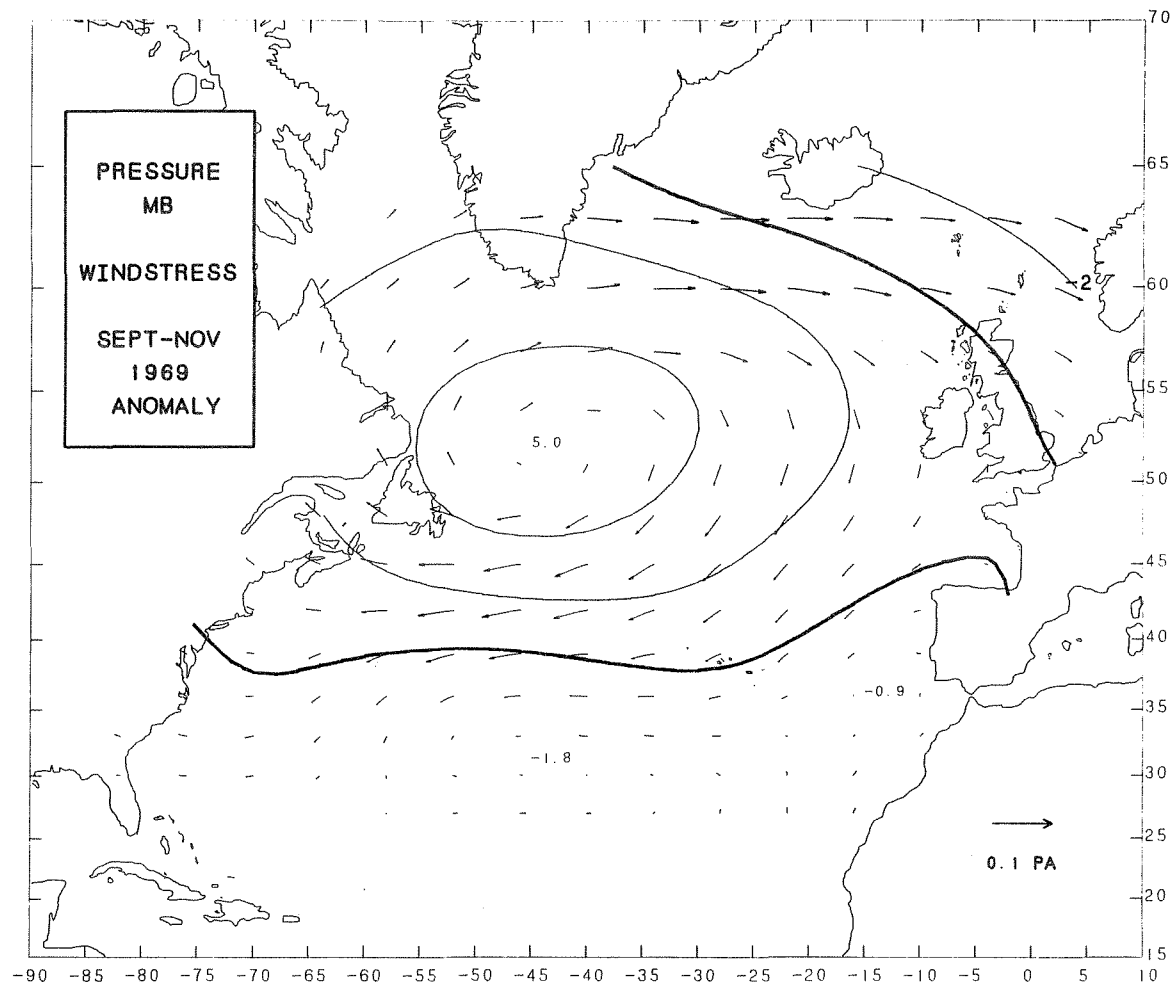


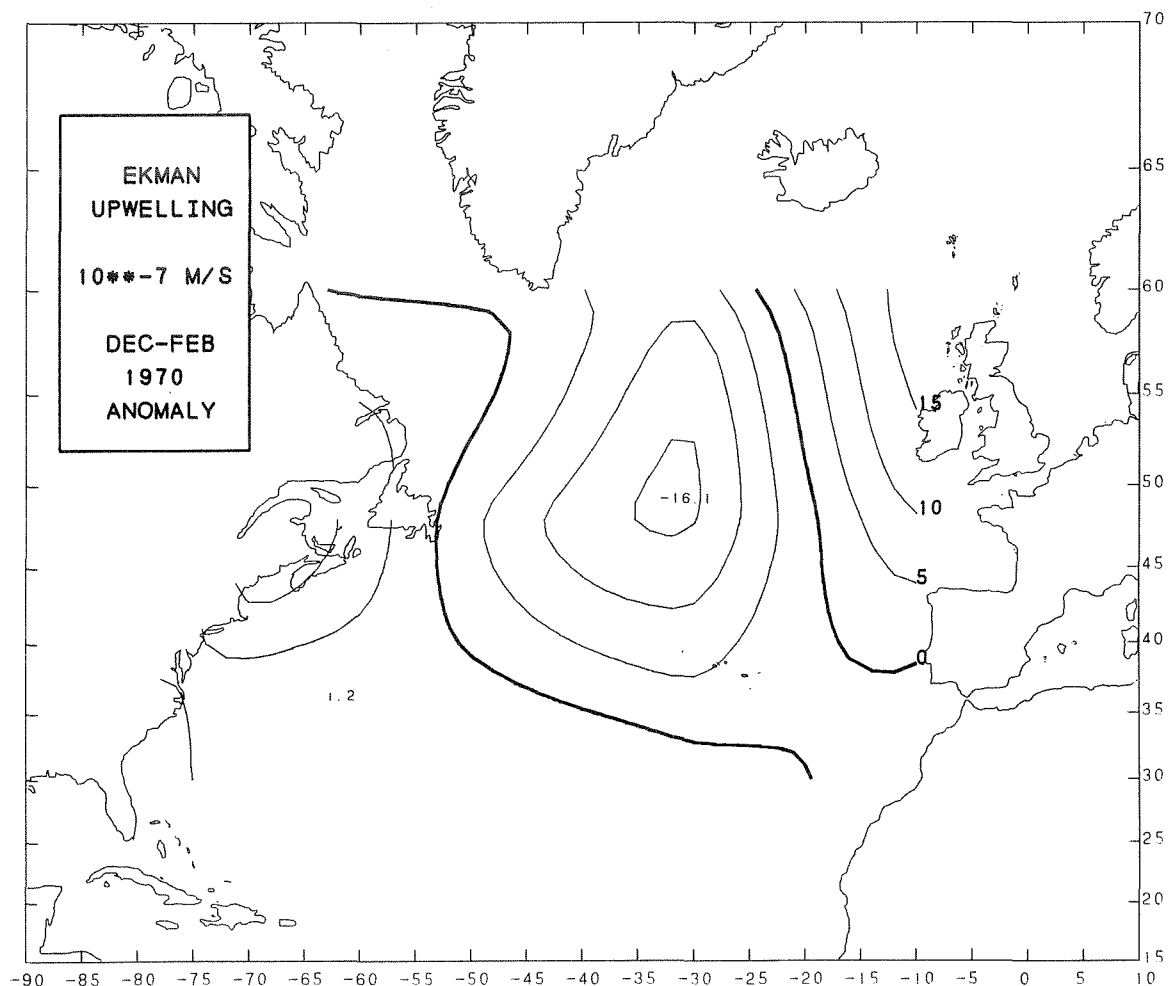
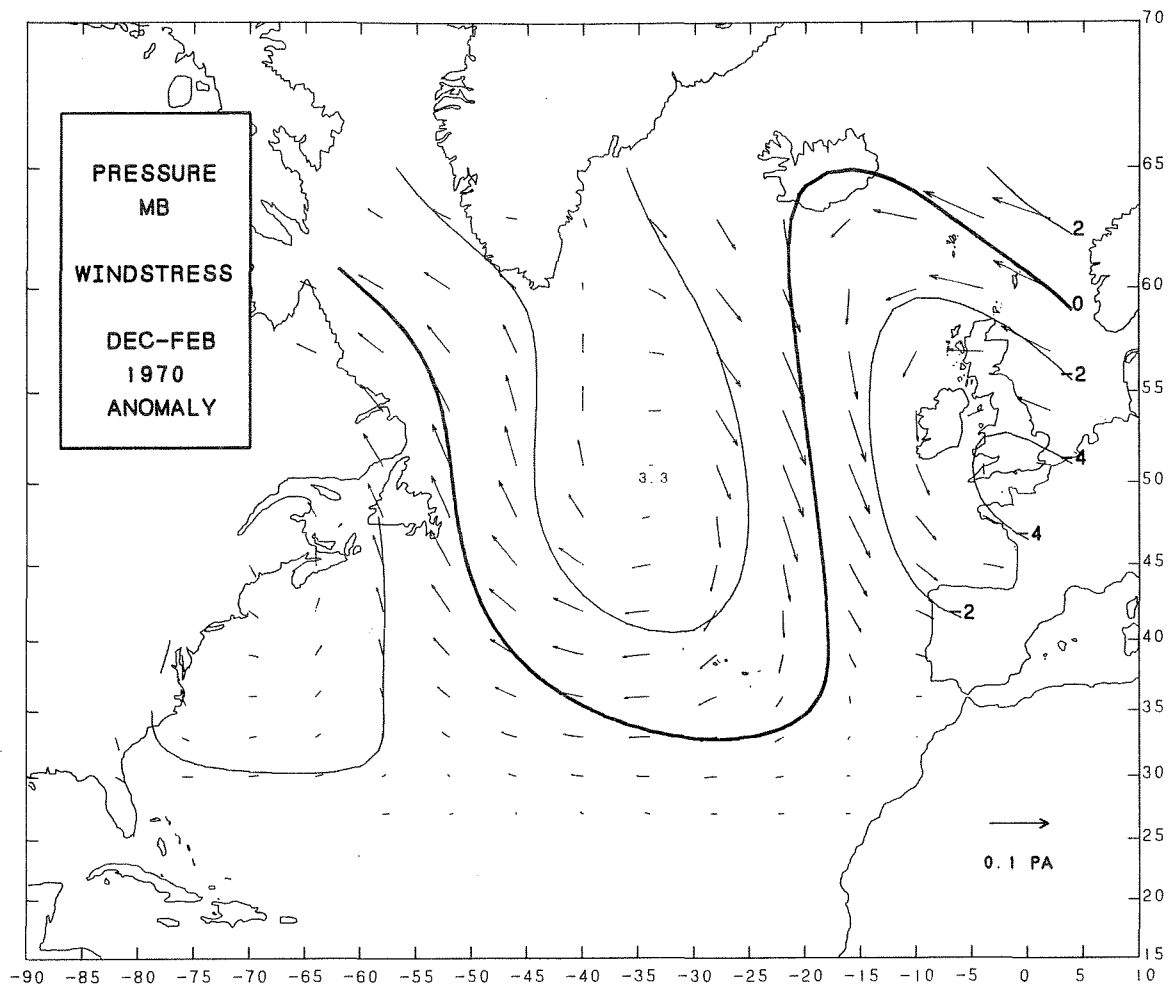


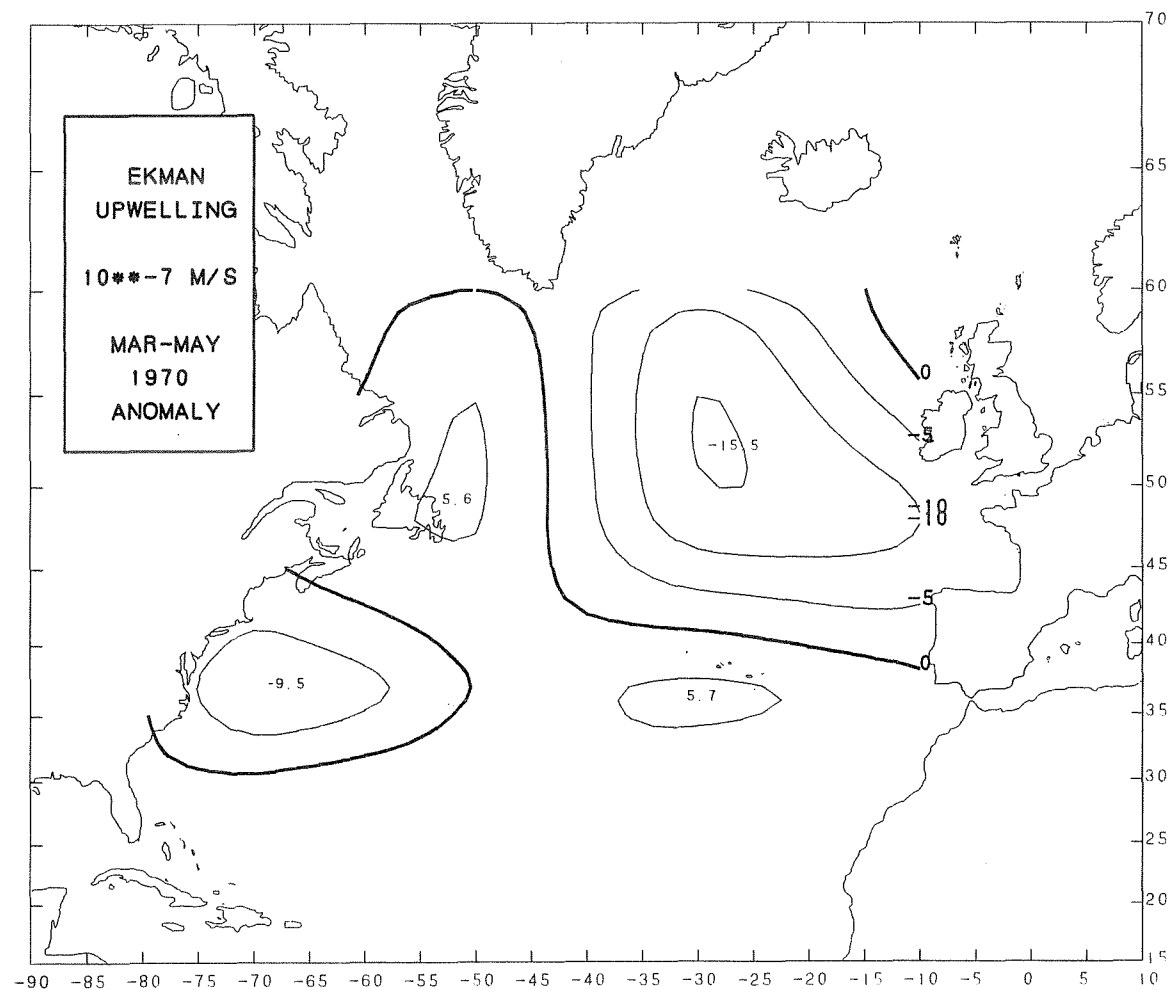
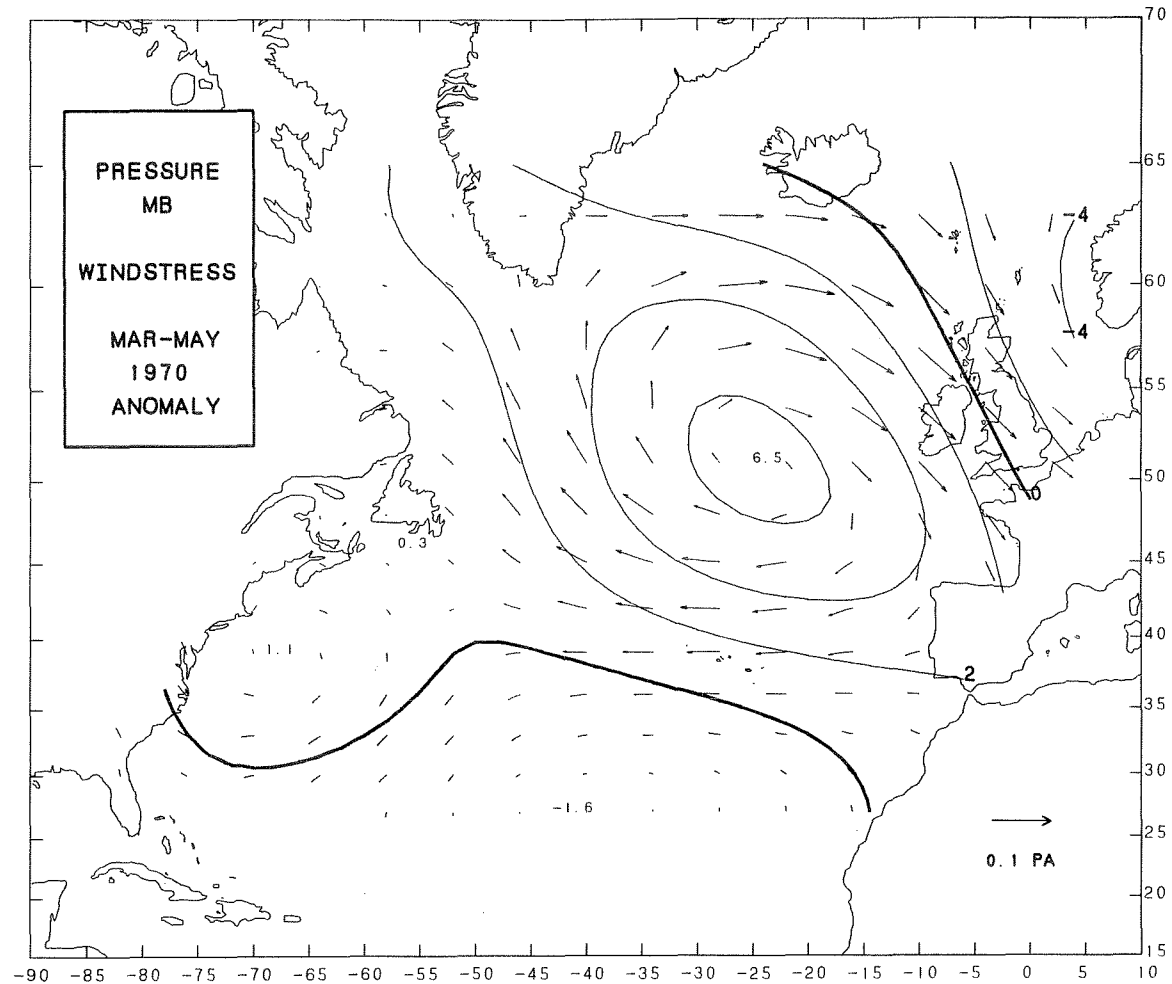


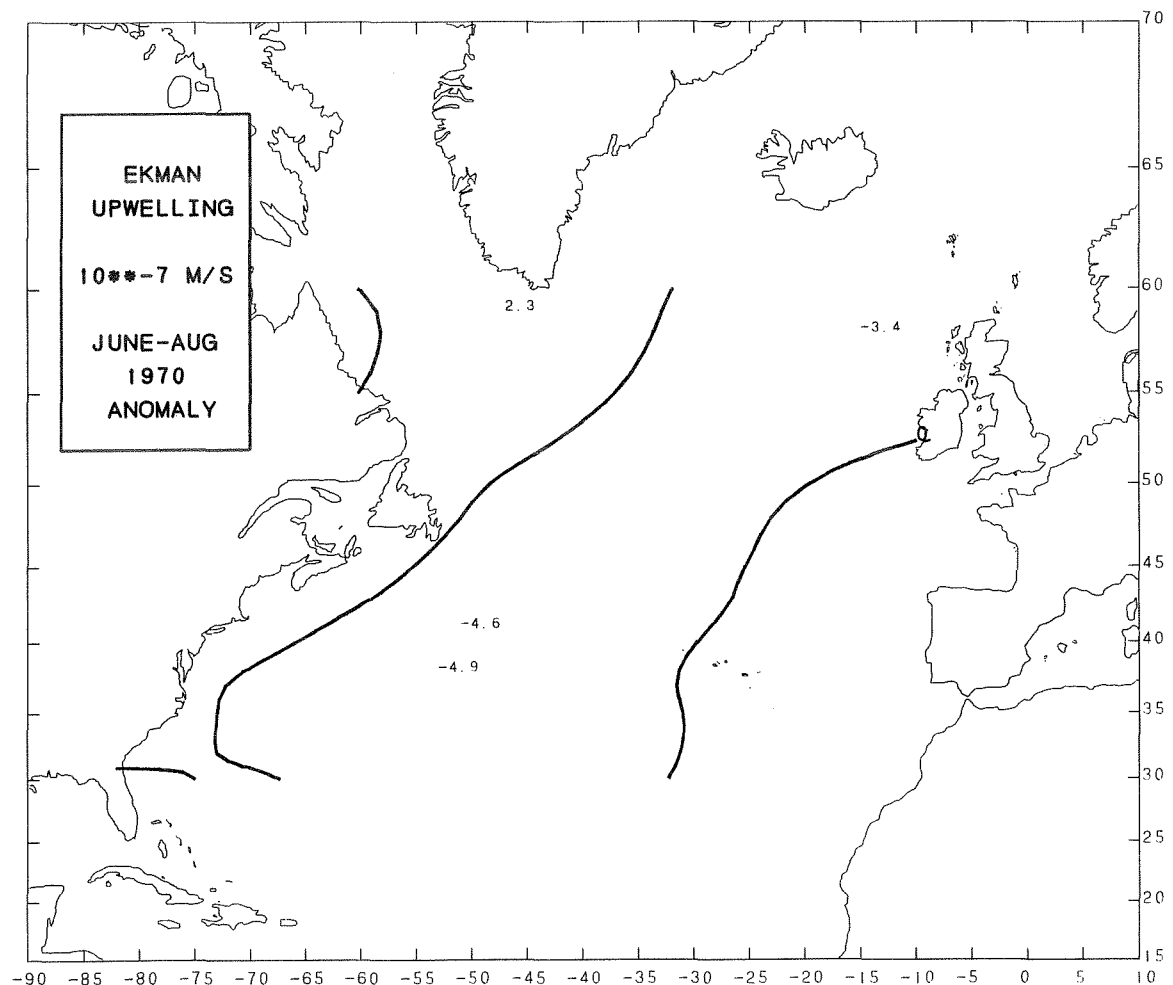
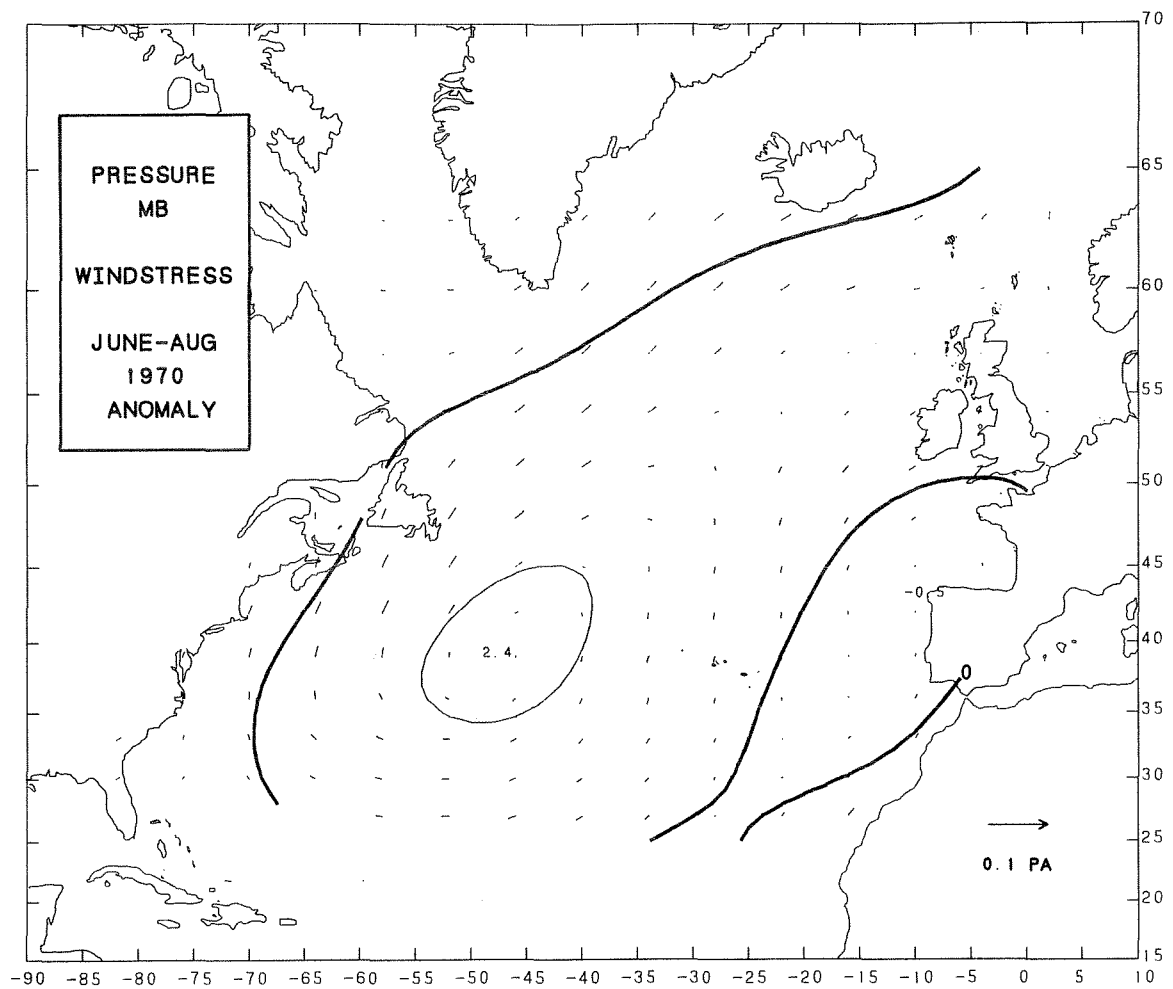


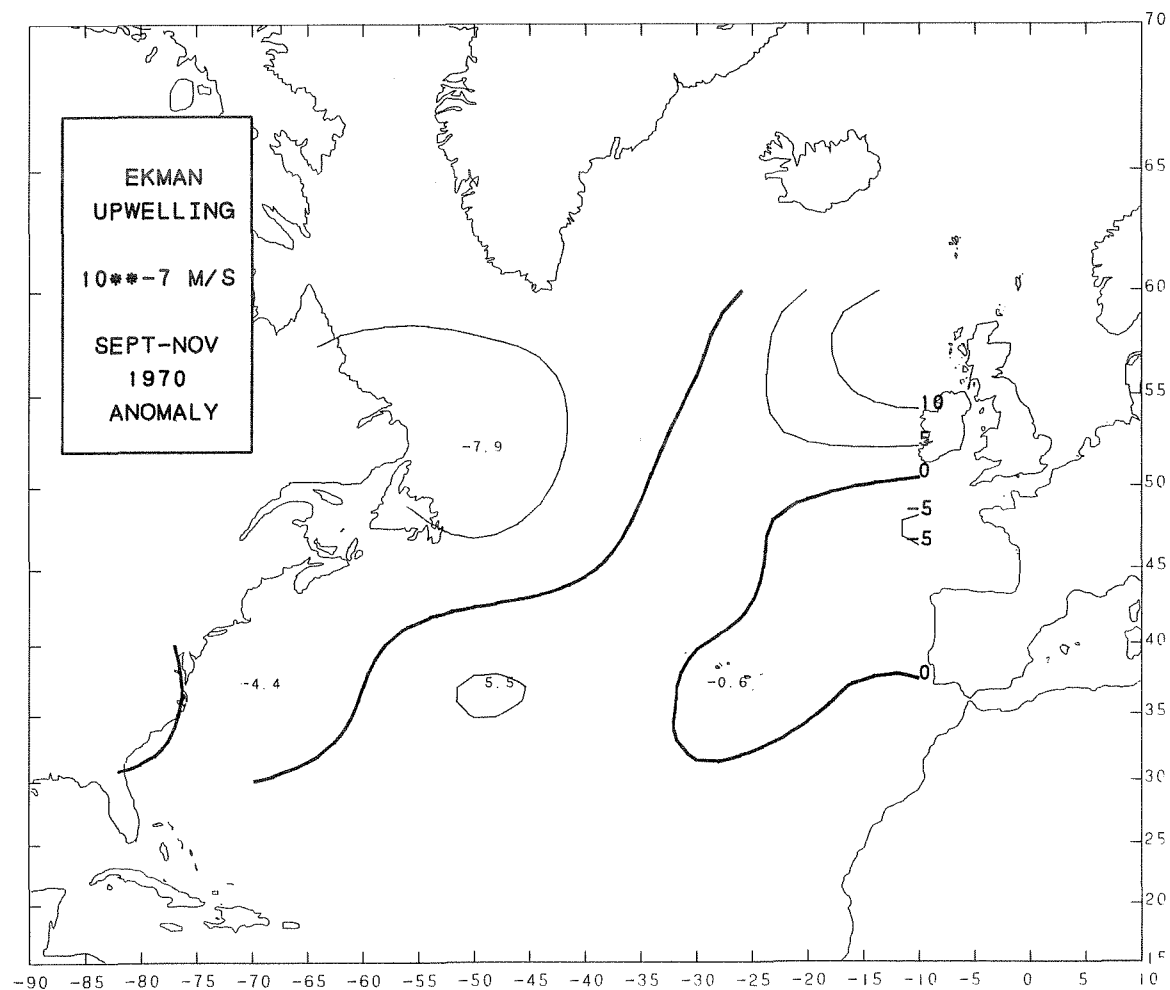
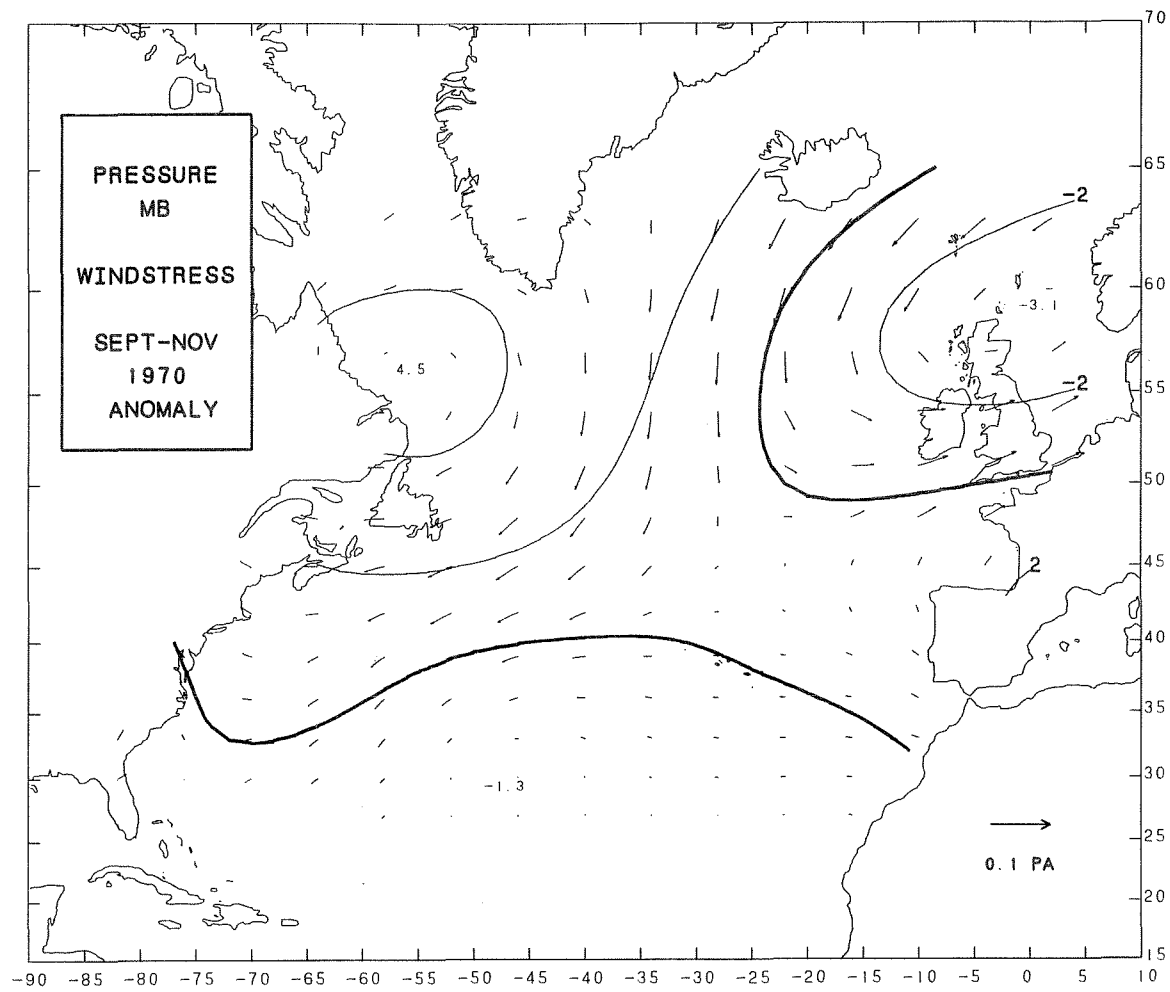


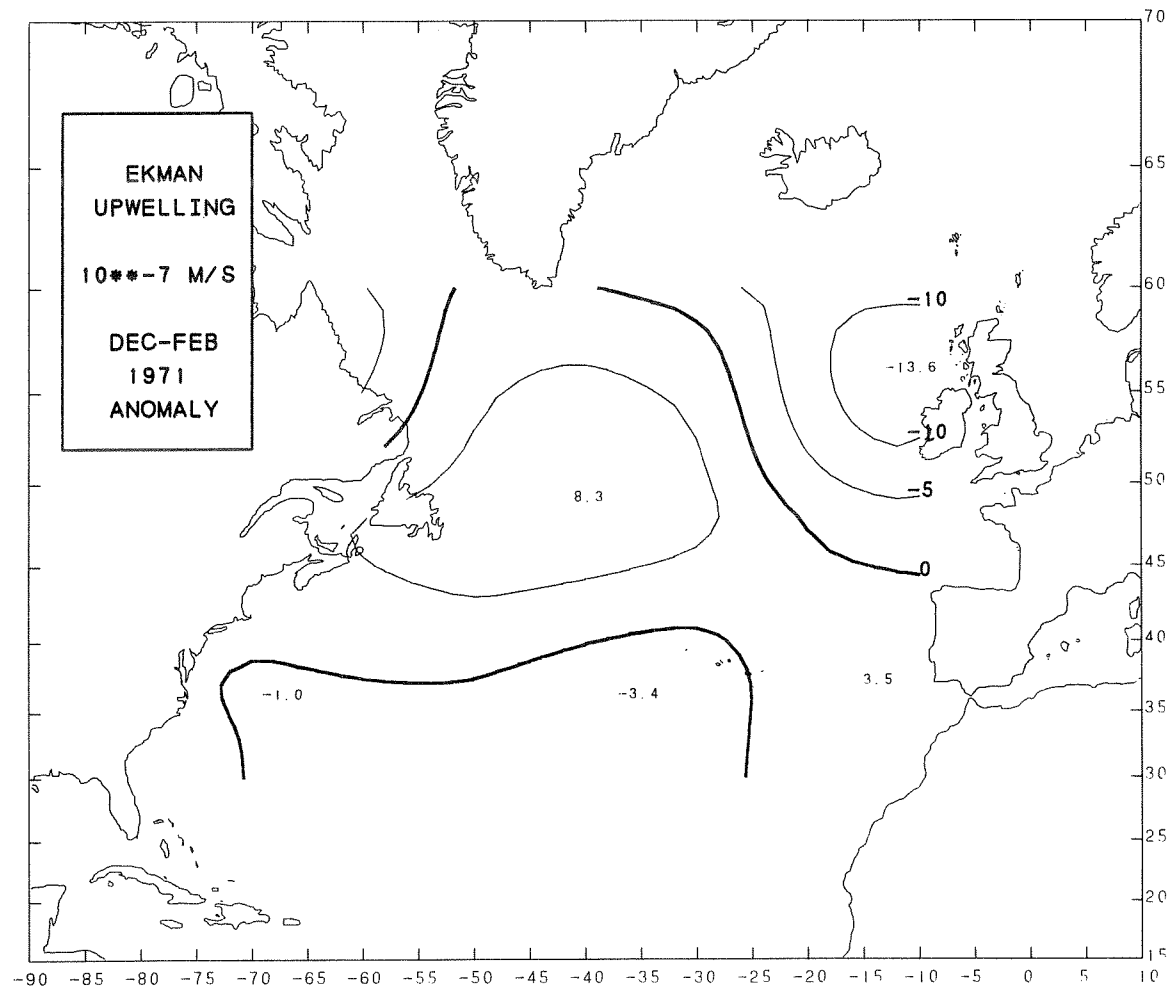
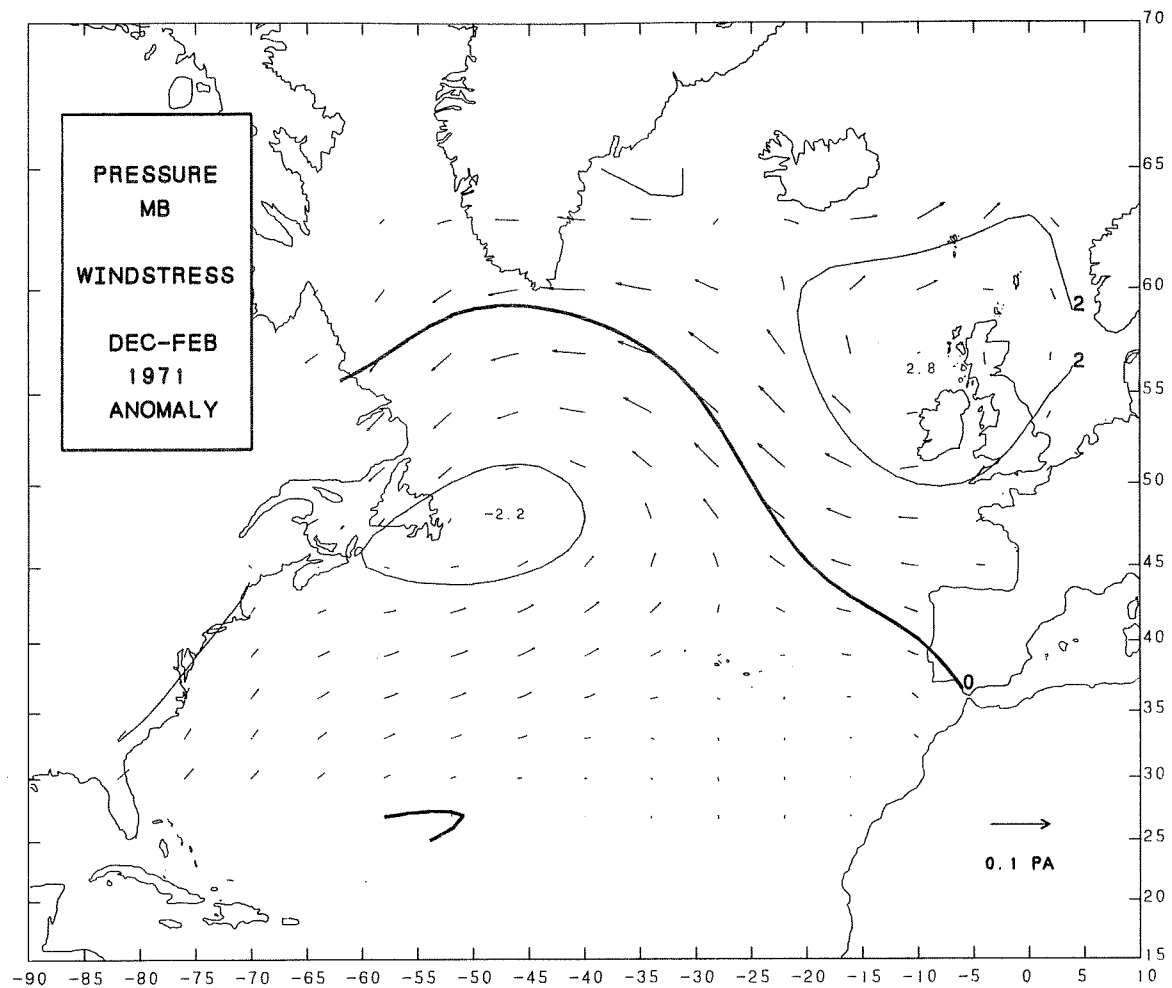


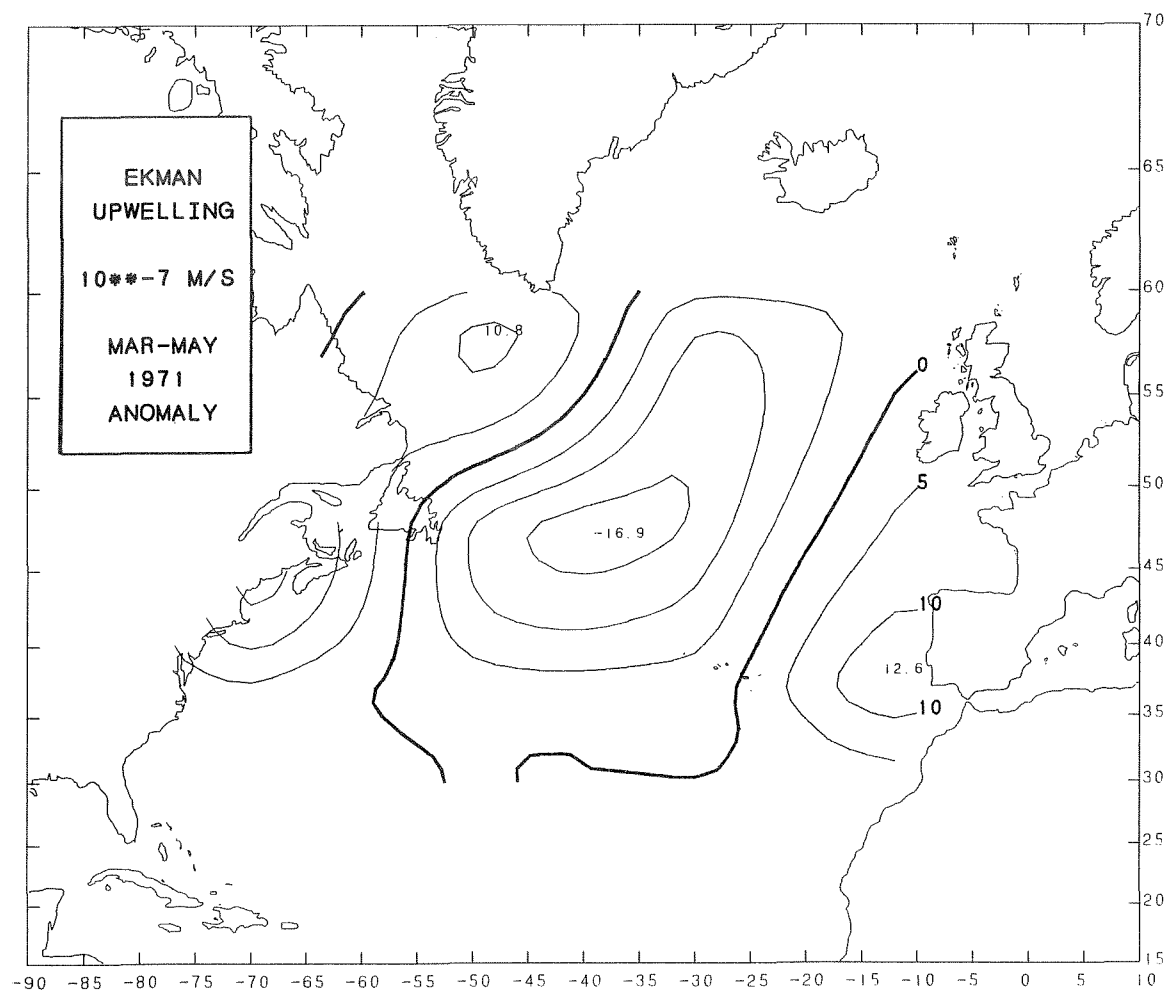
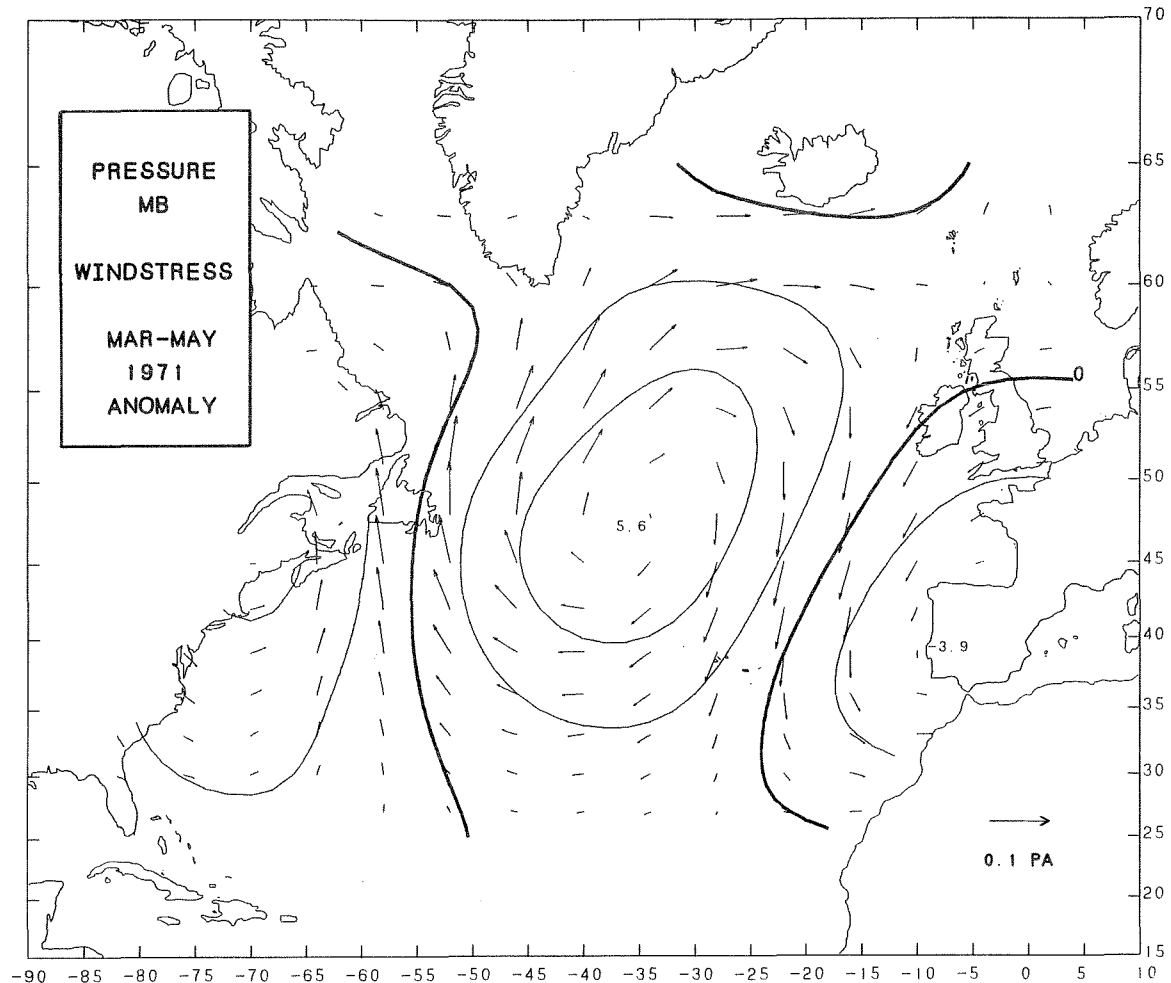


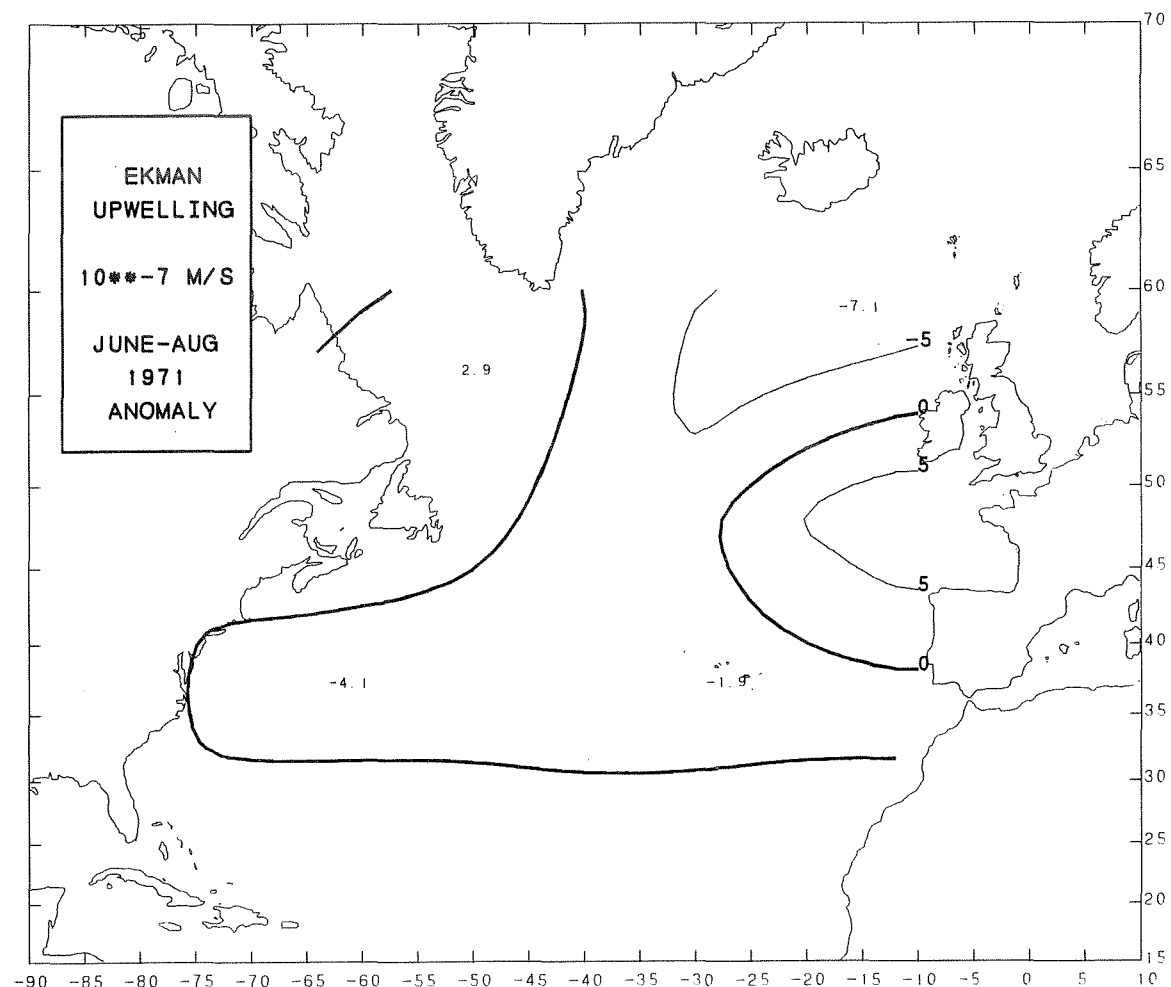
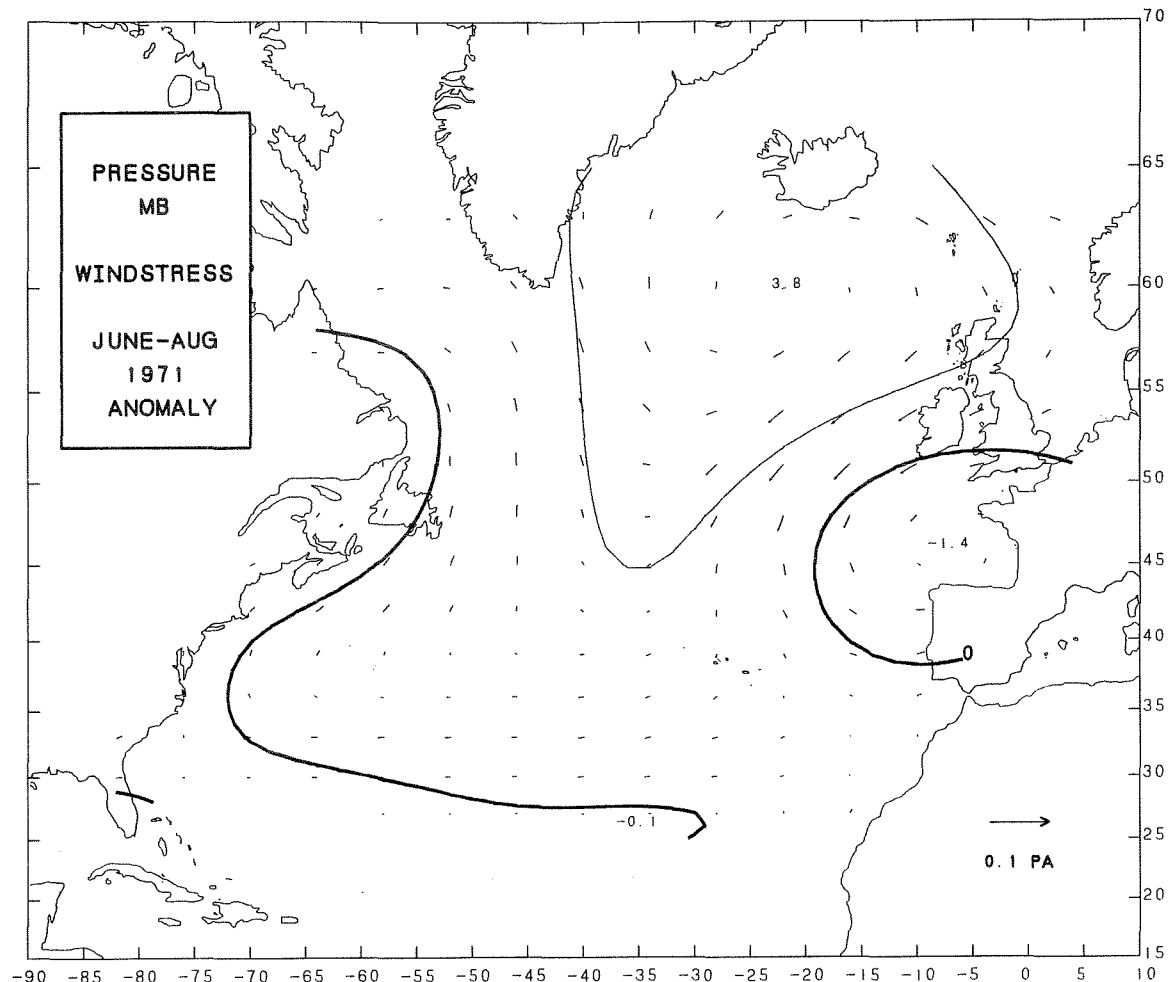


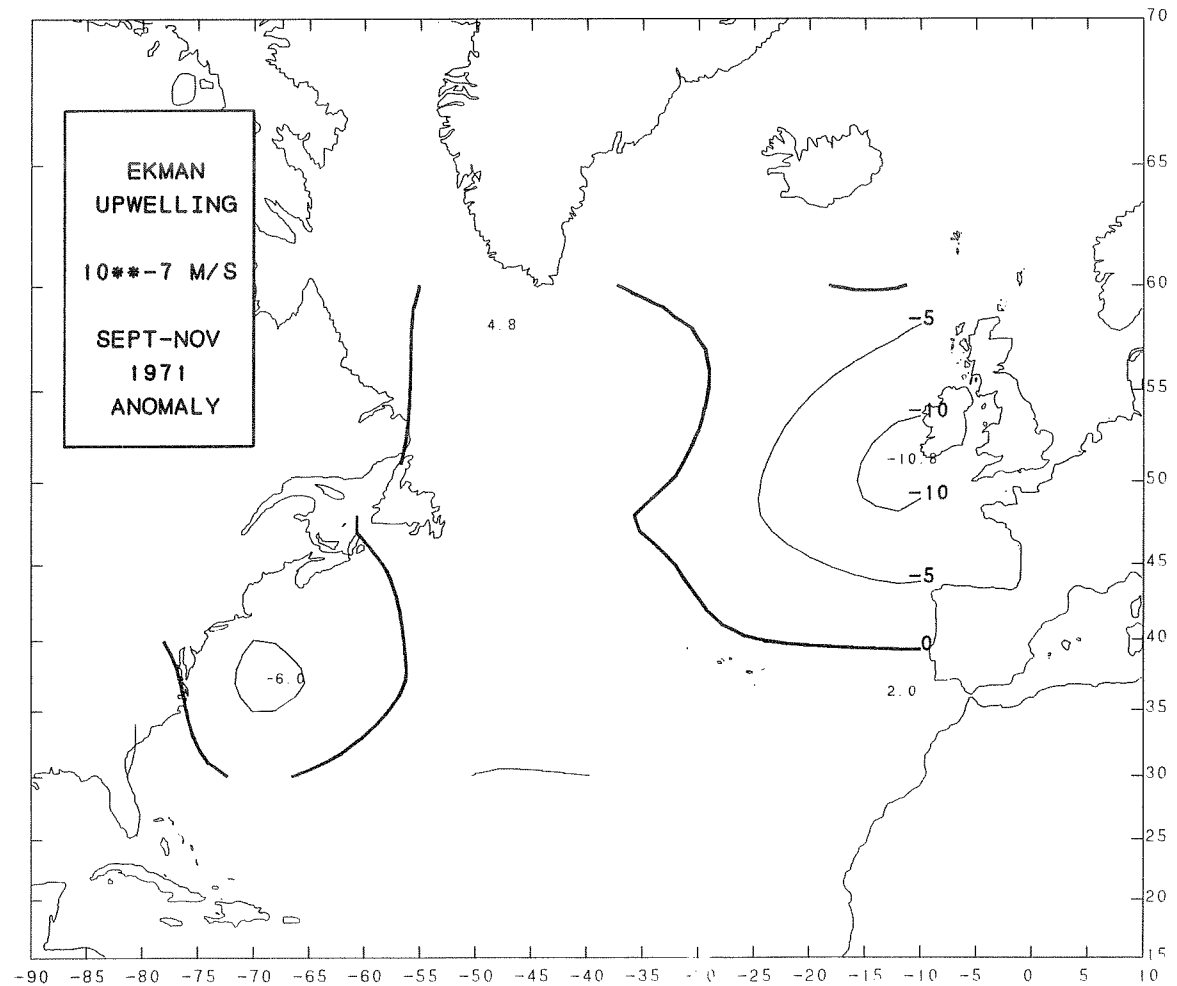
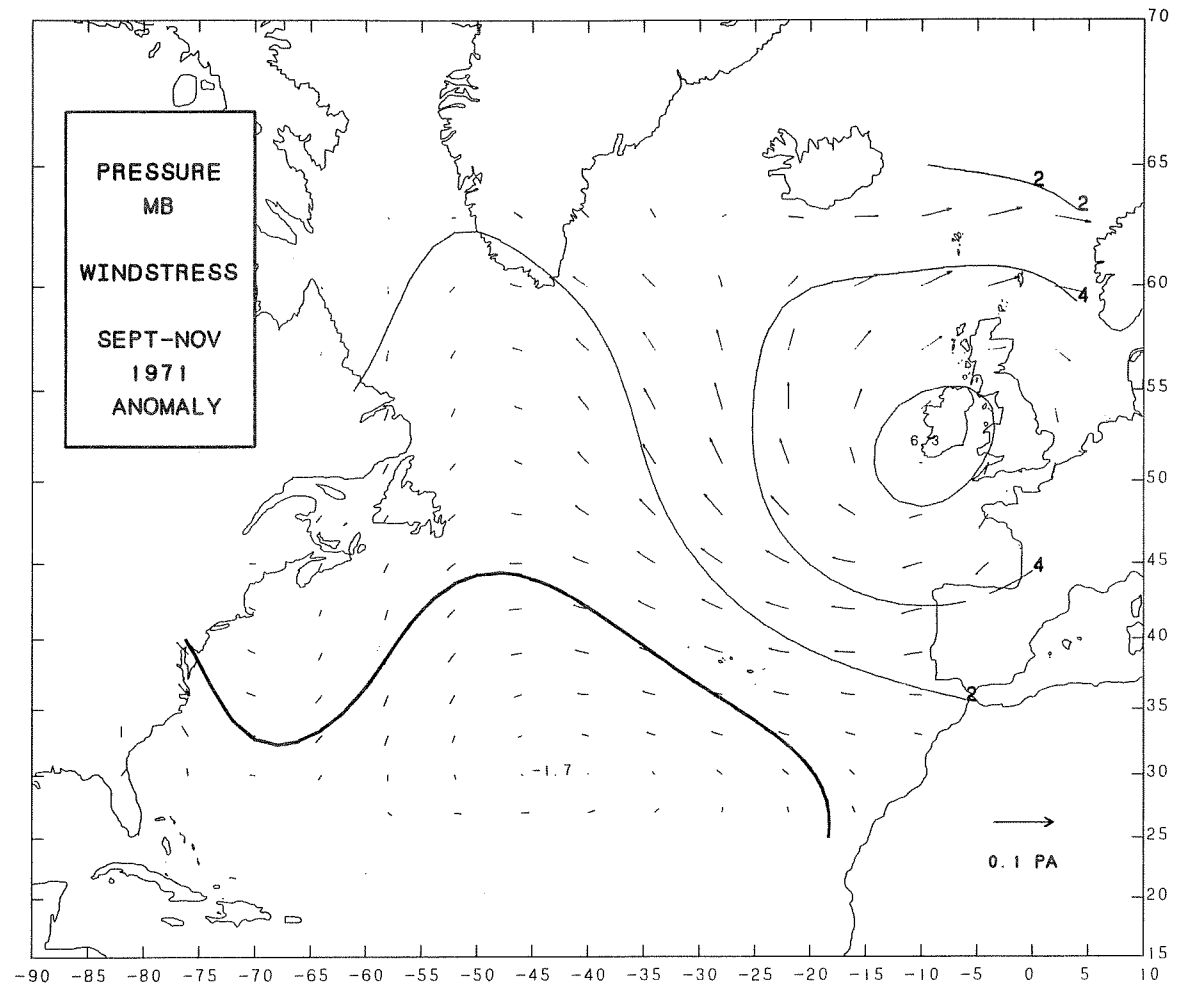


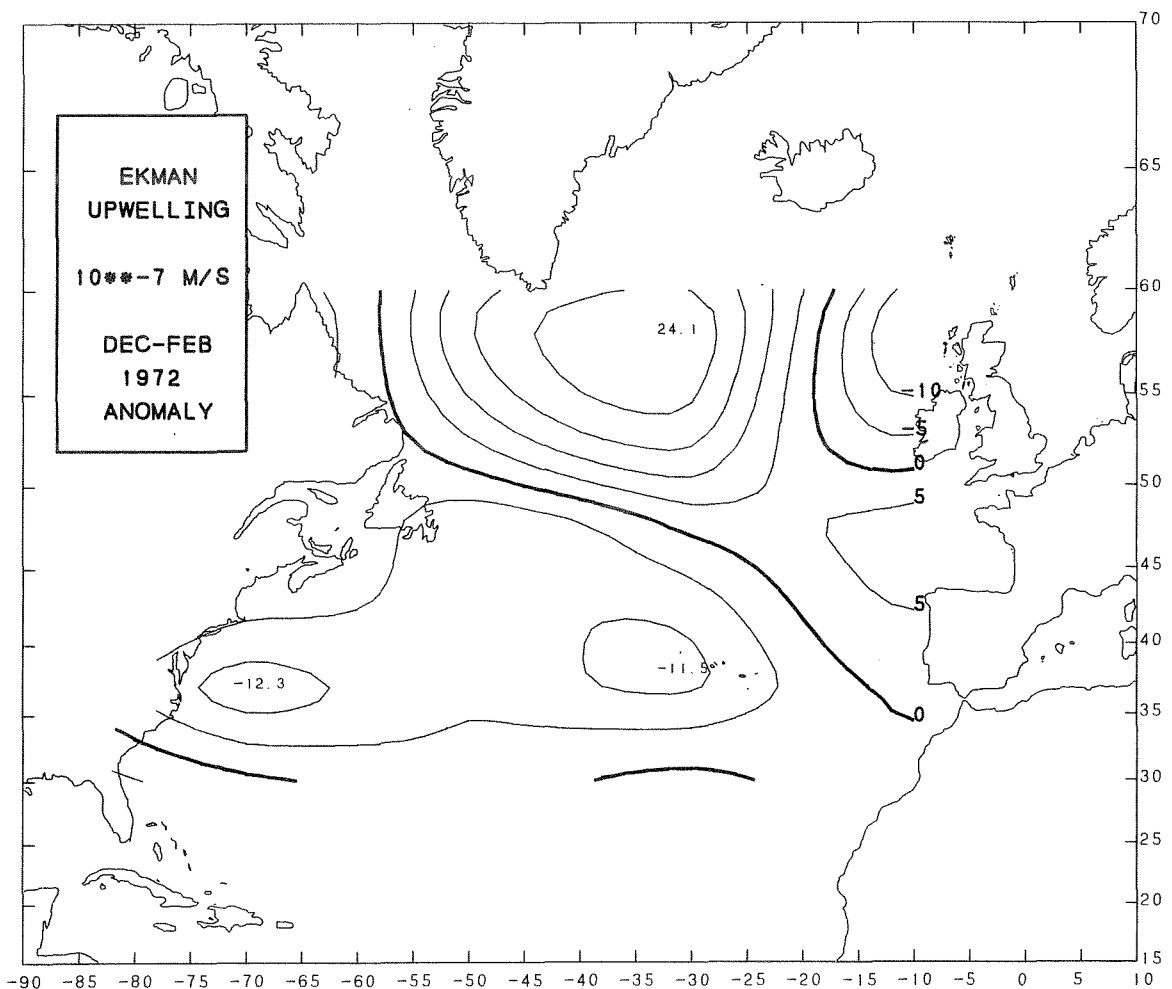
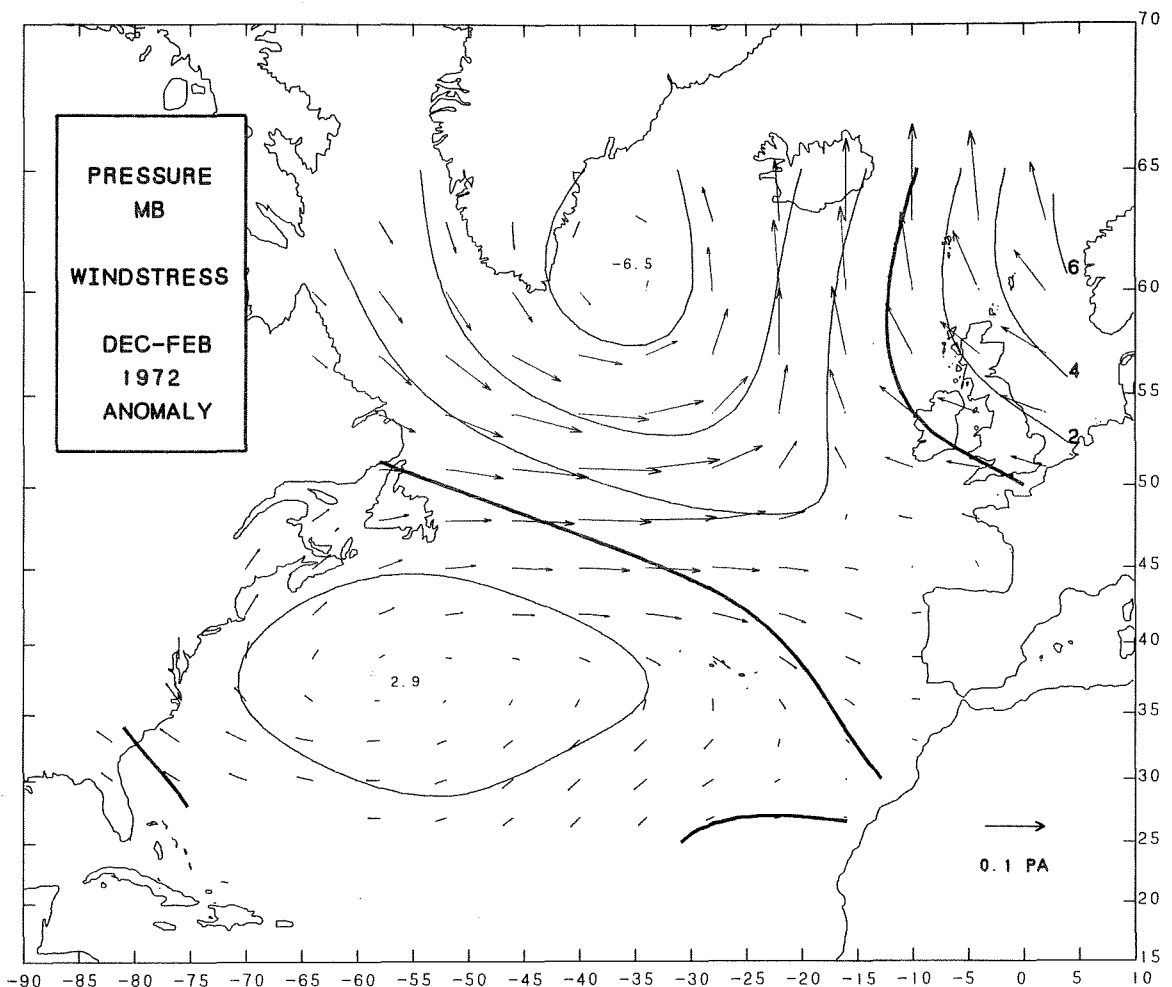


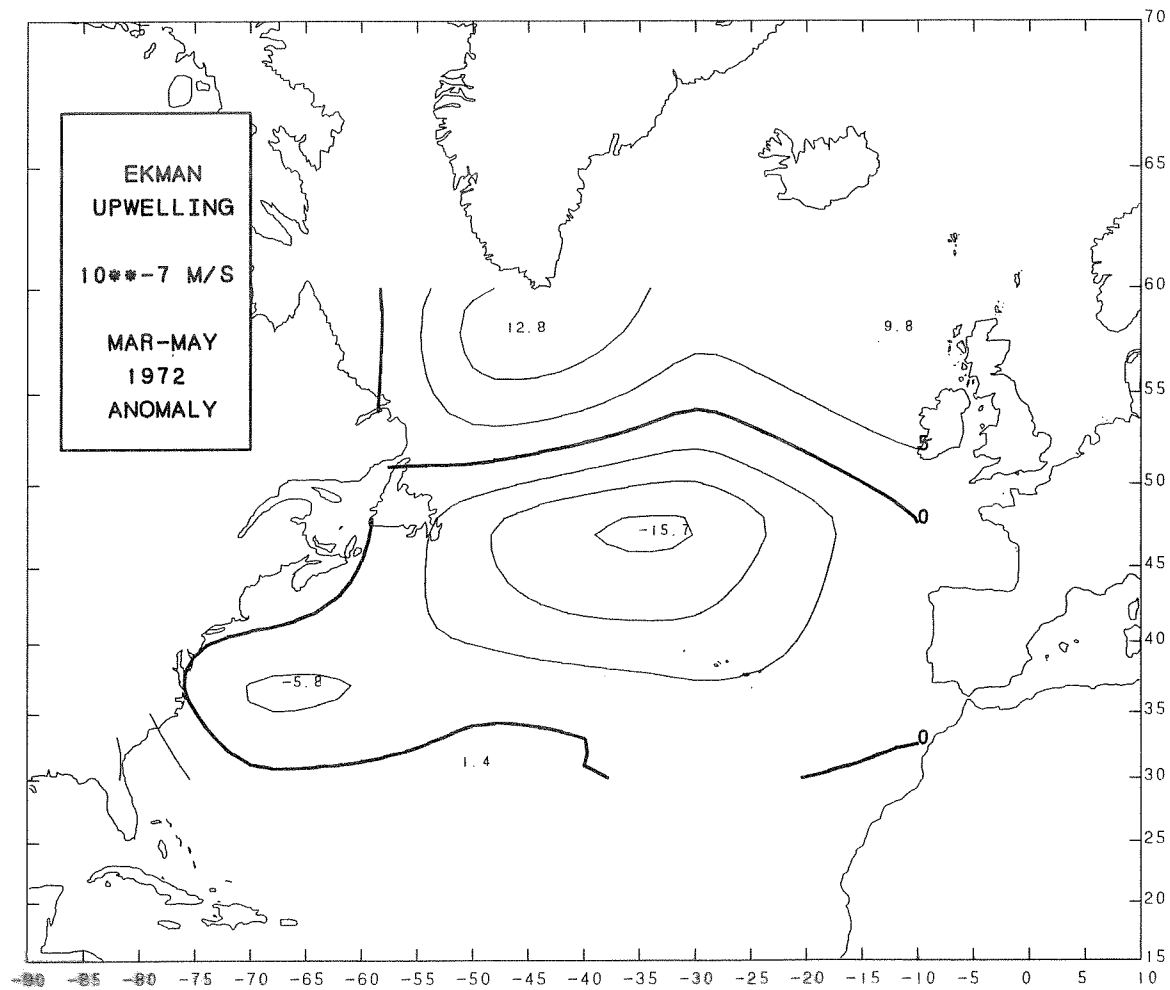
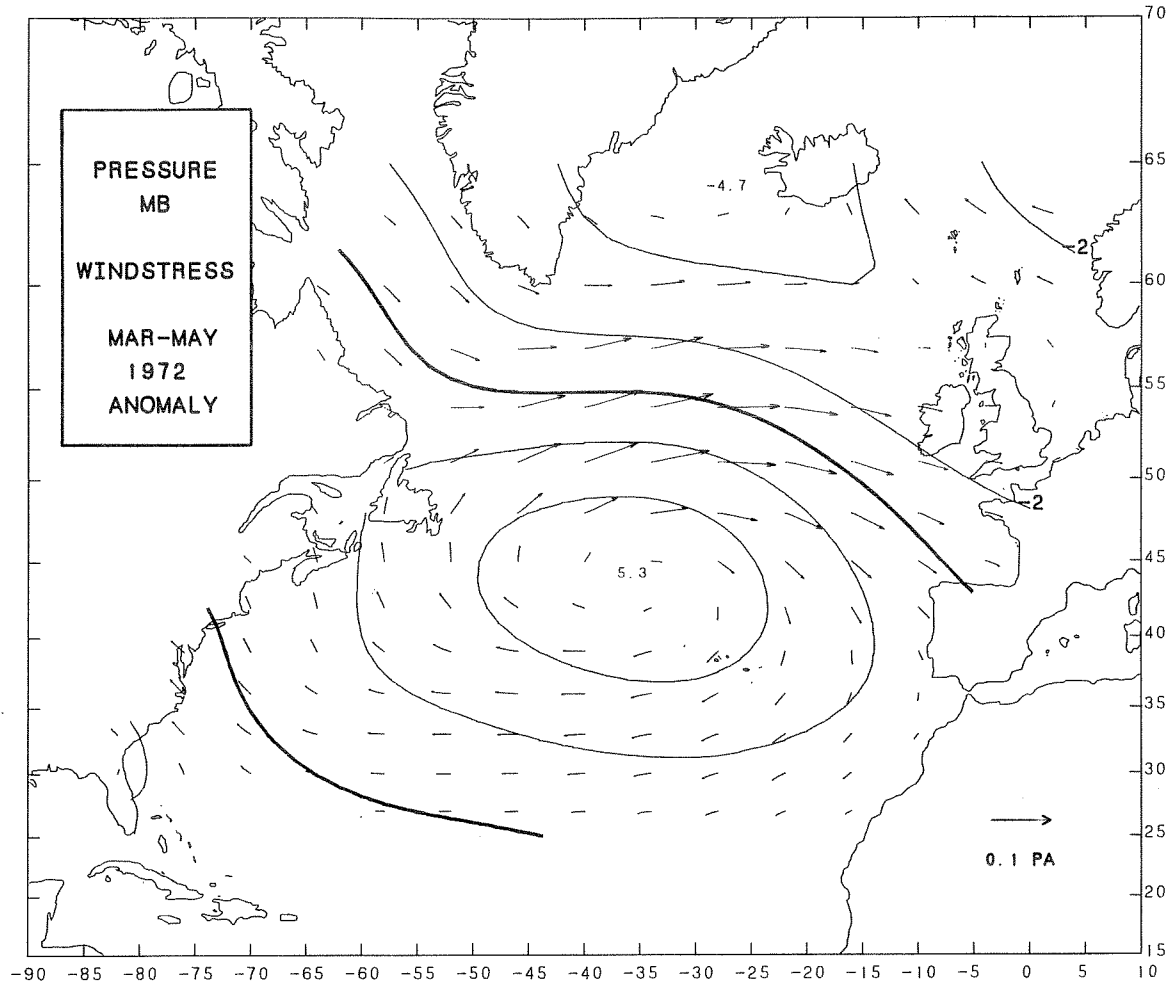


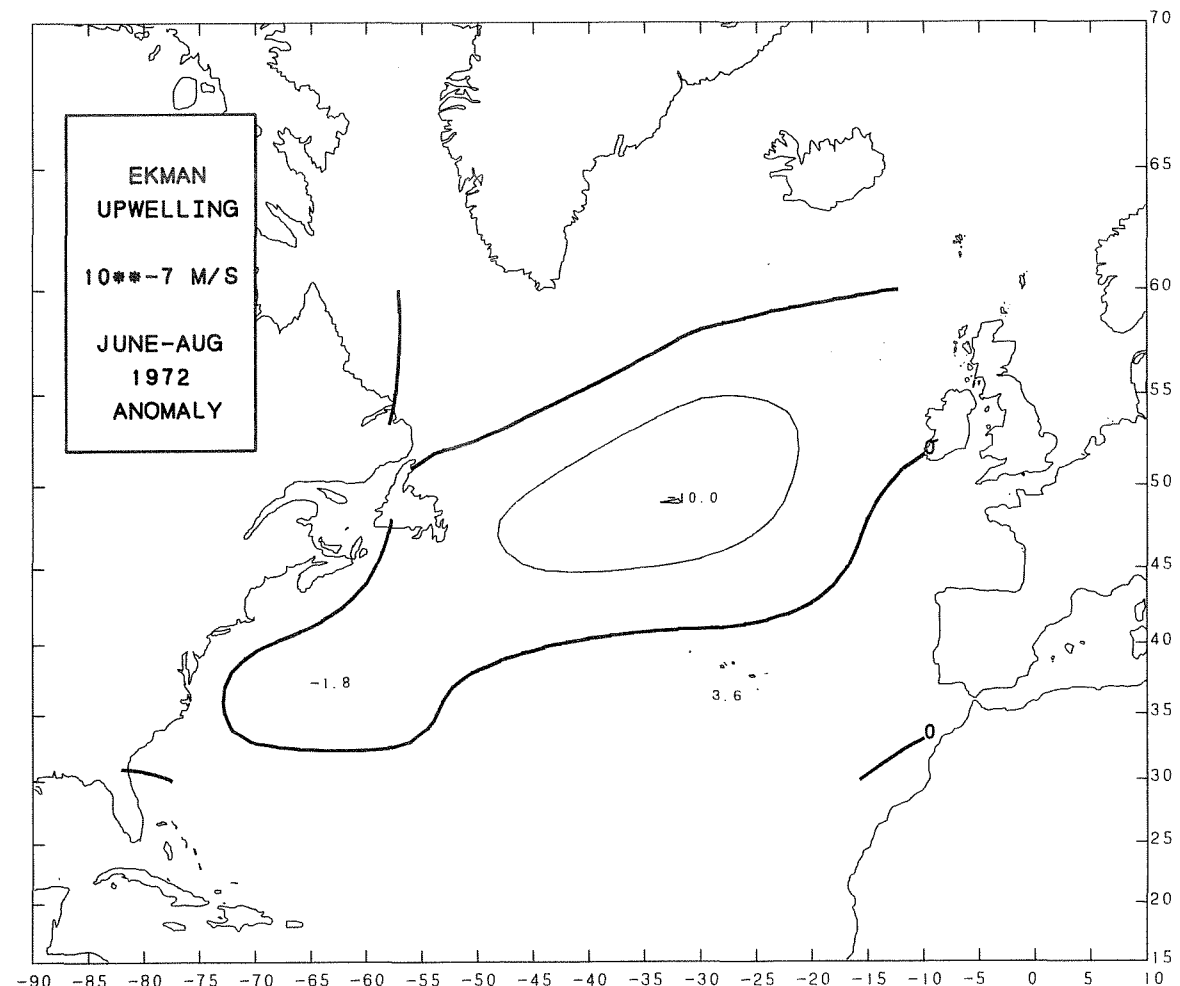
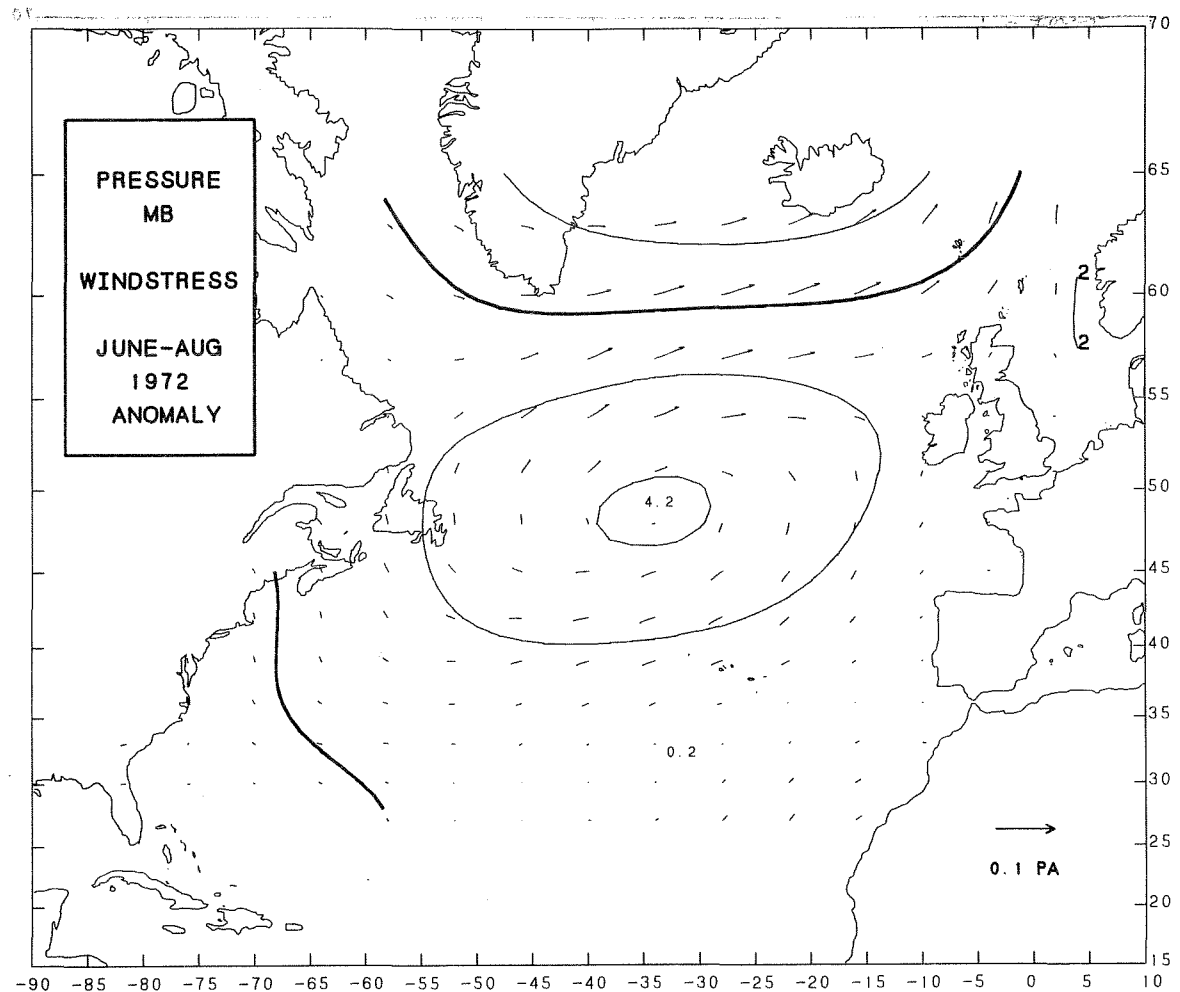


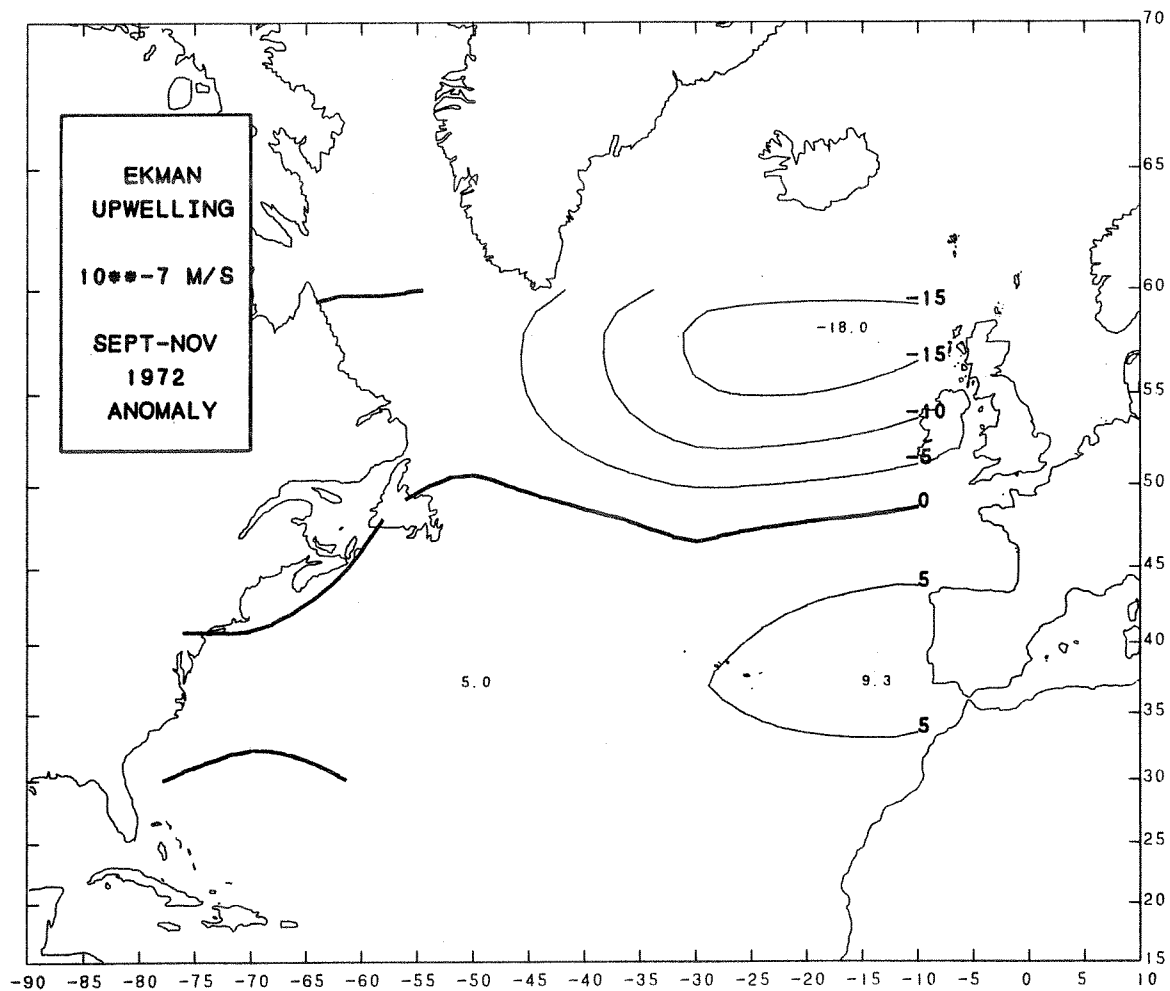
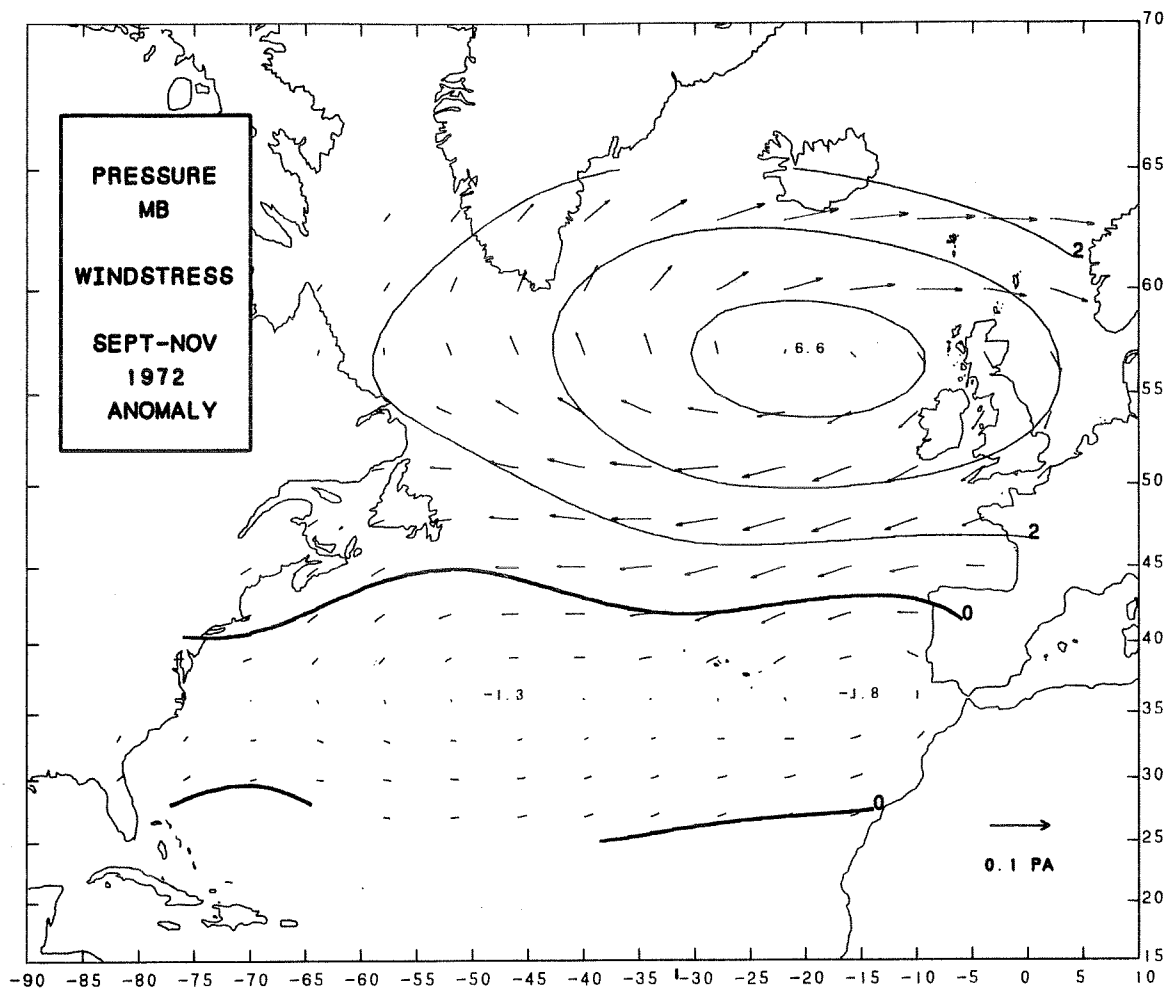


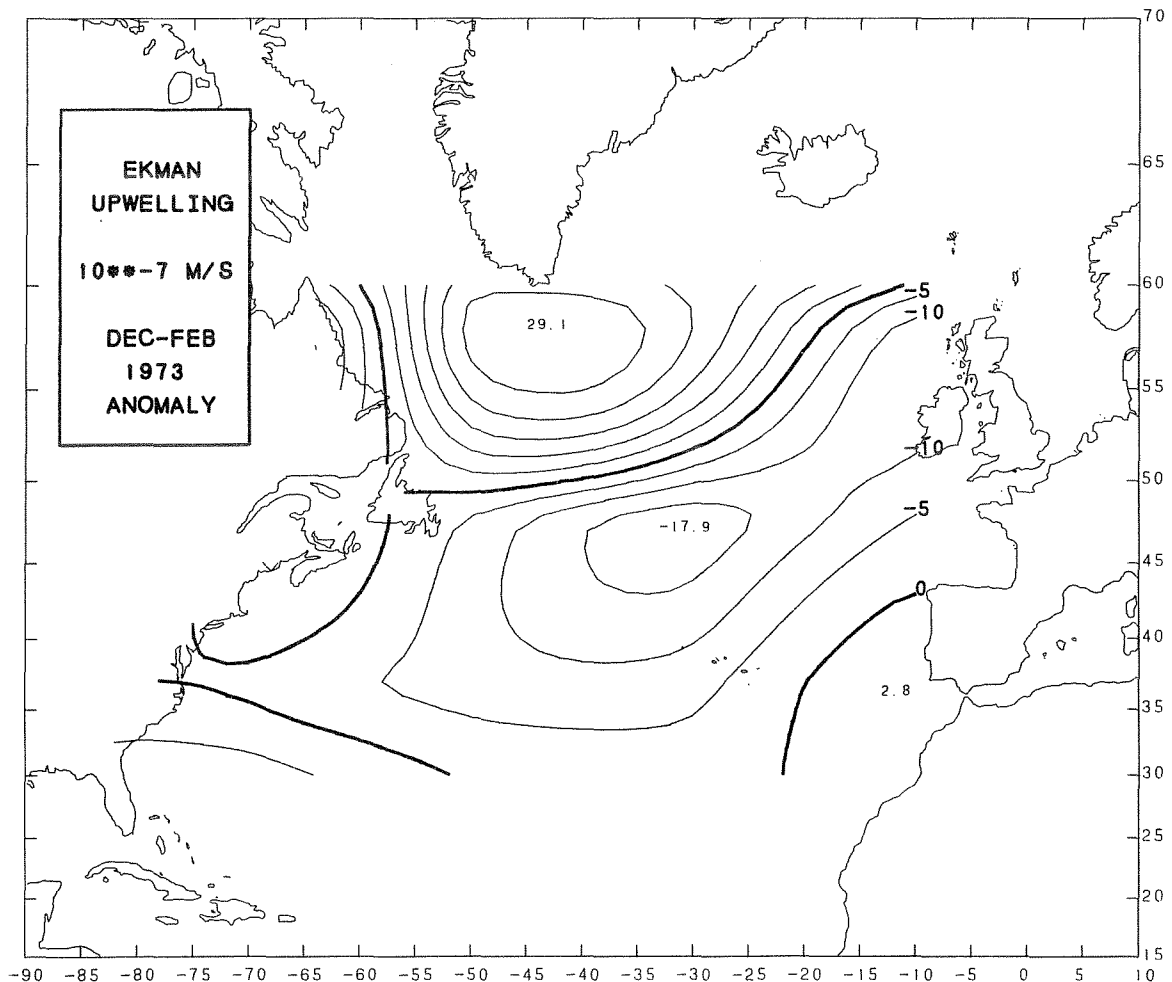
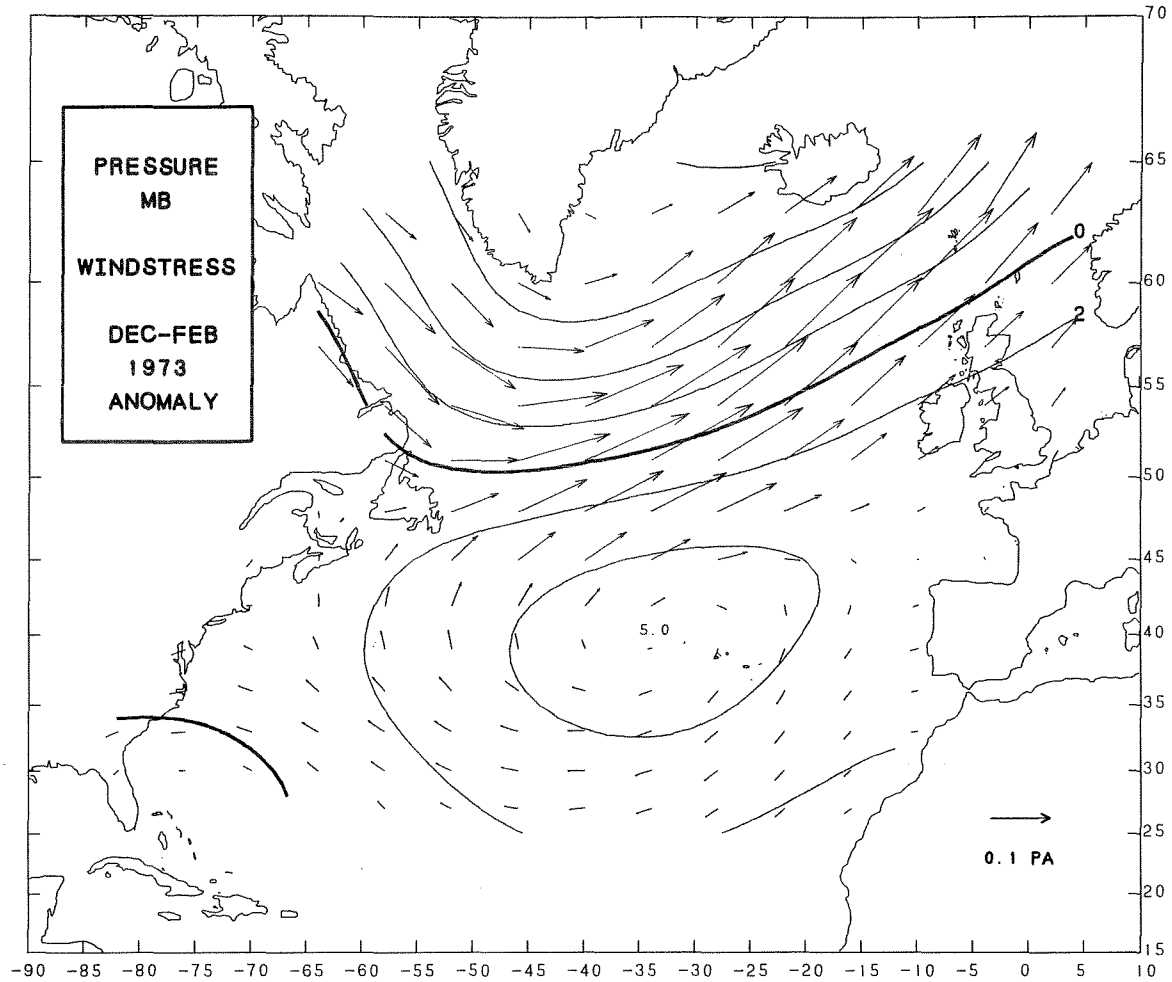


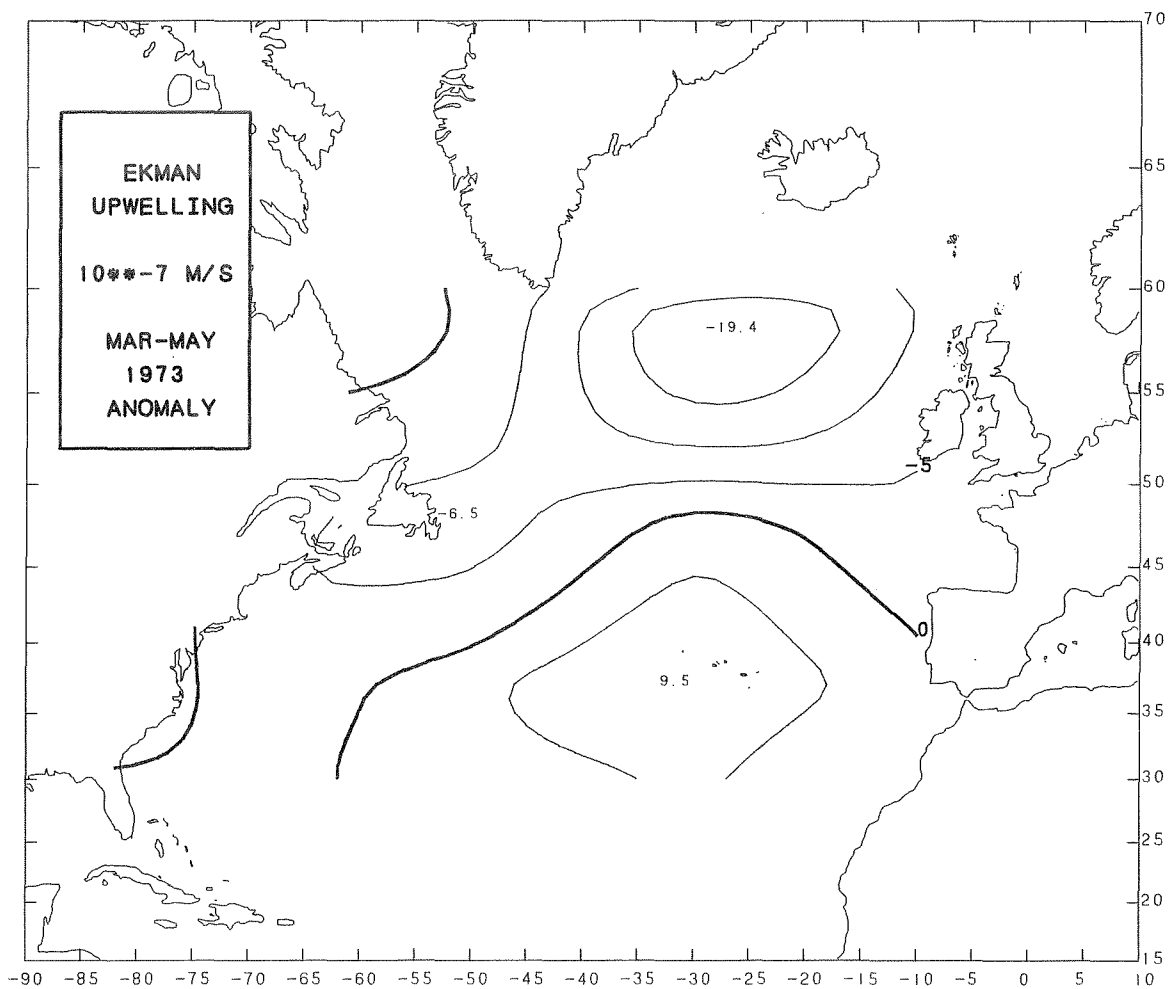
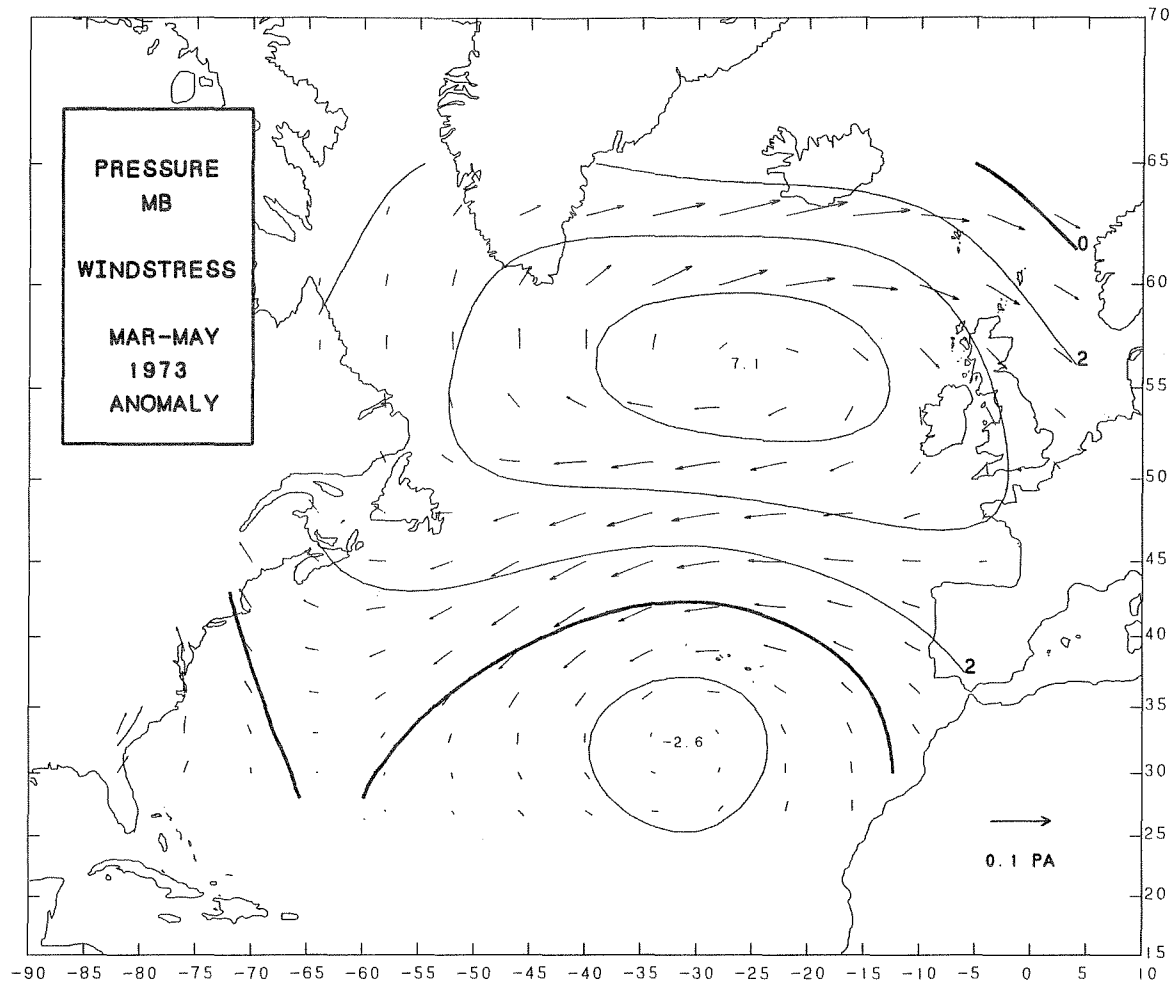


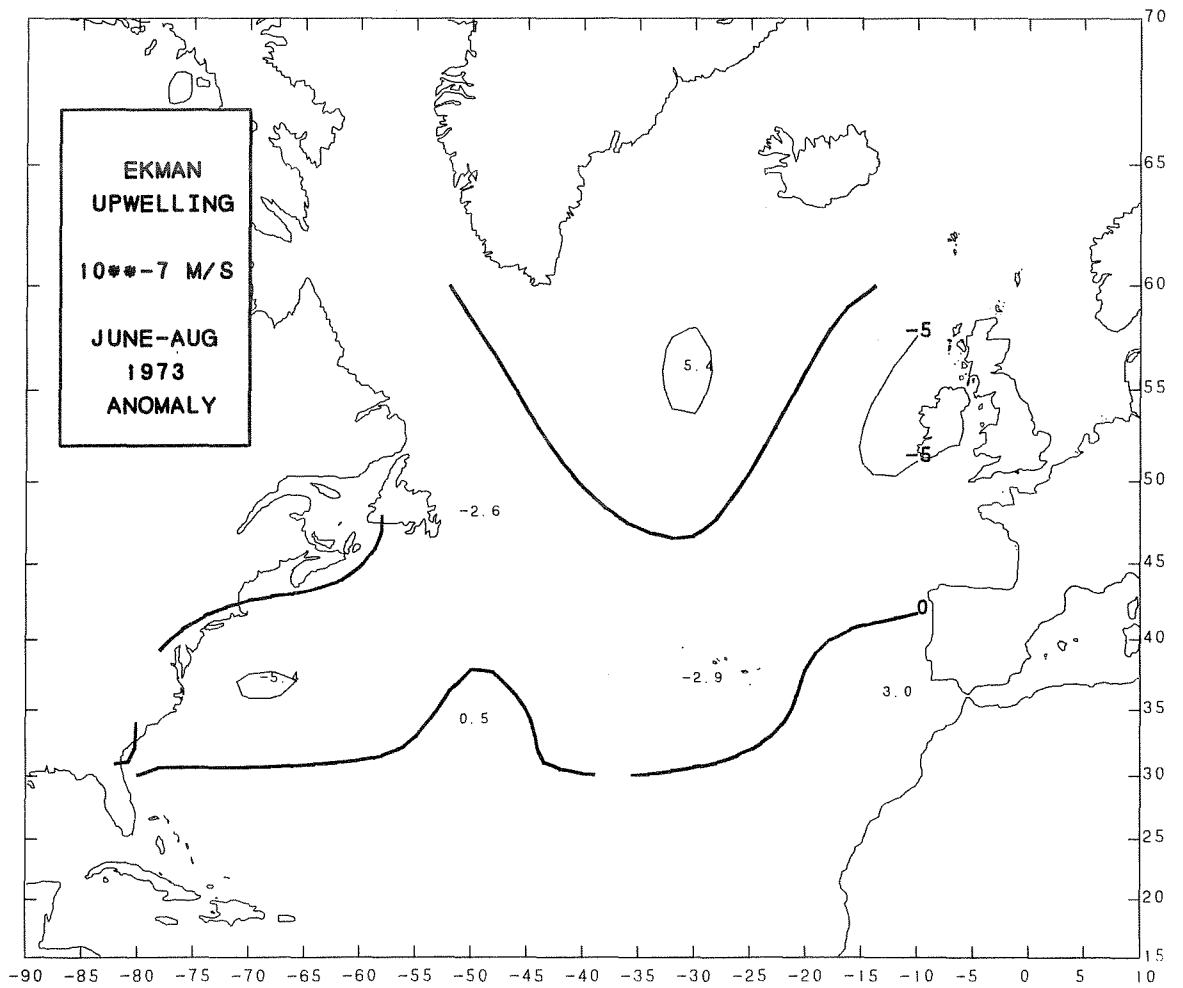
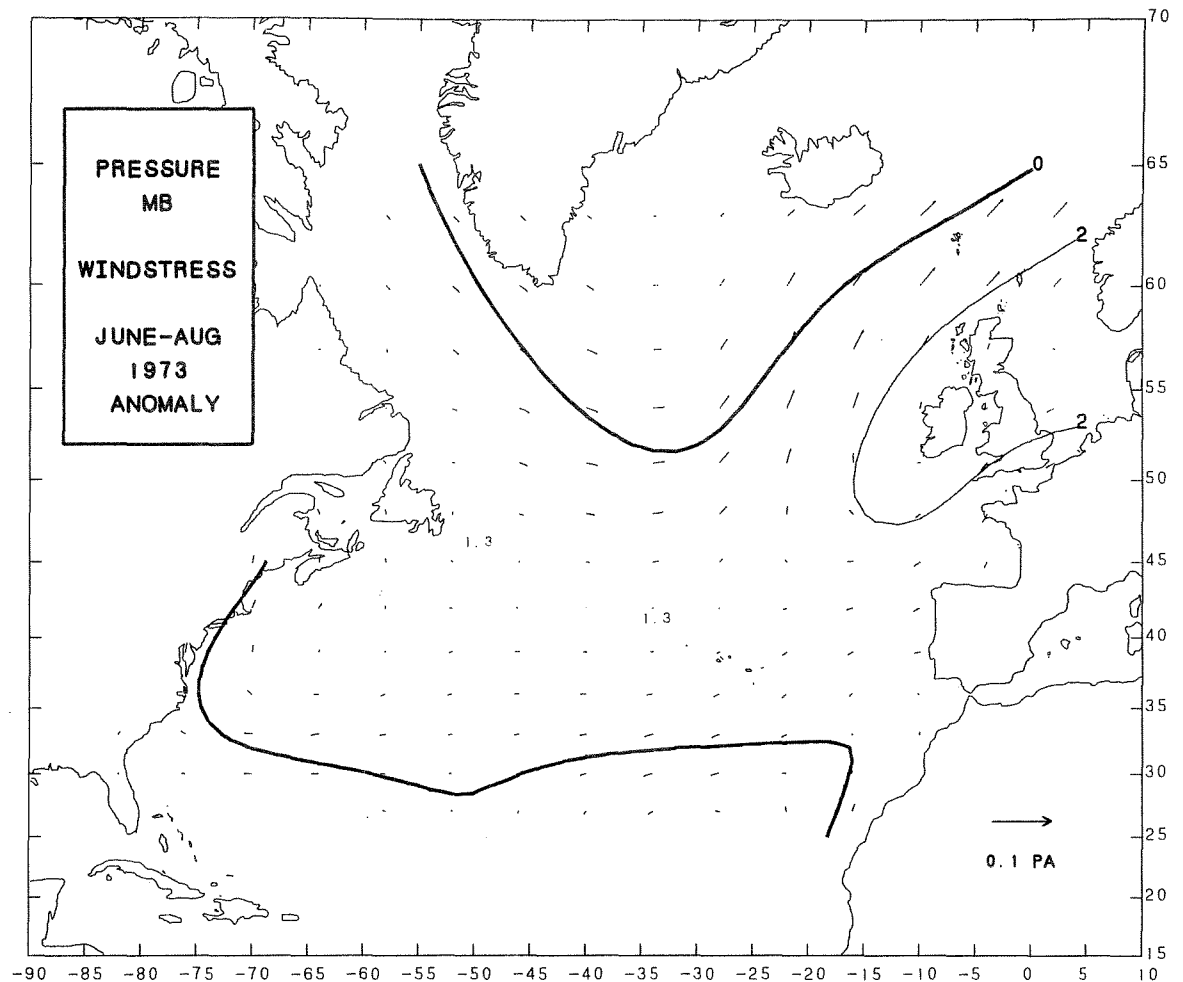


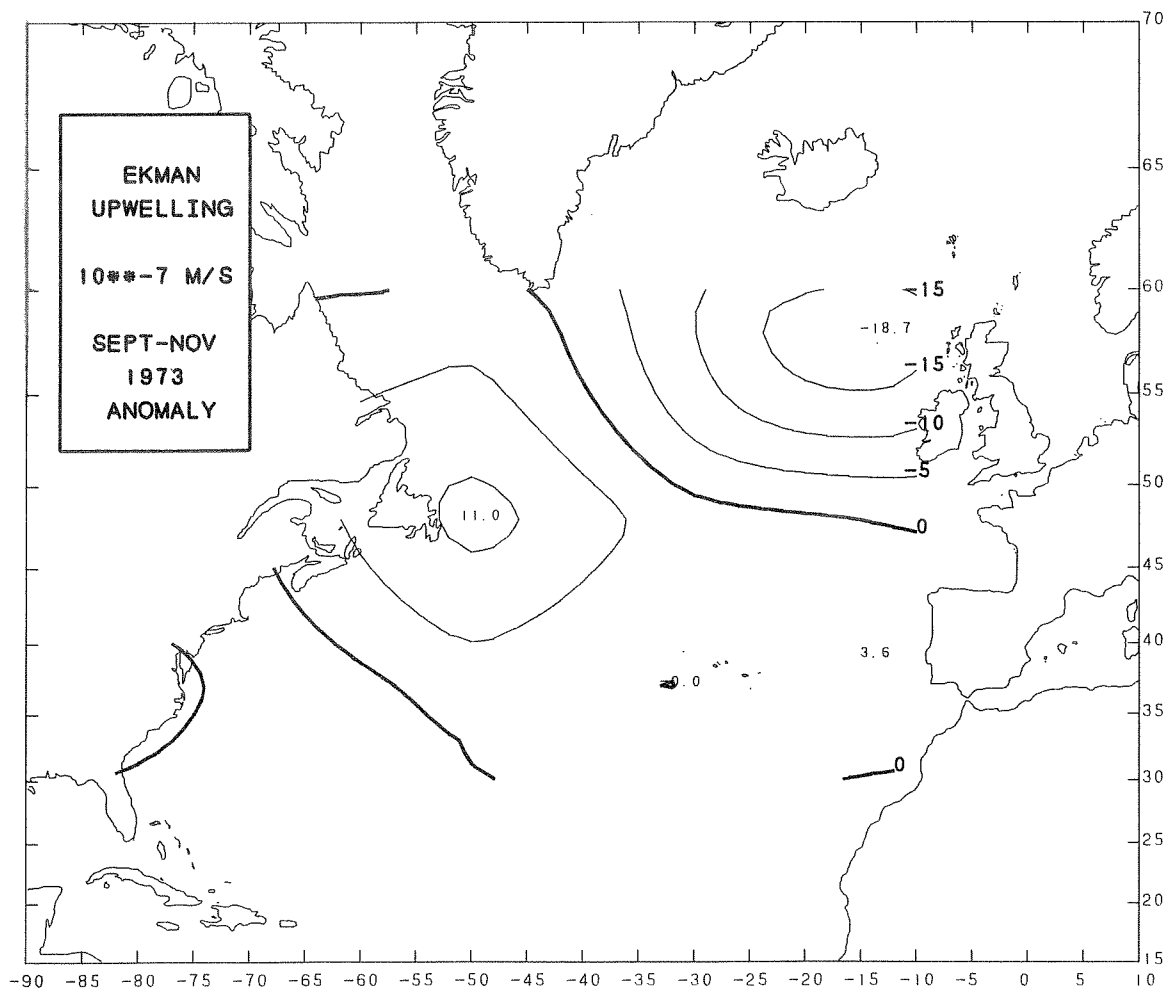
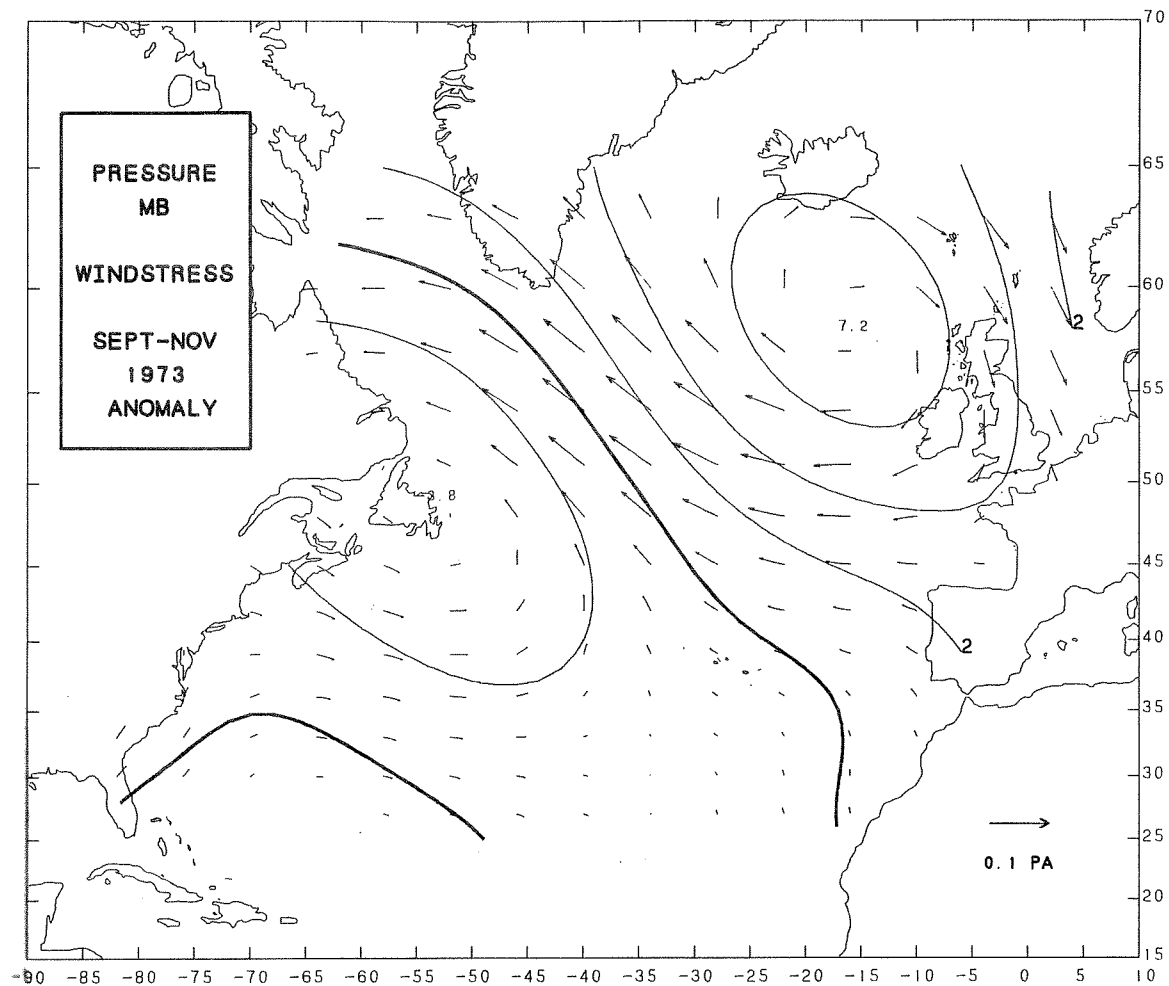


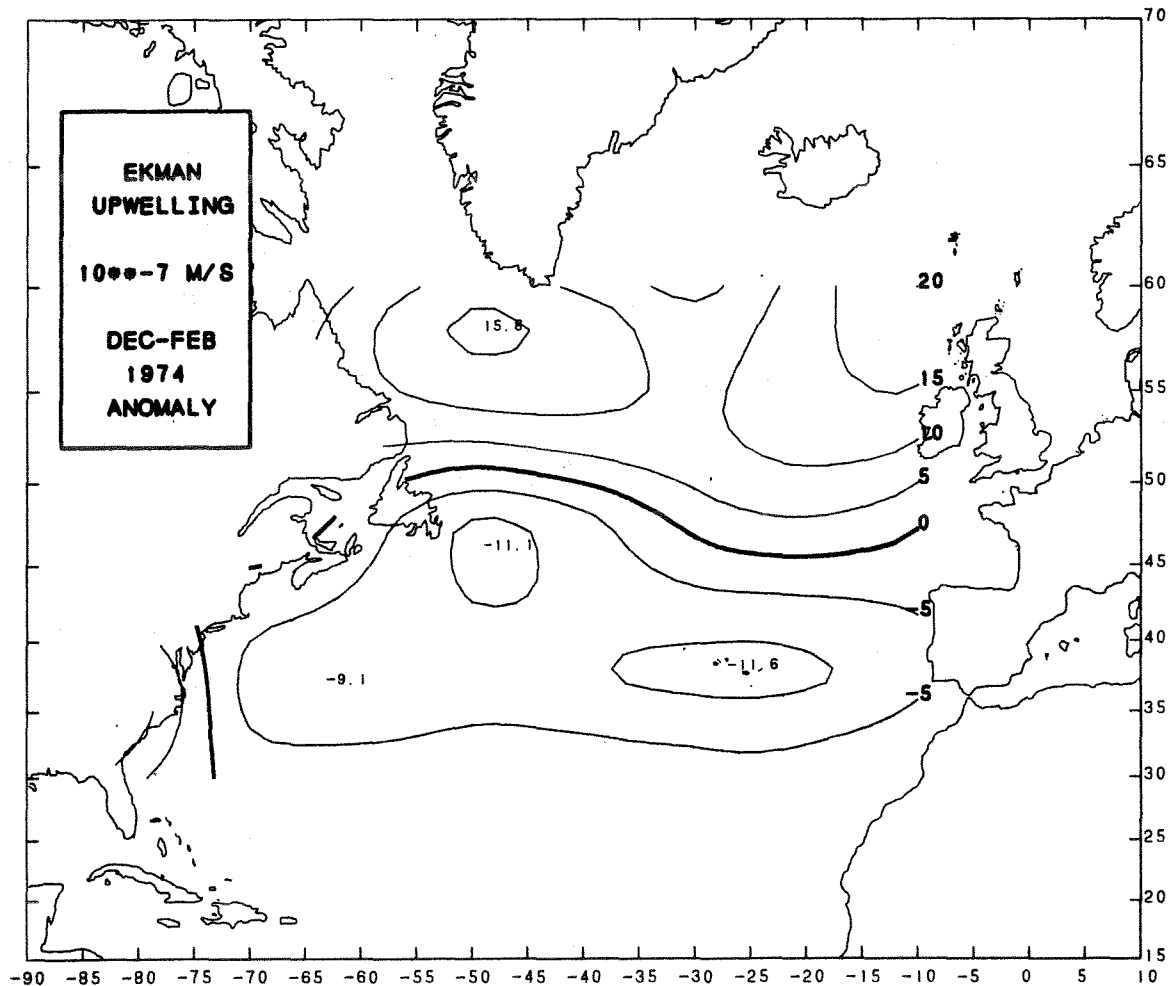
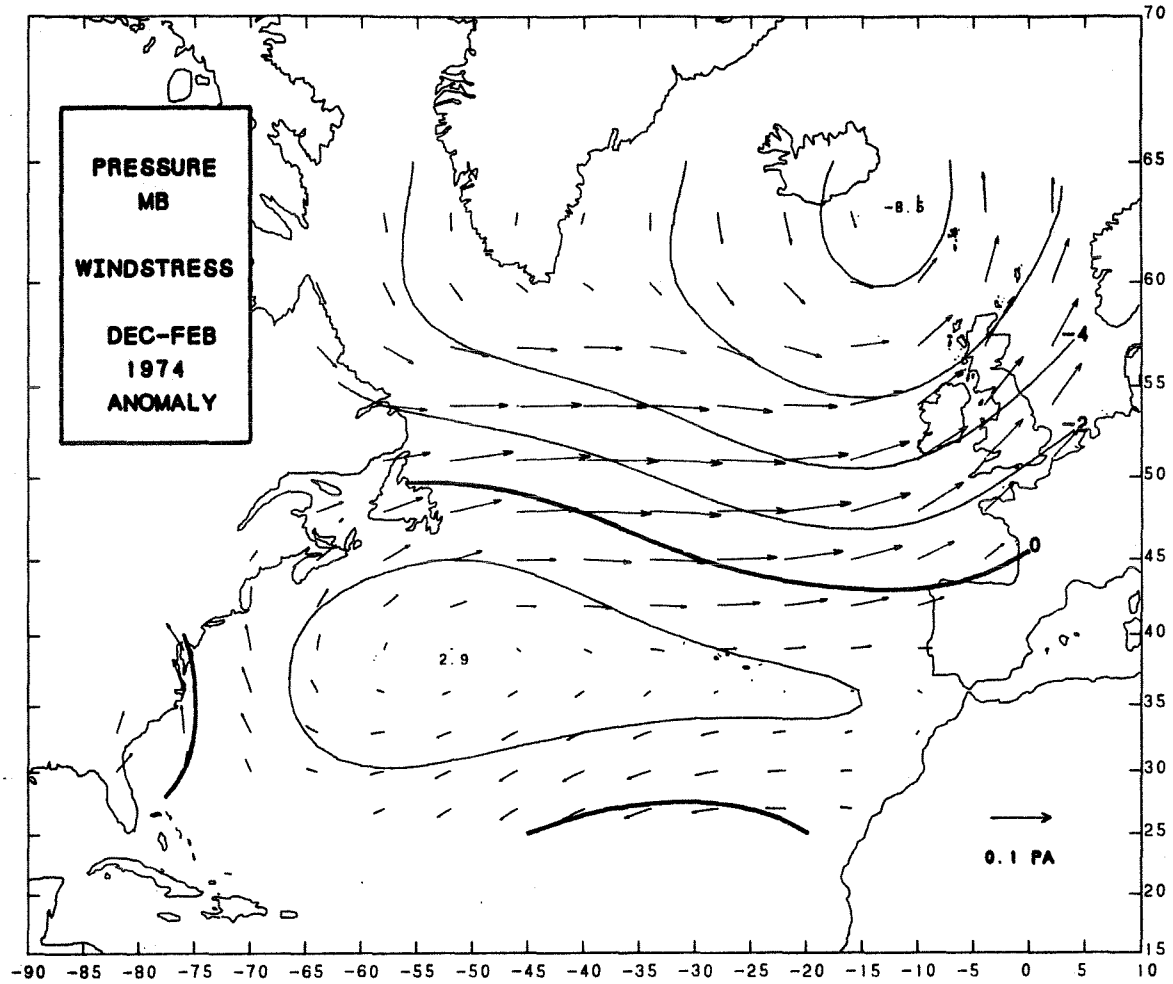


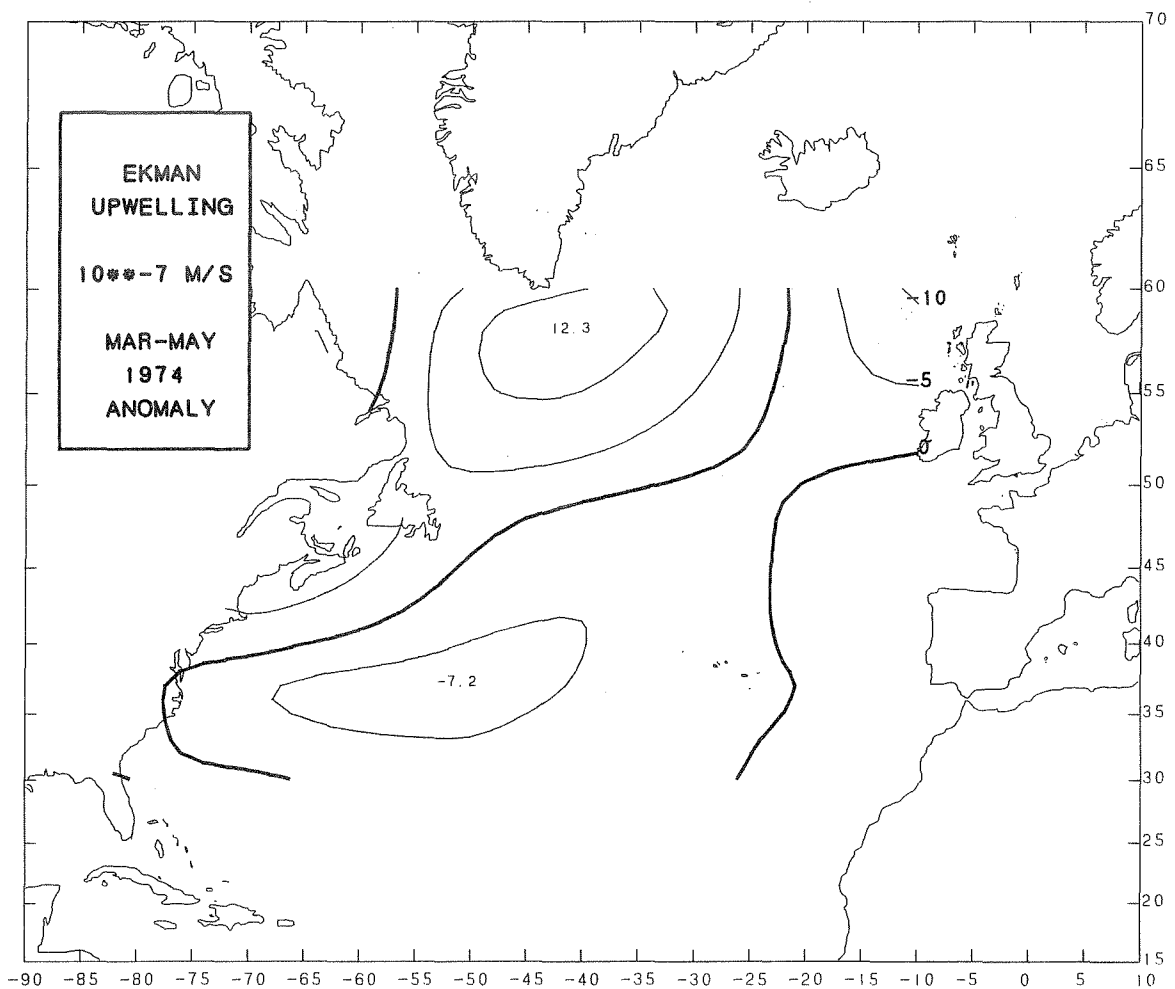
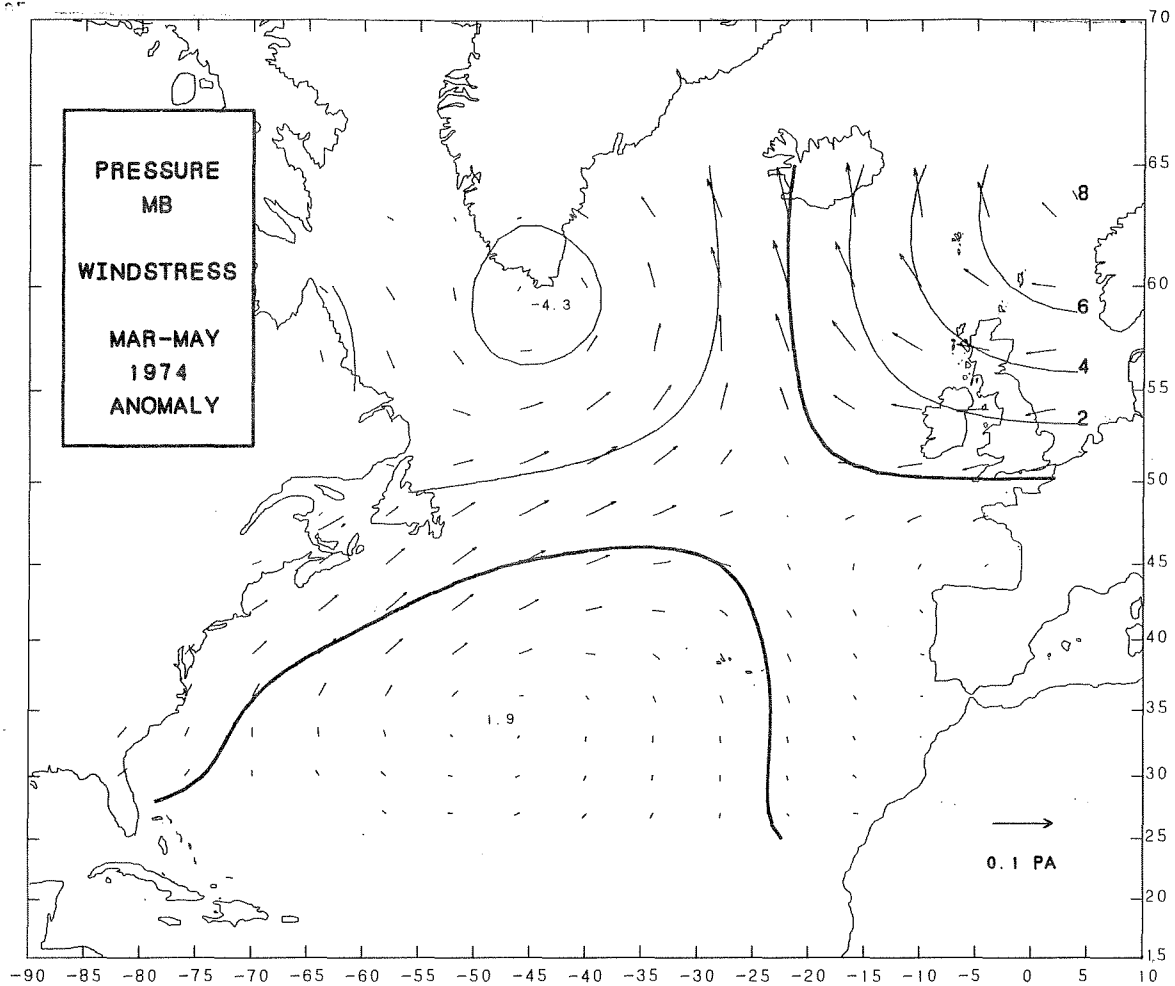


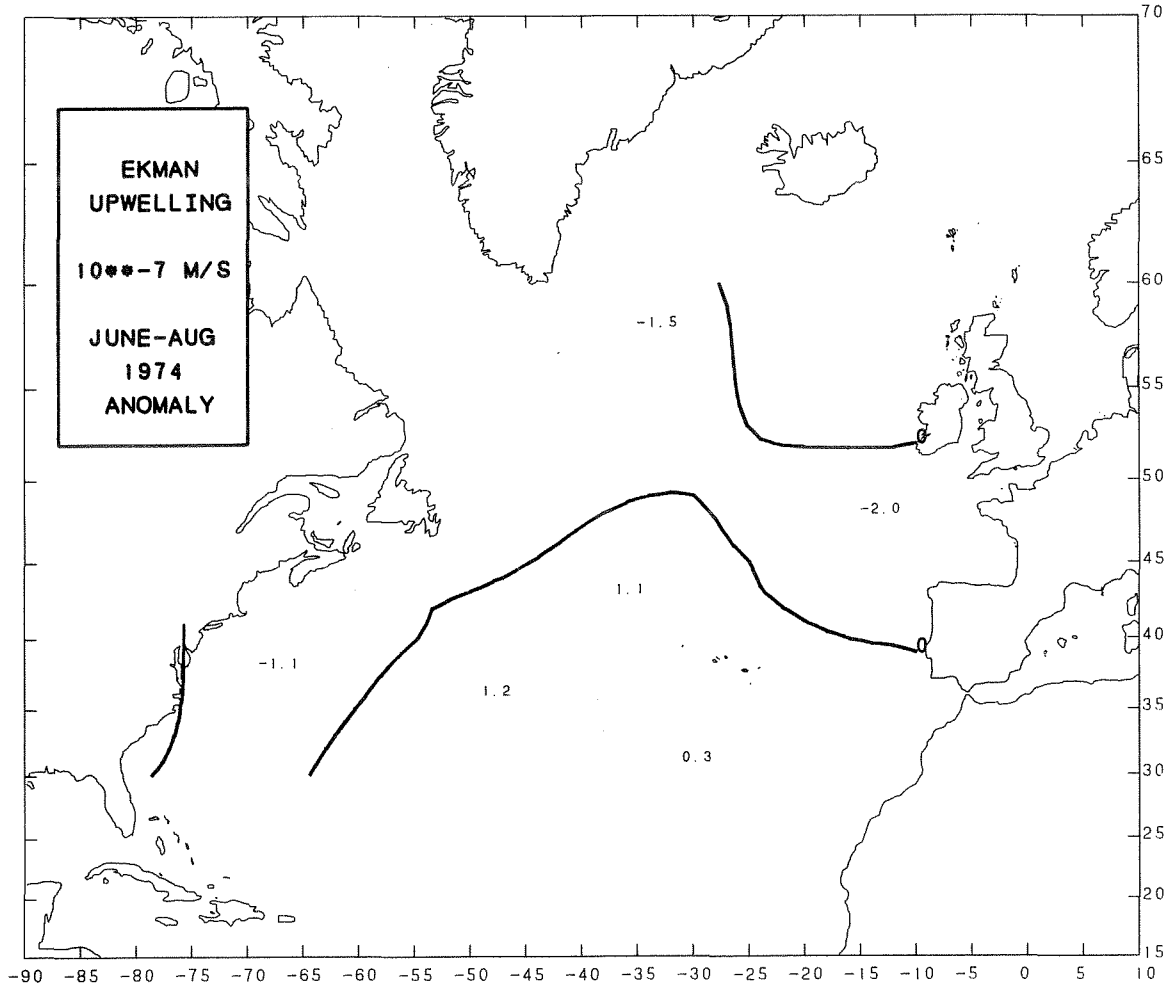
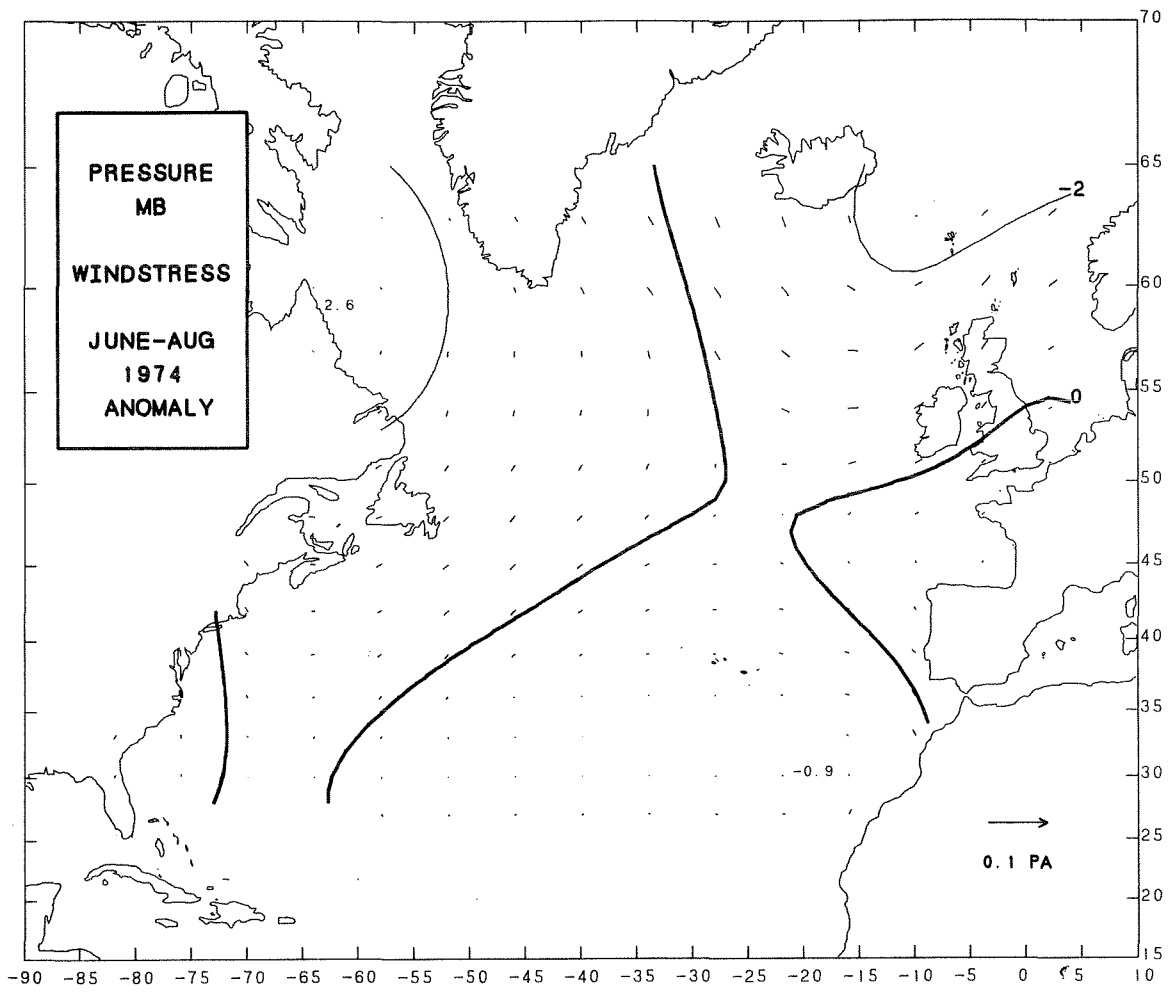


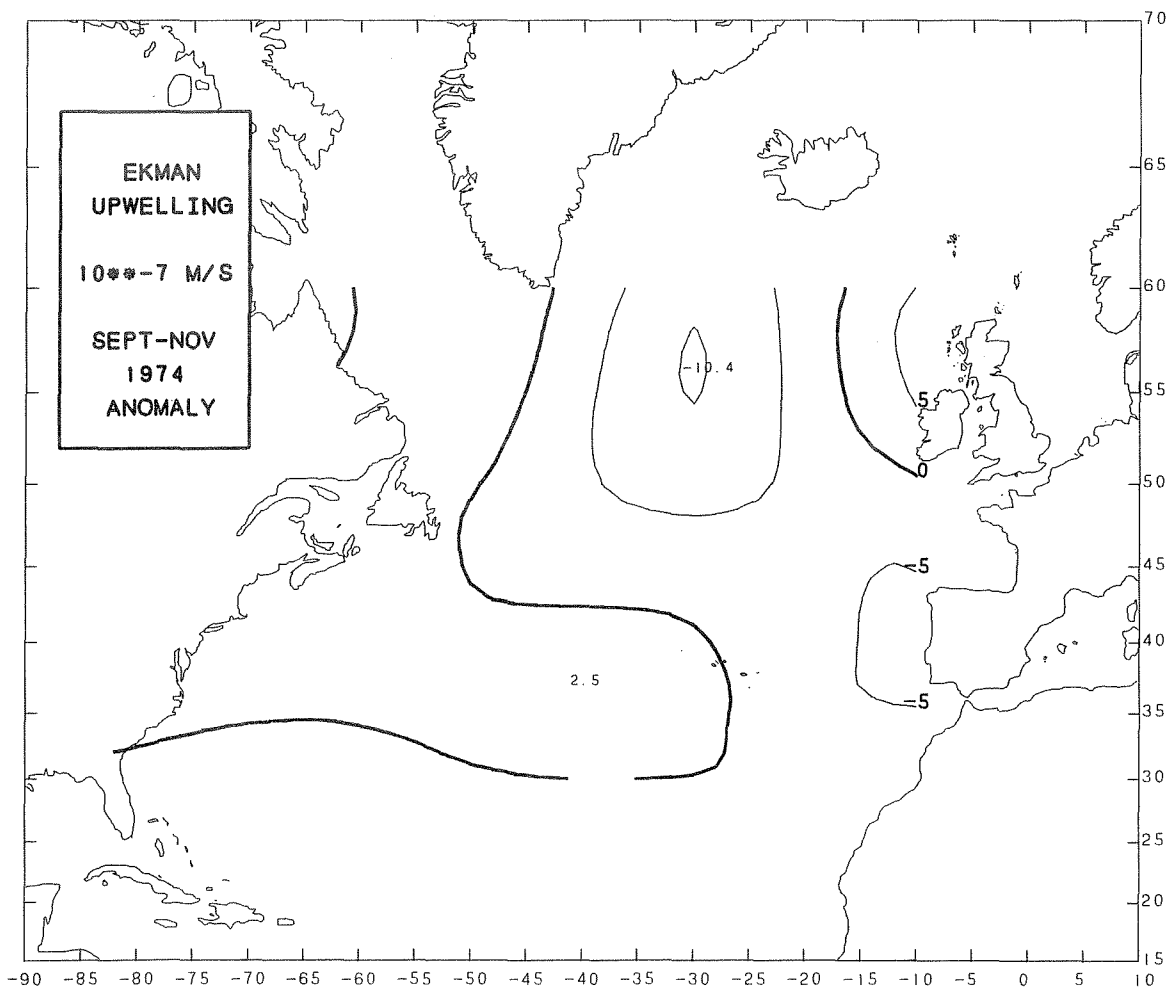
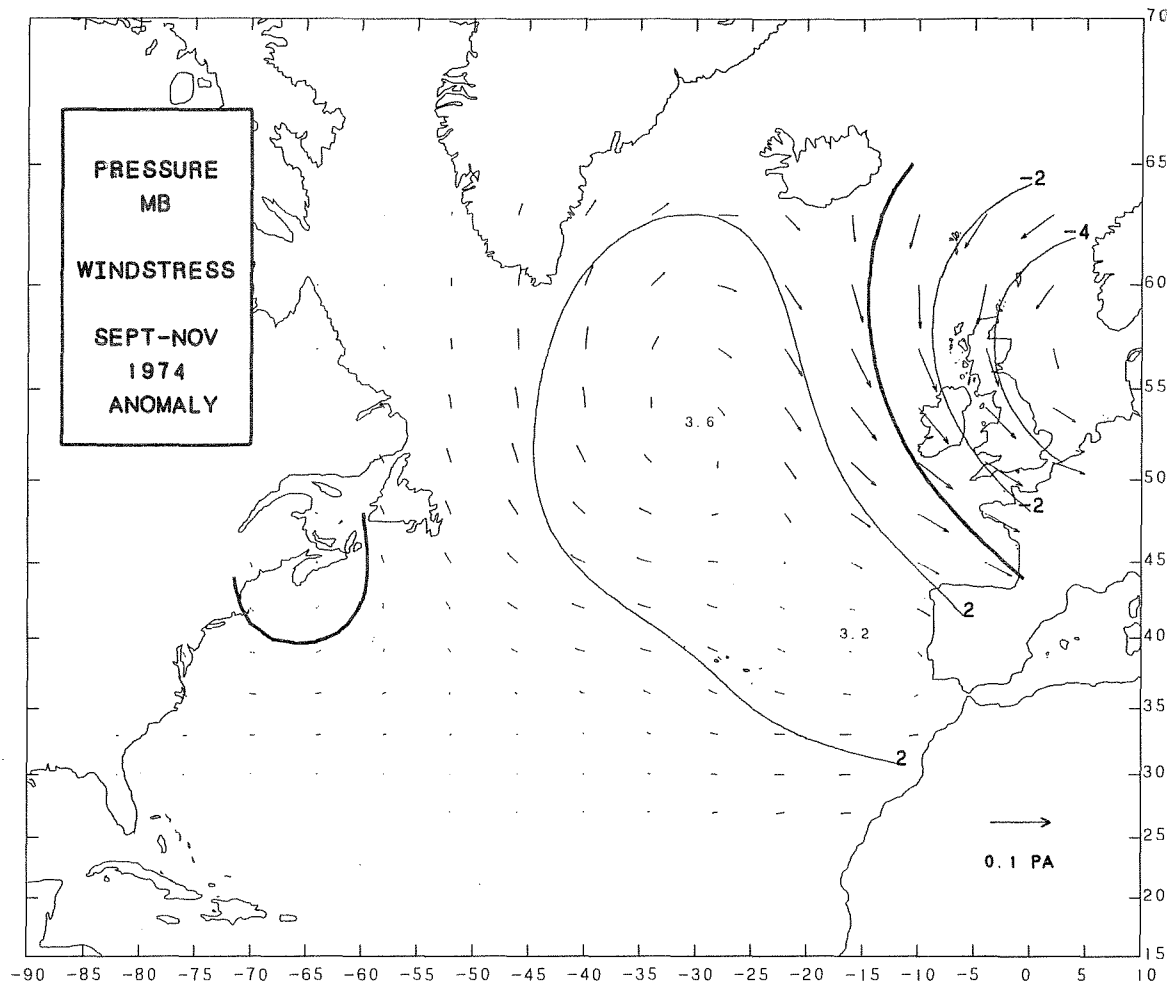


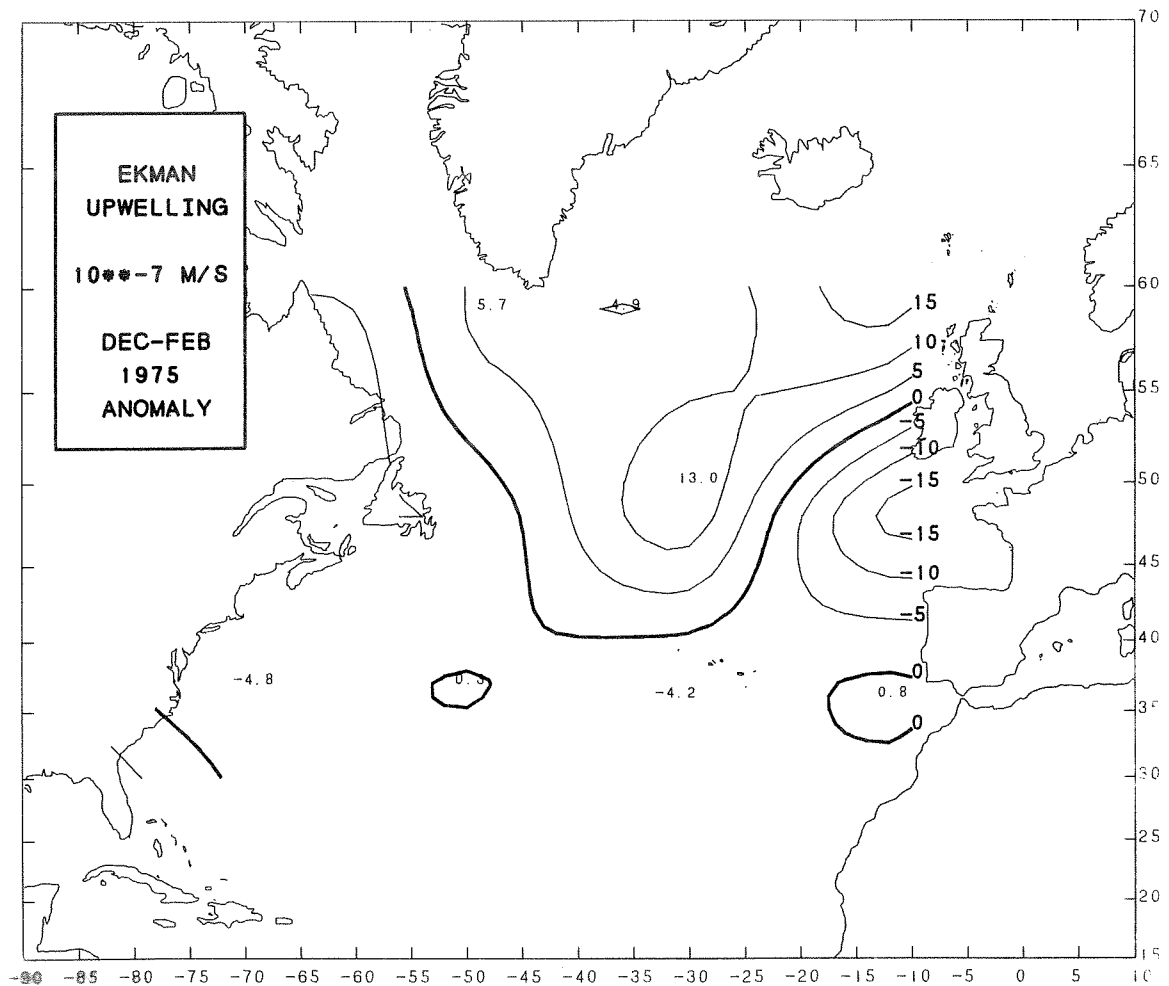
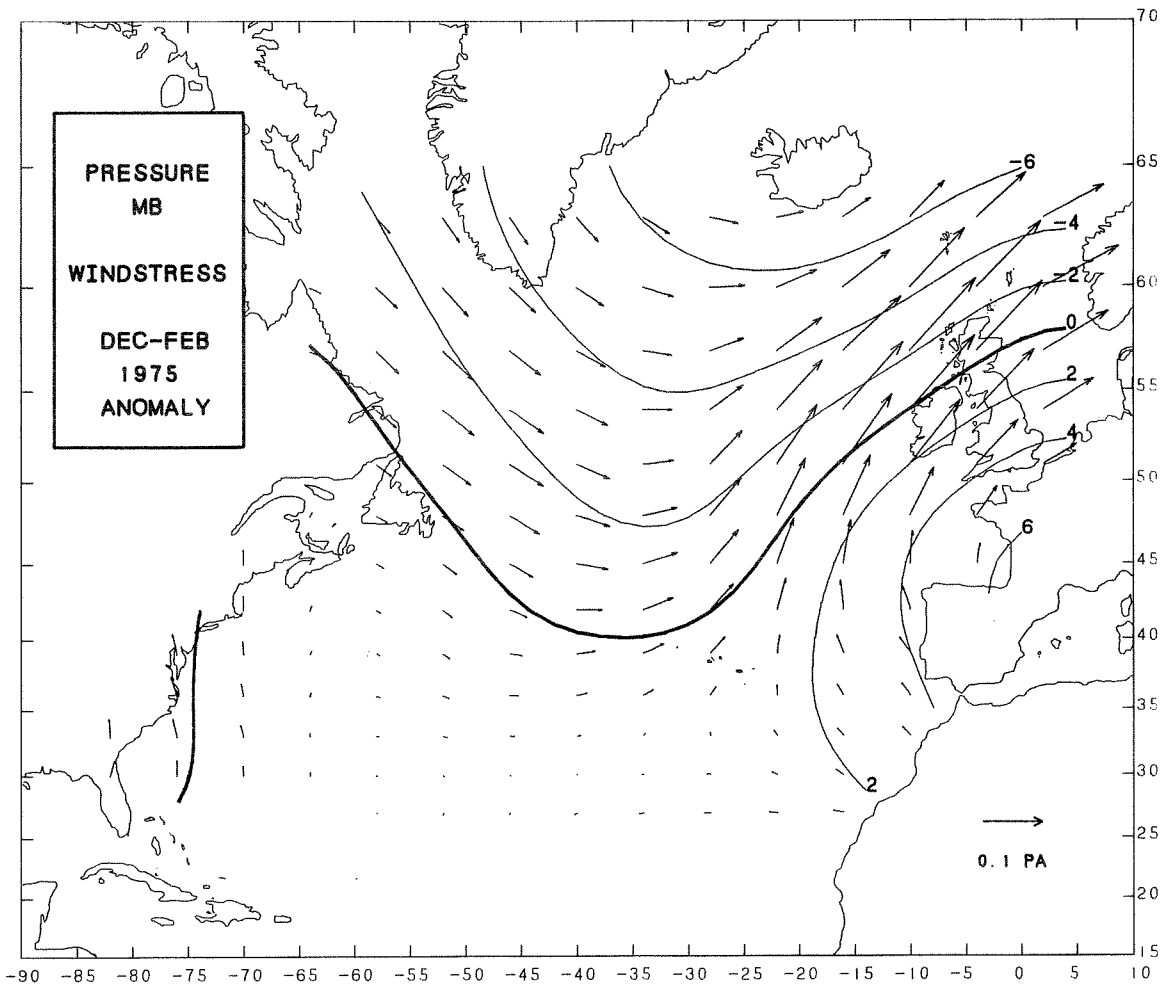


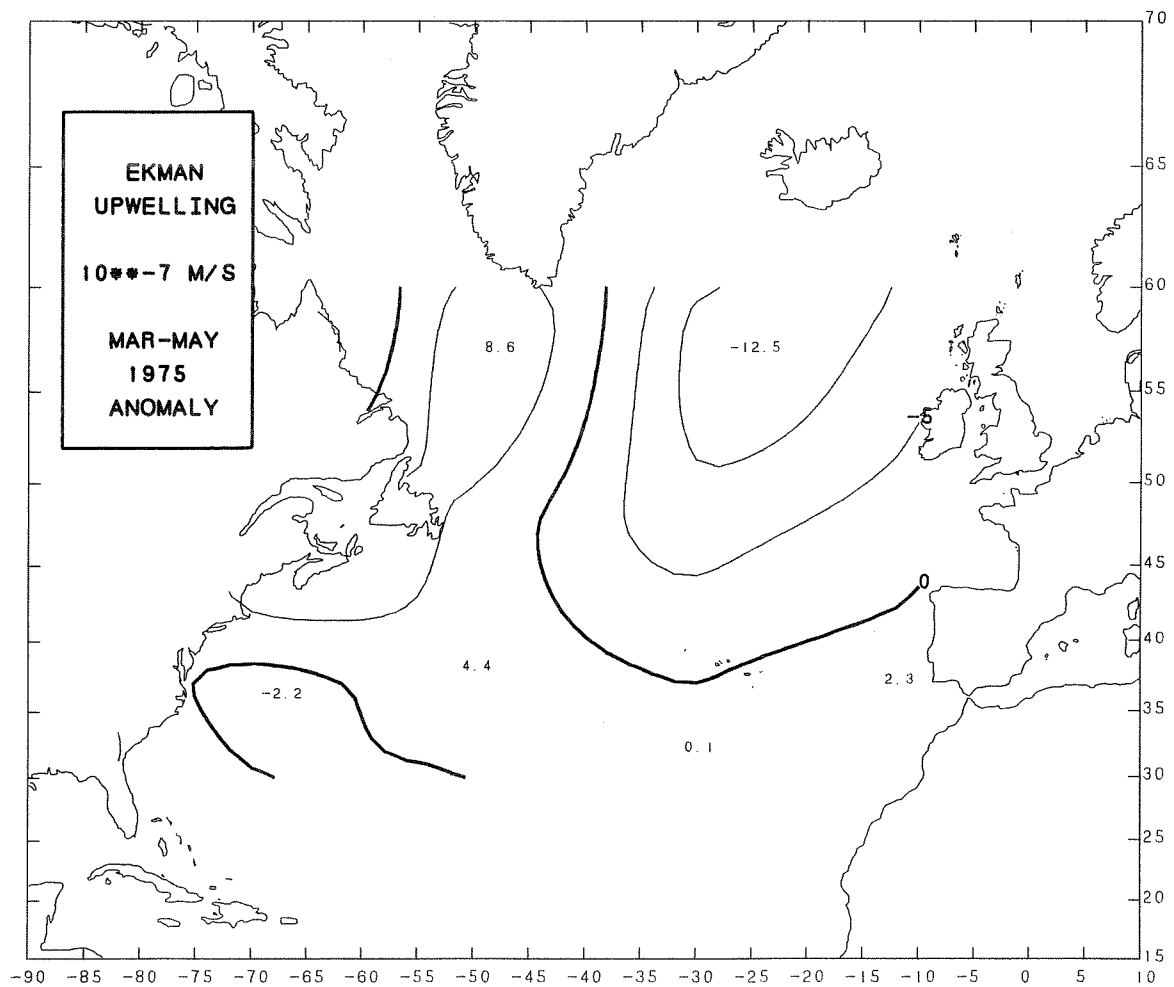
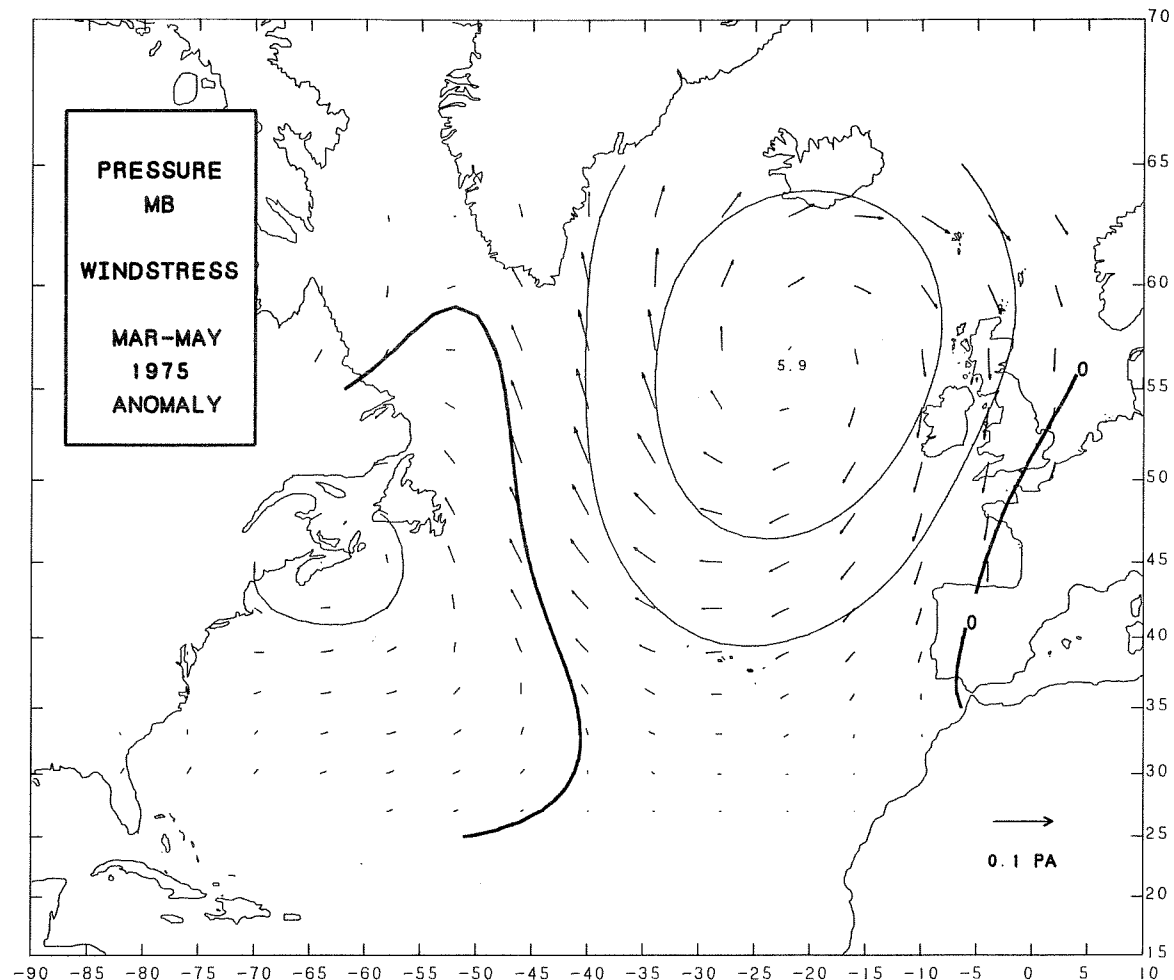


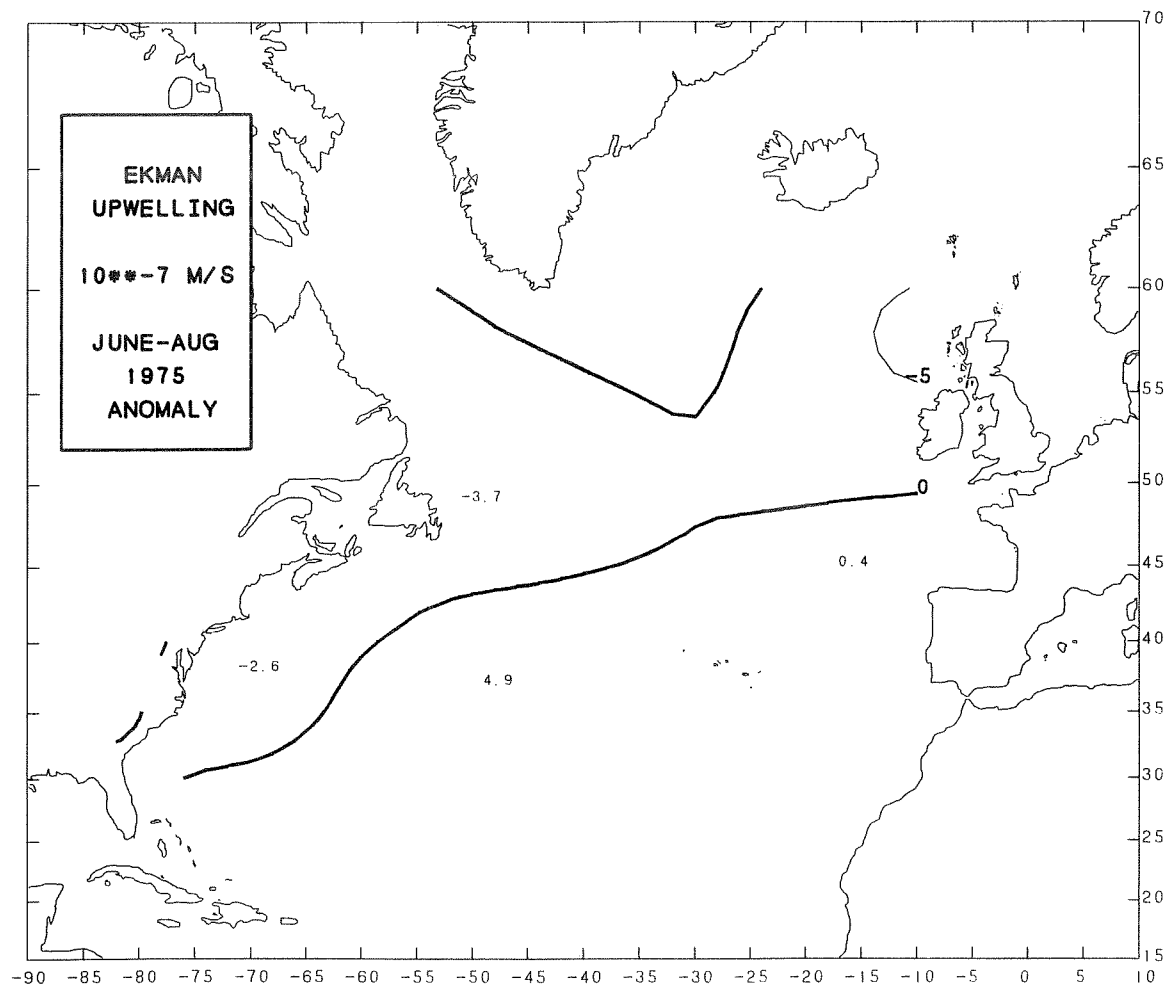
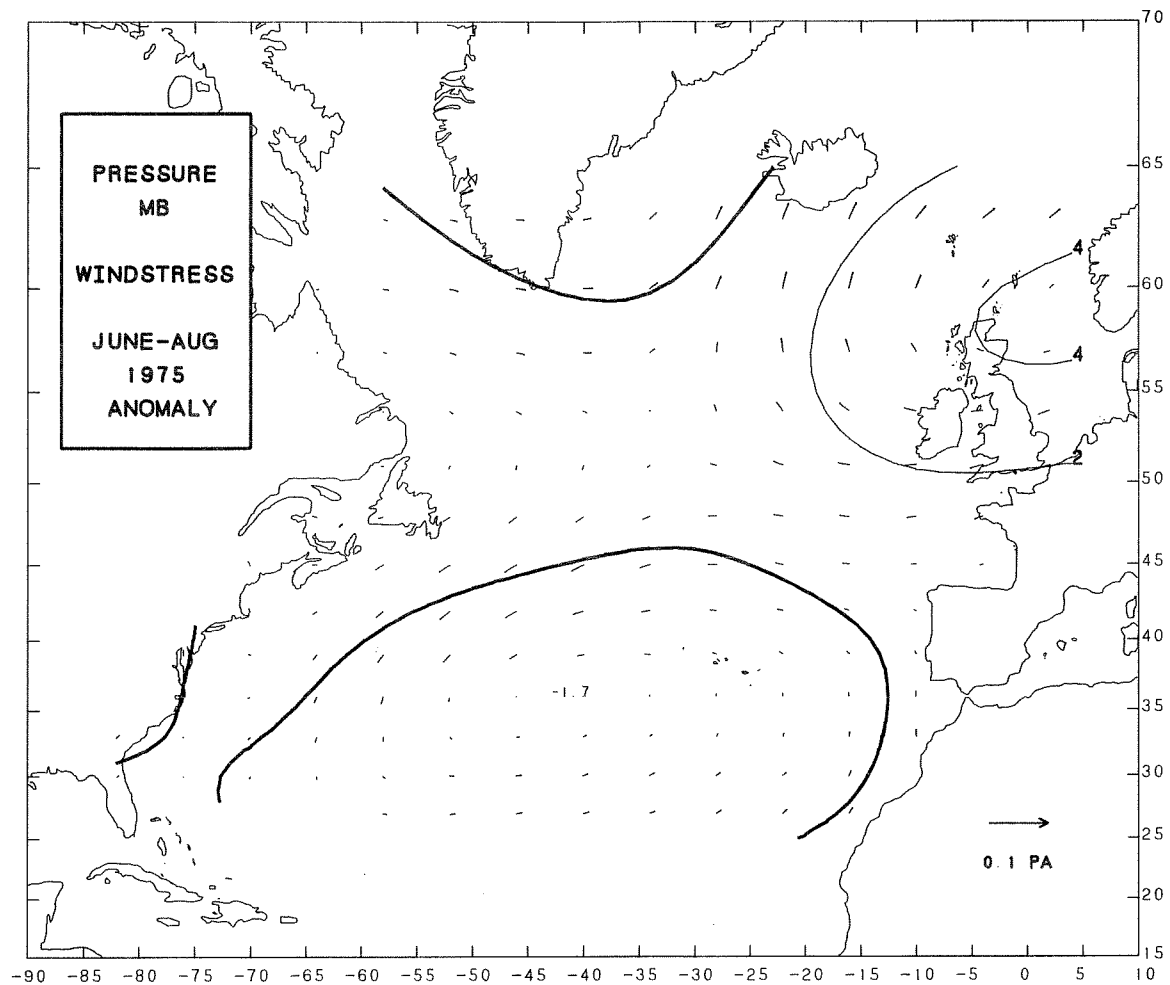


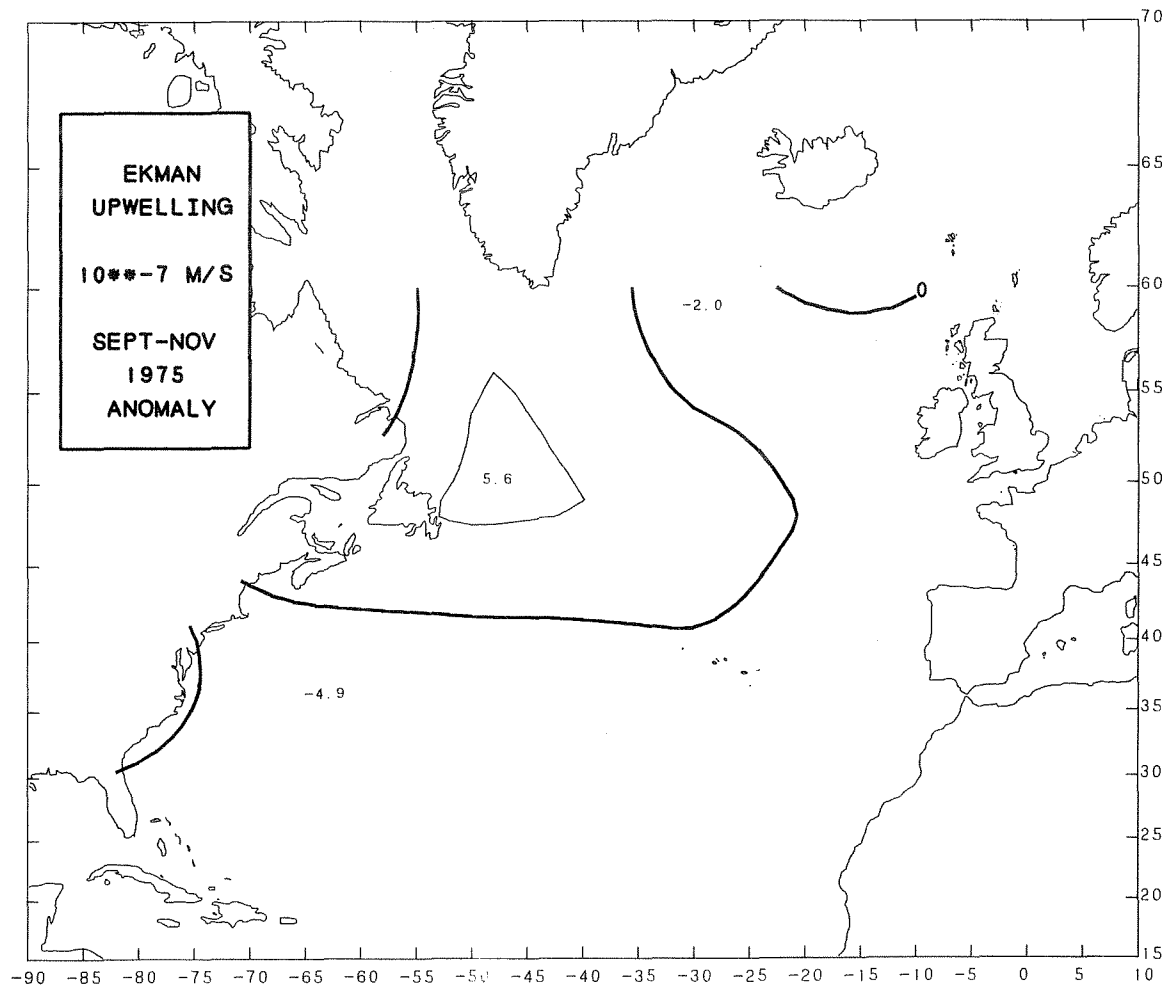
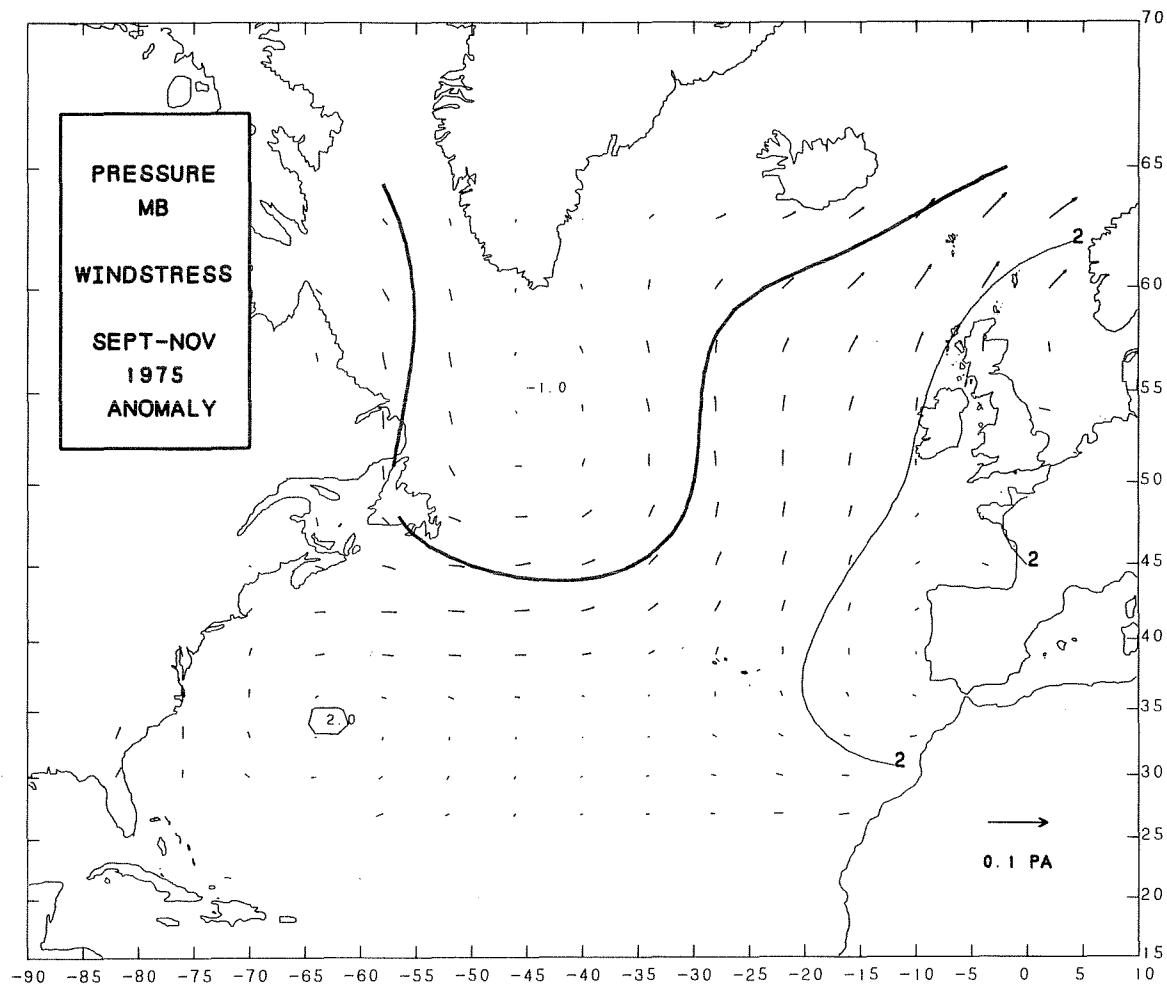


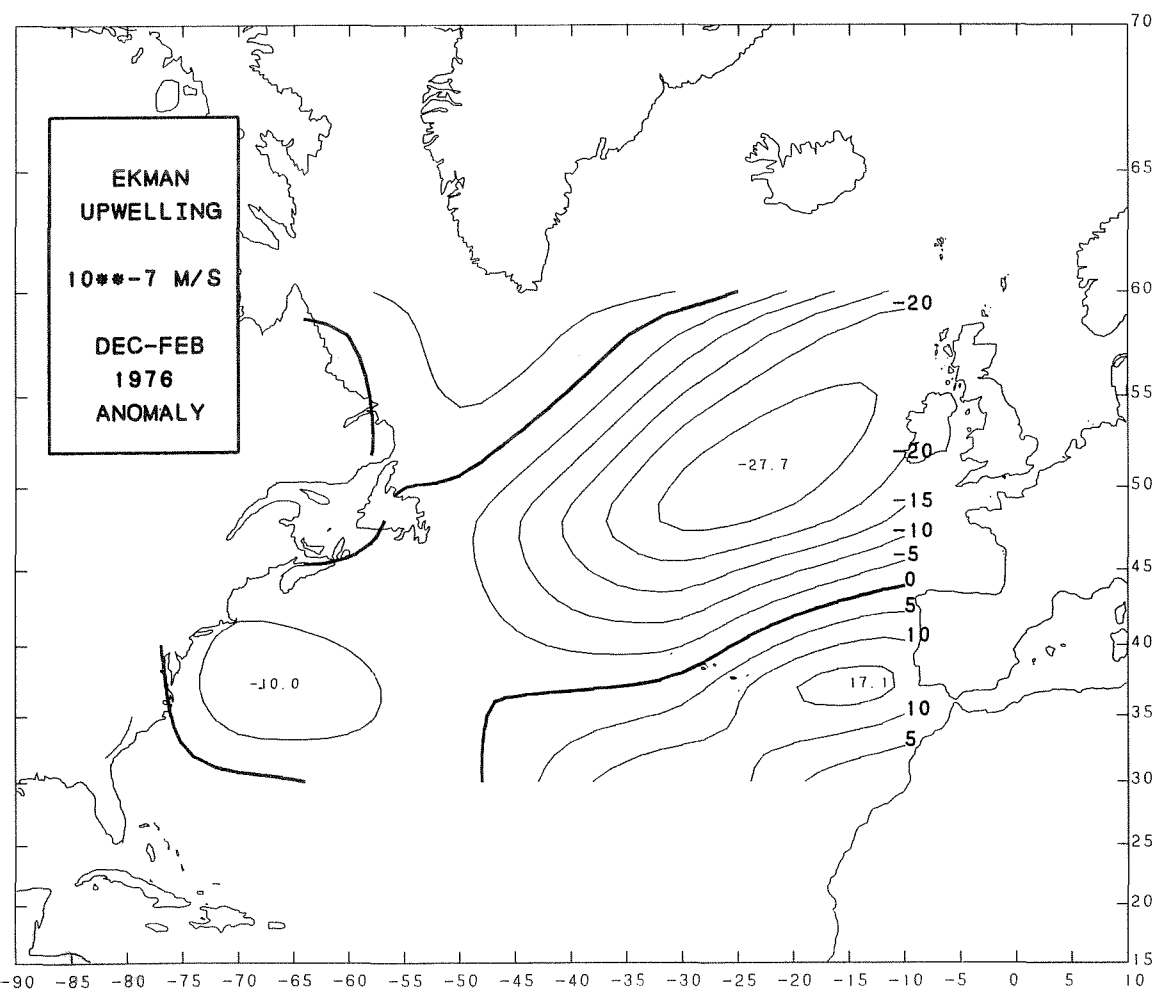
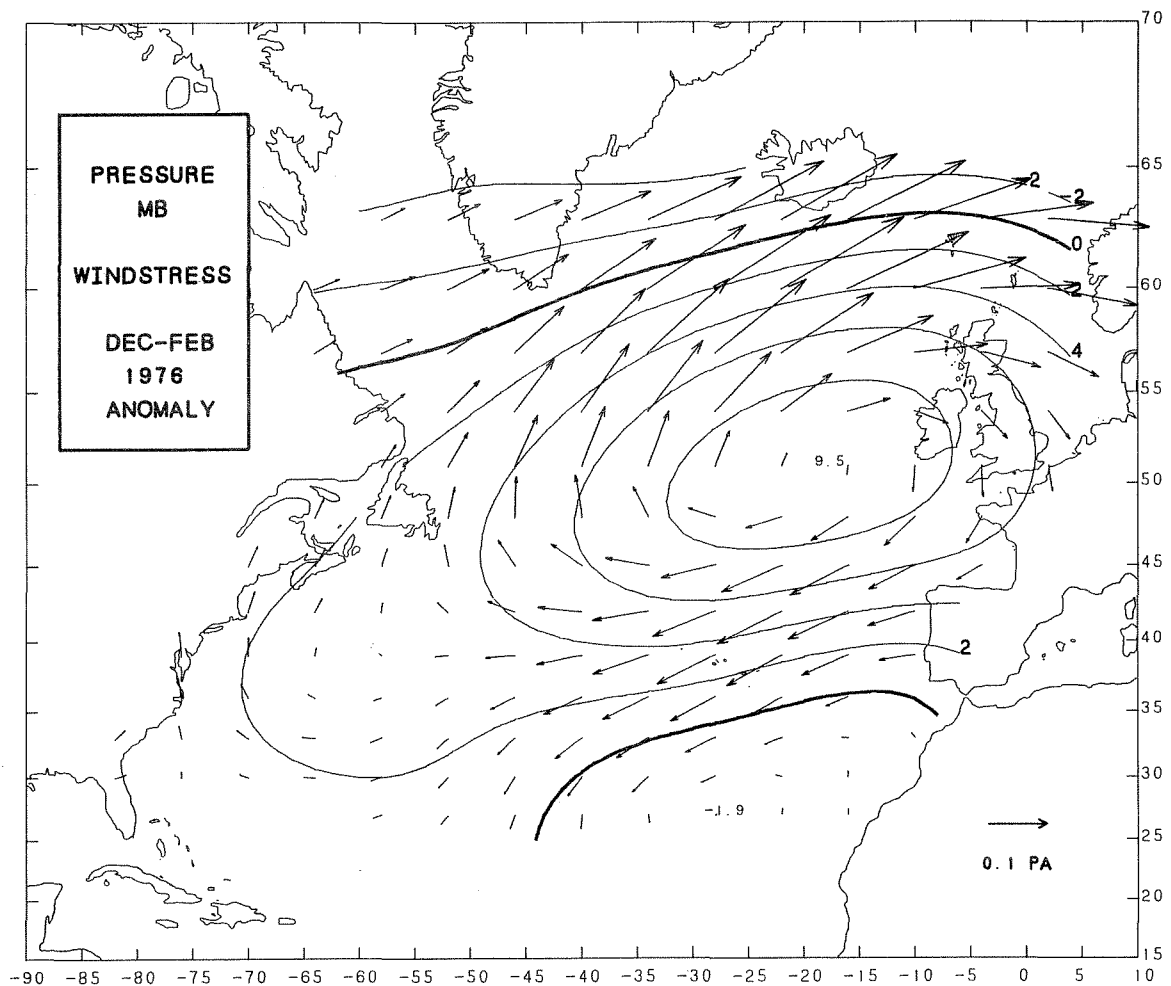


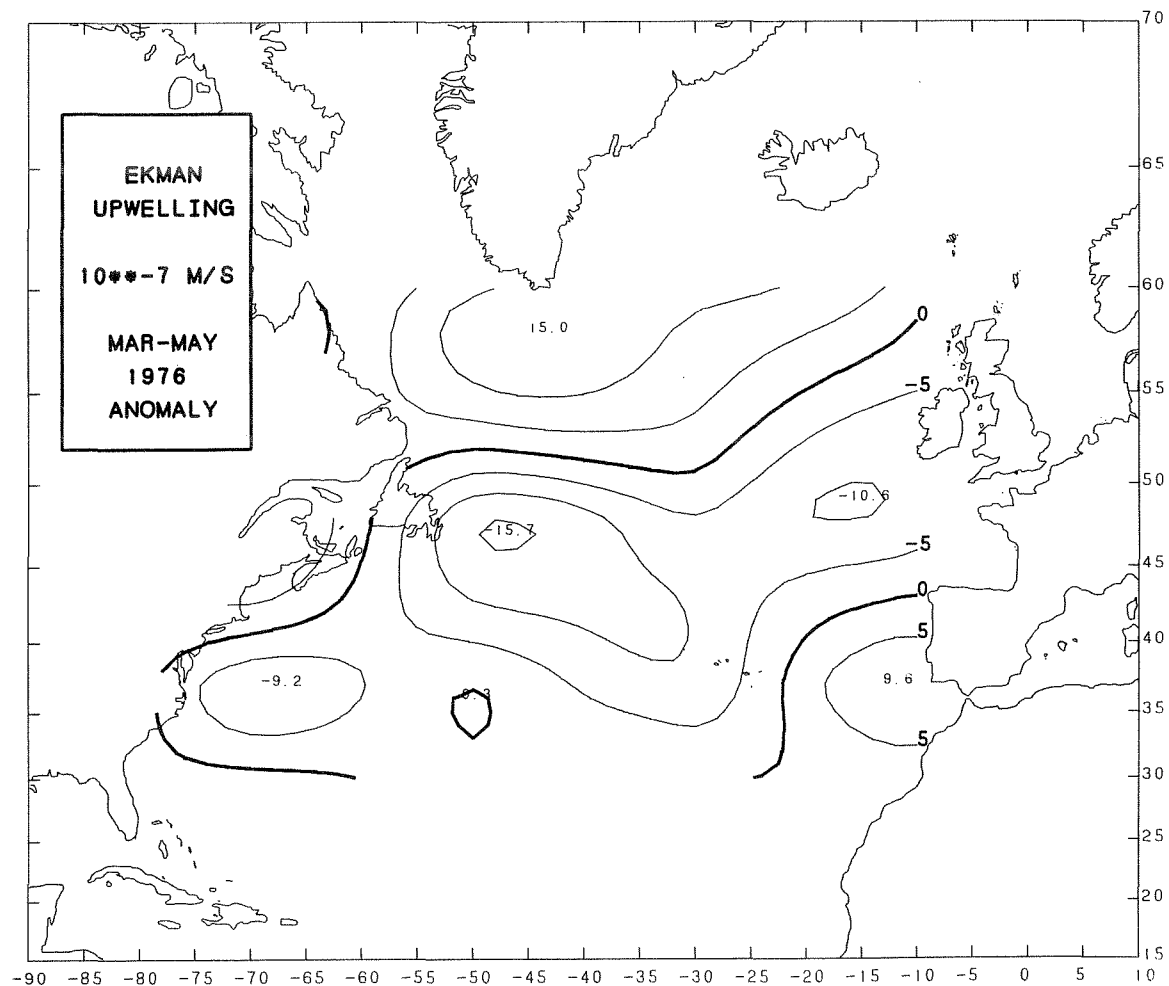
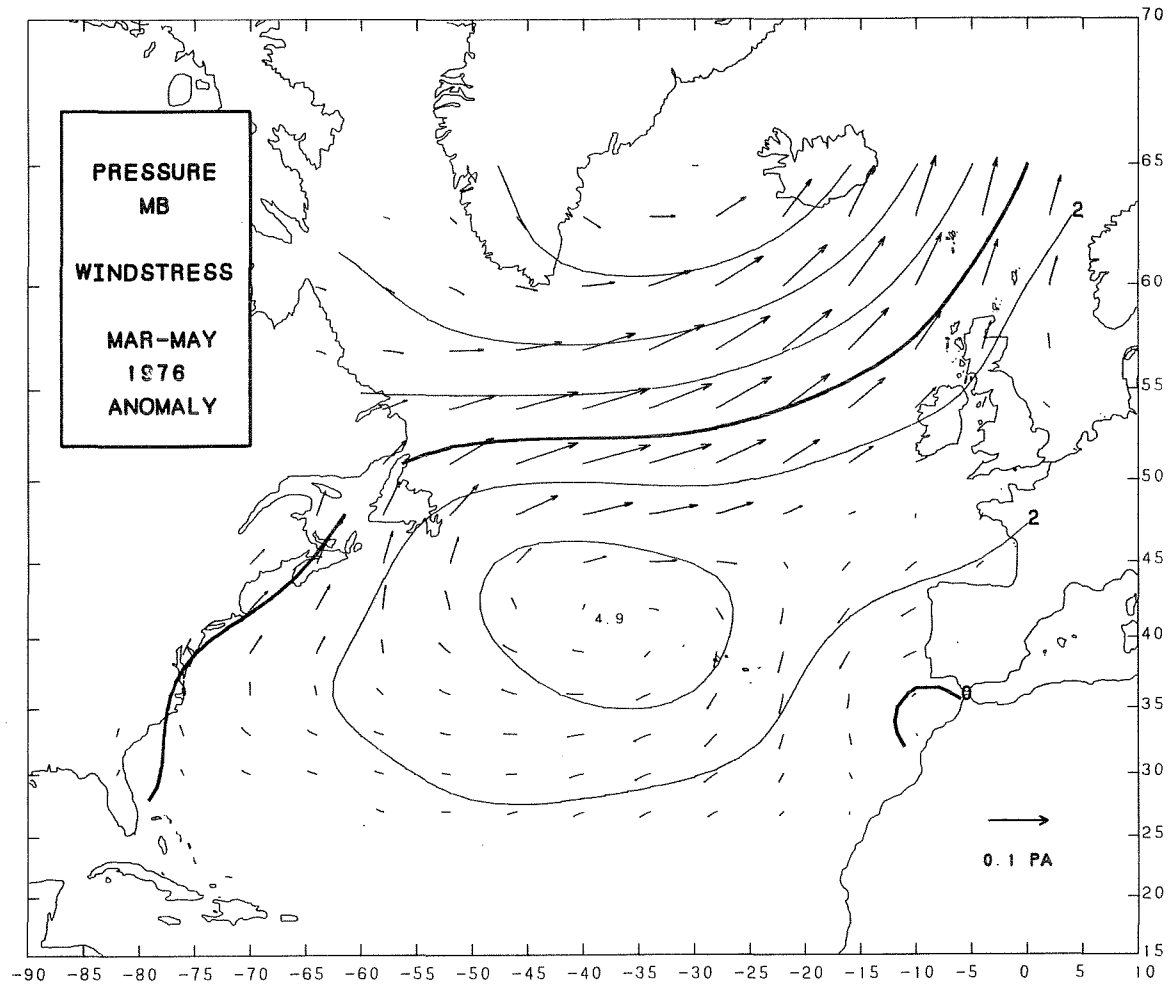


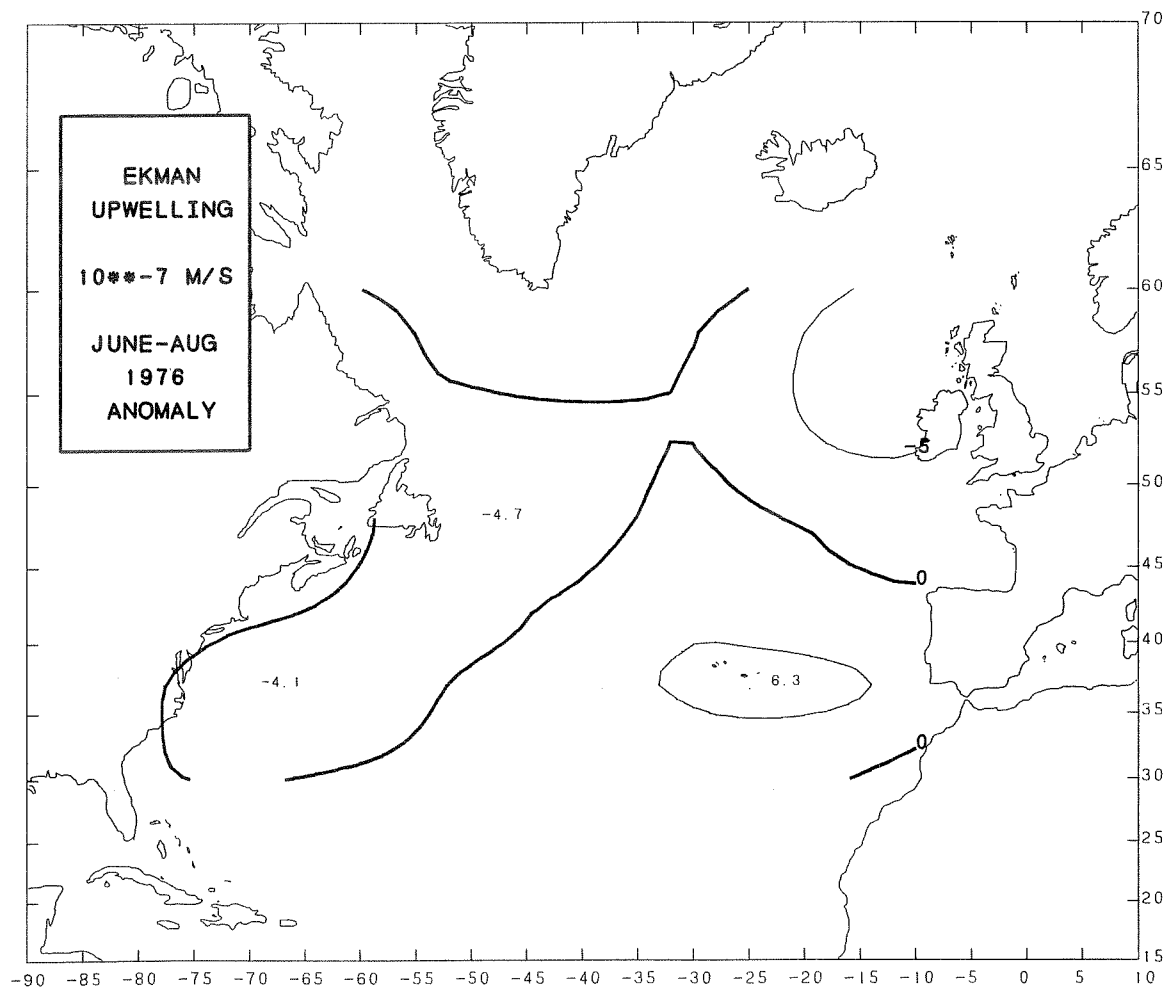
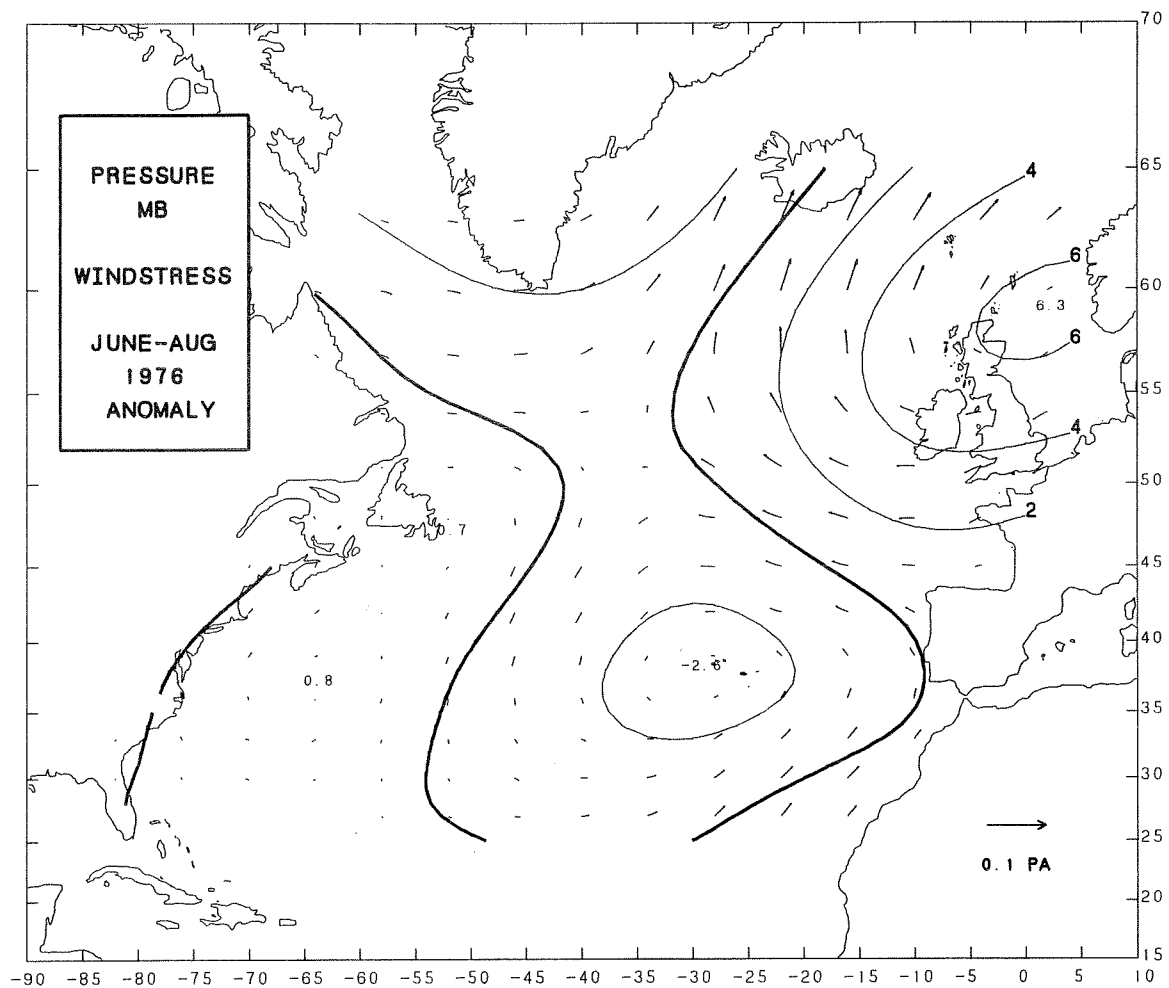


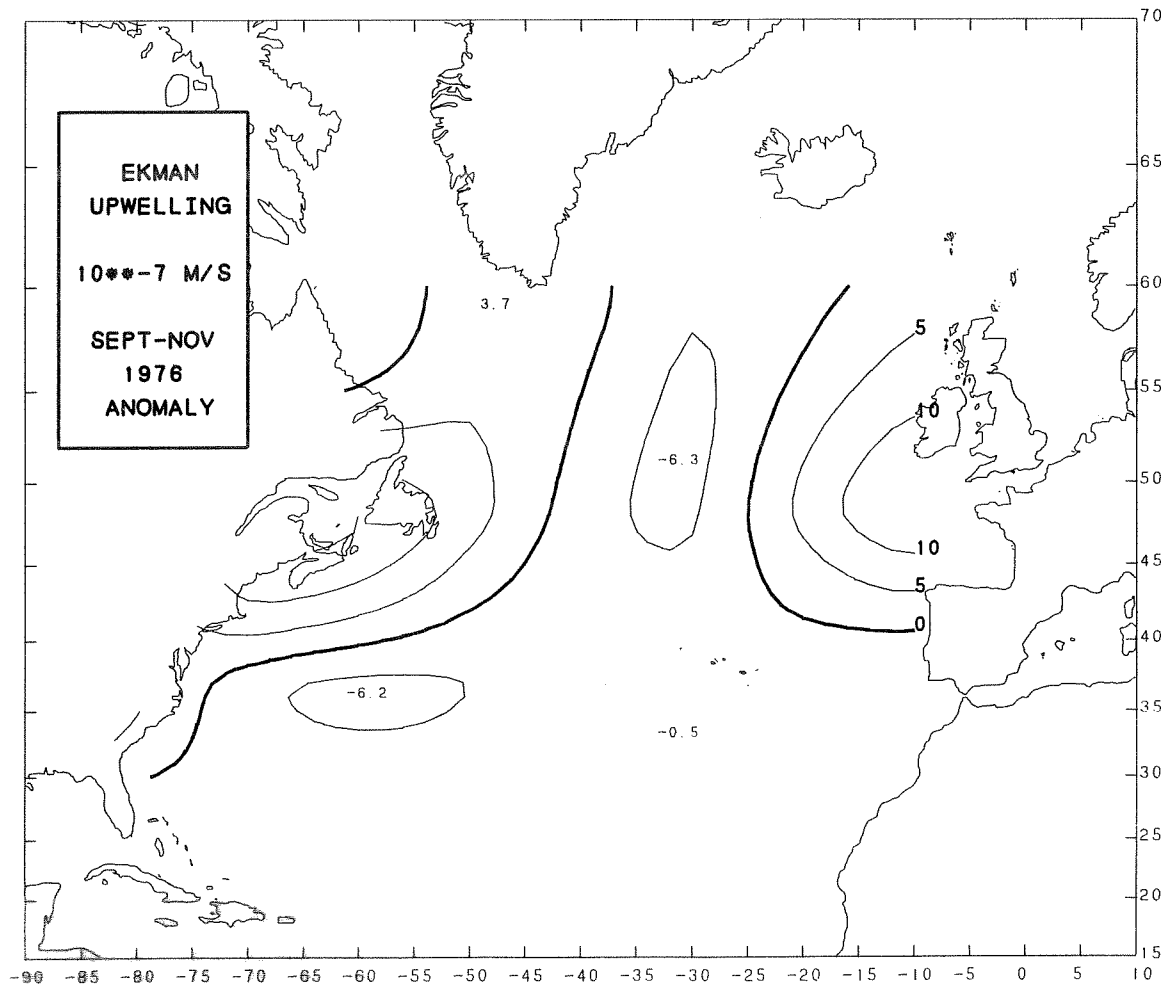
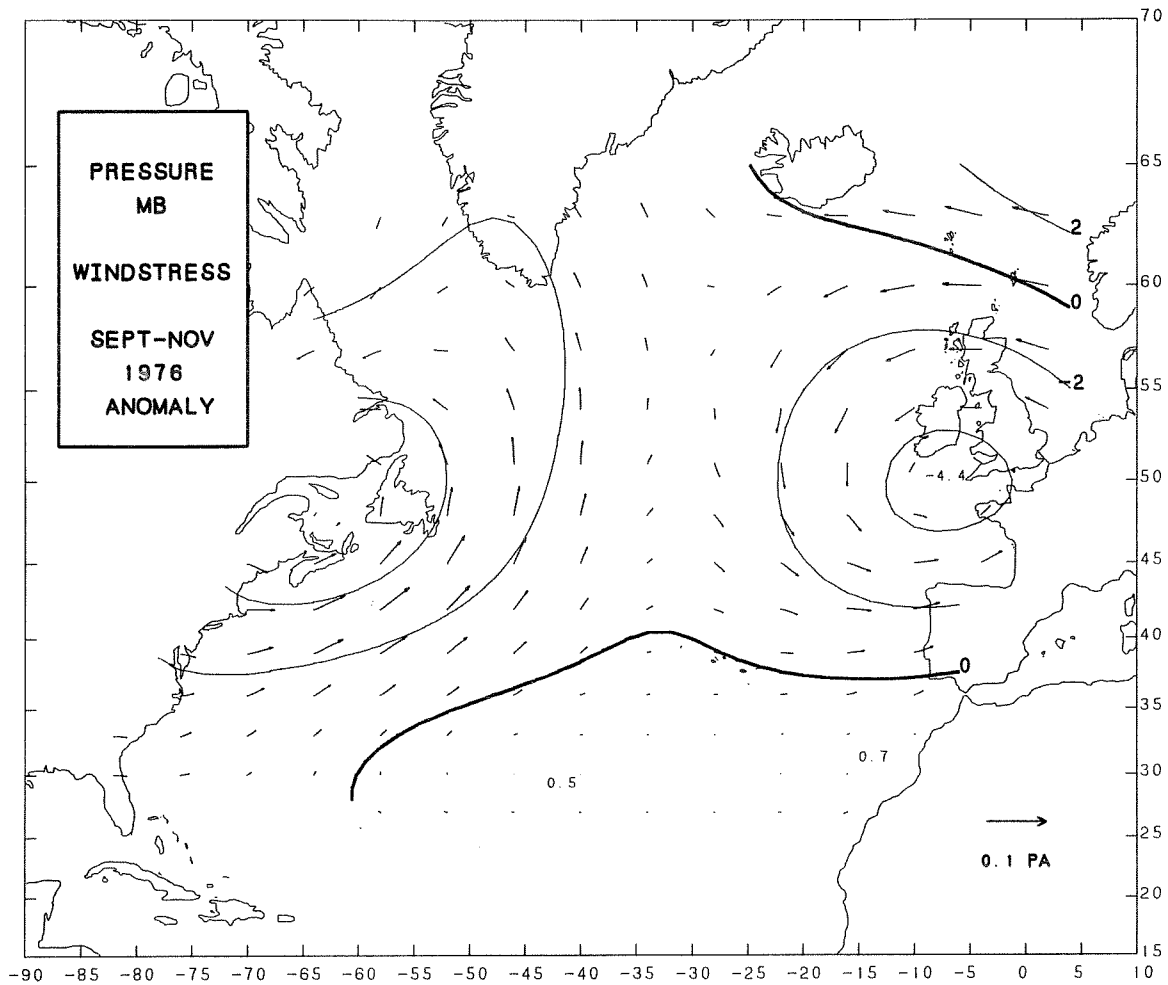


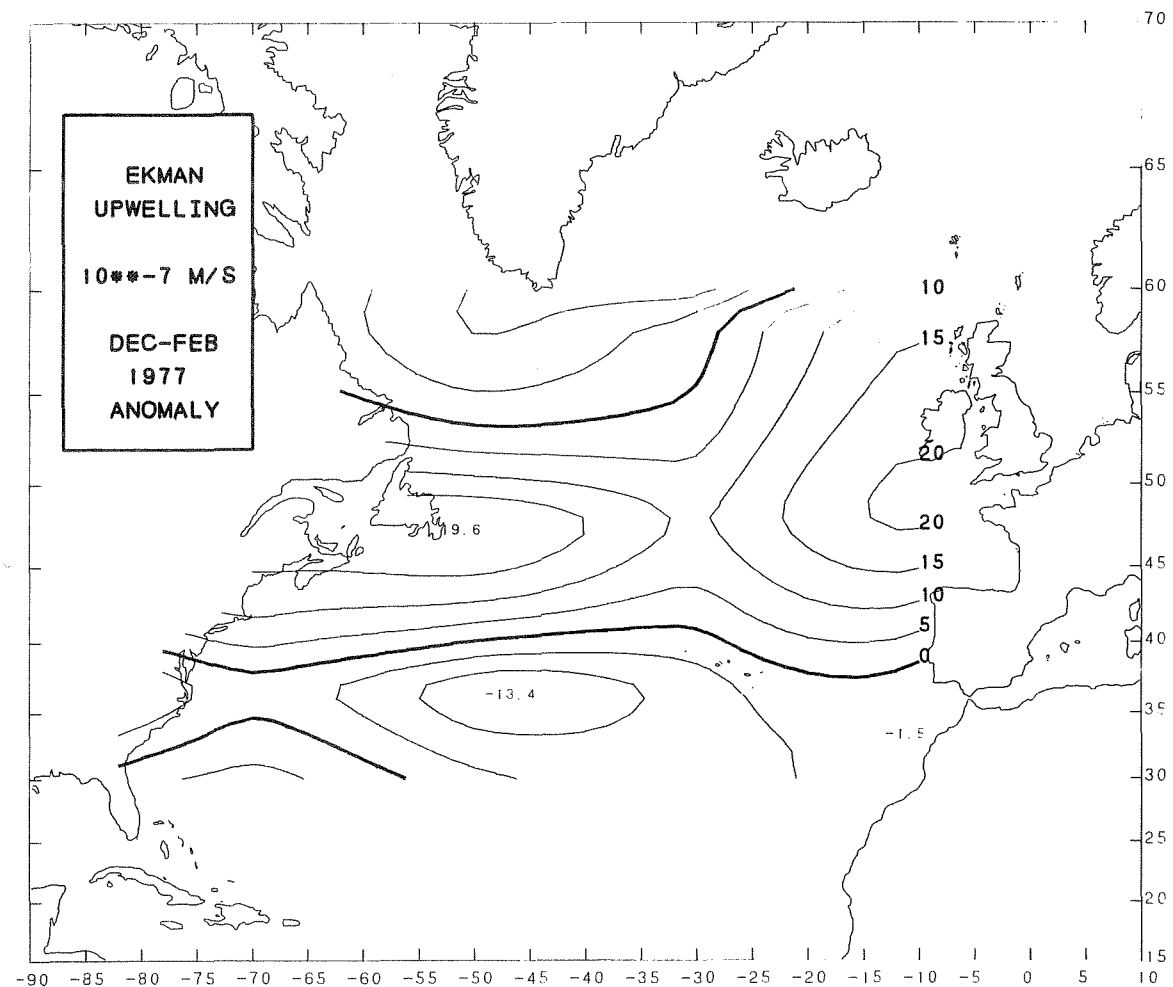
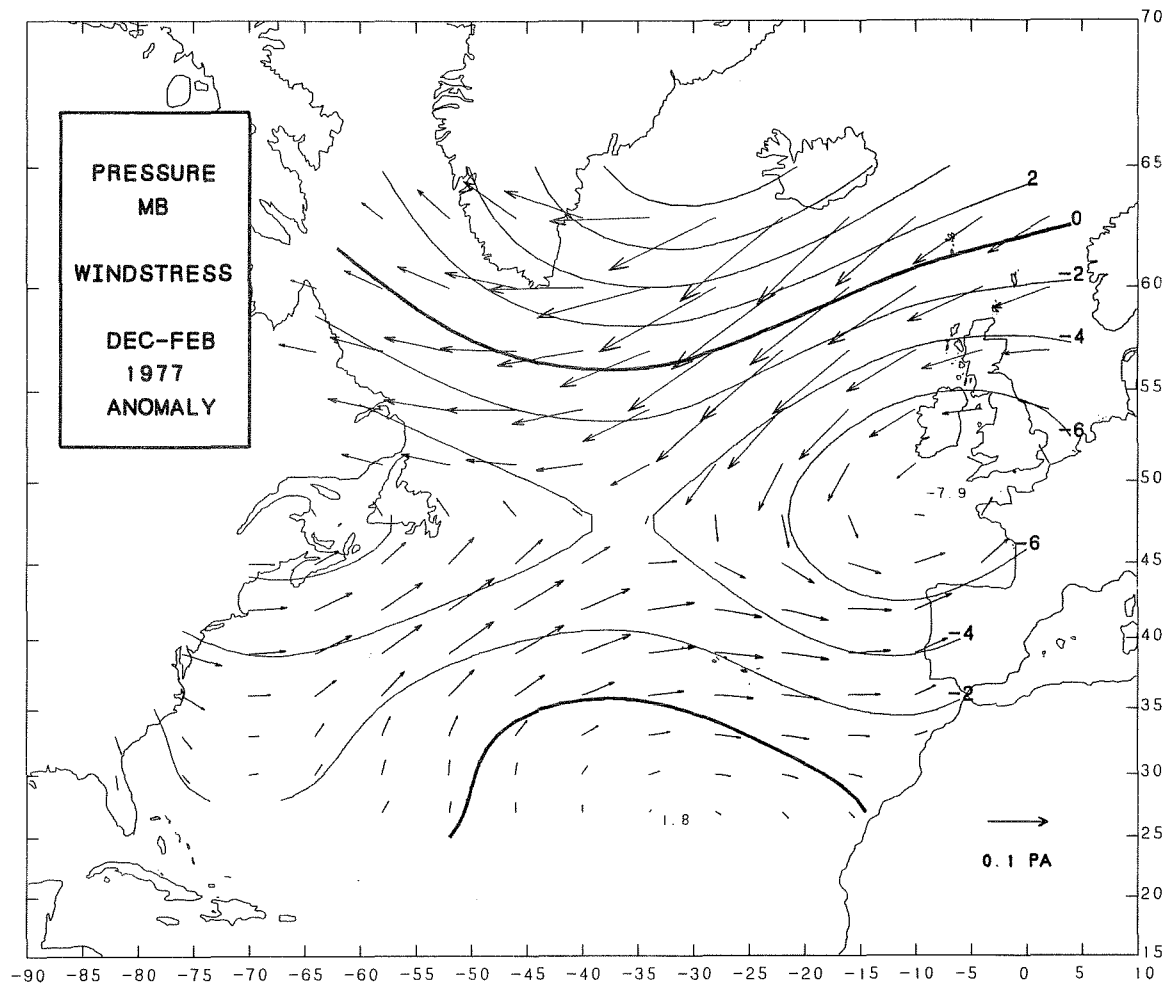


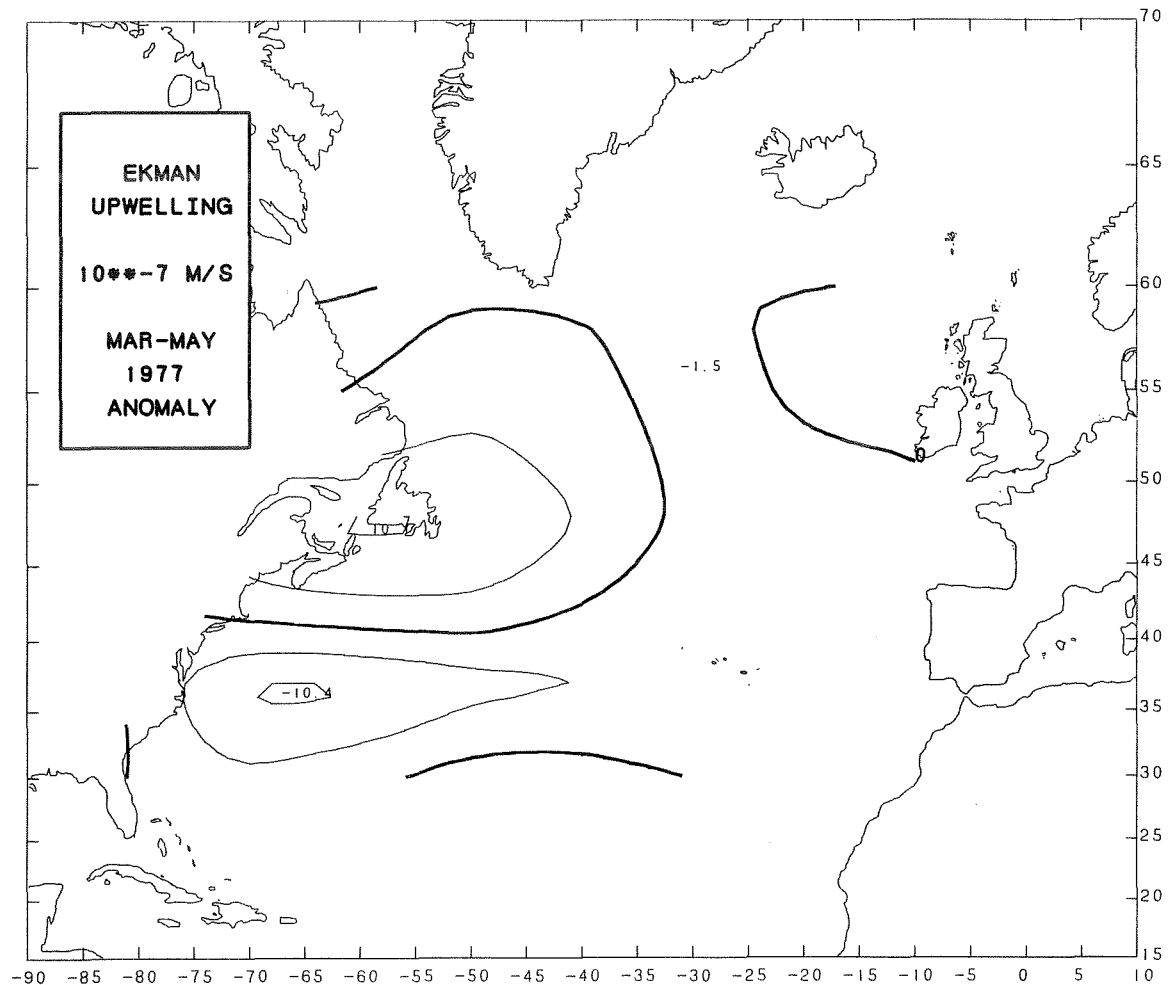
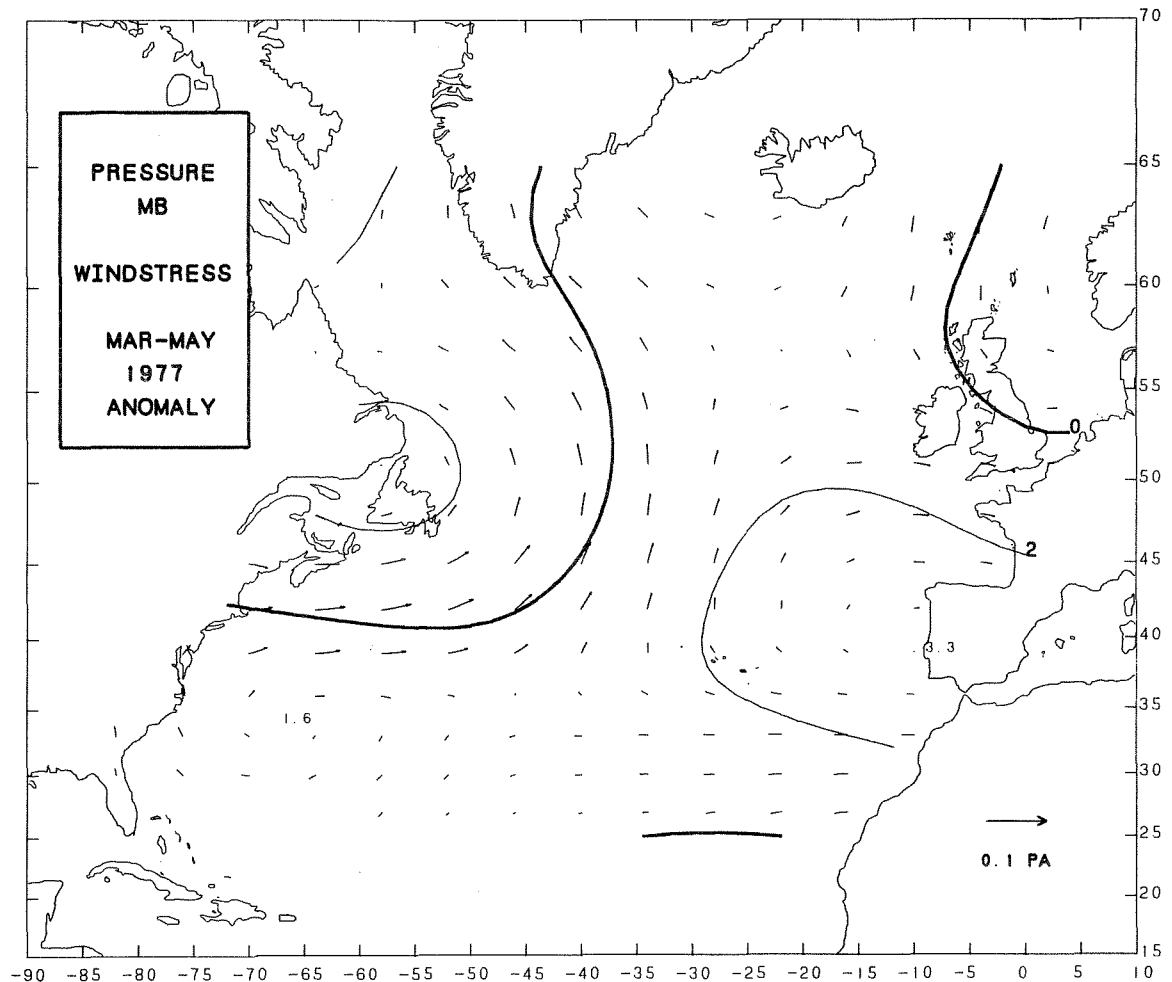


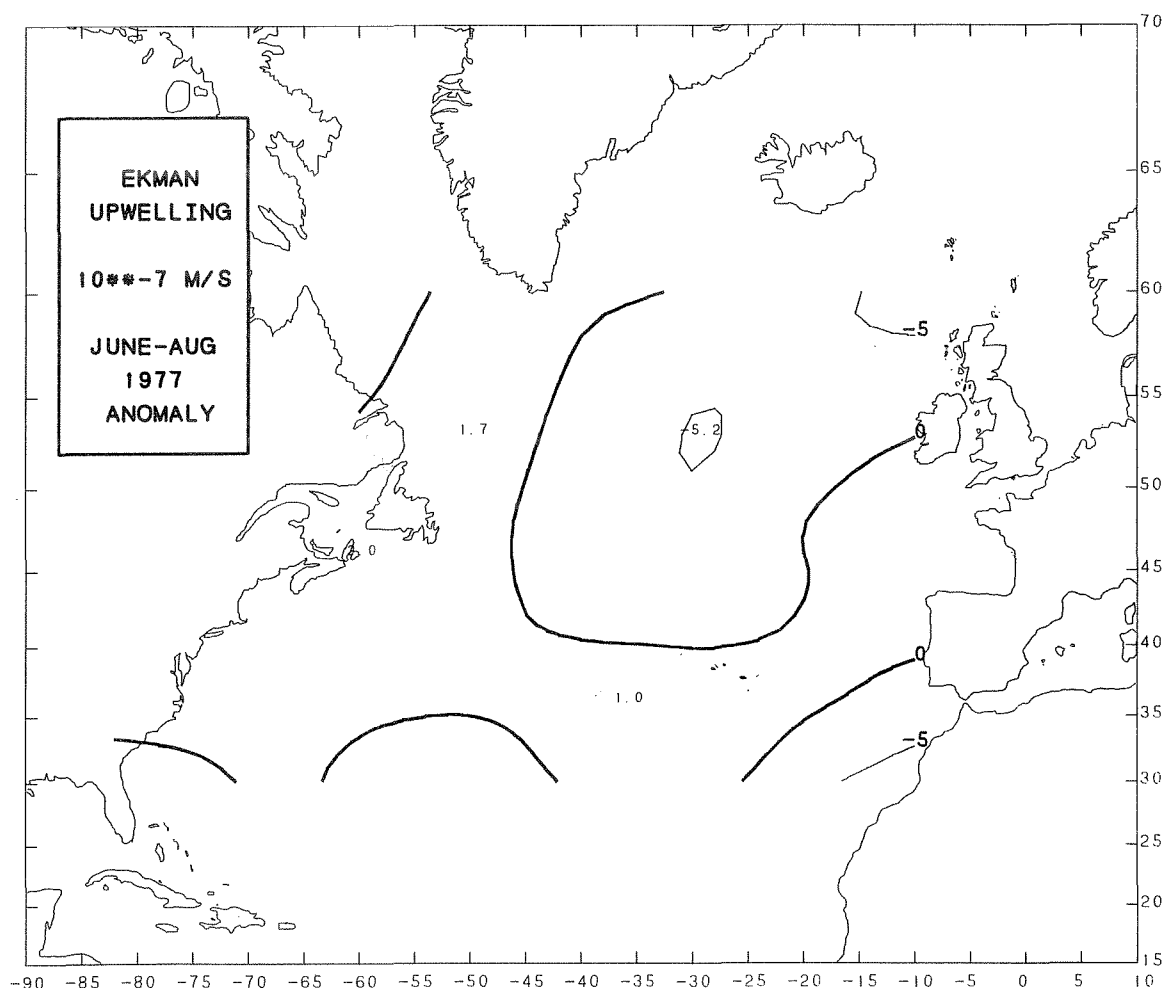
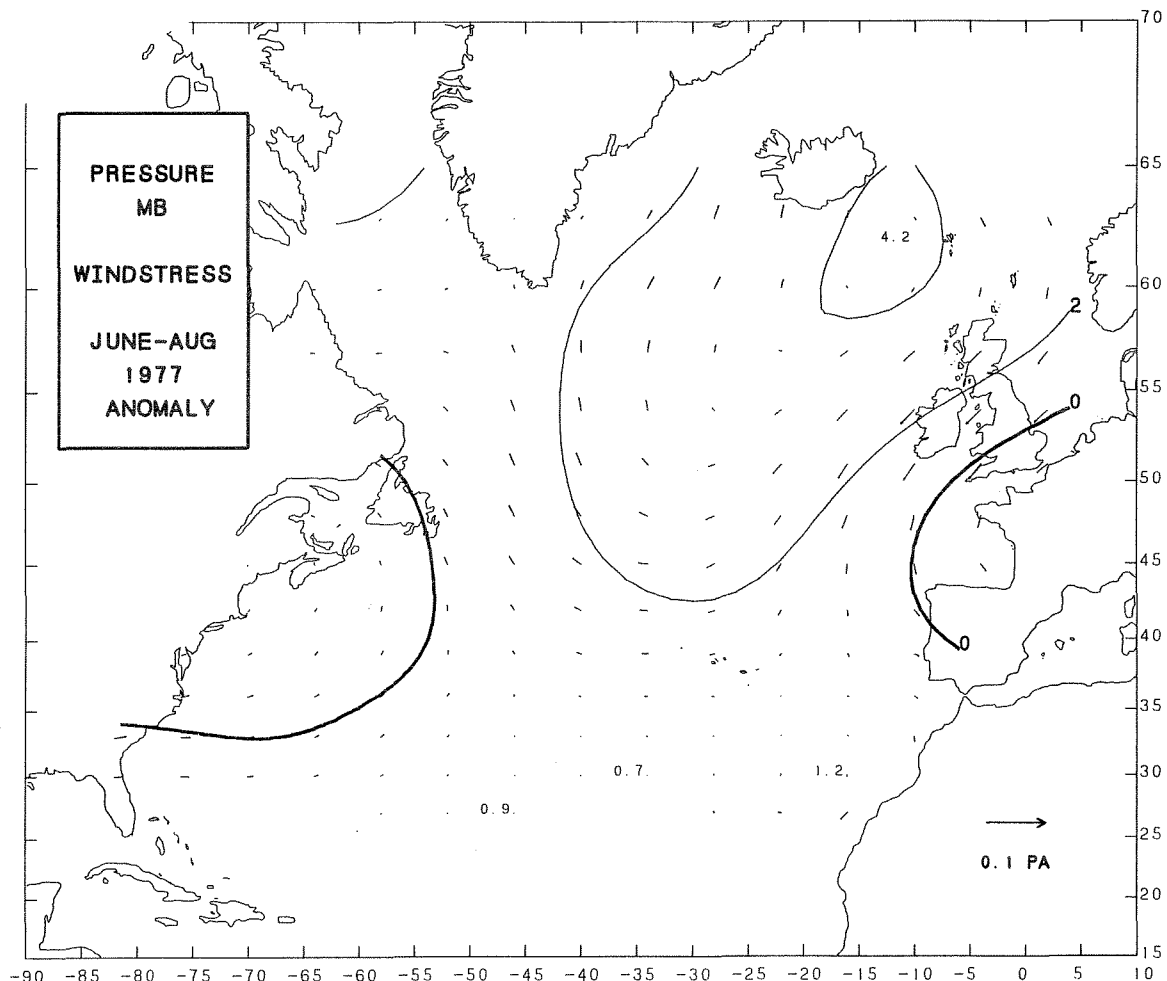


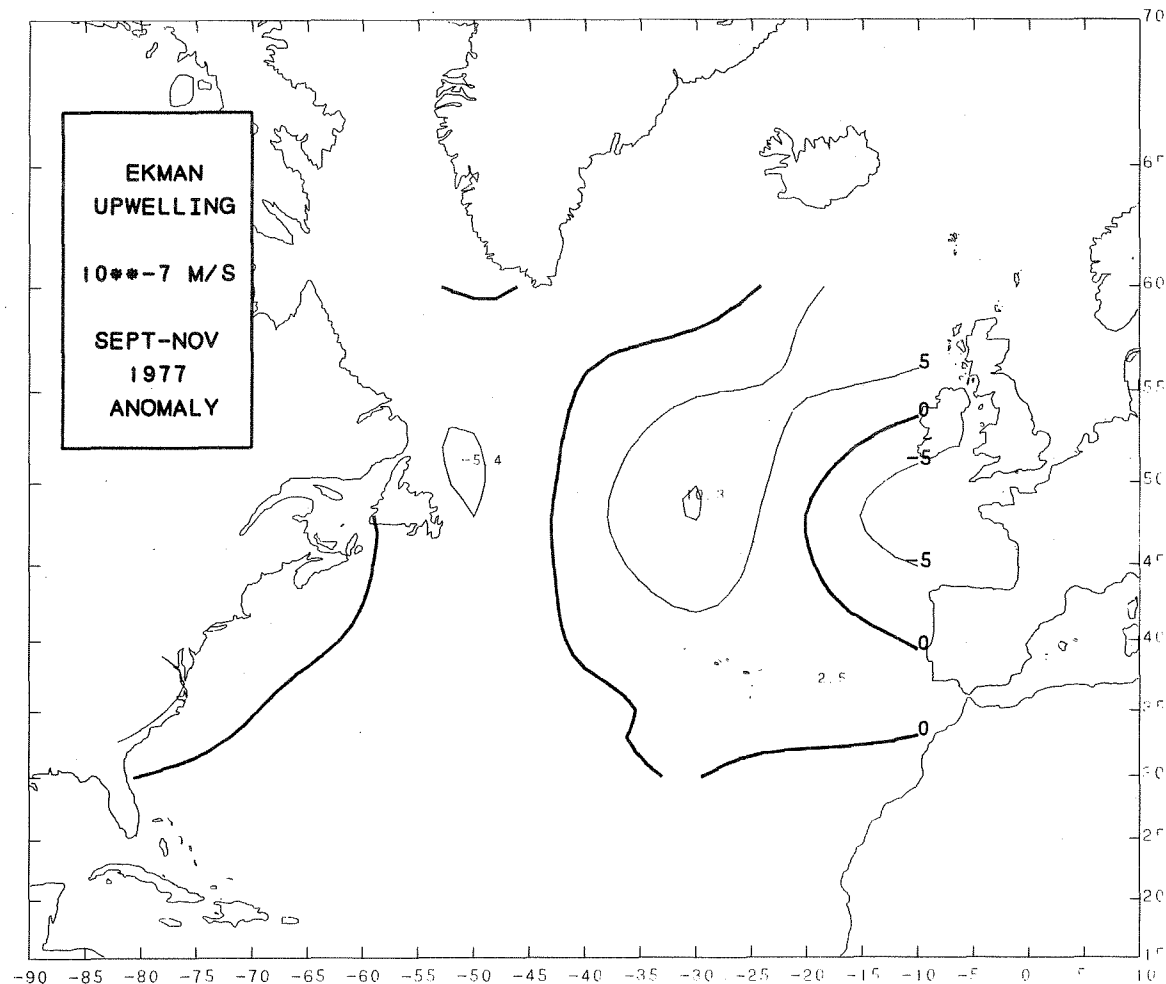
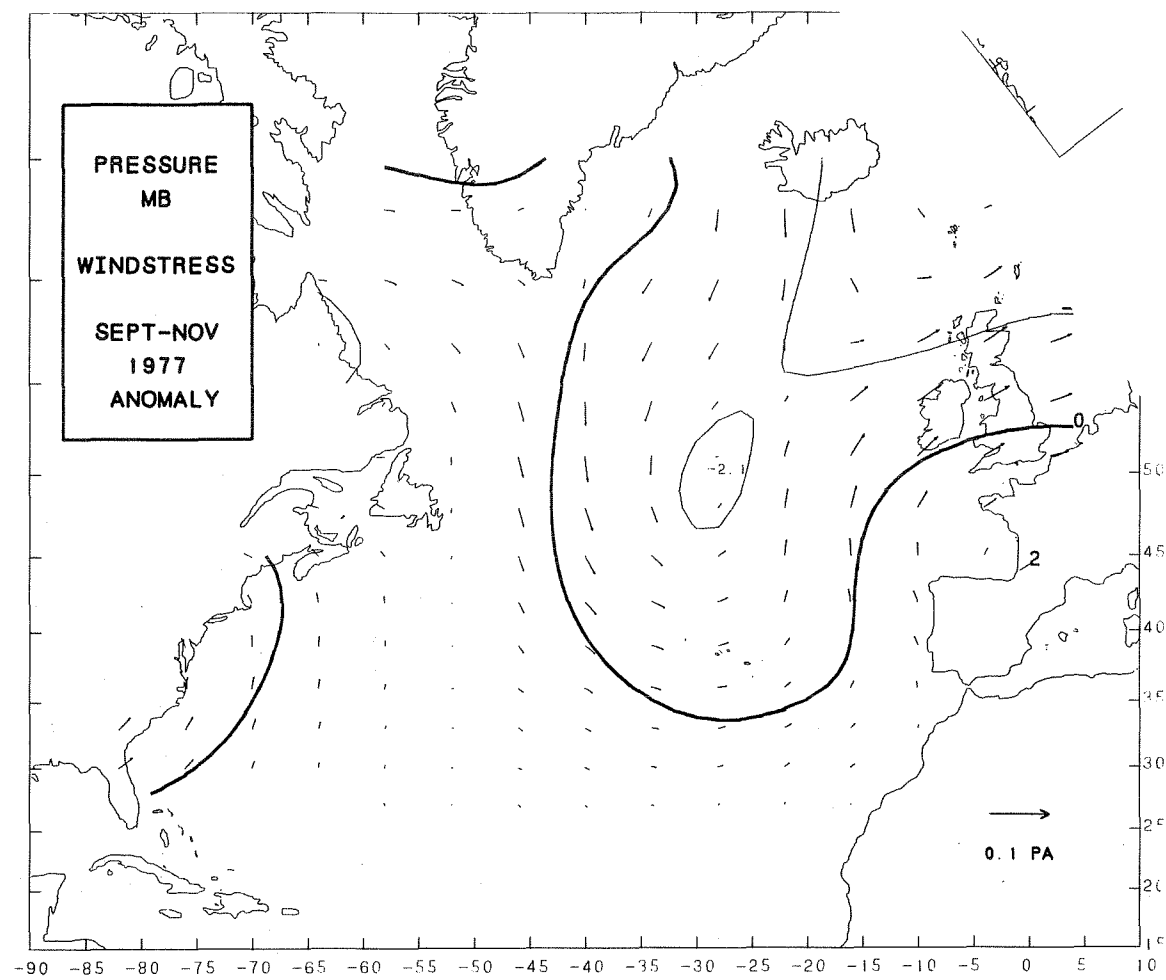


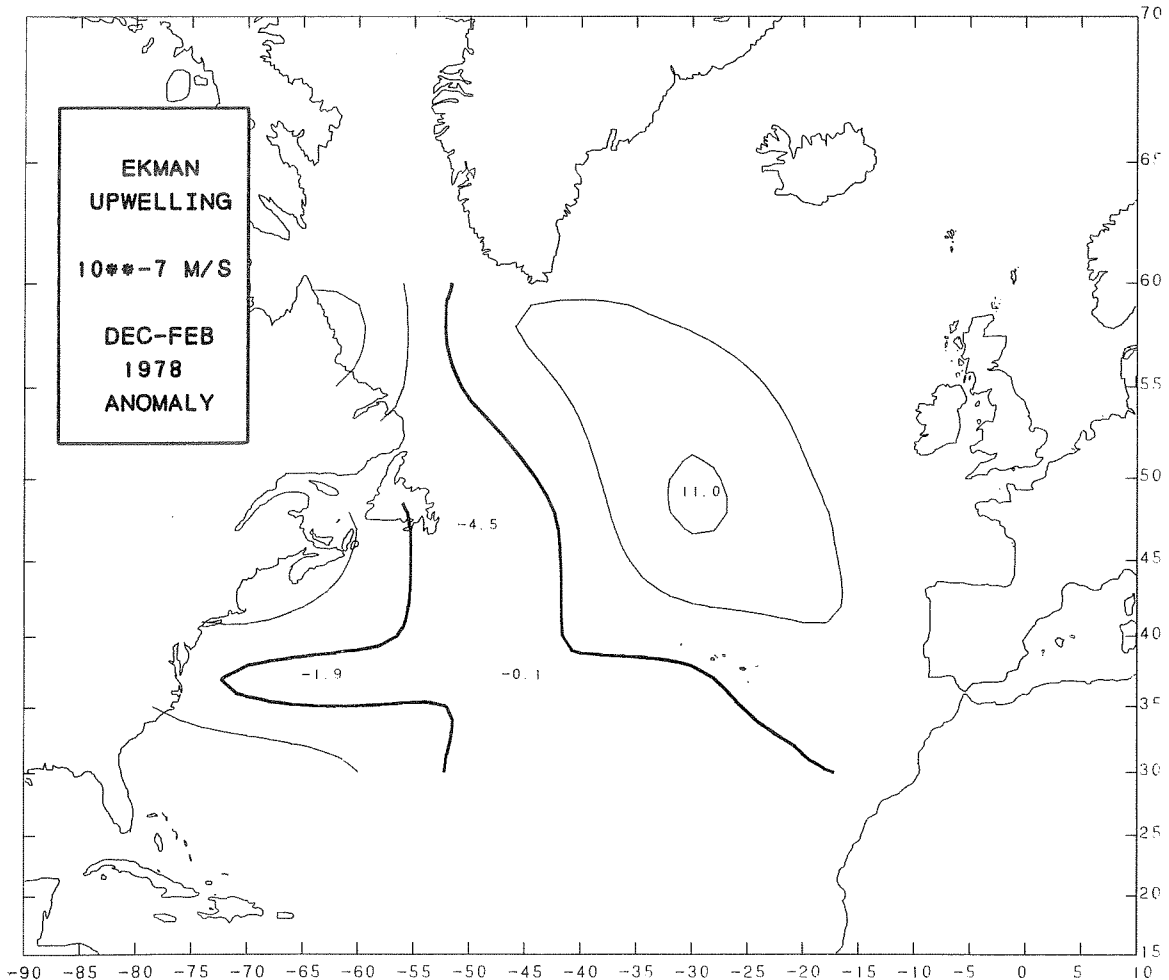
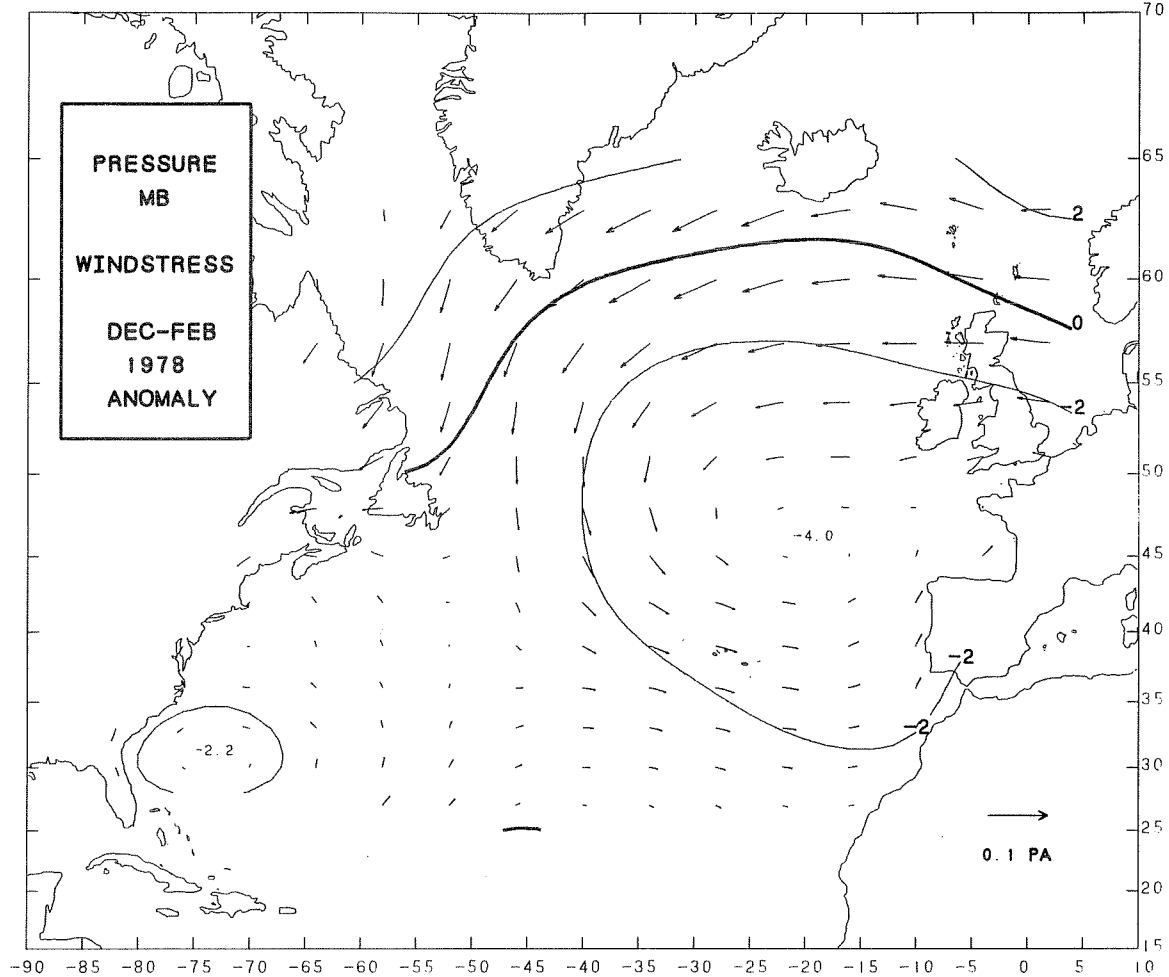


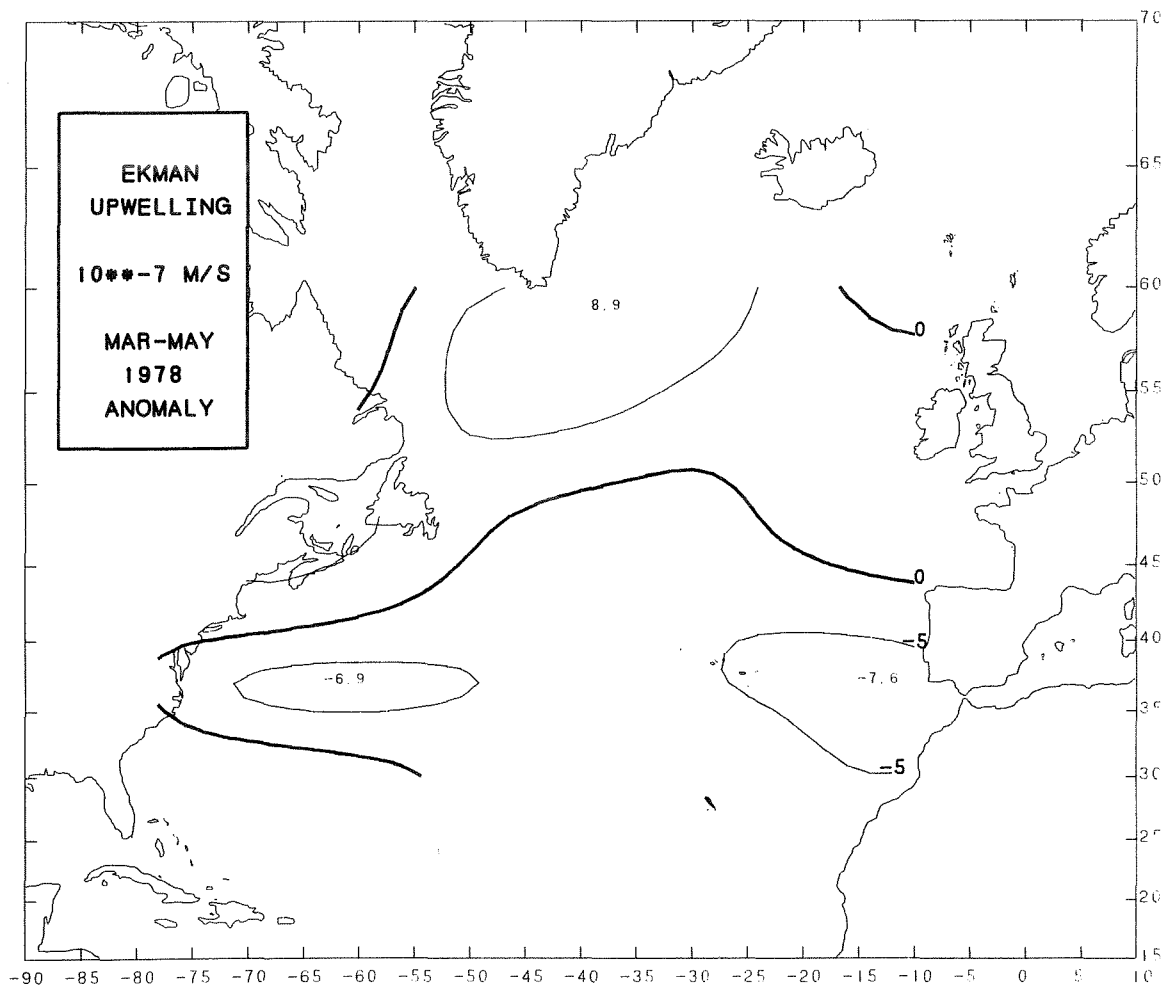
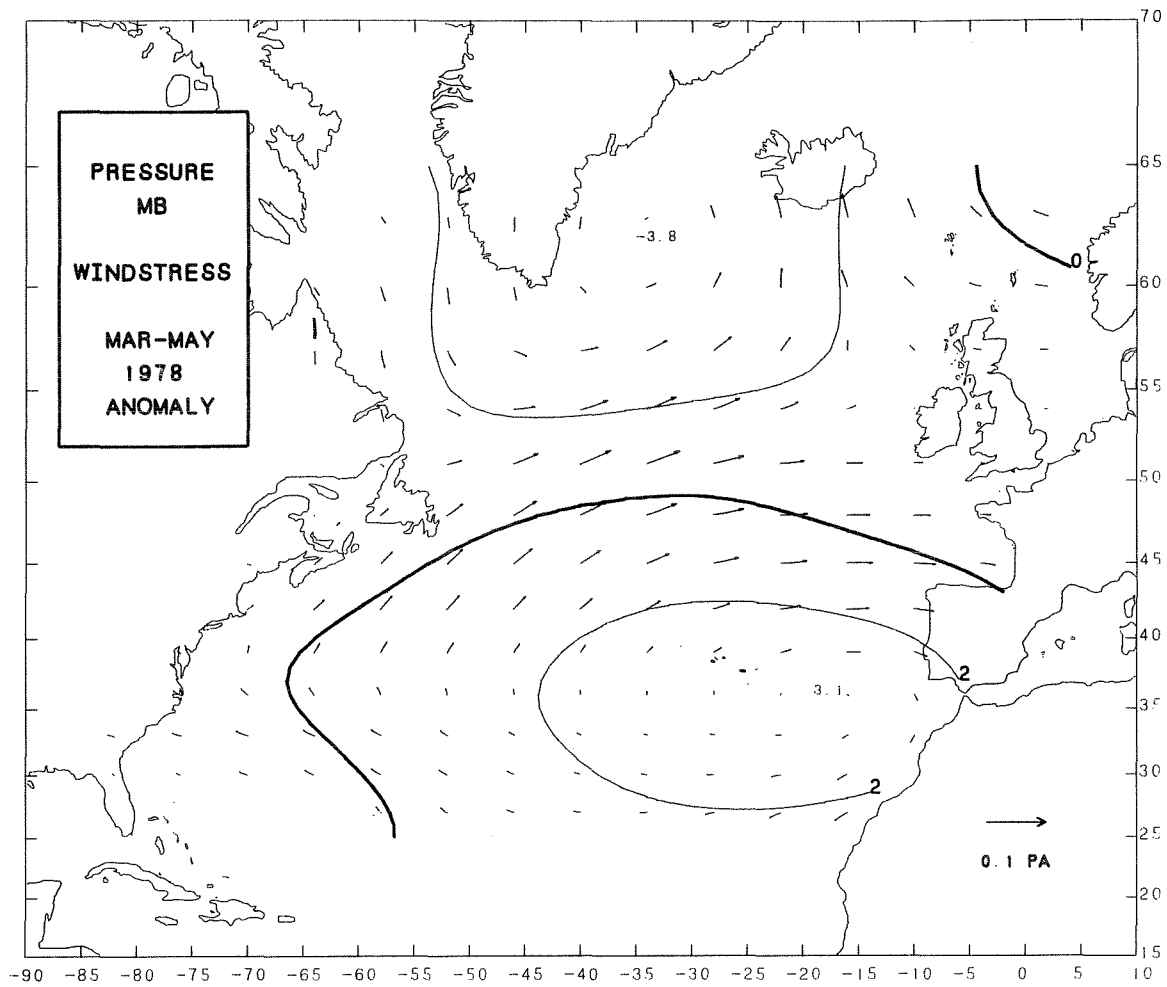


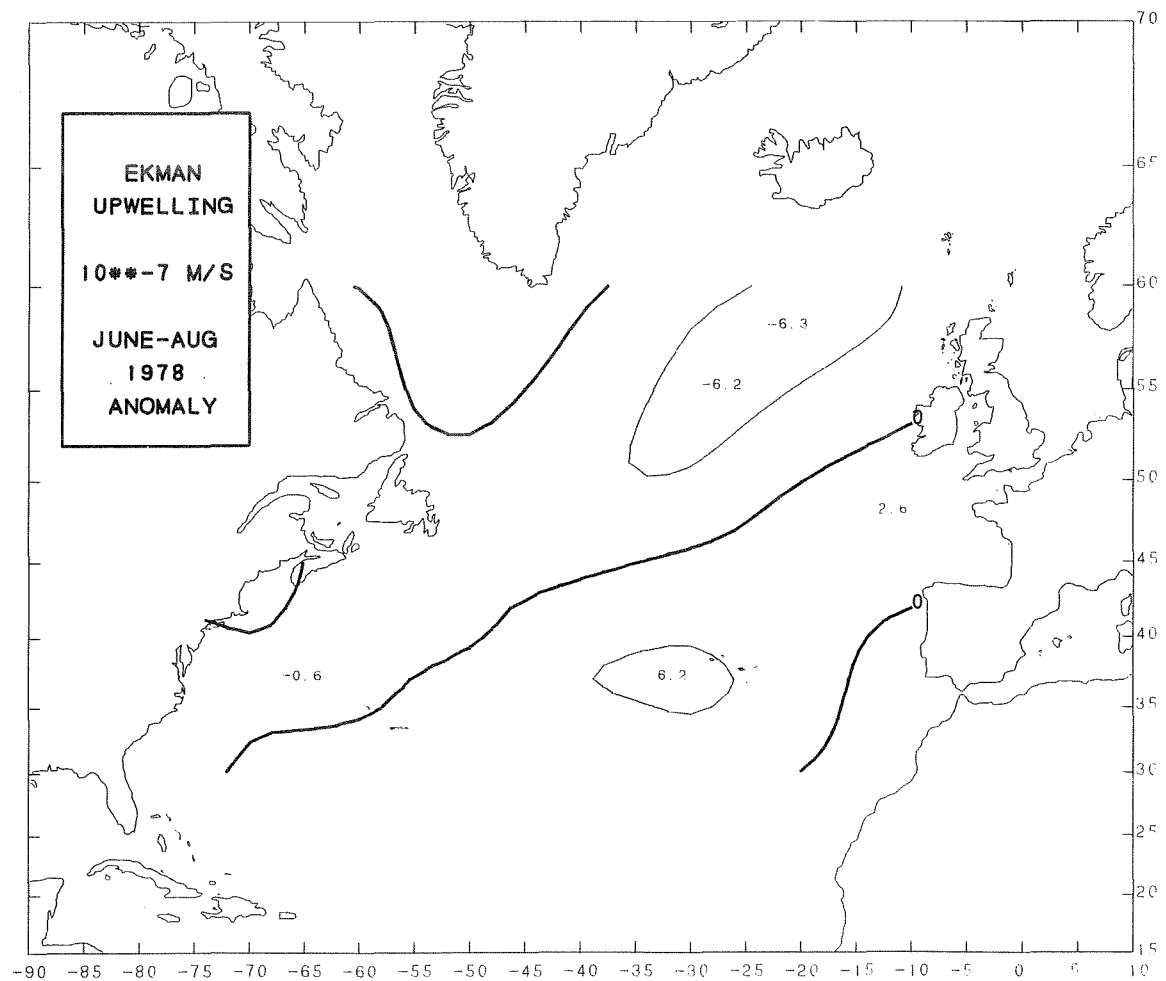
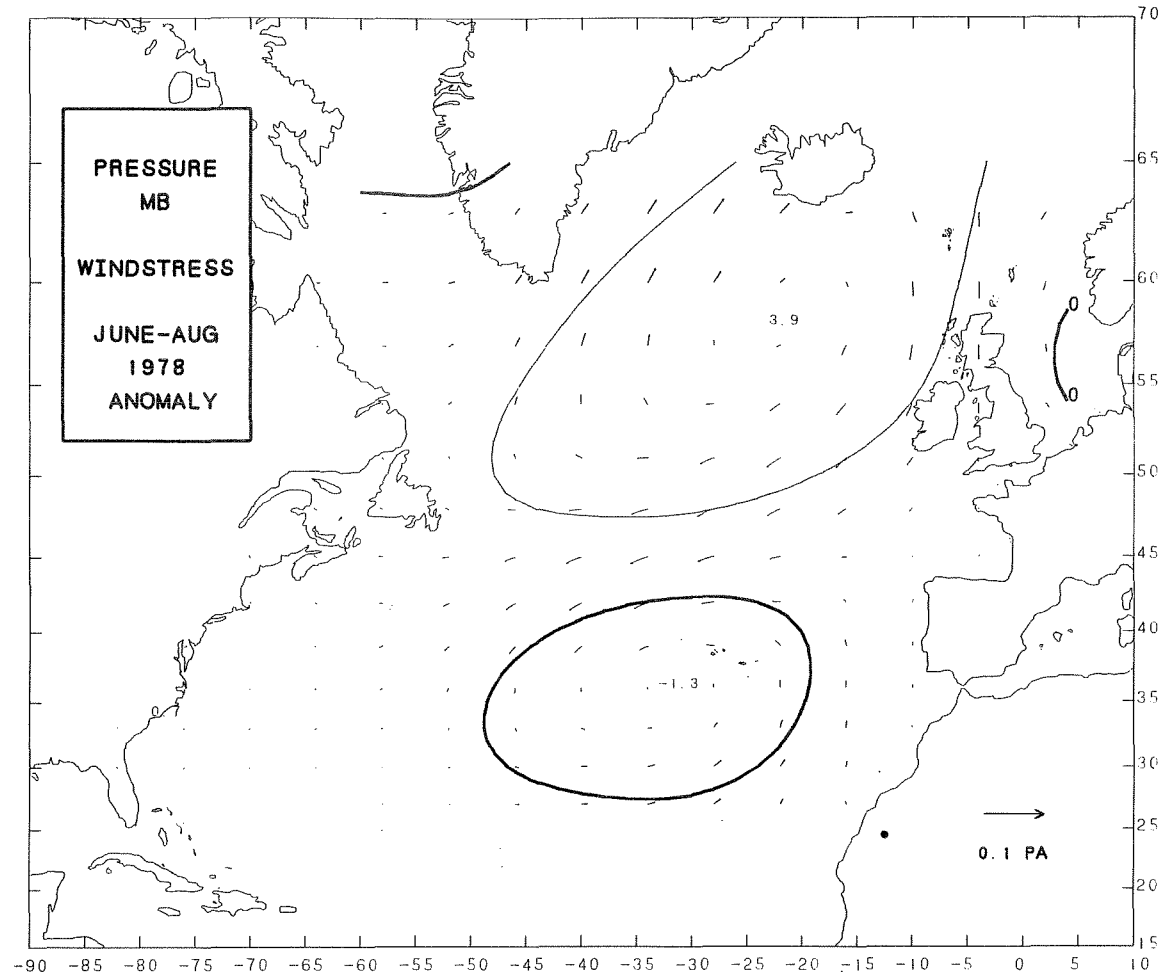


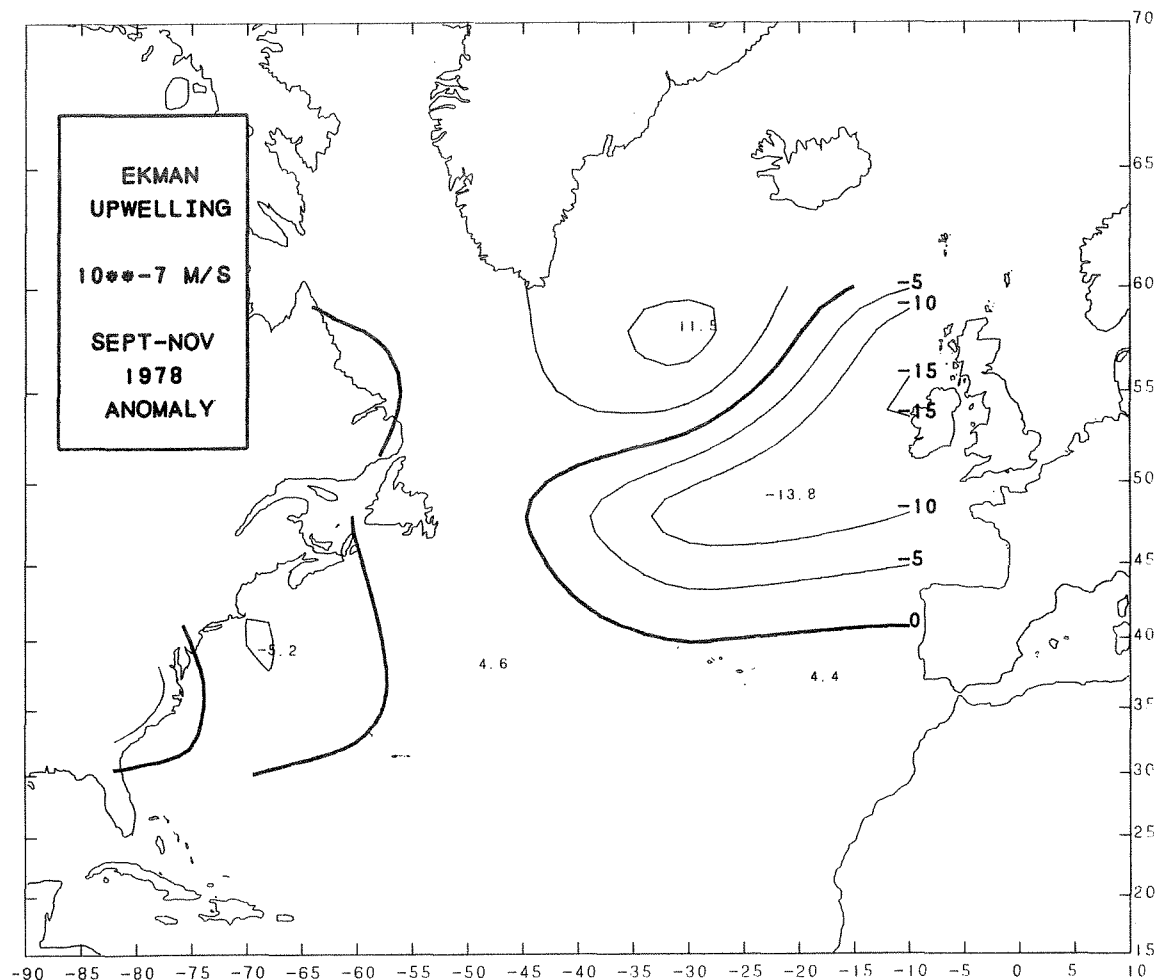
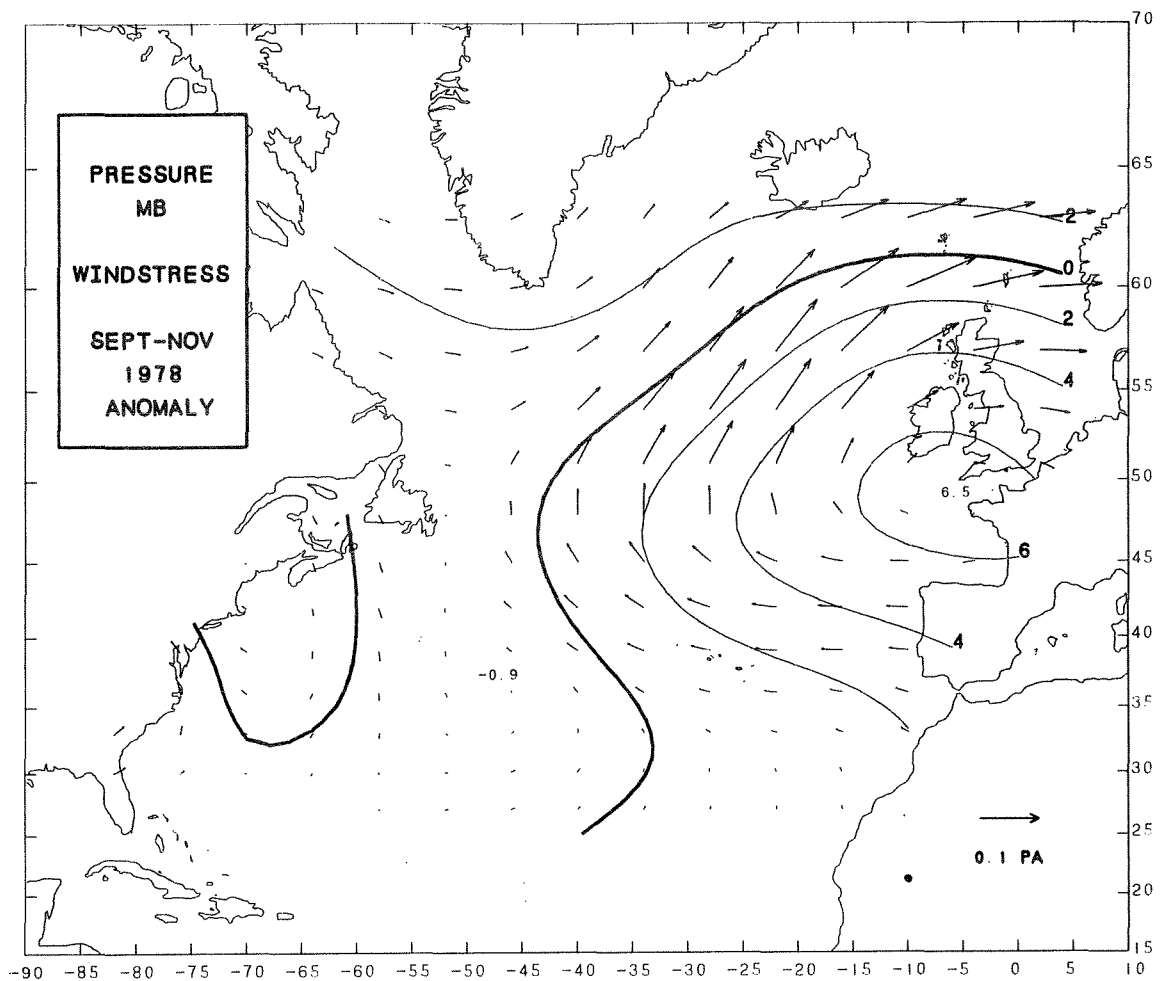


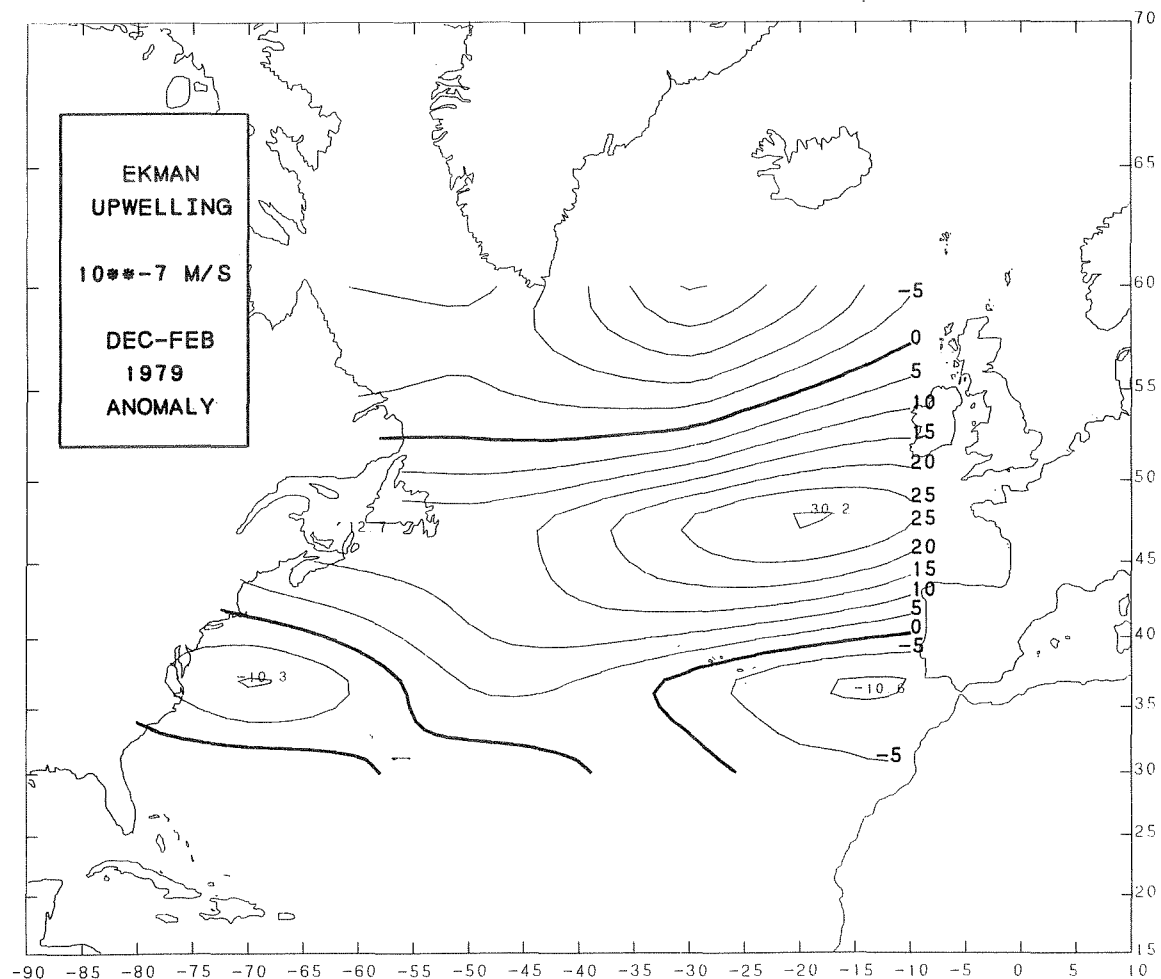
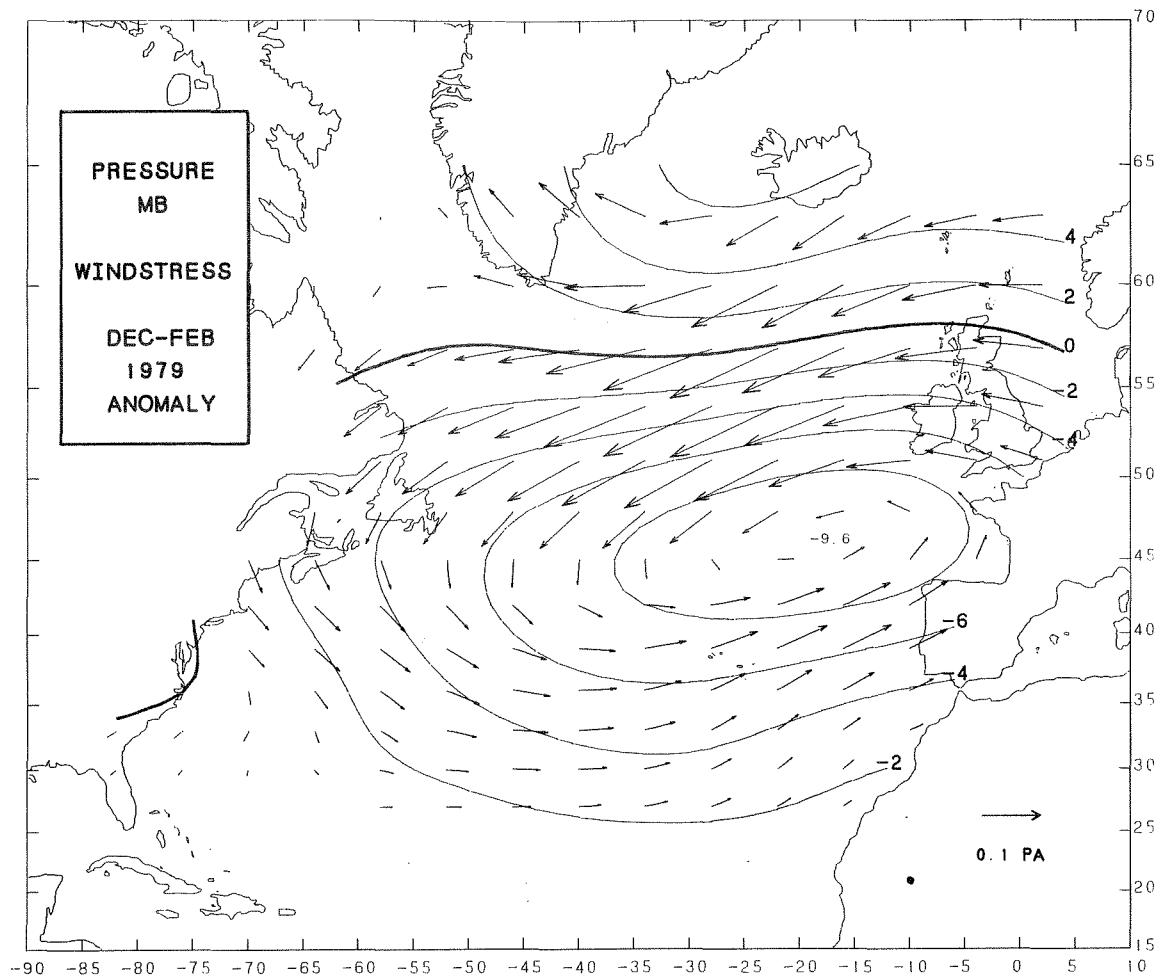


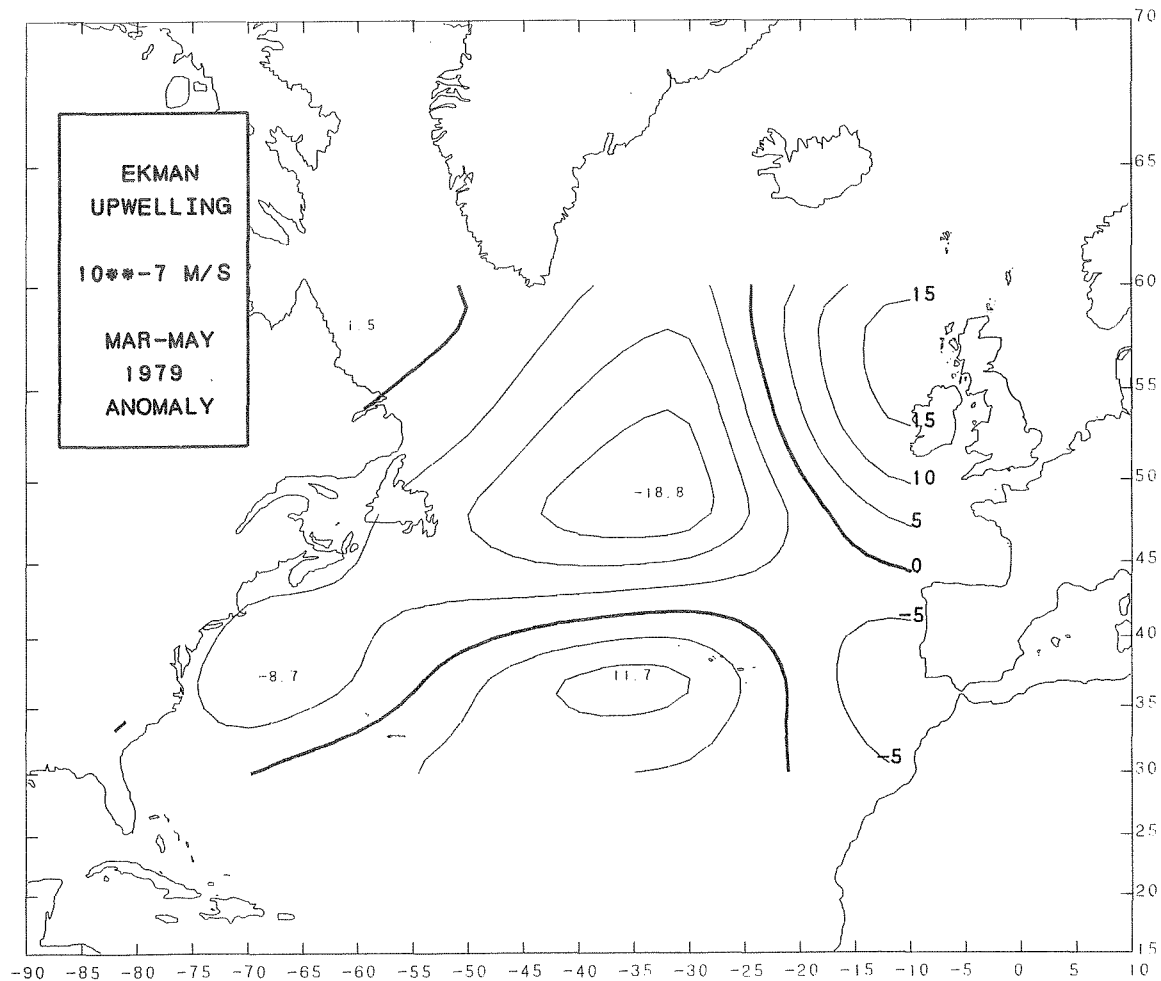
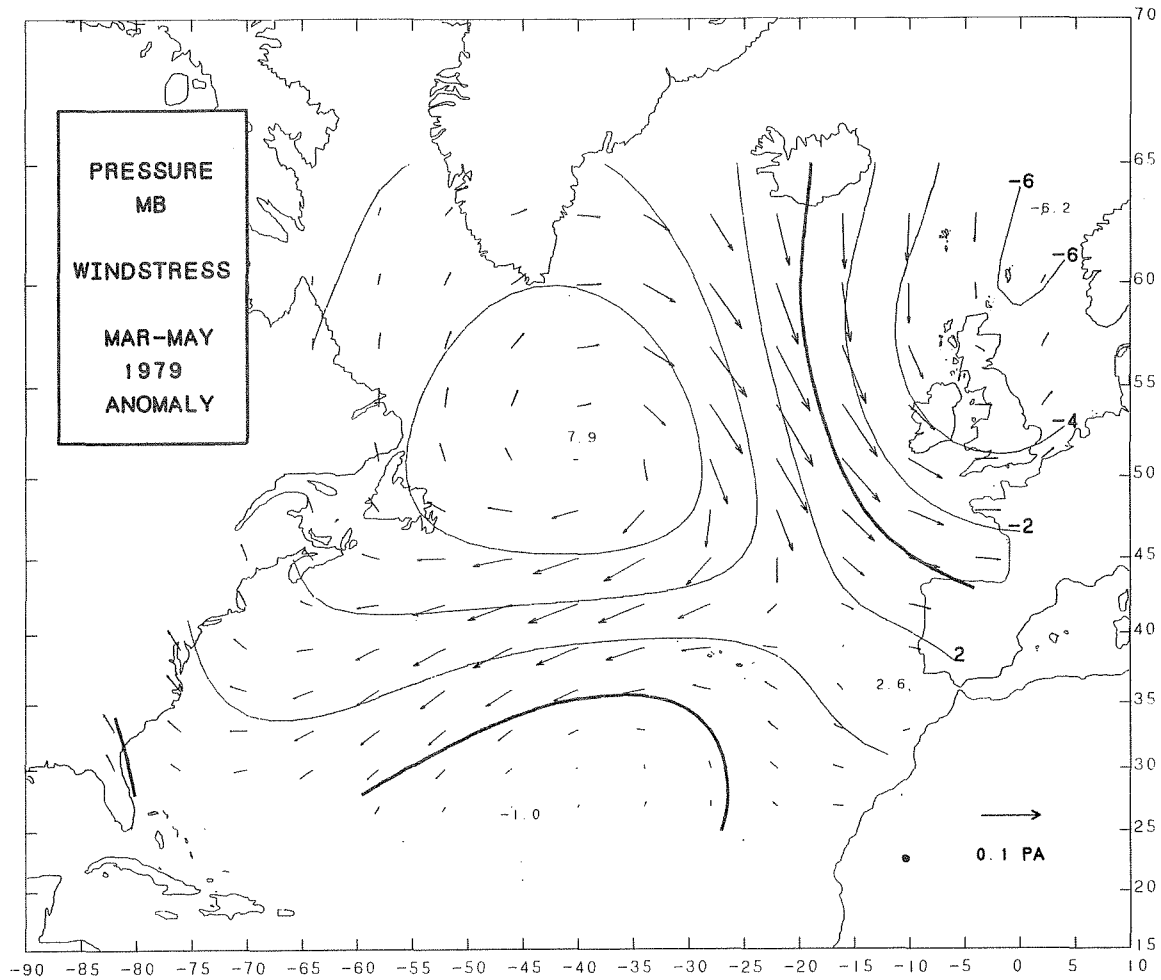


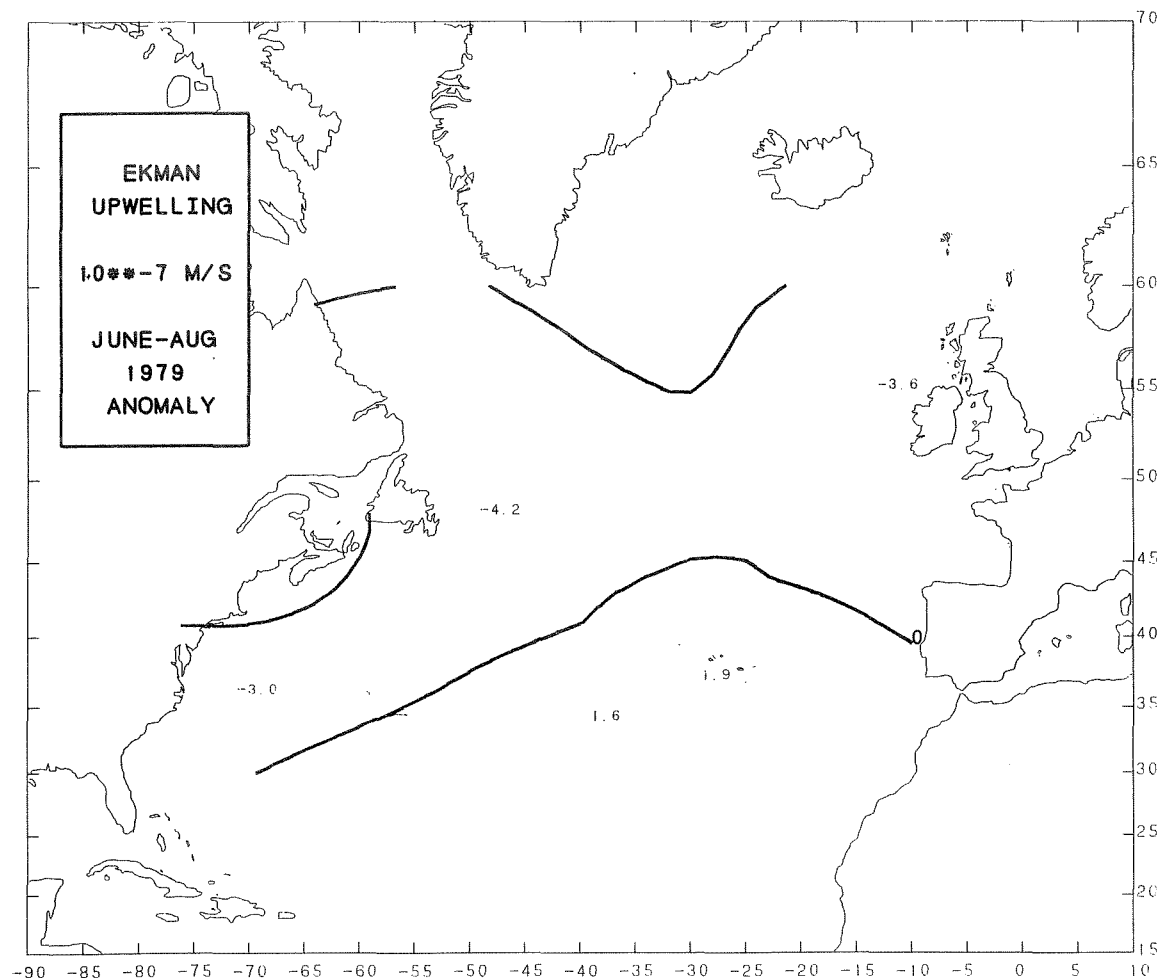
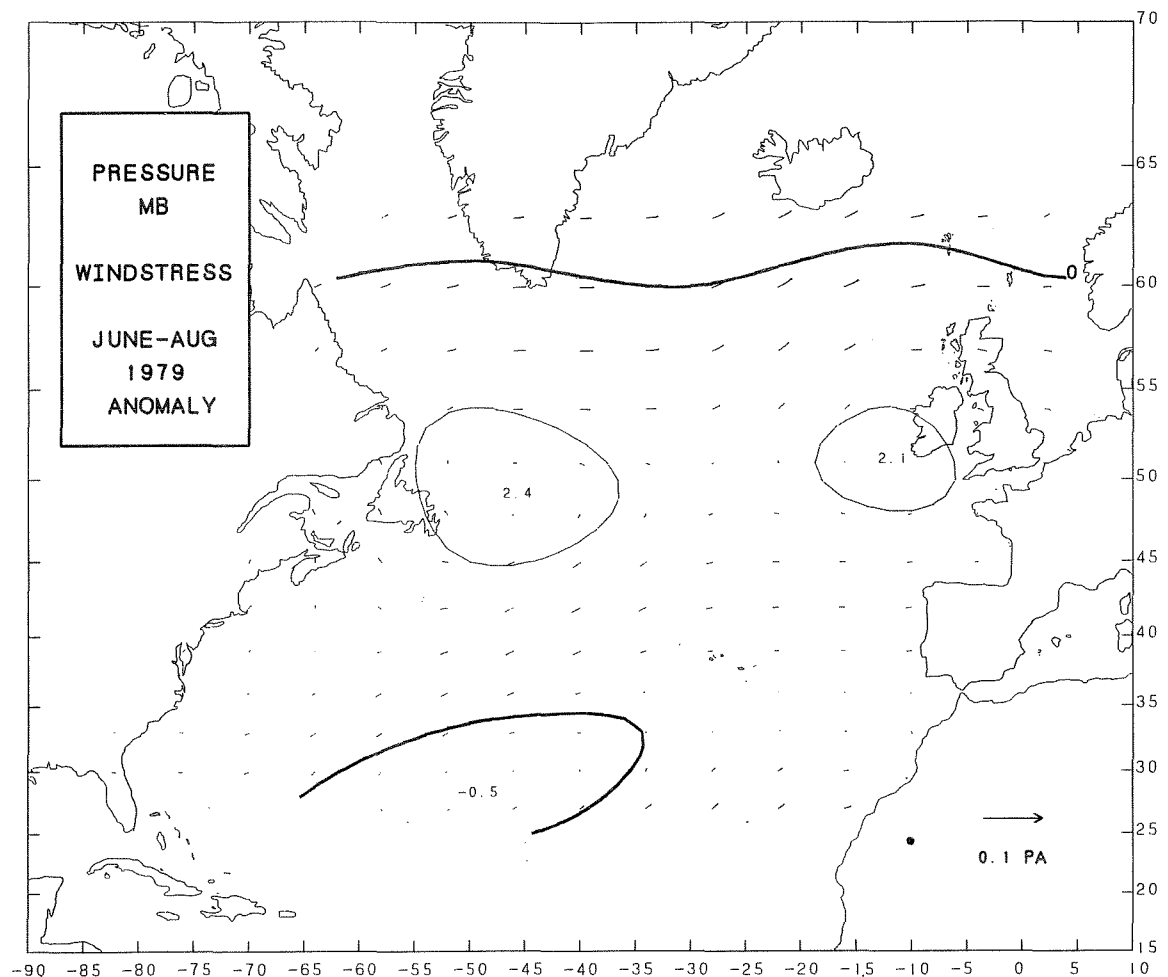


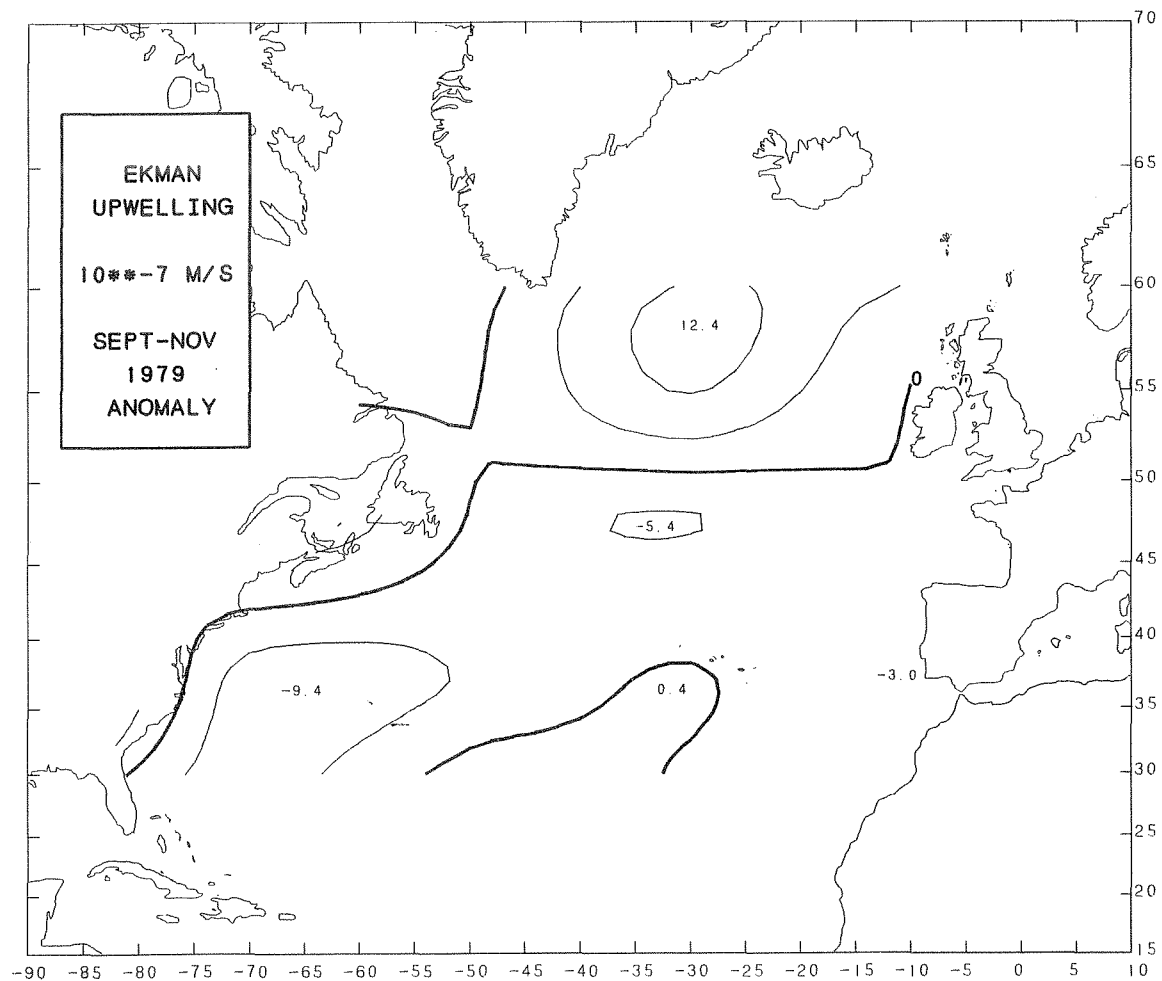
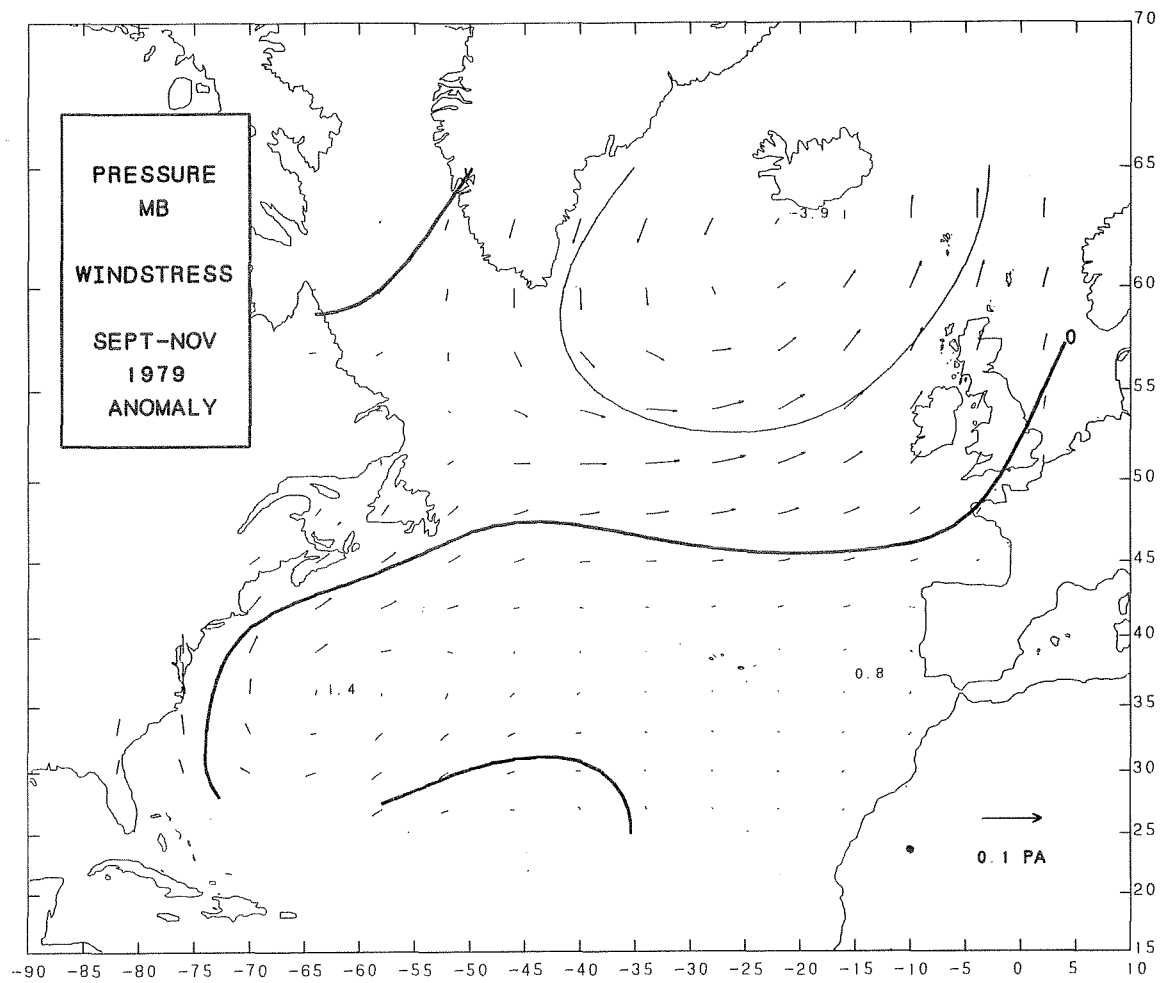


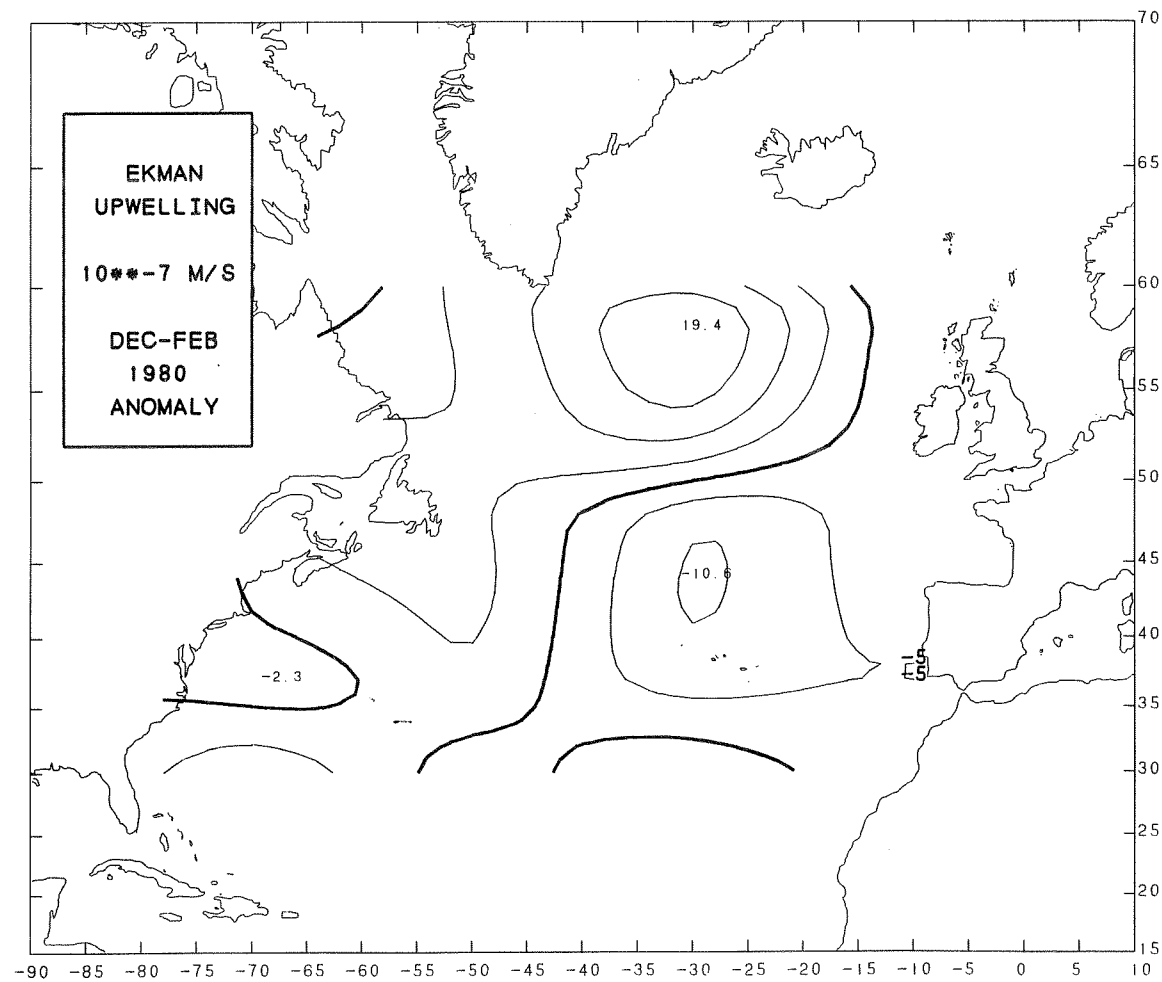
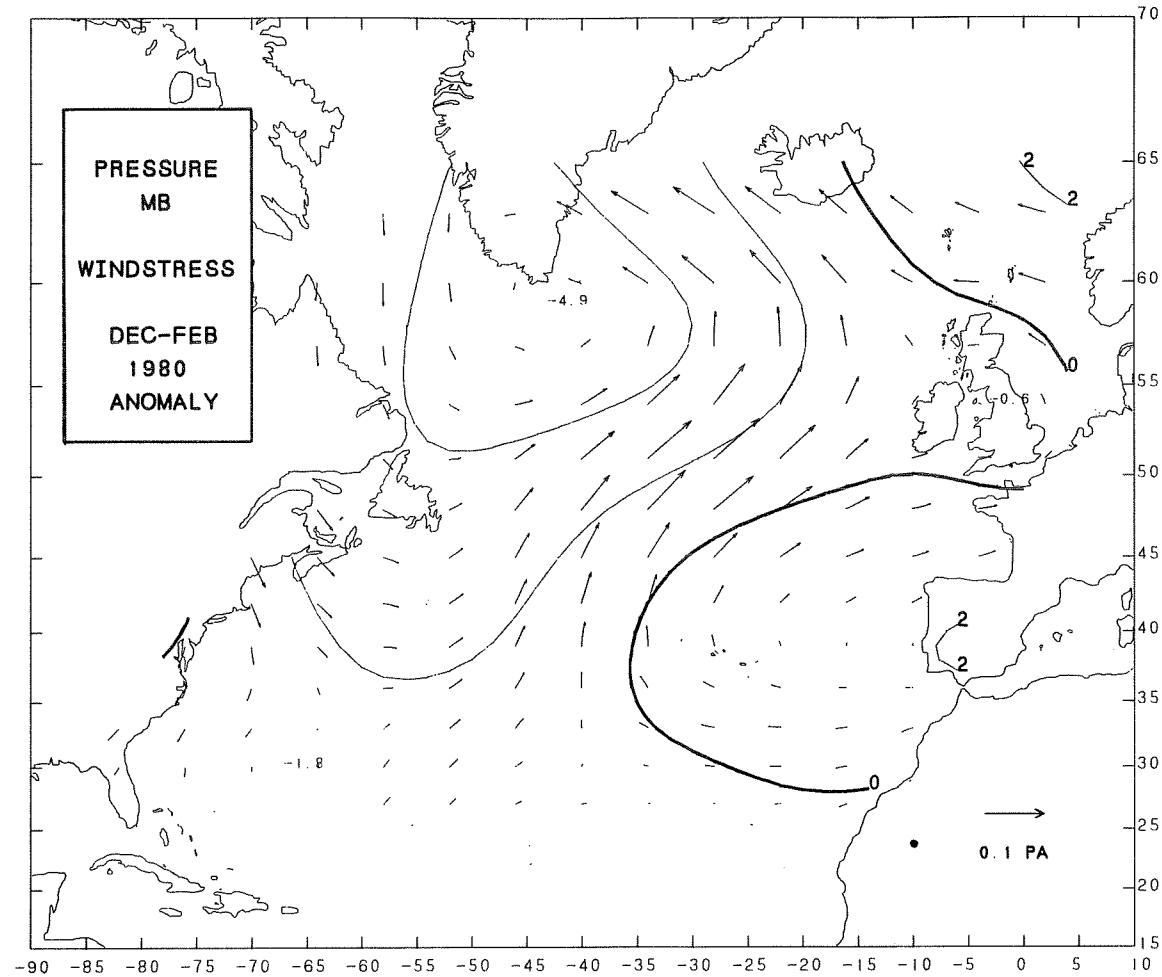


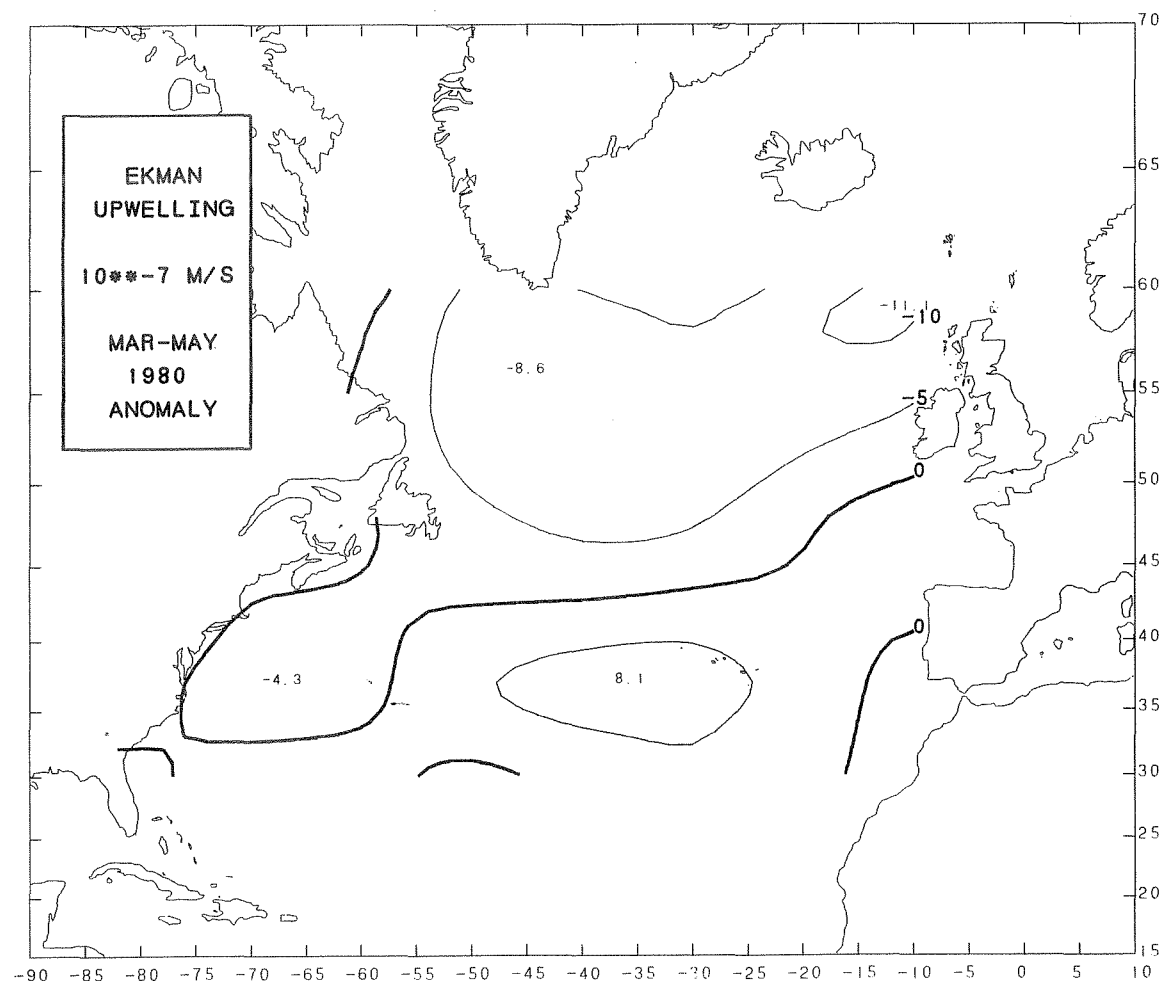
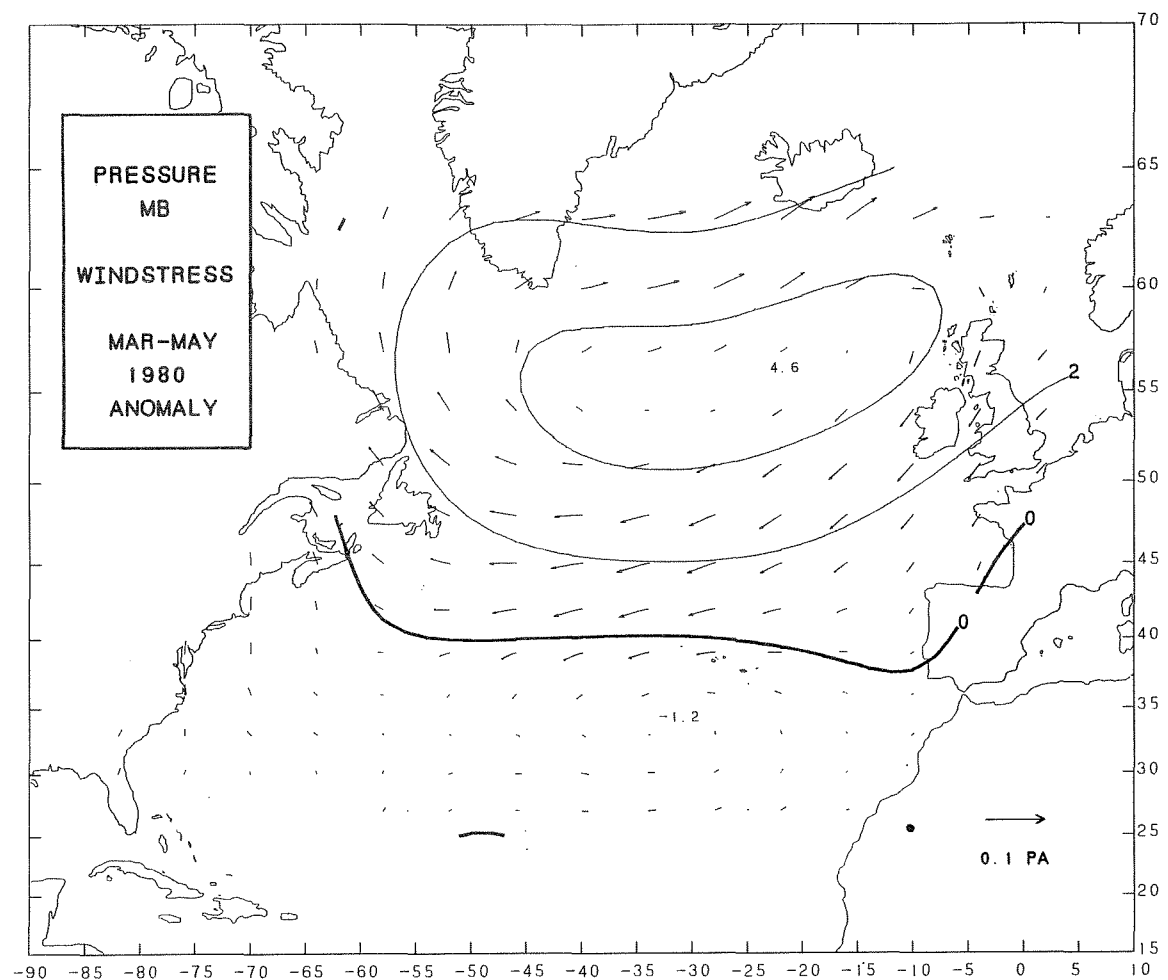


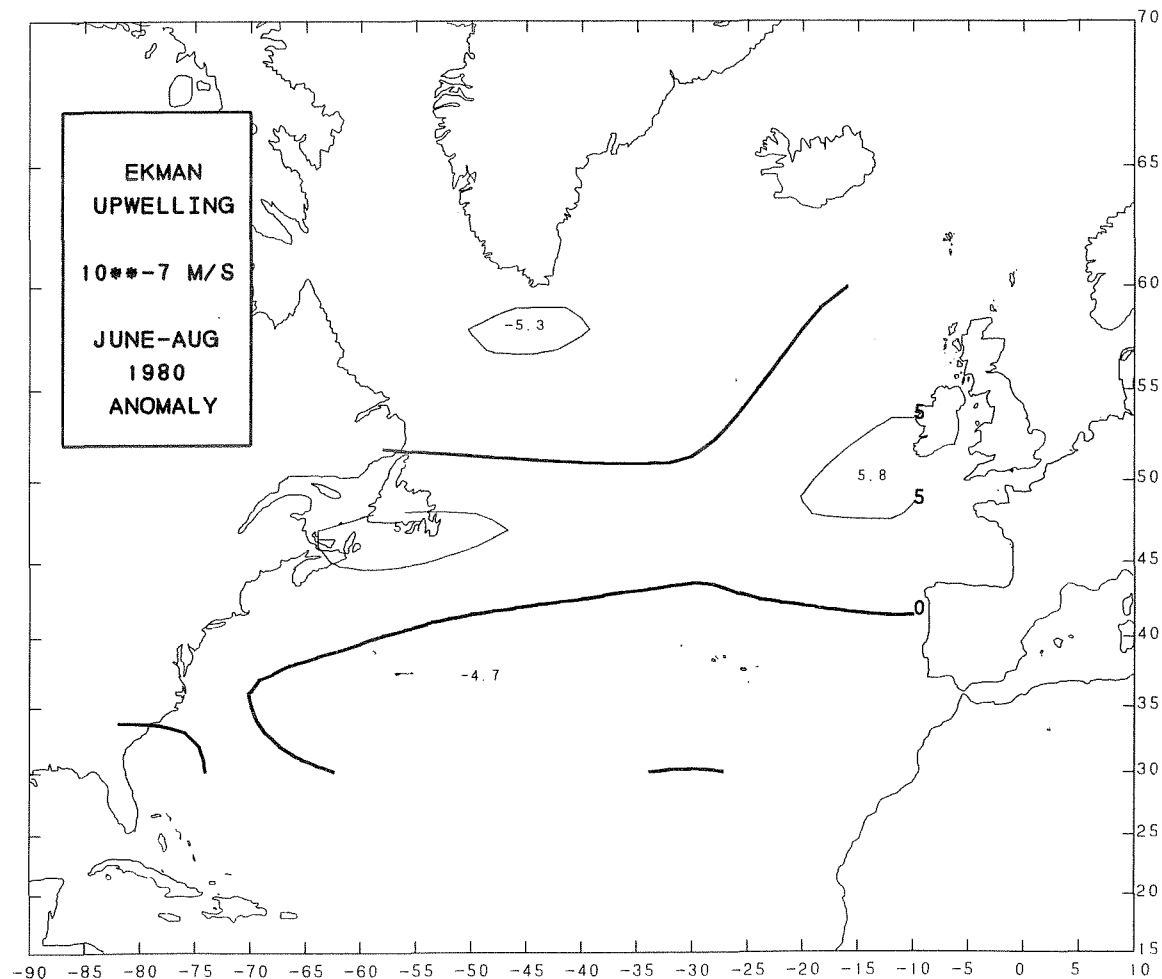
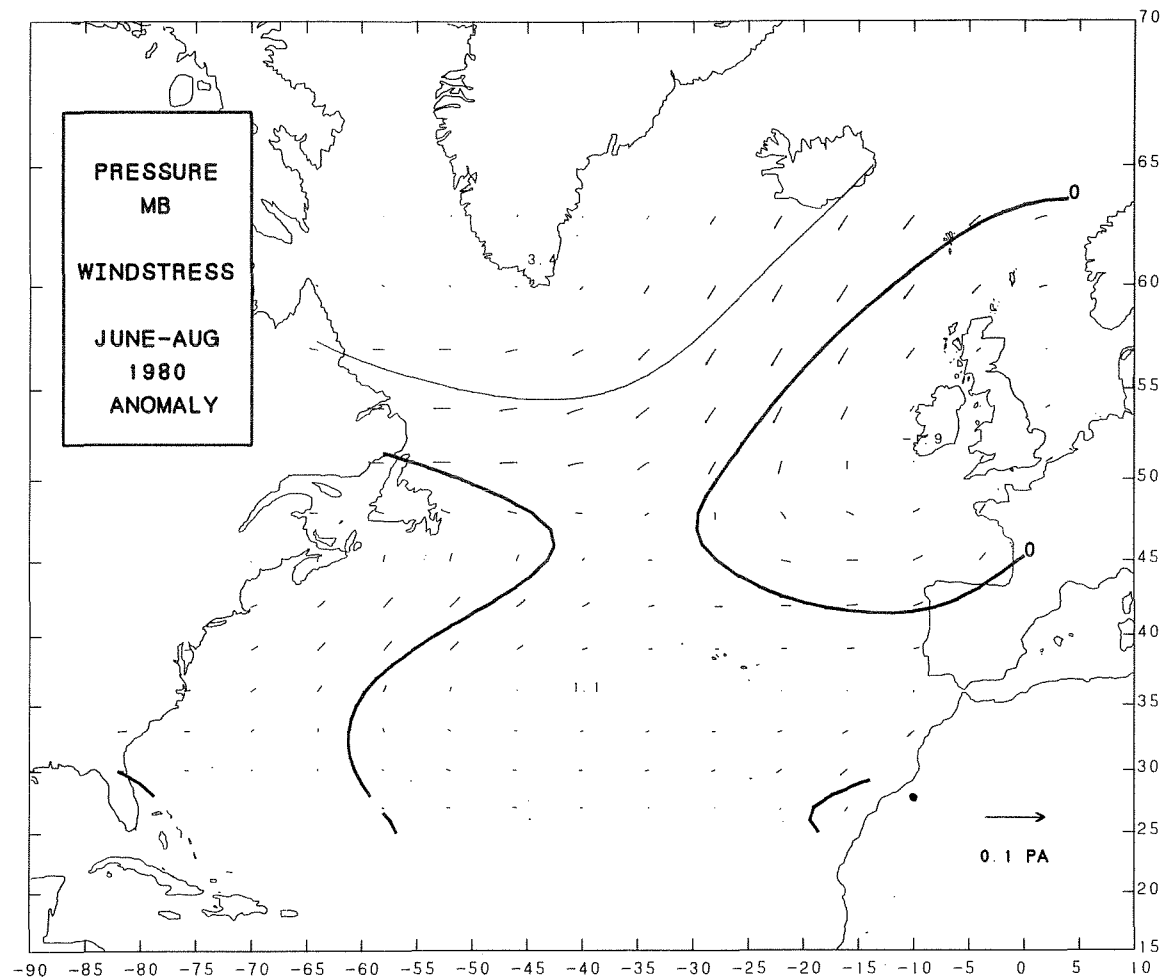


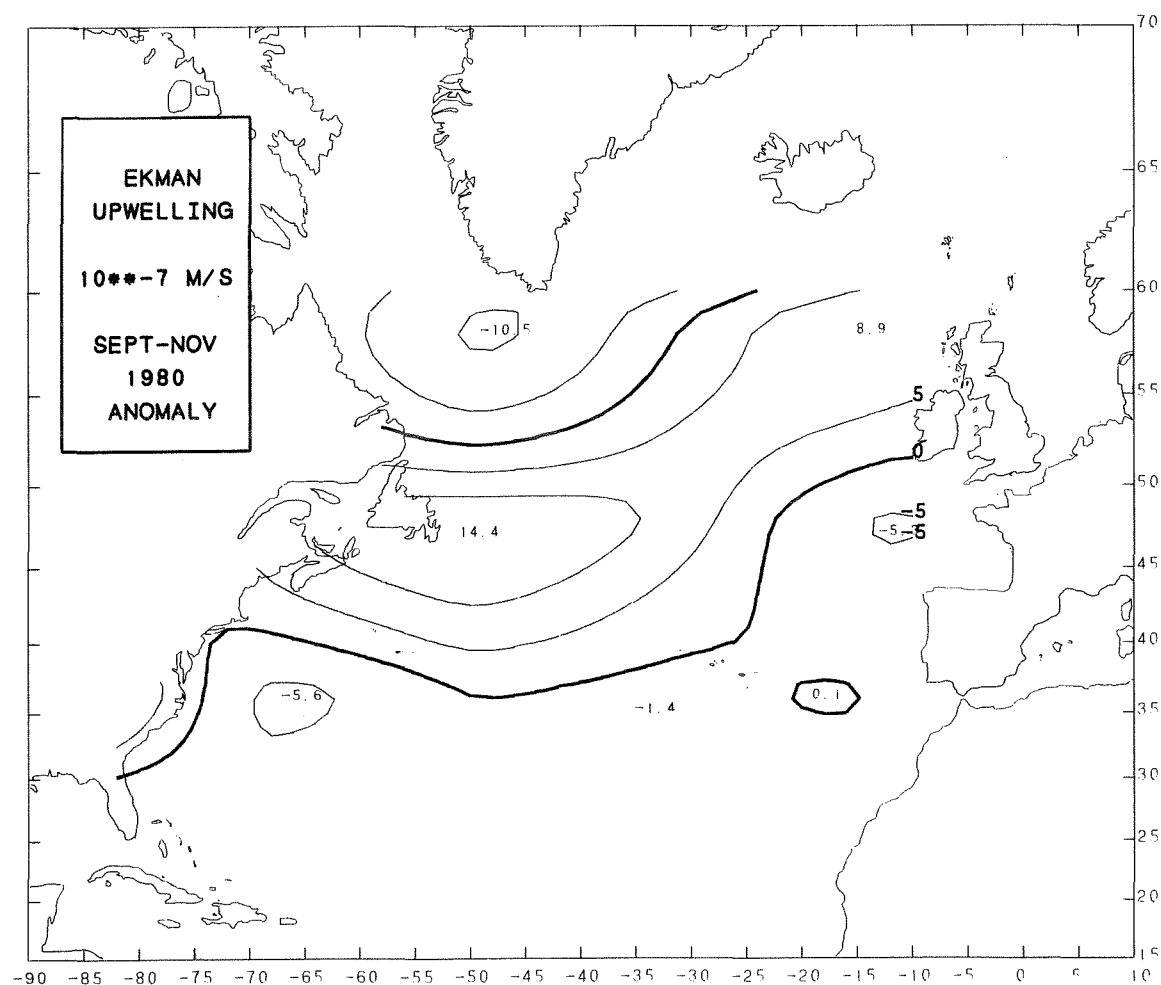
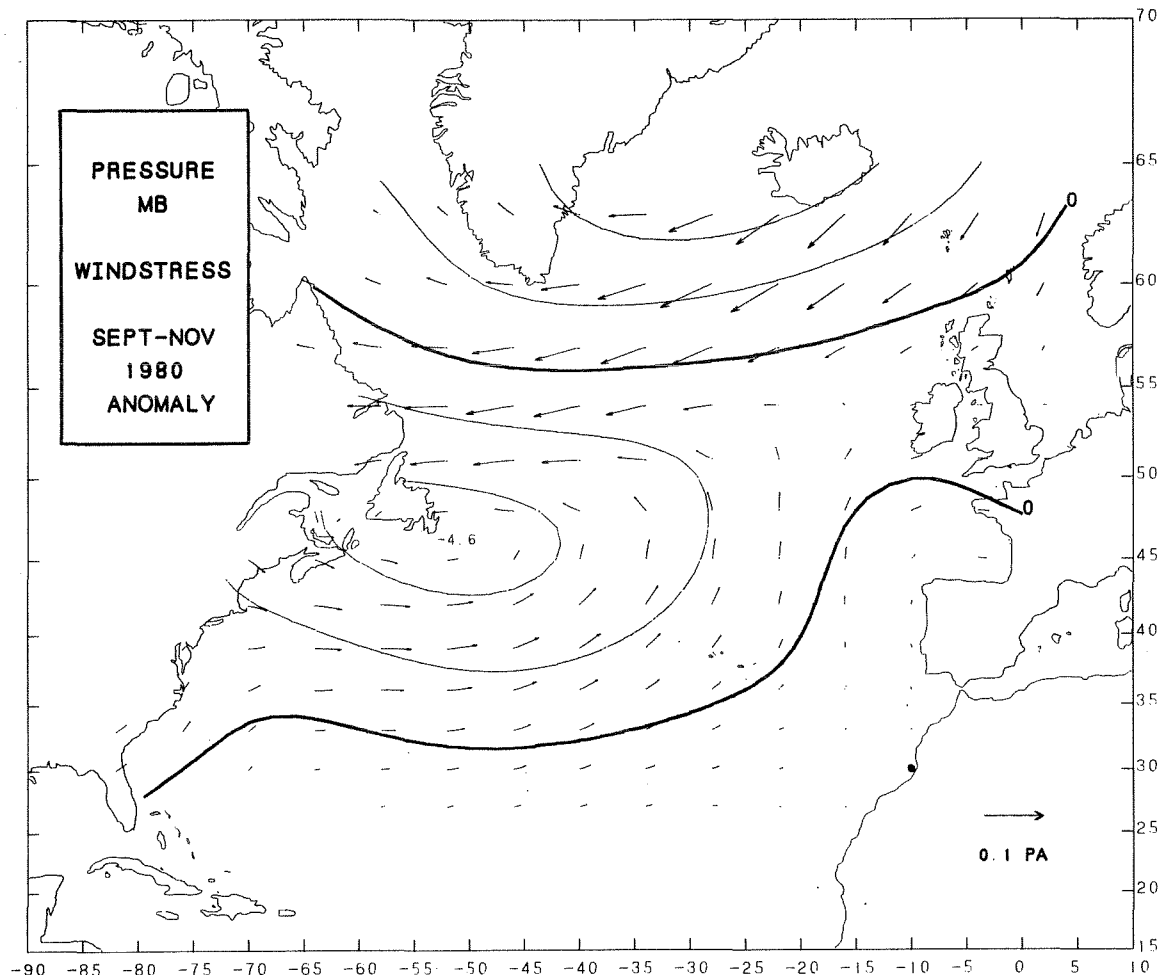












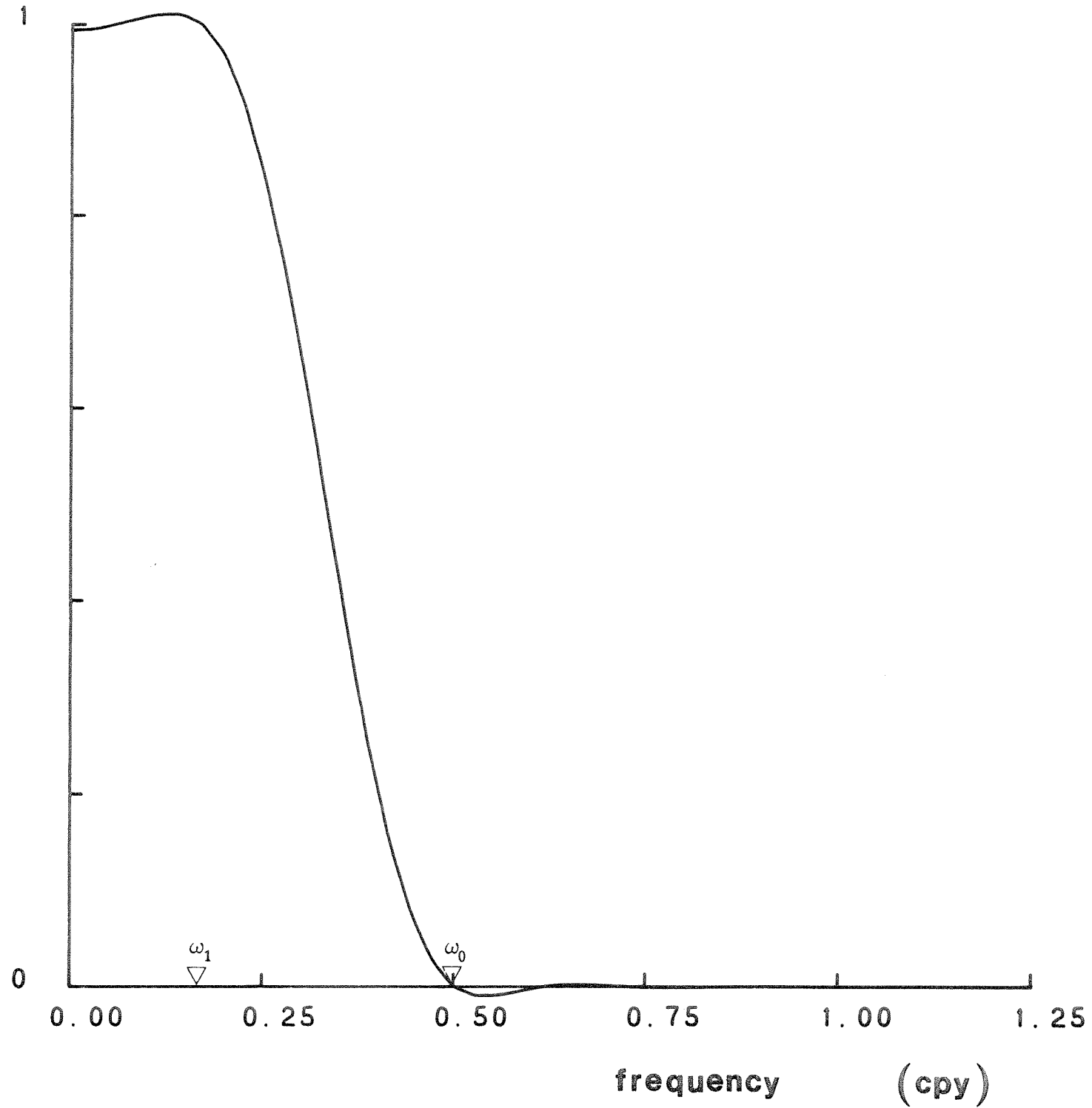


Figure 7

Response function of the lowpass filter applied to the wind stress and Ekman upwelling time series shown in Figure 9 and 10. The response function equals 0 and 1 for  $\omega_0 = 1/2$  cpy and  $\omega_1 = 1/6$  cpy respectively.

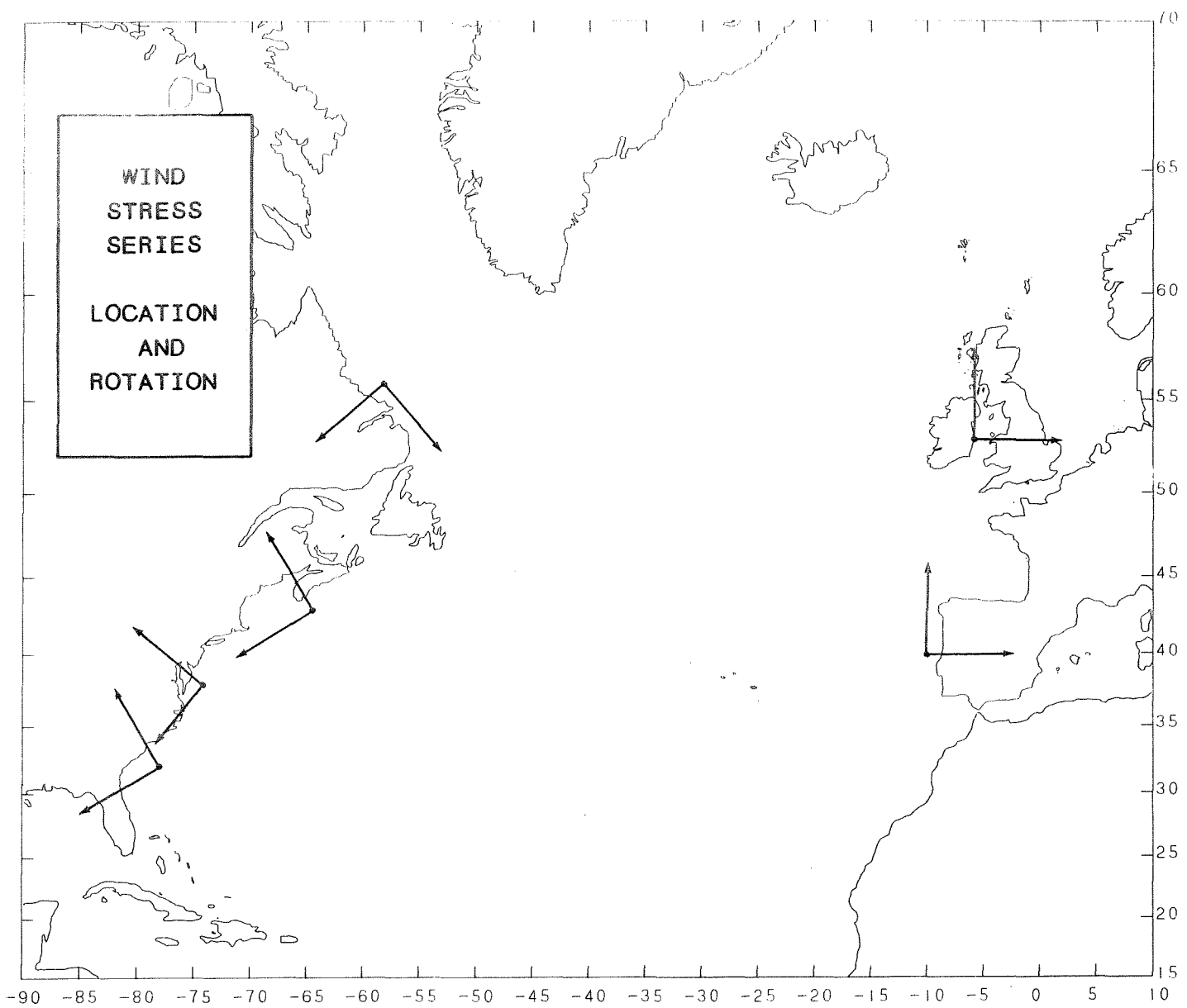
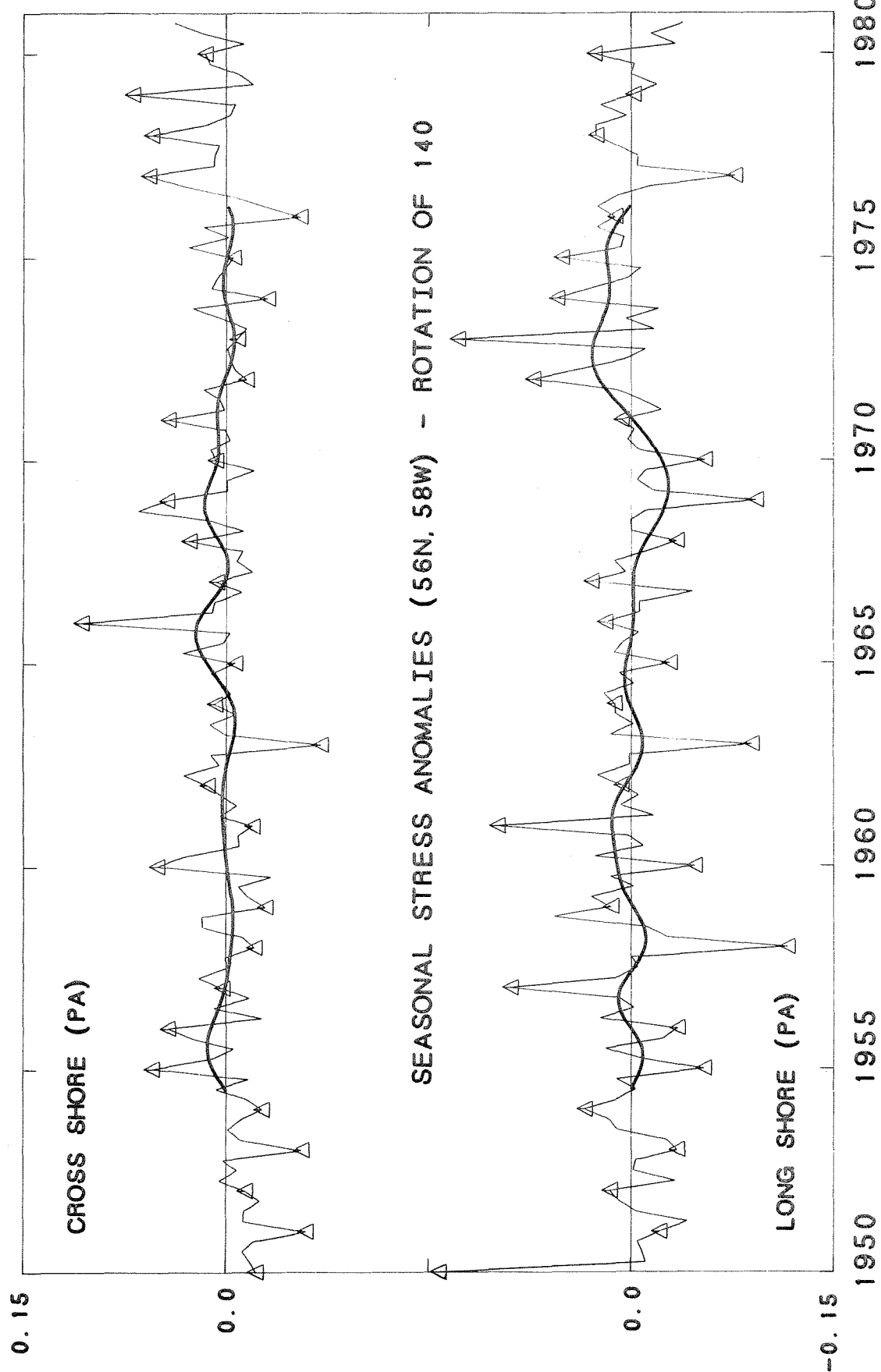


Figure 8

Locations for which wind stress time series have been plotted. The local orientation of the coordinate system, chosen to coincide with longshore and cross-shore, is also shown.

Figure 9

Longshore and cross-shore seasonal anomalies of wind stress. The appropriate seasonal variation given in Figure 4 has been removed from each series. The triangle marks the winter value and the continuous line shows the low-frequency component obtained by applying the lowpass filter (see Figure 7).



(a) Labrador Coast. The longshore component along this straight narrow shelf will drive coastal upwelling.

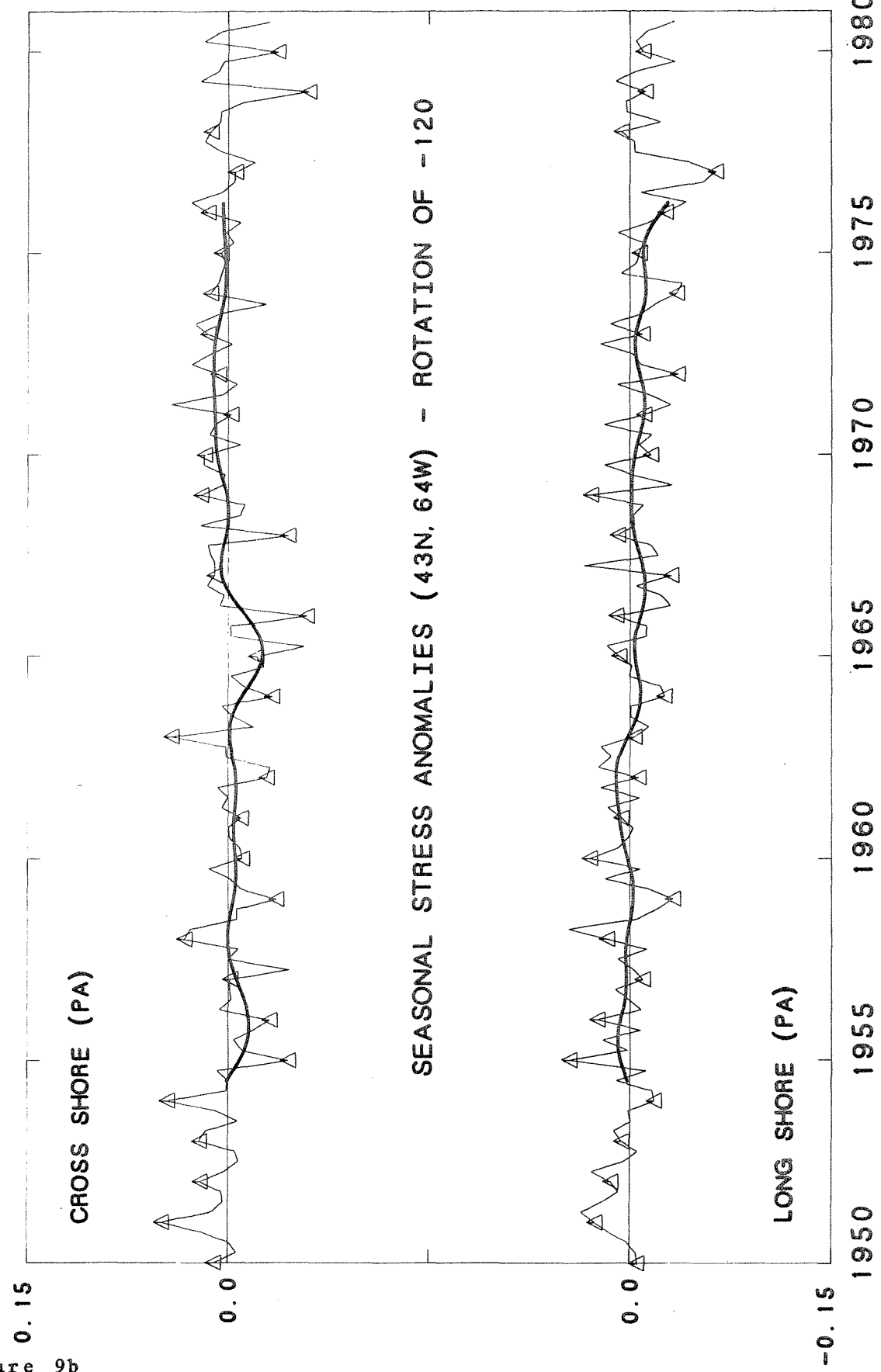
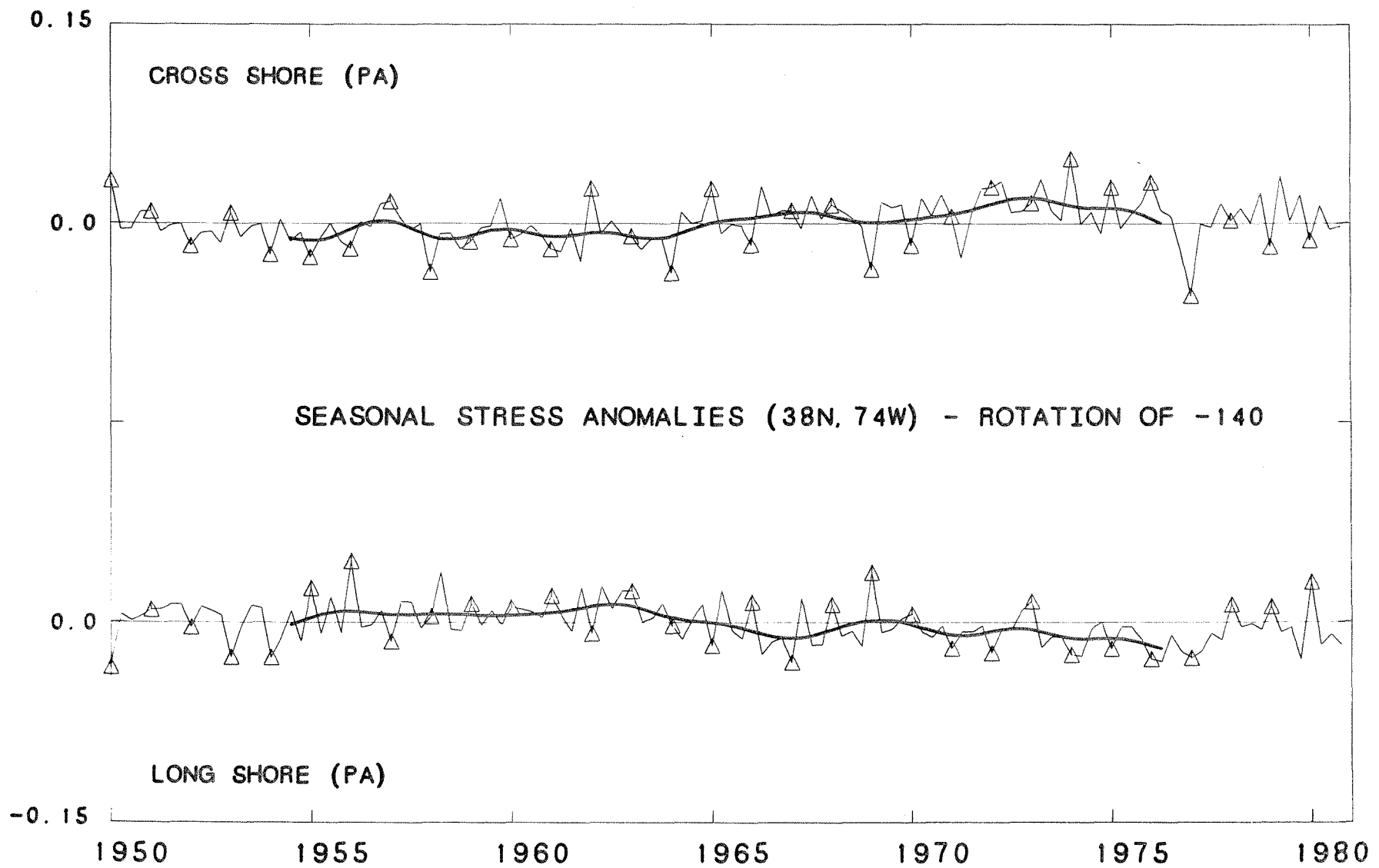


Figure 9b

Scotian Shelf and Gulf of Maine.

Mid-Atlantic Bight.

Figure 9c



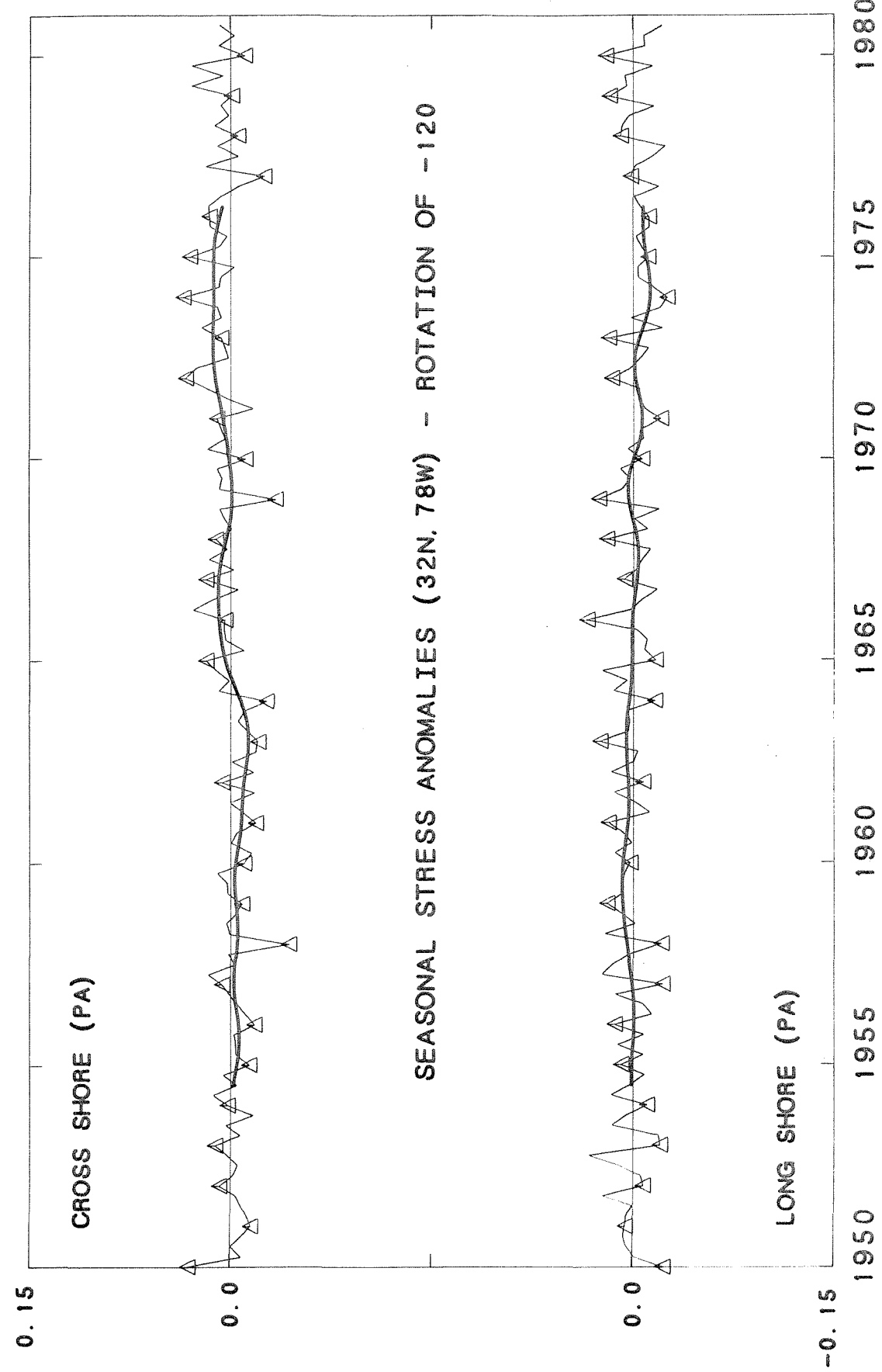


Figure 9d

South Atlantic Bight.

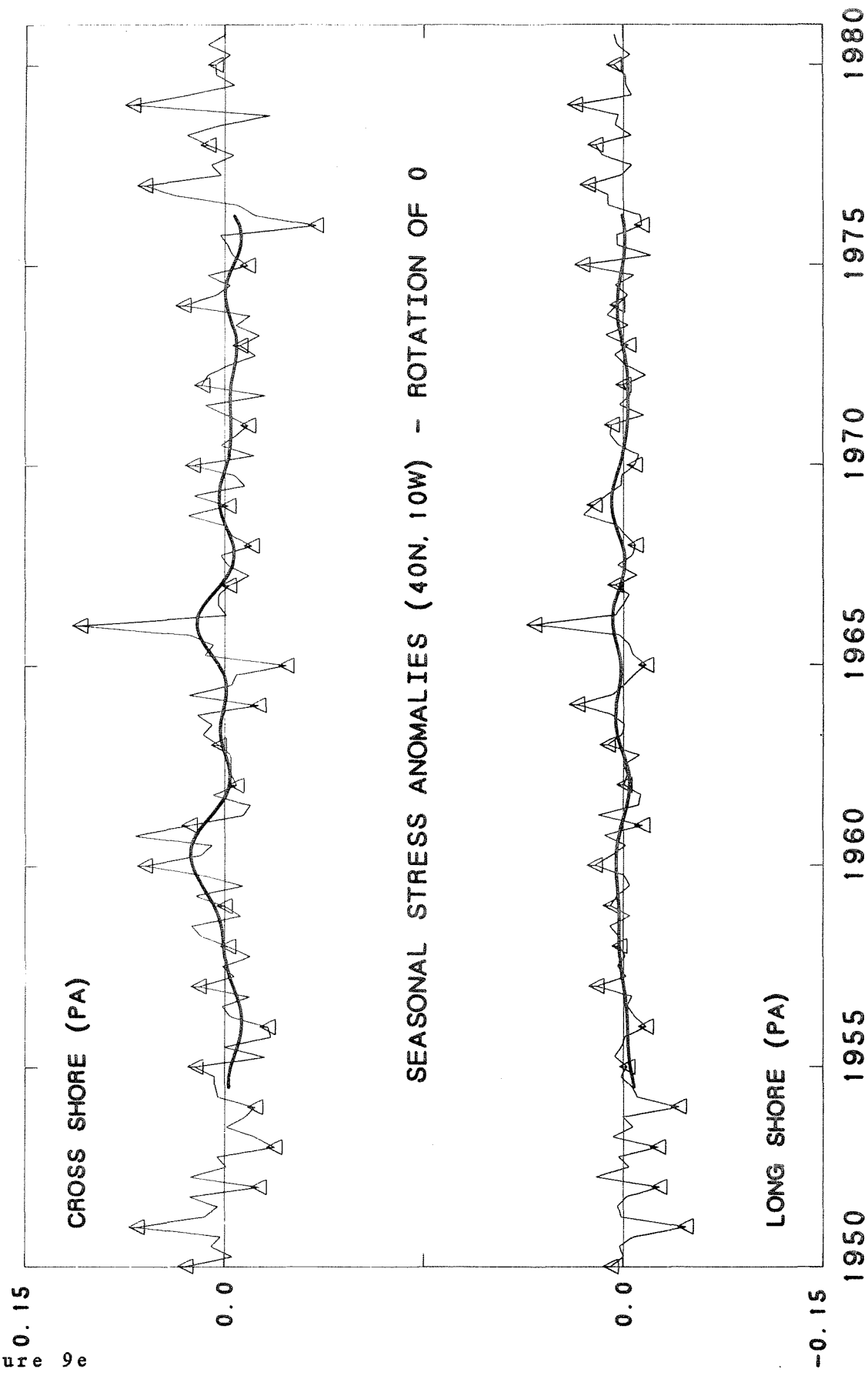
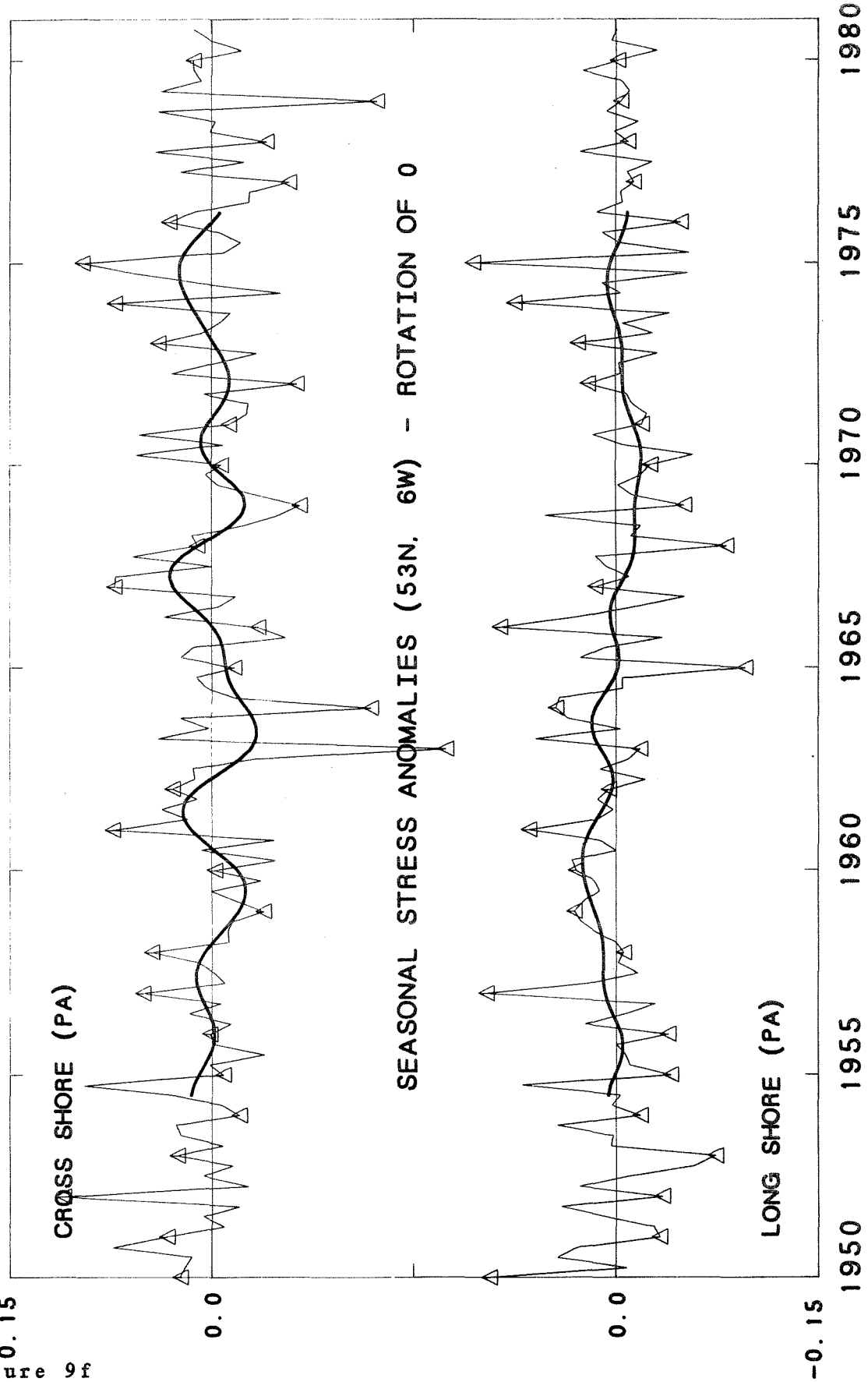


Figure 9e

Portuguese Coast. The longshore component along this straight, narrow shelf will drive coastal upwelling.



Northwest European Shelf Seas. Cross-shore corresponds to easterly stress.

**Figure 10**

Seasonal upwelling anomalies at 3 positions in the interior of the North Atlantic. Winter values are marked by a triangle and the low-frequency component by a continuous line.

50

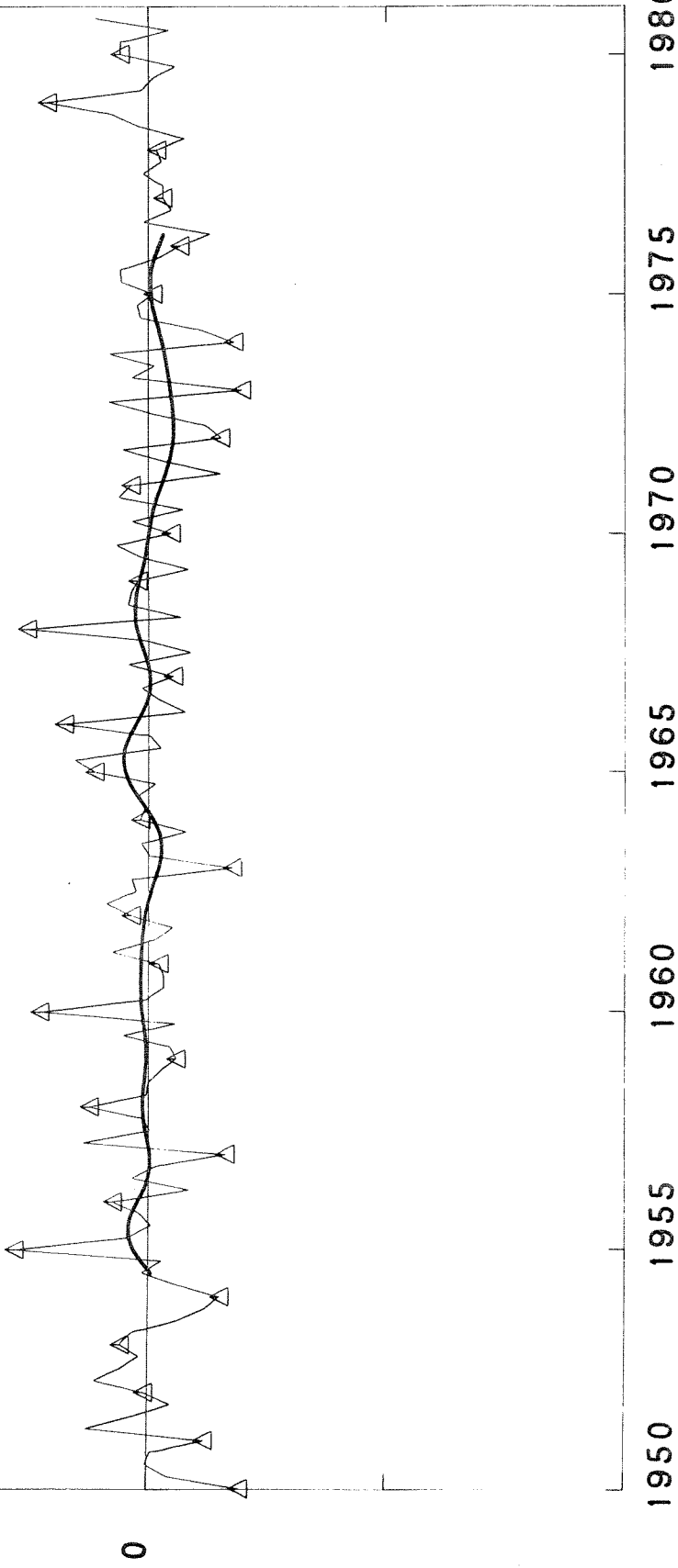
SEASONAL EKMAN UPWELLING ANOMALIES (50N, 36W) IN  $10^{-7}$  M/S

0

1950 1955 1960 1965 1970 1975 1980

50

SEASONAL EKMAN UPWELLING ANOMALIES (40N, 46W) IN 10\*\*-7 M/S



50

SEASONAL EKMAN UPWELLING ANOMALIES (30N, 56W) IN 10\*\*-7 M/S

